# The Descent: Geographical Information System Mapping as a Method of Quantification in Osteoarchaeological and Taphonomic Analysis of Early Neolithic Human Remains from Cave Burials in North-Western England

**by**

**Keziah Claire Warburton**

A thesis submitted in partial fulfilment for the requirements for the degree of Doctor of Philosophy at the University of Central Lancashire

September 2023

# RESEARCH STUDENT DECLARATION FORM

**Type of Award** **_____Doctor of Philosophy_____**

**School** **_____School of Law and Policing_____**

**Concurrent registration for two or more academic awards**

I declare that while registered as a candidate for the research degree, I have not been registered candidate or enrolled student for another award of the University or other academic or professional institution.

**Material submitted for another award**

I declare that no material contained in the thesis has been used in any other submission for an academic award and is solely my own work.

**Use of a Proof-reader**

No proof-reading service was used in the compilation of this thesis.

**Signature of Candidate** _____

# ABSTRACT

Caves have long been recognised as an important aspect of Neolithic burial practice and our understanding around such practices has been supported by taphonomic analysis and re-analysis of original excavations. This research aims to assess whether Geographic Information Systems (GIS) can be used as a tool for exploring taphonomy, currently underutilised in human cave assemblages. Through our understanding of taphonomic patterns at an element, body and stratigraphic level, site specific inferences of burial practices can be reconstructed and patterns across cave burials assessed.

Two main sites were selected for analysis, Cave Ha 3 (Yorkshire) and Heaning Wood (Cumbria). Bone fragments were assessed for taphonomic modifications and mapped onto templates of bones in QGIS. This has created visual and quantitative data of changes at a body level. Spatial archive data was examined and taphonomic modifications were geographically referenced in QGIS. This provided information of its distribution, allowing for analysis of the movement of skeletal elements and possible locations of geological processes within the cave system.

Analysis of Cave Ha 3 has highlighted possible burial locations and position of bodies, adding support to earlier narratives. Spatial data for Heaning Wood was less detailed, however analysis has indicated burial sequences. Eight of the nine individuals recovered from Heaning Wood have been radiocarbon dated, showing distinct episodes of burial spanning from the Early Mesolithic through to the Early Bronze Age. The research provides the most comprehensive report on Heaning Wood to date, with radiocarbon dates challenging previous discourse around the absence of Early Neolithic cave burials along the south coast of Cumbria. The Early Mesolithic date also provides support for the reoccupation of Britain occurring in the North West, simultaneous with occupation in the South.

Results suggest that QGIS can provide excellent visualisation of taphonomic modifications, regardless of whether a site has spatial legacy data. It has allowed analysis of intra and inter-body taphonomic changes. For sites that do have context data, QGIS provides a more traditional use, mapping where these modifications have occurred within the cave. This has

implications for understanding original deposition, geological processes and the relationship between the buried bodies and cave.

ACKNOWLEDGMENTS XVIII

LIST OF FIGURES XX

LIST OF SUPPLEMENTARY FIGURES XXVI

LIST OF TABLES XXVII

LIST OF SUPPLEMENTARY TABLES XXVIII

CHAPTER 1: INTRODUCTION 1

CHAPTER 2: NEOLITHIC BRITAIN 4

**2.1: The Neolithic Transition** **4**

**2.2: Neolithic Burials** **7**

**2.3: Cave Burial in Yorkshire** **15**

**2.4: Caves and the Ancestors, a Place of Spirituality?** **17**

CHAPTER 3: CAVES AND TAPHONOMY 20

**3.1: Cave Formation and Geology** **20**

**3.2: Taphonomy** **25**

3.2.1: Weathering 27

3.2.2: Fluvial Transport 29

3.2.3: Animal Agents 32

3.2.4: Natural Traps 36

3.2.5: Burial 39

3.2.6: Decomposition, Body Movement and Skeletal Part Representation 40

CHAPTER 4: QUANTIFICATION IN ARCHAEOLOGY 44

CHAPTER 5: ARCHAEOLOGY AND GIS 55

**5.1: Quantification and GIS** **56**

**5.2: Taphonomy and GIS** **61**

**5.3: Site Level Distribution and GIS** **66**

CHAPTER 6: AIMS AND OBJECTIVES 71

**6.1: Aims** **71**

**6.2: Objectives** **71**

CHAPTER 7: METHODOLOGY 72

**7.1: Terminology and Codes** **72**

**7.2: Identification of Human Remains** **74**

**7.3: Databasing** **75**

**7.4: Quantification** **77**
7.4.1 Minimum Number of Elements (MNE) and Minimum Number of Individuals (MNI) 77
7.4.2: Dentition 79

**7.5: Biological Profiling** **79**
7.5.1: Sex Estimation 79
7.5.2: Stature Estimation 80
7.5.3: Age at Death Estimation 81

**7.6: Geographical Information Systems (GIS)** **82**
7.6.1: GIS and MNI 82
7.6.2: GIS and Taphonomy 86
7.6.3: Creation of GIS Templates 90
7.6.4: Mapping the Body 94
7.6.5: Taphonomy and Bodies in Space 98

**7.7: Analysis** **101**
7.7.1: Skeletal Part Representation 101
7.7.2: Analysis of Whole Body Taphonomy 102
7.7.3: Spatial Analysis 105

CHAPTER 8: CAVE HA 3 – AN OVERVIEW 108

**8.1: Site Stratigraphy and Original Excavations** **108**

**8.2: Previous Analysis** **110**

CHAPTER 9: CAVE HA 3 QUANTIFICATION 114

**9:1: NISP and MNI** **114**

**9.2: Bone Representation Index** **115**

**9.3: Preservation According to Anatomical Side** **116**

CHAPTER 10: CAVE HA 3 DEMOGRAPHICS 118

**10.1: Individual 1** **118**
10.1.1: Age at Death Estimation 118
10.1.2: Skeletal Sex and Stature 118

**10.2: Individual 2** **120**
10.2.1: Age at Death Estimation 120
10.2.2: Genetic Sex 121

**10.3: Individual 3** **121**
10.3.1: Age at Death Estimation 121

**10.4: Individual 4** **123**
10.4.1: Age at Death Estimation 123

CHAPTER 11: CAVE HA 3 TAPHONOMY 125

**11.1: Individual 1** **125**
11.1.1: Bone Representation 125
11.1.2: Whole Body Taphonomy 127
11.1.3: Destruction 129
11.1.4: Fractures 133
11.1.5: Tufa Deposits 136
11.1.6: Staining 139
11.1.7: Processing Modifications 143
11.1.8: Animal Activity 144
11.1.9: Invertebrate Activity 145
11.1.10: Root and Weathering 146

**11.2: Individual 2** **146**
11.2.1: Bone Representation 146
11.2.2: Whole Body Taphonomy 147
11.2.3: Destruction 149
11.2.4: Fractures 150
11.2.5: Tufa Deposits 152
11.2.6: Staining 154

11.2.7: Invertebrate Activity 156
11.2.8: Animal Activity, Root Action, Butchery, and Weathering 157

**11.3: Individual 3 157**
11.3.1: Bone Representation 157
11.3.2: Whole Body Taphonomy 158
11.3.3: Destruction 160
11.3.4: Fractures 162
11.3.5: Tufa Deposits 164
11.3.6: Staining 166
11.3.7: Invertebrate Activity 168
11.3.8: Animal Activity, Root Action, and Weathering 168

**11.4: Individual 4 169**
11.4.1: Bone Representation 169
11.4.2: Whole Body Taphonomy 170
11.4.3: Destruction 172
11.4.4: Fractures 174
11.4.5: Tufa Deposits 176
11.4.6: Staining 178
11.4.7: Invertebrate Activity 180
11.4.8: Animal Activity, Root Action, and Weathering 180

**11.5: Assemblage Taphonomy 181**

CHAPTER 12: CAVE HA 3 SPATIAL ANALYSIS 182

**12.1: Assemblage - Distribution of Fragments 182**

**12.2: Assemblage – Element Distribution 183**

**12.3: Individual 1 - Element Distribution 184**
12.3.1: Crania 185
12.3.2: Vertebra 186
12.3.3: Long Bones 187
12.3.4: Flat/Irregular 189
12.3.5: Hands, Feet & Patellae 190

**12.4: Individual 1 - Taphonomic Distribution 192**
12.4.1: Fracturing 192
12.4.2: Destruction 192
12.4.3: Tufa Deposits 193
12.4.4: Staining 194

12.4.5: Processing Modifications 197
12.4.6: Animal Activity 197
12.4.7: Invertebrate Activity 197
12.4.8: Root and Weathering 197

**12.5: Individual 2 – Distribution of Fragments 198**

**12.6: Individual 2 – Element Distribution 198**
12.6.1: Crania 199
12.6.2: Vertebra 200
12.6.3: Long Bones 200
12.6.4: Flat/Irregular 203

**12.7: Individual 2 – Taphonomic Distribution 204**
12.7.1: Fracturing 204
12.7.2: Destruction 204
12.7.3: Tufa Deposits 205
12.7.4: Staining 206
12.7.5: Invertebrate Activity 207
12.7.6: Processing Modifications, Animal Activity, Root, and Weathering 207

**12.8: Individual 3 – Distribution of Fragments 208**

**12.9: Individual 3 – Element Distribution 209**
12.9.1: Crania 210
12.9.2: Vertebra 210
12.9.3: Long Bones 211
12.9.4: Flat/Irregular 211

**12.10: Individual 3 – Taphonomic Distribution 212**
12.10.1: Fracturing 212
12.10.2: Destruction 212
12.10.3: Tufa Deposits 213
12.10.4: Staining 213
12.10.5: Invertebrate Activity 214
12.10.6: Processing Modifications, Animal Activity, Root, and Weathering 214

**12.11: Individual 4 – Distribution of Fragments 215**

**12.12: Individual 4 – Element Distribution 216**
12.12.1: Crania 216
12.12.2: Long Bones 217
12.12.3: Flat/Irregular 218

**12.13: Individual 4 – Taphonomic Distribution** **219**
12.13.1: Fracturing 219
12.13.2: Destruction 220
12.13.3: Tufa Deposits 221
12.13.4: Staining 222
12.13.5: Invertebrate Activity 222
12.13.6: Processing Modifications, Animal Activity, Root, and Weathering 223

**12.14: Spatial Summary of Cave Ha 3** **224**

CHAPTER 13: HEANING WOOD – AN OVERVIEW 225

**13.1: Site Stratigraphy and Original Excavations** **225**

**13.2: Radiocarbon (C-14) Dating** **227**

CHAPTER 14: HEANING WOOD QUANTIFICATION 229

**14.1: NISP AND MINI** **229**

**14.2: Bone Representation Index** **230**

**14.3: Preservation According to Anatomical Side** **232**

CHAPTER 15: HEANING WOOD DEMOGRAPHICS 234

**15.1: Bronze Age - Individual A** **234**
15.1.1: Age at Death Estimation 234
15.1.2: Skeletal Sex and Stature 235
15.1.3: Paleopathology 235

**15.2: Bronze Age - Individual D** **236**
15.2.1: Age at Death Estimation 236
15.2.2: Skeletal Sex and Stature 237

**15.3: Early Neolithic - Individual B** **238**
15.3.1: Age at Death Estimation 238
15.3.2: Skeletal Sex and Stature 239

**15.4: Early Neolithic - Individual C** **239**
15.4.1: Age at Death Estimation 239
15.4.2: Skeletal Sex and Stature 241

**15.5: Early Neolithic - Individual E** **242**
15.5.1: Age at Death Estimation 242

**15.6: Early Neolithic - Individual H** **243**
15.6.1: Age at Death Estimation 243

**15.7: Mesolithic - Individual F** **244**
15.7.1: Age at Death Estimation 244

**15.8: Undated - Individual G** **245**
15.8.1: Age at Death Estimation 245

CHAPTER 16 HEANING WOOD TAPHONOMY 246

**16.1: Bronze Age - Individual A** **246**
16.1.1: Bone Representation 246
16.1.2: Whole Body Taphonomy 247
16.1.3: Destruction 249
16.1.4: Fractures 253
16.1.5: Tufa Deposits 255
16.1.6: Staining 257
16.1.7: Large Animal and Invertebrate Activity 260
16.1.8: Weathering and Surface Effects 261

**16.2: Bronze Age - Individual D** **263**
16.2.1: Bone Representation 263
16.2.2: Whole Body Taphonomy 264
16.2.3: Destruction 266
16.2.4: Fractures 268
16.2.5: Tufa Deposits 270
16.2.6: Staining 272
16.2.7: Large Animal and Invertebrate Activity 275
16.2.8: Weathering and Surface Effects 276

**16.3: Summary of Early Bronze Age Taphonomy** **279**

**16.4: Early Neolithic - Individual B** **280**
16.4.1: Bone Representation 280
16.4.2: Whole Body Taphonomy 281
16.4.3: Destruction 283
16.4.4: Fractures 285
16.4.5: Tufa Deposits 287
16.4.6: Staining 290
16.4.7: Large Animal and Invertebrate Activity 292
16.4.8: Weathering and Surface Effects 293

**16.5: Early Neolithic - Individual C** **295**
16.5.1: Bone Representation 295
16.5.2: Whole Body Taphonomy 297
16.5.3: Destruction 299
16.5.4: Fractures 301
16.5.5: Tufa Deposits 302
16.5.6: Staining 304
16.5.7: Large Animal and Invertebrate Activity 307
16.5.8: Weathering and Surface Effects 307

**16.6: Early Neolithic - Individual E** **309**
16.6.1: Bone Representation 309
16.6.2: Whole Body Taphonomy 310
16.6.3: Destruction 312
16.6.4: Fractures 313
16.6.5: Tufa Deposits 314
16.6.6: Staining 315
16.6.7: Large Animal and Invertebrate Activity 316
16.6.8: Weathering and Surface Effects 316

**16.7: Early Neolithic - Individual H** **317**
16.7.1: Bone Representation 317
16.7.2: Whole Body Taphonomy 317

**16.8: Summary of Early Neolithic Taphonomy** **319**

**16.9: Mesolithic - Individual F** **319**
16.9.1: Bone Representation 319
16.9.2: Whole Body Taphonomy 320

**16.10: Undated - Individual G** **321**
16.10.1: Bone Representation 321
16.10.2: Whole Body Taphonomy 322
16.10.3: Destruction 324
16.10.4: Fractures 326
16.10.5: Deposits 326
16.10.6: Staining 326
16.10.7: Large Animal and Invertebrate Activity 328
16.10.8: Weathering and Surface Effects 328

**16.11: Assemblage Taphonomy** **328**

CHAPTER 17: HEANING WOOD SPATIAL ANALYSIS 329

**17.1: Assemblage - Distribution of Fragments 329**

**17.2: Distribution According to Burial Period 331**
17.2.1: Dated Samples 331
17.2.2: Early Bronze Age Distribution 332
17.2.3: Early Neolithic Distribution 334
17.2.4: Mesolithic Distribution 335
17.2.5: Unassigned Material Distribution 336

**17.3: Assemblage - Element Distribution 337**

**17.4: Individual A (Early Bronze Age) – Distribution of Fragments 338**

**17.5: Individual A (Early Bronze Age) - Element Distribution 339**
17.5.1: Crania 340
17.5.2: Vertebra 341
17.5.3: Long Bones 343
17.5.4: Flat/Irregular 344
17.5.5: Hands, Feet & Patella 345

**17.6: Individual A (Early Bronze Age) - Taphonomic Distribution 346**
17.6.1: Fracturing 346
17.6.2: Destruction 346
17.6.3: Tufa Deposits 347
17.6.4: Staining 347
17.6.5: Invertebrate Activity 347
17.6.6: Root and Weathering 349

**17.7: Individual D (Early Bronze Age) - Distribution of Fragments 349**

**17.8: Individual D (Early Bronze Age) - Distribution of Elements 350**
17.8.1: Crania 351
17.8.2: Vertebra 352
17.8.3: Long Bones 354
17.8.4: Flat/Irregular 355
17.8.5: Hands, Feet and Patella 355

**17.9: Individual D (Early Bronze Age) - Distribution of Taphonomy 356**
17.9.1: Fracturing 356
17.9.2: Destruction 356
17.9.3: Tufa Deposits 357
17.9.4: Staining 357

17.9.5: Invertebrate Activity 358
17.9.6: Root and Weathering 358

**17.10: Individual B (Early Neolithic) - Distribution of Fragments 359**

**17.11: Individual B (Early Neolithic) - Distribution of Elements 360**
17.11.1: Crania 360
17.11.2: Vertebra 362
17.11.3: Long Bones 363
17.11.4: Flat/Irregular 364
17.11.5: Hands, Feet and Patella 365

**17.12: Individual B (Early Neolithic) - Distribution of Taphonomy 366**
17.12.1: Fracturing 366
17.12.2: Destruction 366
17.12.3: Tufa Deposits 367
17.12.4: Staining 367
17.12.5: Invertebrate Activity 367
17.12.6: Root and Weathering 368

**17.13: Individual C (Early Neolithic) - Distribution of Fragments 368**

**17.14: Individual C (Early Neolithic) - Distribution of Elements 369**
17.14.1: Crania 370
17.14.2: Vertebra 371
17.14.3: Long Bones 372
17.14.4: Flat/Irregular 373
17.14.5: Hands, Feet and Patella 373

**17.15: Individual C (Early Neolithic) - Distribution of Taphonomy 375**
17.15.1: Fracturing 375
17.15.2: Destruction 375
17.15.3: Tufa Deposits 375
17.15.4: Staining 375
17.15.5: Invertebrate Activity 377
17.15.6: Root and Weathering 377

**17.16: Individual E (Early Neolithic) - Distribution of Fragments 379**

**17.17: Individual E (Early Neolithic) - Distribution of Elements 380**

**17.18: Individual E (Early Neolithic) - Distribution of Taphonomy 382**

**17.19: Individual H (Early Neolithic) – All Distributions 383**

**17.20: Individual F (Mesolithic) - Distribution of Fragments** **383**

**17.21: Individual F (Mesolithic) - Distribution of Taphonomy** **385**

**17.22: Individual G (Undated) - Distribution of Fragments** **385**

**17.22: Individual G (Undated) - Distribution of Elements** **386**

**17.23: Individual G (Undated) - Distribution of Taphonomy** **388**

**17.24: Spatial Summary of Heaning Wood** **388**

CHAPTER 18: DISCUSSION 390

**18.1: Readdressing the research question** **390**

**18.2: Cave Ha 3** **391**
18.2.1: Quantification and Individuation 391
18.2.2: Individual 1 393
18.2.3: Individual 2 396
18.2.4: Individuals 3 and 4 398
18.2.5: Assemblage 398

**18.3: Heaning Wood** **401**
18.3.1: Individuation of Commingled and Fragmented Assemblages 401
18.3.2: Radiocarbon Dating: Changing the Narrative 404
18.3.3: Bronze Age Burials 407
18.3.4: Neolithic Burials 409
18.3.5: Mesolithic Burial 414
18.3.6: Undated Burial 414
18.3.7: Assemblage 414

**18.4: Geographical Information Systems (GIS) as an Analytical Tool** **416**
18.4.1: Templates and Recording Issues 416
18.4.2: Placement of Fragments 418

CHAPTER 19: CONCLUSION 422

**19.1: The Bigger Picture: Heaning Wood and Cave Ha 3 in Context** **422**
19.1.1: Cave Morphology 422
19.1.2: Mesolithic Cave Burials 423
19.1.3: Neolithic Cave Burials 424
19.1.4: Bronze Age Cave Burials 425

**19.2: Where Next? Implications for Future Research** **426**

19.2.1: Alternative Visualisations 427
19.2.2: Histological and Microscopic Analysis 430
19.2.3: Biochemical Analysis 431
19.2.4: Ancient DNA and Isotope Analysis 431
19.2.5: Excavation and Faunal and Artefact Analysis 431

**19.3 Conclusion 432**

REFERENCES 434

APPENDICES 1

APPENDIX ONE: METHODOLOGY 2

**1.1: Bone Names and Associated Codes 2**

**1.2: QGIS Codes 5**
1.2.1: Field Attributes for GIS 5
1.2.2: Taphonomy Codes for GIS 6

**1.3: Cave Ha 3 Discrepancies 9**

**1.4: Osteology Observation Forms 10**
1.4.1: Observational notes 10
1.4.2: Adult Skeletal Sketch 11
1.4.3: Infant Skeletal Sketch 12

**1.5: Skeletal Zones 13**
1.5.1: Adult Zones 13
1.5.2: Infant Zones 19

**1.6: Zonation Forms 21**

**1.7: Example Dental Inventory Form 22**

**1.8: Gross Taphonomy 24**

**1.9: Criteria for Taphonomy Observations 25**

**1.10: Cave Ha 3 Archive 29**

**1.11: Georeferenced Taphonomy Tables 30**
1.11.1 Cave Ha 3 Attribute Spreadsheets 30
1.11.2 Heaning Wood Attribute Spreadsheets 30

APPENDIX TWO: CAVE HA 3 QUANTIFICATION 31

**2.1: Cave Ha 3 Master Spreadsheet** **31**

APPENDIX THREE: CAVE HA 3 DEMOGRAPHICS 32

**3.1: Metrics** **32**
3.1.1: Individual 1 32
3.1.2: Individual 2 34
3.1.3: Individual 3 35
3.1.4: Individual 4 36

APPENDIX FOUR: CAVE HA 3 TAPHONOMY 37

**Appendix 4.1: Individual 1** **37**

**Appendix 4.2: Individual 2** **38**

**Appendix 4.3: Individual 3** **39**

**Appendix 4.4: Individual 4** **40**

APPENDIX FIVE: HEANING WOOD QUANTIFICATION 41

**5.1: Heaning Wood Master Spreadsheet** **41**

**5.2: Heaning Wood Unassigned Fragments** **41**

APPENDIX SIX: HEANING WOOD DEMOGRPAHICS 42

**6.1: Individuals E and F X-Rays** **42**

APPENDIX SEVEN: HEANING WOOD TAPHONOMY 43

**Appendix 7.1: Individual A** **43**

**Appendix 7.2: Individual D** **43**

**Appendix 7.3: Individual B** **43**

**Appendix 7.4: Individual C** **43**

**Appendix 7.5: Individual E** **44**

**Appendix 7.6: Individual G** **44**

# ACKNOWLEDGMENTS

Firstly, thank you to my supervisors Dr Rick Peterson, Dr Catherine Tennick and Dr Patrick Randolph-Quinney for their support during both this journey and my masters, where all this started. Thank you to Pat for introducing me to those 15 sacks of Heaning Wood bones back in 2017 and for believing that I could continue the process. Thanks to Cat, not only for the academic support, but also for all the emotional support and "you've got this" memes. A huge thanks to Rick for entertaining all my questions (even when I knew the answer), reading countless drafts and always making himself available. You have PhD supervising down to a fine art.

Thank you to the rest of the UCLan Archaeology team, particularly Professor Duncan Sayer, Peter Cross, Professor Dave Robinson, Rachel Cunliffe, Dr Sam Walsh, Dr Clare Bedford, and Irene Van Zwieten for their advice, support, and practical help. A special thank you to Dr Jim Morris who gave invaluable feedback and assistance with data during the transfer process.

Thank you to Charlotte Hawley from the Dock Museum, Barrow-in-Furness for the loan of the Heaning Wood material and an enormous thank you to Tom Lord at Lower Winskill farm. Tom not only loaned the Cave Ha 3 material for analysis but sent archive records, shared his knowledge freely and welcomed us to his farm for project work. Thank you to Martin Stables for the excavation of Heaning Wood Bone Cave, without which this project would not exist and to Lisbeth R. Redshaw for welcoming us onto her property.

To the PhD society and members; Alex, Ellis, Vicki, Suse, Alison, Nicola, and Naomi. I am so grateful for the online and in-person working sessions. Thank you for holding me accountable, supporting me during stressful periods and for transforming the journey from one of isolation to one of friendship and belonging.

I would like to thank my family. My dad, Geoff Warburton, for his unwavering support, help with diagrams, conference run throughs, and generally being my number one fan. My mum, Katherine Warburton for taking me to task on my errant commas, as well all the emotional support. My sisters Bethany and Lily for always believing I could finish this even when I didn't. Thank you to my son Jacob, I promise that now this is finished I will come to the gym with

you. Finally, Adam. I am lost for words on how to express my gratitude. You are the calm to my storm. Without you, I would not have finished.

# LIST OF FIGURES

**Figure 1.1: Known caves in Ireland and Britain with radiocarbon dated human remains from the Neolithic period. The grey circles show the positions of caves in both countries with human remains of any date (taken from Peterson, 2019, fig. 1.1). 1**

**Figure.3.1: Development of vadose and phreatic cave systems. The dashed line represents the water table. Figure (a) shows phreatic development before becoming a vadose system (b to d). (Lewin and Woodward, 2009). 21**

**Figure 3.2: Example of calcite deposits on a calcaneus (photo: K.Warburton, 2021) 24**

**Figure 3.3: Example of a tibial shaft showing manganese staining and iron oxides (Randolph-Quinney et al., 2016, p. 2) 24**

**Figure 3.4: Stages one to five showing progression of weathering (taken from Behrensmeyer, 1978, fig.2). 27**

**Figure 3.5: A distal tibia showing cracking and delamination after 150 wet-dry cycles (taken from Pokines et al., 2018, fig.3). 28**

**Figure 3.6: Examples of A) sediment impaction, B) acid etching, C) discolouration, D) invertebrate activity, and E) cracking as a result of fluvial transport (taken from Evans, 2013, figures 6.1a, 6.2c,6.4b, 6.5c and 6.5e). 31**

**Figure 3.7: Examples of A) gnawing, B) gastric erosion, C) punctures, D) rounding, pitting and striations as a result of dog gnawing (taken from Pokines, 2013a, figures 9.6, 9.7, 9.8a, and 9.11a). 35**

**Figure 3.8: A transverse fracture on mineralised bone, with rough edges (taken from Outram, 2001, fig.3). 37**

**Figure 3.9: Helical fracture lines radiating from point of impact in fresh cattle bone (taken from Outram, 2001, fig.2). 37**

**Figure 3.6: Diagram showing factors influencing decomposition and bone displacement (Schotsmans *et al.*, 2022, fig. 27.9). 41**

**Figure 4.1: Zoned tibia (taken from Dobney and Rielly, 1988, fig. 13). 50**

**Figure 4.2: Zoned tibia (taken from Knüsel and Outram, 2004, fig. 10). 51**

**Figure 5.1: Example of fragments placed on digital templates (taken from Marean *et al.*, 2001, fig. 5). 57**

**Fig 7.1: Example of a zoned femur (adapted from Knüsel and Outram, 2004). 77**

**Figure 7.2: Example of a template photograph for GIS. 82**

**Figure 7.3: Vector polygon layered over raster image, set to 33% opacity to ensure accurate tracing of bone contours. 83**

**Figure 7.4: Template of the four views of a right femur. 84**

**Figure 7.5: Specimen image overlaying the reference template. Note how the margins do not line up. 85**

**Figure 7.6: Example template of zoned atlas. Showing superior, inferior, anterior, posterior, and lateral views. 89**

**Figure 7.7: Manually recorded staining on femur. Colour indicated severity and staining type. 90**

**Figure 7.8: Image of the combined elements, creating a full body template. 91**

**Figure 7.9: Image of the combined elements, creating sub-adult templates (A. Birth - 1 years, B. 1- 3 years, C. 3+ years) 93**
**Figure 7.10: Ulna with destruction, fractures, staining, absent bone, rodent markings, and deposits recorded in GIS. 95**
**Figure 7.11: Workflow for QGIS mapping. 97**
**Figure 7.12: 1955 excavation and finds map with 2022 survey. 99**
**Figure 7.13: Example of the group stats function in QGIS. 103**
**Figure 7.14: Analysis of body taphonomy. 104**
**Figure 7.15: Example of the query builder in QGIS. 105**
**Figure 7.16: Process of spatial analysis 107**
**Figure 8.1: Location of the Cave Ha Complex. 108**
**Figure 8.2: The interior of Cave Ha 3 (Photograph: Peterson, 2019, p.144) 109**
**Figure 8.3: Hand drawn map of finds (Lord, 2004). 112**
**Figure 8.4: Digitised and georeferenced map of Cave Ha 3. 113**
**Figure 9.1: Graph showing BRI % for grouped bones – excluding unidentified cranial fragments. 116**
**Figure 9.2: Percentage of fragments according to anatomical side (Cave Ha 3). 117**
**Figure 10.1: Mandible showing area of bone lesion. 119**
**Figure 10.2: Specimen CH3.73.36 Ld$M_1$ with incomplete root formation. 122**
**Figure 10.3: Embedded mandible. 122**
**Figure 10.4: Deformed parietals from Individual 4. 124**
**Figure 11.1: Bone representation for Individual 1, Cave Ha 3. 125**
**Figure 11.2: Ribs excluded from GIS due to uncertainty around position (Individual 1). 126**
**Figure 11.3: Distribution of all taphonomic modifications across Individual 1. 128**
**Figure 11.4: Distal portion of radius showing area of crush damage. 130**
**Figure 11.5: Distribution of crushing across Individual 1. Red dot = area of crush damage. 131**
**Figure 11.6: A talus showing areas of 'exposure of trabecular bone' (red arrows) consistent with sediment abrasion. 132**
**Figure 11.7: Distribution of fracturing across Individual 1. 134**
**Figure 11.8: Blue arrows showing incomplete fractures radiating from areas of destruction. 135**
**Figure 11.9: Distribution of fragments affected by tufa deposits for Individual 1. 137**
**Figure 11.10: a) GIS diagram of the plantar and dorsal view (respectively) of deposits embedding the right foot. B) photograph of the foot in plantar view. 139**
**Figure 11.11: Image showing black-grey staining on the posterior surface of a patella. 140**
**Figure 11.12: Distribution of fragments affected by staining for Individual 1. 141**
**Figure 11.13: Image showing notch defect (blue box) on smashed tibia. 143**
**Figure 11.14: Smashed tibia showing area of deposit covering internal bone surface (blue arrow) and deposit crossing fracture (red arrow). 144**
**Figure 11.15: Left ulna showing area of rodent gnawing. 145**

**Figure 11.16: Graph showing bone representation for Individual 2, Cave Ha 3. 147**
**Figure 11.17: All taphonomic modifications across Individual 2. 148**
**Figure 11.18: Fracture distribution for Individual 2 151**
**Figure 11.19: Tufa distribution for Individual 2 153**
**Figure 11.20: a) Tibia and fibula adhered by tufa b) Represented in QGIS 154**
**Figure 11.21: Staining distribution for Individual 2 155**
**Figure 11.22: Graph showing bone representation for Individual 3, Cave Ha 3. 158**
**Figure 11.23: All taphonomic modifications across Individual 3. 159**
**Figure 11.24: Crush distribution for Individual 3. 161**
**Figure 11.25: Fracture distribution for Individual 3 163**
**Figure 11.26: Tufa distribution for Individual 3. 165**
**Figure 11.27: Staining distribution for Individual 3 167**
**Figure 11.28: Graph showing bone representation for Individual 4, Cave Ha 3. 169**
**Figure 11.29: Image showing all taphonomic modifications across Individual 4. 171**
**Figure 11.30: Crush distribution for Individual 4. 173**
**Figure 11.31: Fracture distribution for Individual 4 175**
**Figure 11.32: Tufa distribution for Individual 4 177**
**Figure 11.33: Staining distribution for Individual 4 179**
**Figure 12.1: Distribution of fragments according to NISP counts. 182**
**Figure 12.2: Distribution of fragments according to element group for all individuals. 183**
**Figure 12.3: Distribution of fragments from Individual 1 according to NISP counts. 184**
**Figure 12.4: Distribution of fragments according to element group - Individual 1. 185**
**Figure 12.5: Dispersal of the occipital in relation to the mandible – Individual 1. 186**
**Figure 12.6: Dispersal of the occipital in relation to the atlas and axis – Individual 1. 187**
**Figure 12.7: Distribution of long bone fragments – Individual 1. 188**
**Figure 12.8: Distribution of irregular bones – Individual 1 189**
**Figure 12.9: Distribution of hands, feet, and patellae - Individual 1 190**
**Figure 12.10: Possible sequences of movement for elements of the feet – Individual 1. 191**
**Figure 12.11: Distribution of crush damage and cortical removal - Individual 1. 193**
**Figure 12.12: Distribution of fragments embedded in tufa – Individual 1. 194**
**Figure 12.13: Distribution of staining - Individual 1. 195**
**Figure 12.14: Distribution of fragments with dark staining - Individual 1. 196**
**Figure 12.15: Distribution of fragments from Individual 2 according to NISP counts. 198**
**Figure 12.16: Distribution of fragments according to element group - Individual 2. 199**
**Figure 12.17: Distribution of cranial fragments - Individual 2. 200**
**Figure 12.18: Distribution of long bone fragments - Individual 2. 201**
**Figure 12.19: Possible body position of Individual 2. 202**
**Figure 12.20: Distribution of irregular and flat fragments - Individual 2. 203**

**Figure 12.21: Distribution of fragments with peri-mortem fracture - Individual 2. 204**
**Figure 12.22: Distribution of fragments with evidence of crushing - Individual 2. 205**
**Figure 12.23: Distribution of fragments with dark staining - Individual 2. 206**
**Figure 12.24: Distribution of fragments with invertebrate modifications - Individual 2. 207**
**Figure 12.25: Distribution of fragments from Individual 3 according to NISP counts. 208**
**Figure 12.26: Distribution of fragments according to element group - Individual 3 209**
**Figure 12.27: Distribution of cranial fragments - Individual 3. 210**
**Figure 12.28: Distribution of irregular/flat fragments - Individual 3. 211**
**Figure 12.29: Distribution of fragments with evidence of crushing - Individual 3. 212**
**Figure 12.30: Distribution of fragments with tufa embedding - Individual 3. 213**
**Figure 12.31: Distribution of fragments with staining - Individual 3. 214**
**Figure 12.32: Distribution of fragments from Individual 4 according to NISP counts. 215**
**Figure 12.33: Distribution of fragments according to element group - Individual 4 216**
**Figure 12.34: Distribution of cranial fragments - Individual 4. 217**
**Figure 12.35: Distribution of long bones - Individual 4. 218**
**Figure 12.36: Distribution of flat/irregular bones - Individual 4. 219**
**Figure 12.37: Distribution of fragments with incomplete or peri-mortem fractures - Individual 4. 220**
**Figure 12.38: Distribution of fragments with peri-mortem crushing - Individual 4. 221**
**Figure 12.39: Distribution of fragments with dark staining - Individual 4. 222**
**Figure 12.40: Distribution of fragments with invertebrate modifications - Individual 4. 223**
**Figure 13.1: Location of Heaning Wood Bone Cave 225**
**Figure 13.2: Plan, north-facing, and west-facing views of Heaning Wood Bone Cave 226**
**Figure 14.1: Total BRI % for grouped bones, excluding and including unassigned fragments, 230**
**Figure 14.2: BRI % for grouped bones – excluding unidentified and unassigned fragments. 231**
**Figure 14.3: BRI % by period. 232**
**Figure 14.4: Percentage of fragments according to anatomical side. 233**
**Figure 15.1: Mandibular dentition for Individual A. 234**
**Figure 15.2: Frontal bone from Individual A showing area of porotic hyperostosis to the supraorbital ridge. 236**
**Figure 15.3: Mandibular dentition for Individual D. 237**
**Figure 15.4: Partial fusion of first and second sacral elements. 238**
**Figure 15.5: Partial fusion of the medial epiphyseal flake of the clavical. 240**
**Figure 15.6: Mandibular dentition for Individual C. 241**
**Figure 16.1: Bone representation for Individual A, Heaning Wood. 246**
**Figure 16.2: Distribution of all taphonomic modifications across Individual A. 248**
**Figure 16.3: Distribution of destruction across Individual A. 250**
**Figure 16.4: Distribution of crushing across Individual A. 252**
**Figure 16.5: Distribution of fracturing across Individual A. 254**

**Figure 16.6: A) East view, across main chamber, B) West View, along fissure (photos by Martin Stables). 255**
**Figure 16.7: Right foot showing increased coverage of calcite deposits. 256**
**Figure 16.8: Tibia showing different stain types. 257**
**Figure 16.9: Distribution of staining across Individual A. 258**
**Figure 16.10: Staining spanning two fragments (blue arrow). 259**
**Figure 16.11: Soil embedded in exposed trabecular bone. 260**
**Figure 16.12: Example of circular areas of cortical removal consistent with invertebrate activity (taken from Warburton, 2017) 261**
**Figure 16.13: Distribution of weathering across Individual A. 262**
**Figure 16.14: Bone representation for Individual D, Heaning Wood. 264**
**Figure 16.15: Distribution of all taphonomic modifications across Individual D. 265**
**Figure 16.16: Distribution of destruction across Individual D. 267**
**Figure 16.17: Distribution of fracturing across Individual D. 269**
**Figure 16.18: Distribution of deposits across Individual D. 271**
**Figure 16.19: Distribution of staining across Individual D. Blue box indicates differential staining to femurs. 273**
**Figure 16.20: Darker staining to the Redshaw specimens. 274**
**Figure 16.21: Example of linear cracking to a tibial diaphysis. 276**
**Figure 16.22: Distribution of weathering across Individual D. 277**
**Figure 16.23: Delamination spanning two fragments, HBC011 and HBC401 (blue arrow). 279**
**Figure 16.24: Bone representation for Individual B, Heaning Wood. 280**
**Figure 16.25: Distribution of all taphonomic modifications across Individual B. 282**
**Figure 16.26: Distribution of destruction across Individual B. 284**
**Figure 16.27: Distribution of fracturing across Individual B. 286**
**Figure 16.28: Build-up of calcite to the right humerus. 287**
**Figure 16.29: Distribution of deposits across Individual B (patches of embedded deposits marked with blue box). 288**
**Figure 16.30: Build-up of deposit to the right humerus (HBC157/HBC158) 290**
**Figure 16.31: Distribution of staining across Individual B. 291**
**Figure 16.32: Area of focussed invertebrate pitting to the lateral, right parietal (blue arrow). 293**
**Figure 16.33: Distribution of weathering across Individual B. 294**
**Figure 16.34: Bone representation for Individual C, Heaning Wood. 296**
**Figure 16.35: Distribution of all taphonomic modifications across Individual C. 298**
**Figure 16.36: Distribution of destruction and fractures across Individual C. 300**
**Figure 16.37: Area of cortical removal because of fracturing. 301**
**Figure 16.38: Distribution of deposits across Individual C. 303**
**Figure 16.39: Distribution of staining across Individual C. 305**
**Figure 16.40: Staining crossing fracture margin (blue arrow). 306**

**Figure 16.41: Distribution of weathering across Individual C. 308**
**Figure 16.42: Bone representation for Individual E, Heaning Wood. 310**
**Figure 16.43: Distribution of all taphonomic modifications across Individual E. 311**
**Figure 16.44: Distribution of destruction and fractures across Individual E. 313**
**Figure 16.45: Distribution of deposits across Individual E. 314**
**Figure 16.46: Distribution of staining across Individual E. 315**
**Figure 16.47: Distribution of weathering across Individual E. 316**
**Figure 16.48: Bone representation for Individual H, Heaning Wood. 317**
**Figure 16.49: Distribution of all taphonomic modifications across Individual H. 318**
**Figure 16.50: Bone representation for Individual F, Heaning Wood. 319**
**Figure 16.51: Distribution of all taphonomic modifications across Individual F. 320**
**Figure 16.52: Bone representation for Individual G, Heaning Wood. 322**
**Figure 16.53: Distribution of all taphonomic modifications across Individual G. 323**
**Figure 16.54: Distribution of all taphonomic modifications across Individual G. 325**
**Figure 16.55: Distribution of staining across Individual G. 327**
**Figure 17.1: Distribution of fragments according to NISP counts. 330**
**Figure 17.2: Illustration of talus formation with associated run off. 331**
**Figure 17.3: Distribution of radiocarbon dated samples. 332**
**Figure 17.4: Distribution of fragments assigned to Early Bronze Age individuals. 333**
**Figure 17.5: Distribution of fragments assigned to Early Neolithic individuals. 334**
**Figure 17.6: Distribution of fragments assigned to the Mesolithic individual. 335**
**Figure 17.7: Distribution of unassigned fragments. 336**
**Figure 17.8: Concentration of fragments according to element group. 338**
**Figure 17.9: Distribution of fragments assigned to Individual A. 339**
**Figure 17.10: Concentration of fragments according to element group assigned to Individual A. 340**
**Figure 17.11: Distribution of cranial fragments assigned to Individual A. 341**
**Figure 17.12: Distribution of vertebral fragments assigned to Individual A. 342**
**Figure 17.13: Distribution of long bone fragments assigned to Individual A. 343**
**Figure 17.14: Distribution of long bone fragments assigned to Individual A. 344**
**Figure 17.15: Distribution of hand, foot and patella fragments assigned to Individual A. 345**
**Figure 17.16: Frequency counts for invertebrate modifications across the whole assemblage 348**
**Figure 17.17: Distribution of fragments assigned to Individual D. 350**
**Figure 17.18: Concentration of fragments according to element group assigned to Individual D. 351**
**Figure 17.19: Distribution of cranial fragments assigned to Individual D. 352**
**Figure 17.20: Distribution of vertebral fragments assigned to Individual D. 353**
**Figure 17.21: Distribution of long bone fragments assigned to Individual D. 354**
**Figure 17.22: Distribution of hand, foot and patella fragments assigned to Individual D. 355**
**Figure 17.23: Distribution of fragments assigned to Individual B. 359**

**Figure 17.24: Concentration of fragments according to element group assigned to Individual B. 360**
**Figure 17.25: Distribution of cranial fragments assigned to Individual B. 361**
**Figure 17.26: Distribution of vertebrae fragments assigned to Individual B. 362**
**Figure 17.27: Distribution of vertebrae fragments assigned to Individual B 363**
**Figure 17.28: Distribution of flat/irregular fragments assigned to Individual B 364**
**Figure 17.29: Distribution of hands, feet and patellae fragments assigned to Individual B 365**
**Figure 17.30: Distribution of fragments assigned to Individual C. 369**
**Figure 17.31: Concentration of fragments according to element group assigned to Individual C. 370**
**Figure 17.32: Distribution of cranial fragments assigned to Individual C. 371**
**Figure 17.33: Distribution of long bones fragments assigned to Individual C. 372**
**Figure 17.34: Distribution of hand, foot and patella fragments assigned to Individual C. 374**
**Figure 17.35: Distribution of staining across the skull versus long bones for Individual C. 376**
**Figure 17.36: Distribution of root embedding for all individuals. 378**
**Figure 17.37: Distribution of fragments assigned to Individual E. 380**
**Figure 17.38: Distribution of cranial and long bone fragments assigned to Individual E. 381**
**Figure 17.39: Distribution of fragments assigned to Individual F. 384**
**Figure 17.40: Distribution of fragments assigned to Individual G. 386**
**Figure 17.41: Distribution of all fragments assigned to Individual G. 387**
**Figure 18.1: Sequence of events post deposition for Individual 1. 395**
**Figure 18.2: Sequence of events post deposition for Individual 2. 397**
**Figure 18.3: Sequence of taphonomic processes at Cave Ha 3 399**
**Figure 18.4: Radiocarbon modelled dates for Heaning Wood (Jazwa, 2022). 405**
**Figure 18.5: Example of staining following meningeal grooves in the parietal (blue box). 408**
**Figure 18.6: Layers with higher frequencies of modifications 412**
**Figure 18.7: Sequence of depositions for Individuals A-D, Heaning Wood. 413**
**Figure 18.8: Archive map for Sewell's Cave {Citation} 419**
**Figure 18.9: Finds list for Sewell's Cave {Citation} 420**
**Figure 19.1: Distribution of fragments from Individual A according to depth. 428**
**Figure 19.2: Distribution of fragments from Individual B according to depth. 429**

# LIST OF SUPPLEMENTARY FIGURES

**Figure 1.5: Adult sketch for initial observations 11**
**Figure 1.5: Adult sketch for initial observations 12**
**Figure 1.6: Cranial Zones (Lateral view) 13**
**Figure 1.7: Cranial Zones (frontal and posterior view) 14**
**Figure 1.8: Upper Limb Zones 15**
**Figure 1.9: Vertebral Zones 16**

**Figure 1.10: Axial Zones** **17**
**Figure 1.11: Lower Limb Zones** **18**
**Figure 1.12: Infant Cranial Zones** **19**
**Figure 1.13: Infant Upper Limb Zones** **20**
**Figure 1.14: Infant Lower Limb Zones** **20**
**Figure 6.1: X-rays of HBC012 (E),HBC260 (E) and HBC238 (F) (left to right)** **42**
**Figure 6.2: X-rays of HBC237 (E), HBC252 (E) and HBC256 (F) (left to right)** **42**

# LIST OF TABLES

**Table 7.1: List of age and sex categories.** **74**
**Table 7.2: List of age and sex categories** **78**
**Table 7.3: Example of scapula zonation counts** **78**
**Table 7.4: Taphonomy assessment criteria and subcategories.** **87**
**Table 7.5: List of element groups, (according to Robb, 2016).** **102**
**Table 8.1: Dating results taken from Peterson (2019) for Cave Ha 3** **110**
**Table 9.1: Total figures for NSP, NISP, NUSP, faunal remains and non-bone specimens.** **114**
**Table 9.2: Demographics for identified individuals.** **115**
**Table 9.3: Frequencies of fragments according to anatomical side (Cave Ha 3).** **117**
**Table 10.1: Genetic results taken from Booth (2019) for Individual 2** **121**
**Table 11.1: Fragments excluded from Individual 1 GIS mapping.** **126**
**Table 11.2: Deposit frequencies and percentages according to element group for Individual 1.** **138**
**Table 11.3: Fragments from Individual 2 with peri-mortem crushing.** **149**
**Table 13.1: Radiocarbon dating results.** **228**
**Table 14.1: Summary of Heaning Wood demographics** **229**
**Table 14.2: Frequencies of fragments according to anatomical side.** **232**
**Table 16.1: Adjusted and unadjusted frequencies of destruction.** **268**
**Table 16.2: Staining frequencies according to classification and anatomical view for Individual D.** **275**
**Table 17.1: comparison of destruction counts per layer, including and excluding additional vertebral views.** **356**
**Table 17.2: comparison of destruction counts per layer, including and excluding additional vertebral views.** **357**
**Table 18.1: Evidence for and against curated burials at Heaning Wood.** **415**

# LIST OF SUPPLEMENTARY TABLES

**Table 1.1: List of skeletal elements and codes** **2**

**Table 1.2: Field names for GIS** **5**

**Table 1.3: GIS codes for taphonomy subcategories** **6**

**Table 1.4: Cave Ha 3 discrepancies to Leach (2006a)** **9**

**Table 1.5: Descriptive criteria for Taphonomy observations from Hawks et al., 2017** **25**

**Table 3.1: Metrics for Cave Ha 3 Individual 1** **32**

**Table 3.2: Metrics for Cave Ha 3 Individual 2** **34**

**Table 3.3: Metrics for Cave Ha 3 Individual 3** **35**

**Table 3.4: Metrics for Cave Ha 3 Individual 4** **36**

**Table 4.1.1: Fragments from Individual 1 with peri-mortem crushing.** **37**

**Table 4.2.1: Fragments excluded from Individual 2 GIS mapping.** **38**

**Table 4.3.1: Fragments from Individual 3 with peri-mortem crushing.** **39**

**Table 4.4.1: Fragments excluded from Individual 4 GIS mapping.** **40**

**Table 4.4.2: Fragments from Individual 4 with peri-mortem crushing.** **40**

# CHAPTER 1: INTRODUCTION

Cave burials have formed a part of funeral ritual across pre-history and have long been recognised as an important aspect of Neolithic burial practice. While they are considered to be "well understood" (Peterson, 2019, p. 1) caves in the North of England do not appear to have the same patterns of use as those in the south (figure 1.1).

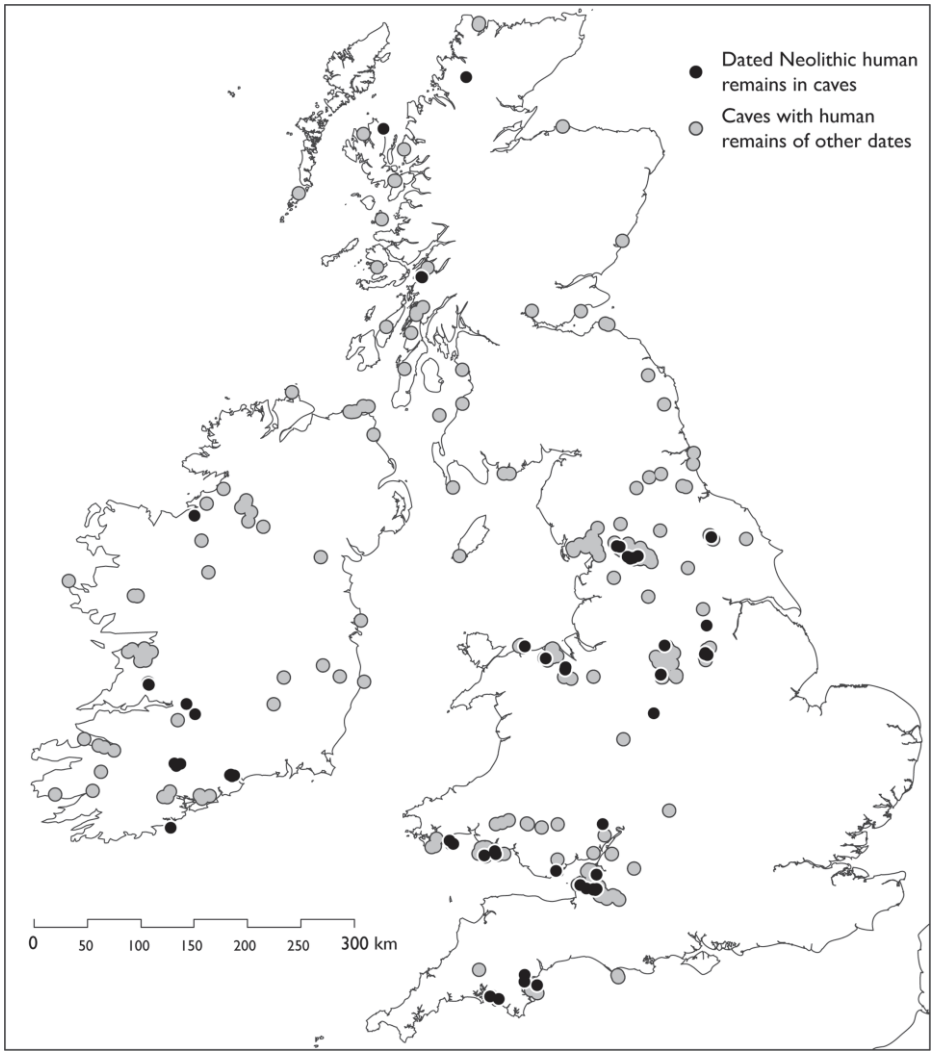


Figure 1.1: Known caves in Ireland and Britain with radiocarbon dated human remains from the Neolithic period. The grey circles show the positions of caves in both countries with human remains of any date (taken from Peterson, 2019, fig. 1.1).

Peterson (2019) discusses how this pattern is not just a reflection of biases in fieldwork and refers to an absence of Neolithic remains located along the south coast of Cumbria, despite research being conducted in the area (Smith, 2012). Heaning Wood, is one of two cave

assemblages presented in the following thesis and is located in Cumbria. Radiocarbon dating presented in the following pages challenges this view, with evidence of at least four individuals deposited at Heaning Wood dating to the Early Neolithic. Further to this, one individual was dated to the Early Mesolithic (9290-8930 Cal BC and 9115-8635 Cal BC) and two to the Early Bronze Age. Mesolithic burials are rare, both in the UK and Europe (Orschiedt, 2012; Hodgkins *et al.*, 2021) and in the North of Britain burials from this early in the Mesolithic are limited to Kent's Bank Cavern where a portion of femur was dated to 9100 ± 35 $^{14}$C a BP (Smith, Wilkinson and O'Regan, 2013). The Early Mesolithic date is particularly significant, making it the earliest known burial from Northwest England. This makes Heaning Wood an important site in our understanding around burial practices in North West Britain. It is an example of successive use of a site, spanning several periods, with long hiatuses between use. The site was assessed in 2017 (Warburton, 2017), however between 2016 and 2019 more human and faunal material was excavated. A portion of the assemblage is also held at the Dock Museum, Barrow-in-Furness, comprising material from excavations conducted in 1958 and 1974. These remains were also not included in the 2017 analysis; therefore, the following research is the most comprehensive and detailed analysis of the human remains to date.

Burials can be used to provide insight into belief systems and wider societal practices (Cummings, 2017, p. 24) but to do this the 'burial narrative' needs to be reconstructed. Robb (2016, p. 684) proposes two most common initial questions when faced with a commingled assemblage: "how many people were deposited, and how they were deposited?". This project initially aimed to focus on the answering these first questions by applying digital methods to quantification, such as those proposed by Marean and colleagues (2001). This approach did not offer any improvement to quantification than more traditional methods (White, 1953; Dobney and Rielly, 1988; Knüsel and Outram, 2004); it did however offer a novel solution for taphonomic analysis.

The second stage to understanding burial narrative is to look at the taphonomic changes. Cave assemblages are usually fragmented and commingled; it therefore becomes important to unravel the acting agents to understand whether the depositions are part of an extended burial ritual, or primary depositions altered by geological processes occurring within the cave. The second stage of the project aimed to expand methods developed by several researchers

looking at using Geographic Information Systems (GIS) as a method of bioarchaeological analysis (Herrmann, 2002; Herrmann and Devlin, 2008; Parkinson, 2013, 2018; Herrmann, Devlin and Stanton, 2014; Parkinson, Plummer and Bose, 2014; Stavrova *et al.*, 2019).

Traditional methods of taphonomic analysis typically rely on recording the presence or absence of a modification, location, and a description (Buikstra and Ubelaker, 1994, p.105; Leach, 2006a, 2006b; Beckett, 2011; Hawks *et al.*, 2017). The output of these analyses is often in the form of binary databases, alongside descriptions, making interpretations subjective. Heaning Wood was originally analysed using such a method (Warburton, 2017) but the need to combine the disparate assemblages offered an opportunity to apply a digital approach. By treating the body as a mappable space, it is possible to quantify changes occurring to the body, look for patterns and in some cases ascertain information such as burial position or location.

Cave Ha 3 is an example of Early Neolithic, successive, multi-stage burial and was introduced as a case study to support the Heaning Wood analysis. This was due to it having previously been analysed by Leach (Leach, 2006b, 2006a, 2008) with a good understanding of the practices involved. While the re-analysis of Cave Ha 3 did not change the burial narratives, the process of using GIS to record the taphonomy has highlighted new information about the burial positions of two of the individuals deposited there, reinforcing the value of GIS for taphonomic interpretation.

By applying new methodology to taphonomic analysis of commingled and fragmented cave burials it is possible to understand the processes acting on bodies and reconstruct the burial narratives, shaping our understanding of burial practices across several periods in North West Britain.

# CHAPTER 2: NEOLITHIC BRITAIN

## 2.1: The Neolithic Transition

The Neolithic period saw the introduction and spread of agricultural practices and stone tools, with a shift from hunter gatherer lifestyle to the cultivation of cereals and domestication of animals. Key aspects of the Neolithic are domesticated animals and cereals, bowl pottery, monuments, and stone tools, however changes to the Neolithic looked different in different areas and occurred at different times (Smith and Brickley, 2009, p.9; Thomas, 2013, p.1; Cummings, 2017, p.28). The global expansion of Neolithic practises did not occur uniformly. Areas constrained by geographical barriers saw the transmission of ideas much later; for example, the submerging of Doggerland around 6500-6200 BC resulted in the loss of a physical link between Britain and Europe (Bocquet-Appel *et al.*, 2009; Smith *et al.*, 2011). Some, however, argue that this should not be seen as a barrier, but rather a method of transformation and that the shift to Neolithic life was a result of both adaptations of indigenous people, as well as migration, through the process of acculturation (Thomas, 2013, pp.213-214; Griffiths, 2014). The debate surrounding mechanisms of change during the transition from Mesolithic to Neolithic is ongoing. The following section explores this debate and provides a general overview of Neolithic burial before exploring the Yorkshire cave burials specific to this research.

Neolithic practices spread from the near east around 10,000 BC and through South-East Europe in 7000 BC but for Britain it was initially estimated as occurring as late as 4000 BC (Cummings, 2017, p.35). The nature of archaeology means that with the advancement of new methods, such as the introduction of radiocarbon dating and the application of Bayesian statistics, our understanding is continually shifting (Whittle and Bayliss, 2007). Prior to 2011 there was a degree of contention surrounding when the shift to the Neolithic occurred in Britain, as well as discussion around how ideas and practices were transmitted (Thomas, 2003, 2004; Sheridan, 2004, 2007, 2010). In their seminal work “Gathering Time” Whittle and colleagues (2011b), with the use of Bayesian modelling, demonstrated that the spread of Neolithic activity in Britain was gradual. Beginning in the South-East of England around cal BC 4100 it then spread to the remainder of Britain and Ireland around 3800 cal BC (Whittle, Healy and Bayliss, 2011a, p. 1). The strongest data for this lies in southern Britain, where the authors

sampled most sites. Further work showed a "rapid and abrupt transition to agriculture c. 3750 cal BC" in Ireland (Whitehouse *et al.*, 2014, p. 180). Although there was an earlier date produced for cereal grain it lacked clarity and caution against using this as dating evidence was advised by the authors. Griffiths (2014) identified the 38th century cal BC as a period of significance for Humberside and Yorkshire, an area also not covered in detail by Whittle and colleagues' (2011b) study. Using radiocarbon dates Griffiths (2014) applied calibration and Bayesian modelling to estimate the start of the Neolithic in Yorkshire and Humberside, estimating it as "3920-3720 cal BC (95% probable) most probably 3840-3740 cal BC (68% probable)" (Griffiths, 2014, p. 16). Both support the work done initially by Whittle and colleagues (2011b) and since 2011 there has been broad agreement around the timing of the Early Neolithic in Britain.

Despite agreement around the timing of the transition, an enduring debate within archaeology is the around what drove the transition from a hunter-gatherer society of the Late Mesolithic to one of agriculture, characteristic of the Neolithic. Two main arguments have defined the decades long debate; rapid uptake due to colonisation, and the uptake of Neolithic practices by indigenous communities because of acculturation (Thomas, 2004; Sheridan, 2010; Whittle, Healy and Bayliss, 2011b; Griffiths, 2014).

With the earliest material evidence first appearing in the South East, dating between 4315-3985 cal BC (95% probability, probably in 4145-4005 cal BC 68% probability) (Bayliss *et al.*, 2011, p. 731) the subsequent spread took around 100 years to appear outside of this area (Griffiths, 2014; Whitehouse *et al.*, 2014; Cummings, 2017, p.35). Whittle and colleagues (2011b) "demonstrated variability in both timing…and changes in the tempo of the spread of these traditions" (Griffiths, 2014, p. 5), with the authors arguing that the evidence suggested "indigenous acculturation from early on" (Whittle, Healy and Bayliss, 2011b, p. xiii). Prior to the publication of 'Gathering Time' Sheridan (2004, 2007, 2010; Pailler and Sheridan, 2009) and Thomas (2003, 2004) were key contributors to the discussion, with polarised perspectives. Sheridan (2004, 2007, 2010) theorised that the introduction of Neolithic to Britain and Ireland was the result of colonisation. She argued that Britain during the Mesolithic was most likely isolated from the continent until various conditions on the continent, including internal conflicts, lead to the migration of people to Britain. The movement of people may

only have been small but led to a scattered but simultaneous spread across Britain (Sheridan, 2004; Pailler and Sheridan, 2009). Colonisation resulted in the appearance of Neolithic practices. Contrary to this Thomas (2003, 2004) argued that rather than a 'package' resulting from the migration of people from the continent, that the Neolithic was more of a 'repertoire', "an interrelated set of material and symbolic resources from which different communities could draw in different ways" (Thomas, 2003, p. 72). He debated that a lack of direct continental parallels in all aspects of Neolithic culture in Britain indicated that they were the result of "inventiveness and bricolage on the part of the indigenous population" rather than the result of colonisation (ibid. p.73).

Despite seeming to agree with Thomas (2003) that uptake across Britain was simultaneous, in her 2010 paper Sheridan goes on to describe the transition as "by no means a unitary phenomenon, nor did it happen abruptly" (Sheridan, 2010, p. 89), this is at odds to her discussion around pottery where Sheridan (2004, p. 12) argues that dating evidence "suggests that there was no significant time lag between its appearance in different parts of Britain and Ireland". Thomas (2003, p. 72) also refers to the "synchronic appearance" of resources and a rapid uptake of Neolithic practice. Within the debate there are those that argue for a combination of colonisation and acculturation. Colonisation either becomes a driver for acculturation within indigenous populations (Whittle, 2007) or both processes are occurring but in different areas. Cummings and Whittle (2004) have suggested that there is evidence for colonisation in the East, compared to the acculturation in the West, however these combined arguments are less frequent within the debate (Whittle, Healy and Bayliss, 2011a).
Sheridan (2010) claims that her view of colonisation is not at odds with proponents of a combined theory, but Whittle and colleagues (2011) offer a compelling critique of her evidence. There is little to support the theory that Britain was isolated. Evidence of domesticates at Ferriter's Cove opens "the possibility, from at least as far back as the middle of the fifth millennium cal BC, of movement by boat up and down the western side of Britain and Ireland" (Whittle, Bayliss and Healy, 2011, p. 849). The direction of this contact is not clear, however, and could have occurred in either direction.

Dating from the Western Isles, Caithness, and the Orkney and Shetland Islands was consciously omitted from Whittle and colleagues' (2011b) study; however, these areas and

the associated western sea way is considered key to understanding the transition of Britain to the Neolithic (Garrow *et al.*, 2017). This omission of key areas forms a large part of the criticisms of 'Gathering Time', its focus on 'well-dated' south and east causewayed enclosures runs the risk of missing evidence of early contact in other regions of Britain (Sheridan and Pétrequin, 2014; Garrow *et al.*, 2017). While Garrow and colleagues (2017) found no evidence of earlier contact for 48 sites across the Channel Islands, Isles of Scilly, Isle of Man, Outer Hebrides, and Orkney, they strongly highlight the biases in both their study and similar research. Differential priorities in excavation across regions along with the exclusion of undated or undatable evidence mean that chronological studies of the transition only provide part of the picture (Garrow *et al.*, 2017). The application of more robust procedures and precise methods will add weight to the interpretative aspect of archaeology. Whittle and Bayliss (2007) hint at this when discussing the application of Bayesian statistics to interpret radiocarbon dates when they say that "archaeology needs to embrace" these developments (Whittle and Bayliss, 2007, p. 21). It is not unusual for reanalysis of remains to result in a revision of dates, however any discussions must consider biases in the archaeological record and that loss occurs at both a preservation and observational level (Perreault, 2019, p.80).

## 2.2: Neolithic Burials

"Burials have long been used by archaeologists to provide insight into belief systems" (Cummings, 2017, p. 24) and understanding Early Neolithic burials, particularly in comparison to Mesolithic practices, can offer further understanding of hunter-gatherer to agricultural transitions. Despite Late Mesolithic evidence of formal burial in other areas of Europe, evidence of such is lacking Britain and Ireland. Excarnation and the circulation of bones in Europe dates to the Upper Palaeolithic and the continuation of this during Late Mesolithic Britain suggests that hunter-gatherers, if aware of European formal burial, consciously decided not to follow the practice. This has been used to suggest, due to the similarity to animal body deposition, that hunter-gatherers had different beliefs about the animal world to agricultural societies (Cummings, 2017, p.25). Isotopic analysis of remains from caves in the Mendip region of Britain have also shed light on the characteristics of the Mesolithic-Neolithic transition, despite the proximity to the coast, cave remains dated to the Early Neolithic lacked evidence of a marine diet, reflective of the overall dietary pattern in Britain during the

Neolithic (Schulting, Chapman and Chapman, 2013). Schulting, Chapman and Chapman (2013) argue that this supports the argument for a rapid and complete change from the use of marine to terrestrial resources.

A distinctive aspect of the Neolithic period was architecture, particularly the building of large timber halls and monuments with most of these monuments containing human remains (Smith and Brickley, 2009; Cummings, 2017). Neolithic burials recovered from monuments are well documented (see discussions by Wysocki and Whittle, 2000; Whittle, Bayliss and Wysocki, 2007; Smith and Brickley, 2009) however, with most excavations and reports happening prior to 1945 advancements in research, including the use of Bayesian statistics and taphonomic analysis, have offered new insights into old collections (Smith and Brickley, 2009; Whittle, Healy and Bayliss, 2011a; Griffiths, 2014; Whitehouse *et al.*, 2014).

Remains recovered from monuments are rarely articulated and complete. Excarnation, multi-stage burials rites and circulation of bones have been discussed as a 'normal' feature of Neolithic practice, involving transformation of remains (Leach, 2008; Smith and Brickley, 2009p.11; Cummings, 2017 p.,25; Peterson, 2019, p.2). Most skeletal assemblages from this period are disarticulated, highly fragmented, and commingled (Beckett and Robb, 2006; Smith and Brickley, 2009, p.11). In their review of British and Irish Neolithic burial ritual, Beckett, and Robb (2006, p. 60) posit that while primary inhumations are "the most commonly identified rite", later disruption and damage was common. This was usually deliberate or a result of successive internments. While disarticulated and commingled remains are common, there are cases of articulated burials, including evidence of in-situ decomposition (Whittle, Bayliss and Wysocki, 2007; Whittle *et al.*, 2007; Leach, 2008).

Evidence suggests that remains were sometimes subject to manipulation and movement as a means of excarnation, this included leaving bodies exposed to scavengers and open air, multiple burials, or manual disarticulation (Smith and Brickley, 2009, p.39; Cummings, 2017, p.25). Once disarticulated there is evidence that burial rituals involved the movement, and reburial of remains. In their re-analysis of Fussell's Lodge long barrow remains, Wysocki and colleagues (2007) discussed depositional evidence from a taphonomic perspective. They agreed with earlier interpretations by Ashbee (1966) that there was evidence of

transportation of older remains to the site. They did, however, state it was possible that some bodies had been deposited fleshed. What was clear was the burial rites were complex and involved curation of older remains and re-ordering of bones. However, not all monument assemblages show evidence of deliberate manipulation. Disarticulation and commingling may also be a result of destructive processes, including the addition of new bodies, resulting in the movement and disarticulation of previous burials (Beckett and Robb, 2006; Robb, 2016). In caves the movement of sediment, including bones, can occur through several processes including water flow, sediment infills, and collapse (Andrews, 1990, p.91). It cannot be assumed that commingling or disarticulation is always down to deliberate manipulation or interference.

Thomas (2000) argued that movement and reburial was an important aspect of Early Neolithic burial. The idea of a person as an 'individual' is a modern concept, and it may be that, even during life, it was not of the same concern in the Early Neolithic as we afford it today (Thomas, 2000). In their discussion of assemblages recovered from chambered long cairns in Southeast Wales, Wysocki and Whittle (2000) found that distinct deposits of bones had been made that represented an individual human skeleton but were comprised of different individuals. This suggests that there were "concerns with the representation of physical entities and the concept of a human body" (Wysocki and Whittle, 2000, p. 599) but less concern over retaining the individual after death. Thomas (2000) summarised several Early Neolithic sites where evidence of fully articulated bodies was found alongside "disordered" piles of remains further into chambers, arguing that this movement was more than just creating space for new bodies. The circulation of bones is said to have occurred across the landscape as part of a gift economy where "movement of disarticulated remains from person to person and place to place served not simply to create relationships between givers and receivers, but also between the living and the dead" (Thomas, 2000, p. 662). Thomas (2000) uses ethnographic parallels to explain commingling and manipulation of bones, leading to an emphasis on multi-stage rites. Contrary to this, those that use a taphonomic perspective tend to interpret such movement as a result of successive inhumations (Peterson, 2019, p.46). A more in-depth discussion around these differing interpretations of burial is provided in chapter 2.3.

Neolithic burials are not limited to monuments, with remains being recovered from “caves, enclosures, single graves, and ‘stray’ bones” (Smith and Brickley, 2009, p. 13). While single graves are considered rare, Schulting (2007, p. 3) argues that how these bodies are recovered results in an assumption of rarity, “rather than demonstrated”. The recovery of Neolithic remains is low in number, including those from monument burials, with the total number of Neolithic remains making up a relatively small amount in comparison to other periods and the relative population of the time (Roberts and Cox, 2003; Smith and Brickley, 2009, p.42; Cummings, 2017, p.91). It is possible that many depositions during the Early Neolithic resulted in the complete destruction of skeletal elements, for example through water depositions that were occurring at the time. Human crania have been recovered from rivers, in the 1880’s twenty-three crania were recovered from Preston Docks along with ungulate remains (Turner, Gonzalez and Ohman, 2002). Dates for the crania recovered from Preston Docks span millennia but have returned several dates from the Neolithic (*ibid*.). In their discussion Turner and colleagues (2002) argue that taphonomic evidence does not suggest a sinister reason behind deposition, however there is little to show how or why the deposits ended up there. It is possible that these are not deliberate depositions, but rather the result of drownings or movement of burials from riverbanks (Schulting, 2007). If, however, burials in water were occurring then this, along with leaving bodies exposed to scavengers, may have led to remains being archaeologically unavailable due to destruction (Smith and Brickley, 2009, p.42; Cummings, 2017, p.91). Additionally, some remains, including those from caves, have in the past been incorrectly dated through artefact association (Leach, 2006a; Dowd, 2008, p.63). The reanalysis of many of these finds has resolved this issue but older literature should be treated with caution and the method of dating critically considered.

Conventional dating through artefact association relies on the assumption that the burial environment is closed. Caves, whilst seemingly closed, cannot be reliably dated through artefact association. Movement because of natural forces, or successive use of the space, can result in the misdating of remains (Schulting, Chapman and Chapman, 2013). This was highlighted by Leach (2006a) where a number of cave remains, such as Thaw Head cave in the Yorkshire Dales, had been dated by artefact association. Subsequent radiocarbon dating came back with much earlier dates, placing the remains in the Early Neolithic rather than later periods. The interpretations made around cave use in these cases was then adjusted. It is for

this reason that Peterson (2019, p.5) argues that when studying cave burials that only those "with direct dates on human bone should be considered", particularly when making comparisons and interpretations of the past. Research conducted by Leach (2006a, 2006b, 2008, 2015) into cave burials in the Yorkshire Dales has played a pivotal role in dating cave remains.

While there is a wealth of literature around Early Neolithic burials of all types (Wysocki and Whittle, 2000; Leach, 2006b, 2006a, 2008; Schulting, 2007; Smith and Brickley, 2009; Cummings, 2017; Peterson, 2019) caves are recognised as an important aspect of Neolithic burial practices (Chamberlain, 1996; Schulting, 2007). Straus (1997, p. 2) argued that the study of caves is vital to "interpret the regional adaptations of prehistoric humans" but warns of placing too much emphasis on the significance of cave burials. The act of moving or placing a body within a cave allows survival and is therefore more likely to result in recovery by archaeologists than subaerial depositions (Straus, 1990, 1997; Pokines *et al.*, 2011; Schulting, 2016).

Despite humans utilising caves since the Lower Paleolithic (Berger *et al.*, 2015; Dirks *et al.*, 2015) their use as burial sites declined after c. 10,000 cal BP (Schulting, 2016) and after 5000 BC there are "no known examples" of cave burials in Britain until a reappearance in Early Neolithic (Cummings, 2017, p. 24). Dating work conducted by Chamberlain demonstrated that cave burials then occurred "continuously from the early Neolithic onwards" (Chamberlain, 1996, p. 951). Hellewell and Milner (2011) disagree with this. While there are few human remains dating back to the Mesolithic, there are some, particularly cave burials, originating from this period. The authors argue that there is no way to separate the way the dead were treated during the Mesolithic and the Neolithic; burial in caves was a practice of continuity rather than novelty, citing dates from Fox Hole Cave in Derbyshire (Hellewell and Milner, 2011). These dates are not reliable, however, due to an incident of known contamination at the Oxford laboratory (Schulting *et al.*, 2013). During a reanalysis of human remains from another Foxhole cave in Gower, South Wales, Schulting and colleagues (2013; 2020) found more than a millennium between Late Mesolithic and Early Neolithic cave remains (5522-5375 cal BC 95% probability and 3912 - 3660 cal BC 95% probability respectively) (Schulting *et al.*, 2013, p. 12). Similar gaps have been found at other sites, such as Totty Pot cave (Schulting,

Chapman and Chapman, 2013), suggesting that cave burial in the Neolithic was not a result of continuity. Others have suggested that the gap considered by Chamberlain (1996) and Schulting and colleagues (2013; 2020) is not as clear cut. There is evidence that suggests a stronger overlap between Mesolithic and Neolithic practices, particularly in Yorkshire and Humberside (Griffiths, 2014). Griffiths (2014) goes as far as to exclude caves with earlier dates on the basis that they could feasibly have been used by either hunter-gatherers or farmers (Peterson, 2019, p. 98). In addition to this, in their research into Mesolithic and Neolithic deposits from Vlasac, the Danube Gorges, Boric and Griffiths (2015) found evidence for continuation of burial traditions despite gaps of several centuries between burials, suggesting evidence for "long-term remembering or recognition and visibility" (Borić and Griffiths, 2015, p. 355). In their study of human bones recovered from a Mesolithic midden in Cnoc Coig, Oronsay, Meiklejohn and colleagues (2005, p. 102) argue that the depositional pattern of the remains indicates a "purposive cultural act", and suggest that it could mirror Neolithic social customs, comparing the depositions to those found at Carding Mill Bay. It is possible, however, that the late date of the human remains from Cnoc Coig (4400 – 3800 cal BC) mean that Mesolithic people were mimicking burial styles from nearby farming communities, rather than it being evidence of continuity. Even the authors say there is "insufficient evidence to fully defend the equivalence" of the Cnoc Coig bones to those found at Carding Mill Bay (Meiklejohn *et al.*, 2005, p. 103).

This is where accurate dating is, again, a matter of importance. There is merit in conducting reanalysis, particularly as methods improve, as found by Schulting and colleagues (2013), Leach (2006a; 2006b; 2008), and Dowd (2008, p.63). It does not, however, all hinge on dating. As raised by Griffiths (2014) it is possible that remains returning Early Neolithic dates could have been burials conducted by those yet to transition to Neolithic practices, as argued by Peterson (2019, p. 113) "Whether the people who used these caves were farmers or hunter-gatherers can only be resolved by a detailed examination of the surviving archaeological evidence from each site". While it has been discussed that artefact association should not be relied on for dating purposes, it does provide context around depositional narratives and may offer insight into whether cave burials were a continuing or novel practice in the Early Neolithic.

With a 'shared architecture of passages and chambers' (Barnatt and Edmonds, 2002; Peterson, 2019, p. 3) burial practices in caves often reflect how bodies were treated in other burial types, such as monuments. Prior disarticulation, excarnation and reordering of bones as well as taphonomic processes arising from multi-stage burials are evident in both caves and monument depositions (Schulting, 2007; Schulting *et al.*, 2013; Cummings, 2017; Peterson, 2019). In Leach's (Leach, 2006a, 2006b) reanalysis of 20 subterranean burial sites across Yorkshire there was evidence of burial that was "deliberate" and "cultural" in origin (Leach, 2006a, p. 148) due to recovering only cranial elements. The absence of postcranial elements and a lack of evidence of carnivore activity and weathering suggests that the crania had been moved from a prior location. In her further work Leach (2008) suggested that whole body burials in Yorkshire caves were a result of deviant burial. Lord and Howard (2013) interpret Leach's words as saying that these burials reserved for those who were sick or disabled and may somehow represent "malign souls" (Lord and Howard, 2013, p. 244), however this is not the impression Leach (2008) gives. While she discusses the possibility that these individuals were kept separate from the 'collective' dead, in the form of articulated burials, Leach (2008) acknowledges their uniqueness. The amount of recovered remains from the Neolithic is low in comparison to the estimated population (Roberts and Cox, 2003). The very nature of these burials means these remains "represent a select group - deliberate, meaningful deposition" (Leach, 2008, p. 52). It is possible that the location of the cave, and the beliefs of those using it, are the determining factors into what and how was placed in them.

Schulting (2007) argued that a plausible explanation for cave burials is that they were reserved for those with lower social standing. Similarly Leach (2008) found evidence of disability and wear and tear because of manual labour, so while the burials were seen as "meaningful", they supported Schulting's (2007) initial theory. He posited this theory based on the labour required for monuments in contrast to caves being "found places". This "claim of legitimacy and ownership" (Schulting, 2007, p. 591) appears to have grounding, however it could be argued that we are placing Western, modern centric ideology onto prehistoric culture; buying into the idea that beliefs around ownership is something that is invariable across time. As put by Barnett and Edmonds "we cannot assume that prehistoric communities necessarily drew the same sharp lines between the found and the made that we tend to acknowledge today" (Barnatt and Edmonds, 2002, p. 114). Schulting (2013) has subsequently altered his position

on cave burial and social standing arguing that a “lack of any clear isotopic difference between those buried in caves and those buried in monuments in general” raises important questions as to who was buried and where (Schulting, Chapman and Chapman, 2013, p. 22).

Cummings (2017), while acknowledging evidence that caves and monuments were possibly used interchangeably, argues that "people are unlikely to have thought about the two in the same way" (Cummings, 2017, p. 92). Similarly, in her discussion around Irish caves, Dowd (2015) argued that distinctions were made between caves and monuments through use and “perception” (Dowd, 2015, p. 110). The separation of natural spaces from constructed ones is something that should not be assumed, when making comparisons across such extended time periods our current way of thinking will influence our interpretations: “Western modernity has given rise to quite unique, perhaps even aberrant, ways of being human” (Thomas, 2000, p. 658). As Dowd (2015) questions, why do we not consider that natural features were thought of as important places, rather than something in comparison to built structures?

Hellewell and Milner (2011) made this comparison in their discussion around Mesolithic-Neolithic transition. Caves were seen as “mysterious places” (Hellewell and Milner, 2011, p. 65) where disarticulation is seen as a method of transition, both metaphorically and physically, to ancestral form. They argue that the introduction of monument burials in the Neolithic could be seen as a “reaffirmation” of these beliefs, expanding rituals from caves to constructed spaces. The issue with this is the lack of evidence surrounding continuity. While cave burials are not new to the Neolithic, with evidence of cave remains dating back to the Pleistocene (Bonsall and Tolan-Smith, 1997; Barton *et al.*, 2008; Gibbon *et al.*, 2014; Berger *et al.*, 2015), as discussed earlier there remains a question over whether cave burials were a result of continuing Mesolithic traditions or a novel practice. More importantly there are clear distinctions in how caves were used in comparison to monuments (Dowd, 2015, p.110). Through analysing the use of spaces, we can gain insight into what people may have thought about them, something that is otherwise inaccessible.

The idea of ancestry in archaeology, particularly during the British Neolithic, is well accepted (Parker Pearson and Ramilisonina, 1998; Robb, 2020). Whitley (2002) discusses this preoccupation with ancestors, the origins of which stem from ethnographic and theoretical

frameworks, arguing that it should not always be the forefront interpretation of burial rituals, however others argue that the connections between caves and spirituality was prominent during the Early Neolithic (Dowd, 2015, p.124). Connections between spirituality, ritual, and caves are returned to and examined in detail in chapter 2.4.

## 2.3: Cave Burial in Yorkshire

Yorkshire and Humberside, with its wealth of Neolithic monuments, sites, and materials, has been an area of focus since the 19th century. It is a key area for Neolithic activity in the North and sits third only to the Cotswolds-Severn and Wessex for mortuary monuments (Griffiths, 2014). The Yorkshire Dales boasts some of Britain's "best developed and best-known limestone landforms", with the "country's longest cave system" (Waltham and Lowe, 2013, p. 1).

Prior to the Neolithic, human cave use in Yorkshire appears to be limited with evidence of short, distinct periods of use evident during the Later Upper Palaeolithic before a gap because of a cold event (Lord and Howard, 2013). There is evidence of human activity in caves during the Late Mesolithic in Yorkshire, but it is indicative of a short event, unrelated to mortuary practice. Arcow Wood Caves evidenced human exploration around 5800 BC and between 5298-5057 BC at Victoria Cave. After this there appears to be a break in human activity consistent across the region between around 5400 BC and 3900 BC (Lord and Howard, 2013). A resurgence of human use of caves in the Dales coincided with the onset of the Neolithic. Dates for the human remains at Kinsey Cave, Yorkshire suggest they were deposited around 3977-3791 cal BC, contemporary with depositions occurring in Torbryan Valley, Devon (*ibid*.). Lord and Howard (2013) discuss the sequences of depositions occurring in the Dales, positing that Cave Ha 3 mirrored sequences at Torbryan valley, where interment of human remains followed the deposition of processed animal bones. Sequences at other caves are less clear, particularly for Kinsey and Greater Kelco Caves, and the authors suggest that more dating is needed. They argue the possibility that burial in this region is phasic, with burials occurring "generations apart" (Lord and Howard, 2013, p. 243). If cave depositions are discontinuous this has implications behind the motive for burial, indicative of external factors driving the practice (Lord and Howard, 2013). Leach (2008, p. 51) suggests that cave burials were used as

a method of separating specific individuals “from the ancestral community of the dead”, perhaps due to disabilities. While data on disease prevalence is limited, Roberts and Cox (2003) have shown evidence of joint, congenital, and dental disease in the Neolithic. Evidence is limited to diseases that leave traces on bones and it is possible that others had disabilities no longer present in the archaeological record (Leach, 2008). It is unlikely, however, that this would explain the generational gap, as people across generations would likely suffer the same illnesses.

Many of the Yorkshire cave systems are situated within the Great Scar Limestone and as of 2013, approximately 80 caves in the Dales had been excavated (Lord and Howard, 2013) Further excavations continue, including secondary excavations occurring more recently at Heaning Wood Bone Cave, a vertical shaft in Great Urswick, Cumbria. Despite being originally excavated in 1958 (Holland, 1960) excavations have yielded more finds. Reanalysis of previous finds for several Yorkshires caves have offered new insights and the advancement of radiocarbon dating has furthered knowledge previously inaccessible to early researchers (Lord and Howard, 2013). Thirty-five caves out of the 80 Yorkshire caves excavated have been methodically examined, with radiocarbon dates associated with 22 caves in the area (*ibid*.). The purpose of this research is to re-examine caves from the Yorkshire area, originally discussed by Leach (2006b, 2006a, 2008), applying new methods of quantification using a geographical information system (GIS). Additional taphonomic analysis will add evidence to help answer questions around timings and change during the Early Neolithic in Yorkshire. As put by Schulting, Chapman and Chapman (2013, p. 23) “thorough osteological analysis” can “provide a very useful baseline for comparison with contemporary assemblages from caves and monuments and may provide insights regarding the decision of where to place the dead”.

The following section returns to discussions around spirituality and caves, following which the geological and taphonomic processes associated with caves are covered. Details of the caves specific to this research are covered in the chapters eight and thirteen.

## 2.4: Caves and the Ancestors, a Place of Spirituality?

The human use of caves spans geographical and temporal space, with use traceable back to our hominid ancestors (Bonsall and Tolan-Smith, 1997; Dirks *et al.*, 2015). Throughout prehistory to the present day, caves have been seen as unique and special places. Our fascination with these dark spaces and their links to mythology, crime, tourism, shelter, and more are well summarised by Leach (2006b, 2006a) and Dowd (2015). It is not the intention here to repeat such an overview, rather to provide a brief discussion around ritual and domestic use. This is pertinent to the area of study and reveals possible motives for the depositions in the caves studied here. The remainder of the section explores cave geomorphology and the taphonomy around bone accumulations in subterranean contexts.

In the closing chapter of their book, Bonsall and Tolan-Smith (1997, p. 217) argue that cave use can be split "loosely" into economic purpose and the disposal of waste. There is clear evidence, however, of continuing ritual use. Such a divide could be considered too simple. Ideas and connections to caves are much more complex with ritual and domestic use continuing to this day. Evidence of habitation and ritual use has been found across the world and although it is thought that economic and spiritual use are rarely simultaneous (Bonsall and Tolan-Smith, 1997) there are instances when they occur together. When they do occur together the darker, less accessible areas tend to be reserved for ritual and burial practices. The Grotta Scaloria cave, Italy, has evidence of both, with light levels dictating use (Whitehouse, 2016; Rellini *et al.*, 2020). Similarly, at Grotto Mora Cavoro, Central Italy and Mayan caves in Suchitepéquaz and Sololá, chambers away from natural light were more heavily used for rituals (Ishihara-Brito and Guerra, 2012; Silvestri *et al.*, 2020). Tomkins (2012, p. 108) describes the predominant areas used for depositions, during prehistoric times, as "focused in the darkest parts of the cave". He argues that the nature of Cretan caves is such that they are unlikely to have been used for domestic purposes during the Neolithic. Despite domesticity forming the dominant discourse around prehistoric cave use in Greece, Tomkins (2012, p. 107) considers it a misnomer that Neolithic people were "cave dwellers". It is the dark nature of caves, difficult access, and their ethereal qualities, that has resulted in them being places strongly associated with ritualism and spirituality. The language used for caves further heightens their 'otherworldliness'. Caves in Guatemala have been called 'Ventana'

(window) and 'Encantos' (spells/charms) (Ishihara-Brito and Guerra, 2012) and the Irish 'uath' can simultaneously be used to mean "fear, horror or terror" (Dowd, 2015, p. 6). The language surrounding caves evokes the idea that they can act as portals to communicate with ancestors or are spaces to be feared.

Darkness may have had additional meaning during the Neolithic with connections drawn "between darkness, birth and regeneration" (Hensey, 2016, p. 8). The inaccessibility of some caves, particularly chambers away from the entrance may have been a means of limiting access to select people. Robb (2020), in a discussion around the nature of Neolithic cave art, suggested that the art itself was important from a ritual perspective rather than a representational one, particularly cave art that is hidden from view. He argues that during the Neolithic people had a "preoccupation with ritual activities" and that societal hierarchies may have been built around ritual knowledge rather than socioeconomic factors. Dowd (2015, p.10) touches on a similar theory; the darkest areas of caves may have been limited to spiritual leaders, with rules around who was able to enter. Entrances to caves also held significance, with evidence of bone deposits discovered at entrances (Dowd, 2015, p.3) and should not be overlooked. Constructed 'mesas' (altars) outside Guatemalan caves have been documented, as well as local folklore about a 'gallo' (rooster) that would appear in front of caves to lure people in (Ishihara-Brito and Guerra, 2012). If the darkest areas of caves were reserved for individuals with spiritual importance, then it is possible that rituals extended to entrances, to allow participation of other society members, much like the modern practices documented in Guatemala.

The darkness in caves can alter the senses creating an out-of-body experience. The heightening of other senses when in complete darkness can act to achieve "a spiritually better state" (Whitehouse, 2016, p. 34). Caves altering consciousness has been discussed in reference to cave art (Lewis-Williams and Clottes, 1998) and the intense effect caves can have on our sensory experienced highlighted (Ustinova, 2009; Mlekuž, 2012; Dowd, 2015, p.147). It is these liminal spaces that Tomkins (2012) found were characteristic of Neolithic cave sites in Crete; "all Cretan Neolithic caves emerge as liminal places, entry into which involves dramatic changes in light, sound, smell and freedom of movement" (Tomkins, 2012, p. 116). More recently evidence has been found of the consumption of oral hallucinogens at Pinwheel

Cave, California (Robinson *et al.*, 2020). The idea of sensory alterations, whether through the aid of hallucinogens or as a function of the cave atmosphere itself, tie into the idea of transformation. Darkness becomes a metaphor for transition and funeral rites in the Neolithic are argued to be a process of managing transformations of death (Parker Pearson, 2000; Peterson, 2019, p.47). The moment when a living body is removed from its social role but has not yet taken up another, such as the role of ancestor, involves a period of transition (Whitehouse, 2016). The darkness of the cave acts as a liminal space, driving the transformation (Leach, 2008; Dowd, 2015, p.2; Freikman, 2017; Peterson, 2019; Badiella, 2020). Evidence of the manipulation of the dead in Scaloria support this theory of taking a body from the realm of the living and transforming it (Robb *et al.*, 2015; Rellini *et al.*, 2020). A similar process can be seen in depositions at Grotto Mora Cavoro. An upper room contained partially articulated remains; in the lower chamber the commingled remains of several bodies were "chaotically piled" (Silvestri *et al.*, 2020, p. 31). The paper focused their discussion on the possibility that movement had either occurred due to down sloping of the cave or from subsequent interments pushing bodies back. An intermediate room, however, is described as devoid of light. If this was used to deposit whole bodies, then it may be indicative of spiritual practices around darkness providing a means of spiritual passage. Intermediate spaces in caves can offer a "twilight" zone or "physical threshold that marks departure from the world of the living and entry into the subterranean realm" (Dowd, 2015, p. 3). A better understanding into the movement of the assemblages, through taphonomic analysis, between the two sections of Grotto Mora Cavoro may aid understanding of ritualism and burial practices.

Examining the taphonomy of assemblages to interpret depositional processes, particularly in relation to stratigraphy and cave geomorphology, is critical to understanding funeral rites. The excavation site of remains does not necessarily reflect the place of deposition (Peterson, 2019) and understanding this can help interpret possible ritualistic use. To make sense of the movement of remains the formation of caves and assemblages needs to be considered. The collections examined in this research originated from limestone caves in Yorkshire and Cumbria. While there are different types of caves, the following examines the formation processes of limestone caves due to its pertinence to the assemblages.

# CHAPTER 3: CAVES AND TAPHONOMY

## 3.1: Cave Formation and Geology

Limestone caves form when weak acids in rain dissolve limestone along joints, bedding planes, and fractures formed during tectonic deformation (Waltham and Murphy, 2013). Limestone is formed of layers and fractures act as conduits for water. Some layers will contain a higher percentage of magnesium, making them more resistant to dissolution. Other layers, more susceptible to dissolution, will widen as water passes through them. The dissolution of limestone creates passages and voids, voids beneath the subsurface flood and fill with water to the point of saturation (at the ground water table). The level of the water table is controlled by local streams; erosion causes streams to deepen, resulting in the lowering of the water table. The lowering of the water table allows the flooded voids to drain, abandoning upper chambers. Caves formed below the ground water table form evenly due to the consistent flow of water, creating tube-like passages, and are referred to as phreatic. Vadose caves erode at the cave floor, with water only filling a portion of the void with free air at the surface (Waltham and Murphy, 2013) and result in canyon shaped caves. As the water table drops, caves that initially underwent phreatic development may be subjected to vadose erosion, resulting in a multi-phase cave passage, with a keyhole profile (Waltham and Murphy, 2013).

As the water table sinks new caves form, speleothems grow, and chambers are enlarged by hydraulic action, corrosion, and abrasion. The development of vadose and phreatic cave systems is depicted in figure 3.1 (taken from Lewin and Woodward, 2009).

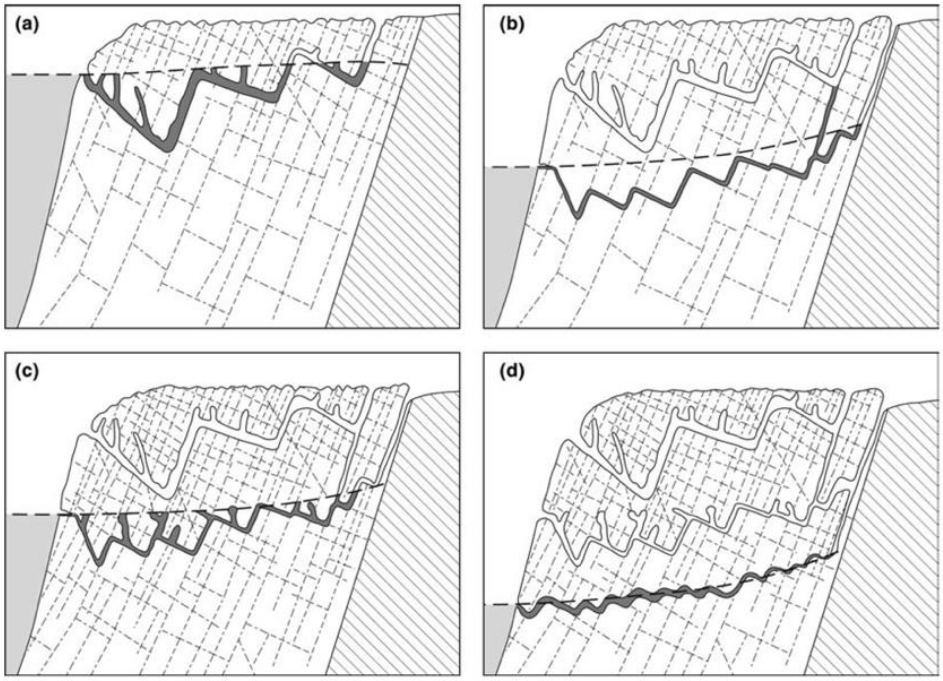


Figure.3.1: Development of vadose and phreatic cave systems. The dashed line represents the water table. Figure (a) shows phreatic development before becoming a vadose system (b to d). (Lewin and Woodward, 2009).

"Caves are open cavities in the Earth. As such they are natural sediment traps" (White, 2007). They contain complex deposits along with sediment transported by varying methods. Fragmentation and decay of walls and roofs cause the introduction of sediment from the surface. Large sediment infills may occur during periods of heavy erosion, additionally calcite deposits may act to partially block passages. Such processes can cause access routes and entrances to caves to change (Waltham and Murphy, 2013). Interpretations of deliberate burial in caves should consider geological changes to cave stratigraphy that may leave prehistoric entrances closed or blocked in the modern day. While limestone caves are slow forming, the "location, configuration, shape, and size of their *mouths* can and do change relatively rapidly" (Straus, 1990, p. 258).

Collapse in more mature caves results in infilling and destruction, while surface erosion can simultaneously lead to roof collapse. The majority of Yorkshire caves started as phreatic until they were large enough to allow water to freely drain; subsequently passages have developed through both vadose and phreatic processes, with many high-level passages no longer active. New cave passages have developed beneath these larger ones and continue to be active. Sediment infills and surface erosion, resulting in blockages, have prevented the mapping of

some of the high-level areas (Waltham and Murphy, 2013, p. 126). Infilling in Yorkshire caves has tended to be a result of wall destruction, adding to floor debris. Avens can also introduce sediment, including bone, further adding to build up (Andrews, 1990). Some clastic sediments in Yorkshire have measured at least 30 metres deep. Streams that flow across the floor further act as a method of debris removal and enlargement of chambers; caves developed through vadose processes are likely to see the input of material through streams (Waltham and Murphy, 2013; Peterson, 2019, p.61). Fluvial action and periods of flood will act to further redistribute debris. Caves that are cut off from the surface will have a stable and humid atmosphere and sediment accumulation will be limited, made up from sources within the cave. Water flows can wash out finer sediment leading to compaction of remaining materials and major collapse. Skeletal remains are not spared from this movement, periods of collapse can result in the crushing and damage of bone and water flows can disperse skeletal elements. The formation of rockshelters follow similar mechanisms, often the result of wall collapse. Deposits placed within rockshelters may, however, experience different climates to those in internal chambers due to exposure to the surface and light.

Alongside movement, collapse, infilling, and fluvial action, chemical deposits form within caves. Speleothems are secondary deposits formed in caves from calcite, aragonite, or gypsum. The most common is calcium carbonate and caves that sit at the water table, with circulating air, will see the formation of stalagmites, stalactites, and flow stones (Peterson, 2019). Stalagmites and stalactites are unlikely to form in lighter areas of caves due to "turbulent" air flow (Peterson, 2019, p. 63). At Grotta Scoloria, Italy, there is evidence of deliberate collection of water from beneath stalactites. The pottery vessels used for collection became integrated with the forming stalagmite below (Whitehouse, 2015; Peterson, 2019, p.19; Rellini *et al.*, 2020). This suggests a ritualistic association with water, which is echoed at Mayan caves in Guatemala (Ishihara-Brito and Guerra, 2012). Tufa, another speleothem, does accumulate in lighter areas of caves and there is evidence to suggest that tufa held meaning during the Neolithic (Peterson, 2019, p.64). Tufa forms from calcium carbonate in the ground water around organic matter (*ibid*.). Characteristic of moist environments, tufa often contains fossilised remains, including faunal elements. Its laminar characteristics and mineral content make it ideal for stratigraphic study and dating (Dabkowski, 2014). Leach (2008) discussed the preservative nature of tufa and the possibility that it served a particular purpose for Neolithic

burials. Several Early Neolithic remains found in Yorkshire caves were found to be coated in tufa deposits. Leach (2008) offers two views around its preserving quality. Tufa may have served to prevent transformation to the spirit or ancestral world, particularly with burials that seemed to be against the norm. Alternatively, it may have been seen as a "living rock", something ritually significant that acted as part of the transformation, rather than against it. This links to Parker Pearson and Ramilisonina (1998) who described the idea that during the Neolithic stone structures were built for ancestors, paralleling the wooden constructs of the living. The embedding of pottery at Grotta Scoloria may add to this argument of the sanctity of natural substances. Research into tufa and its archaeological significance appears scant, perhaps due to the difficulty in establishing its symbolic use (Davies and Robb, 2002). Whether it was ritually significant or not, there is some evidence to suggest that it played a role in Neolithic life. Lewis and colleagues (2019) discuss the significance of tufa during the Late Mesolithic and Early Neolithic, where there is evidence that it was hand moulded into balls. While possible ritual aspects of deposits are important, deposits also play an important part in taphonomic analysis and understanding deposition. At Cave Ha 3, Yorkshire, surrounding tufa deposits preserved some anatomical articulations, allowing interpretations to be made that the body had been likely to be introduced to the cave in a whole, fleshed state (Leach, 2008).

Other deposits can provide similar information. Calcite, commonly found in caves in the Dales, is white or translucent in its pure form. Iron oxides in water can make calcite appear off-white or cream (figure 3.2). Clay can leave dirty grey deposits and hydrated iron sulphates, carbonates, and compounds such as copper can leave blue/green deposits (Waltham and Murphy, 2013).

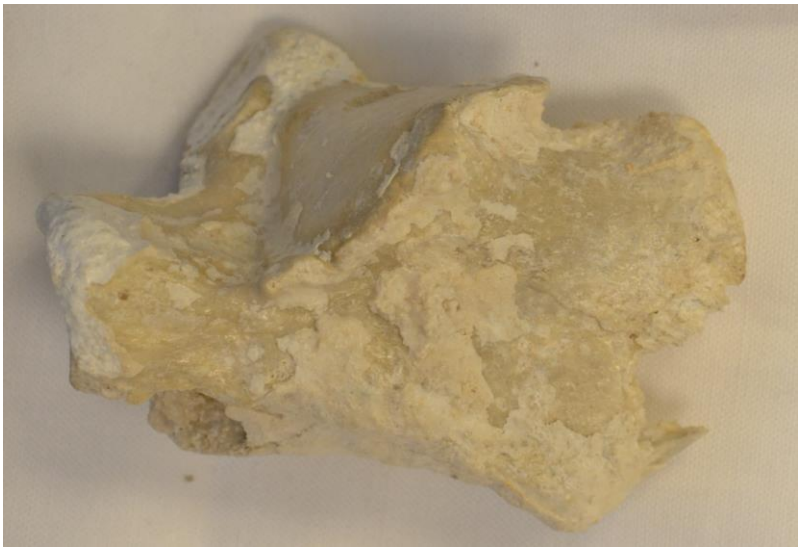

Figure 3.2: Example of calcite deposits on a calcaneus (photo: K.Warburton, 2021)

The latter are less common in Yorkshire caves but not absent (*ibid*.). Blue calcite flow has been documented in Wizards Chasm, west of Malham (Waters and Lowe, 2013, fig. 2.28) and in North Yorkshire manganese deposits were found at Black Reef Cave (Murphy and Hodgson, 2017). Such deposits are often found on bones deposited in caves; bones may also be stained as a result of lying-in particular substances. Manganese can leave black staining on bones, usually as a 'stippling' effect and iron oxides can leave bones stained red or red-brown (figure 3.3) (Pokines *et al.*, 2013; Fernández-Jalvo and Andrews, 2016, p.156-158; Randolph-Quinney *et al.*, 2016).

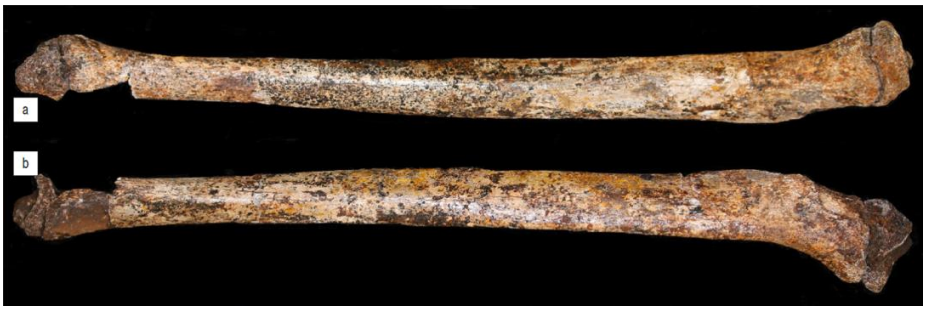


Figure 3.3: Example of a tibial shaft showing manganese staining and iron oxides (Randolph-Quinney et al., 2016, p. 2)

The distribution of coatings can provide information on the state of bones on deposition. For example, fewer deposits (or lighter deposits) on articulating surfaces can suggest burial in an articulated state as these surfaces will have been exposed for shorter lengths of time (Fernández-Jalvo and Andrews, 2016, p.156). Dirks and colleagues (2015) argued that the

"lack of surface modifications and stain patterns" suggested a more recent deposition when compared to other remains that had more prolific staining. Tide lines can also indicate orientation or partial burial (Evans, 2013; Randolph-Quinney *et al.*, 2016).

The geology of caves is a complex subject, with the above providing a brief overview of some processes likely to impact depositions. Bone assemblages in caves may be exposed to a variety of mechanisms: changing the appearance, structure and placement of skeletal elements. There are several ways in which bones can accumulate in caves: natural accumulation through geological forces, predation, death (faunal traps), and deliberate accumulation through burial (Andrews, 1990, p.93; Dirks *et al.*, 2015). Additionally, remains, especially those of smaller mammals, may accumulate a result of natural death whilst seeking shelter (Andrews, 1990). This is not limited to smaller mammals, primates such as Chacma Baboons have been known to use caves in the Dronkvlei cave in South Africa for shelter (Barrett *et al.*, 2004) and more recent research shows that "they commonly occupy caves" (Val, Taru and Steininger, 2014, p. 57). It is possible that, while using caves as shelter, natural deaths occur. Val, Taru and Steninger (2014) found that taphonomic evidence, cave stratigraphy and the mortality profile of a primate assemblage from Cooper's D, South Africa indicated accumulation was most likely through natural death. Applying taphonomic criteria to archaeological remains has allowed "a more contextual and nuanced picture of decomposition" (Peterson, 2019, p. 54). Understanding changes and dispersal of an assemblage, in relation to geological processes can provide insight into the method of accumulation as well as exposure to taphonomic agents.

The next section introduces taphonomy with reference to processes most likely seen in cave assemblages, before introducing research specific to the aims and objectives of this project.

## 3.2: Taphonomy

Taphonomy is "the study of the transition, in all details, of organics from the biosphere in the lithosphere or geological record" (Lyman, 1994b, p. 1). First introduced into palaeontology by Efremov (1940), it has found its way to both forensic and archaeological practice via the discipline of zooarchaeology (Lyman, 2010; Pokines, 2013b). For archaeologists the

relationship of an object within the environment can provide invaluable insight into patterns of human behaviours (Scott and Connor, 1997; Lyman, 2010). This is especially useful in prehistoric contexts where written accounts are not available. The application of taphonomic analysis to subterranean, Neolithic remains helps interpretations of deposition practices: by considering taphonomy in a spatial context, movement and manipulation of bones can be understood.

There are myriad systems involved when a person dies, the body is disposed of, recovered, and even beyond excavation. These can be split into processes that occur naturally and those that occur because of human (or animal) manipulation. These mechanisms result in 'taphonomic effects', namely: disarticulation, dispersal, fossilisation, and mechanical modification (Lyman, 1994b, p.36). Taphonomic research is based within the concept of uniformitarianism resulting in experimental models and analogues (Lyman, 1994b, p.47). The underlying assumption is that modern-day processes will have the same effect as the equivalent process during the Neolithic. It is therefore possible to compare modifications on historical bones to modern criteria and infer the underlying processes. Such research has been conducted on weathering (Behrensmeyer, 1978; Pokines *et al.*, 2018), fluvial transport (Boaz and Behrensmeyer, 1976; Coard and Dennell, 1995; Coard, 1999; Evans, 2013; Gümrükçü and Pante, 2018), carnivore activity (Brain, 1981, p.56-108; Bunn, 1983; Marean and Spencer, 1991; Lam, 1992), bone fractures (Symes, L'Abbé, Stull, *et al.*, 2013; Galloway, Zephro and Wedel, 2014), butchery (Brain, 1981, 30-55; Bunn, 1981; Marean, 1991), soil staining (López-González, Grandal-d'Anglade and Vidal-Romaní, 2006; Pokines *et al.*, 2013), cremation (Bennett, 1999; Symes, L'Abbé, Pokines, *et al.*, 2013; Snoeck, Lee-Thorp and Schulting, 2014), root etching (Pokines and Baker, 2014), and invertebrate surface modification (Andrews, 1995; Zanetti, Visciarelli and Centeno, 2014), all of which can provide evidence into burial processes.

The following does not aim to provide a complete discussion on the issues of taphonomic analysis. Perreault (2019) provides a useful resource into both criticism of taphonomy and the nature of archaeological assemblages. Lyman (1994b) has also covered vertebrate taphonomy in depth. The next section offers an overview of research into modifications likely to occur on bone assemblages from UK caves.

### *3.2.1: Weathering*

In 1978 Behrensmeyer wrote her seminal work on the weathering of mammal bones in the Amboseli Basin, South Kenya, leading to the development of six-stage criteria to assess the level of subaerial exposure (figure 3.4).

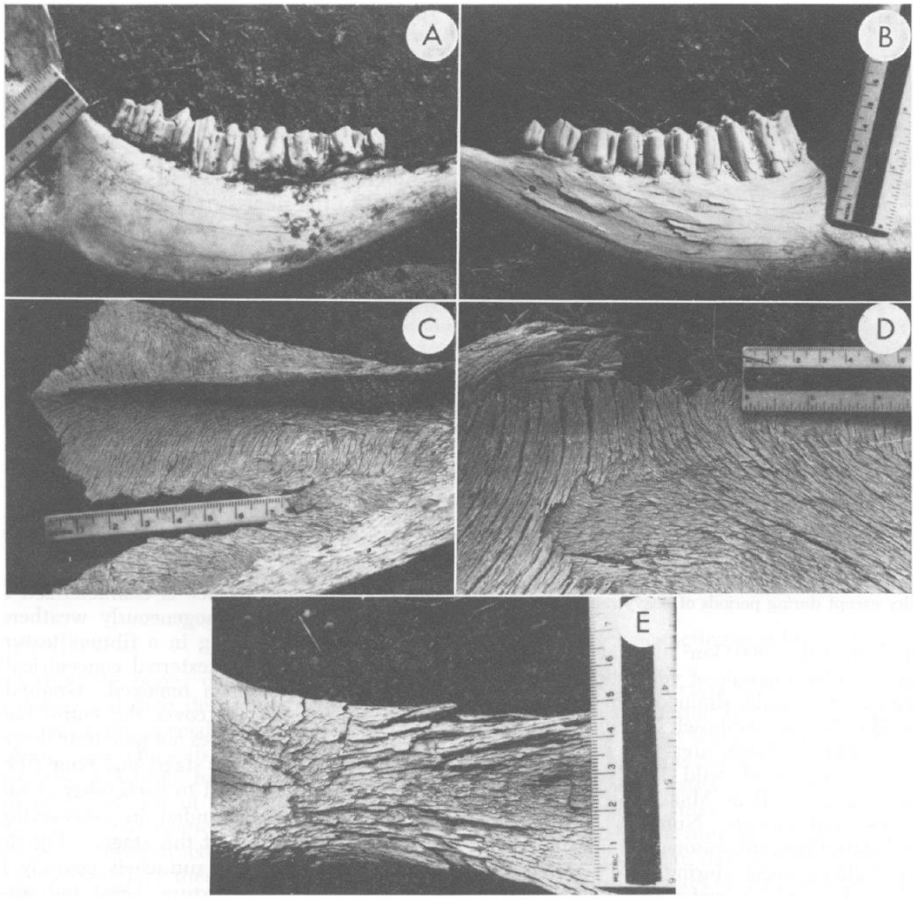


Figure 3.4: Stages one to five showing progression of weathering (taken from Behrensmeyer, 1978, fig.2).

Weathering is commonly used to describe changes to bones that have been exposed to subaerial conditions. Burial does not, however, prevent weathering of bones (Lyman and Fox, 1989; Scott and Connor, 1997) and using a weathering score to determine exposure is problematic. Weathering is an umbrella term covering several processes that can occur because of exposure. This can include "ultraviolet exposure, mineral leaching, mineral recrystallization, thermal expansion/contraction, freezing/thawing, and wetting/drying" (Pokines *et al.*, 2018, p. 433). The research conducted by Behrensmeyer (1978) was specific to a dry, arid climate (Kenya) and to surface exposure. Behrensmeyer herself urged that

"sampling over a broad range of climatic regimes will be essential" and that for "temperate climates, the added effects of freezing and thawing will need to be tested" (Behrensmeyer, 1978, p. 160). This has implications for UK cave burials where bones can be subjected to periods of flooding and sediment infill. Areas away from the daylight zone usually maintain consistent temperatures, offering a "climatically stable environment" (Murray and Kunz, 2005) with no ultraviolet exposure. Sediment accumulation may result in the 'burial' of bones, or in the case of Cave Ha 3, build-up of tufa results in the obscuring of bone surfaces. All these factors will impact the degree of weathering to bone surfaces.

Lyman and Fox (1989) offered a critique of Behrensmeyer's stages of weathering, highlighting several issues with the method. Despite Lyman and fox (1989) arguing that there are flaws with applying weathering stages to the passage of time, it is still routinely applied to prehistoric collections. Behrensmeyer's (1978) weathering stages can provide useful information, but other evidence should be considered when used to interpret deposition.
Pokines and colleagues (2018) demonstrated that the cracking associated with weathering can occur solely through the process of wetting and drying (figure 3.5).

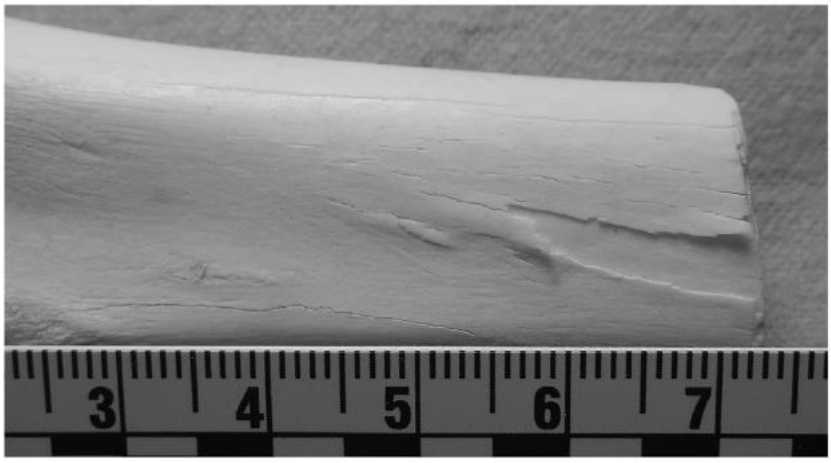


Figure 3.5: A distal tibia showing cracking and delamination after 150 wet-dry cycles (taken from Pokines et al., 2018, fig.3).

While their research was focussed on subaerial processes, they describe open karst systems as an environment where prolonged exposure to "seasonal wet-dry cycling" may result in cracking without evidence of other weathering (Pokines *et al.*, 2018, p. 438). The area of interest would have seen cave interiors "become wetter […] as a result of the higher rainfall"

during the onset of the Holocene (Lord *et al.*, 2007, p. 693); this, coupled with the length of time the bones remained there, could result in cortical cracking. Dirks and colleagues (2015) argued that lower stage weathering patterns on the recently discovered hominin species *Homo naledi* were indicative of direct burial in a cave environment due to their climatic consistency. Further analyses of *Homo naledi* fossil remains by Hawks and colleagues (2017, p. 40) distinguished cracking, because of "fluctuations in moisture content", from secondary characteristics of surface exposure such as "delamination, deep patination, bleaching or cortical exfoliation". Hawks and colleagues (2017) provide a comprehensive checklist that divides the characteristics of surface exposure, allowing for splitting in bone from wet/dry cycles. By creating sub-characteristics such as delamination, peeling, cracking, and bleaching, more specific processes indicating surface and subsurface exposure can be identified. In their related paper Dirks and colleagues (2015, p. 22) suggest that a lack of "bleaching, cortical exfoliation, delamination or deep patination" indicated that the bones had not been exposed to solar radiation, thus differentiating from subterranean weathering. Pokines and colleagues (2018, p. 438) suggest, however, that the cracking seen in the *Homo naledi* fossils was "more consistent with sediment loading" and that further research is needed specific to karstic environments. Care should be taken when interpreting taphonomic modifications. The issue of equifinality, the same modification resulting from different agents, is inherent in taphonomy. It is this process of gaining an overall picture of all modifications, rather than a single criterion, that provides insight into the underlying processes. It is possible to extend Leach's (2006a, 2006b) taphonomic analysis by applying an adaptation of Hawks and colleagues' (2017) criteria, to gain a full picture of changes occurring.

### *3.2.2: Fluvial Transport*

Natural accumulation can occur because remains are washed into a cave system because of fluvial transport or mudflow. Sediment, including bones that are lying on surrounding surfaces, can be washed into a cave system through avens (Andrews, 1990, p.92). Research into the effects of river transport has shown that water has the potential to move remains across great distances and has serious effects on preservation (Nawrocki *et al.*, 1997; Evans, 2013). Nawrocki and colleagues (1997) provide a summation of the transport effects of water. They describe the characteristics of fluvial transport during 'phase three' (remains that are skeletonised and disarticulated) as including: preferential movement of elements according

to size, high energy flow more likely to transport larger elements, mixing of distinct depositions, concentration of elements in accordance to morphological class, differential movement in accordance to density and shape, orientation of elements (in line with the flow of water), degree of sediment influencing movement, and abrasion (dependent on distance travelled and mode of transport) (Nawrocki *et al.*, 1997, p. 603). This is where burial context and the quality of excavation comes into play. Knowing the stratigraphic relationship of elements can provide evidence of movement by water, particularly if there is concentration or dispersal of morphologically similar elements. Abrasion and polishing occur on bones because of sediment in water flow during fluvial transport; wind abrasion and trampling can also cause similar effects. The orientation and location at excavation can provide indication as to which mechanism is behind the changes (Fernández-Jalvo and Andrews, 2016, p.169).

Evans (2013) summarises the characteristics of fluvial transport as consisting of: abrasion, acid etching, discolouration, invertebrate activity, sediment impaction and cracking (figure 3.6).

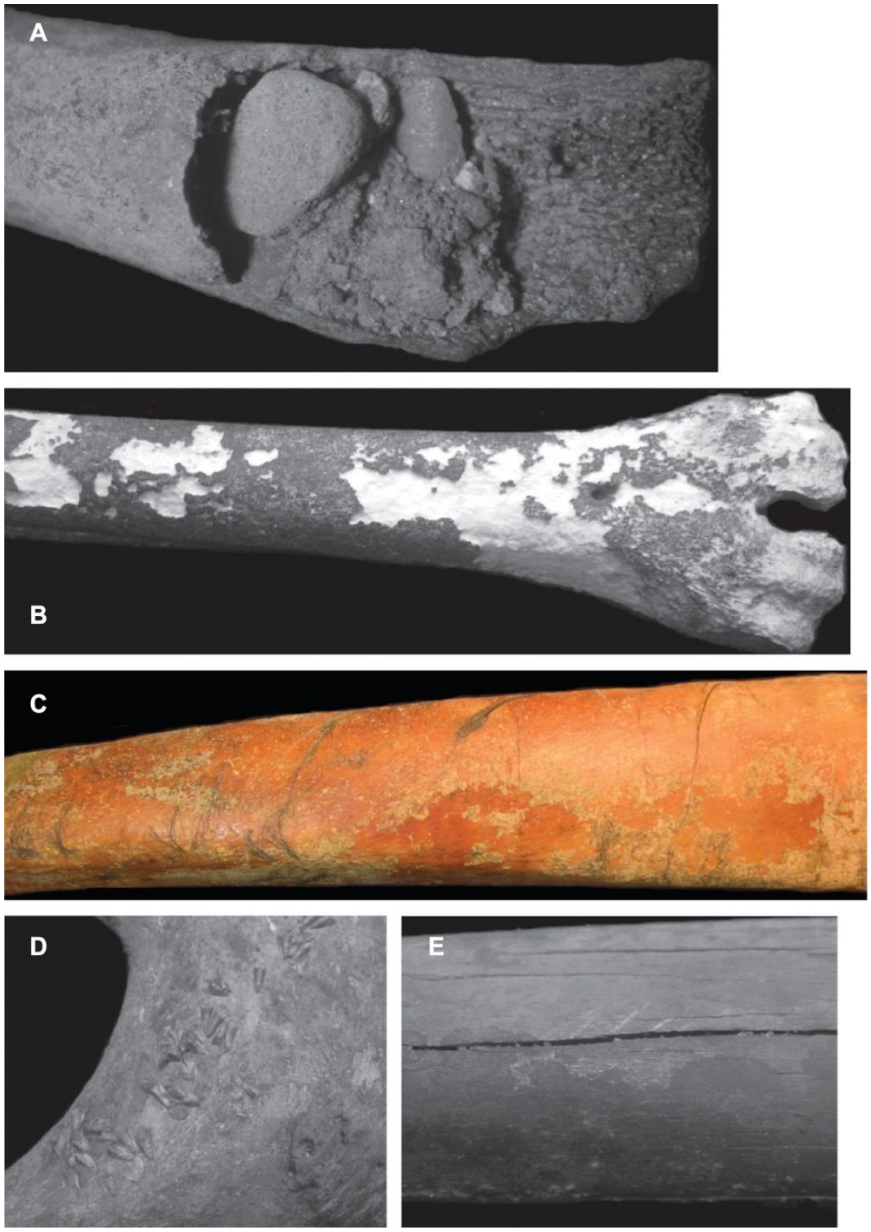


Figure 3.6: Examples of A) sediment impaction, B) acid etching, C) discolouration, D) invertebrate activity, and E) cracking as a result of fluvial transport (taken from Evans, 2013, figures 6.1a, 6.2c,6.4b, 6.5c and 6.5e).

They highlight, however, that there is a paucity of literature and what exists is small scale or observational. Evans (2013) also suggests that interpretation of remains from fluvial environments is complex, a viewpoint they still hold nearly a decade later (Evans, 2021). Nawrocki and colleagues (1997) also describe individual characteristics, however, suggest that there is not a single modification that indicates fluvial transport but "rather, it is the overall pattern or gestalt that reflects their unique taphonomic histories" (Nawrocki *et al.*, 1997, p. 608). This is where the application of GIS has the potential to highlight such patterns. Breaking

down the analysis into distinct modifications, then looking at how these are distributed, along with an understanding of the depositional environment may help determine acting agents.

### *3.2.3: Animal Agents*

Deposition in caves and subterranean contexts may not always be a result of deliberate disposal. Actions such as fluvial transport or carnivore activity may result in bones left in subaerial conditions being transported into caves, with predation considered the most common cause of bone accumulation (Brain, 1981; Andrews, 1990, p.95; Sauqué *et al.*, 2018). Accumulators can either be animal or human agents (Brain, 1981; Bunn, 1981, 1986; Binford, 1985; Blumenschine, 1988; Andrews, 1990; Fernández-Jalvo and Andrews, 2016). Human accumulation, burial aside, is usually the result of butchery. This has led to discussion around how to distinguish between marks left by carnivores and cutmarks because of human processing (Brain, 1981, p.17-20; Bunn, 1983; Eickhoff and Herrmann, 1985; Cruz-Uribe, 1991; Andrews, 1995; Pickering, 2002). The focus of discussion on cutmark and butchery evidence has been on faunal remains however human butchery is not limited to animals. The earliest evidence of cannibalistic consumption dates to c. 780,000 BP (Fernández-Jalvo *et al.*, 1996, 1999) and is seen up to modern day, including during the Neolithic (Villa *et al.*, 1986; Santana *et al.*, 2019; Marginedas *et al.*, 2020). There are strong links to ritualistic behaviours (Bello, Parfitt and Stringer, 2011; Bello *et al.*, 2015; Marginedas *et al.*, 2020), however, not all cannibalism is related to ritual practices and identifying ritual intention is not always possible (Fernández-Jalvo *et al.*, 1999; Saladié and Rodríguez-Hidalgo, 2017; Marginedas *et al.*, 2020). Cannibalism is not without controversy and usually determined from a combination of modifications rather than a singular type of damage. Marks considered to be characteristic of cannibalism include abundant cut marks, stone tool cutmarks, percussion damage on long bones and skulls, peeling, human tooth marks, boiled bones, scattered and mixed remains, (rarely) cremation, and skull caps (Villa *et al.*, 1986; Fernández-Jalvo *et al.*, 1999; Bello, Parfitt and Stringer, 2011; Bello *et al.*, 2015, 2017; Morales-Pérez *et al.*, 2017; Saladié and Rodríguez-Hidalgo, 2017; Santana *et al.*, 2019; Marginedas *et al.*, 2020). Cut or tool marks on human bone are often first interpreted as the result of "defleshing and dismemberment, as a means of hastening the process of transformation from a fleshed corpse to disarticulated remains" (Schulting *et al.*, 2015, p. 38), especially in the absence of other changes such as those described above. Schulting and colleagues found evidence in Kent's Cavern of marrow

extraction of an ulna that also had evidence of cutting. They were unable to determine the purpose behind such processing, especially since it was limited to a single bone, but did not rule out the possibility that marrow extraction could also serve as a ritual activity, as opposed to cannibalism (Schulting *et al.*, 2015). At Cave Ha 3 a single left tibia was recovered in three sections with evidence of processing for marrow extraction. Leach (2006a, 2006b, 2008) describes the reason as 'unclear', and describes animal bones from the same locations as exhibiting similar damage.

In his study on bone accumulations in African cave taphonomy, Brain (1981) found that many hominid remains were accumulated though predation. The following wild animals have been evidenced during the Neolithic: beaver, wolf, dog, wild cat, mountain hare, otters, pine martens, badgers, wild boar, wild cattle, and red deer (Harcourt, 1974; Serjeantson, 2014; Clark, 2015; Pollard, Serjeantson and Field, 2015; Sykes, 2017). The largest predators in the area of interest (North West UK) during the Neolithic would have been foxes, other canids, and Eurasian Lynx. Wolves and bears, while possibly still present, would likely have been rare in the area (Lord *et al.*, 2007). Human bodies are not exempt from predation and animal attacks still occur (Pokines, 2013a; Bombieri *et al.*, 2018, 2019), additionally bones present nutritional value in the form of bone marrow and are therefore vulnerable to scavenging (Pokines, 2013a). Hyenas have been known to scavenge human remains (Brain, 1981, p.4) and were once native to the UK during the Late Pleistocene (Rivals *et al.*, 2022), however in the area of interest they became extinct at around the time of the last ice age c. 11,000 years ago (Stiner, 2004).

Excarnation has been documented in some cases in Neolithic burials (Leach, 2008; Smith and Brickley, 2009, p.42; Cummings, 2017, p.94; Peterson, 2019) and while carnivores are known to accumulate bones in caves through predation, carnivore activity on Neolithic human bones is much more likely to be a result of deliberate exposure. Such exposure could indicate multi-burial rites or burial practices that have left bodies accessible (Smith, 2006). Evidence at Adlestrop indicated that scavenging was prevented or stopped at a similar point for four bodies. Smith (2006, p. 682) argues that this implies the possibility of "direct observation" of the process and even that excarnation was done using domesticated dogs rather than wild canids. It is possible then, that if there is evidence of carnivore activity on bones recovered

from caves, that this has resulted from deliberate, human exposure, rather than predation. Binford (1981) documented differences between “boredom chewing” and meat consumption. At kill sites of wolves, he documented less pitting and scoring in comparison to dog yard or wolf den assemblages where excessive chewing led to “extensive pitting, scoring and more extreme furrowing” (Binford, 1981, p. 49). Smith (2006) postulates that these differences can indicate the length of time an animal has had access to a bone, and therefore evidence of deliberate excarnation.

Evidence of animal activity includes digestion, gnawing, disarticulation, breakage, abrasion, gouges, linear marks, notches, pits, punctures, rounding and furrows (Pokines, 2013a; Fernández-Jalvo and Andrews, 2016, p.4) (figure 3.7).

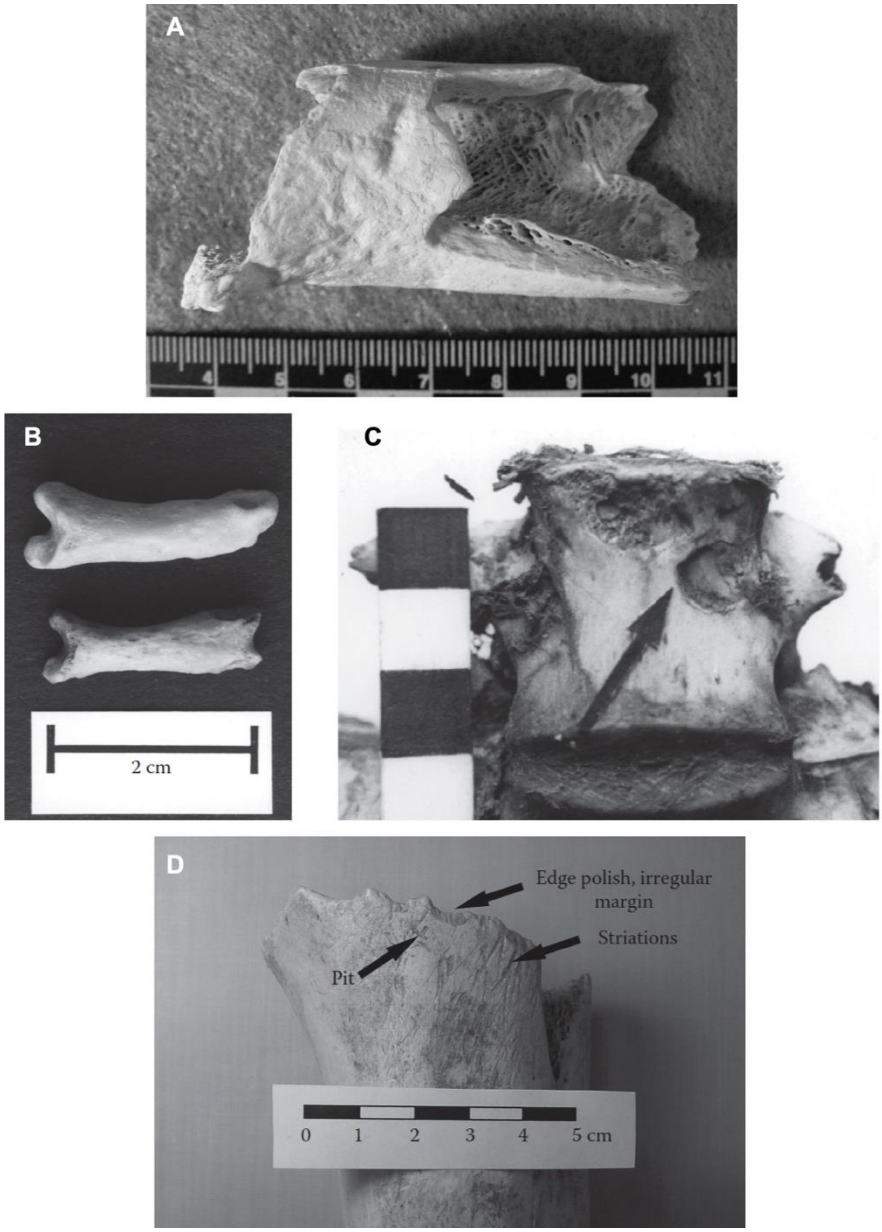


Figure 3.7: Examples of A) gnawing, B) gastric erosion, C) punctures, D) rounding, pitting and striations as a result of dog gnawing (taken from Pokines, 2013a, figures 9.6, 9.7, 9.8a, and 9.11a).

Many of these characteristics can be due to other agents, for example, carnivore chewing marks have been shown to present in a similar way to damage from falling blocks and trampling at the Senéze (Haute Loire, France) site (Fernández-Jalvo and Andrews, 2016). It is also possible that more than one agent is acting on the bone. Both Pokines (2013a) and Fernández-Jalvo and Andrews (2016, p.101) argue that with careful examination these marks can be distinguished. For example, pit and puncture diameters can help assist in determining the size of the animal and the shape, size, and micrology of linear marks can determine the acting agent (U-shape is consistent with animal activity compared to V-shaped tool marks). In

Hawks and colleagues (2017) macroscopic taphonomic analysis they split animal agents into different groups: processing modifications (human action such as notch defects), rodent damage, and carnivore. Carnivore damage was then split into subcategories, coding the presence or absence of bone cylinders, tooth pits, tooth scores, end scalloping and gastric corrosion. This should act as the first stage of analysis, with patterns and locations of damage also noted to gain a fuller picture. Where required, microscopy should be employed to determine smaller features, as seen with their determination of invertebrate activity (Hawks *et al.*, 2017).

### *3.2.4: Natural Traps*

Limestone caves can act as natural faunal or 'death' traps, with narrow openings in comparison to lower chambers creating inverted funnels (Andrews, 1990, p.94-95; Pokines *et al.*, 2011). Cave morphology is important to understand when discussing cave assemblages. Of the sites examined for this research only Heaning Wood had the potential to act as a natural trap. Ceiling openings can become disguised resulting in animals falling into the cave, the fall is either sufficient to kill the animal or death occurs later due to an inability to climb out resulting in starvation. Larger animals can become trapped themselves either through falling or because of attempting to scavenge remains of smaller, trapped animals (Andrews, 1990, p.95; Pokines *et al.*, 2011). Due to the nature of natural traps the animals represented in the assemblage reflect the living population. There may be a higher concentration of carnivores due to scavenging earlier victims, but there is usually a range of remains from all size classes and all, or most skeletal elements will be represented (Andrews, 1990, p.98; Kos, 2003; Pokines *et al.*, 2011; Sauqué *et al.*, 2018; Castaños *et al.*, 2019; Pelletier *et al.*, 2020). Evidence suggests that a lack of bias in age classes is also characteristic of natural traps (Kos, 2003; Pokines *et al.*, 2011; Pelletier *et al.*, 2020), this is contrary to predation where prey preferences may tend towards "weak, young and old prey" (Stiner, 1994, p. 296).

Breakages on bones differ for several reasons, including "morphology, structural integrity, mineralization and density", in addition to the type of force applied to cause the break (Zephro and Galloway, 2014, p. 33). The biomechanics of a bone change depending on their level of degradation and as collagen decays, the flexibility and elasticity of bone lessens (Moraitis and Spiliopoulou, 2006; White, Black and Folkens, 2011, p.35). Dry bone, where little to no

collagen remains, will fracture differently from wet bone. Transverse, diagonal, and longitudinal fractures with rough textures, perpendicular to the cortical surface are characteristic of dry bone fracture (Outram, 2001, fig. 3) (figure 3.8).


Figure 3.8: A transverse fracture on mineralised bone, with rough edges (taken from Outram, 2001, fig.3).

Such fractures suggest that the bone has broken post-mortem and after a period of decay. Incomplete or fresh fractures where the surface is smooth, with "a helical or spiral fracture outline" are referred to as greenstick fractures (Outram, 2001, p. 403), evidence of which can suggest that a bone was broken close to or at the point of death (peri-mortem) (figure 3.9).

Figure 3.9: Helical fracture lines radiating from point of impact in fresh cattle bone (taken from Outram, 2001, fig.2).

Greenstick fractures in a cave assemblage can be indicative of a fall and therefore can be used to reinforce evidence of a natural trap (Kos, 2003; Pokines *et al.*, 2011). An absence of greenstick fractures is not, however, always evidence that a site did not act as a natural trap. Both Pelletier and colleagues (2020) and Sauqué and colleagues (2018) found minimal evidence of greenstick fractures in their study of faunal natural trap remains. Most fractures were consistent with post depositional processes and had occurred post-mortem. Skeletal part representation, demographic profile, and site morphology, alongside an absence of evidence of other agents, led to an interpretation of a natural trap. The comparison of site stratigraphy to taphonomy is vital to make inferences around accumulation. Caves that have easy exit routes are unlikely to result in the trapping of an animal whereas steep entrances or vertical drops are more likely to act as natural traps.

Fractures in the remains of two hominids (*Australopithecus sediba*) discovered at the Malapa site in the Cradle of Humankind, South Africa provided evidence that humans, and their ancestors, can fall victim to natural traps. L'Abbe and colleagues (2015) used trauma analysis on two Malapa hominids. Such analysis is typically difficult in the fossil record due to quality and preservation issues of assemblages. The remains from this case were in good condition and partial articulations allowed for analysis, particularly of the fracture patterns in the right upper limb of one individual. The analysis showed evidence for bracing and the injuries were "highly consistent with a fall from a height" (L'Abbe *et al.*, 2015, p. 6). Unfortunately, such interpretations are harder to make in fragmentary and disarticulated assemblages characteristic of Early Neolithic cave burials. While the type of trauma analysis applied in the aforementioned research is unlikely to be possible, fractures can be classified according to fracture angle and outline and edge or by fracture type (Villa and Mahieu, 1991; Galloway, Zephro and Wedel, 2014; Hawks *et al.*, 2017). Differentiation between peri-mortem and post-mortem fractures can be determined though analysis of "staining/color of fracture surfaces, anatomical location of injury, fracture pattern morphology, angle of fracture margins, and context dependent damage" (Galloway, Zephro and Wedel, 2014, p. 50). An assessment of recent edgewear can also be determined by colour differentiation at the fracture juncture (Hawks *et al.*, 2017). This is particularly important in determining fracture timing. Burial conditions affect bone decomposition with temperate climates and neutral soils with good drainage offering the best conditions for survival (White, Black and Folkens, 2011, p.462). In a

cave setting, humidity, coupled with acidity, can result in the interior of the bone corroding extensively, leading to collapse of the cortical surface. This can result in crushing and fracture due to rock collapse (White, Black and Folkens, 2011, p.463; Fernández-Jalvo and Andrews, 2016, p.110). Determining fracture mechanisms and timing can unpick causes of breakage.

### *3.2.5: Burial*

Deposition is not the same as burial and the length of time and processes bones undergo prior to burial can vary considerably (Lyman, 1994b; Sorg and Haglund, 2002). Burial is described by Lyman (1994b, p. 406) as "the covering of faunal remains with sediments" and processes that occur pre-burial need to be distinguished from post-burial processes. It is often the absence of evidence of pre-burial processes that leads to the interpretation of burial; however, evidence of subaerial deposition does not preclude eventual burial. Primary burial refers to the final internment of a body on first deposition, secondary (or multi) burial refers to the further manipulation or movement of a body or bones after their initial deposition (Lara *et al.*, 2017). While there is an abundance of research around other taphonomic characteristics, such as carnivore activity, there is a paucity around burials. As described by Pokines (2013b, p. 11) "Without thinking much about it, archaeologist and biological anthropologists recognize the characteristics of a primary burial or secondary burial…" and it is a pattern of modifications that indicate burial. This includes "articulation of skeletal elements, a largely complete skeleton, soil staining and/or adherence, plant root damage and invasion, erosion (in acidic soil) of cortical surfaces, and a lack of weathering" in primary burials and most of the above "but with disarticulation of the skeletal elements, loss of smaller skeletal elements, and other markers of having been transported and reburied…"in secondary burials (Pokines, 2013b, p. 11). Skeletal part representation will be covered in more detail in section 3.2.6.

Multi-stage burial rites have been evidenced during the Neolithic (Leach, 2008; Smith and Brickley, 2009, p.11; Cummings, 2017, p.136; Peterson, 2019, p.2) and in such cases evidence of both exposure and (re)burial have been used to interpret movement. Leach (2006b, 2006a) discusses this in her analysis of the remains from Thaw Head cave. The articular ends of long bones and pelvic region of the main burial had evidence of scavenging by both carnivores and rodents. Due to the location of the bones, Leach (2006b, 2006a) interpreted that the remains

had initially been buried toward the back of the cave and subsequently moved toward the front due to scavenging. This contrasts with a single ulna shaft that had "extensive evidence of carnivore chewing" (Leach, 2006a, p. 75), the lack of any other associated elements led Leach (2006b, 2006a) to interpret that this element had been introduced *into* the cave by carnivores.

### *3.2.6: Decomposition, Body Movement and Skeletal Part Representation*

It has been argued that the human body, when protected from certain taphonomic factors, follows a set pattern of disarticulation. Known as 'rank disarticulation', less stable (labile) joints will disarticulate first, followed by more stable (persistent) joints (Roksandic, 2002; Bello and Andrews, 2006; Duday, 2009; Knüsel, 2014; Knüsel and Robb, 2016; Mickleburgh and Wescott, 2018; Schotsmans *et al.*, 2022). Rank disarticulation has implications for both movement and the preservation of skeletal elements. The use of bone representation indices (BRI), developed by Dodson and Wexler (1979), can be used along with stratigraphic analysis of elements within the depositional environment to explore preservation and movement. Understanding how the body disarticulates allows natural processes such as carnivores, scavengers, fluvial transport, and other geological processes to be differentiated from funerary practices (Knüsel, 2014).

The presence of elements associated with earlier disarticulation is often used to indicate the absence of larger taphonomic agents, as well as indicating a primary burial. This is because loose bones will be more prone to loss when a body is moved. Likewise, the opposite has been applied, the absence of smaller bones, disarticulation, or "disorder"(Schotsmans *et al.*, 2022, p. 512) of the skeleton is indicative of handling or secondary deposition. This does not necessarily hold true. Movement of bone has been evidenced despite an absence of manipulation (Wilson *et al.*, 2020). While a single case study, Wilson and colleagues (2020) offer evidence of movement as a result of decomposition, rather than by external agents, demonstrating the complexity of skeletal movement during burial. Bone representation indices can also be affected by excavation. Skill in bone recognition; particularly small, unfamiliar, or juvenile bones, and excavation techniques, may lead to the appearance of differential preservation (Robb, 2016). These bones may simply have been overlooked, rather than missing.

Schotsmans and colleagues (2022) raise concerns about over-interpretation by archaeologists. Researchers do not all agree on which joints can be considered labile or persistent. There is contradictory evidence regarding the breakdown of the atlanto-occipital joint, some evidence describes it as a labile joint, others a persistent one (Duday, 2009; Knüsel, 2014; Knüsel and Robb, 2016; Schotsmans *et al.*, 2022). Schotsmans and colleagues (2022, p. 533) argue that "archaeo-anthropologists require knowledge about all stages of decomposition" to understand depositional history, and that due to variations in decomposition "there is no single sequence of dis-articulation" (Schotsmans *et al.*, 2022, p. 533). This is further supported by other researchers who have similarly found no set pattern and argue that the burial context can also alter disarticulation sequences (Roksandic, 2002; Mickleburgh and Wescott, 2018).

Figure 3.6 (Schotsmans *et al.*, 2022, fig. 27.9) shows factors influencing disarticulation and movement of bones.

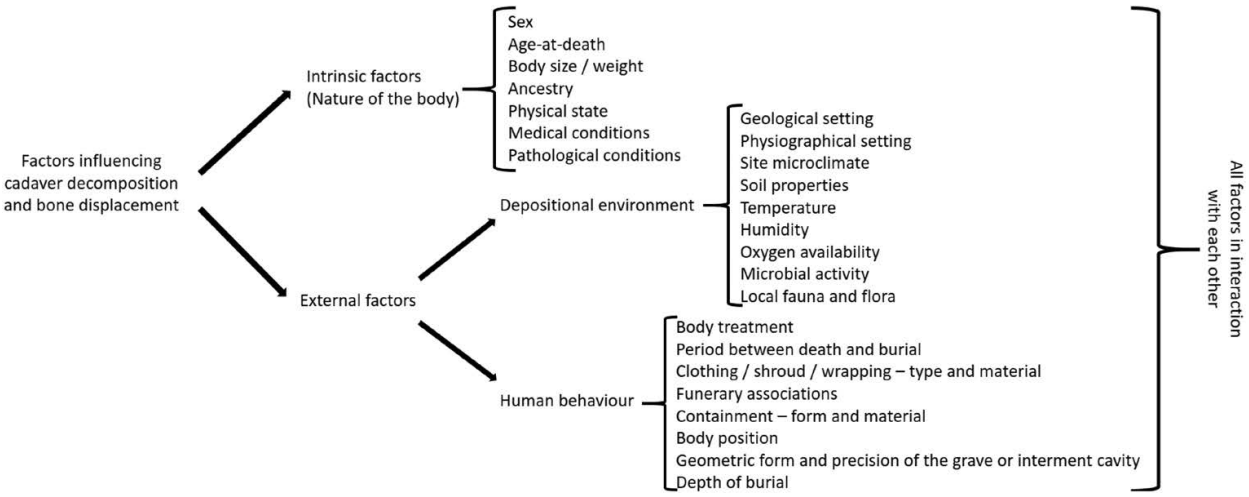


Figure 3.6: Diagram showing factors influencing decomposition and bone displacement (Schotsmans *et al.*, 2022, fig. 27.9).

While there are many factors that may impact how a body disarticulates, there is a consensus regarding some areas of the body. The metacarpals, metatarsals, tarsals (excluding the talus and calcaneus), carpals, phalanges, and patella appear to be consistently labelled as labile joints (Bello and Andrews, 2006; Duday, 2009; Knüsel, 2014; Knüsel and Robb, 2016;

Schotsmans *et al.*, 2022). It may be sufficient to consider the presence of these elements as evidence of primary burial (Duday, 2009; Schotsmans *et al.*, 2022), although care should be taken when applying this logic. Mummified bodies moved to a second location may have a BRI indictive of primary deposition, despite movement. Context is, therefore, important, prior to interpreting burial practices, observations of taphonomy need to be understood, as well as the spatial relationship of bones, cave geology and stratigraphy, in addition to the wider societal context.

In her analysis of the remains from subterranean burials in Yorkshire Leach (2006b, 2006a, 2008) looked at limited taphonomy. In her 2006 research she covered five aspects of taphonomy: cut marks/processing evidence, weathering (as defined by Behrensmeyer, 1978), animal modification, surface condition, and fragmentation/fracturing. While Leach (2006b, 2006a) splits the five taphonomic modifications into subcategories in her written methodology, they become less clear in the databases. These criteria provided information around depositional processes (there was strong evidence for carnivore activity at Thaw Head). The analysis consisted of coding, limited to a spreadsheet and descriptive interpretations. Making interpretations by human eye risks 'cherry picking' data, relying on an "intuitive assessment" of surface damage (Shipman, 1981, p. 358). What looks interesting or is consistent with the researcher's hypothesis is what ends up being discussed. Perreault (2019) touches on this in his discussion around how archaeological research is conducted. The tendency for archaeologists to ignore alternative hypotheses because the data is consistent with their own can lead to confirmatory bias. This amplifies "the underdetermination problem that plagues archaeology" (Perreault, 2019, p. 10). It is not the intention to suggest that Leach's (2006b, 2006a) taphonomic interpretations were incorrect. The aim of this research is to add weight to inferences in the form of quantitative and qualitative reassessments. To achieve this a more detailed macroscopic taphonomic analysis will be conducted, using Hawks and colleagues (2017) recording system as a starting point. A Geographical Information System (GIS) will then be used to highlight underlying taphonomic patterns that might otherwise go unseen, providing a quantitative interpretation of the modifications (Madgwick and Mulville, 2015). Discussed in detail in chapter 5, GIS can handle larger data sets than manual methods and allows the exploration of multiple hypotheses. Additionally, results can be expressed quantitatively removing issues of vagueness or imprecision (Perreault, 2019). Visualisations

and qualitative assessments will, however, be used to complement quantitative assessments. Prior to applying taphonomic analysis to remains the assemblage is usually quantified, and a discussion of potential methods follow.

# CHAPTER 4: QUANTIFICATION IN ARCHAEOLOGY

Archaeological and forensic researchers have adapted quantitative methods originally used in palaeontology and zooarchaeology and applied them to the analysis of human remains (Herrmann, Devlin and Stanton, 2014). Archaeological analysis usually begins with two fundamental questions: "How many people were deposited, and how?" (Robb, 2016, p. 684). It is the answers to these questions that start to shape interpretations around prehistoric societies and their beliefs. Contention around which method provides the most accurate quantification has, however, existed for decades. This research reanalyses Early Neolithic cave burials from North West England, revisiting the key questions outlined by Robb (2016). An open-source Geographic Information System (GIS), QGIS, will be used as part of this analysis. First traditional and manual methods of quantification will be outlined, before discussing GIS and their application to taphonomic analysis.

Different methods of counting have been adopted to answer the first question, "How many people were deposited?". The most common counts include number of identified specimens (NISP), minimum number of elements (MNE) and minimum number of individuals (MNI), a derivative of MNE. This is not an exhaustive list. In his discussion around terminology, Lyman (1994a) lists over a hundred different terms, highlighting ambiguity around definitions and uses. This ambiguity is not new; Casteel and Grayson (1977) attempted to address this issue in 1977, with Lyman (1994a, 2018) continuing the discussion decades later. In the United Kingdom, Márquez-Grant, and colleagues (2016) found that the most used references for human remain analysis were 'Standards for data collection from human skeletal remains' (Buikstra and Ubelaker, 1994) and 'Guidelines to the standards for recording human remains' (Brickley and McKinley, 2004), since updated (Mitchell and Brickley, 2017). Both of which use MNE and MNI counts. While these guidelines are generally accepted as standard practice, there is no formal agreement as to a specific method of quantification. 'Standards for data collection from human skeletal remains' (Buikstra and Ubelaker, 1994) lends itself better to single inhumations or larger skeletal fragments rather than commingled, fragmentary remains (Knüsel and Outram, 2004; Outram *et al.*, 2005). This poses a problem when working with British Neolithic remains since single, articulated inhumations are rarely recovered (Smith and

Brickley, 2009). Many assemblages are fragmented and commingled, particularly remains recovered from caves where active geological processes result in movement, re-deposition, and commingling (Peterson, 2019, p.5).

In Brickley and McKinley (2004) procedures for dealing with commingled remains are separated from those dealing with articulated or cremated assemblages. The guidelines state that the minimum number of individuals should be calculated using "the most commonly occurring skeletal element…in association with clear distinctions in age" (Brickley and McKinley, 2004, p. 14). Additional guidance is given regarding more fragile remains in archaeological settings, recognising the need for more careful and meticulous methods when dealing with fragmentary remains. An updated version of the guidelines acknowledges the need for using databasing software for larger collections, immediate electronic recording, and the use of refitting and landmarks when quantifying (McKinley and Smith, 2017). This highlights the need to continually review and update any attempts at standardised practices. The guidelines do not discuss that refitting is not always possible, and often unlikely, in fragmented collections. The Science and Technology in Archaeology and Culture Research Center (STARC) at the Cyprus Institute published a guide specifically for the 'excavation and study of commingled human skeletal remains' (Nikita, Karligkioti and Lee, 2019). While this aims to set out guidelines, the authors highlight that they are precisely that: guidelines. The authors successfully capture the essence of such research in one sentence: "The high variability in the characteristics of commingled skeletal assemblages suggests that any strategy for retrieval and study has to be case specific" (Nikita, Karligkioti and Lee, 2019, p. 5).

Over time different methods of quantification have come in and out of fashion, with longstanding discussions around their accuracy and statistical integrity (Casteel, 1977; Grayson, 1984; Marshall and Pilgram, 1993; Lyman, 1994a, 1994b, 2008a; Domínguez-Rodrigo, 2012; Cannon, 2013; Lambacher *et al.*, 2016; Morin *et al.*, 2017a, 2017b; Lyman, 2018, 2019; Morin *et al.*, 2019; Palmiotto, Brown and LeGarde, 2019). The ambiguity around counting assemblages along with inherent weaknesses in counts makes comparing reports, particularly those that are less specific about the procedures employed, difficult at best. There is a risk of inconsistency and incorrect interpretations around burial practices (Lyman, 1994a). As focus and knowledge around taphonomic process has increased, the focus of quantification

has moved from NISP and MNI to MNE (Lyman, 1994a), and more recently a return to NISP (Lyman, 2018). Not only are there different ways of quantifying an assemblage, but there is also a multitude of methods for each type of count. As stated by Robb (2016, p. 685) "the MNE and MNI for an assemblage are not absolute estimates but a range, contingent upon various analytical decisions". These analytical decisions will shape the results and interpretations. There is certainly a need for a set of standards in osteoarchaeology, standards that are reviewed and adjusted as methods are refined, but also ones that are most appropriate to the condition of the assemblage. Rigidly sticking to a method without considering the factors which may bias counts risks the discarding of data and incorrect inferences. Interestingly several papers discussing the merits of one method, relative to another, express that the method used should be chosen specifically in line with the analytical question and condition of the assemblage (Ubelaker, 2014; Lyman, 2019; Palmiotto, Brown and LeGarde, 2019). While the following touches on some issues surrounding quantification, a full discussion is outside the scope of this research. Brief definitions and a discussion of manual methods is provided but for a critical review of the last 30 years of quantification trends Lyman (2019) acts as a useful starting point.

It is important to note that when referring to an assemblage this is not an identical representation of the initial deposit. Referred to as the "identified assemblage" (Lyman, 2008a, p. 23), the assemblage that ends up being analysed is a representation of the initial deposit, with loss occurring due to various mechanisms including taphonomic processes, dispersal, incomplete recovery, and rejection of unidentifiable fragments. When discussing the analysis of assemblages, it is this "identified assemblage" which is being referred to. The purpose of quantification is usually to estimate the actual number of individuals (ANI) deposited within a specific site or locus. It is not, and may never be, possible to know the ANI in prehistoric, multiple burials, so why count at all? Analysing assemblages and creating a digital database allows researchers to develop an idea of 'normal' patterns. Having "a set of rules of thumb" (Robb, 2016, p. 692) provides a background against which anomalies or unusual patterns can be compared. Such analyses need to be conducted with careful consideration of the issues surrounding quantification and when reported, the protocols used need to be explicit.

The number of identified specimens (NISP) is a count of how many of a defined specimen per taxon is present in an assemblage. The taxon can be defined as "subspecies, species, genus, family, or higher taxonomic category" (Lyman, 1994b, p. 125). The minimum number of elements (MNE) is calculated as the minimum number of skeletal elements required to account for the identified specimens, for example, if an assemblage has three distal right femurs and two proximal right femurs, the NISP would be calculated as five, but the MNE would equal three (Lyman, 1994a). The minimum number of individuals (MNI) is traditionally calculated by separating 'the most abundant element' of the target taxon into anatomical sides and taking the highest count. For example, in a count of six left and four right tibia the final MNI count would be six (White, 1953, p. 397). Alternatively, the MNI can be calculated by dividing the most abundant MNE count by the number found in the whole animal. In some cases, this formula may result in a fraction. While for most cases the final count is given in integers, Binford (1981) argues that fractions should remain. In his research into butchering practices, he highlights that if butchered remains are shared among households spread over a distance, then it is possible that only a fraction of a body was initially present. The error that is made when calculating MNI in the above manner is that the assumption is made that the entire body was disposed of at that site. This may not be the case even in human depositions, particularly if multi-stage burial rites have been enacted. Fractional MNIs have the possibility of revealing interesting patterns in depositions and should not necessarily be ignored.

White (1953) warned that there was a potential for MNI estimates to be conservative due to not factoring in inter-specimen variation such as age, sex, or size. Having a right and left portion of an element does not automatically mean they are associated; this can lead to the underestimation of the number of individuals in an assemblage. By applying a process of 'pair matching' and ontological analysis the MNI count is thus altered. Pair matching has been shown to have varying error rates as it is usually conducted subjectively through visual assessment of bone size and morphology (Karell *et al.*, 2016). Despite attempts to improve osteometric pair matching, including 3D mesh to mesh comparisons, geometric morphometrics and cross-sectional geometric properties (Karell *et al.*, 2016; Bertsatos and Chovalopoulou, 2020; Fancourt *et al.*, 2021), fragmented remains have "been a neglected area of research in 3D computational methods" (Fancourt *et al.*, 2021, p. 14). It is not the aim here to discuss in depth methods of osteometric pair matching, rather it is to demonstrate

that additional methods may need to be employed to gain a proper picture of MNI estimations. Such methods may include the analysis of unidentifiable fragments.

It is not unusual for fragments to be disregarded during analysis of a skeletal assemblage if they are not identifiable (Outram, 2001). The practice of disregarding remains is long-standing. Klein and Cruz-Uribe (1984) suggested that non-identifiable bones provided no more information than their corresponding identified ones and could therefore be ignored. This inevitably included large numbers of long bone shafts which have fewer discernible landmarks. Outram (2001) highlights that ignoring such fragments is detrimental to analysis, leading to distortion of quantification. The identification of shafts is possible, moreover fragments that cannot be identified can still, and should be, classified. Outram (2001) posits that identification to taxon may not be needed at all but was specifically looking at grease exploitation and marrow extraction. When quantifying human assemblages and using the results to make inferences around burial then identification to taxon is crucial. Yet the techniques employed by Outram (2001) can still provide important information when applied to fragments that have been determined as human, but no further identifications are possible. It can provide information around the degree of fragmentation of the assemblage as well as offering insight into how much data has been lost.

Traditional measures of fragmentation include NISP:MNE ratios (Lyman, 1994b, p.281) and 'percent completeness' (Morlan, 1994). A more comprehensive way to understand fragmentation is to measure fragments, sorting them into size classifications (Lyman and O'Brien, 1987; Villa and Mahieu, 1991; Lyman, 1994b; Outram, 2001; Cannon, 2013). Outram (2001) measured fragments in 10mm groupings and suggested that, in addition to measuring size, mass should be taken into consideration. The mass of unidentified fragments compared to the overall mass of the assemblage can indicate the significance of the loss. Stavrova and colleagues (2019) found this when the 56% of their assemblage was unidentifiable but only equated to 1% of the total mass, indicating the comminuted nature of those fragments. Contrary to this Smith (2006) identified only 39% of the assemblage in his study of bones chewed as evidence of excarnation but no further information was given as to any analysis of the unidentifiable fragments. Smith's (2006) surface analysis was conducted only on identified elements, meaning that interpretations based on patterns of carnivore chewing were made

on less than half an assemblage. Understanding what proportion (in mass terms) the unidentified elements consisted of would go some way to indicate whether this was a significant loss in data.

Other classifications can be made of unidentifiable fragments such as bone type; spongy, cancellous, or trabecular or dense, cortical bone, and for larger fragments whether they originated from the axial or appendicular skeleton. Such information can provide insight into depositional processes, especially if a particular type of bone is overrepresented in the unidentified portion of an assemblage. Absence of elements may be due to 'analytical absence' rather than taphonomic absence and by quantifying unidentifiable portions of an assemblage we can better understand concepts such as skeletal part representation (Outram, 2001). Taphonomic information such as fracture type, "carnivore and rodent gnawing, burning, butchery and modern breakage" can also be discerned without identification to skeletal element (Outram, 2001, p. 404).

Watson (1979) suggested a method to estimate MNE using diagnostic zones. These zones are species-specific, morphological features of bones. The fragment is identified to element and counted when more than half of a zone is present. The problem with only counting fragments where more than fifty percent of a zone is present is that it potentially rejects large numbers of fragments in assemblages that are highly fragmented. Watson (1979) counters this by suggesting using small zones. Smaller zones are less prone to fragmentation, for example, foramina. The use of smaller zones goes some way to counter this issue, but it does not completely remove the potential of distinct skeletal elements being rejected, particularly in bones that have featureless areas such as the diaphysis of long bones. In addition to this, when a zone is close to fifty percent present it adds in an element of subjectivity with the researcher. Watson (1979) does not specify zones, rather he leaves adaptation of these up to the individual researcher. This introduces more subjectivity and makes comparisons across collections more difficult. Using zones reduces the chance of double counting skeletal elements and allows easy calculation of MNI from the frequencies. Zones should, however, be predetermined and logical to facilitate cross-research comparison.

Dobney and Rielly (1988) created the zonation method, an extension of Watson (1979) for use on animal assemblages (figure 4.1).

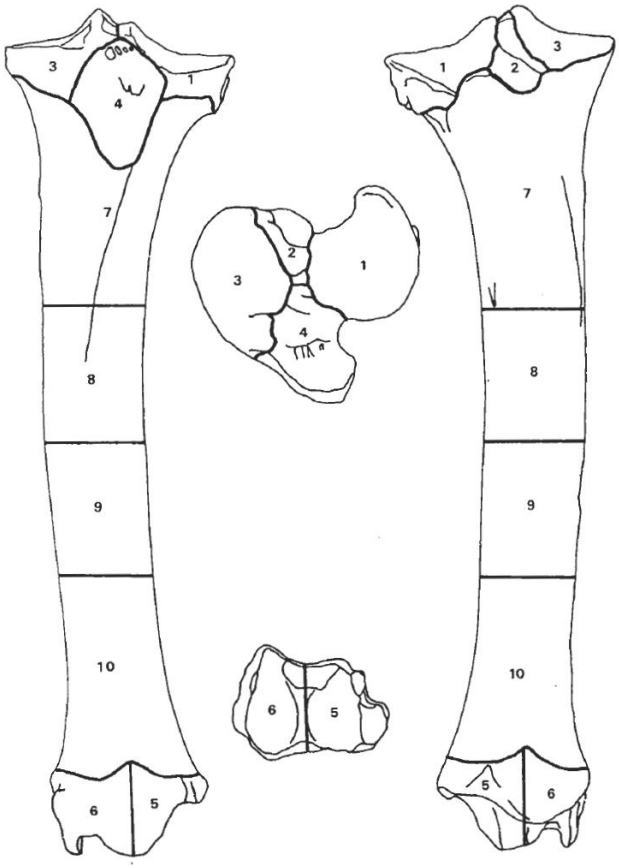


Figure 4.1: Zoned tibia (taken from Dobney and Rielly, 1988, fig. 13).

This provided better standardisation but was, however, still open to the same issues. The zones are represented by a numerical code and marked according to whether more or less than fifty percent of the zone is present. The idea behind this is that if more than fifty percent of the zone is present then it is not repeatable. While this method records fragments with less than fifty percent of a zone, the final MNI estimation still excludes them. The MNI was "made from the zone most frequently recorded as greater than 50% complete" (Dobney and Rielly, 1988, p. 82). As with Watson's (1979) method, there is a possibility that these smaller fragments are distinct skeletal elements, which would add to the final MNI count. The use of zones does allow for a standardised way of coding fragments, which provides a system for relating taphonomic modifications as well as an understanding of breakage patterns and survival patterns, however, the potential to underestimate the MNI needs to be addressed.

The zonation method has continued to be used in archaeology, with Knüsel and Outram (2004) developing it for use on human remains (figure 4.2).

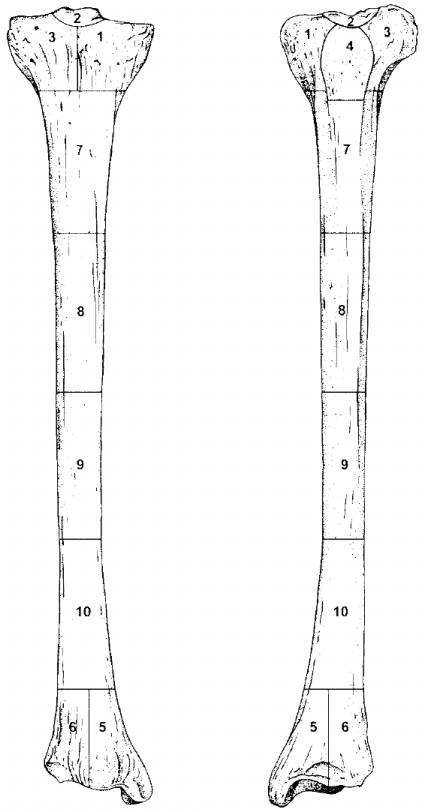


Figure 4.2: Zoned tibia (taken from Knüsel and Outram, 2004, fig. 10).

They suggested that using the same method would allow better comparisons across human and faunal remains and used the method to examine patterns of fragmentation in assemblages. They adapted the animal zones as closely as possible, with juvenile remains sharing the same zones but using codes for unfused epiphyses and proximal/distal ends, for example, “PUF” for proximal unfused (Knüsel and Outram, 2004, p. 87). Unlike Dobney and Rielly (1988), all zones were recorded even if the whole portion was not present. Fragments that were not identified were also counted by grouping them according to fragment size. Zones were coded allowing tallying: the zone with the highest count would provide the MNE calculation, which forms the basis of the MNI calculation. The inclusion of all zones, regardless of percent complete, answers the problem of potential underestimation along with tallies making room for easier recalculations should the assemblage be added to, or the aggregates

altered. The zonation method also helps reduce inter-analyst variation by providing a "standardized (sic) and replicable method" (Palmiotto, Brown and LeGarde, 2019, p. 130).
Both Dobney and Rielly (1988) and Knüsel and Outram (2004) fail to address the issue of overlapping fragments in their papers. Knüsel and Outram (2004, p. 87) refer to "any number of standard anatomy texts" to help assist with overlapping but lack specificity on how to counter this issue. Without looking at areas of overlap, portions of zones are recorded that do not overlap with another fragment from the same zone; this would be counted as two elements despite potentially originating from a single skeletal element. In such cases this would lead to an inflated MNI count and is a particular problem when including all identifiable fragments regardless of percentage completeness. Despite criticism over the accuracy of the zonation method it is still used to this day (Osterholtz, 2019; García-Sagastibelza *et al.*, 2020; Villotte *et al.*, 2020). The method is intuitive and allows for easy recalculation. Other researchers have taken the zonation method and adapted it to facilitate looking for overlapping bones (Villotte *et al.*, 2020). By adapting the zones to follow common fracture patterns the system allows for consistent recording of fragmented collections and providing a visual representation of skeletal representation.

Mack and colleagues (2016) calculated MNE using landmarks. Landmarks consisted of discrete anatomical features "such as tubercles, articular surfaces and processes" or areas that had "clearly defined boundaries" (Mack *et al.*, 2016, p. 527). It was argued that by removing the zones characterised by Knüsel and Outram (2004), and focusing on distinct features, an element of subjectivity would be removed. Where less than half of the landmark was present it was not counted, this was to reduce the chance of double counting elements, but like the original zonation method (Watson, 1979), runs the risk of producing a diminished MNE count. MNE was calculated from the largest number of non-repeating landmarks and from that MNI was calculated by taking the highest MNE count from a single anatomical side. Age was factored into the MNI calculations. Both zonation and landmark methods encounter similar issues, in attempting to address one problem such as subjectivity, they fail to answer the overarching issue of overlapping fragments. Methods that rely on landmarks or anatomical features run the risk of disregarding fragments with no discernible features, risking a conservative count of MNE. Knüsel and Outram (2004) zones factor in the entire bone, thus reducing this risk, and provide a strong basis for quantifying fragmented remains.

In their study of a Spanish medieval cemetery, Lambacher and colleagues (2016) compared three methods used to quantify assemblages: traditional MNI by White (1953); the zonation method by Künsel and Outram (2004); and the landmark method by Mack and colleagues (2016). They came to different values for both MNE and MNI counts for all three methods. The study was not conducted on a known collection and therefore an assessment of how accurately the counts reflected the ANI was not made. The study highlights that methodological decisions influence count, supporting the argument that analytical decisions shape data (Robb, 2016). They found that using White's (1953) traditional method of MNI produced the highest counts, despite previous discussions claiming this method potentially creates more conservative counts. This was discussed as arising from double counts of bones, particularly when refitting was not conducted. The potential for lower counts because of left and right elements being counted as originating from the same individual, even in cases where they may not, is outweighed by errors in double counting fragments that do not overlap.

The decision as to which method of quantification to use in research will depend on the condition of the assemblage as well as the type of research questions asked. Both Watson (1979) and Dobney and Rielly (1988) developed their methods to quantify faunal remains. Knüsel and Outram (2004) adapted their methods to allow for comparison of human remains to faunal assemblages. Whilst measures of abundance form an integral part of zooarchaeology, in the case of funerary archaeology it is often the case that human and faunal comparisons are not the first stage of analysis, nor are they always conducted. Analysis of human assemblages are more focussed on who the people are and why they have been buried there. Recording NISP and MNE initially provides a baseline from which other calculations can be made. How those calculations are derived should be explained explicitly within any project and need to be appropriate to the quality of the material. Applying a method not suited to severe fragmentation will only lead to biased and incorrect results. Additional procedures that have been employed, peripheral to the main methodology, such as refitting, are often not described in detail. References to the procedures are either placed in supplementary material or only made in passing. In her study of subterranean burials, Leach (2006a) describes using a "process of refitting" with little reference to the procedure or criteria employed (Leach, 2006a, p. 28). Simply referring to a 'process' will not provide enough specificity to either critique or compare results.

This research is not an to attempt to create an alternative method of counting. This has been tried and to date no single count has been found to be perfect. It is suspected that due to the unknown nature of the original deposits such a count does not exist. Rather the intention here is to acknowledge the limitations of existing methods of quantification and to show that despite these flaws the estimates they provide still give insight into archaeological processes and depositions. MNI, when applied to human remains, gives us a number from which inferences can be made. Potential inaccuracies in count may impact interpretations and therefore need to be fully understood.

The methods discussed above, even when not made explicit by the researchers, show that a process of refitting or checking for overlap can reduce double counts of bones. Marean and colleagues (2001) refer to refitting and overlap assessments as the 'overlap method', a procedure also discussed by Binford (1978). The overlap method involves placing fragments of skeletal elements in anatomical position and checking if there is any crossover between fragments. Where two fragments overlap it means they must have originated from more than one bone. Manually refitting fragments is, however, time consuming, especially with larger and more fragmented assemblages. For even larger collections there are often space constraints, making it difficult to lay out the bones as required. The decision about what overlaps is also subjective and relies on the researcher's level of experience in identifying remains. These factors can lead to differences in counting between researchers, potentially increasing the larger the assemblage is (Marean *et al.*, 2001). To solve the cumbersome nature of manual refitting Marean and colleagues (2001) developed a method using Geographical Information System Mapping software, arcGIS. Their method, alongside other applications of GIS in osteoarchaeological research are discussed in the following section.

# CHAPTER 5: ARCHAEOLOGY AND GIS

Geographic Information Systems (GIS) are designed to "combine, manipulate, and analyse geographically referenced data of different types" (Nigro *et al.*, 2003, p. 318) and have been used in archaeology for decades, usually in the context of spatial distributions of artefacts and site mapping (*ibid*). GIS was widely adopted in the early 1990s as a way of applying quantitative data to archaeological thinking (Gillings, 2017) and its application is now being extended beyond just geographical spatial relationships. Gillings, Hacigüzeller, and Lock (2018, p. 11) differentiate between two key aspects of GIS; its ability to manage, integrate and display large spatial datasets, and its potential for spatial analysis. The combination of these offers a powerful tool for understanding past human relationships with space, a central concept to archaeology (Gillings, Hacıgüzeller and Lock, 2018). Researchers have since extended the use of GIS, applying it to skeletal analysis, dental topography, taphonomy, and bone histology (Zuccotti *et al.*, 1998; Ungar and Williamson, 2000; Marean *et al.*, 2001; Herrmann and Devlin, 2008; Rose *et al.*, 2012; Herrmann, Devlin and Stanton, 2014; Parkinson, Plummer and Bose, 2014; Garcia Moreno *et al.*, 2015; Parkinson, 2018; Stavrova *et al.*, 2019; Parkinson *et al.*, 2022).

GIS's ability to provide visualisations, coupled with its analytical tools underpin the objectives for this research. Traditional methods of taphonomic analysis rely on recording the presence or absence of a modification, location, and a description (Buikstra and Ubelaker, 1994, p.105; Leach, 2006a, 2006b; Beckett, 2011; Hawks *et al.*, 2017). The output of these analyses is often in the form of binary databases, alongside descriptions. This makes assessments of patterns difficult at best. While certain descriptive statistics, such as frequencies, are possible, additional data such as the location of the modification and clustering is lost. GIS has the potential to provide in-depth data regarding taphonomic modifications in addition to a visual 'map' of the body. Furthermore, the ability to look at multi-scale data, from the body level through to site distribution, allows deeper understanding of potential taphonomic agents.

The following section provides a brief overview of the use of GIS in zooarchaeological and osteoarchaeological research, focusing on quantification and taphonomic analysis. An

exploration of the use of GIS at site level follows before the aims and objectives of this research are outlined.

## 5.1: Quantification and GIS

Marean and colleagues (2001) proposed a new method of estimating minimum number of elements (MNE) using ArcView GIS software and GIS has since been applied to quantification, taphonomy, and analysis of bone surface modifications in faunal remains (Parkinson, Plummer and Bose, 2014; Garcia Moreno *et al.*, 2015; Parkinson, 2018; Stavrova *et al.*, 2019; Parkinson *et al.*, 2022). Despite an uptake in use for bone surface modifications, the number of papers applying GIS to human osteology is limited (Herrmann and Devlin, 2008; Herrmann, Devlin and Stanton, 2014). Guidelines in recording fragmented human remains, with specific reference to archaeological remains, urge the use of electronic databases at point of recording to ensure "rapid detailed interrogation of data" as well as pointing out the need to lay out "large parts of an assemblage" to aid the process of refitting (McKinley and Smith, 2017, p. 20). Using GIS to quantify bones offers the possibility to look for overlap without the need for cumbersome manual methods. In addition to this, GIS works as a database providing the same benefits as other database software such as MS Access and FileMaker, whilst also allowing spatial analysis and visualisation of data (Aldenderfer, 1996). By using GIS to analyse collections it becomes possible to share information across researchers without the need for direct access to remains. This fulfils the parameters set out in the Chartered institute for Archaeologists (CIfA) guidelines, where digital records of remains are encouraged to reduce further, potential damage (McKinley and Smith, 2017).

Another benefit of using GIS is the availability of open-source software through QGIS. While commercial products are available, QGIS provides free to use 2D software, alongside a large community offering support and additional plugins. While Marean and colleagues (2001) initially developed their method for use with a commercial GIS system, ArcView, it is understood that a current project is underway to develop a workflow using QGIS (Farhey, P. 2020 personal communication). Additionally, the use of GIS allows analysis of data that "can be performed either on the single artifact or extended to the whole landscape in the same

georeferenced space" (Landeschi *et al.*, 2019, p. 2807). This creates the possibility of looking at individual specimens as well as whole bodies within the cave landscape.

In an attempt to solve some of the issues that arise when quantifying remains Marean and colleagues (2001) used ArcView to digitise the process and estimate MNE in zooarchaeology. This was achieved by placing digitised images of fragments of bone over a template of the whole element within ArcView (figure 5.1).

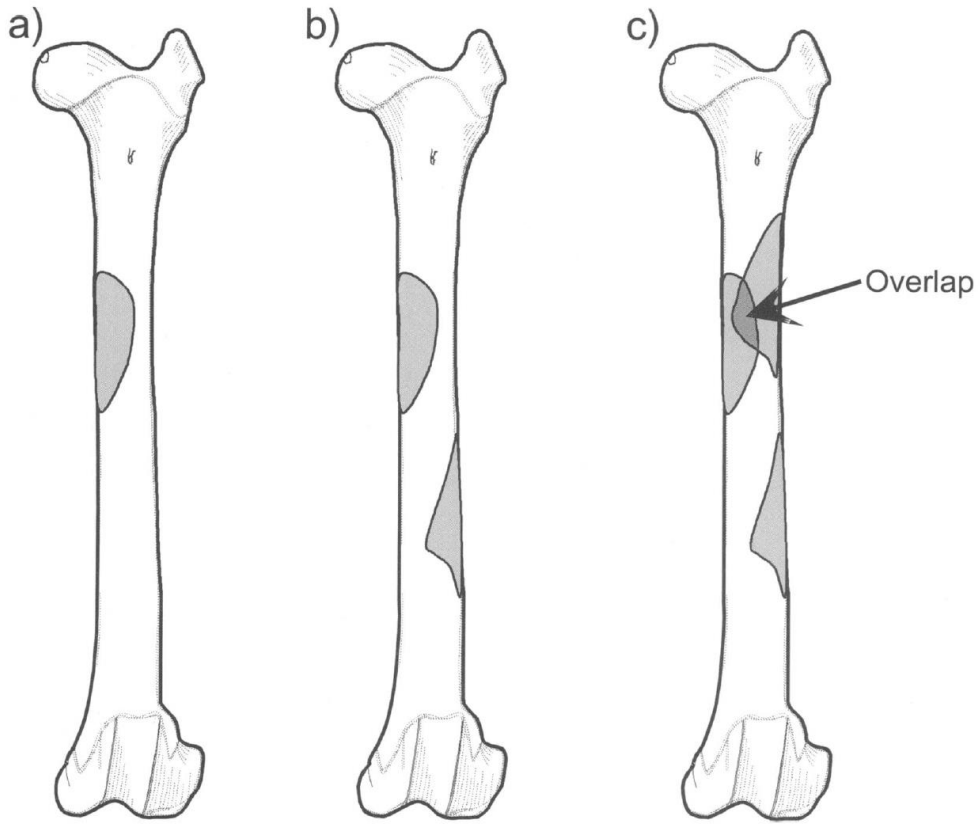


Figure 5.1: Example of fragments placed on digital templates (taken from Marean *et al.*, 2001, fig. 5).

The authors found that previous manual methods of refitting, such as tracings of fragments layered over one another, ran into issues as the size of the assemblage grew. By introducing a computer-based system, larger collections could be analysed more easily, reducing errors in manual methods. The authors conducted their study on bovine bones using a system of size classification based on Brain (1981). There is no such size classification system in humans. As the method involves placing fragments over templates some scaling must be first employed, this was done using a four-point grid that had been referenced within ArcView. The authors

acknowledge that even within species, such as bovids, there may be morphological differences (Marean *et al.*, 2001, p. 342). To counter this, they recommend producing different templates, however construction of the templates is time consuming (Herrmann, 2020 personal communication.). In the case of transferring the method for use in human bones, intrapopulation size differences are said to be eliminated through scaling during the digitisation process. For this reason, a generic set of templates can be used for adult remains. Templates for subadults and infants would, however, need to be additionally created (Herrmann, Devlin and Stanton, 2014). True metric measurements can be recorded within the attribute tables associated with digitised fragments as well as any assignment made to individuals, however the deformation caused by scaling could be considered an issue (Stavrova *et al.*, 2019). QGIS offers six different algorithms in the georeferencing process (Sutton *et al.*, 2023) each one impacts the data differently, therefore, an understanding of the impact on the data is essential prior to processing. Further to this Lyman (2008b) tested the reliability of fragment digitisation based on Marean and colleagues' (2001) methodology. Fragment digitisation was found to be consistent on repeated drawings, but size and location varied, resulting in errors of overlap. These errors increased as the number of identifiable landmarks decreased (Lyman, 2018). Contrary to this Parkinson, Plummer, and Bose (2014) found that there was consistency across researchers in both fragment replication and MNE estimations. It was suggested that the skill level of the researcher influenced the errors found in Lyman's (2008b) experiment. Location of fragments is an issue that needs to be acknowledged with the method, however, and is discussed in more detail below. While Parkinson, Plummer, and Bose (2014) supported the use of GIS for estimation of MNE, they highlighted that it may lead to underestimations due to ontological differences being ignored. GIS is not a replacement to manual methods and the process of individuation can alter the final minimum number of individuals (MNI).

Herrmann, Devlin, and Stanton (2014) compared analyses of human remains from the Walker-Noe site in Kentucky using a landmark approach based on Giovas (2009) and GIS analysis. For the GIS analysis they focused solely on the cranial elements of the collection due to the condition of the remains. The fragments all had evidence of cremation, and most were under three centimetres in diameter (Herrmann, Devlin and Stanton, 2014), making identification of long bone shafts difficult. While their justification for using just cranial elements: high

recovery, readily identifiable, and multiple identifiable features, seems sound, excluding postcranial fragments could have distorted MNE calculations. This is highlighted by research conducted by the authors themselves. The original GIS analysis of the Walker-Noe site was published in 2008 with a calculation of 21 for MNE (Herrmann and Devlin, 2008, p. 264). When making comparisons in 2014, their final MNE calculation was 41 (Herrmann, Devlin and Stanton, 2014, p. 233). This difference is due to the inclusion of temporal bones that were previously left out of final calculations. This is a significant increase and could have a profound influence on the interpretations made of the site. The question remains as to whether the inclusion of postcranial elements would further alter MNE estimations.

While the MNE calculations in Herrmann, Devlin, and Stanton's (2014) work could be questioned, this is due to analytical decisions made to exclude certain elements rather than errors relating directly to the method. With any assemblage there will be decisions such as these that have to be made, and it may not always be possible to conduct the desired analysis due to the fragmented nature of the remains. The purpose of their paper was to compare and examine the methodology used. In that respect the count using GIS was very close to that using the landmark database (GIS MNE: 41, Landmark MNE: 40) (Herrmann, Devlin and Stanton, 2014, p. 230), suggesting consistency between methods.

It is clear from Herrmann and colleagues' (2008; 2014) work that GIS is not applicable to all fragment classes. Marean and colleagues (2001) do not discuss issues regarding 'placeability' of fragments, however Herrmann, Devlin, and Stanton (2014) discuss this issue in depth. Lyman (2008b) also touched on this when he found the inconsistencies in location placing during repeated analyses. QGIS works in 2D, this means that 3D bones, are being rendered in 2D and then placed on a 2D template. This issue is countered by using the four views: anterior, posterior, lateral, and medial. Herrmann, Devlin, and Stanton (2014) encountered problems placing some fragments, particularly with frontal bones. They found that in some views the observer was able to place the fragment easily (anterior and posterior views for the frontal bone), but for other views (lateral) it was difficult to "determine accurate outlines" (Herrmann, Devlin and Stanton, 2014, p. 233). The authors originally rejected an MNE estimation of 26 due to the difficulties in placing frontal elements in their initial analysis in 2008. It was suggested that 3D scanning of fragments, placed onto 3D templates of bones would counter

this issue. Using 3D scanning would not completely erase the issue of 'placeability'. The fragments would still need to be identified and placed within the template regardless of the dimension used. Whether drawing fragments manually or digitally, the accuracy of the drawing will impact whether fragments overlap or not. Lyman's (2008b) finding that reduced visible anatomical landmarks affected the accuracy of overlap assessment is in accord with Herrmann, Devlin, and Stanton (2014) and their issues with determining outlines. It is possible to reject fragments that have unclear outlines or limited landmarks, but this introduces a different bias - the loss of data.

In an analysis of long bone breakage patterns Stavrova, Borel and Vettese (2019) used cattle bones from a previous experiment. Despite all bones being collected, and therefore an expected survivorship of 100%, the authors found otherwise. Due to the large number of bones used in the original experiment some fragments were either lost or mixed up and they were unable to reassign some fragments to the original bones. Only 44% of the fragments were identified to element and side. A major limiting factor of Marean and colleagues' (2001) GIS method relates to the identification of fragments. To accurately place a fragment, it must be identified to element, side, and location. Relying solely on this method to calculate MNE results in large numbers of fragments, and therefore potential data, being rejected. In the case of Stavrova, Borel and Vettese (2019) this amounted to 56% of the entire collection, however, this only represented 1% of the weight of the entire assemblage (Stavrova *et al.*, 2019, p. 8). The bones Stavrova, Borel and Vettese (2019) were analysing were from a known collection, where refitting and identification would be considered more accurate than if they had worked with an unknown collection. This creates a potential for a higher percentage of fragments being rejected in unknown, comingled collections. It is likely, however, that these fragments would also be rejected in traditional, manual methods which also rely on identification and placement. The questions with using GIS for quantification is whether it simplifies the handling and refitting of larger assemblages.

## 5.2: Taphonomy and GIS

Since the introduction of GIS to osteological analysis, GIS software has extended from MNE calculations to the analysis of taphonomic modifications and how they are distributed on the bone, in particular butchery marks on faunal remains.

Butchering marks concern the modifications left on bones because of "human reduction and modification of an animal carcass into usable or consumable parts" and include percussion, cut, sawing and chopping marks (Lyman, 2008, p. 279). The identification of butchery marks is well documented (see Harris *et al.*, 2017, p. 70 for an overview of the history of bone surface modifications in relations to cutmarks and butchery) and, while evidence of butchery on human remains has been found (Villa *et al.*, 1986; Santana *et al.*, 2019; Marginedas *et al.*, 2020), for the most part discussions concerning butchery have centred around the human processing of animal bones. While this research focuses on human remains, GIS research of butchery marks on faunal remains has the potential to be adapted for other taphonomic modifications and applied to human assemblages, including forensic applications such as trauma and dismemberment.

GIS was introduced as a method to improve inter-comparability in cutmark analysis (Abe *et al.*, 2002) and has subsequently been used to understand butchery, bone surface modifications (BSM) and canid damage (Parkinson, Plummer and Bose, 2014; Parkinson, 2018; Stavrova *et al.*, 2019; Parkinson *et al.*, 2022). Abe and colleagues (2002) offer an in-depth summary of the approaches taken in the analysis of cut marks and argue that traditional methods of recording, the overlaying of cutmark diagrams over skeletal elements, lead to "qualitative and subjective assessments" (Abe *et al.*, 2002, p. 645). Similarly, more quantitative assessments of taphonomic marks, using scoring and databasing can also result in subjective assessments or some patterns being missed.

In cut mark analysis researchers have predominately tallied the number of specimens displaying marks (fragment count), while others have focused on the frequency of the cut marks themselves (cut mark count) (Abe *et al.*, 2002). Fragment counts can then be expressed either in terms of the number of identified specimens (NISP), i.e., number of cut marked

specimens or by MNE, i.e., number of cut marked elements. Typically, this is then expressed as a proportion:

**MNE cutmarks / Total MNE**

Expressing counts in this way can be applied to other derived counts that originate from MNE such as the minimum number of individuals (MNI). It is argued that expressing proportions by MNE is more appropriate for comparison than cut mark frequency due to differential survival of skeletal elements (Abe *et al.*, 2002). Tallying by specimen introduces what Abe and colleagues (2002, p. 646) refer to as "the fragmentation problem". Their concern is that counting by specimen runs the risk of undercounting marks due to analytically absent fragments. The more fragmented an assemblage the more fragments will be unidentifiable or destroyed. This renders neo-taphonomic studies (the recreation of taphonomic processes in experimental settings) incomparable as they often use assemblages that are either unfragmented or deliberately fragmented, without subjection to other destructive taphonomic processes (Abe *et al.*, 2002).

Abe and colleagues (2002) suggest that the fragmentation problem can be negated by describing cut mark frequency as a proportion of the total surface area examined rather than as a proportion of NISP or MNE. They made a basic assumption that the relationship between number of cutmarks and surface area size is linear, i.e., the larger the surface area analysed the more cut marks found (*ibid*.). Abe and colleagues (2002) used GIS to calculate the surface area of the fragments analysed to estimate the actual frequency of cut marks should the whole bone be analysed. A two-dimensional measurement of the fragments, using pixel counts, provided a calculation for the surface area analysed. They then calculated a "corrected number of cut marks (CNC)" using the following formula:

**Number of cuts/% surface area analysed x 100 = CNC**

The problem with CNC is that it assumes that cut marks are randomly distributed across bones (Lyman, 2008b). CNC takes a cut mark count and, using the surface area analysed, extrapolates out to estimate how many cut marks would be present across the missing surface. It has been shown that cut mark frequencies vary between identical anatomical

regions (Pobiner and Braun, 2005), contrary to the assumption underpinning Abe and colleagues' (2002) CNC. Lyman (2008b) criticises Abe and colleagues (2002) assumptions further, arguing that fragmentation is more likely to increase cut mark frequencies. If a single mark is split across fragments there is a risk of double counting. This is especially pertinent if an assemblage is fragmented but not to a point of high destruction.

While there are issues regarding the use of CNC it is not related to the use of GIS, rather an issue with the underlaying assumptions. GIS was used to facilitate the calculation of analytic surface area (Abe *et al.*, 2002) and offers an effective way of doing so. The digitising of fragments into GIS, however, involves the transformation of 3D objects into 2D. This introduces distortion and it could be argued that using GIS and pixels to calculate surface area may not be a true reflection of the actual surface area studied. The problems described above are pertinent to taphonomic analysis when using calculations of surface area. Abe and colleagues (2002) introduced the application of GIS to the study of taphonomy, providing an objective understanding of the distribution of taphonomic modifications and the opportunity to apply spatial statistics to data.

Parkinson, Plummer, and Bose (2014) expanded on previous research using GIS for bone surface modifications (BSM) (Marean *et al.*, 2001; Abe *et al.*, 2002) to canid modifications. The focus of carnivore activity in taphonomy has historically centred on hyaenids and felids, particularly in Africa (Parkinson, Plummer and Bose, 2014). Parkinson, Plummer, and Bose's (2014) aimed to create an experimental analogue for large canids, specifically wolves, that would have overlapped with pre-modern humans and would be more relevant to North America, Eurasia, and the northern hemisphere. Parkinson, Plummer, and Bose (2014) plotted tooth marks by type within a single layer in GIS. This was done over the template of the element, per the methodology described in Marean and colleagues (2001). Information about each modification was recorded in the associated database. Using average nearest neighbour distance (NND), a spatial analyst tool within ArcGIS 9.2, they tested for significant spatial clusters and heat maps were produced using the Kernel Density tool, creating visual representations of clusters. Fragments were layered over in one composite layer to show if there was a pattern in element survivorship. This can be applied at whole body and element level. Using GIS Parkinson, Plummer, and Bose (2014) showed variability in tooth mark

frequencies across bones, identified areas of significant clusters of tooth pits and identified patterns of bone damage. While they acknowledged that the method can be time consuming the authors highlight that using GIS can pinpoint finer variations in taphonomic modifications that may otherwise be missed. Their focus was on frequencies and clusters, rather than measures of surface area, reducing issues of potential distortion discussed above. The authors, however, were working on experimentally derived assemblages. In archaeological samples it is likely that there would be greater loss of fragments, and therefore a loss of clustering evidence. Interpretations of taphonomic modifications, irrespective of the method of analysis, must consider that some modifications will be lost to destruction. What is absent may be more significant than what is present (Gillings, Hacıgüzeller and Lock, 2018).

Stavrova and colleagues (2019) aimed to use GIS to create neo-taphonomic data of long bone breakage patterns. They applied NND to assess distribution of percussion marks and visual representations, using GIS kernel density analysis, to indicate clusters of marks. The authors also applied an adaptation of the CNC calculation (Abe *et al.*, 2002) while acknowledging the issues raised by Lyman (2008b). The authors accept that CNC is not a predictor of destroyed marks but offers a way to 'calculate the frequency of cortical bone survivorship". GIS can measure the area of a polygon, allowing Stavrova and colleagues (2019) to estimate the percentage of preserved cortical bone surface in relation to the whole element. Not only did bone survivorship provide information regarding fragmentation it also provided an opportunity to look at potential relationships between percussion marks and the total recovered bone. Importantly, Stavrova and colleagues (2019) highlight the importance of defining methodological procedures. For percussion marks they use the central point of the mark for the location in GIS. While this may not reflect the true origin of the mark it allows standardisation across studies. Using a single point rather than lines and polygons for marks also facilitated the visualisation and spatial pattern analysis.

There are issues with using non geographical data in GIS, particularly the deformation that occurs to metric measurements because of scaling to uniform templates. To minimise problems, specific protocols need to be defined including "the placement of points (percussion marks) or outlines of polygons (fragments)" (Stavrova *et al.*, 2019, p. 17). If these are done properly then GIS is a powerful tool for analysing large amounts of data and is able

"to explore a variety of questions in a short amount of time" (Stavrova *et al.*, 2019, p. 19). GIS has the potential to explore issues such as equifinality (Brouwer Burg, 2017), create experimental models in taphonomy (Parkinson, Plummer and Bose, 2014), and provide analysis at varying levels, even to artefact or bone level (Garcia Moreno *et al.*, 2015).

GIS not only offers accurate recording and better visualisation of taphonomic data (Parkinson, Plummer and Bose, 2014; Garcia Moreno *et al.*, 2015; Parkinson, 2018; Stavrova *et al.*, 2019) but also the option of spatial statistical analysis. However, with GIS comes uncertainty. As with quantification, the application of GIS to archaeological data needs to account, or at least acknowledge, the uncertainty in its models. There is a "basic scientific requirement of being able to describe how close (their) information is to the truth it supposedly represents" (Hunter, 2005, p. 633). Differential preservation, recovery and equifinality all introduce uncertainty into archaeological data, with the use of GIS potentially compounding this (Brouwer-Burg, 2017). While there may be a level of uncertainty with GIS and its application to archaeology, it is not a reason to reject it. The pragmatic approach would be to accept, and acknowledge that this uncertainty exists, and work critically. Gillings, Hacigüzeller, and Lock (2018, p. 12) highlight the importance of approaching spatial data critically, urging evaluation of "the quality of spatial data" and "the validity of arguments based on spatial information".

While offering several benefits, it is worth returning, momentarily, to the issue of 'placeability'. GIS as a tool, for both quantification and taphonomic analysis, is limited to fragments that can be accurately identified to location and element. MNE count can be changed drastically with the inclusion (or exclusion) of elements (Herrmann and Devlin, 2008; Herrmann, Devlin and Stanton, 2014) and the tallying of taphonomic modifications can be biased by fragmentation (Abe *et al.*, 2002; Lyman, 2008b; Stavrova *et al.*, 2019). GIS does not offer a single, standardised method for the analysis of human bones, rather it offers another tool which may lend itself to certain assemblages. Bias will influence data from the moment of discovery, during excavation and analysis, particularly when working with historic collections, or with excavations conducted by non-specialists. Assemblages where identification is limited can further reduce inferences that can be made. Using GIS to refit/overlap involves placing a fragment of bone in its exact location and relies on confident identification of species, bone element, and anatomical side. If a fragment cannot be

confidently identified but is still placed, it is done so falsely and communicates that the researcher knows exactly where the fragment comes from. Any conclusions drawn from this may be misleading. On the other hand, discarding any fragments that are not 'placeable' then creates a bias in the other direction, unnecessarily eliminating potentially useful data. The unplaceable fragments may still provide information (Outram, 2001) but, by blindly following one method, data is lost.

By applying multiple methods to fragmented assemblages, extraction of data is maximised, allowing all levels of fragmentation to be included. The method should be driven by the condition of the assemblage. Fragments that can only be assigned to taxa can be classified according to fragment size: the inferences that can be made from this are limited but degree of fragmentation can provide insight into post depositional processes. Fragments that can be identified to element but not side or location can be tallied within the zonation method (e.g., rib head/rib ends). All identifiable fragments can then be processed using a method of MNE calculation, such as the zonation method. Finally fragments that are 'placeable' can be subjected to an additional level of analysis using GIS and refitting. Together, the combination of manual and GIS methodology allows a multi-dimensional picture from which interpretations can be made. A multidisciplinary approach supports Verhagen (2018, p. 13) in their argument that GIS should "never be a stand-alone approach".

## 5.3: Site Level Distribution and GIS

The section above focused on analysing body-level changes but distributions of skeletal elements and taphonomy within the burial environment are equally important for interpretating burial practices. Despite a proliferation of the use of GIS in archaeology since the 1990s (Nigro *et al.*, 2003; Gillings, Hacıgüzeller and Lock, 2018) its uptake for intra-site spatial analysis is limited, particularly at fragment level (Marín-Arroyo, 2009). A few researchers have focused on its potential to examine zooarchaeological deposits on a micro scale (Nardini and Salvadori, 2003; Nigro *et al.*, 2003; Katsianis *et al.*, 2008; Marín-Arroyo, 2009; Mainland *et al.*, 2014) with fewer applying it to the distribution of commingled human remains (Herrmann, 2002; Beckett and Robb, 2006; Tomé, Díaz-Zorita Bonilla and Silva, 2017; Thompson *et al.*, 2020). The following section examines different methodologies,

demonstrating that GIS has the potential to investigate patterns in commingled, collective depositions that may be unclear when examined by eye.

Marín-Arroyo (2009) applied several statistical models (crossed correlation index, principal component analysis, correspondence analysis, and local density analysis) to the spatial distribution of faunal deposits remains from the El Mirón Cave, Spain. The remains originated from three excavation areas, with evidence of discrete, short periods of occupation. The spatial data for each stratum was well documented, allowing analysis of 0.25 $m^2$ units. Using GIS databases, they were able to explore distributions of remains by taxon, element group, and taphonomic modifications. The nature of their data: a large sample size and good spatial references, allowed them to pinpoint areas of differential accumulation, including differences across temporal space (*ibid*.). Relating densities of taphonomic alterations to the geology of the cave, they were able to make inferences about agents acting on the bones. Additionally, the spatial distribution of different species offered insight into selective transport strategies (Marín-Arroyo, 2009, p. 517).

Other research applying GIS to the distribution of taphonomy on a faunal assemblage has highlighted areas of methodology that need refinement, particularly around visualisations and treatment of frequency data. Channaraypatna and colleagues (2018) explored three taphonomic modifications: exfoliation, weathering, and erosion, on faunal remains from Isernia La Pienta. While this was a preliminary study, some of the frequency maps produced were difficult to understand. They explored density of the remains and in two additional maps used pie charts to show frequencies of alterations and taphonomy. In their final map showing frequency of altered remains, it has not been adjusted to reflect differential densities within each area. If there are more bones in a grid square, then the likelihood of having bones with alterations is increased. Additionally, the use of a pie charts shows information only in relation to the number of fragments per square, however the authors are not clear on these counts. Due to the nature of archaeological material, counts are unlikely to be absolute. Using a pie chart indicates a proportion of 100%, when final recovery is likely to be less than this. A map showing density of each alteration across the site, adjusted for relative fragment density may have better reflected taphonomic distributions. Additionally, bar charts showing actual counts would have been easier to understand, and better reflect differences across the assemblage.

Mainland and colleagues (2014) expanded on distribution analysis when excavating a faunal deposition at the Ness of Brodgar, Orkney. Their method used a combination of 3D spatial recording at the point of excavation and GIS to analyse distributions of remains according to element type, taphonomic alterations and bone orientation. Mainland and colleagues (2014) were able to interpret that the assemblage was the result of either "a single depositional event, or at the very least a series of events occurring over a fairly short time period" (Mainland *et al.*, 2014, p. 875). Both Marín-Arroyo (2009) and Mainland and colleagues (2014) had large sample sizes and *x, y, z* coordinates, meaning that analysis of the data worked well with GIS. Although Marín-Arroyo (2009, p.509) was working with retrospective data, El Mirón Cave was described as having a "long, well-preserved stratigraphic sequence". The authors describe a paucity of bones with all three coordinates, however their sample sizes in comparison to human deposits in caves was large, numbering in the thousands for Red Deer and Ibex. Their suggestion that similar research employ methods of spatial correlation assumes a quality of data that is often missing from older excavations. Similarly, Mainland and colleagues (2014) were able to apply specific, high-resolution recording at the point of excavation. This provided a level of detail down to the orientation of several fragments. The time and financial cost may be prohibitive in future excavations, and the spatial data needed absent from older projects.

Papers using GIS in the analysis of human remains tend to work with historic data, as opposed to applying high-resolution, 3D or GIS methodologies at the point of excavation. Two papers, however, have been able to use GIS from excavation onwards. Herrmann (2002) published their research on the Río Talgua Cave, Northeast Honduras, looking at using GIS to reconstruct burial contexts. In the case of their research, they applied GIS methods *in-situ*. This was due to restrictions regarding the removal of bones by the Honduran government. Herrmann (2002, p. 21) categorised the bones into: "cranial, axial, appendicular or indeterminate", as well as looking at paired elements. Herrmann (2002) highlighted possible bone bundles, with crania placed next to, or on top of them. This was confirmed with clustering in GIS. The method introduces the idea that GIS can be used to look at burial contexts, away from the burial site. While they were working *in-situ* through necessity, the mapping of fragments provides a method for older assemblages where the bones are no longer in context. Provided there is

sufficient spatial data, it is possible to reconstruct the burial environment and understand depositional sequences. Although Herrmann (2002) alludes to the possibility, they did not expand the analysis to incorporate distribution of taphonomy. Combining the analysis of taphonomic spread with bone dispersal would use more contextual information, providing nuance to interpretations, thus providing greater support.

Beckett and Robb (2006) used GIS to analyse the movement and distribution of fragmented skeletal elements in a case study on collective burials in Neolithic Ireland. Three sites in Ireland, Poulnabrone, Poulawack and Parknabinnia, had a combined total of over 20,000 fragments of human remains. During excavation these had been geographically located within the tombs. Focusing on the Parknabinnia site, Beckett and Robb (2006) had primary location data allowing them to look at element distributions. When the assemblage was looked at as a complete unit, there did not appear to be any significance to the spread of bones. Clusters were subsequently identified when element groups were analysed independently. These were a combination of articulated groups, but also disarticulated remains that had retained proximity (*ibid*.). Beckett and Robb (2006) also looked at pair matching identifying 118 bone groups. By using GIS, they tracked movement of the bone groups. They found that 65% of the bone groups moved less than 30 cm. Long bones, however, were shown to move up to 60 cm. This suggested that there had been deliberate movement during "tomb cleaning, "paving" to seal levels, and further depositions" (Beckett and Robb, 2006, p. 64).
Again, Beckett and Robb (2006) recorded taphonomic modifications but did not use GIS to look at that distribution. Both Herrmann (2002) and Beckett and Robb (2006) demonstrate that GIS can be used to "identify patterns too subtle to be immediately apparent in the data" (Beckett and Robb, 2006, p. 61). Inferences made using the dispersal of skeletal elements must consider extrinsic (and intrinsic) agents acting on the bones. By looking at the spread of taphonomy alongside bone dispersal, interpretations of depositional narrative would be further strengthened.

Thompson and colleagues (2020) used spatial analysis and GIS to understand burial practices in late Neolithic Malta, this time using retrospective data. They used excavation records from the Xaghra Circle Hypogeum, Gozo and scale drawings of skeletal remains to input data into GIS. This allowed them to look at burial density across the East and West caves, as well as

looking at differential temporal densities of burials. By inputting the finds into GIS Thompson and colleagues (2020) identified previously unrecognised articulations that spanned excavation grid squares. Further analysis looked in-depth at a single 1 $m^2$ deposit, creating visualisations in GIS of bone fragments. This resulted in being able to infer details such as the flexed burial of an adolescent, the orientation of other burials and pinpoint temporal changes in depositional practices. Their research is an example of the power of "working with archival and post-excavation data" (Thompson *et al.*, 2020, p. 84) and taking a detailed look at multiple aspects of a single assemblage. It is evident that even when high-resolution excavation data, such as that described by Mainland and Colleagues (2014), is absent, re-analysis using GIS is possible, and moreover offers insights into prehistoric funerary practices.

There is less research looking at using GIS for burial contexts in comparison to research such as lithics refitting (Beckett and Robb, 2006) or landscape archaeology, however, its application to human assemblages and taphonomy appears to be increasing (Herrmann, 2002; Beckett and Robb, 2006; Herrmann and Devlin, 2008; Herrmann, Devlin and Stanton, 2014; Tomé, Díaz-Zorita Bonilla and Silva, 2017; Thompson *et al.*, 2020). The above acts as a sample of such research to demonstrate the power of applying GIS to both historic and current data. It is possible to unpick micro-scale information such as body position, burial sequences, and manipulation, helping to shape our understanding of burial practices. Some papers feature heavy use of statistical analysis (Marín-Arroyo, 2009; Mainland *et al.*, 2014), while others combine density analysis with visualisations and qualitative descriptions (Beckett and Robb, 2006; Herrmann and Devlin, 2008; Herrmann, Devlin and Stanton, 2014; Tomé, Díaz-Zorita Bonilla and Silva, 2017; Thompson *et al.*, 2020). Whether statistical analysis can be applied will depend on the nature of the spatial data available, but GIS can still act as a useful analytical tool for qualitative discussion and visualisations. As Marín-Arroyo (2009, p. 507) suggests "GIS must be complemented by other techniques to enlarge its capabilities"; it is with this in mind that the following section describes the aims and objections of this project.

# CHAPTER 6: AIMS AND OBJECTIVES

## 6.1: Aims

This research aims to assess whether Geographic Information Systems (GIS) can be used as a tool for exploring taphonomy, currently under researched in human assemblages. Using GIS will allow a multiscale examination, aiming to highlight taphonomic patterns at an element, body, and stratigraphic level. Site specific inferences of burial practices will be constructed and taphonomic patterns across cave burials assessed.

## 6.2: Objectives

- Taphonomic observations of assemblage fragments will be recorded on element templates in GIS.

- Taphonomy across individual bodies will be examined to investigate distribution across elements and anatomical regions, aiming to identify deposition narratives.

- Fragments will be georeferenced to their original find location (Cave Ha 3) or layer (Heaning Wood) to examine:
    - Inter and intra-body taphonomic patterns.
    - Distributions of skeletal elements.
    - The distribution of modifications, collectively, within the cave environment.

- Two cave sites (Heaning Wood and Cave Ha 3) will be analysed and compared to:
    - Improve understanding of Heaning Wood, which lacks detailed stratigraphic data.
    - investigate possible patterns of taphonomy in cave burials.

# CHAPTER 7: METHODOLOGY

Two assemblages from limestone caves in North West England were assessed. Cave Ha 3 was used as a test case as it had strong excavation and stratigraphic information as well as previous reporting. Heaning Wood was introduced as a second case study. While Heaning Wood had previously been reported on, the findings were limited, unpublished, and the stratigraphic information less extensive. Previous assessments have been made to identify the human from faunal remains for both assemblages. Heaning Wood had additional finds that were not previously sorted, and Cave Ha 3 was last quantified in 2006, therefore a secondary assessment was made to verify identification for both collections.

## 7.1: Terminology and Codes

Terminology and its ambiguity in archaeology has been discussed in detail (see Lyman, 1994a; Knüsel, 2014) . Terminology needs to be explicit to avoid ambiguity therefore some terms are defined below to ensure specificity:

**Specimen** relates to a discrete archaeological unit (per Lyman, 1994a, p. 39). For the most part this refers to either a fragment of, or whole bone.

**Fragment** is used interchangeably with specimen and refers to a portion of an element.

**Element** relates to an entire anatomical skeletal unit (*ibid*). This distinction is vital to avoid confusion around fragments being inferred to be whole if referred to as an element.

**NSP** refers to the number of specimens (irrespective of identification) and provides a count of all units within the assemblage.

**NUSP** is the number of unidentified specimens. Initially a category of “faunal” was assigned to bones that were not human and “unidentified” to bones that were queried, pending a second opinion. For analysis, NUSP refers to faunal remains, inorganic specimens and

unidentifiable fragments. This was because faunal remains were not formally identified to taxon.

**NISP** is the number of identified (human) specimens. The NISP should be considered a *minimum* number of identified specimens (Lyman, 1994a, p. 44) as some fragments, in all assemblages, were unidentifiable.

If teeth were still fixed, they were not counted as additional specimens but rather included as a single NISP count for either the fragment of mandible or maxilla they were contained in, they were, however, given an individual specimen number to allow easier documentation. Loose teeth counted toward the final NISP. Likewise, elements that were embedded into tufa and indistinguishable were counted as a single specimen within the NUSP category. Specimens that were embedded in tufa, but clearly distinct, counted individually towards the NISP.

**MNE** is the minimum number of (human) elements, irrespective of sex, age, side, or side. MNE was calculated from the highest portion of an element, for example the humeral head, with left and rights totalled (as per Stiner, 1991 cited in Lyman, 1994a, p. 43). **MNI** is the minimum number of individuals.

Standard anatomical names were used for bones and codes were assigned to allow easier recording. Bone codes were adapted from Klein and Cruz-Uribe (1984) with additional codes created for cranial and juvenile elements (appendix 1.1).

Age and biological sex codes were adapted from Buikstra and Ubelaker (1994, p.9) and Scheuer and Black (2000, pp. 468–469) respectively (table 7.1):

Table 7.1: List of age and sex categories.

| | Code | Description | | |
|---|---|---|---|---|
| **Sex** | M? | Probable Male | | |
| | M | Male | | |
| | F? | Probable Female | | |
| | F | Female | | |
| | U/D | Undetermined | | |
| | **Code** | **Description** | **Age Range** | **Notes** |
| **Age** | NN | Neonate | Birth – 1 month | |
| | YI | Young Infant | < 6 months | |
| | OI | Older Infant | 6-23 months | |
| | YC | Young Child | 2-7 years | |
| | J | Juvenile | 7-10 years | |
| | AD | Adolescent | 10-17 years | |
| | YA | Young Adult | 18-25 years | |
| | MA | Middle Adult | 26-45 years | |
| | OA | Older Adult | >45 years | |
| | SA | Subadult | <18 years | No other indications of age |
| | AU | Adult age unknown | >18 years | No other indications of age |
| | UA | Unknown Age | | |

Other coding systems were used throughout, particularly during the digitisation process with QGIS. These codes are detailed in the relevant sections and listed in appendix 1.2.

## 7.2: Identification of Human Remains

The Human Bone Manual (White and Folkens, 2005), Juvenile Osteology: A Laboratory and Field Manual (Scheuer, Black and Schaefer, 2008), cast and real reference skeletons were used to identify human specimens from animal. Expert opinions were sought for fragments that were more difficult to assess.

Some cranial elements, particularly the juvenile remains, were difficult to identify. Leach (2006a) categorised most of these fragments as “cranial fragments”, using the code $CR_{fg}$. An attempt was made to be more specific with placement and identification. Some cranial fragments are described as “probably indistinguishable from other vault fragments” (Scheuer, Black and Schaefer, 2008, p. 32) and in the absence of distinguishing characteristics remained unidentified. For this reason, several fragments have retained the identification of $CR_{fg}$. For

cranial fragments that are not identifiable they have been sorted into juvenile and adult, based on size and thickness, but not allocated to specific individuals.

## 7.3: Databasing

The remains from Cave Ha 3 had previously been kept in a private collection. They were lent to the University of Central Lancashire (UCLan) for research purposes. The remains were contained in eight lightly packed plastic boxes, labelled with a context number and brief description. The boxes were numbered one to eight and each box contained a description of context that related to the original excavation notes. These details were recorded on the spreadsheet as "context" and "context description". A total NSP, NISP and NUSP for each box was recorded.

Each specimen had previously been marked with the cave ID and find location. A portion of the remains also had an assigned finds number. These numbers relate to handwritten documents and maps, allowing their original discovery location to be traced.

The human specimens were documented in the following format:

| | **CAVE CODE** | **FIND LOCATION** | **FIND NUMBER** |
|---|---|---|---|
| ***EXAMPLE*** | *CH3* | *69* | *72* |

For remains where there was no find number the specimen was recorded with just the cave code and find location. Any files pertaining to specific specimen (e.g., GIS files) were also saved with the element code and side:

| | **CAVE CODE** | **FIND LOCATION** | **FIND NUMBER** | **ELEMENT** | **SIDE** |
|---|---|---|---|---|---|
| ***EXAMPLE*** | *CH3* | *69* | *72* | *FE* | *L* |
| ***Resulting code*** | *CH3.69.72 FEL* | | | | |

The human remains were cross checked with Leach's (2006a, 2006b) database, some errors were found. A number of these were simple mis-documenting of find numbers and easily rectified. Other discrepancies were more difficult to resolve, an overview of these differences

is provided in appendix 1.3. Leach's original specimen numbers were documented but for ease of analysis new specimen numbers were assigned using a three-digit number, prefaced with CH3.

The remains from Heaning Wood originated from a private collection and a large proportion of the specimens had previously been analysed (Warburton, 2017 unpublished). These were documented in the following format:

| | **CAVE CODE** | **SPECIMEN NUMBER** |
|---|---|---|
| ***EXAMPLE*** | *HBC* | *001* |

Newly recovered fragments were assigned specimen numbers following on sequentially from the initial spreadsheet. As the original spreadsheet for Heaning Wood was created by the author, this spreadsheet was added to and amended rather than creating a new one. Some fragments for Heaning Wood were related to layer numbers, and some were stored in bags with a context description. This was entered into the spreadsheet. An added complication of Heaning Wood was that remains from the first excavation in 1958 were held at the Dock Museum, in Barrow-in-Furness. The author had previously databased the collection and these were combined into the master spreadsheet. These specimens were later loaned to UCLan and individuation was completed a second time.

Each specimen, for both assemblages, was analysed macroscopically with observational notes documented on forms 1-3 (appendix 1.4). Initial metric measurements, ontological assessments, bone condition, completeness, a description of observational taphonomy, and suitability for GIS placement were recorded.

## 7.4: Quantification

### *7.4.1 Minimum Number of Elements (MNE) and Minimum Number of Individuals (MNI)*

An estimation of the minimum number of elements (MNE) and minimum number of individuals (MNI) was done using an adaptation of the zonation method (Knüsel and Outram, 2004), considering ontological and size differences.

The zonation method divides each element into segments that have been derived from common fracture patterns in fragmented remains (figure 7.1). Fragments were sided and placed on the area of bone they originated from. The zone numbers for the fragment were recorded along with anatomical side, for example a fragment originating from the left femoral head and neck area may result in a code of FE(L)4,5. All zones can be found in appendix 1.5.

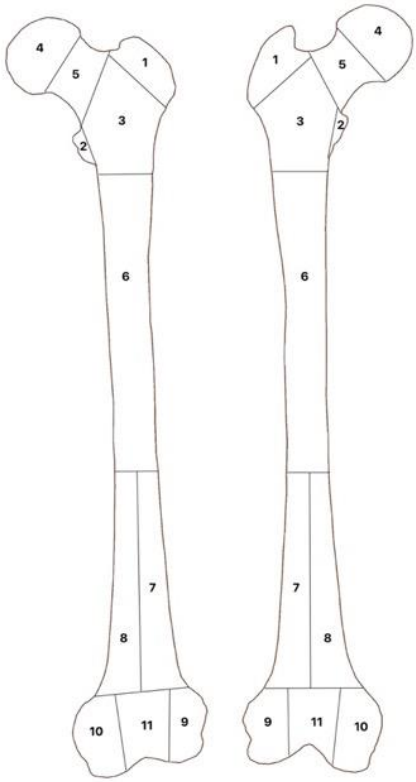


Fig 7.1: Example of a zoned femur (adapted from Knüsel and Outram, 2004).

The number of fragments from each element and zones were tallied on a zonation form (appendix 1.6).

Infant remains were recorded using templates (appendix 1.5.2) and a zonation form (appendix 1.6) specifically developed for unfused remains. An assessment of fusion was made where appropriate and recorded as:

Table 7.2: List of age and sex categories

| | |
|---|---|
| **DUF** | Distal unfused |
| **PUF** | Proximal unfused |
| **UF** | Both proximal and distal both unfused |
| **PF** | Partial fusion |
| **FF** | Fully fused |

Prior to calculating the MNI, refitting was conducted. If a zone from one side showed more than one fragment these fragments were checked for overlap. If the fragments overlapped each other, they were considered to have originated from more than one individual. If there was no overlap, or the fragments refitted, then it was possible they originated from the same person and therefore the MNI remained unchanged.

An estimate for minimum number of element (MNE) was then made based on the maximum zone and side count. Table 7.3 shows an example of zone counts for scapula. This would result in an MNE of four for scapula.

Table 7.3: Example of scapula zonation counts

| | **Left** | | | **Right** | | |
|---|---|---|---|---|---|---|
| **Zone ->** | **1** | **2** | **3** | **1** | **2** | **3** |
| *Scapula* | *3* | *3* | *3* | *1* | *1* | |

The MNI was calculated initially calculated taking the maximum count for a side. This assumes that left and right are paired (originating from the same individual). This can be expressed as the following formula (L = number of lefts of a single element, R = number of rights of a single element) (Adams and Königsberg, 2004):

$$Max\ (L, R)$$

Should the left and rights have originated from different individuals the calculation would underestimate the MNI. The MNI, however, is a **minimum** count. It was therefore felt that this calculation was most appropriate at this stage. Subsequent individuation offered the opportunity to reassess the minimum.

Specimens were assigned to a body using repetition of elements, robusticity, and age markers. While a previous estimation had been made on the number and age estimations of individuals for both Cave Ha 3 (2006a, 2006b) and Heaning Wood (Warburton, 2017 unpublished), individuation was repeated blind to avoid bias. It also allowed new fragments to be included in the individuation process (Heaning Wood). MNI was then recalculated based on pairings of elements.

#### *7.4.2: Dentition*

Dental inventory forms were completed where appropriate (appendix 1.7) and taphonomy was not recorded for dentition unless still in the crypt.

## 7.5: Biological Profiling

#### *7.5.1: Sex Estimation*

Sex estimation for the adult remains was made using metric measurements of long bones (Spradley and Jantz, 2011) and morphological features of the mandible, the greater sciatic notch and preauricular sulcus of the pelvis (Buikstra and Ubelaker, 1994, p.16-20; Walker, 2005). While non-metric assessment of sex has been criticised for its potential to lack objectivity (Bruzek, 2002), the innominate "has been a key area for assessing" sex (Jilala *et al.*, 2021, p. 1) and assessments "can be performed quickly and do not require specialized equipment" (Klales, Ousley and Vollner, 2012, p. 104). Further to this, metric measurements in fragmented remains can be difficult, or at times absent.

It is argued that Neolithic humans lack correspondence to our modern ancestral groups (Günther and Jakobsson, 2016; Posth *et al.*, 2016) and the extent to which Neolithic ancestry shapes modern Europeans is also debated (Bramanti *et al.*, 2009). A full discussion around this issue, and more wide-reaching ethical problems with ancestry estimations (historically

referred to as race in biological anthropology) is outside of the scope of this research. It is important to note, however, that due to these reasons, and an absence of morphological identifiers, an assessment of ancestry was not conducted. This resulted in using sectioning points for both black and white Americans for metric sex estimations (per Spradley and Jantz, 2011). The sample used by Spradly and Jantz (2011) consisted of data from the Forensic Anthropology Data Bank which is both population-specific to America and was also derived from modern data. Neolithic humans were reportedly smaller on average than modern humans, estimated at between 162 -177cm for males and 151cm- 161cm for females (Roberts and Cox, 2003). In comparison the average modern British height range for males is 170-180 cm (Cox *et al.*, 2019). It is therefore possible that sex estimations based on metric measurements are interpreted as female, when male, due to their smaller stature.

Sex estimation was not conducted on juvenile and infant remains due to children following a similar pattern of growth until puberty, therefore proving difficult to accurately assess sex from both metric and non-metric traits (Scheuer and Black, 2000; Stull *et al.*, 2020; Lamer, Spake and Cardoso, 2021). While attempts have been made to develop a method of sexing younger remains using long bone measurements (Stull, L'Abbé and Ousley, 2017), they have lacked validity when tested across independent samples (Lamer, Spake and Cardoso, 2021) and were beyond the scope of this project.

### *7.5.2: Stature Estimation*

Stature estimation was estimated using maximum femoral length (Trotter and Gleser, 1952; Trotter, 1970). Where intact femurs were unavailable, stature was based on equations by Simmons and Colleagues (1990). While methods for stature estimation are possible from other, fragmented long bones (Steele and McKern, 1969; Simmons, Jantz and Bass, 1990; Holland, 1992; Bidmos, 2008), they often require specific landmarks, such as the tibial condyles (Holland, 1992), and are considered less accurate than estimations made from complete elements (Simmons, Jantz and Bass, 1990).

Later methods of stature estimation have used the metatarsals (Wilbur, 1998; De Groote and Humphrey, 2011) and calcaneal measurements (Bidmos and Asala, 2005), however,

estimations from metatarsals involve estimating femoral length first. Since an intact femur was present for the Cave Ha 3 adult it was considered that this was the most appropriate element to use. An additional estimation was calculated using an intact radius. Three of the Heaning Wood adults had fragmented femurs, allowing stature estimation. The remaining adults had metatarsals present, however, confidence in individuating these elements is low, and therefore it was considered that they would be unsuitable for use in stature estimation.

The issue of Neolithic statures in comparison to modern-day populations is encountered again. The methods for stature estimations rely on data from specific populations that may not relate to Neolithic people. Preservation makes formulating methods specific to pre-historic populations difficult (Mahler, 2022) and there is varying accuracy in biological stature estimations (White and Folkens, 2005, p.398). It is emphasised that the stature ranges provided in this study are estimations rather than absolutes.

### *7.5.3: Age at Death Estimation*

Age at death estimation was initially done on an element-by-element basis and split into adult or non-adult categories as per Nikita, Karligkioti and Lee (2019). More specific age estimations were then made on elements that could provide such information.

Foetal age at death estimations were done using post cranial metrics, using an average of three measurements per element (Scheuer, Black and Schaefer, 2008). Infant age at death estimations were done using post cranial metrics, using an average of three measurements per element (Scheuer, Black and Schaefer, 2008) and dental development (Ubelaker, 1989; Liversidge and Molleson, 2004; AlQahtani, Hector and Liversidge, 2010).

The adult elements were aged using epiphyseal fusion (Scheuer and Black, 2000; Scheuer, Black and Schaefer, 2008), dental attrition (Brothwell, 1981, p.69; Lovejoy, 1985), third-molar eruption (AlQahtani, Hector and Liversidge, 2010) and age-related changes (Todd, 1920; McKern and Stewart, 1957; Lovejoy *et al.*, 1985; Brooks and Suchey, 1990; Buckberry and Chamberlain, 2002; Snodgrass, 2004). While there were sternal ribs ends available it was felt that a combination of damage, the presence of glue as a preservative (Cave Ha 3) and a lack of confidence in seriation meant that methods utilising rib ends (İşcan, Loth and Wright, 1984;

Hartnett, 2010) were compromised. Other methods of aging, such as cranial suture closure (Meindl and Lovejoy, 1985), were unavailable due to fragmentation and damage.

It should be noted that there are issues with accuracy in biological assessments, it is emphasised that age and sex estimations are exactly that, estimations and should not be confused with age at death or sex determination.

## 7.6: Geographical Information Systems (GIS)

### *7.6.1: GIS and MNI*

To assess the applicability of Geographical Information Systems (GIS) as a means of MNI quantification, a modified method from Marean and colleagues (2001) was applied.

Images of left and right plastic, cast skeletal elements were taking using a Nikon digital camera, fitted with an AF-NIKKOR 35mm 1:1 8G lens. The photographs were taken on a black background with a calibrated, science grade photography scale (figure 7.2). The cast skeleton was described as “male”.

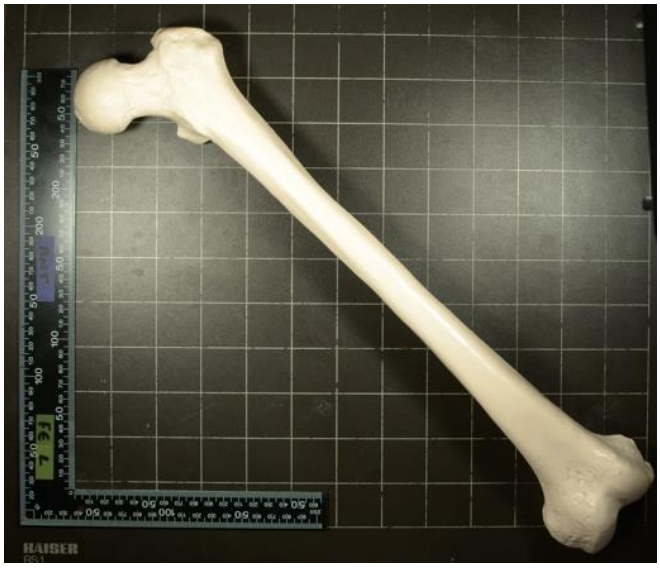


Figure 7.2: Example of a template photograph for GIS.

The template photographs were imported as a raster image into QGIS 3.16 Hannover (Long-term release) *(QGIS 3.16 Hannover is shortened to **QGIS** henceforth for brevity. When referring to generic GIS systems the term **GIS** is used)* using the georeferencer (QGIS.org, 2021).

Reference points were plotted along the X and Y coordinates at centimetre intervals. The transformation setting was set to linear, and the image imported. A new layer was created, and a vector polygon traced over the image. The zoom function, coupled with the opacity set to 33%, was used to ensure that the vector lines followed the edges of the bones as accurately as possible (figure 7.3).

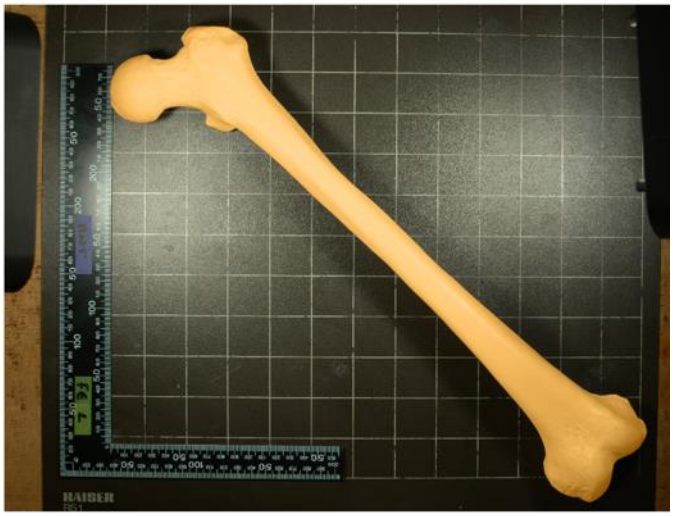

Figure 7.3: Vector polygon layered over raster image, set to 33% opacity to ensure accurate tracing of bone contours.

This process was repeated for the four views (anterior, posterior, medial, and lateral) for each element, with separate shape files for left and rights. All four views were created as polygons within the same vector layer. The view was recorded in the attribute table for each shape (figure 7.4).

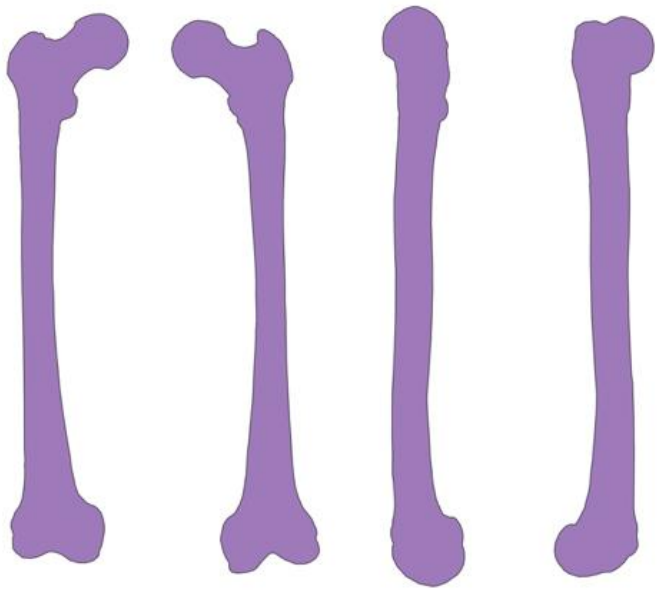

Figure 7.4: Template of the four views of a right femur.

Using the Georeferencer, a raster image of a skeletal fragment from Cave Ha 3 was imported into QGIS. It was decided that due to potential size differences of elements the reference points would be determined from the map canvas rather than using the scale ruler in the photograph. It was anticipated that this would allow the image to be scaled proportionally.

Key landmarks were mapped from the element photograph to the template. This was tested initially by using specimens that were known to be whole. On the first import there were gaps on the edge of the bone and the template. A whole element should fill the template completely. This has the potential to skew MNI counts if further elements are layered on top. To solve the scaling problem, the image was re-imported using the scale ruler rather than landmarks, however the distortion was increased.

Different transformation types were tested as well as trying the method without a coordinate reference system (CRS) and with the CRS set to WGS84 EPSG:4326, neither of these solved the distortion. The first overlay attempt was done using a whole patella. As there are few distinct landmarks on the patella, it was re-attempted using a femur from both anterior and posterior angles. Seven (anterior view) and nine (posterior view) points of reference were used (figure 7.5). Due to damage, landmarks such as the lesser trochanter and the epicondyles were either missing or difficult to determine. The purpose of this method is to provide an improved

method of quantifying MNI in fragmented remains. The difficulties experienced with minimally fragmented specimens would only be exacerbated in more damaged assemblages.

Figure 7.5: Specimen image overlaying the reference template. Note how the margins do not line up.

Despite an increase in available landmarks, the specimen image failed to fit within the template margins. There are a couple of possibilities for this, the key one being morphological differences within humans. This has the potential to be magnified by using a modern skeletal cast in comparison to a prehistoric assemblage. The other reason could have been due to photographic angles. A copy stand, sand tray (to hold elements in place) and references were

used to ensure both the bones and references for templates were photographed in the correct plane. Even with these measures in place there is a possibility that bones were 'off-angle' and therefore did not relate to the reference template.

It was felt that after making several attempts to make this method work that there was too much room for error. The difficulty in controlling the variables meant that it would not offer a more precise MNI calculation in comparison to the zonation method. The zonation method, based on Knüsel and Outram (2004), manual refitting and biological assessments were used to calculate the final MNI.

### *7.6.2: GIS and Taphonomy*

Taphonomy was recorded using an alpha-numeric coding system (appendix 1.2.2) and initial taphonomic assessments were recorded in an Excel spreadsheet (appendix 1.8). The specimens were assessed for general preservation, mineral staining, fracture pattern, surface effects, cortical removal, modification of mineral deposit, destruction, fluvial markers, processing modifications, carnivore modifications, rodent activity, burning, and root erosion based on Hawks and colleagues (2017) (appendix 1.9). These were split into 42 subcategories (table 7.4) with tufa and calcite initially added as distinct categories.

Table 7.4: Taphonomy assessment criteria and subcategories.

| Taphonomic trace | Feature |
|---|---|
| **General preservation** | |
| **Mineral staining** | Iron (red)<br>Manganese (black)<br>Stain pattern<br>Calcite<br>Soil<br>Tide mark |
| **Fracture pattern** | Peri-mortem<br>Post-mortem<br>Crushing<br>Recent fracture or edge wear |
| **Surface effects** | Cracking<br>Crack penetration<br>Patination (mosaic cracking)<br>Delamination/peeling<br>Bleaching |
| **Cortical removal** | Possible invertebrate<br>Striations<br>Pitting<br>Furrow<br>Gouge |
| **Modification of mineral deposit** | Penetrates existing mineral surface |
| **Destruction (underlying structure exposed)** | Epiphyses/joint surface<br>Non-epiphyseal<br>Coffin wear |
| **Fluvial** | Dissolution<br>Smoothing<br>Polish<br>Frosting<br>Window or aperture |
| **Processing modifications** | Cut mark<br>Peeling/shaved<br>Point insertions/notched defects<br>Slot fractures<br>Chop marks/scoop defects |
| **Carnivore Modifications** | Bone cylinder<br>Tooth pit<br>Tooth score<br>Scalloped end<br>Gastric corrosion |
| **Rodent** | |
| **Burning** | |
| **Roots** | Embedding<br>Etching |

Grey concretions were classed as tufa and white deposits classed as calcite. Despite calcareous tufa being “a brown to cream coloured deposit of calcium carbonate” that differs “from the calcite deposits of caves” (Pentecost, 2013, p. 111), due to not testing the composition of the deposits and that “a continuum of forms exists between the two” (*ibid*) the two classifications were subsequently combined into one assessment, referred to as deposits.

All fragments were assessed macroscopically, and several fragments were identified as needing microscopy. This was conducted using the Keyence VHX-2000E microscope with VH-Z20R lens, providing 20-200 X magnification. Where appropriate research analogues were consulted to make an inference of taphonomic agent. Due to project scope micro-CT, histology, and additional X-rays were not conducted. X-rays had been taken in 2017 and those results have been used here (Warburton, 2017).

The element templates described above (section 7.6.1) were adapted to make zoned, paper templates (figure 7.6). These were used to manually map taphonomic modifications. It was decided that anterior and posterior views were sufficient to gain an understanding of modifications. The exception of this was for a tibia that had been split along the coronal plane. For this specimen all four views were retained. Generic templates were made for cervical, thoracic, and lumbar vertebrae. These were split into upper and lower (cervical and lumbar) and upper, middle, and lower (thoracic). Separate templates were made for the atlas, axis and twelfth thoracic. This was due to considerations around identification of vertebral position. In assemblages where the vertebrae can be positioned with confidence, templates can be split and numbered. For assemblages where placement is not possible the generic categories can be employed. A similar approach was taken for ribs. Templates for the first and twelfth ribs were made, and a generic template created for middle ribs.

The plastic cast vertebrae and ribs were difficult to photograph accurately for the QGIS templates, therefore, an alternative reference (3D 4Medical Essential Anatomy 5 v5.0.8) was used. Additional views were created for more complex bones, such as vertebrae (figure 7.6). All templates were printed and, using the Excel spreadsheet as a guide, the taphonomy drawn by hand.

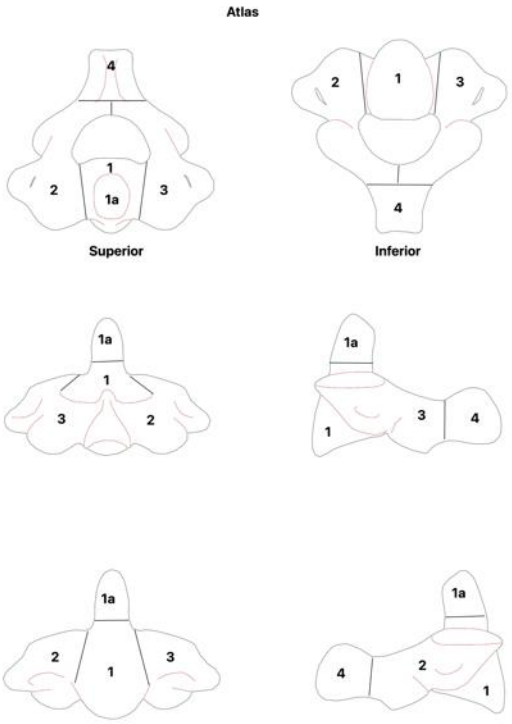


Figure 7.6: Example template of zoned atlas. Showing superior, inferior, anterior, posterior, and lateral views.

A separate template was used for each taphonomic characteristic (figure 7.7). Due to the homogenous nature of the Cave Ha 3 assemblage most elements were only mapped for calcite deposits, staining, fractures, and cortical removal. Destruction was recorded on the same template as fracture patterns. Heaning Wood was equally homogenous, resulting in most elements being mapped for fracture patterns, destruction staining and deposits. For elements that showed other modifications (invertebrate, weathering, butchery, and root etching) further templates were used. Fractures and destruction were recorded first, areas of destruction were then traced onto subsequent templates to ensure the outlines of fragments were consistent. Modifications were mapped using landmarks and zones to ensure accurate location. Areas where modifications overlapped were traced to ensure the overlap was correctly indicated and colours were used to indicate severity.


Figure 7.7: Manually recorded staining on femur. Colour indicated severity and staining type.

Where the margins of calcite build-up extended beyond the bone edges the extent was drawn and coloured around the bone template.

All modern sampling artefacts were excluded from GIS analysis as they do not offer insight into modifications prior to excavation.

### *7.6.3: Creation of GIS Templates*

Prior to mapping the taphonomy into QGIS, the individual element shapefiles were combined to create a full body layout (figure 7.8). When combined some elements were poorly arranged, these were repositioned into the correct anatomical place. The use of alternative references for the vertebrae and ribs also resulted in different scaling. This was corrected by scaling the templates by 0.02 using the affine transform tool.

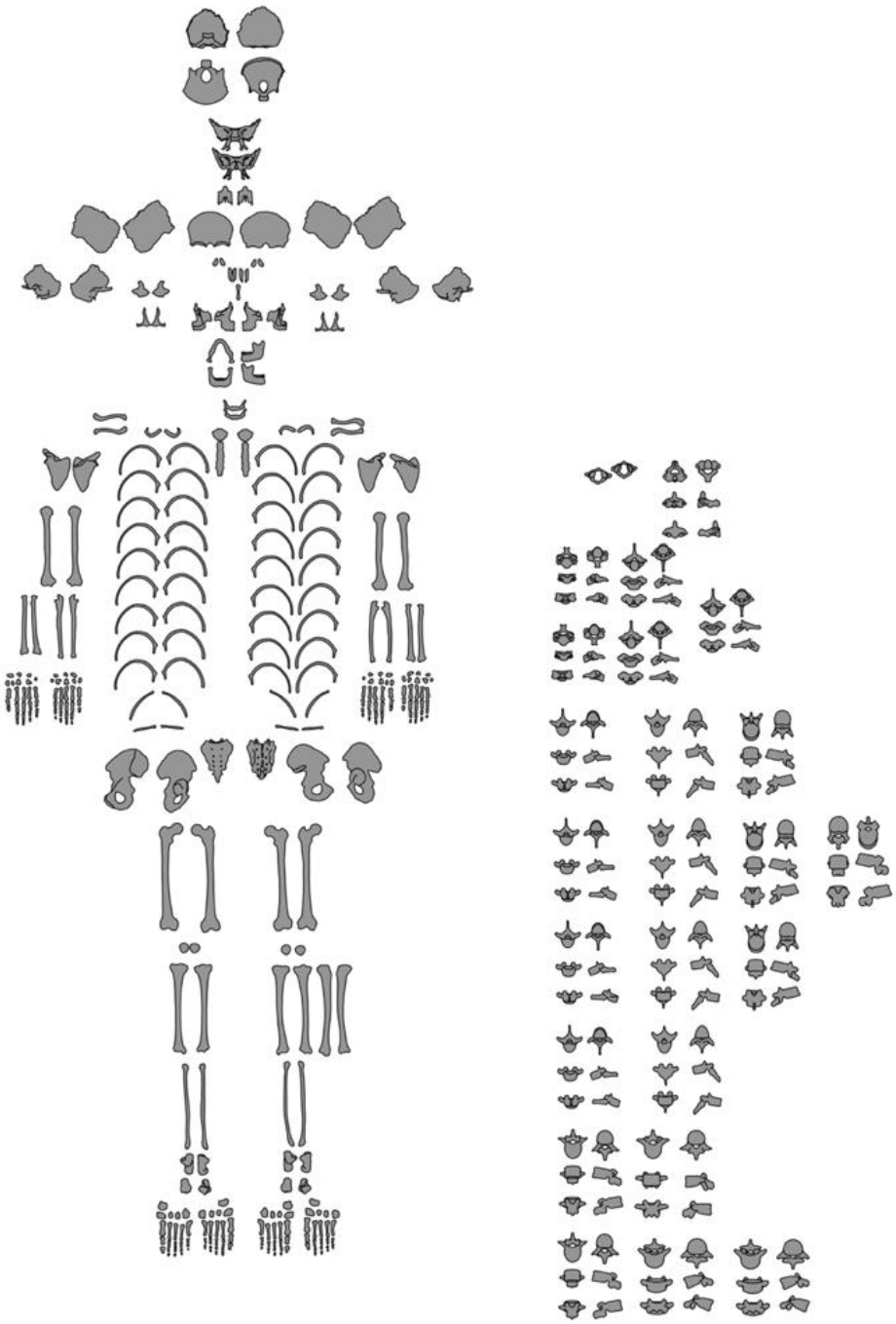

Figure 7.8: Image of the combined elements, creating a full body template.

The template does not mimic traditional recording forms. The anterior and posterior views of elements are positioned next to each other to provide a better view of taphonomy over the whole bone, rather than having to switch between two layouts. The vertebrae and ribs were split to allow numbering when positioning was possible.

Due to morphological differences in juveniles, new element templates were created for the subadult material. Due to a lack of suitable juvenile cast models for the ages required, photographs were sourced from Scheuer, Black and Schaefer (2008) to create templates. These templates were created as a whole body made up of layered elements, ensuring correct positioning from the outset.

The subadults for both Cave Ha 3 and Heaning Wood were estimated as older infant (OI), young infant (YI) and neonatal (NN). This meant that, while there was relatively similar morphology in most elements, there were sufficient differences in fusion for the older infants to necessitate different templates (figure 7.9). This was mainly in the cranial elements. Should future work involve older children, then templates accommodating differential fusion and epiphyseal appearance will be required.

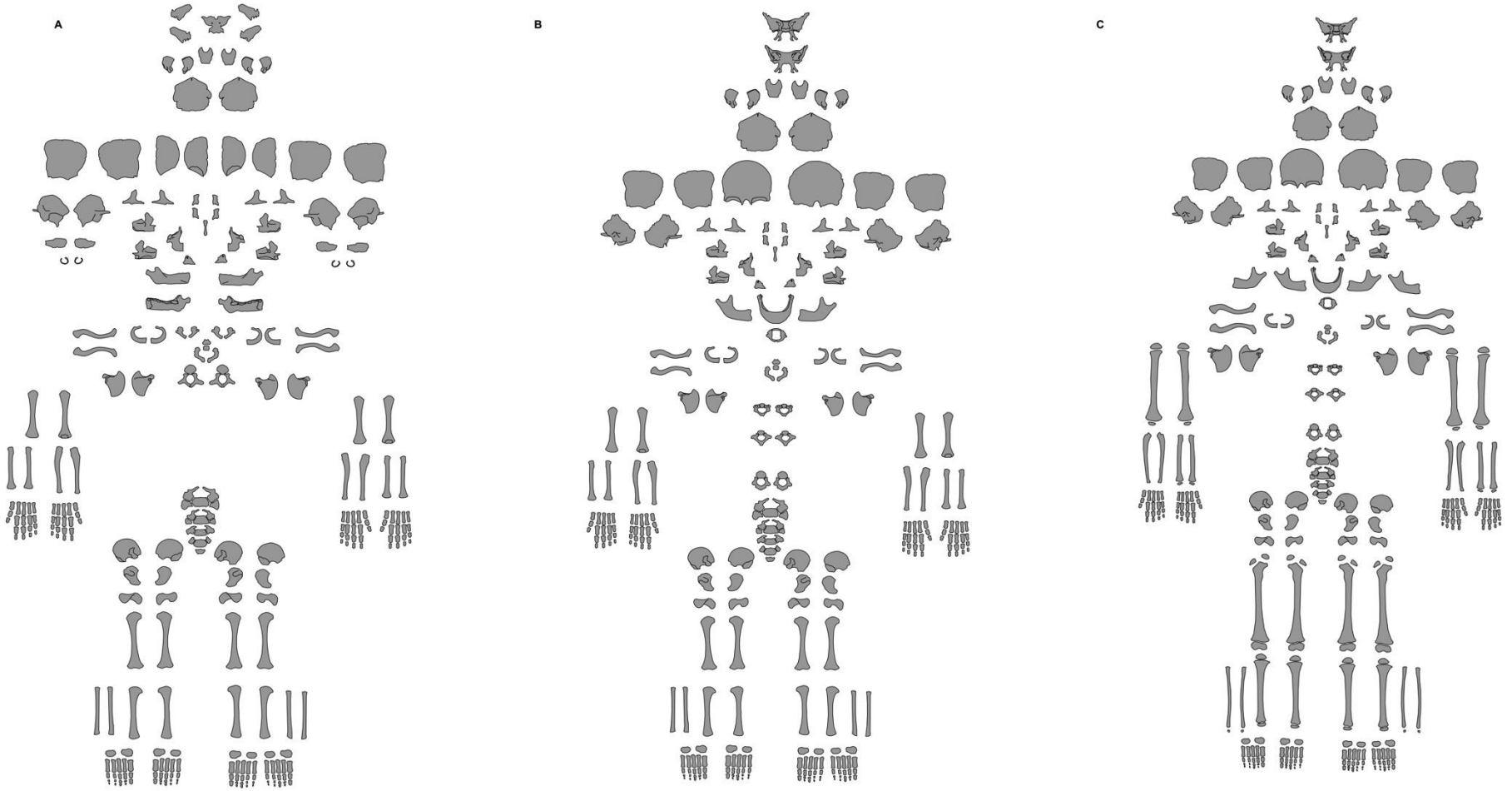


Figure 7.9: Image of the combined elements, creating sub-adult templates (A. Birth - 1 years, B. 1- 3 years, C. 3+ years)

*7.6.4: Mapping the Body*

Initially, for the first adult (Individual 1, Cave Ha 3), a master project for each element was created (elements represented by more than one fragment were recorded in the same project). The specimen ID was used for the project file reference, followed by the element code and side (for example CH3.13.460 SCl for the left scapular from Cave Ha 3). The projects were created with no coordinate reference system (CRS), since at this stage the elements were not spatially referenced.

The hand-mapped templates were scanned and imported as raster images into QGIS. The raster files were georeferenced, using map to canvas, to the shapefile element templates. While there were issues referencing fragment photographs to templates, the mapping of taphonomic modifications were done on exact replicas of corresponding QGIS templates, allowing accurate placement. While some accuracy over fragment shape will be compromised, the shape and relative location of modifications on the bone were maintained and considered precise enough for the intended analyses.

Modifications were traced as lines or polygons over the element template (figure 7.10). Each modification type was recorded in separate layer and characteristics were coded in an attribute table along with specimen code, element, anatomical side, and view (appendix 1.2.1). Layers were saved using the specimen code and modification type (for example: CH3.65.76 ULr Fractures, see figure 7.10).

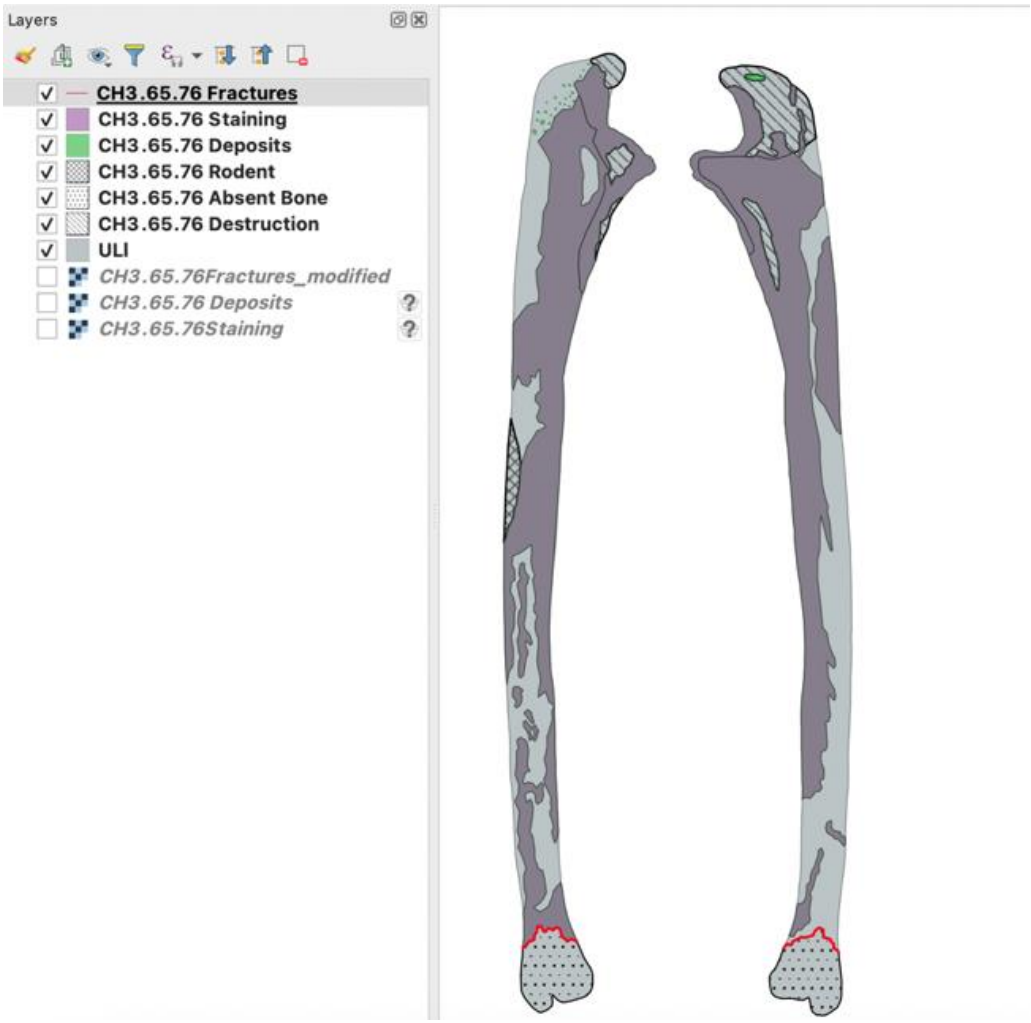


Figure 7.10: Ulna with destruction, fractures, staining, absent bone, rodent markings, and deposits recorded in GIS.

Where modifications shared boundaries with other modifications, or met the edge of an element, the SAGA 7.3.0 vector point tool was used (QGIS.org, 2021). This enabled snapping and tracing to vector points, allowing polygons to be drawn accurately without unintentional overlap. If overlap were to occur incorrect assessments would be made during the analysis stage. This is particularly pertinent where modifications adjoin areas of absent or destroyed bone. Modifications were classified in attribute tables using numeric and descriptive data, this included the modification type as well as, where appropriate, additional information such as timing, location and whether it overlaid existing modifications (appendix 1.2.1).

Some amendments were made to categories when it came to recording in QGIS. Initial taphonomic databasing recorded invertebrate modifications in separate categories: cortical removal, pitting, and furrow or gouge. To simplify this, invertebrate modifications were

entered in QGIS as a single layer. These were then coded within the attribute table for modification type (furrow, gouge, striation, or pitting), spread (focussed, multifocal, diffuse, or singular) and location (random/diffuse, adjacent to joint, or distal to joint).

Cracking was initially only included in surface effects (according to Hawks *et al.*, 2017) however two types of cracking were identified. Cracks consistent with weathering and cracks consistent with fracture or destructive damage. The fracture layer, therefore, included an assessment on cracking and a separate layer was created to record weathering cracking. Similarly, there were areas of peeling and delamination that were post depositional and associated with damage rather than a result of UV exposure. This was recorded within the category 'destruction'. Finally, rodent and carnivore modifications were combined into an 'animal' layer and sub-divided accordingly. Due to an absence of burning and fluvial modifications these were not coded for in GIS.

Once all fragments from an individual were recorded in GIS at an element level, the layers were combined into the whole-body template. Due to the number of fragments this resulted in over 80 layers for one individual, slowing QGIS down. Before mapping the rest of the assemblage, it was decided to create a master vector layer for each modification type. Modifications were then traced within the whole-body template, saved at an element level, and then copied into the master vector layer. This allowed individual layers for each fragment to be created but reduced the number of layers needed when viewing all fragments as a whole body. The workflow is described in figure 7.11.

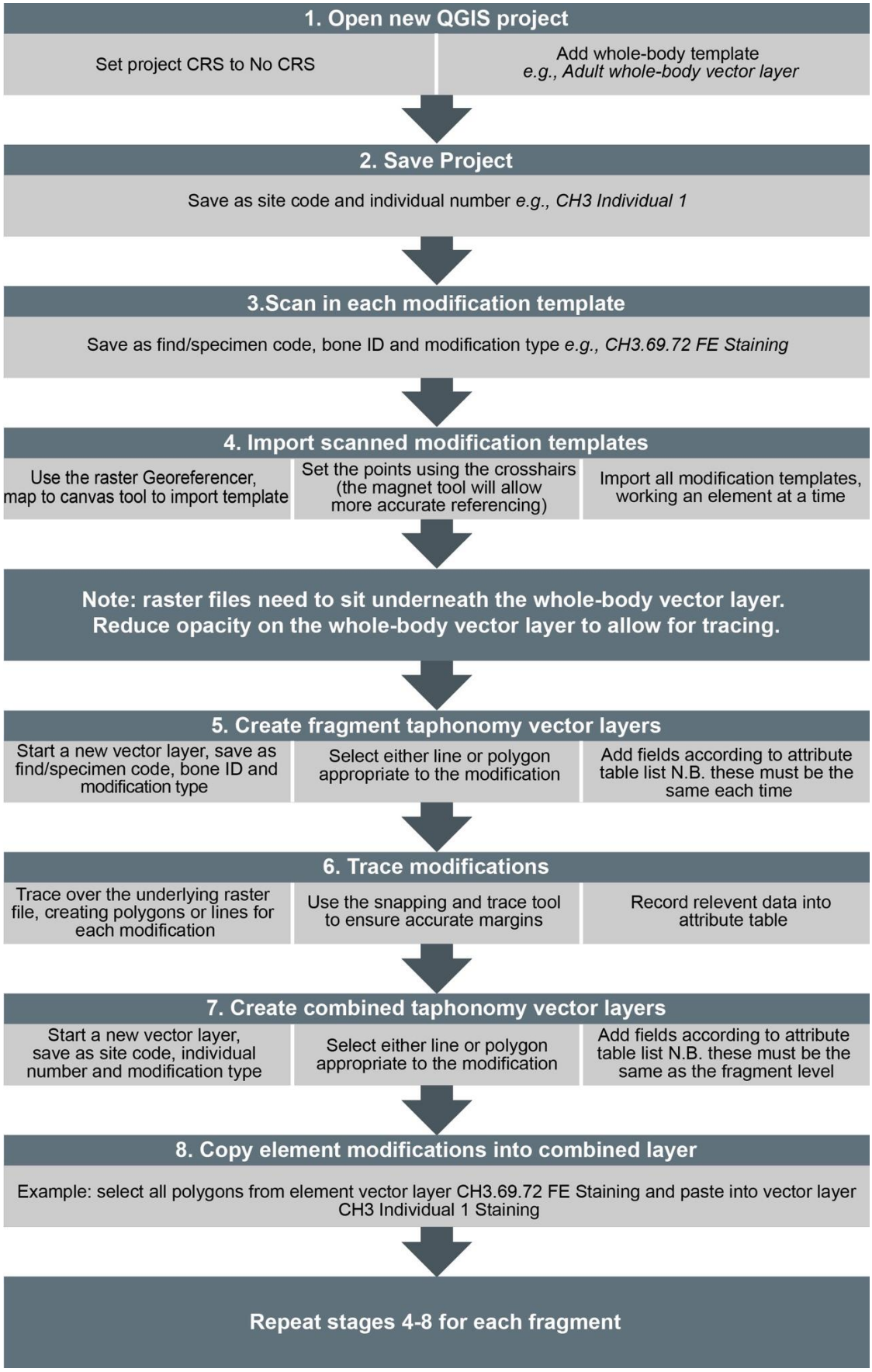


Figure 7.11: Workflow for QGIS mapping.

*7.6.5: Taphonomy and Bodies in Space*

Cave Ha 3 had handwritten logbooks that related find locations to a grid square, 1 foot x 1 foot; these were digitised independently to this research. A temporary coordinate reference system in feet was established using the site excavation grid with values of 100.100.500 for northings, eastings, and elevation. Some find locations were missing grid coordinates, but auxiliary context information provided enough detail to relate these to an approximate grid square. Initially all coordinates were arbitrary in terms of geographic location but accurate in terms of spatial relationship to each other. Once access to the site was permitted it was possible to adjust these coordinates to reflect their geographic location in line with British National Grid coordinates and were converted to 0.5 m x 0.5 m squares (appendix 1.10). Figure 7.12 shows the original 1955 finds map in relation to the 2022 site survey.

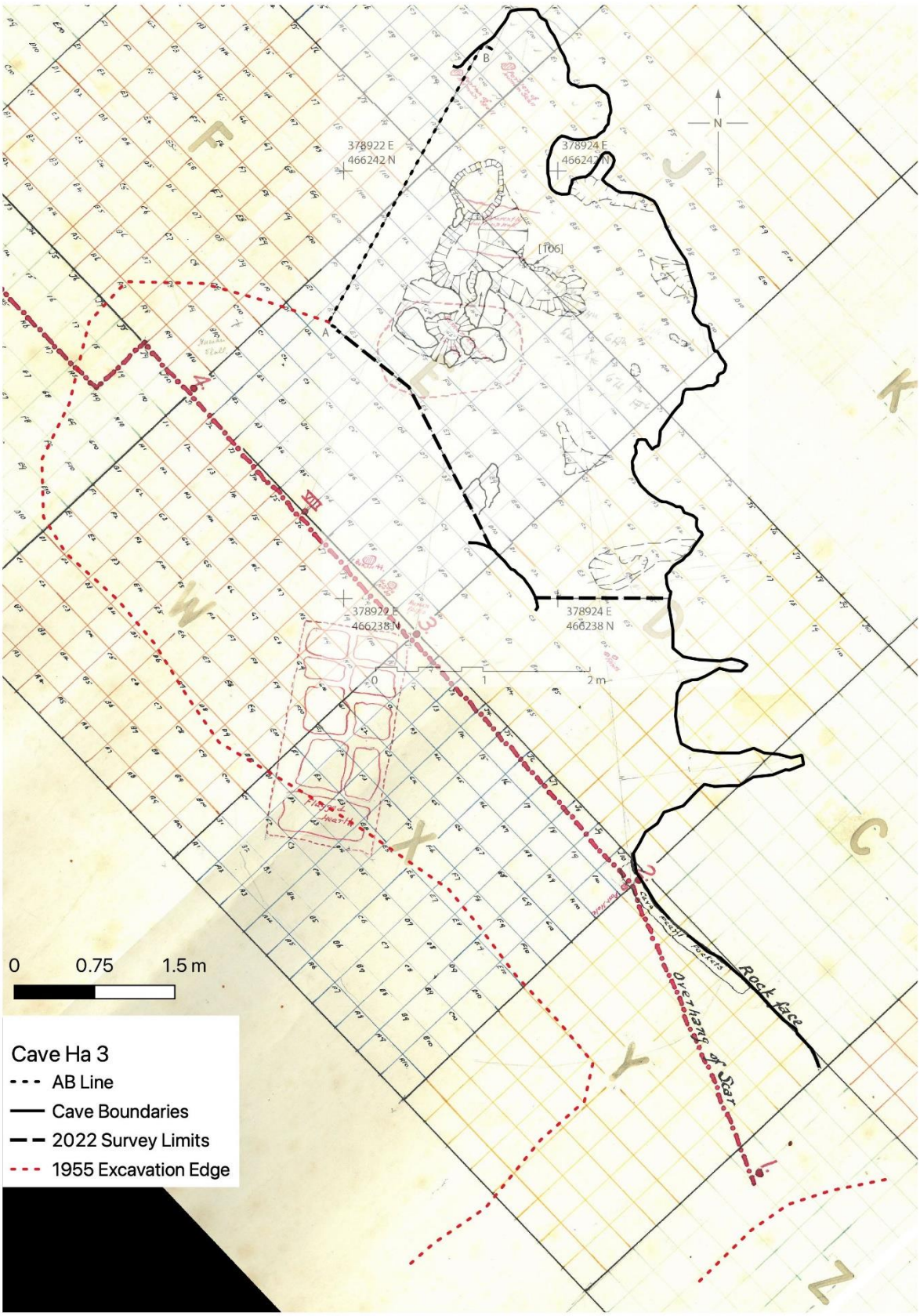


Figure 7.12: 1955 excavation and finds map with 2022 survey.

Each attribute table associated to taphonomic modifications was extracted from QGIS and placed into a spreadsheet (appendix 1.11.1). The tables were combined for all individuals but kept separate for each modification category (fractures/cracking, deposits, staining, destruction, absent bone, animal, invertebrate, processing, weathering). Using the information from the find location and archive spreadsheet, the northing, eastings, and elevation were added into each spreadsheet. This resulted in a coordinate for every mapped taphonomic modification. As the location of each fragment was based on the location number, rather than the find number, multiple fragments shared the same geographical location. This was the extent of the spatial accuracy Cave Ha 3 legacy data allowed.

Most elements were placed with confidence, however due to fragmentation not all specimens were possible to place. Fragments that were not placeable within QGIS were photographed and the modifications manually added to each modification spreadsheet. While it was not possible to position the fragments onto the body, by excluding the fragments completely, it would skew skeletal part representation. The modifications could still be spatially referenced from the find location. Data for each polygon or line was extracted from GIS into the respective spreadsheet; for example, if there were individual flakes of tufa on the same surface these would show as multiple data points in GIS. Fragments that were manually databased, therefore, followed the same protocol. When classifying areas of spotted staining, these were either mapped as an area if the spots were highly concentrated, or individual spots if diffuse.

The same approach was applied to Heaning Wood; the attribute tables for each modification were extracted and combined for all individuals (appendices 1.11.2). Initially, due to the limited spatial recording, no northings, eastings, or elevations were recorded. The layer number or context description was entered instead. Subsequent review of excavation journals provided information on layer depth. Spatial information was limited to a depth measurement, with each layer approximately 0.125 metres deep. There was no information regarding where, within a layer, fragments were found.

## 7.7: Analysis

### *7.7.1: Skeletal Part Representation*

Skeletal part representation was assessed using the Bone Representation Index (BRI). This was done using the following formula:

$$BRI = \frac{Minimum\ number\ of\ elements\ (MNE)}{Number\ of\ elements\ in\ complete\ skeleton\ x\ MNI}\ x\ 100$$

The expected number of elements in a complete skeleton were split into four categories:

- Adult (Over 18)
- Child (One-three years)
- Infant (Under one year)
- Neonate (Birth)

This was in accordance with the ages recovered within the assemblages and reflective of Bello and Andrews (2006), who caution against using only two age classifications: adult and sub-adult.

Separate epiphyseal bones were only scored if they would be identifiable at that age. By initially splitting into age categories this meant that a 0% BRI was not indicated for bones that would not have been present at the age of death (should older remains be found then this would need adapting to account for the appearance of epiphyseal plates). For bones that consist of separate centres, the expected number for a complete skeleton was adjusted; for example, in younger infants the pelvis comprises of the ischium, ilium and pubis (expected count of six for left and right combined). In comparison, the pelvis is fully fused by 18 years, and therefore the expected count for an adult would be two.

A tally of one was given for any element represented by a fragment or fragments, irrespective of the percentage of the element it represented. This was an assessment of which elements

were present in the assemblage rather than an assessment of preservation. Once separate element assessments had been made the counts were grouped as follows (table 7.5):

Table 7.5: List of element groups, (according to Robb, 2016).

| **Group** | **Elements** |
|---|---|
| Crania | Cranium, mandible |
| Vertebrae | Vertebrae |
| Long Bones | Clavicle, humerus, radius, ulna, femur, tibia, fibula |
| Flat/irregular bones | Scapula, sternum, *ossa coxae* (pelvis), sacrum |
| Hands and feet | Carpals, tarsals, metapodials, phalanges, patellae |

Patellae were included in the category "hands and feet" due to the ease in which they become disarticulated (Bello and Andrews, 2006); see section 3.2.6 for a discussion regarding rank disarticulation during decomposition. Bone representation indices were calculated for both individuals and combined to give a BRI for the whole assemblage.

Recovery per anatomical side was assessed at an individual and assemblage level. Specimens assigned to individuals were extracted from the main database, where an element was represented by more than one specimen only one count was retained. The percentage distribution per side was calculated (specimens where anatomical side could not be determined were coded as **unclassified**; specimens that are anatomically unilateral were coded as **unsided**). The distribution per side was the recalculated for the whole assemblage, to include fragments that were not assigned to an individual. Where fusion would not have occurred, such as juvenile frontal bones, were recorded according to left or right. Comparatively, in adult remains, these would be recorded as unsided.

### *7.7.2: Analysis of Whole Body Taphonomy*

Distribution of taphonomic modifications were first explored at body level, by category. For some modifications, such as invertebrate activity, all subcategories were of interest. For others, such as crush damage within the destruction layer, the '*extract by attribute tool'* was used to create a new vector layer of polygons with a specific attribute.

Frequencies of modifications across anatomical view, side, and element group were calculated for each individual using the *'group stats'* plug in (QGIS, 2021). Most modifications had subcategories and the 'group stats' function operates like a pivot table (figure 7.13), allowing frequencies of modifications to be split by category and area of interest e.g., anatomical view. Images of the distribution of taphonomy were used to aid qualitative discussions.

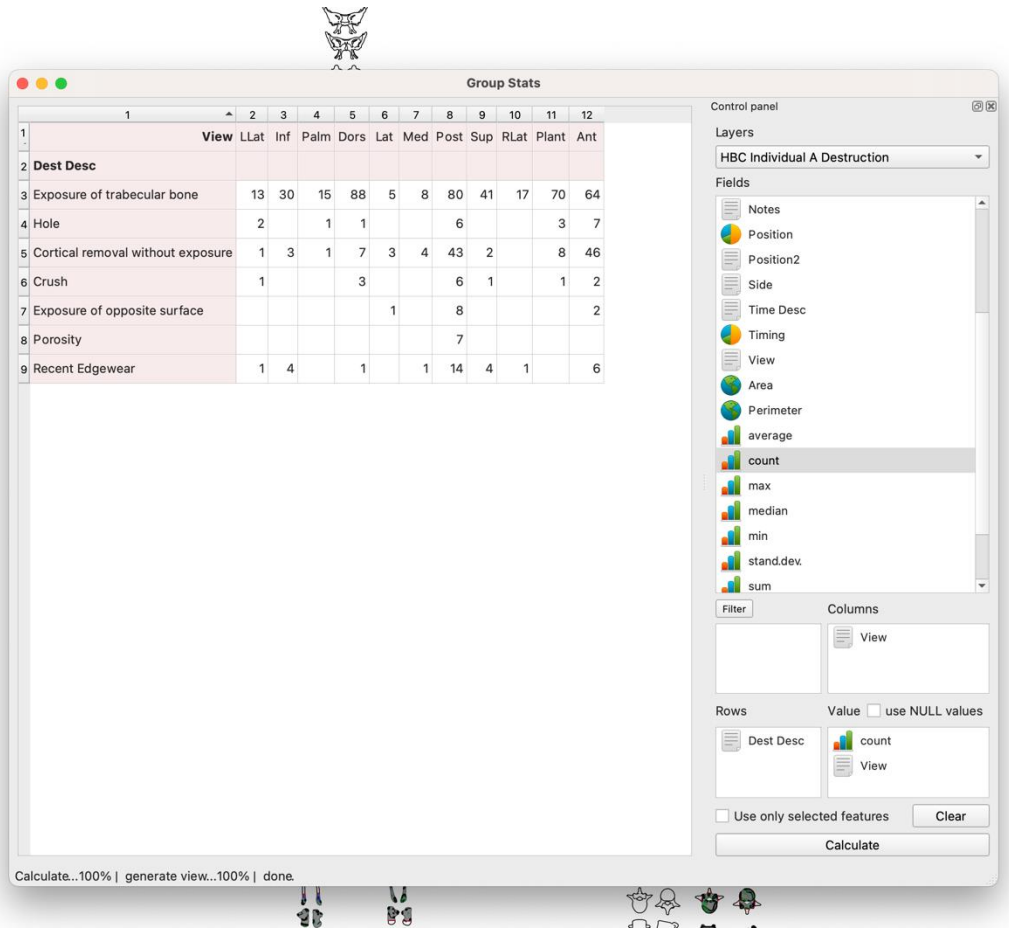


| 1 | View | LLat | Inf | Palm | Dors | Lat | Med | Post | Sup | RLat | Plant | Ant |
|---|---|---|---|---|---|---|---|---|---|---|---|---|
| 2 | **Dest Desc** | | | | | | | | | | | |
| 3 | Exposure of trabecular bone | 13 | 30 | 15 | 88 | 5 | 8 | 80 | 41 | 17 | 70 | 64 |
| 4 | Hole | 2 | | 1 | 1 | | | 6 | | | 3 | 7 |
| 5 | Cortical removal without exposure | 1 | 3 | 1 | 7 | 3 | 4 | 43 | 2 | | 8 | 46 |
| 6 | Crush | 1 | | | 3 | | | 6 | 1 | | 1 | 2 |
| 7 | Exposure of opposite surface | | | | | 1 | | 8 | | | | 2 |
| 8 | Porosity | | | | | | | 7 | | | | |
| 9 | Recent Edgewear | 1 | 4 | | 1 | | 1 | 14 | 4 | 1 | | 6 |

Figure 7.13: Example of the group stats function in QGIS.

Figure 7.14 shows the flow of analysis for taphonomy on the body for clarity

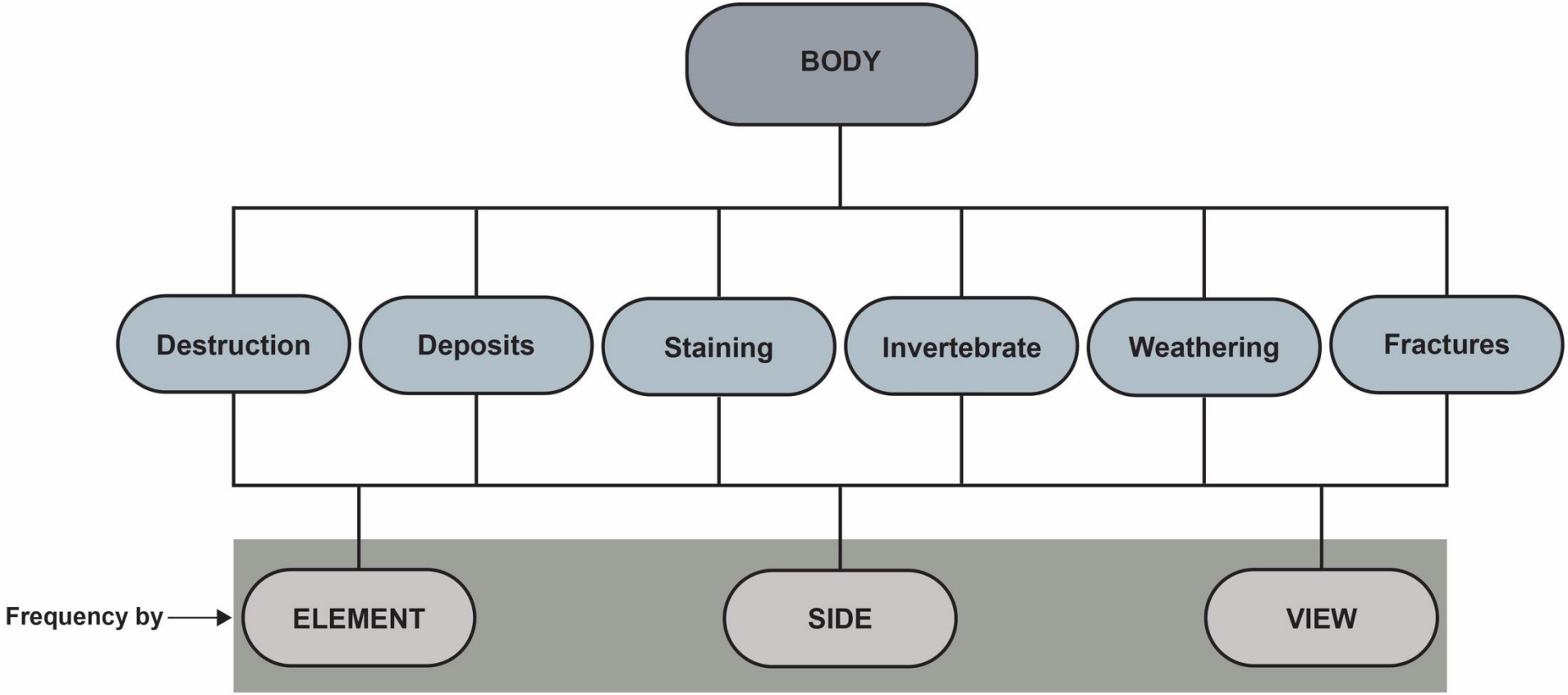


Figure 7.14: Analysis of body taphonomy.

### *7.7.3: Spatial Analysis*

The specimen spreadsheet for Cave Ha 3 was imported into QGIS with X and Y coordinates placing specimens within the centre of the grid square they were found in. For Heaning Wood fragments were georeferenced to the centre point of layer. Distribution of fragments was explored at an assemblage level for both sites, initially with all specimens combined, and then looking at element group. For Cave Ha 3, maps showing the frequency by element group per grid square were created. Heat maps were produced to show concentrations of element groups for Heaning Wood due to the nature of the spatial data.

Specimens were then filtered, using the 'query builder' within QGIS (figure 7.15), to explore fragment distribution per individual. For Heaning Wood, the distribution of fragments according to burial period was also explored. The distribution of elements was looked at in detail, exploring movement across either grid squares (Cave Ha 3) or layers (Heaning Wood), including relationships of broken fragments or elements usually anatomically associated.

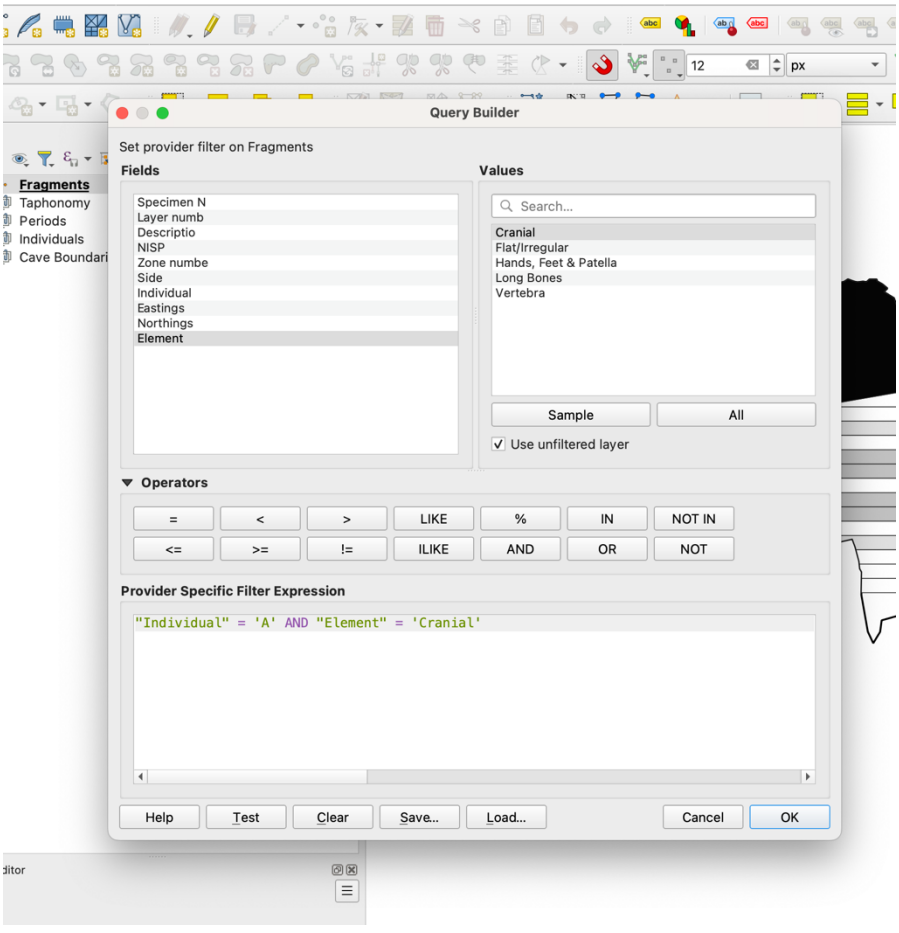


Figure 7.15: Example of the query builder in QGIS.

The taphonomic spreadsheets were imported into QGIS and using the query builder, modifications were filtered according to individual. These were then split to filter for modification subcategories, allowing for analysis of concentrations of modification types. Figures 7.16 shows the flow of analysis for clarity.

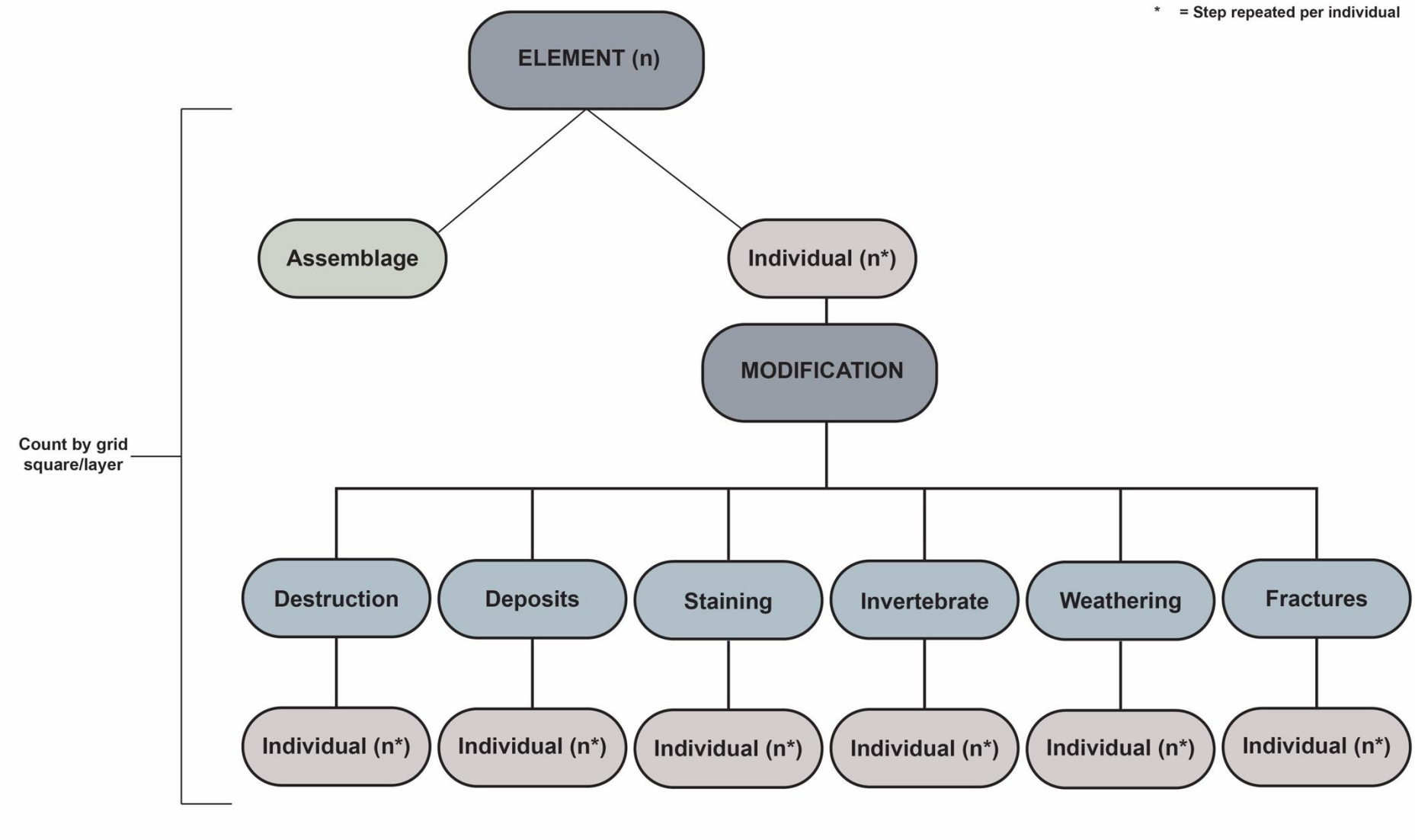


Figure 7.16: Process of spatial analysis

# CHAPTER 8: CAVE HA 3 – AN OVERVIEW

## 8.1: Site Stratigraphy and Original Excavations

Cave Ha 3 is a medium-sized rock shelter that forms part of a complex of four rock shelters in North Yorkshire (NGR SD 7890 6624; figure 8.1), situated in the limestone cliffs in Giggleswick, north-west of Settle (Hughes, 1874; Leach, 2006a).

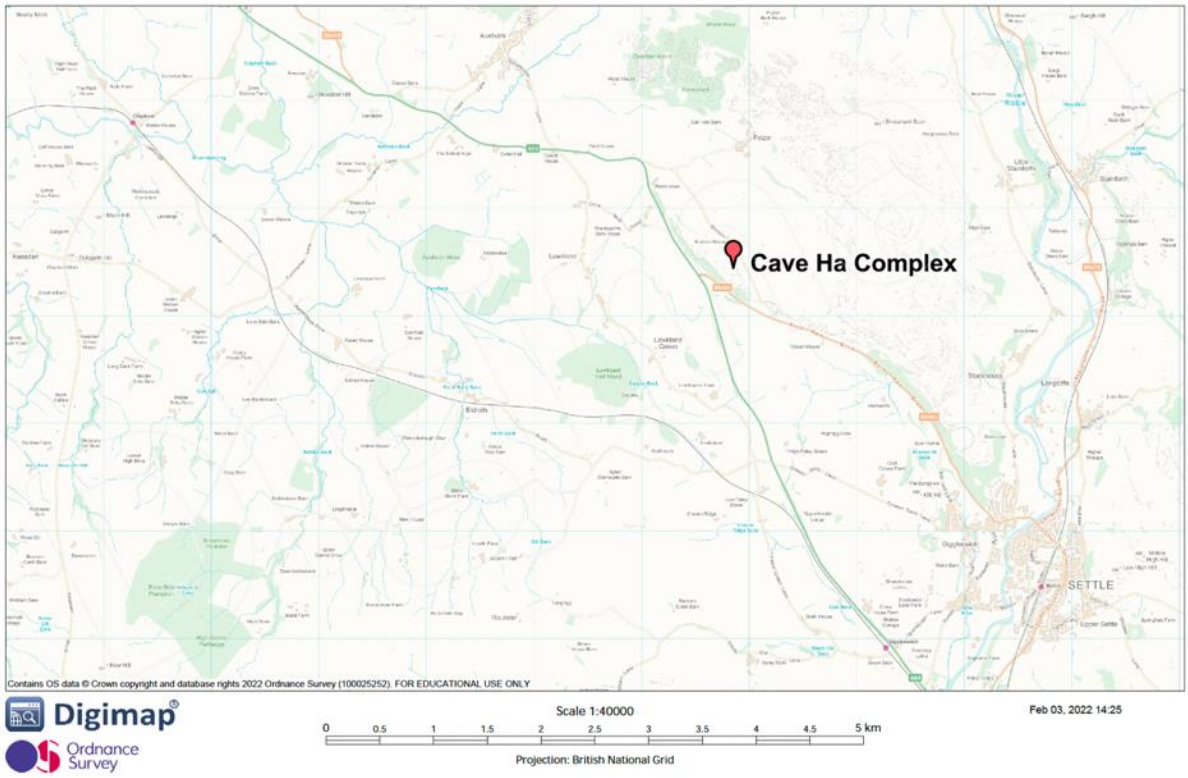


Figure 8.1: Location of the Cave Ha Complex.

Original excavations conducted in the 19th century focused on Cave Ha 1, the largest of the complex. Hughes, assisted by Tiddeman, Lyell and Sedgwick (1874) found owl and kestrel pellets, charred wood, antique knives, extinct Celtic Ox bones, stone beads, flint flakes, bones of recent animals, and pottery (Hughes, 1874, p. 384). Samples of Neolithic pottery were found, but as they were fragmented and mixed in with other modern specimens because of burrowing of rabbits and badgers, they were disregarded as having little evidentiary value (Hughes, 1874). Similarly, the flints were believed to be modern in use, possibly related to pistols or guns. Leach (2006a) gives an overview of Hughes (1874), reporting that the location

of the flints and stone bead are unknown. No human remains were reported, and the excavation of the other rock shelters was ruled out due to the considerable “labour of opening them” (Hughes, 1874, p. 387).

The remaining rock shelters were revisited during the mid-20th century. Excavations remain incomplete, particularly Cave Ha 4 where it is understood further human remains are visible (Leach, 2006a). Leach (2006a) gave an overview of the Cave Ha 3 excavations using unpublished archived reports from Tobin (1955 cited in Leach, 2006a). Cave Ha 3 has “natural cavities or niches in the back wall of the shelter” and it is in two of these recesses and near a “large hearth” that most human remains were recovered (Leach, 2006a, p. 153). The adult bones were found across a recess, adjacent to where the subadult remains were found. The area near the hearth was reported to have yielded an abundance of charcoal and fragmented animal remains (figure 8.2).

Figure 8.2: The interior of Cave Ha 3 (Photograph: Peterson, 2019, p.144)

Cave Ha 3 has both hard, stone-like tufa deposits and tufa that is softer with a “soft creamy ‘porridge-like’ consistency and green thick liquid” (Leach, 2006a, p. 154). Evidence shows that tufa was still forming during, and after, the Neolithic (Pentecost *et al.*, 1990) and a large portion of the bones were described as coated in tufa deposits. The significance of this is raised by Leach (2008), who posits that the placement of the Cave Ha 3 bodies in a tufa-rich

environment offered a means of preservation, suggesting the intention was “to separate these individuals from the collective dead” (Leach, 2008, p. 51).

## 8.2: Previous Analysis

Initial biological profiles referred to subadults and a mature male until the remains were reanalysed by Leach (2006a). Radiocarbon C14 dating of the human remains produced dates between 4800 BP and 4600 BP (3660 BC and 3100 cal. BC) (Leach, 2006a). The final minimum number of individuals (MNI) was estimated as four: one mature, adult male; two infants and a neonate. This was at odds with original assessments that suggested there were only two infants present (Lord, 2004).

The Individuals dated by Leach (2006a) and are summarised in table 8.1.

Table 8.1: Dating results taken from Peterson (2019) for Cave Ha 3

| | Lab no. | Bone Sampled | Date BP | Cal. Date ranges BC (2 ∑) | δ13 C (‰) |
|---|---|---|---|---|---|
| Individual 1 (Mature Adult) | OxA-13539 | Tibia | 4808 ± 32 | 3655–3620: 3610-3520 BC | -21.0 |
| Individual 2 (Older Infant) | OxA-14266 | Mandible | 4595 ±40 | 3515–3395: 3385-3320: 3275-3265: 3240-3110 | -22.0 |

Individual 2 was re-sampled for aDNA (Booth, 2019; Brace *et al.*, 2019). This returned a different date of 4808 ± 32 BP (3515-3113 BC, OxA-13539) due to updated calibration curves. For this report the most recently produced dates will be used; between 3660 BC and 3113 BC for Cave Ha 3.

Of note were a smashed left tibia from the adult, and associated bones of the feet embedded in tufa. The adult male also exhibited evidence of potential facial disfigurement, characterised by a mandibular lesion and the short nature of the long bones were remarked on. Disfigurement and disability were hypothesised, leading to the theory of deviant burial (Leach, 2008). Leach (2006a) concluded that while there was evidence of whole-body deposition due

to the articulation of the foot and skeletal part representation, there was some evidence of fragmentation and processing. This is supported by the notching and fracture patterns of the left tibia, and indicative of "the practice of manual disarticulation of the corpse during the intermediary period"; something rarely evidenced in the British Early Neolithic (Peterson, 2019, pp. 145–146). Leach's (2006a) analysis supports the conclusion that these were successive burials, with movement of bodies towards the back of the cave. The skeletal part representation in the smaller two infants was described as consistent with a whole burial and subsequent recovery, suggesting more direct deposition into the niches (Peterson, 2019, p.146).

Leach's (2006a) analysis of the Cave Ha 3 remains was thorough, and while elements of this research repeat the initial analysis, it was felt that Cave Ha 3 provided an appropriate prototype due to the wealth of data behind it and there was opportunity to provide new support to the existing knowledge. The stratigraphic data consist of hand drawn maps and record books (figure 8.3). The specimens were labelled with a find number in addition to a context number, allowing placement of fragments to the nearest foot square.

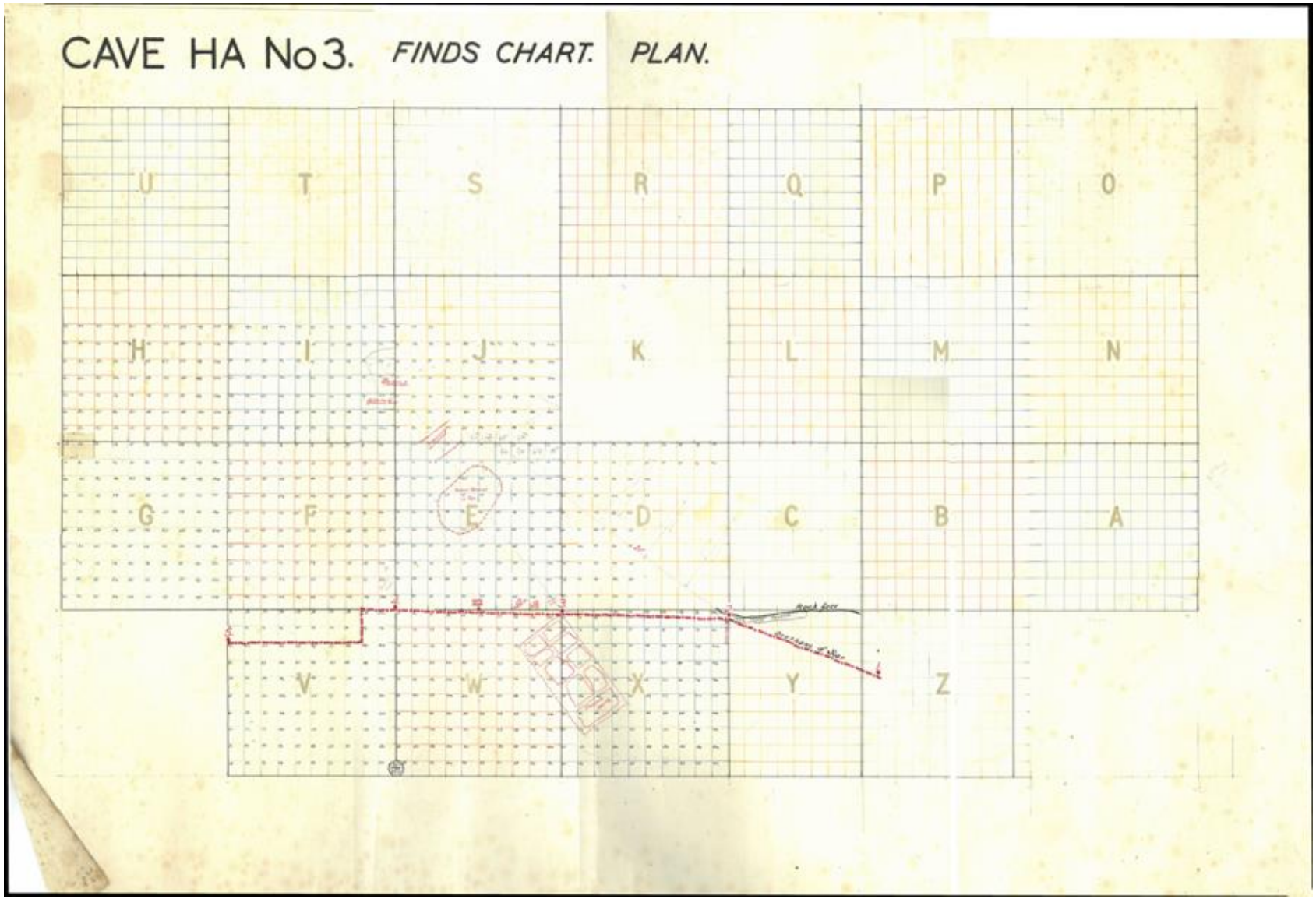


Figure 8.3: Hand drawn map of finds (Lord, 2004).

Tertiary excavations were undertaken in 2022 and digital scans and maps of Cave Ha 3 were made (figure 8.4). Due to license limitations, digging was only conducted to the point of the earlier excavations. The area to the far Southwest of the original maps was not reproduced in the updated diagrams. No significant finds were reported; all bone fragments recovered in 2022 were small, and either animal or unidentifiable.

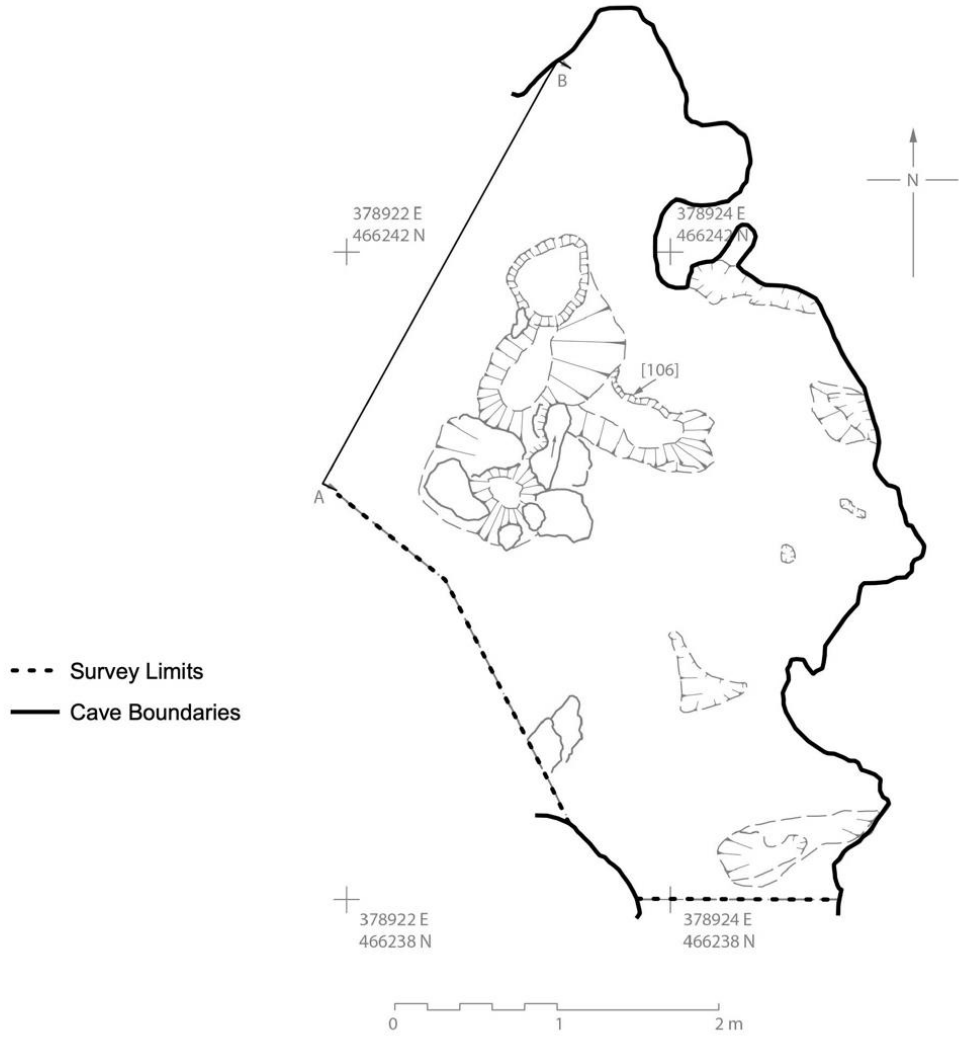


Figure 8.4: Digitised and georeferenced map of Cave Ha 3.

# CHAPTER 9: CAVE HA 3 QUANTIFICATION

## 9:1: NISP and MNI

A total of 202 fragments were identified as human, 1299 fragments were identified as animal and there were 78 non-bone specimens including shells, lithics, cave pearls, charcoal, potential pottery, and a previously identified bone hook (table 9.1). Non-human specimens have been logged but this is the extent of their analysis due to the research scope. A complete spreadsheet of the human remains can be found in appendix 2.1.

Table 9.1: Total figures for NSP, NISP, NUSP, faunal remains and non-bone specimens.

| Site | Box | Context | NSP | *NISP* | *NUSP* | *Animal* | *Shell* | *Lithics* | *Cave Pearls* | *Charcoal* | *Pottery* | *Hook* |
|---|---|---|---|---|---|---|---|---|---|---|---|---|
| Cave Ha 3 | 1 | VIII | **94** | 20 | 0 | 73 | 1 | 0 | 0 | 0 | 0 | |
| | 2 | IX | **102** | 46 | 0 | 56 | 0 | 0 | 0 | 0 | 0 | |
| | 3 | VII | **229** | 1 | 0 | 228 | 0 | 0 | 0 | 0 | 0 | |
| | 4 | VII | **118** | 85 | 0 | 33 | 0 | 0 | 0 | 0 | 0 | |
| | 5 | VI | **243** | 5 | 0 | 238 | 0 | 0 | 0 | 0 | 0 | |
| | 6 | II | **191** | 0 | 0 | 191 | 0 | 0 | 0 | 0 | 0 | |
| | 7 | I | **516** | 4 | 6 | 429 | 25 | 2 | 15 | 30 | 4 | 1 |
| | 8 | V + IV | **92** | 41 | 0 | 51 | 0 | 0 | 0 | 0 | 0 | |
| | | ***Totals*** | ***1585*** | *202** | *6* | *1299* | *26* | *2* | *15* | *30* | *4* | *1* |

**Within crypt teeth are excluded from this count, NISP with teeth counted totalled 211.*

Due to methodological issues (see section 7.4) with using GIS, the final estimation of minimum number of individuals (MNI) was determined using an adaption of the zonation method (Dobney and Rielly, 1988; Knüsel and Outram, 2004). The MNI was estimated at four: one adult; two infants and one neonate. Of the human bones identified, an additional human ulna was recovered from Cave Ha 4; its presence increased the MNI to two adults and a total MNI of five. This bone was excluded from analysis because of its recovery from a different cave; it was therefore suspected to be a different burial. It is considered significant and further excavation of Cave Ha 4 is advised.

Some differences were found from Leach's (2006a) original report and are listed in appendix 1.3; the final MNI was not, however, altered. Some cranial fragments that are likely to have

originated from the infants were not assigned due to identification issues. They did not, however, make up more than would be expected from the MNI described below. The remains were disarticulated and commingled, therefore, apart from articulations because of tufa embedding, the remains were individuated based on size, robustness, and age.

While individuation was facilitated by the lack of cross over with age at death estimations, it is still possible that the remains originated from more than the number of individuals cited here. Table 9.2 summarises the estimated minimum number of individuals.

Table 9.2: Demographics for identified individuals.

| Individual | Age | Sex | Stature |
|---|---|---|---|
| **1** | 45-59 years | Skeletal Male | 154.96 ± 3.94 |
| **2** | 1.5–2.5 years | Genetic Male | Undetermined |
| **3** | 7-9 months | Undetermined | Undetermined |
| **4** | 38-40 weeks | Undetermined | Undetermined |

## 9.2: Bone Representation Index

Elements from all areas of the body are represented. Bone representation indexes (BRI) showed Individual 3 (7-9 months) as having the smallest number of skeletal elements (N =13), and Individual 1 (adult) the most (N = 86). Individual 1 showed only an 8.00% representation of cranial and mandibular elements compared to an overall representation of 42.86%. This was limited to a portion of mandible and a queried fragment of occipital (see section 10.1); no other cranial fragments were attributed to Individual 1. Individuals 2 (N= 33) and 4 (N= 24) showed better representation of cranial elements (34.48% and 20.59% respectively) (figure 9.1). There were no hands, feet or patellae recovered for the subadults.

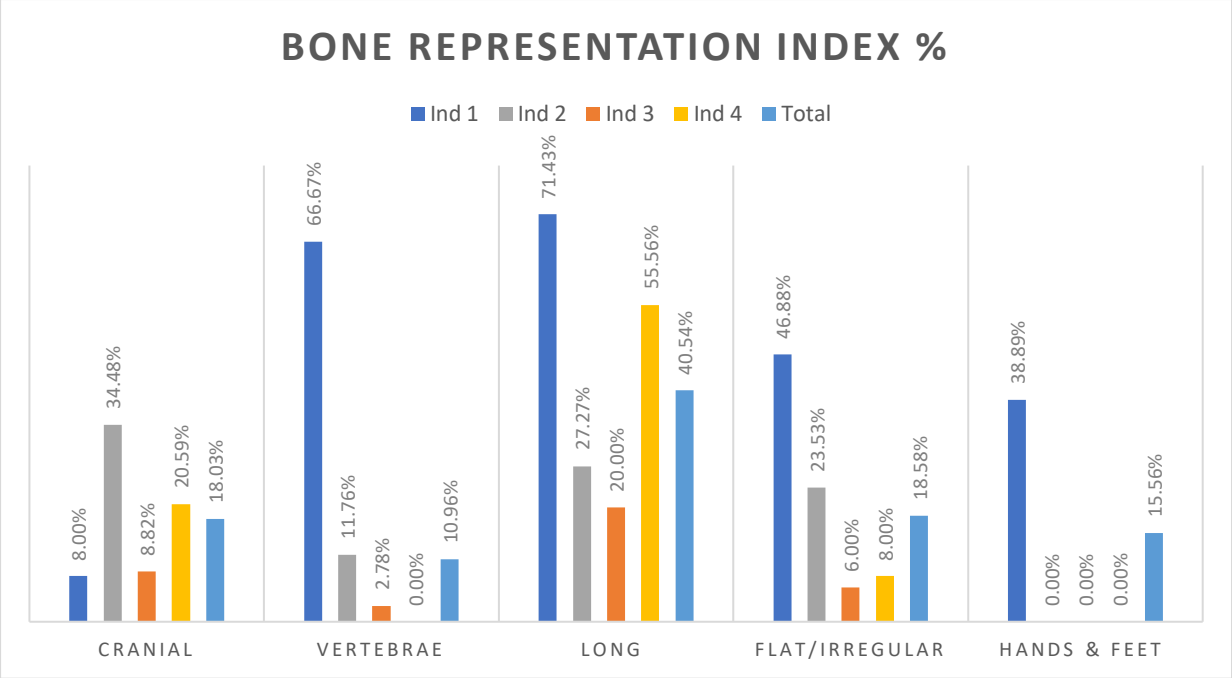


Figure 9.1: Graph showing BRI % for grouped bones – excluding unidentified cranial fragments.

The presence of all element groups indicate that Individual 1 was deposited whole, most likely fleshed. While an absence of smaller, quick to disarticulate, elements can be indicative of secondary burial (Robb, 2016), the absence of hands and feet for the younger individuals is more likely to be due to recovery bias and destructive processes. Smaller infant bones may have been lost due to the abundance of tufa present in Cave Ha 3, which has embedded several elements.

## 9.3: Preservation According to Anatomical Side

There was higher representation of left elements than right for all individuals; 25 fragments were unassigned to an individual and five fragments were unable to be sided. As the frequencies were not normally distributed, the median count of the four individuals was taken (table 9.3 and figure 9.2). This showed only a difference of two between left and rights, indicating little to no preservation bias for anatomical side across the assemblage.

Table 9.3: Frequencies of fragments according to anatomical side (Cave Ha 3).

| Body -> | 1 | 2 | 3 | 4 | Unassigned | Total | Median |
|---|---|---|---|---|---|---|---|
| **L** | 39 | 13 | 6 | 11 | 1 | 70 | 11 |
| **R** | 25 | 9 | 4 | 9 | 1 | 48 | 9 |
| **Unsided (u/s)** | 19 | 9 | 3 | 4 | 23 | 58 | |
| **Unclassified** | 3 | 2 | 0 | 0 | 0 | 5 | |
| **Total** | 86 | 33 | 13 | 24 | 25 | 181 | |

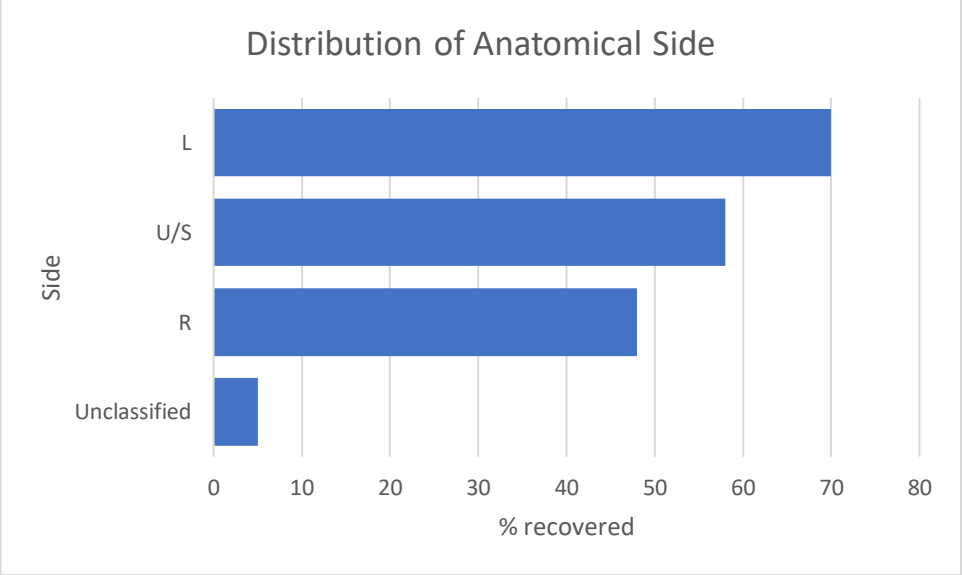


Figure 9.2: Percentage of fragments according to anatomical side (Cave Ha 3).

The absence of a significant difference in the representation of anatomical side indicates that the bodies were not positioned in a manner that resulted in a bias of preservation, likely supine or prone rather than crouched to one side, resulting in destructive processes acting uniformly.

The following section provides an overview of the demographic profiles of each individual; bone representation indices per individual will then be discussed in more detail, along with an exploration of taphonomy (chapter 11).

# CHAPTER 10: CAVE HA 3 DEMOGRAPHICS

## 10.1: Individual 1

### *10.1.1: Age at Death Estimation*

Consistent with Leach (2006a), Individual 1 was estimated to be an older, adult male. Final age estimations resulted in a slightly older estimation than Leach (2006a) of between 45 and 59 years. Tooth wear on a mandibular molar provided an estimation of 45+ years (Brothwell, 1981, p.69). Wear of the acetabulum of the right pelvis (CH3.77.96) was scored at a stage 7 (Ubelaker, 1989), giving an age estimation of 50-59 years. Eight of the twelve thoracic vertebrae and three of the five lumbar vertebrae were identified. While this is not the full vertebral column it was felt there were sufficient vertebrae to make a tentative assessment of age using osteophytic lipping (according to Snodgrass, 2004). Osteophytes on the thoracic vertebrae were variable, with an average score of 0.625. The lumbar vertebrae were more consistent with a score of 2. While the age estimation for thoracic placed Individual 1 at age 40 – 50 years, it is posited that an average score of 2 for lumbar vertebrae rarely happens under 50 years, giving a different age estimation of 50-59 years (Snodgrass, 2004). With the combination of age estimations, it was felt that an older age bracket of 45 – 59 years was most appropriate.

There is a slight difference in age estimation to Leach (2006a), however both age estimations overlap and are therefore not discordant. With limited age markers it is difficult to obtain a more accurate estimation, this is not uncommon in adults once full maturity has been reached.

### *10.1.2: Skeletal Sex and Stature*

All post cranial measurements (table 3.1, appendix 3.1.1) indicated probable female based on Spradley and Jantz (2011), except for the sacrum (CH.21.95). Measurement of the transverse diameter (54.4 mm) indicated probable male. Morphological assessments of the pelvis and mandible indicated male. The pelvis scored four for the greater sciatic notch (Buikstra and Ubelaker, 1994, p.18; Walker, 2005).

Stature was estimated to fall between 155.46 cm and 162.00 cm (Trotter and Gleser, 1952; Trotter, 1970). This falls just below the range for an average male during the Neolithic. Neolithic people were considered to be shorter, however, the average range for males was proposed to be between 162-177cm and 151-161cm for females (Roberts and Cox, 2003). The stature estimation from post cranial elements was therefore borderline. The significance of this will be discussed in section 18.2.2 however, due to the bone representation indices indicating whole body deposition, it is considered most likely that Individual 1 was a male of diminished stature, as proposed by Leach (2006a).

Individual 1 had a large lesion on the right mandible (figure 10.1). Leech (2008, p. 47) proposes either "a large haematoma with secondary infection, or actinomycosis infection" as possible causes. Due to the focus of this project the lesion was not explored in any detail and the above is taken as accurate. Further explorations of the pathology would be encouraged in future research.

Figure 10.1: Mandible showing area of bone lesion.

## 10.2: Individual 2

### *10.2.1: Age at Death Estimation*

Individual 2 was estimated to be a young child aged 1.5-2.5 years (24 –36 months).

Age at death estimation for Individual 2 was conducted using the deciduous teeth present, tooth crown development and adult tooth crowns visible in the crypt of the left maxilla and the mandible. The right maxilla was absent. An absence of deciduous teeth was not taken as an absence of development due to evidence of alveolar eruption. The dentition is summarised below, using Zsigmondy-Palmer notation.

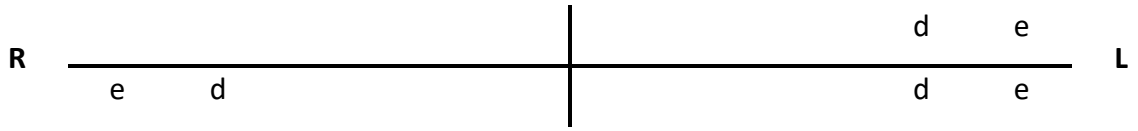


Deciduous dentition present in fractured maxilla and mandible (right maxilla was absent).

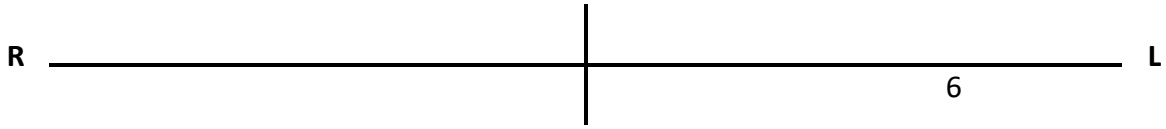


Adult dentition present in fractured mandible, visible by sight.

Tooth development and emergence was compared to the Atlas of Human Tooth Development and Eruption (AlQahtani, Hector and Liversidge, 2010), giving an age estimation of 30 months (2.5 years). Complete eruption of the second, deciduous, mandibular molar indicated a minimum age of 24 months (2.49 ± 0.51 years) (Liversidge and Molleson, 2004).

Metric measurement supported the lower age range derived from dentition. All post cranial measurements (table 3.2, appendix 3.1.2) returned an upper limit of 24 months (2 years). After dentition, the maximum iliac length (55.8 mm) provided the most reliable estimation of 19 -24 months (Scheuer, Black and Schaefer, 2008). Greater weight was placed on estimates derived from dentition due to fragmentation of other elements, and better predictability with tooth eruption. Periods of nutritional or physiological distress can impact post cranial development (Lewis and Flavel, 2006; Niel, Chaumoître and Adalian, 2022). Root development

was not possible to assess due to lack of x-ray access. The age range may be further refined in the future using x-ray.

### *10.2.2: Genetic Sex*

Individual 2 was sampled for aDNA (Booth, 2019; Brace *et al.*, 2019). Individual 2 was assessed as being genetically male (table 10.1).

Table 10.1: Genetic results taken from Booth (2019) for Individual 2

| Element | Petrous |
|---|---|
| Ancient Human DNA | 37-51% |
| Genetic Sex | Male |
| Mitochondrial haplogroup | Ka2 |
| Y-chromosome haplogroup | I2a2a1 |

## 10.3: Individual 3

### *10.3.1: Age at Death Estimation*

Individual 3 was estimated to be a young child aged 7-9 months.

Age at death estimation using dentition was not possible for Individual 3. There was a single, left, first, deciduous, mandibular molar in the assemblage. Crown height (6.4 mm) provided an age estimation of 4 - 10 months (0.6068 $\pm$ 0.25 years) (Scheuer, Black and Schaefer, 2008). Root formation was estimated at R¼ (figure 10.2), placing the age estimation at 5 to 7.5 months (+/- 1 SD) (Scheuer, Black and Schaefer, 2008). The tooth was assigned to this individual as the age estimation was in concordance with other metric estimations, however since the tooth is loose, it is not possible to be certain of its origin.

Figure 10.2: Specimen CH3.73.36 $LdM_1$ with incomplete root formation.

A portion of mandible was present in the assemblage. It was heavily embedded in tufa (figure 10.3). An attempt to x-ray it was made, however the concretions prevented a clear image. The mandible appears to be that of a young infant, with two erupted teeth. It was cautiously assigned to Individual 3 but did not provide any biological information.

Figure 10.3: Embedded mandible.

Most post cranial measurements were partial due to fragmentation (table 3.3, appendix 3.1.3). The maximum length of the left tibia (91.6 mm) provided an age estimation of 6 – 8 months (Scheuer, Black and Schaefer, 2008). The maximum iliac length (46.2 mm) and the maximum iliac width (42.9 mm) provided an age estimation of 7 – 9 months (Scheuer, Black and Schaefer, 2008).

The age at death for Individual 3 was originally estimated at nine to twelve months. This was based on "…dental development, fusion of the cervical vertebra arch and the maximum width of the ilium" (Leach, 2006, p. 167). The cervical vertebral arch was not identified during analysis and maximum width of the ilium returned a different age assessment, perhaps due to the use of a different reference. The final estimation of age at death was seven to nine months, placing it in a younger age bracket than the original analysis. This was decided based on the iliac measurements, supported by the limited dental observations.

## 10.4: Individual 4

### *10.4.1: Age at Death Estimation*

Individual 4 was estimated to be a neonate aged 38-40 gestational weeks.

Age at death was estimated using measurements of both cranial and post cranial elements (table 3.4, appendix 3.1.4). Apart from damaged elements, all were consistent with an age estimation of 38-40 gestational weeks (Scheuer, Black and Schaefer, 2008).

There was evidence of deformation of the parietal plates (figure 10.4). Foetal head moulding occurs during labour to allow the head to pass safely through the vaginal canal (Pu *et al.*, 2011). This, coupled with the absence of a female adult in proximity suggest that the infant had been born. It is not possible to determine whether this was a still or live birth.

Figure 10.4: Deformed parietals from Individual 4.

Demographic assessments agree with Leach's (2006a) findings and remain at four individuals. Radiocarbon dating suggests that these were successive burials, deposited during the Early Neolithic. The following section describes the taphonomic findings from QGIS analysis before exploring spatial distributions of fragments, bodies and taphonomy.

# CHAPTER 11: CAVE HA 3 TAPHONOMY

## 11.1: Individual 1

### *11.1.1: Bone Representation*

Representation of elements was consistent across all groups except for cranial elements (figure 11.1). There is a possibility that elements originated from more than one individual. The pelvis and mandible from a male, and the shorter, post cranial elements from a female. Evidence of composite burials, where apparent single individuals are assembled from distinct bodies (Wysocki and Whittle, 2000; Fowler, 2010; Lorentz, Casa and Miyauchi, 2021), will be discussed in relation to Individual 1 in section 18.2.2, however the BRI, coupled with retained articulations (section 11.1.5) indicate that Individual 1 is not a composite.

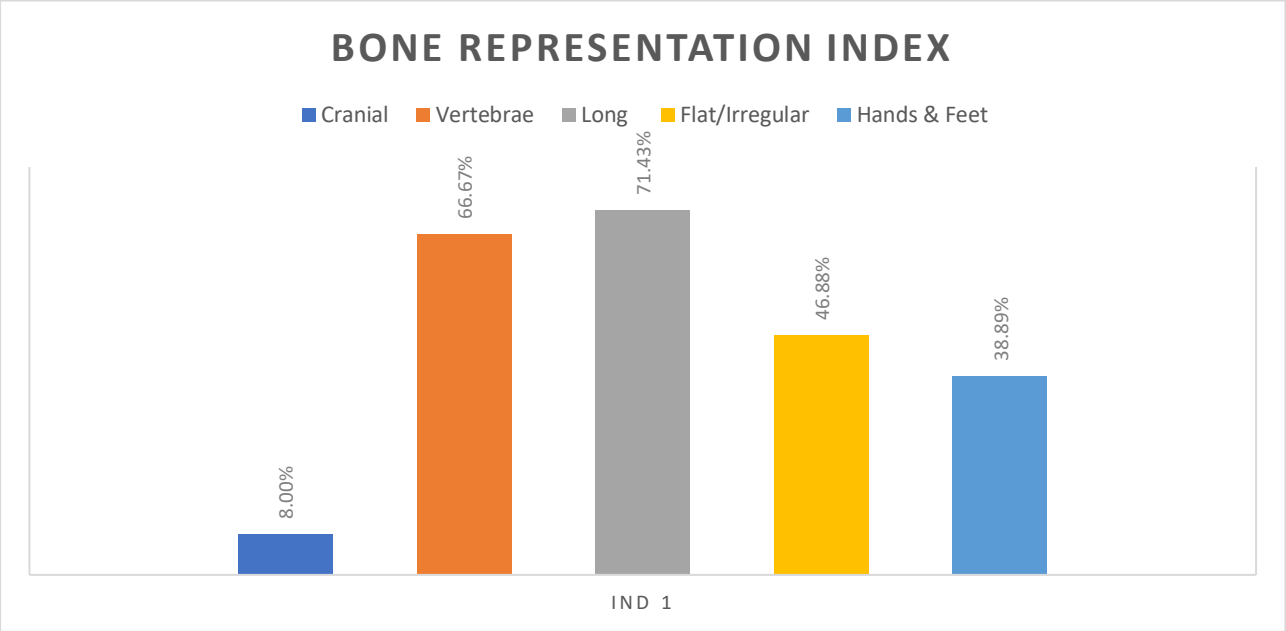


Figure 11.1: Bone representation for Individual 1, Cave Ha 3.

Seven fragments of occipital were identified from the entire assemblage. Overlap and refitting led to a minimum number of elements (MNE) of four. The largest occipital fragment (CH3.14.9) was obscured by heavy tufa embedding. Measurements of occipital chord and arc, and lambda-inion (L-I) chord and arc appeared small. Literature on occipital measurements was scant and was limited to palaeolithic collections originating from areas outside Britain. Discussions around the human cranium from the Peştera cu Oase, Oase 2 (Rougier and Trinkaus, 2013) described adult L-I measurements that were consistent with measurements

taken from CH3.14.9 (L-I chord = 54mm, L-I arc = 60mm). While it is not possible to assign the fragment conclusively to the adult (Individual 1), it is also not possible to rule it out. The fragment was therefore tentatively assigned and recorded as Individual 1.

A total of three ribs were excluded from GIS visualisations but were included in the spatial analysis of modifications (table 11.1 and figure 11.2).

Table 11.1: Fragments excluded from Individual 1 GIS mapping.

| Bone Code | Bone ID | Side | Reason for exclusion |
|---|---|---|---|
| CH3.64.456 | Rib Shaft | Unclassified | Uncertainty around position |
| CH3.64.457 | Rib Shaft | Unclassified | Uncertainty around position |
| CH3.13.448 | Rib | R | Uncertainty around position |

Figure 11.2: Ribs excluded from GIS due to uncertainty around position (Individual 1).

Other ribs present in the assemblage were excluded from analysis due to the possibility that they were faunal. Without histology some animal ribs, especially when fragmented, look very similar to human ribs. The number of possible ribs did not exceed the MNI and were homogenous in taphonomy. It was felt that their inclusion in analysis would not add anything

further to the results and, on balance, it was better to avoid potential biases caused through misidentification.

The following discusses frequencies of modifications, all tables for Individual 1 taphonomy can be found in appendix 4.1.

### *11.1.2: Whole Body Taphonomy*

All fragments from Individual 1 were altered by taphonomic processes (figure 11.3).

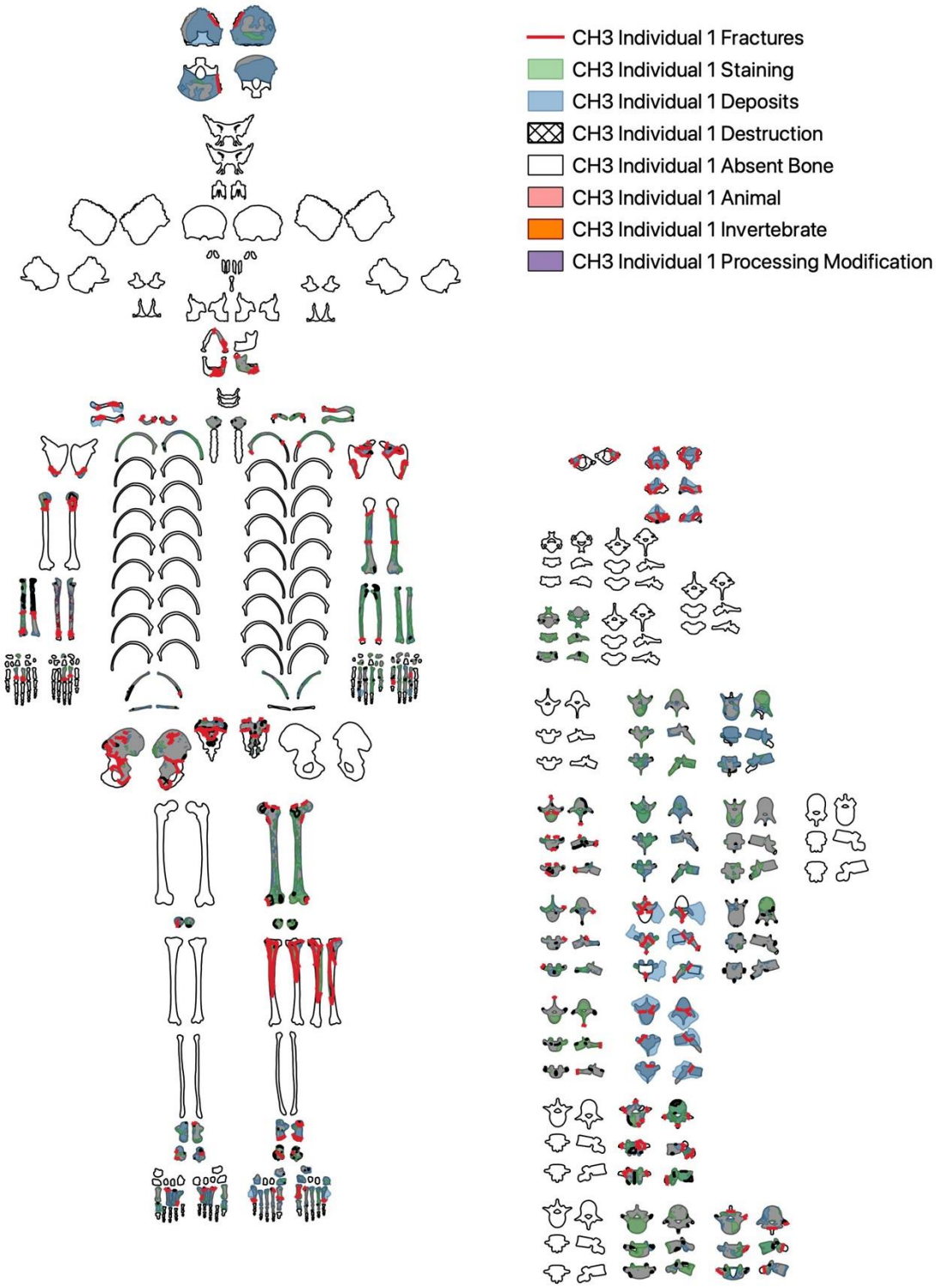


Figure 11.3: Distribution of all taphonomic modifications across Individual 1.

Both left and right anatomical sides and all planes were affected by taphonomy. The left side of the body showed 32.30% of all taphonomic modifications, compared to 26.12% occurring on the right side of the body, the remaining 41.58% of modifications were on unilateral elements. This is reflective of the slightly higher proportion of left sided elements recovered. When this is factored in and all modifications are combined, there is no difference to modification according to anatomical side. There was an even distribution of combined taphonomy across the anterior and posterior surfaces (19.66% and 19.34% of all modifications respectively). Superior and inferior surfaces were similarly affected (12.59% and 11.26% respectively). Most bones were assessed for their anterior or posterior surfaces. Due to the labelling traditions of anatomical planes some surfaces that were included appear to be disproportionately unaffected by taphonomic processes (for example the lingual surface of the mandible, 2.57%). This is not due to differences in taphonomic process, rather a result of only one lingual surface occurring in the body.

### *11.1.3: Destruction*

Ten specimens from Individual 1 exhibited crush damage indicative of peri-mortem destruction (table 4.1.1, appendix 4.1). Retention of small, adherent bone fragments suggest that the damage occurred when some level of elasticity remained (figure 11.4). Determining the point at which this occurred is difficult, however, due to characteristics of peri-mortem trauma extending “well into the post-mortem interval” (Galloway, Zephro and Wedel, 2014, p. 54). It is possible that sediment movement within the cave led to crushing at a point when elements still retained collagen.

Figure 11.4: Distal portion of radius showing area of crush damage.

Crush damage was limited to the post cranial elements. The distribution of damage across left and right anatomical side was roughly even (40% and 50% respectively). Only a single unilateral element was affected (CH3.63.92 LV3). Most of the damage occurred on the anterior surface (55.56% of the total points of crushing), the superior surface was also more affected (22.22%) than posterior surfaces (5.56%). Other surfaces (plantar, lateral, and dorsal) were minimally impacted by crushing (figure 11.5).

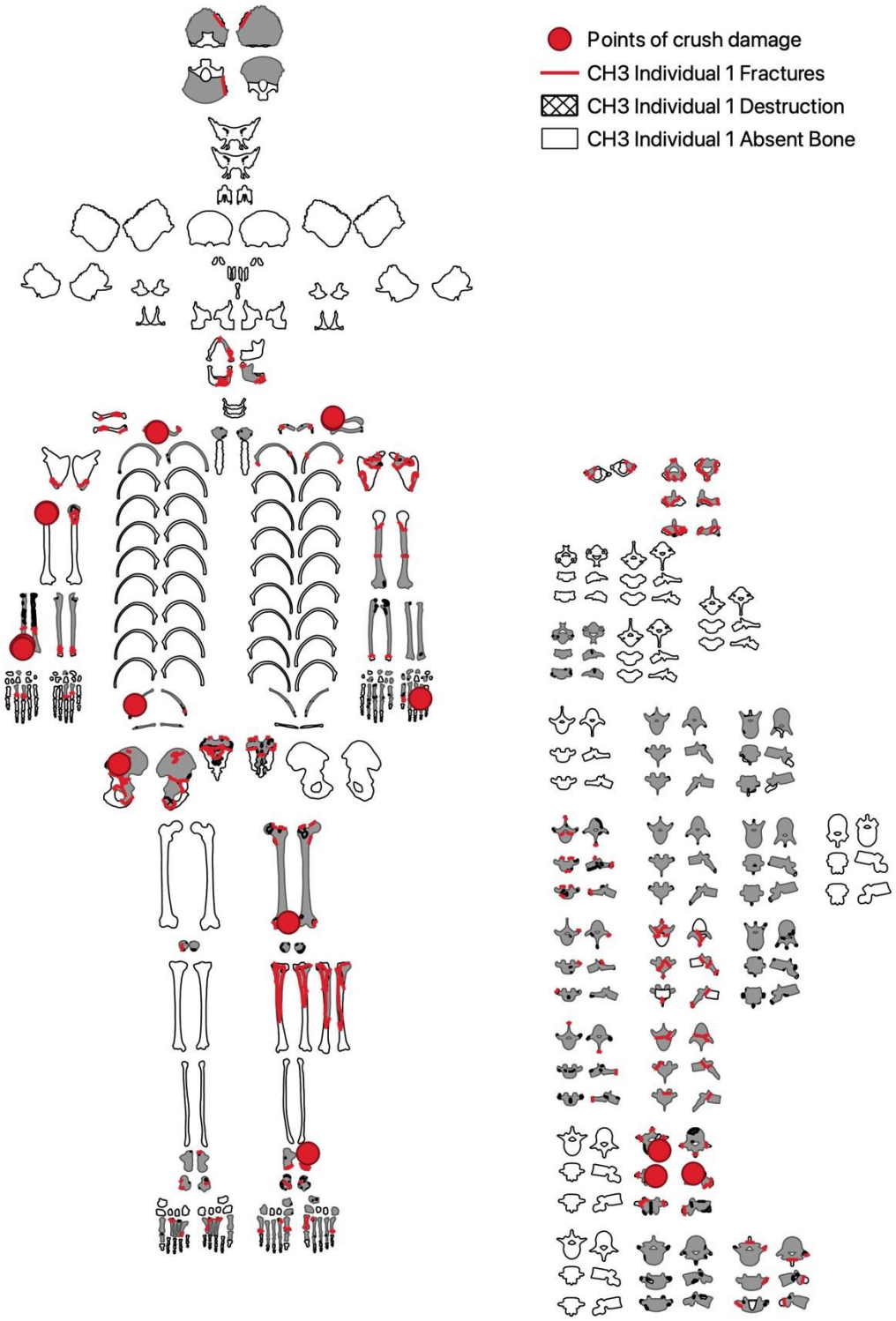


Figure 11.5: Distribution of crushing across Individual 1. Red dot = area of crush damage.

While the bias towards crushing occurring on post cranial elements can be attributed to bone representation rather than an indication of position; the distribution according to plane is interesting and is indicative of the body lying supine. This would expose the anterior surface to damage from falling debris, while protecting the posterior surface.

The remaining classifications of destruction were all indicative of post-mortem damage. Most of the destruction was classified as 'exposure of trabecular bone' (79.03%). These were areas on bones where the cortical surface had been degraded, resulting in the trabecular bone being visible (figure 11.6).

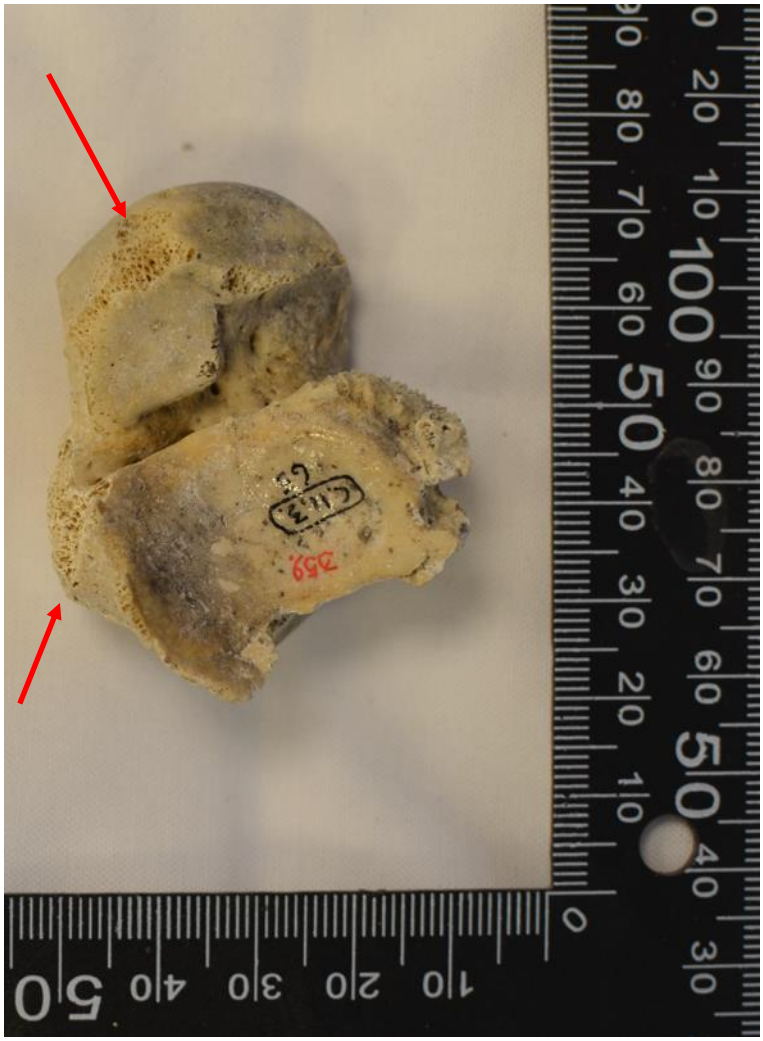

Figure 11.6: A talus showing areas of 'exposure of trabecular bone' (red arrows) consistent with sediment abrasion.

When the additional views were accounted for with vertebrae, the distribution of damage according to element group was even. This shows that damage was occurring across the body and that the whole body was subjected to the same environment.

All post-mortem damage described above was consistent with sediment abrasion and other physical mechanisms of post-depositional damage accordant with the remains lying in a cave.

### *11.1.4: Fractures*

Incomplete and complete fractures were recorded in the same GIS layer. Fracturing occurred across the whole of Individual 1, with 24.76% occurring on the anterior surface compared to 17.59% on the posterior surface (figure 11.7). Complete fractures were recorded on all surfaces they were visible from; therefore, it would be expected that frequencies for anterior and posterior views would be similar.

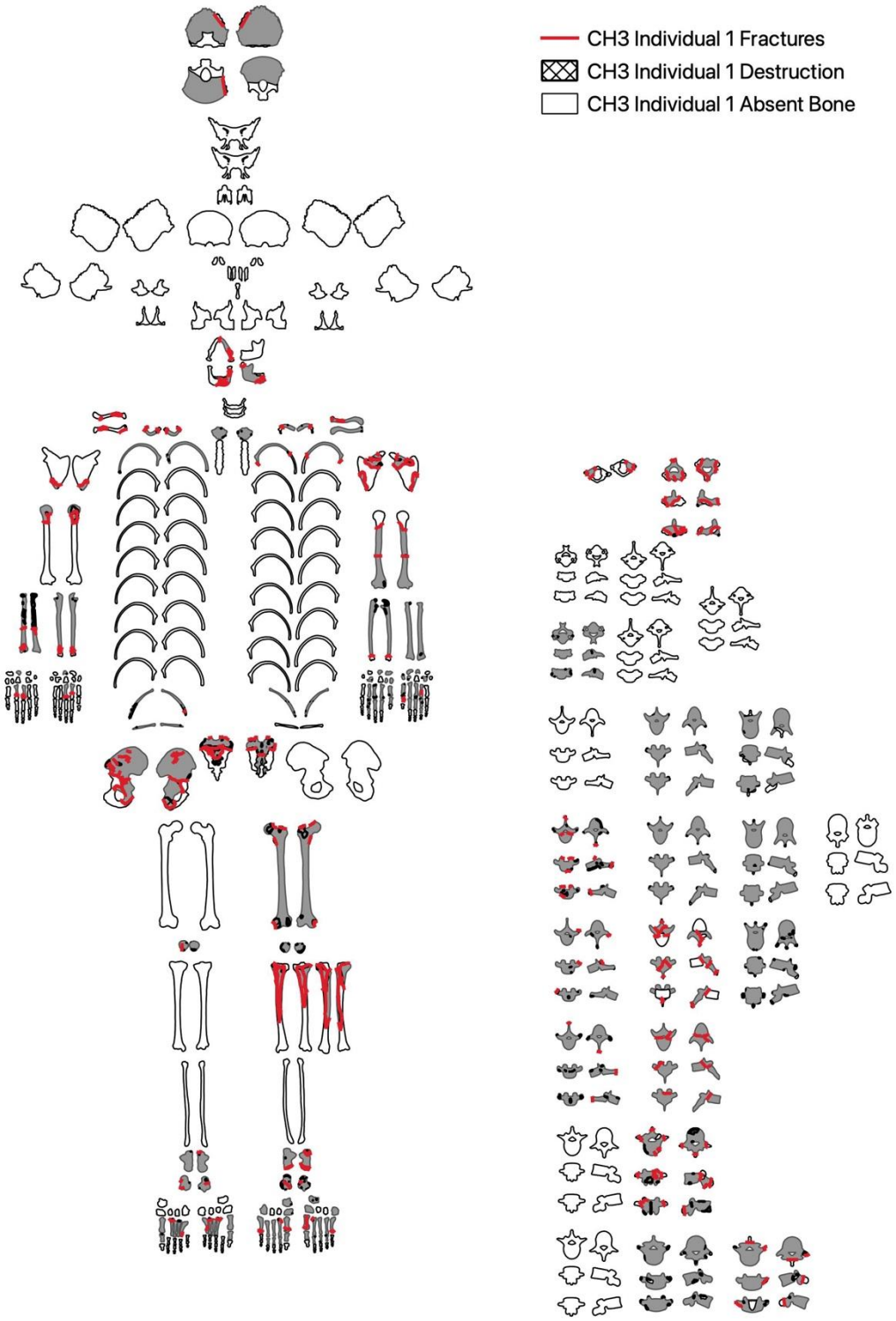


Figure 11.7: Distribution of fracturing across Individual 1.

Of the fractures, 30.62% were classified as incomplete (recorded as cracking in QGIS), often these originated from an area of damage or destruction (figure 11.8).

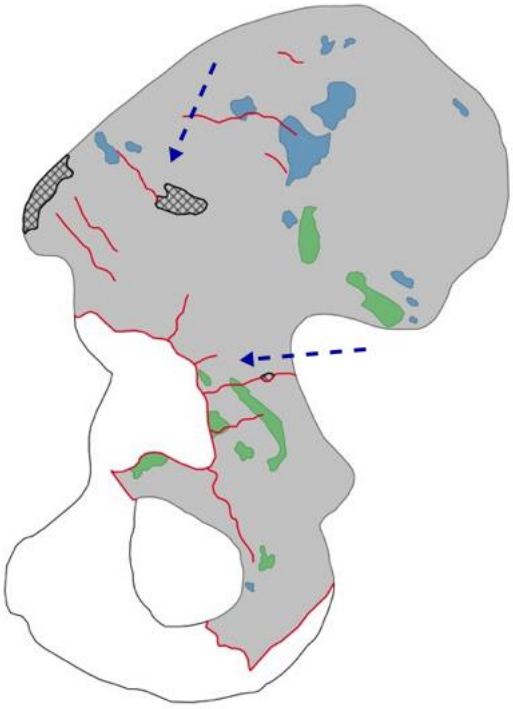

Figure 11.8: Blue arrows showing incomplete fractures radiating from areas of destruction.

Analysis of areas of damage showed a bias towards the anterior surface. When incomplete fractures were removed from counts, the distribution across anterior and posterior views was almost even (21.13% and 21.60% respectively). The distribution of incomplete fractures supports the interpretation around body position.

Most fractures were classified as oblique dry (46%) and 93.43% of fractures were consistent with post-mortem fracture. The remaining 6.57% of fractures were classified as peri-mortem breaks. The peri-mortem fractures were solely concentrated on the left tibia. Fractures were classified as V-shaped, spiral, and oblique wet, and had smooth margins consistent with breakage at a stage when collagen was still present. The pattern of destruction was consistent with butchery processing for marrow extraction. The significance of this is discussed in the following section (page 11.1.7) covering processing modifications.

Most fractures (including incomplete cracking) occurred on the vertebrae (36.81%). Multiple surfaces were recorded for the vertebrae, rather than just anterior and posterior. This was adjusted to look at fractures only occurring on anterior and posterior surfaces and compared again to other groups. Irregular bones then exhibited the most fracturing (22.15%) despite having a lower count in the bone representation index. This is perhaps due to fragility in irregular bones. Irregular bones such as the sacrum and pelvis have shown increased fragmentation in archaeological samples (Bello and Andrews, 2006).

### *11.1.5: Tufa Deposits*

There were tufa deposits on all fragments, ranging from thin flakes to embedded fragments (figure 11.9).

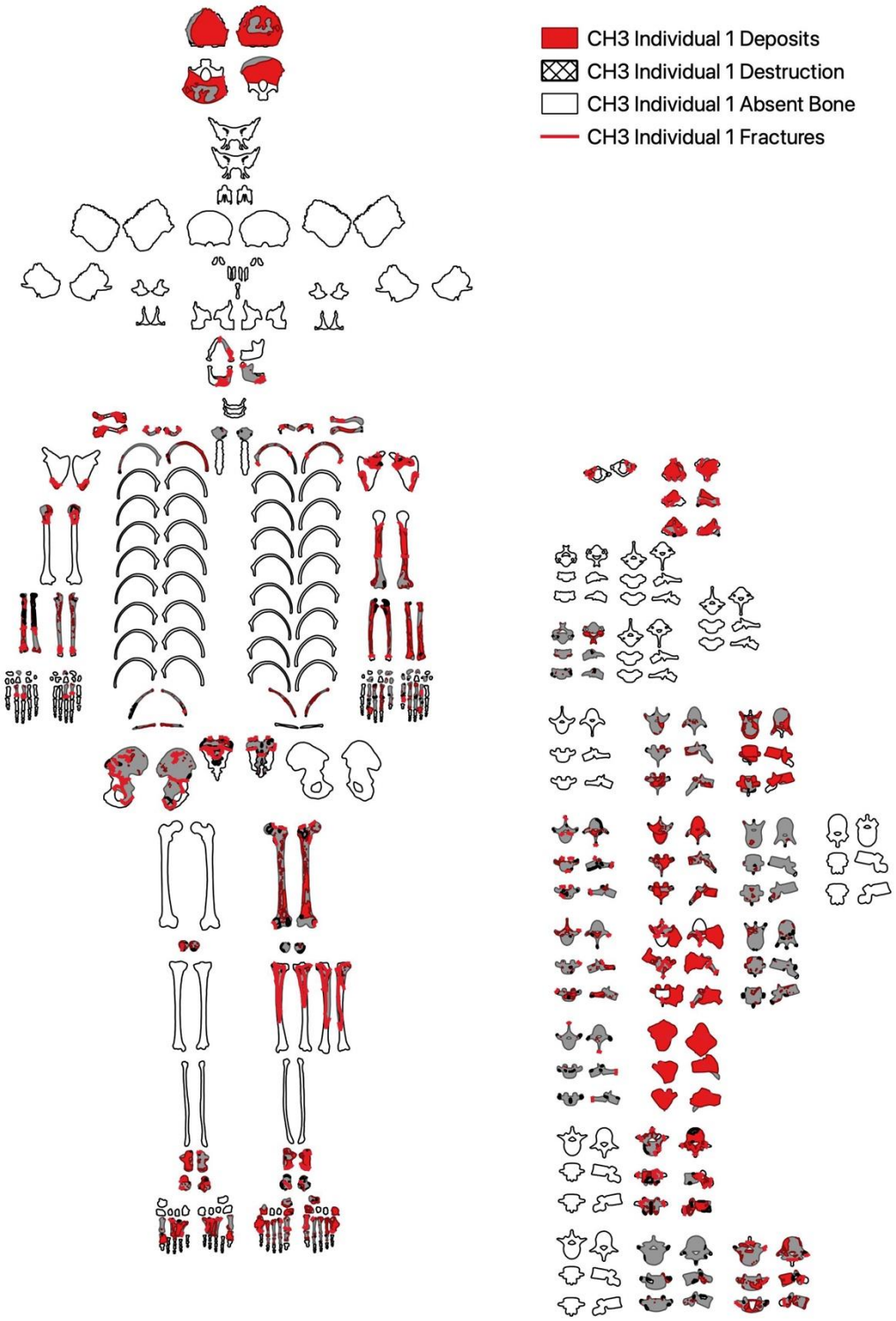


Figure 11.9: Distribution of fragments affected by tufa deposits for Individual 1.

Embedded tufa accounted for 9.35% of all deposits, most deposits were classed as thin/flaked (72.95%).

Most of the embedded tufa occurred on plantar and dorsal surfaces (18.37% and 18.46% respectively). This is different from other taphonomic modifications which mainly occurred on anterior and posterior surfaces. Plantar surfaces are limited to the feet and dorsal surfaces are limited to the hands and feet; a lower frequency of modifications would therefore be expected. The bias in embedding occurring on these surfaces was due to the presence of an articulated foot. The significance of this will be discussed in more detail in section 18.2.2. This is reflected in table 11.2, which shows an almost equal distribution of deposits occurring on the long bones and hands, feet, and patella.

Table 11.2: Deposit frequencies and percentages according to element group for Individual 1.

| **Deposit ↓** | **Long Bone** | **Cranial & Mandible** | **Hands, Feet & Patella** | **Vertebra** | **Vert (just Ant/Post)** | **Irregular** |
|---|---|---|---|---|---|---|
| Embedded | 19 | 2 | 43 | 56 | 15 | 11 |
| Thick/Coated | 40 | 6 | 65 | 118 | 50 | 19 |
| Thin/Flaked | 278 | 2 | 206 | 302 | 112 | 234 |
| **Group %** | 24.1% | 0.7% | 22.4% | 34.0% | 12.6% | 18.8% |

There was no indication of bias on the distribution of embedded fragments according to anatomical side, 20.00% occurred on the right, 35.38% on the left and 44.62% occurred on unsided elements. This is consistent with the bias in representation of side and is not considered indicative of positioning.

The second, third, fourth and fifth metatarsals on the right foot were held in anatomical position by embedded tufa (figures 11.10a and 11.10b). Other tarsals and pedal phalanges could be associated to the embedded foot and appeared to have previously been adhered.


Figure 11.10: a) GIS diagram of the plantar and dorsal view (respectively) of deposits embedding the right foot. B) photograph of the foot in plantar view.

This articulation is reflected in the distribution of embedded tufa for both anatomical plane and element grouping. Retention of articulation suggests that Individual 1 was deposited whole and most likely fleshed. The body was certainly deposited at a point when connective tissue was still present, allowing the tufa to form around the foot, holding it in place.

### *11.1.6: Staining*

The bones were mostly pale in colour, however there was staining evident (figure 11.11).

Figure 11.11: Image showing black-grey staining on the posterior surface of a patella.

The staining was mostly grey-black staining, ranging from light to dark, with either a mottled, 'spotted' appearance or matt coverage. This was consistent with manganese staining, common in limestone deposits (Waters and Lowe, 2013). There were patches of light to dark brown-orange staining, consistent with iron oxide staining, although the presence of these was mostly limited to small patches.

It was beyond the scope of this project to test the chemical composition of stains. Identification was conducted from looking at analogues and geological descriptions. It may be that these stains are caused by different compounds. The remaining results discuss the prevalence and positioning of the staining.

One fragment (8$^{th}$ thoracic vertebrae CH3.73.440) did not show any staining (indicated by the blue box on figure 11.12). It was heavily embedded in tufa so may have staining that was obscured. All other fragments had some form of staining (figure 11.12).

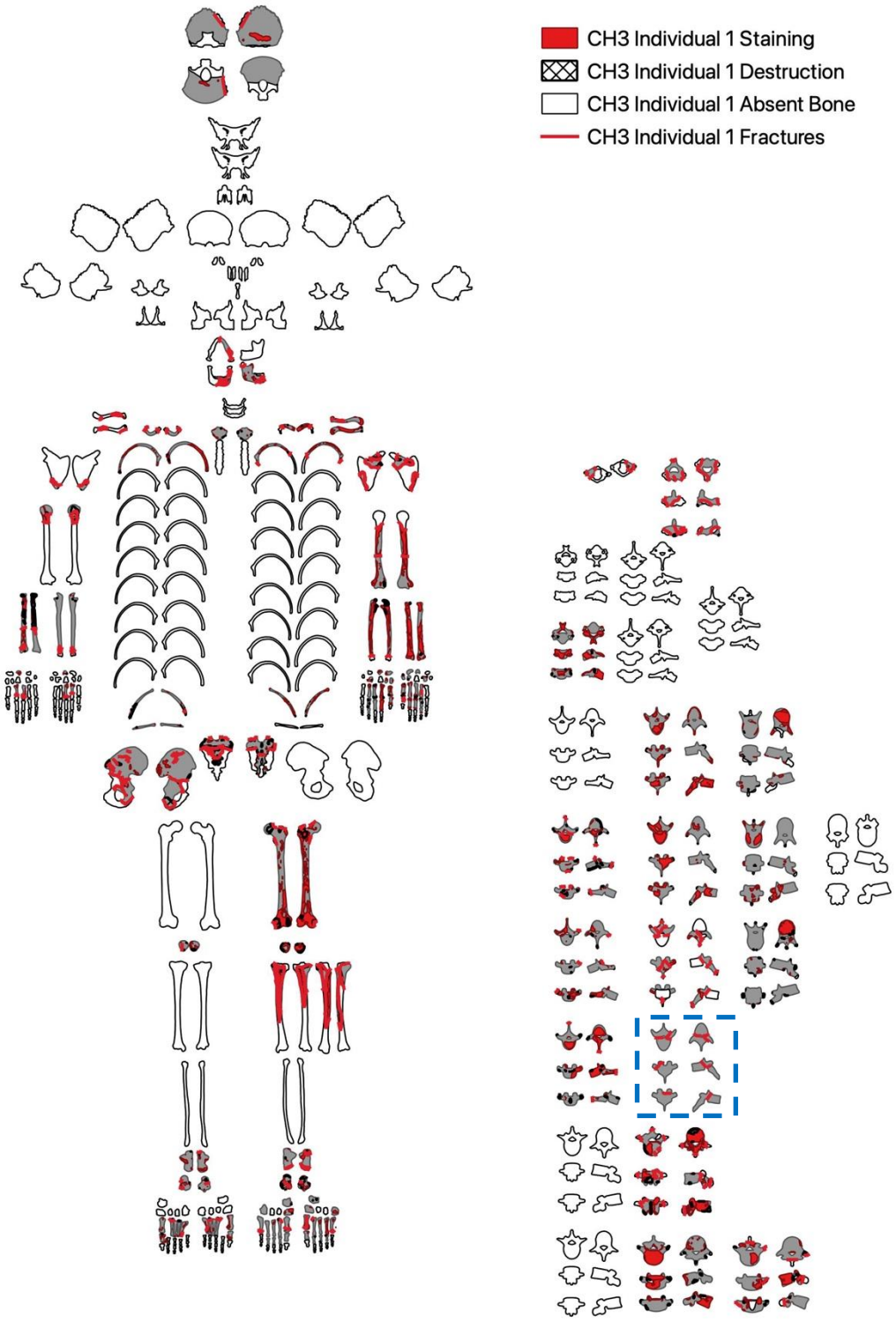


Figure 11.12: Distribution of fragments affected by staining for Individual 1.

Staining occurred evenly across the anterior and posterior view. The lateral views had disproportionately more staining compared to medial surfaces. Right and left lateral views (of the vertebrae) may have accounted for some of this difference by increasing the number of lateral surfaces analysed. When this was accounted for the frequencies were still higher for lateral views than medial (11.02% and 1.17% respectively). The medial surfaces did not show higher levels of deposits, meaning the difference was not due to obstruction. The difference may be due to lateral surfaces having greater contact with external environments, because of their position when the body is articulated.

There was a marginally higher frequency of staining on unsided and left fragments however, as discussed, right sided fragments are underrepresented. There was a higher frequency of staining on the hands, feet, and patella, when assessed by element group. This may be due to those elements disarticulating earlier in the decomposition sequence (Bello and Andrews, 2006; Robb, 2016), and therefore having longer exposure to the cave environment. Irregular bones, however, also showed higher frequency of staining in comparison to other groups (21.37%). Most of this staining occurred on the ribs (14.83%). Less variation in surface structure, resulting in increased surface contact, may explain the higher occurrence of staining to ribs. The innominate and sacrum showed much less staining, perhaps due to the irregularity of the bone reducing surface contact.

It is important to note that, for both deposits and staining, assessment was based on frequencies and not area covered. Long bones in particular show large areas of staining, which if continuous, would be classed as one incidence. Smaller, diffuse patches of staining would have higher frequency counts. The decision to work on frequencies, rather than area, will be discussed in more detail in section 18.4.1.

While there were a few differences in distribution of staining, there was nothing to indicate depositional bias or differential treatment of Individual 1. The staining was considered homogenous in nature and consistent with the body lying in a cave environment for an extended period. The staining was then analysed to assess the sequence of taphonomic changes. By identifying whether staining overlies an existing modification, or whether the staining is in fact underneath a modification, a timeline of events can be established. More

than half of the stains were either modified by deposits or independent of other changes (55.41%), suggesting that staining was generally occurring before tufa deposits.

### *11.1.7: Processing Modifications*

Due to limited modifications, this, and the following section (Animal Activity) are descriptive and frequency tables have been omitted.

The left tibia of Individual 1 had evidence of butchery practice, consistent with marrow extraction. A single notch defect was evident on the medial surface (figure 11.13, marked with blue box). Fracturing was consistent with fresh breakage at a stage when collagen was still present (see section 3.2.4, pages 33-34).

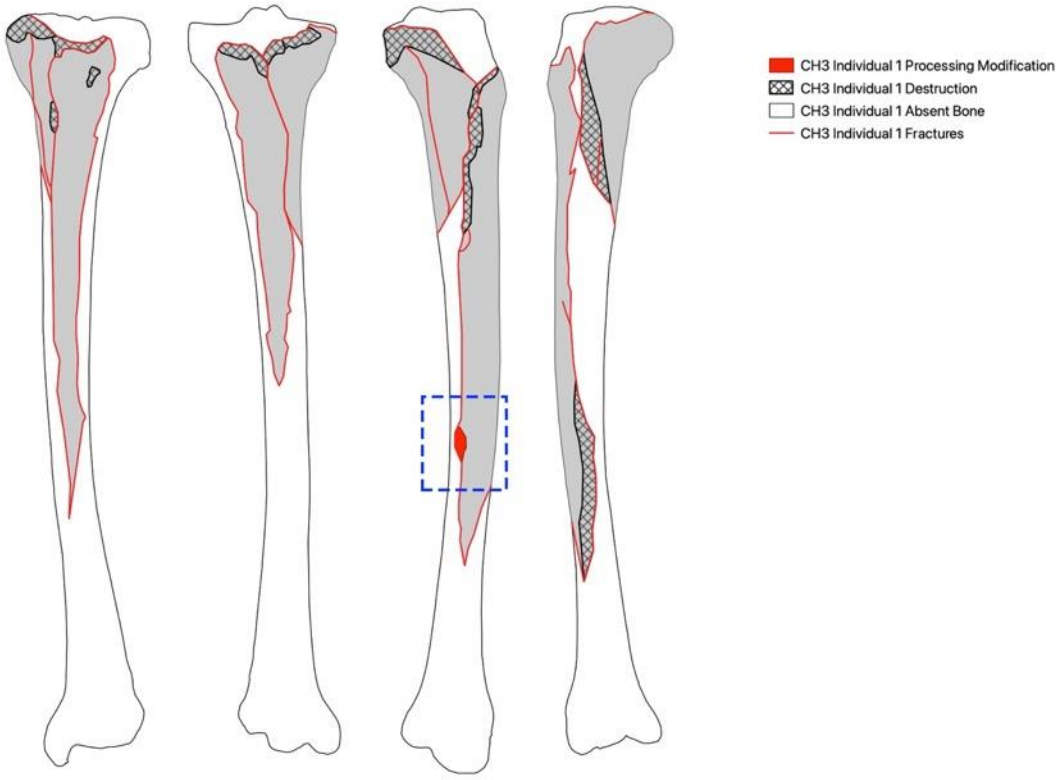


Figure 11.13: Image showing notch defect (blue box) on smashed tibia.

Contrary to the embedded foot discussed in section 11.1.5, the presence of processing modifications suggests access and manipulation at the point of skeletonisation. The pattern of staining and deposits support the sequence of fracturing. None of the deposits, bar one

thin flake (red arrow, figure 11.14) cross fracture margins. An area of deposit (blue arrow, figure 11.14) overlays an area of destruction where the internal surface of the bone is exposed.

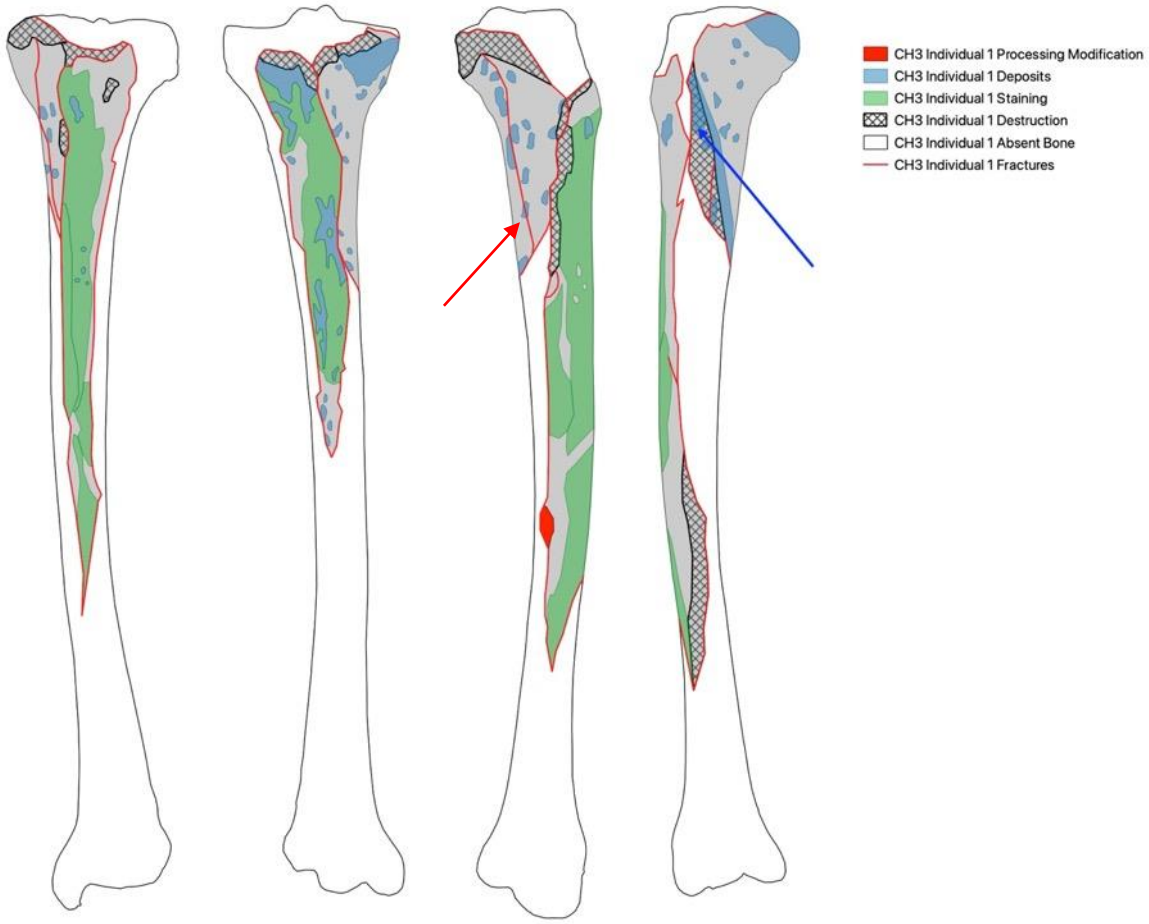


Figure 11.14: Smashed tibia showing area of deposit covering internal bone surface (blue arrow) and deposit crossing fracture (red arrow).

As previously discussed, the peri-mortem period can last for an extended time. This is supported by evidence of a single deposit crossing a fracture margin. This indicates that the bone lay in the cave environment long enough for some tufa to adhere prior to processing, while retaining a degree of bone freshness. The presence of deposits on internal bone surfaces show that once fractured, the bone was returned to tufa-rich environment.

### *11.1.8: Animal Activity*

There was a single patch of animal activity present on Individual 1. This was an area of gnawing consistent with rodents on the medial surface of the left ulna (figure 11.15).

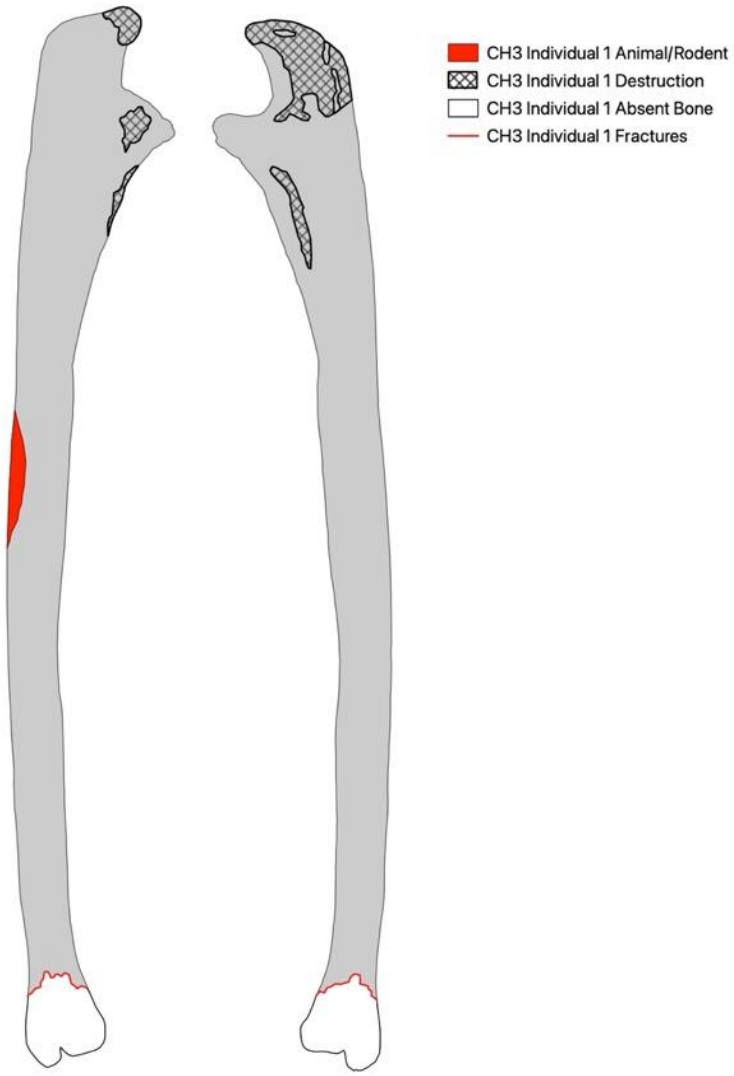


Figure 11.15: Left ulna showing area of rodent gnawing.

There were no other areas of animal activity evident and consistent with Leach (2006a), it appears that the body was protected from access by animals or scavengers. The location of this ulna is explored in section 12.4.6.

### *11.1.9: Invertebrate Activity*

Invertebrate activity was limited to long bones and ribs. A single right ulna showed extensive pitting and some furrows were evident on the posterior surfaces of ribs. A frequency table per anatomical plane has been omitted, most alterations occurred on medial and lateral surfaces. This was, however, due to the right ulna showing a disproportionate amount of invertebrate

activity. Tufa may have obscured observations of invertebrate activity, or acted as a preservative, preventing access and modification.

#### *11.1.10: Root and Weathering*

The assemblage was minimally affected by weathering, with a maximum score of 1 according to Behrensmeyer (1978). No other changes associated with weathering were observed, including an absence of bleaching, cortical exfoliation, delamination, or patination. No root embedding or etching was observed on bone surfaces. This may be due to the tufa acting as a preservative, shielding cortical surfaces from weathering effects and roots, or because of the sheltered nature of Cave Ha 3.

All taphonomic changes to Individual 1 are consistent with a primary, whole-body burial with secondary access and manipulation of a single bone during the peri-mortem stage.

## 11.2: Individual 2

#### *11.2.1: Bone Representation*

Individual 2 had the highest representation for cranial elements and complete absence of hands, feet, and patellae (figure 11.16). As discussed above (section 9.2), the absence of smaller, quick to disarticulate bones is not necessarily indicative of secondary burial. The tufa rich environment of Cave Ha 3 could easily have obscured less recognisable juvenile bones, leading to bias in recovery and destruction. Differential patterns of recovery for sub-adult remains have been well documented (Buckberry, 2000; Bello *et al.*, 2006; Manifold, 2010), with hands and feet often absent, as reflected here.

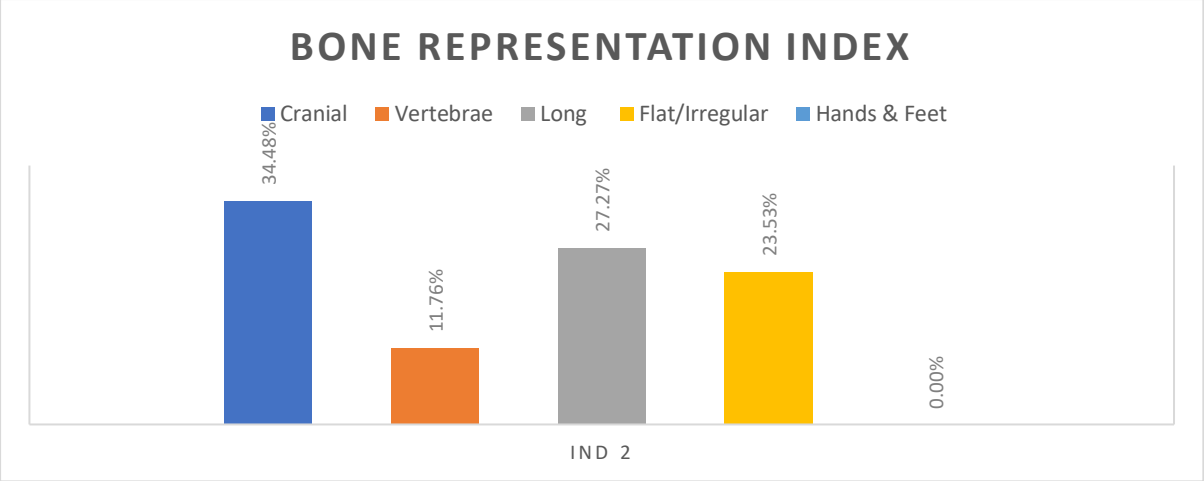


Figure 11.16: Graph showing bone representation for Individual 2, Cave Ha 3.

Individual 2 had the most recovered elements for the sub-adults in Cave Ha 3, with a total representation of 16.43%. The representation for left elements (39.39%) was slightly higher than rights (27.27%) and unilateral elements (33.33%).

It was not possible to sequence the vertebral and rib fragments due to incomplete representation. They were therefore excluded from body level GIS (table 4.2.1, appendix 4.2). They were, however, included in the spatial analysis (section 12.7).

The following discusses frequencies of modifications; all tables for Individual 2 taphonomy can be found in appendix 4.2.

*11.2.2: Whole Body Taphonomy*

All fragments from Individual 2 were altered by taphonomic processes (figure 11.17).

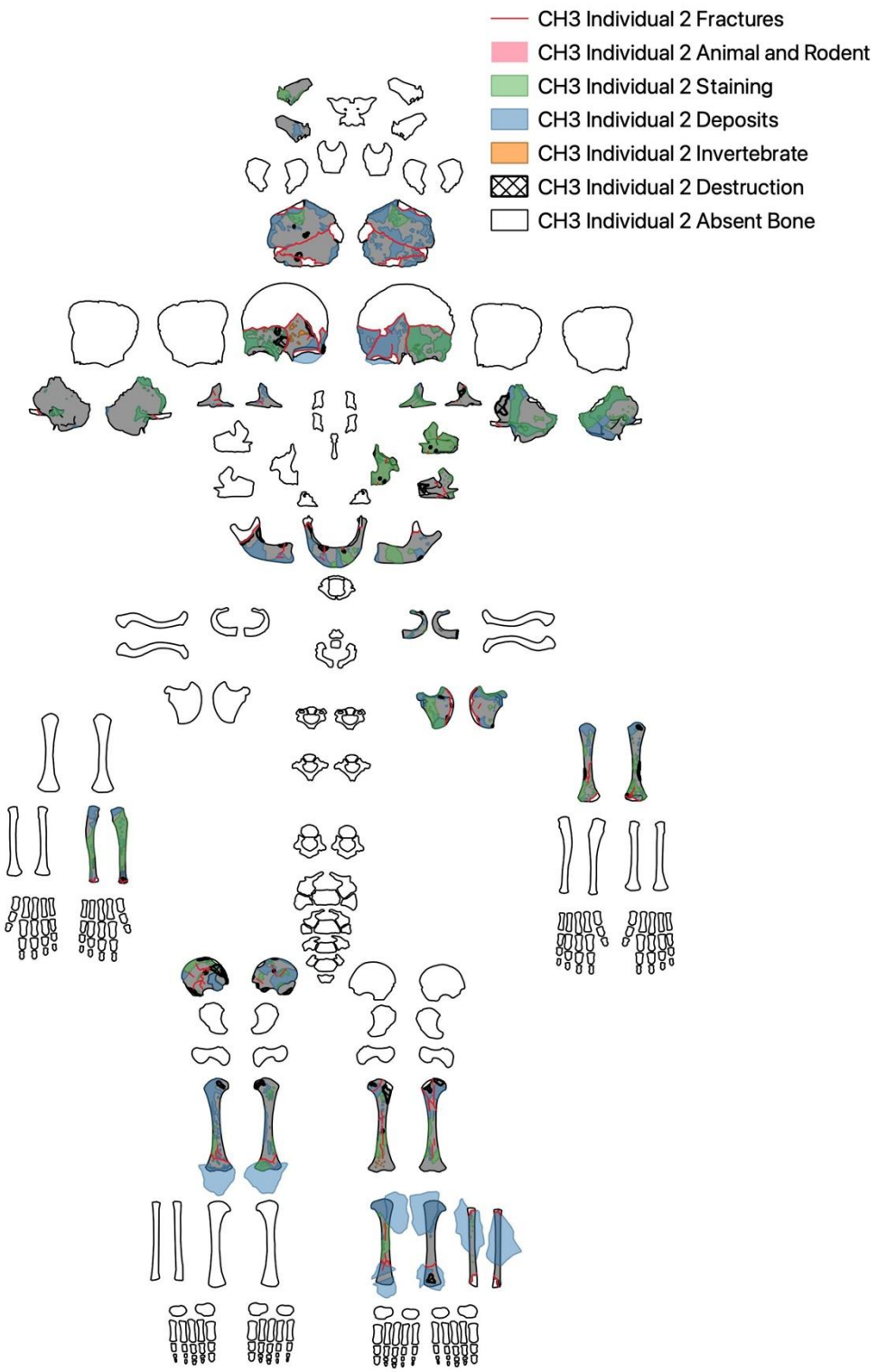


Figure 11.17: All taphonomic modifications across Individual 2.

Both left and right anatomical sides and all planes were affected by taphonomy. Left fragments showed 46.43% of all taphonomic modifications, compared to 26.92% on right fragments. The remaining 26.65% of modifications were on unilateral elements. This is reflective of the slightly higher proportion of left sided elements recovered. The anterior surface showed higher observations of taphonomic modifications (42.55%) than the posterior surface (37.05%). Lateral and medial surfaces were almost even (8.05% and 7.11% respectively), and superior surfaces had slightly higher counts than inferior (3.49% and 1.74% respectively). It is possible that higher occurrences of modifications on the anterior surfaces are indicative of a supine position resulting in exposure of the front of the body.

### *11.2.3: Destruction*

Two specimens from Individual 2 exhibited crush damage indicative of peri-mortem destruction (table 11.3).

Table 11.3: Fragments from Individual 2 with peri-mortem crushing.

| Bone Code | Bone ID | Side |
|---|---|---|
| CH3.70.114 | HU | L |
| CH3.77.239 | PEil | R |

Crushing occurred on both anterior and posterior views and to left and right elements. There was nothing to indicate positional bias for Individual 2 based on crushing.

Destruction was consistent with sediment abrasion and exposure of trabecular bone accounted for most damage. Exposure of trabecular bone was evenly distributed across the anterior and posterior surfaces, however, when all types of destruction were accounted for, most of the damage occurred on the anterior surface (51.8%). Cortical removal without exposure was only present on anterior, superior, and lateral surfaces. This may be indicative of body position since these surfaces would be expected to be exposed if the body was lying supine.

Most damage occurred to cranial elements (44.64%) which is in line with the bone representation indices. The irregular bones showed more damage than long bones (30.36% and 25.00% respectively), despite having lower representation.

### *11.2.4: Fractures*

Fracturing and cracking occurred across 84.2% of the recovered elements of Individual 2. The first rib and the right, greater wing of the sphenoid had no visible fracturing or cracking (figure 11.18).

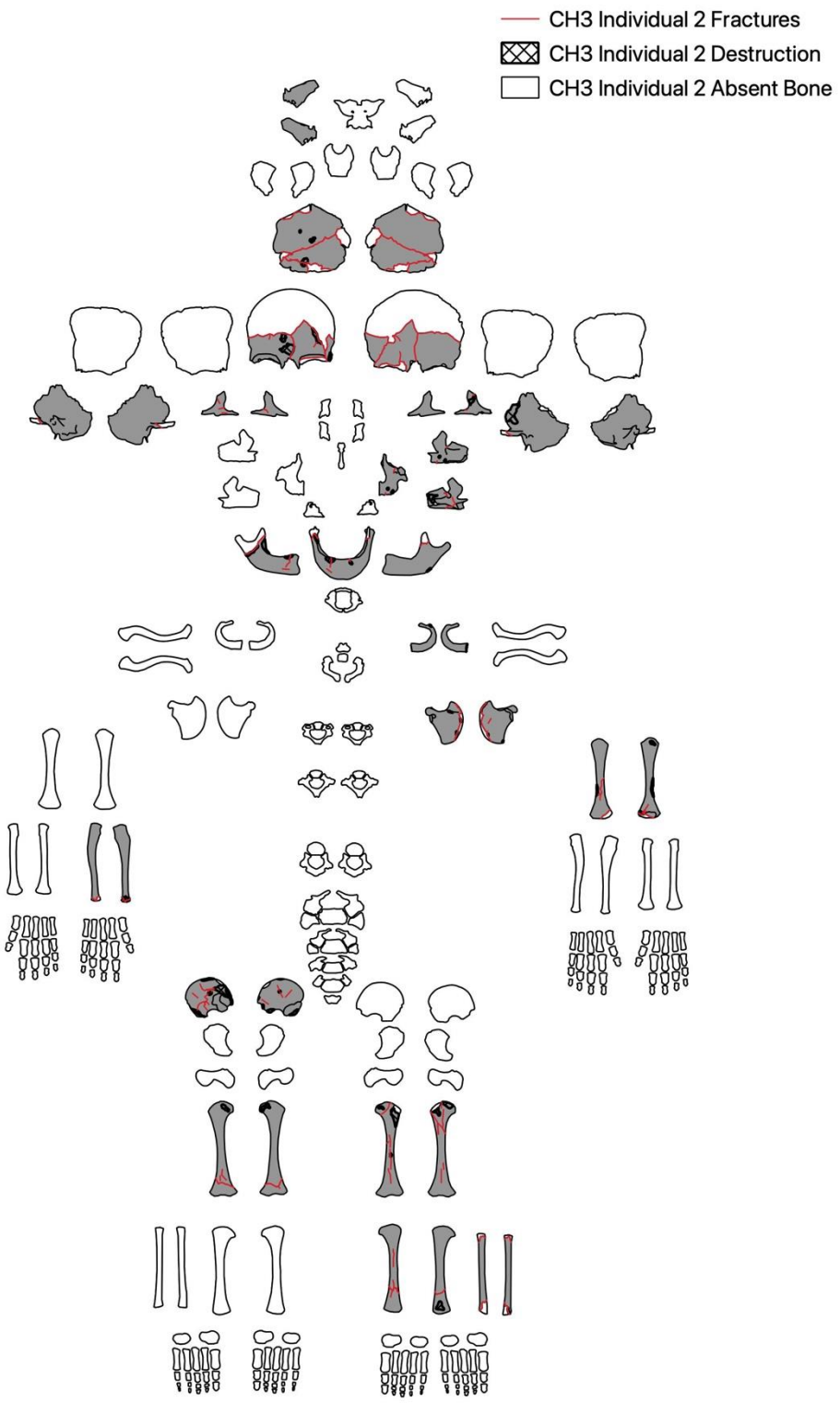


Figure 11.18: Fracture distribution for Individual 2

Incomplete cracking counted for 50.50% of fractures, of those, five cracks originated from areas of crushing and 12 originated from areas of damage. One incomplete fracture on the left femur originated on the posterior surface, crossing to the anterior surface. The fracture was classified as spiral fracturing, commonly seen in femoral shafts due to the application of high force on wet bone (Galloway, Zephro and Wedel, 2014). There was no area of cracked, adherent bone, however the damage was consistent with crushing during the peri-mortem stage. The pattern of fracturing from the left humerus below suggests that the lower region of Individual 2 was subjected to compression while the bone still retained a level of freshness. Most dry fractures were oblique dry (57.69%) and mostly occurred on the anterior surface (48.08%), although the difference was marginal. A disproportionate percentage occurred on lateral surfaces, these surfaces were limited to cranial elements, and, because of recording protocols, the mandible was disproportionately recorded for lateral sides.

The distribution of fractures according to element group is in line with bone representation. While cranial bones showed higher frequencies of fractures this may just be due to there being a higher number of cranial fragments recovered. There is no indication of positional bias for dry fractures.

### *11.2.5: Tufa Deposits*

There were tufa deposits on all fragments, ranging from thin flakes to embedded fragments (figure 11.19).

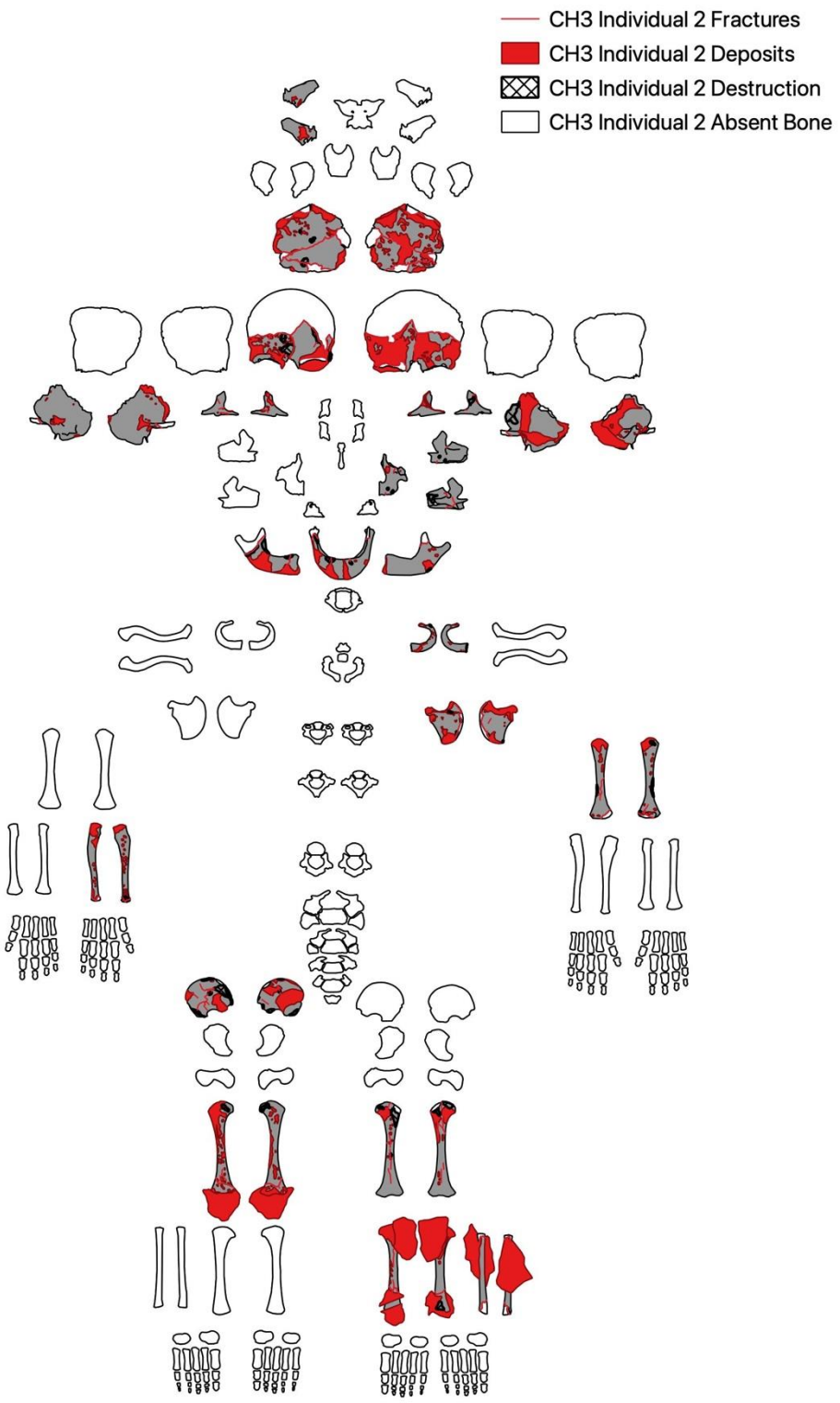


Figure 11.19: Tufa distribution for Individual 2

Most deposits were classed thin/flaked (68.12%) and 10.14% were embedded. There were more deposits to posterior surfaces (43.48%) than anterior (37.68%). This may be indicative of a supine position resulting in posterior surfaces having greater contact with the cave floor.

Embedded deposits mostly occurred on cranial elements (49.86%), including a large area of tufa adhered to the left eye orbit of the frontal bone. The left tibia and fibula were stuck together by a large tufa deposit (figure 11.20). The proximity and adherence indicate that Individual 2 was buried whole, or at the least with their lower limbs articulated.

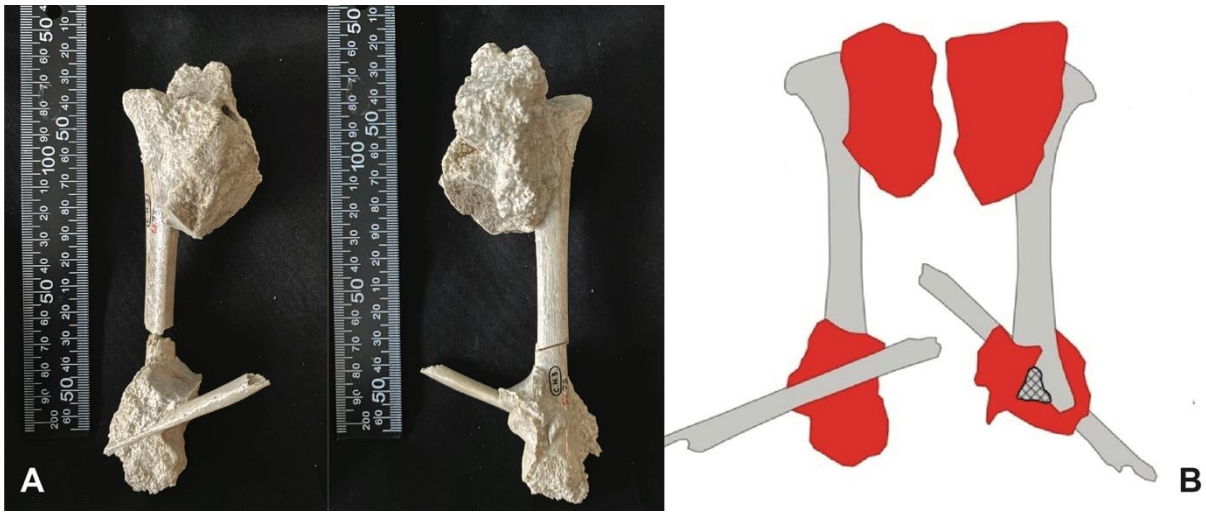


Figure 11.20: a) Tibia and fibula adhered by tufa b) Represented in QGIS

### *11.2.6: Staining*

The bones were a similar, pale colour to Individual 1, with staining occurring on all recovered elements except for the right zygomatic (figure 11.21). Disproportionately more staining occurred on left elements than right (67.15% and 17.87% respectively). The left humerus and fibular had patches of spotted staining. Due to the nature of recording frequencies the individual spots may be skewing the side bias. If the staining is not skewed by the recording system, it may be indicative of positioning, this is explored further in section 12.7.4, in combination with spatial distributions of staining.

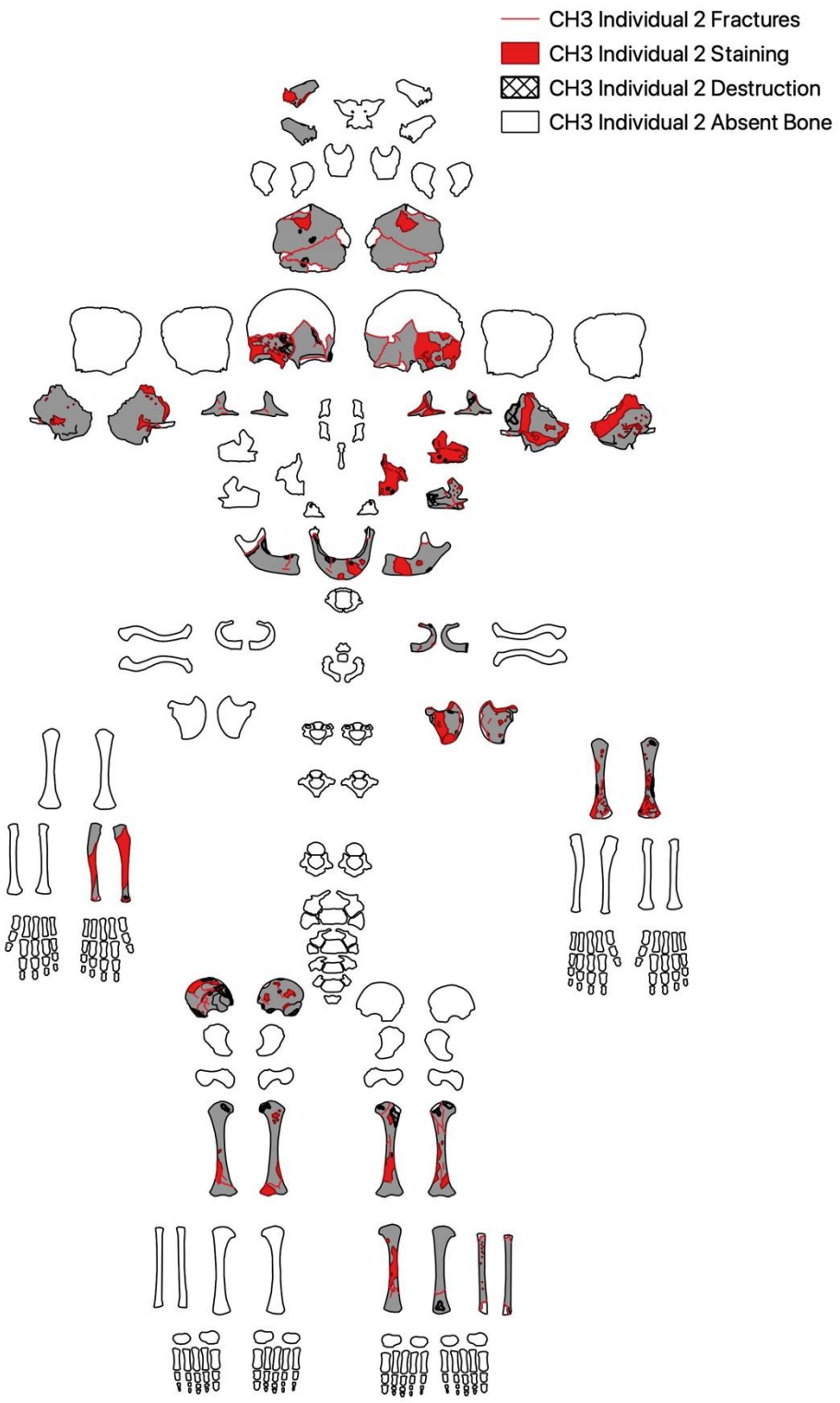


Figure 11.21: Staining distribution for Individual 2

Most of the staining was classified as dark spotted or light matt (39.61% and 39.13% respectively). Both classifications refer to black-grey staining of either a mottled or matt appearance. The staining is consistent with manganese but has not been chemically tested. Staining occurred mostly on the anterior (37.20%) or posterior (32.37%) views, the bulk of the analysis was conducted on these surfaces, which explains the higher frequencies. There was only a marginal difference between the anterior and posterior staining, offering no suggestion of body position.

Staining occurred mostly on cranial elements (48.31%), with most affected by light matt staining. The staining distribution according to element group is reflective of bone representation for Individual 2. There does not seem to be a bias in staining across the body.

Sometimes it was unclear as to whether staining was overlying tufa or whether the tufa itself was grey. There were patches where tufa showed only partial colouration, suggesting that the staining occurred separately, however, it is important to note that some staining may be areas of dark tufa. A precise differentiation was not possible due to time limitations and the focus of this research, but deeper chemical analysis could be of interest for further geological study. Just over half (51.21%) of staining overlaid deposits. This is contrary to the finding in Individual 1 but for both bodies the difference is marginal. It is possible that staining occurred underneath deposits but was obstructed, however, both processes were likely occurring at a similar time and rate. The tufa and staining are consistent with the cave environment and suggest that the body was not exposed to another environment for long enough for taphonomic changes to occur. This supports the theory that the bodies in Cave Ha 3 were primary depositions.

### *11.2.7: Invertebrate Activity*

Invertebrate activity was observed on cranial elements, long bones, and ribs (irregular). All modifications were classified as pitting and the majority were multifocal. The cranial pitting was classified as random whereas the pitting to the long bones was evenly distributed across distal to joint and adjacent to joint. Anterior surfaces showed the highest frequency of pitting (73.68%), with the femur and frontal bone only showing modifications to the anterior surface. There was slightly higher coverage of tufa deposits to the posterior surface of the frontal bone,

possibly obscuring changes or providing protection, however the same was not observed on the femur. It is therefore possible, that the anterior surface had greater exposure, allowing easier access.

### *11.2.8: Animal Activity, Root Action, Butchery, and Weathering*

Individual 2 was minimally affected by weathering, with a maximum score of 1 according to Behrensmeyer (1978). No other changes associated with weathering were observed, including an absence of bleaching, cortical exfoliation, delamination, or patination. No root embedding or etching was observed on bone surfaces. This may be due to the tufa acting as a preservative, shielding cortical surfaces from weathering effects and roots, or because of the sheltered nature of Cave Ha 3. There was an absence of large animal activity, including carnivore, ruling out the possibility of carnivore accumulation. Evidence of deliberate processing or butchery was absent for all sub-adults.

All taphonomic changes to Individual 2 are consistent with a primary, whole-body burial.

## 11.3: Individual 3

### *11.3.1: Bone Representation*

Individual 3 had the lowest total bone representation for all individuals in Cave Ha 3, with a total representation of 5.22%. The highest represented group was long bones and there were limited cranial and irregular bones. Vertebrae were limited to two thoracic neural arches and there was a complete absence of hands and feet (figure 11.22).

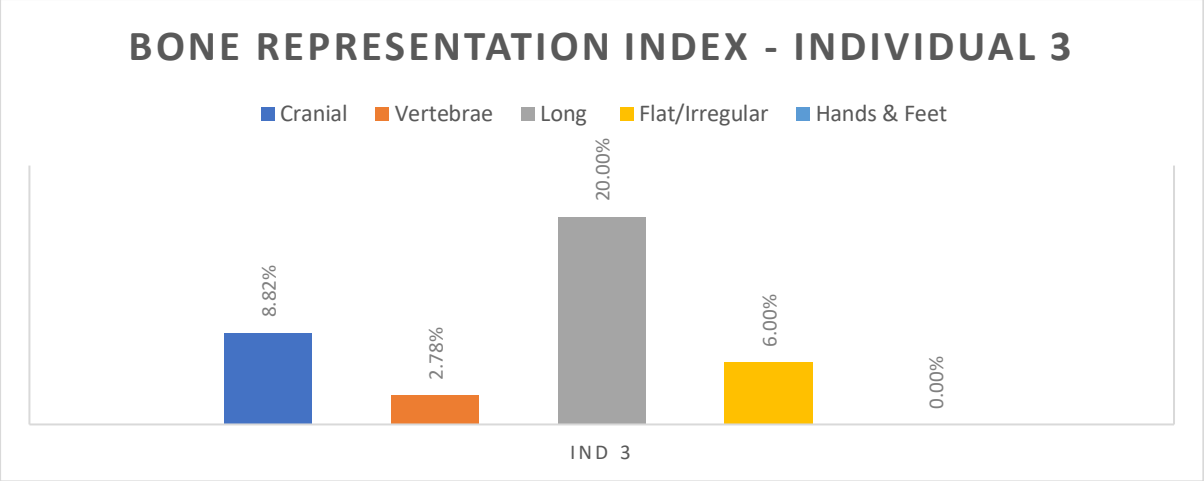


Figure 11.22: Graph showing bone representation for Individual 3, Cave Ha 3.

The representation for left elements (50.00%) was higher than rights (33.33%) and unilateral elements (16.67%).

All fragments assigned to Individual 3 were placeable in GIS. There were 19 cranial fragments that were assessed as juvenile but not identifiable to individual. It is therefore possible that there were more cranial fragments for Individual 3 that are currently unaccounted for.

The following discusses frequencies of modifications, all tables for Individual 3 taphonomy can be found in appendix 4.3.

### *11.3.2: Whole Body Taphonomy*

All fragments from Individual 3 were altered by taphonomic processes (figure 11.23).

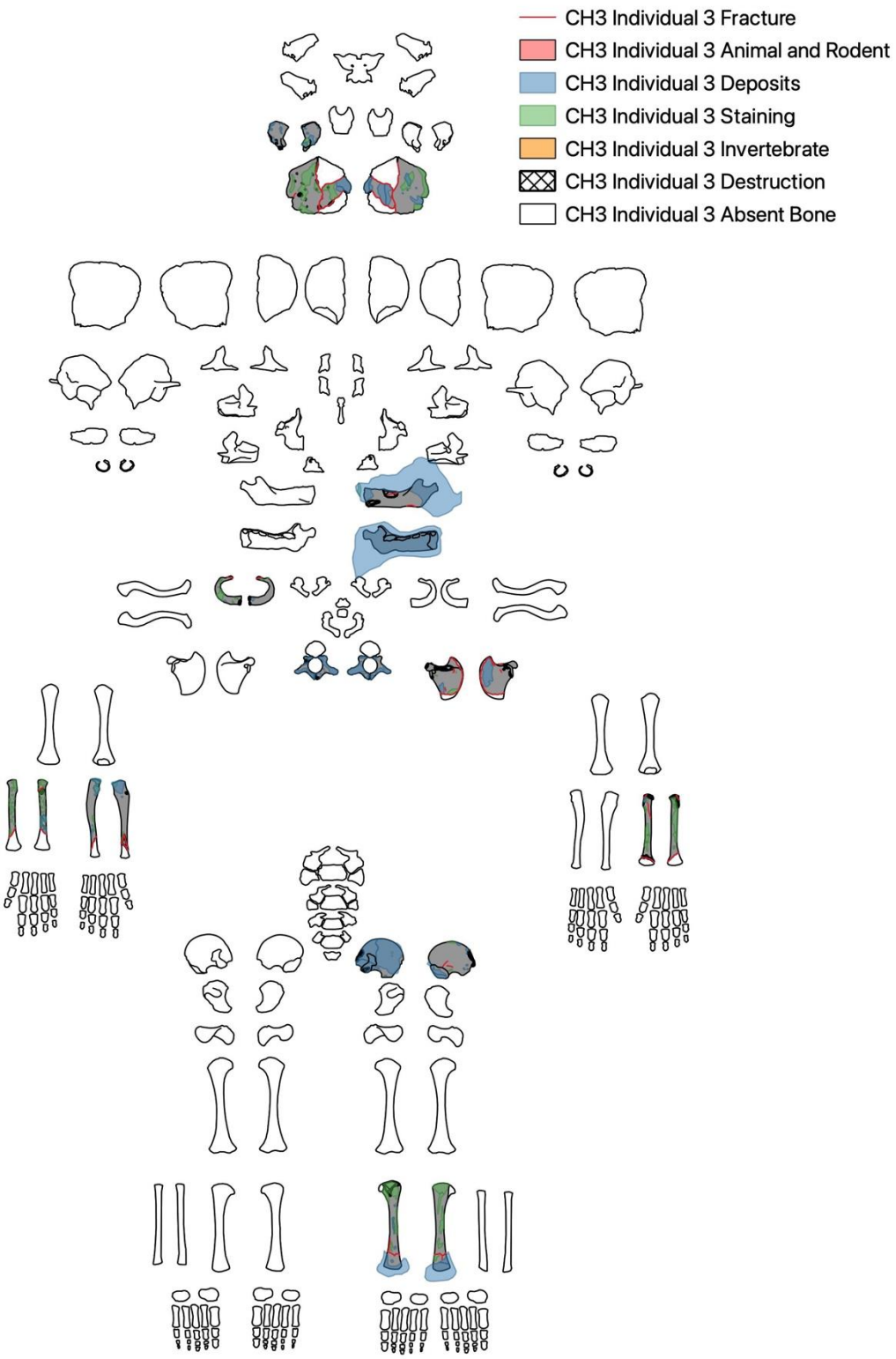


Figure 11.23: All taphonomic modifications across Individual 3.

Left, right and all anatomical planes were affected by taphonomy. Left and right sides were almost evenly affected by taphonomy (37.21% and 39.20% respectively), with the right showing slightly more. The remaining 23.59% of modifications were on unilateral elements. This is contrary to the slightly higher proportion of left sided elements recovered and the patterns of taphonomy showed in Individuals 1 and 2.

The anterior surface showed slightly higher observations of taphonomic modifications (42.19%) than the posterior surface (37.21%). No medial surfaces were analysed due to the nature of the recovered elements and superior surfaces showed higher counts than inferior (11.63% and 6.64% respectively). The following sections discuss the taphonomic modifications separately.

### *11.3.3: Destruction*

Two specimens from Individual 3 had peri-mortem crushing. Crushing occurred on the anterior and posterior views and on left and right elements (figure 11.24). There was nothing to indicate positional bias for Individual 3 based on crushing.

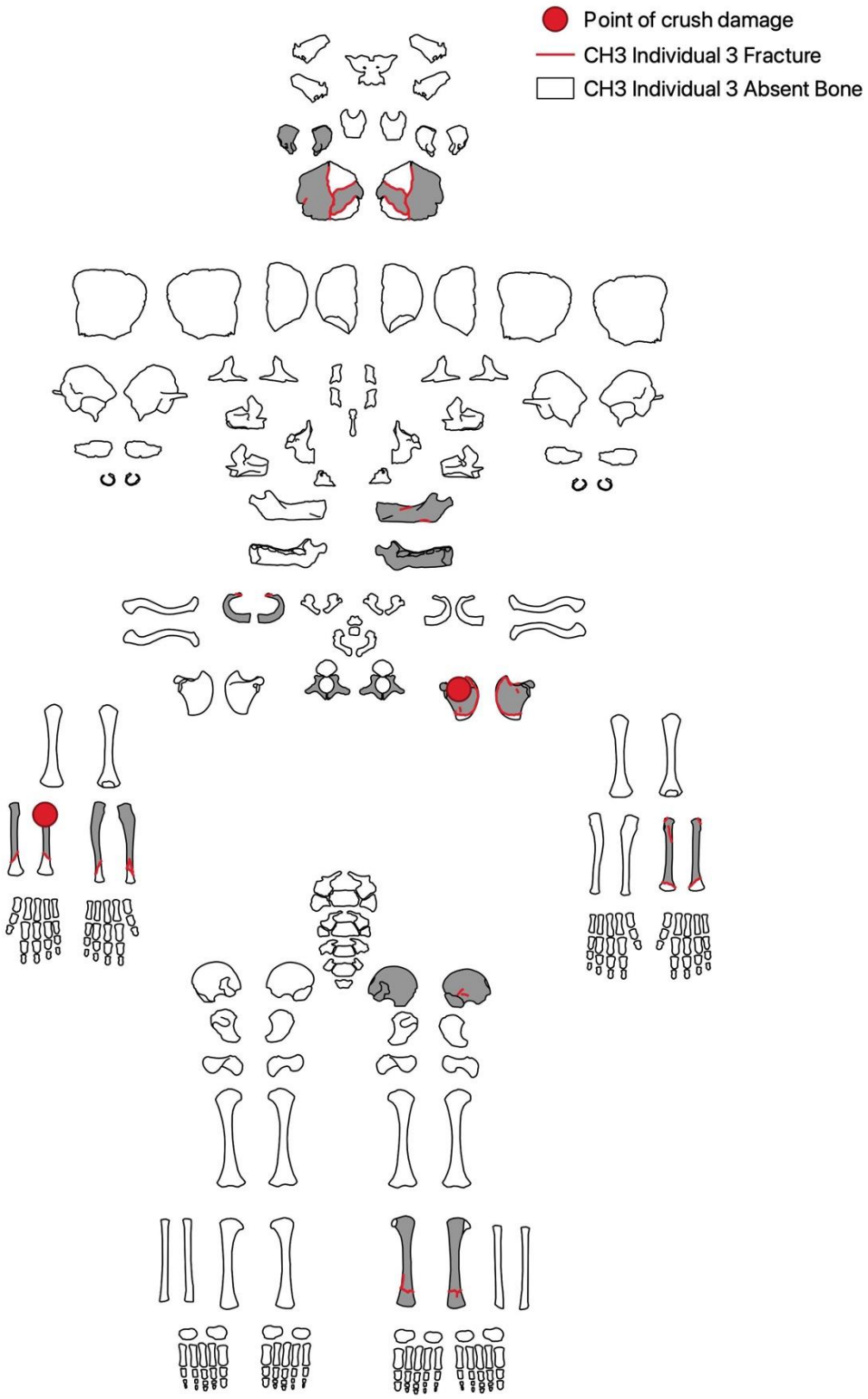


Figure 11.24: Crush distribution for Individual 3.

All damage, except the peri-mortem crushing, was consistent with sediment abrasion. Exposure of trabecular bone accounted for most damage (78.79%) with the majority occurring on the anterior surface. When all types of destruction were accounted for, most of the damage occurred on the anterior surface (51.52%). The higher frequency of destruction occurring on the anterior surface may be indicative of supine body position, however, such a low representation of elements (5.22%) limits analysis of Individual 3.

Most damage occurred to irregular bones (45.45%), of the 13 counts of damage on irregular bones, nine occurred on the scapula. This may be due to the more fragile nature of scapulae, particularly in infants.

### *11.3.4: Fractures*

Fracturing and cracking occurred across all fragments of Individual 3 (figure 11.25) except for the *pars lateralis*, which showed no fracturing and only a small area of damage (exposure of trabecular bone).

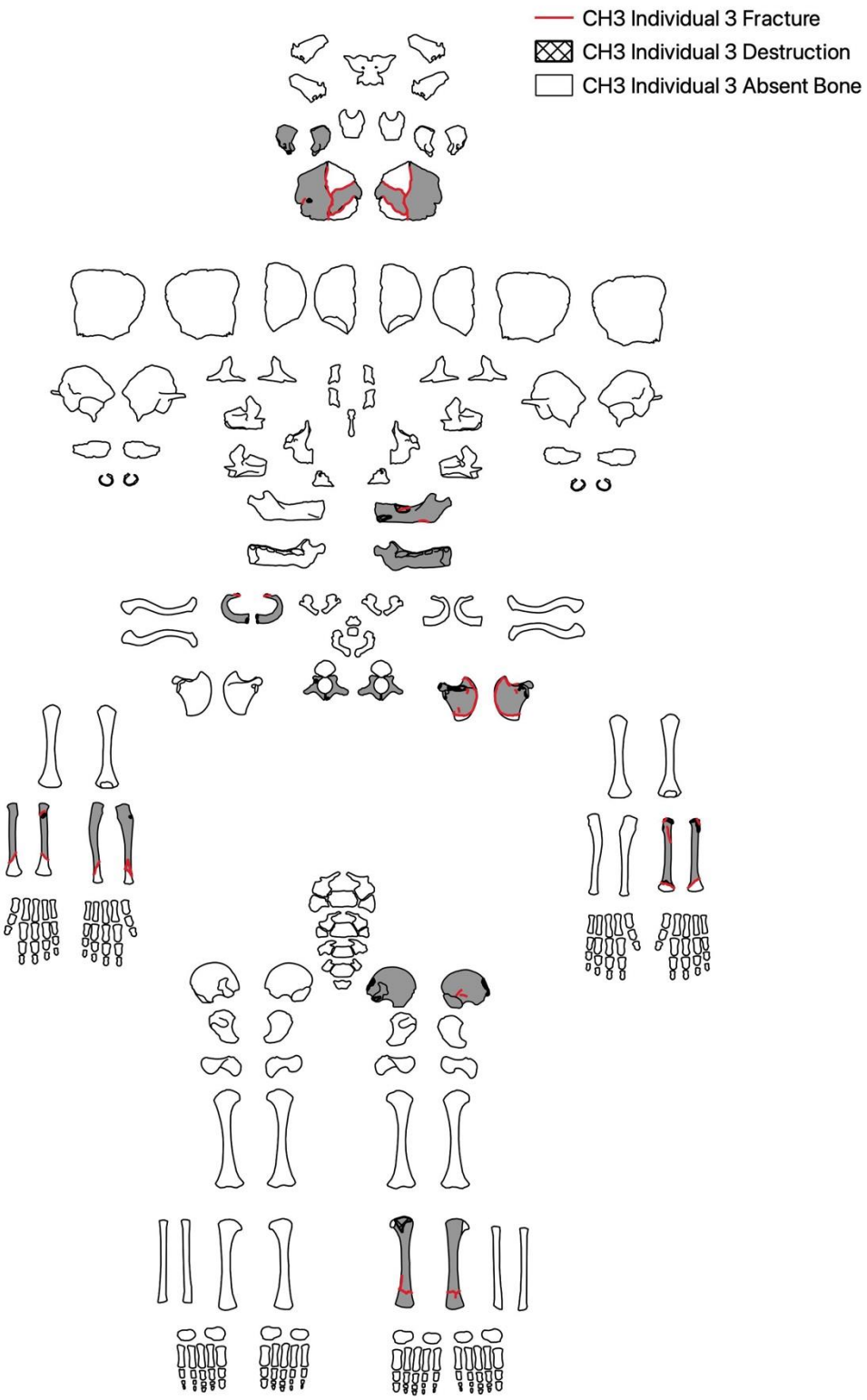


Figure 11.25: Fracture distribution for Individual 3

Incomplete cracking accounted for 39.90% of fractures, of those, two originated from areas of crushing and four originated from areas of damage.

The remaining fractures were all characteristic of post-mortem cracking, with rough margins and areas of lighter bone. Most fractures were classified as oblique dry (68.00%). There was an additional posterior fracture to the right ulna where the bone had split, leaving the anterior surface intact, otherwise, as expected there was an even distribution across surfaces.

Long bones showed the highest proportion of post-mortem fracture (52.00%). The cranium showed a relatively high frequency of fracturing (32.00%) despite only occurring on two elements. The occipital bone in infants is very thin and prone to breakage (Scheuer and Black, 2000). All fractures to Individual 3 were consistent with either peri-mortem crushing or post-mortem fracture patterns, with no indication of deliberate manipulation or antemortem trauma.

### *11.3.5: Tufa Deposits*

Tufa deposits were on all fragments, ranging from thin flakes to embedded fragments (figure 11.26). Embedded fragments accounted for 8.65% of tufa deposits, 66.67% of the embedding was to left fragments.

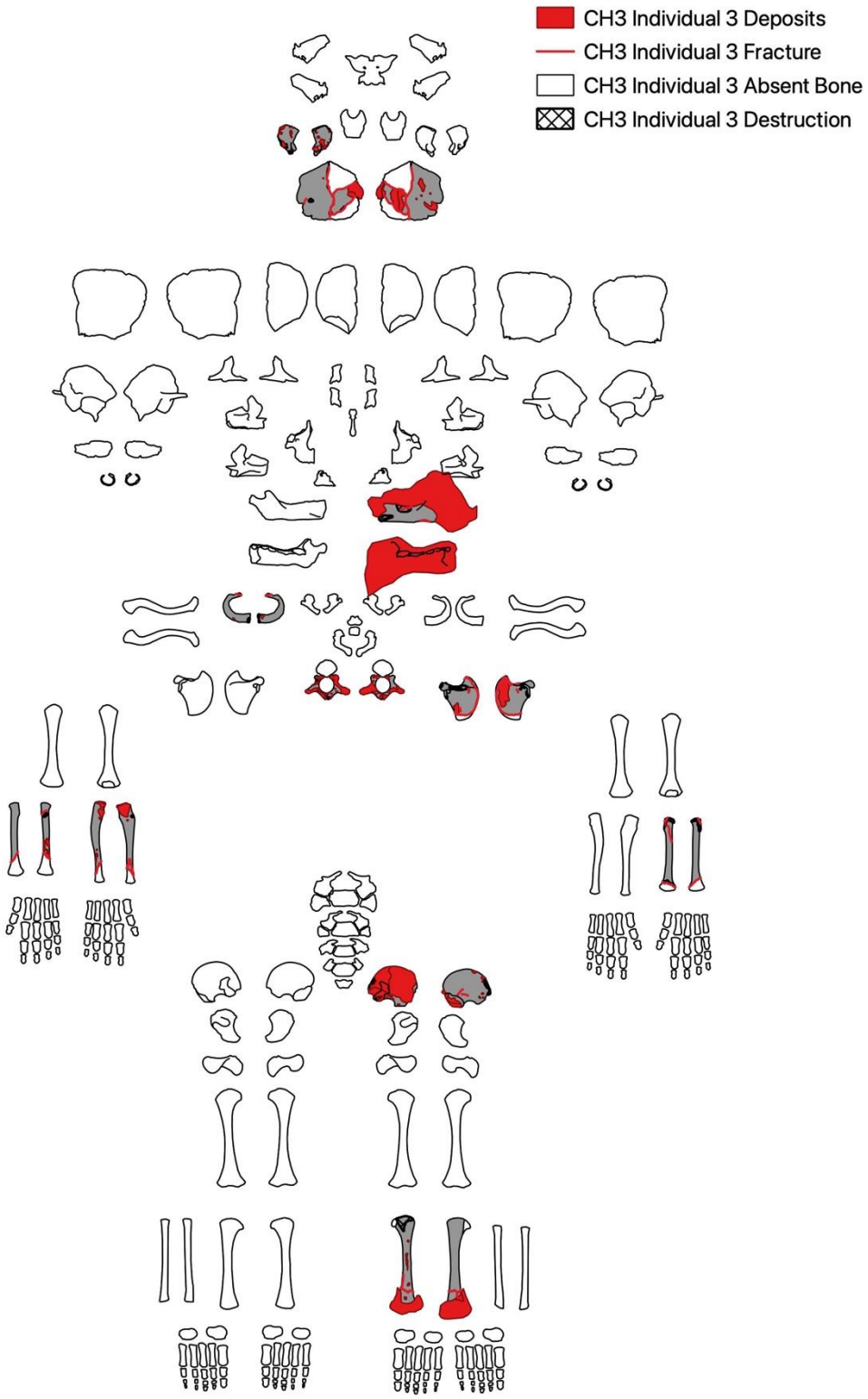


Figure 11.26: Tufa distribution for Individual 3.

A portion of mandible, with deciduous teeth showing, was completely embedded in tufa (figure 10.3, p.118). It was tentatively assigned to Individual 3. Attempts were made to x-ray the mandible, in the hope that an age assessment could be made, unfortunately the tufa was too dense to get a clear image.

Marginally more posterior surfaces had tufa deposits than anterior surfaces (36.54% and 32.69% respectively). Lateral and lingual surfaces were limited to the mandible and were reflective of the large build up described above. Cranial elements showed a slightly higher frequency of deposits (31.73%), despite there being fewer fragments associated to that group. Similarly, the vertebrae had high frequencies of deposits (23.08%) despite only consisting of two fragments. Both vertebral arches and the *pars lateralis* had several smaller spotted deposits, which would explain the higher counts.

There was nothing to indicate a positional bias for both grouped elements and views. The number of fragments associated to Individual 3 was minimal, potentially impacting analysis. There were no elements showing articulations as per Individuals 1 and 2 and the pattern of tufa deposits indicate that the body lay in the cave for an extended period.

### *11.3.6: Staining*

Staining occurring on all recovered elements (figure 11.27). There was only minimal staining to the mandible, and this occurred on the tufa deposit rather than bone surface. More staining occurred on right elements than left (55.75% and 36.28% respectively), despite there being more left fragments recovered. Embedded tufa was mainly on left fragments (66.67%) and may have protected the bone surfaces from staining, resulting in the observed bias.

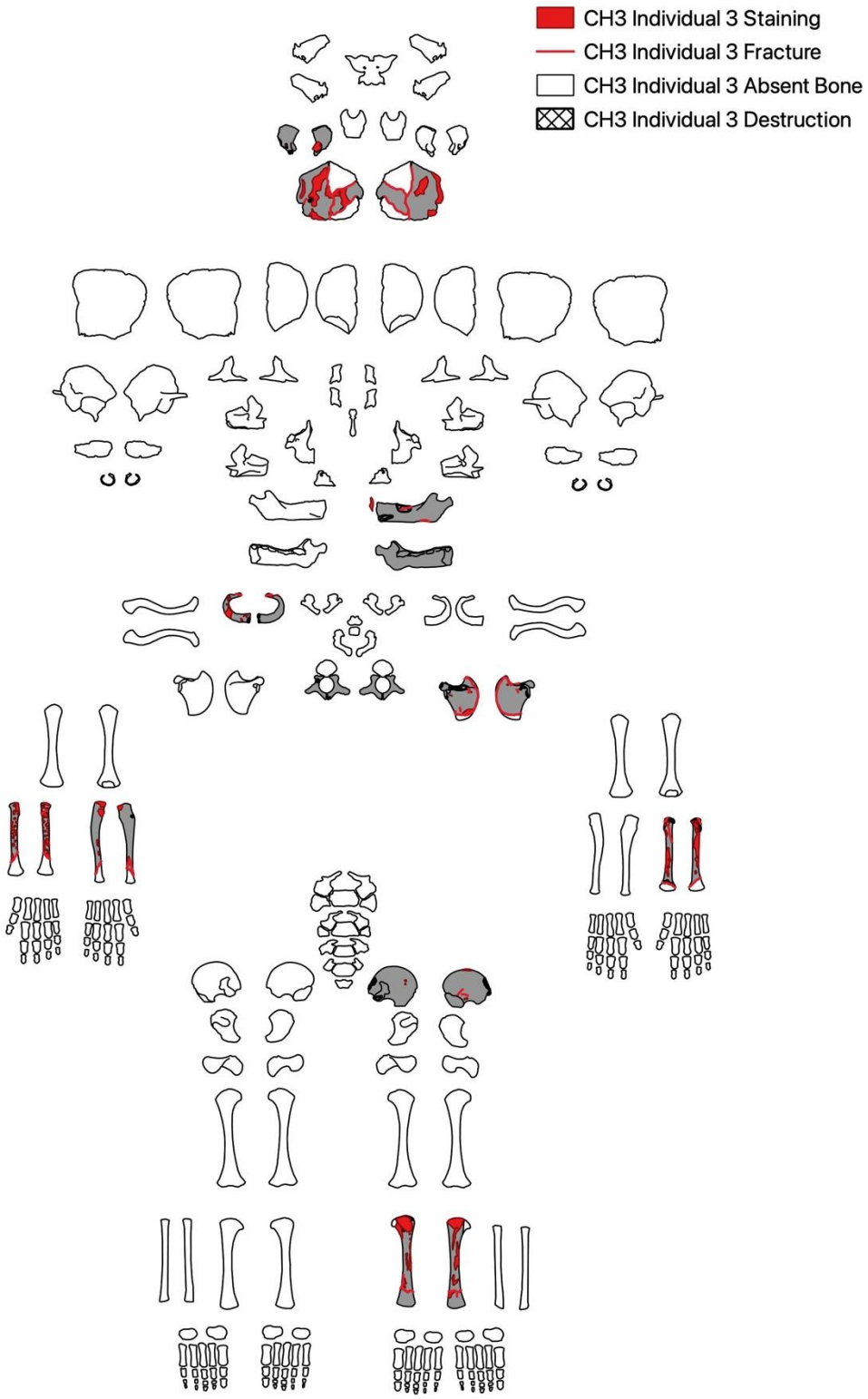


Figure 11.27: Staining distribution for Individual 3

Most staining was classified as light or dark spotted (30.97% and 38.94% respectively). Both classifications refer to black-grey staining of a mottled appearance. The staining is consistent with manganese but has not been chemically tested. Staining occurred mostly on the anterior (42.48%) or posterior (40.71%) views with no suggestion of body position. Light brown/orange staining was limited to the anterior surface but only accounted for 1.77% of the total staining.

Long bones showed the highest counts of staining (64.60%), with most affected by dark spotted staining. The higher counts may be a result of a large patch of spotted staining on the right radius.

Only 14.16% of staining was modifying other modifications, it is possible that further staining was obscured by tufa deposits. Staining was limited to black-grey and brown-orange consistent with manganese and iron-oxides. This, combined with the tufa deposits, is in accordance with Individuals 1 and 2. It is likely that both processes are occurring at the same time, with some deposits overlaying staining and vice versa.

### *11.3.7: Invertebrate Activity*

Invertebrate activity was only observed on the occipital, was all classed as pitting, and only occurred on the anterior surface. It is possible that other processes such as tufa deposits were protecting the bones from access.

### *11.3.8: Animal Activity, Root Action, and Weathering*

Individual 3 was minimally affected by weathering, with a maximum score of 1 according to Behrensmeyer (1978). No other changes associated with weathering were observed, including an absence of bleaching, cortical exfoliation, delamination, or patination. No root embedding or etching was observed on bone surfaces. This may be due to the tufa acting as a preservative, shielding cortical surfaces from weathering effects and roots, or due to the sheltered nature of Cave Ha 3. There was an absence of large animal activity, including carnivore, ruling out the possibility of carnivore accumulation.

The evidence for whole body burial is less clear for Individual 3 than Individuals 1 and 2. The absence of smaller, quick to disarticulate, elements are likely explained by biases in excavation

and destruction, rather than secondary burial. The taphonomy is homogenous, with little to indicate deposition position and there was no evidence of articulations as seen for Individuals 1 and 2. The taphonomy, however, is very similar to the other individuals, occurring across the body. Peri-mortem crushing supports that the deposition of the body occurred at a point when collagen remained. This, coupled with little to no evidence of weathering and the absence of animal activity, indicates that Individual 3 was likely a primary, whole-body deposition.

## 11.4: Individual 4

### *11.4.1: Bone Representation*

Individual 4 had a total representation of 9.21%. The highest represented group was long bones and there were limited cranial and irregular bones. No vertebra, hands, feet, or patellae were recovered (figure 11.28).

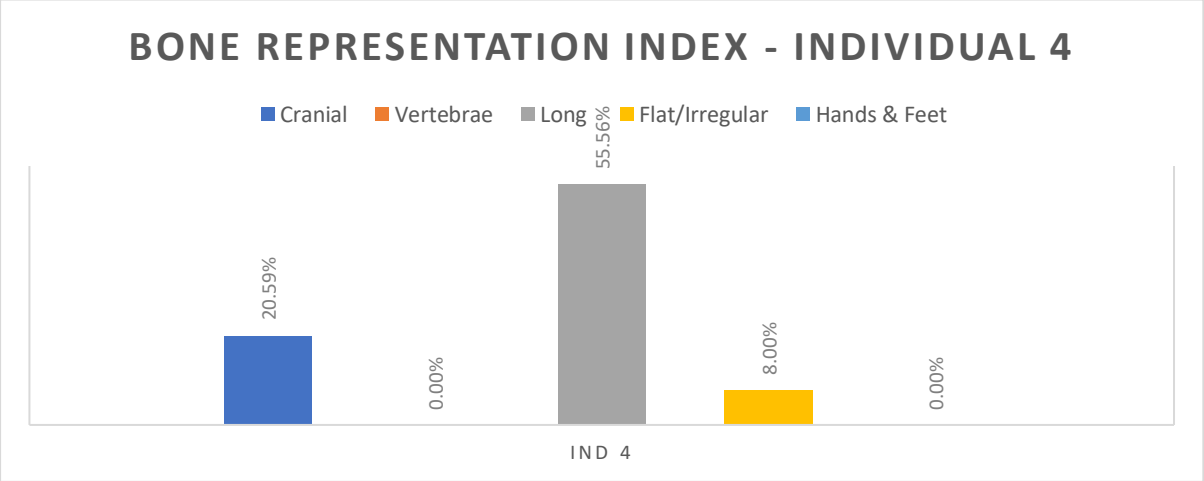


Figure 11.28: Graph showing bone representation for Individual 4, Cave Ha 3.

The representation for left elements (52.38%) was higher than rights (42.86%) and unilateral elements (4.76%). It is possible that there were cranial elements associated to Individual 4 included in the 19 non-associated fragments.

Five fragments (three cranial and two rib) were not recorded in GIS at body level due to uncertainty around position (table 4.4.1, appendix 4.4). These were recorded in the spatial analysis (section 12.13).

The following discusses frequencies of modifications, all tables for Individual 4 taphonomy can be found in appendix 4.4.

### *11.4.2: Whole Body Taphonomy*

All fragments from Individual 4 were altered by taphonomic processes (figure 11.29).

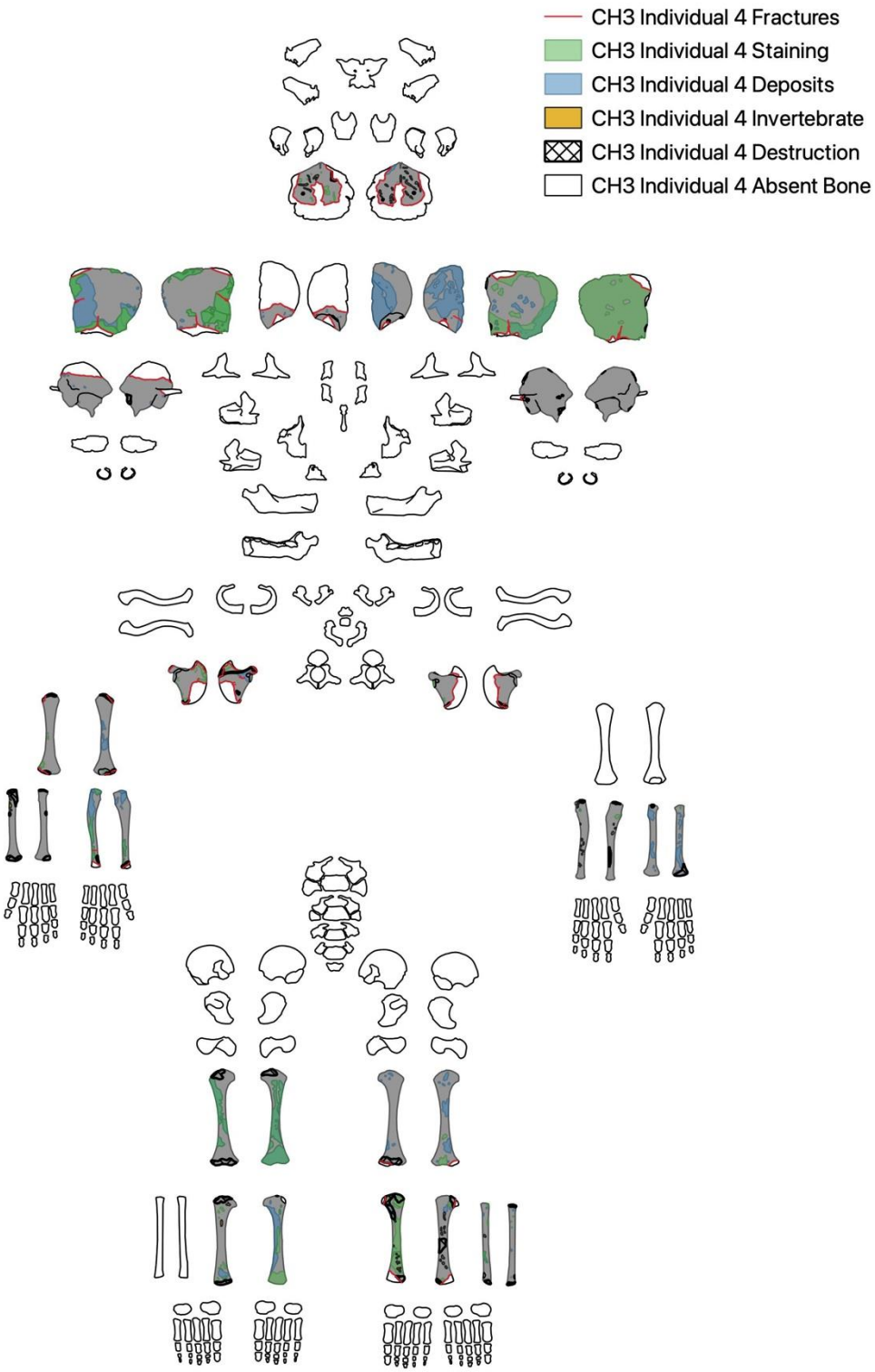


Figure 11.29: Image showing all taphonomic modifications across Individual 4.

Left and right anatomical sides and all planes were affected by taphonomy. The right was disproportionately affected by taphonomy (50.00%), despite having lower representation. The anterior surface showed slightly higher observations of taphonomic modifications than the posterior surface (39.54% and 36.61% respectively). Lateral surfaces were more effected than medial (15.90% and 7.95% respectively). No other planes were analysed for Individual 4 due to the fragments that were recovered.

### *11.4.3: Destruction*

Two specimens from Individual 4 exhibited crush damage indicative of peri-mortem destruction (table 4.4.2, appendix 4.4). The crushing occurred solely on right elements (figure 11.30) suggesting that the right side of Individual 4 was subjected to impact, while the left side remained protected.

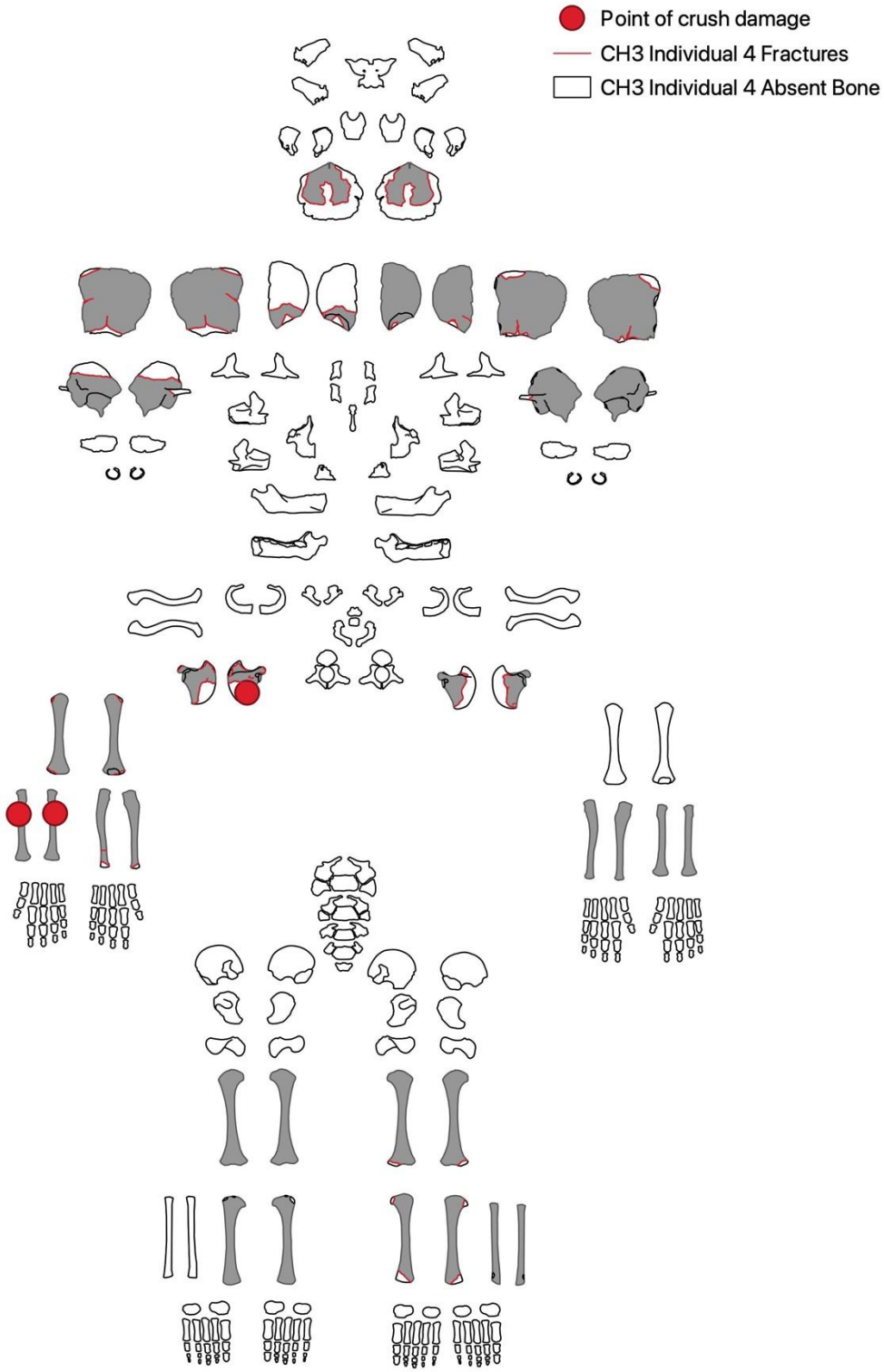


Figure 11.30: Crush distribution for Individual 4.

All post-mortem damage was consistent with sediment abrasion. Exposure of trabecular bone accounted for most damage (69.09%) with slightly more damage occurring to anterior surfaces (45.45%) than posterior (41.82%). No damage was recorded to medial surfaces, compared to 12.73% of total damage occurring to lateral planes. This follows previous trends, indicating a level of protection to the medial surfaces of bones. Analysis of medial and lateral surfaces was limited to the temporal bones. The absence of damage to the medial surface may be a result of remaining protected for longer due to its position in the cranium. There is otherwise nothing to indicate a bias in destruction according to anatomical view.

Most of the damage occurred to long bones (60.00%) and the distribution of damage is consistent with bone representation.

### *11.4.4: Fractures*

Fracturing and cracking occurred across most fragments except for both radii, the left ulna, left fibula, right tibia, and right femur (figure 11.31).

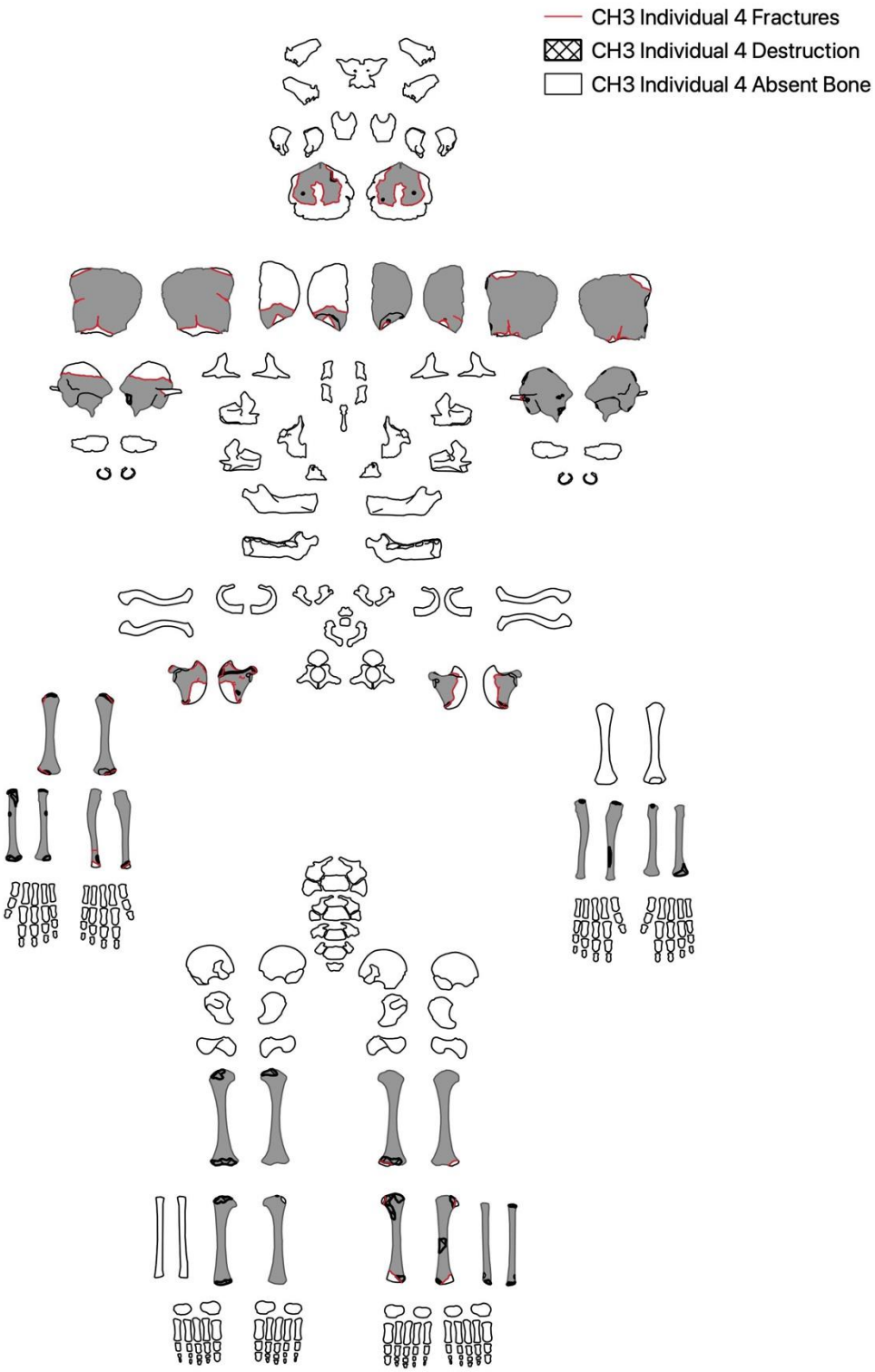


Figure 11.31: Fracture distribution for Individual 4

Incomplete cracking counted for 27.27% of fractures, of those, nine occurred around the crush site of the right scapula and one was a transverse crack to the base of the right ulna. The remaining incomplete fractures occurred to thin cranial edges.

The remaining fractures were all characteristic of post-mortem cracking, with rough margins and areas of lighter bone. Most were classified as oblique dry (47.62%) and were evenly split across the anterior (33.33%) and posterior (33.33%) surfaces. The lateral surface showed slightly more fracturing (19.05%) because fracturing to the zygomatic process was only visible in the lateral view.

The cranium showed the highest frequency of fracturing (52.38%), despite long bones having a higher representation. The fracture classifications for cranial bone were the most variable due to thinness causing breakage in multiple directions.

All fractures to Individual 4 were consistent with either peri-mortem crushing or post-mortem fracturing, with no indication of deliberate manipulation or antemortem trauma.

### *11.4.5: Tufa Deposits*

There were tufa deposits on most fragments except for the right radius and the left temporal bones. There were no embedded fragments and 77.61% were thin/flaked deposits (figure 11.32).

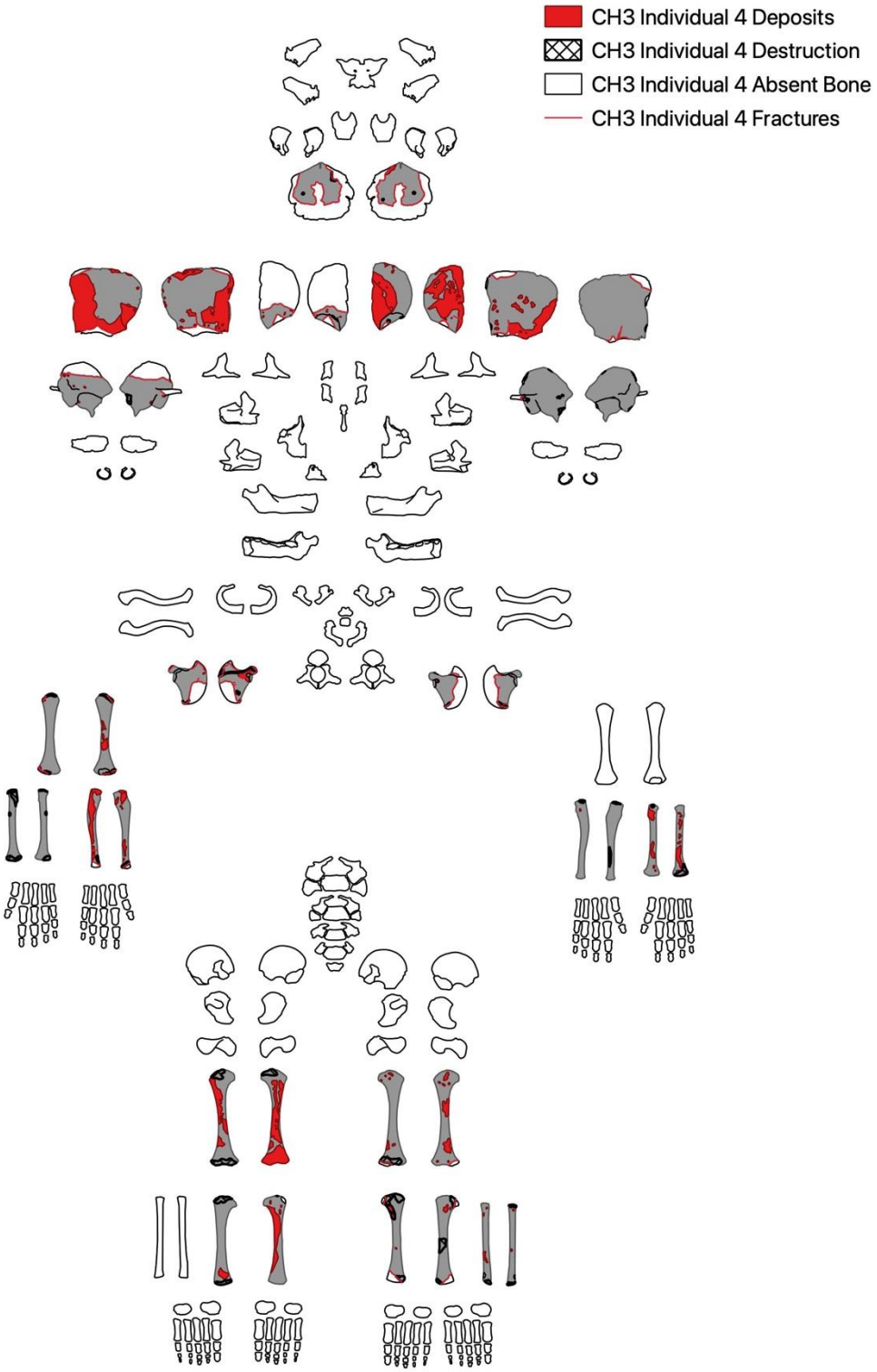


Figure 11.32: Tufa distribution for Individual 4

Posterior surfaces had the most tufa deposits (41.04%), compared to 30.60% to the anterior surfaces. This may indicate a supine position as with Individual 2. Again, the medial surface of the temporal bone showed the lowest frequency for deposits (8.96%), potentially due to being protected for longer while the body was articulated.

Long bones showed the highest frequencies for total tufa deposits (52.99%), with the distribution by element group consistent with bone representation.

Most thick/coated tufa deposits occurred on cranial elements (93.3% of all thick deposits). This suggests that the head may have been positioned in an area with more tufa. Sections 12.12 and 12.13 describe spatial distributions of taphonomy and elements and will explore whether there is any further evidence for this.

### *11.4.6: Staining*

Staining occurring on most fragments, except for the right radius and right temporal (figure 11.33). More staining occurred on right elements than left (60.36% and 31.36% respectively), despite there being more left fragments recovered. This was because the analysis looked at frequencies, when looking at visualisations there is a large area of staining to the left parietal and left femur. These would only count as one occurrence despite the extensive coverage.

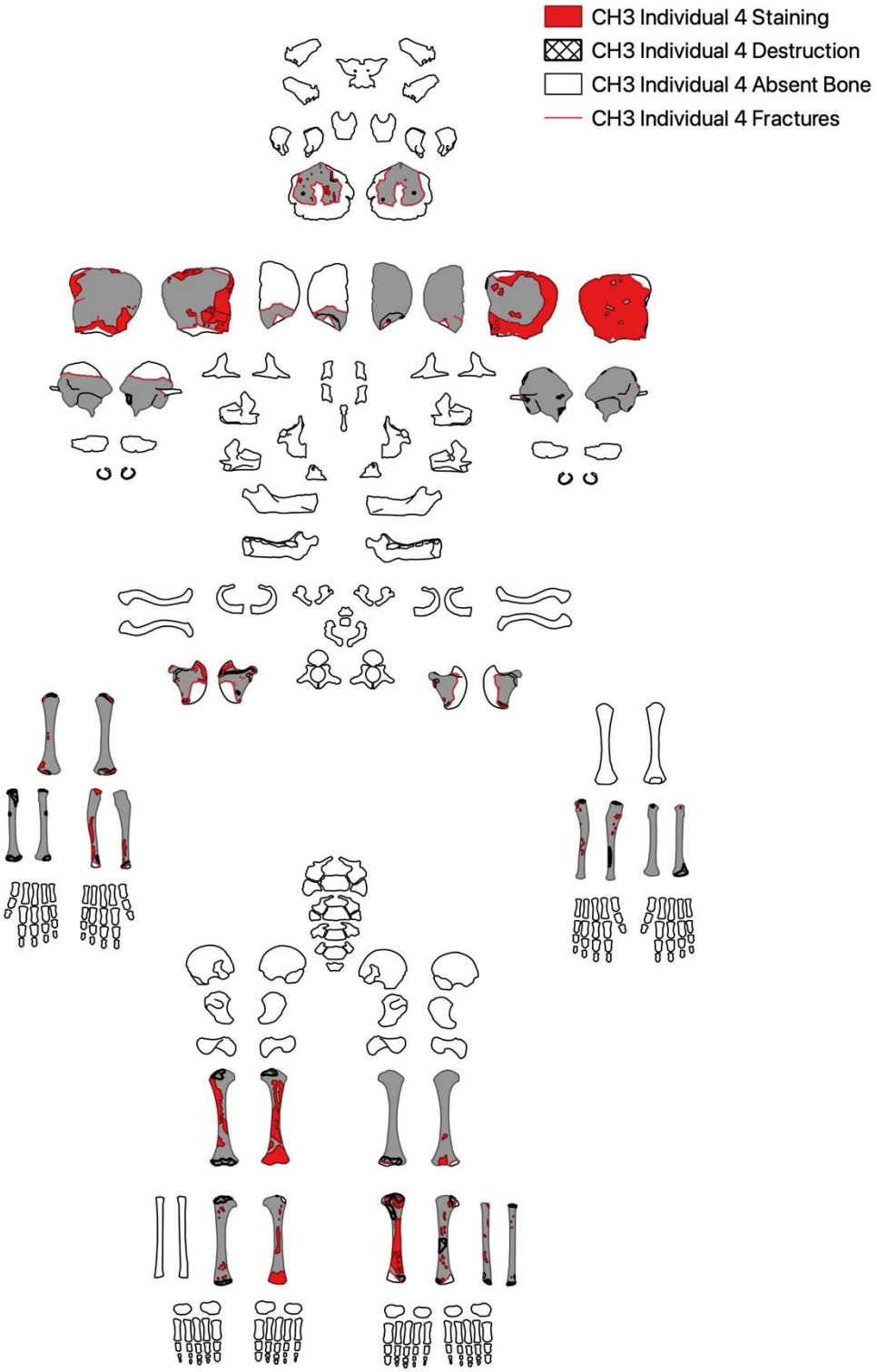


Figure 11.33: Staining distribution for Individual 4

Most of the staining was classified as light matt, light spotted or dark spotted, consistent with manganese. Staining occurred mostly on anterior surfaces (42.60%) compared to the posterior surfaces (25.44%). This may be a result of the higher frequency of tufa deposits occurring on the posterior surface, therefore providing protection from staining, rather than an indication of body position.

Long bones showed the highest counts of staining (46.15%), with most affected by matt, light staining and most of the darker staining occurred to cranial elements. The distribution of staining by element group is consistent with bone representation with no indication of body position.

Most staining was modifying other modifications (57.40%) however, this is a marginal majority and there is potential that tufa was obstructing underlaying staining or providing protection. It is likely that both processes occurred simultaneously. There were no other staining types identified and combined with the tufa deposits, the evidence for Individual 4 is in accordance with the rest of the assemblage.

### *11.4.7: Invertebrate Activity*

Invertebrate activity was observed only on cranial elements (63.2%) and long bones (31.6%). Modifications were evenly split between pits and furrows, with cranial elements only showing furrows. Cranial furrows were classified as random/diffuse, whereas most defects to the long bones were distal to the joint. The anterior surface showed slightly higher defects (52.38%) than the posterior surface (47.62%). There was slightly higher coverage of tufa deposits to the posterior surface of the frontal bone, possibly obscuring changes or providing protection. The difference is marginal and offers no significant indication of body position.

### *11.4.8: Animal Activity, Root Action, and Weathering*

Individual 4 was minimally affected by weathering, with a maximum score of 1 according to Behrensmeyer (1978). No other changes associated with weathering were observed, including an absence of bleaching, cortical exfoliation, delamination, or patination. No root embedding or etching was observed on bone surfaces. This may be due to the tufa acting as a preservative, shielding cortical surfaces from weathering effects and roots, or due to the

sheltered nature of Cave Ha 3. There was an absence of animal activity, ruling out the possibility of carnivore accumulation.

The evidence for whole body burial is less clear for Individual 4 than Individuals 1 and 2. The absence of smaller, quick to disarticulate, elements are likely explained by biases in excavation and destruction, rather than secondary burial. The taphonomy is homogenous, with little to indicate deposition position and there was no evidence of articulations as seen for Individuals 1 and 2. The taphonomy, however, is very similar to the other individuals, occurring across the body. Peri-mortem crushing supports that the deposition of the body occurred at a point when collagen remained. This, coupled with little to no evidence of weathering and the absence of animal activity, indicates that Individual 4 was likely a primary, whole-body deposition.

## 11.5: Assemblage Taphonomy

Retention of articulations and patterns of destruction provide strong evidence for whole body burials for Individuals 1 and 2. The evidence is more challenging to interpret for Individuals 3 and 4, however, the homogeneity of the taphonomy across all individuals and the absence of evidence of other mechanisms of accumulation indicate they were also whole-body depositions. The following section discusses how the taphonomy is spread spatially within the cave to further explore the depositional narrative.

# CHAPTER 12: CAVE HA 3 SPATIAL ANALYSIS

## 12.1: Assemblage - Distribution of Fragments

Each fragment was traced back to a 0.5 x 0.5 m grid square. This was translated from the original imperial measurements. The number of identified specimens (NISP) for each grid square was expressed as a polygon rather than a point to reflect the level of precision of the data. Figure 12.1 shows the distribution of all the human remains recovered from Cave Ha 3.

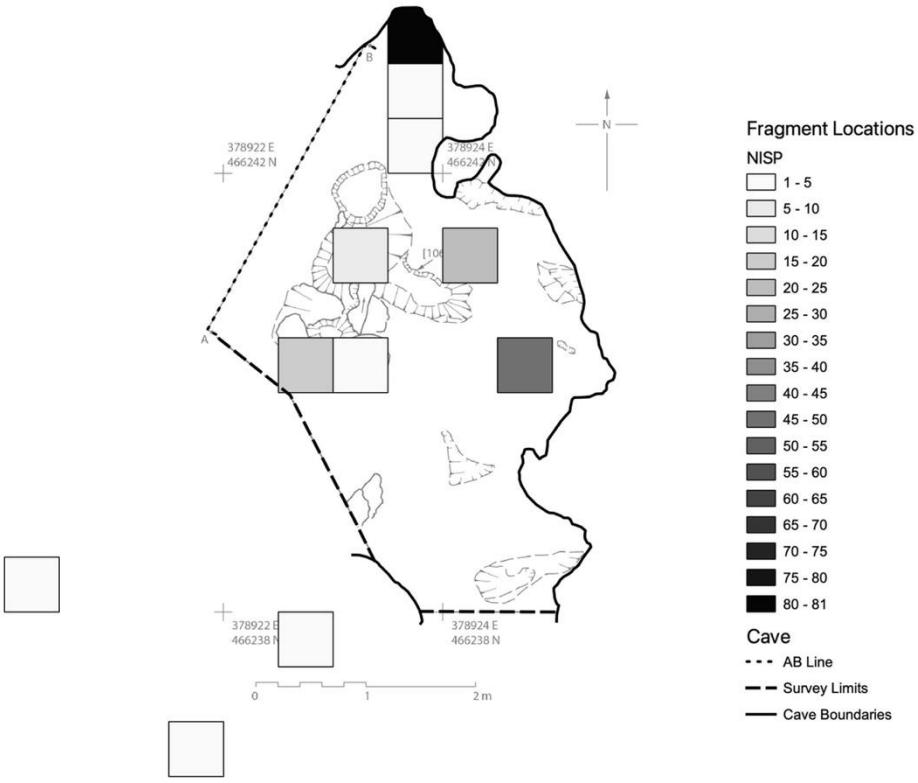


Figure 12.1: Distribution of fragments according to NISP counts.

The highest concentration of elements was towards the back recess and the fewest fragments were recovered to the southwest of the cave. While it appears that there are fragments recovered outside of the cave area, this is due to the map being produced from a survey taken in 2022. The extent of surveying was limited to a smaller area of excavation, the original excavation extended beyond these boundaries and are reflected in the find locations. The

distribution of fragments according to element group will be discussed before exploring element group and distributions of taphonomy per individual.

## 12.2: Assemblage – Element Distribution

The locations of the original depositions are unknown. It is possible that the concentrated areas of fragments are where each body was placed, however the concentrations may be more reflective of recovery than placement. There were 81 fragments where the find location had to be estimated using archive records which will have created a bias in the distribution data. Figure 12.2 shows the distribution of fragments according to element group and the relative frequencies.

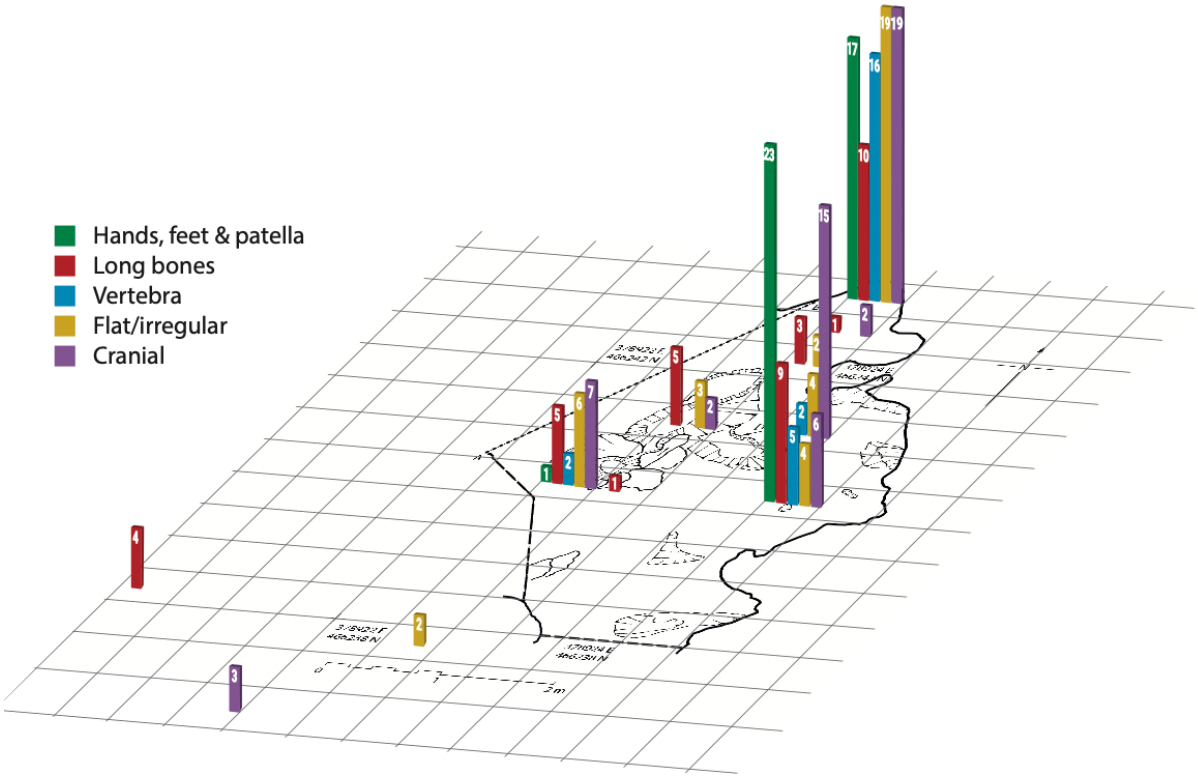


Figure 12.2: Distribution of fragments according to element group for all individuals.

When all individuals are combined, element groups are dispersed around the cave with no apparent significance according to element types. The next section will explore movement of skeletal elements per individual and the distribution of taphonomic modifications, with the view of highlighting potential agents for fragment movement and sequence of events post deposition.

## 12.3: Individual 1 – Distribution of Fragments

Fragments from Individual 1 were concentrated within the back recess (figure 12.3), which is consistent with archive reports.

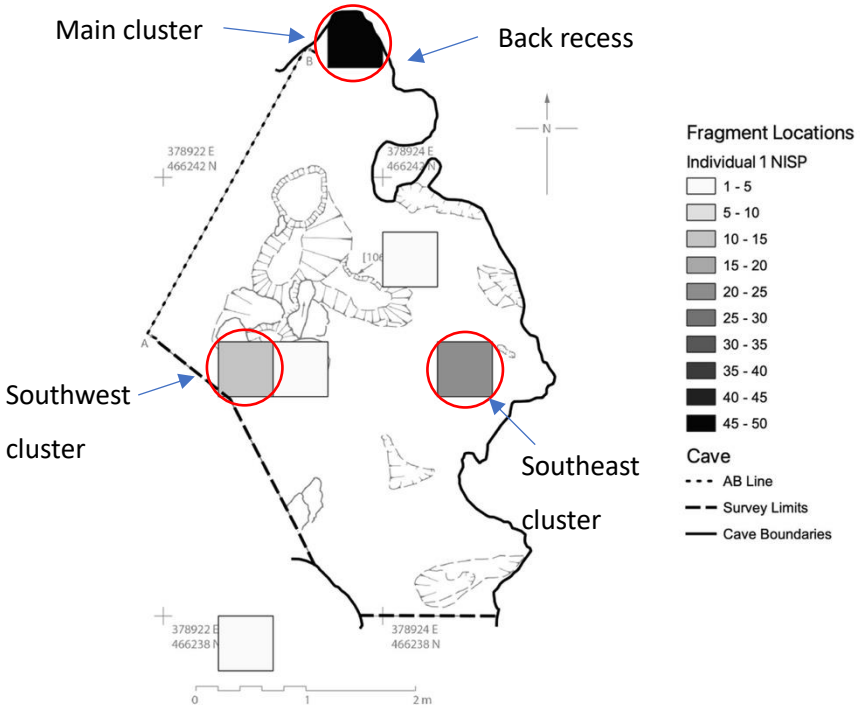


Figure 12.3: Distribution of fragments from Individual 1 according to NISP counts.

Two smaller clusters were recovered to the southeast and southwest of the recess, with the southeast cluster the larger of the two. For ease of discussion the clusters will be referred to as they are labelled in the figure above.

## 12.3: Individual 1 - Element Distribution

There was displacement of all element groups for Individual 1 (figure 12.4).

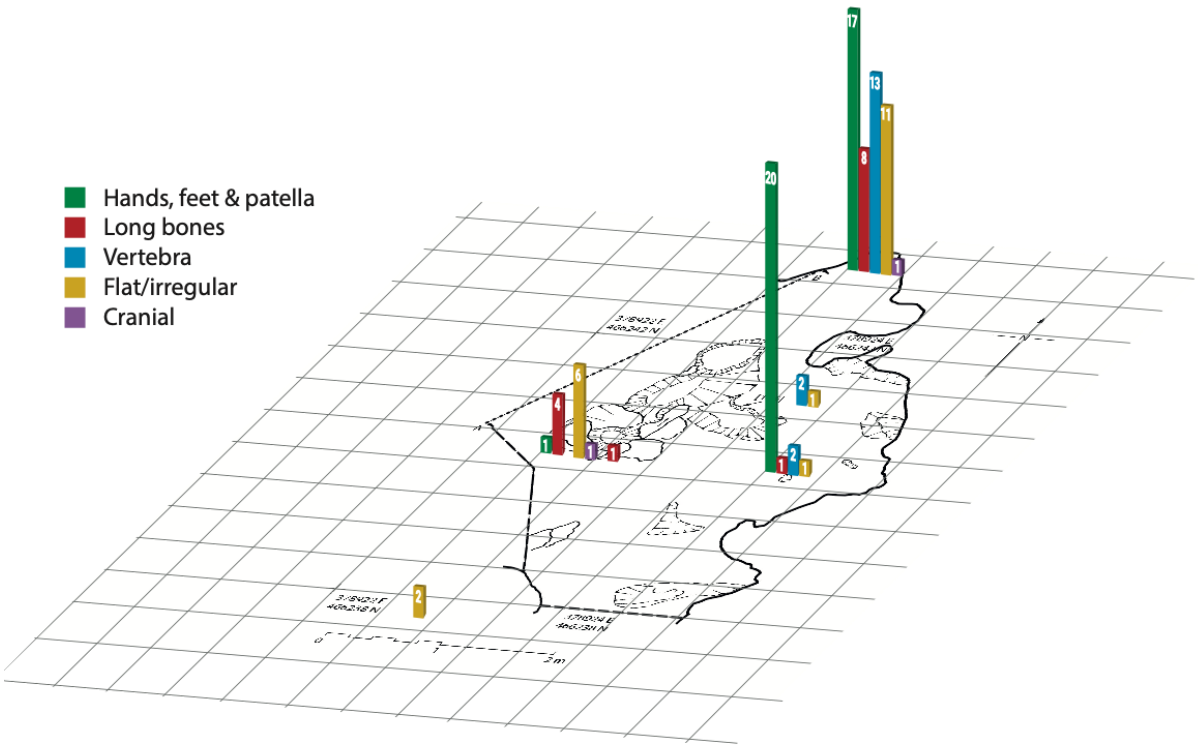


Figure 12.4: Distribution of fragments according to element group - Individual 1.

Based on clustering it could be inferred that Individual 1 was deposited towards the back recess and assessments of movement have been attempted based on this inference. Multi-directional movement has also been explored due to the possibility that the clusters are a result of excavation bias and limitations of the archive.

### *12.3.1: Crania*

Cranial elements were limited to two fragments: a portion of occipital and the mandible. The temporal-mandibular joint is a labile joint, and therefore understood to disarticulate sooner in the decomposition sequence (Mickleburgh and Wescott, 2018). Whether it disarticulates before or after the cranium from the cervical spine is variable and in cases where it disassociates afterwards, displacement often occurs together (Duday, 2009). The mandible was recovered from the main cluster, away from the occipital fragment (figure 12.5).

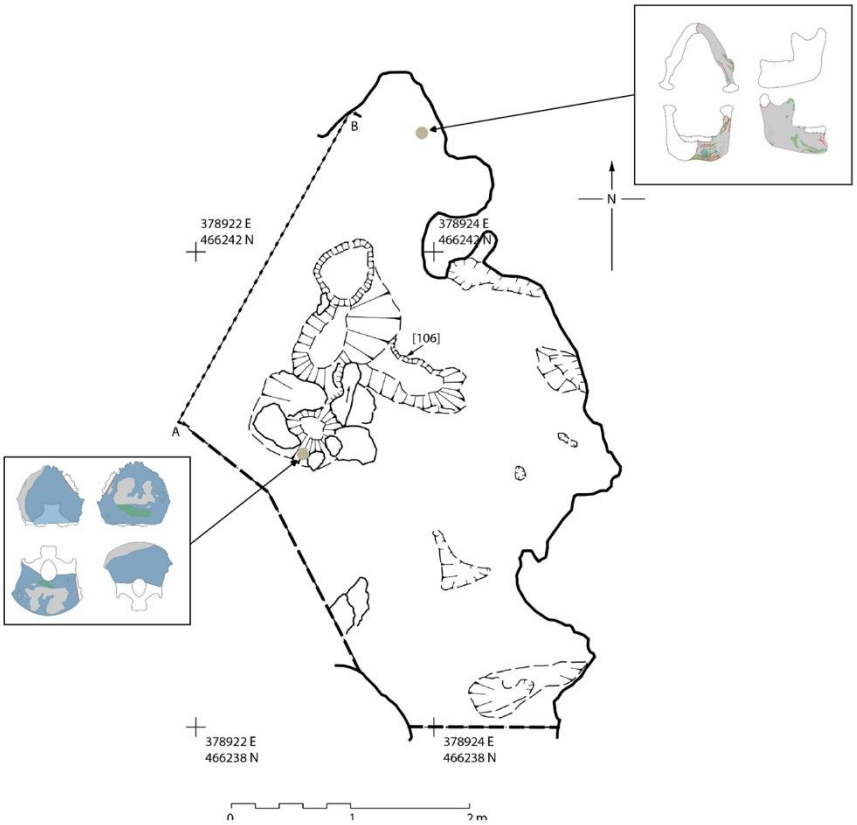


Figure 12.5: Dispersal of the occipital in relation to the mandible – Individual 1.

If the main cluster is the point of original deposition, then this indicates that the mandible disarticulated prior to the movement of the cranium. Without the rest of the crania, it is difficult to infer whether the displacement is a result of the more rounded cranium rolling away from the mandible (Boaz and Behrensmeyer, 1976; Roksandic, Haglund and Sorg, 2002). It is possible that other cranial fragments remain in situ and that only the occipital was displaced.

### *12.3.2: Vertebra*

Most of the vertebrae were recovered from the main cluster. Two thoracic vertebrae were found in the southeast cluster. The first (atlas) and second (axis) cervical vertebrae were recovered away from the rest of spinal column, along with a portion of right pelvis. These were the only fragments recovered in this location that were associated to Individual 1. The atlas was embedded in calcite with the axis. It is understood that detachment of the cranium usually occurs between the axis and third, or third and fourth vertebrae first. Detachment between the atlas and axis can occur early (Roksandic, Haglund and Sorg, 2002; Duday, 2009)

and while Duday (2009) posits that this will usually occur before detachment at the atlantooccipital joint, Roksandic, Haglund, and Sorg, (2002) argue that the cranium frequently separates first. The embedding of the atlas and axis together indicate articulation; however, they were found away from the occipital fragment (figure 12.6). It is likely that disarticulation at the atlantooccipital joint occurred first, resulting in movement of the occipital bone away from the atlas and axis.

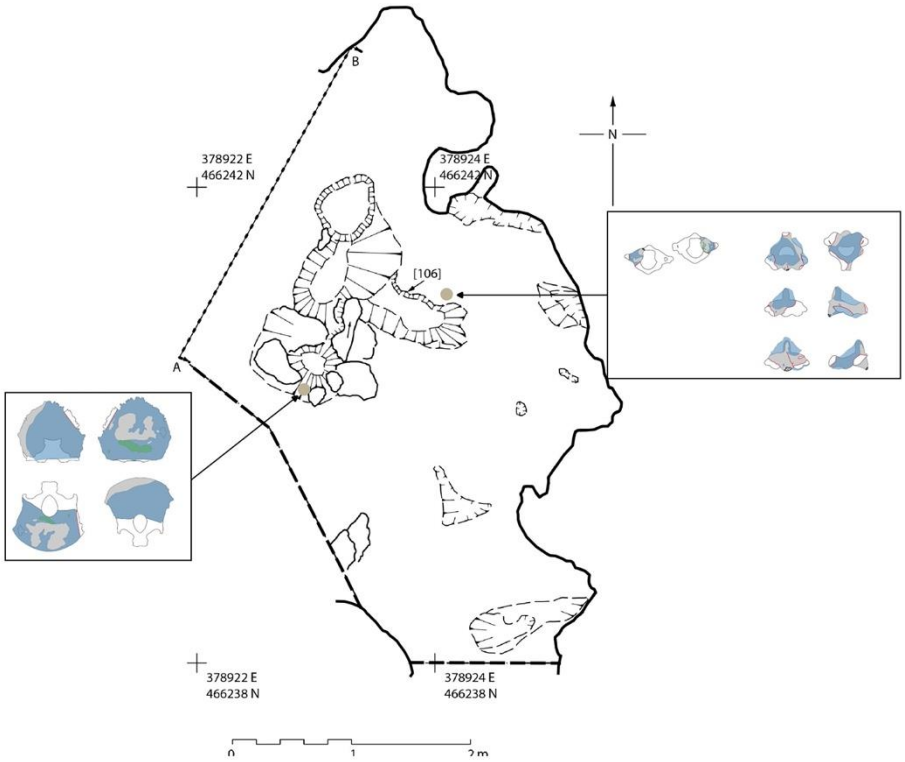


Figure 12.6: Dispersal of the occipital in relation to the atlas and axis – Individual 1.

Reports indicate that fragments were left in situ, it would be worth re-exploring these key areas to check for other fragments of the cranium to further understanding of movement.

### *12.3.3: Long Bones*

Most of the long bones were concentrated towards the back recess. The right clavicle was recovered in two sections (CH3.12.113 and CH3.12.80) and was recovered from the southwest cluster. The right radius was also fractured into two, however the distal portion (CH3.73.220) was recovered in the southeast cluster, away from the main cluster of fragments. This

indicates fracture timing, with the clavicle fracturing after movement and the radius fracturing beforehand (figure 12.7).

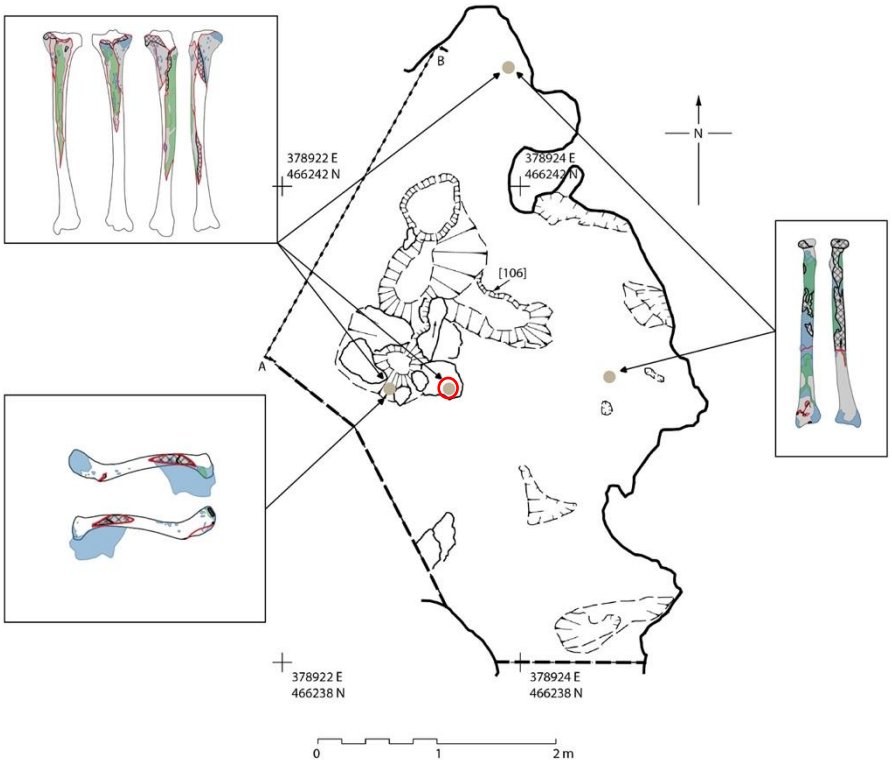


Figure 12.7: Distribution of long bone fragments – Individual 1.

The smashed tibia was recovered in three fragments, the distal portion was absent, and all three fragments were dispersed. One portion was recovered away from any other fragments (red circle, figure 12.7), one was in the main cluster and the third was in the southwest cluster. The absence of defleshing evidence was discussed in section 11.1.7 and indicates that the tibia was likely processed at the point of skeletonisation. If the main cluster was the point of burial, it is possible that the bone was processed in-situ and the other fragments have subsequently moved due to other taphonomic processes. Alternatively, if the tibia was removed to be processed elsewhere, an effort could have been made to place the fragmented element back with the main burial, however this is unlikely due to the dispersal of the other fragments.

### *12.3.4: Flat/Irregular*

Four fragments of left scapula were recovered. Three of these were recovered from the southwest cluster along with a single fragment of right scapula. The other fragment of left scapula was found in the main cluster (figure 12.8, marked with blue circle). This indicates that movement occurred after fracturing. A right section of pelvis was with the atlas and axis and the sacrum was found approximately 3.5 m southwest from the pelvis, and 5.2 m from the main cluster. This was the furthest fragment from the main cluster for Individual 1.

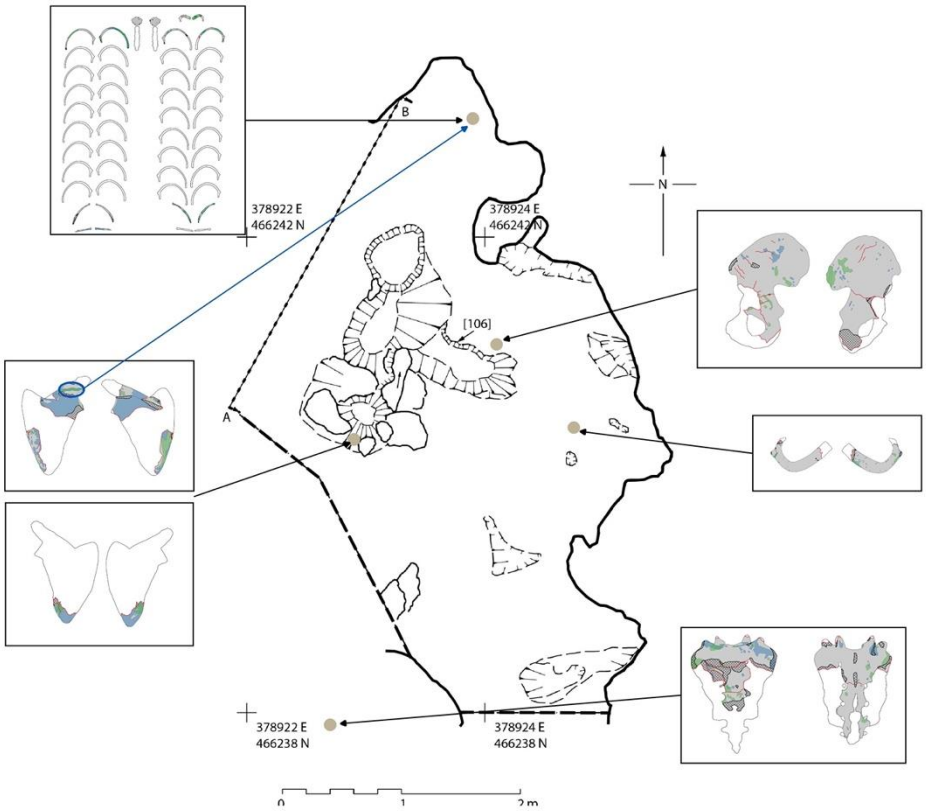


Figure 12.8: Distribution of irregular bones – Individual 1

The sacrum is low density (Boaz and Behrensmeyer, 1976) and "considerable displacement" has been observed (Duday, 2009, p. 40). It is likely that due to its low volume the sacrum is more susceptible to floating and the movement seen here may have been due to fluvial or rainwater action. The first right rib had moved to the southeast cluster and two ribs (one left, one right, un-sequenced) had moved to the southwest cluster. The remaining ribs where all located in the main cluster along with the sternum. The ribs and sternum are also described

as elements that are subject to displacement due to small volumes (Duday, 2009), however appear to have undergone minimal displacement.

### *12.3.5: Hands, Feet & Patellae*

All fragments from the left and right hands were found in the main cluster, except for a fourth, left metacarpal and a proximal phalange located in the southeast cluster. All fragments of the left and right feet were found in the southeast cluster except for a second, left metatarsal and the left talus which were recovered from the main cluster, and a left calcaneus, which was recovered from the southwest cluster (figure 12.9).

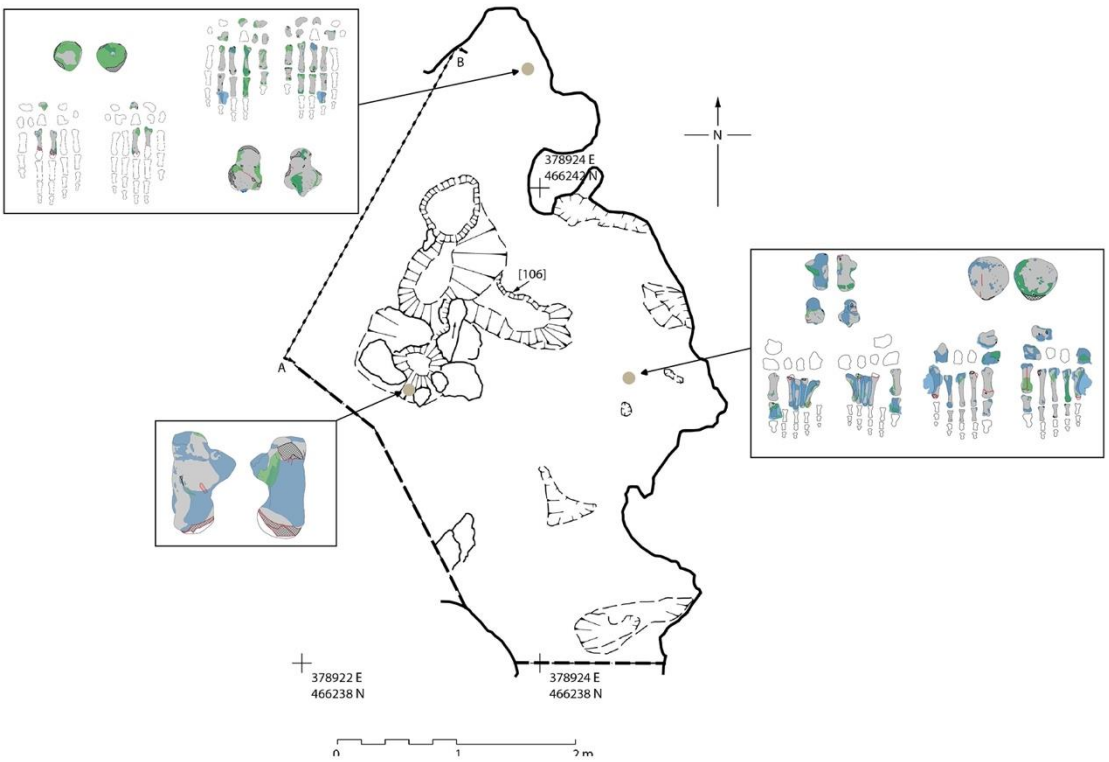


Figure 12.9: Distribution of hands, feet, and patellae - Individual 1

The right foot was recovered articulated, bound by calcite. This indicates that the foot was whole when deposited and would have retained this articulation long enough for calcite to form around the foot. There was no indication of manual disarticulation on the right talus, as would be expected with human processing (Bello *et al.*, 2016). The lower right limbs were absent however, and it is possible evidence of disarticulation was present on the distal ends of the tibia. Lamerton and colleagues (2021) found during a case study assessing skeletal

movement during decomposition that there was complete separation of a single metacarpal, despite retention of articulation of the remaining hand. This may explain the displacement of single elements, while other elements have moved in articulating groups. Anatomically related bones that have moved are likely to have moved prior to the disappearance of all soft tissue, conversely bones recovered away from articulating counterparts indicate movement post-decomposition and disarticulation (Haglund, 1997). Figure 12.10 shows three possible scenarios to explain the movement of the feet, assuming that the main burial is located at the back recess.

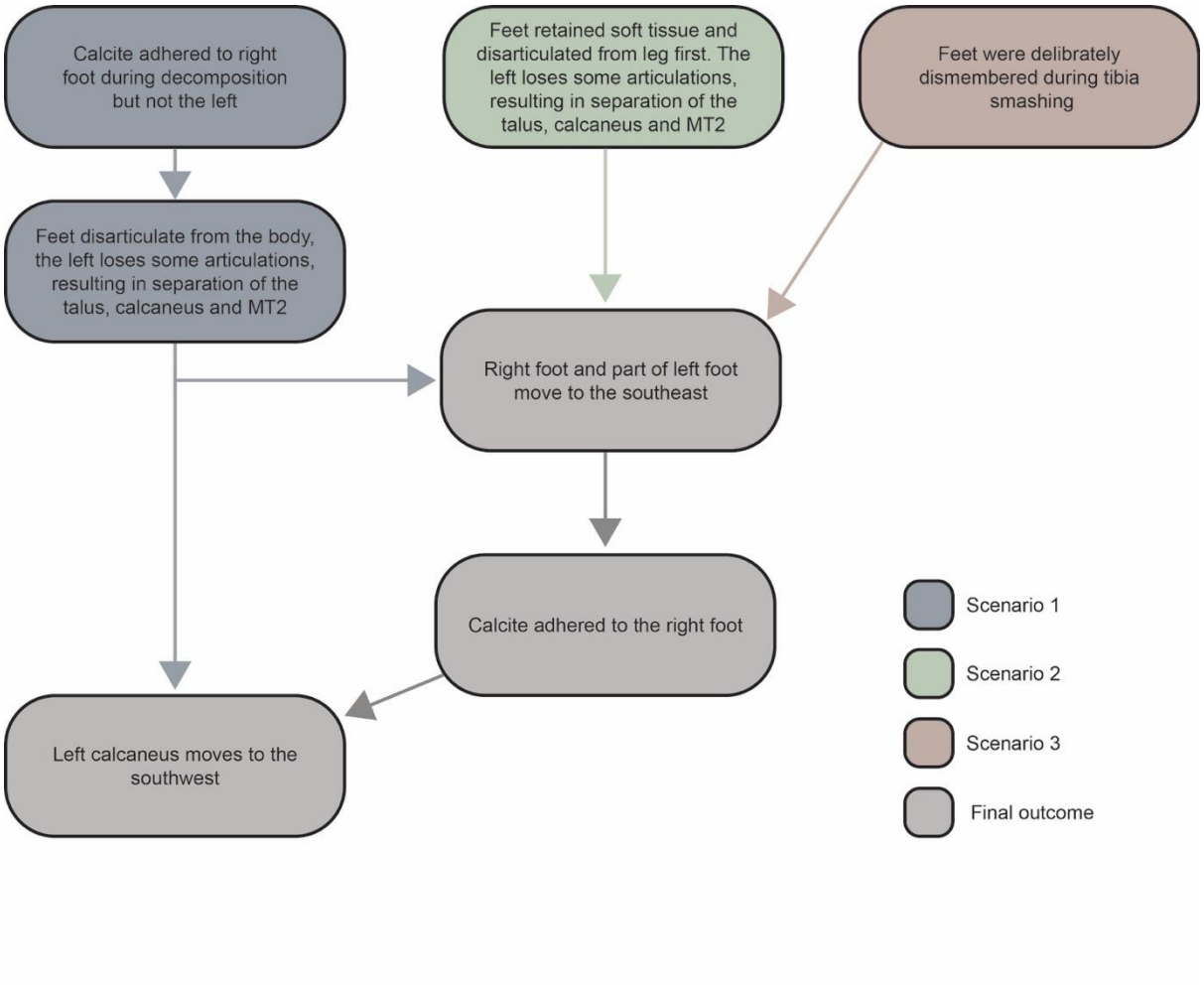


Figure 12.10: Possible sequences of movement for elements of the feet – Individual 1.

Due to the absence of evidence of deliberate dismemberment, it is considered most likely that the feet moved while retaining some soft tissue disarticulations, with tufa adhering after displacement. While it is possible that the foot was embedded prior to movement the nature of the tufa would make this difficult.

## 12.4: Individual 1 - Taphonomic Distribution

### *12.4.1: Fracturing*

Fracturing occurred on fragments recovered from all areas of the cave. There was no significance to where fragments with incomplete fractures or peri-mortem breaks occurred. Refitting of fragments allowed for exploration around movement. Refitting elements that were fractured but recovered from the same location indicate movement prior to breakage. Refitting fragments recovered in different locations indicate movement post breakage. Fragments where this has occurred are discussed above and there does not appear to be any significance around which fragments fractured before or after movement, except for the smashed tibia.

### *12.4.2: Destruction*

Destruction occurred in all areas of the cave where fragments of Individual 1 were recovered. Damage classified as 'exposure of trabecular bone' occurred across all locations, whereas fragments that exhibited cortical removal without exposure were concentrated to the main and southeast cluster. Crush damage was more spread out than cortical removal and did not seem to occur in a specific area (figure 12.11). Due to the timing of the crushing, it is likely that it occurred prior to movement, and therefore its origin is obscured.

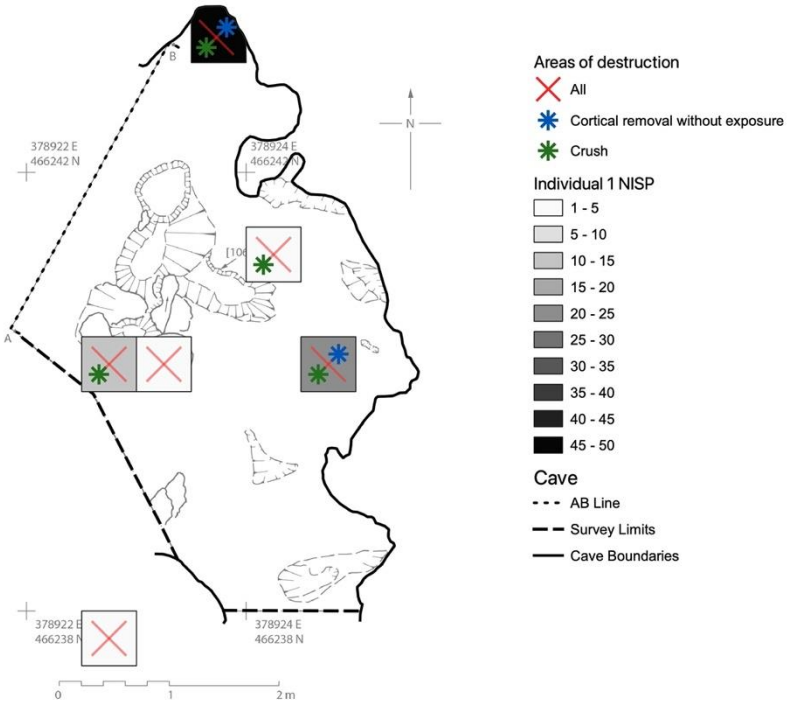


Figure 12.11: Distribution of crush damage and cortical removal - Individual 1.

There is no indication of damage occurring in a localised area. Destruction occurred across the cave which reflects sediment abrasion and damage common in a cave environment (Fernández-Jalvo and Andrews, 2016).

### *12.4.3: Tufa Deposits*

Deposits occurred in all areas of the cave where fragments of Individual 1 were recovered. Embedded fragments were found in all areas where there were multiple fragments recovered (figure 12.12).


Figure 12.12: Distribution of fragments embedded in tufa – Individual 1.

There was no significant area where embedding occurred, and tufa formation was present in the whole area of the cave excavated in 2022. This supports the sequence discussed above (figure 12.10, page 187), in that the embedding of the right foot in tufa is likely to have occurred after movement.

### *12.4.4: Staining*

Staining occurred in all areas of the cave where fragments of Individual 1 were recovered except for a single fragment to the east of the southwest cluster (figure 12.13).


Figure 12.13: Distribution of staining - Individual 1.

Fragment CH3.17.465 was found on its own and was a fragment of the smashed tibia that had no evidence of staining. The remaining two fragments of smashed tibia were found in the main cluster (CH3.65.431) and the southwest cluster (CH3.14.466) and both were stained. Fragment CH3.65.431 had dark grey/black mottled and dark brown/orange matt staining, comparatively fragment CH3.14.466 was only lightly stained with matt grey/black. Figure 12.14 shows all areas where all fragments with dark staining (including dark spotted, dark matt and dark brown/orange) were recovered (see section 11.1.6, figure 11.11 for an example of staining).


Figure 12.14: Distribution of fragments with dark staining - Individual 1.

Staining was only analysed macroscopically and not tested to verify the cause. It was consistent with manganese staining (Waters and Lowe, 2013). The fragments with dark staining assigned to Individual 1 were all recovered from the east border of the cave. This suggests an area of active elements, such as manganese, occurring in this location of the cave. Fragments with light staining may have originally been deposited in these locations and subsequently moved before staining could darken. Alternatively, light staining may be a result of less concentrated elements in other areas of the cave. The smashed tibia provides an example of how this can be used to interpret taphonomic sequences, since the three fragments all have different staining, with no staining crossing fracture margins and were recovered from three different locations. This suggests that staining occurred after processing and that the fragments were likely to have been dispersed at the point of fracture.

All other staining (light spotted, light matt and light orange/brown) occurred across the cave.

### *12.4.5: Processing Modifications*

There was a single notch defect for Individual 1. This was located on the fragment of smashed tibia that was recovered from the main cluster. The movement of the smashed tibia is discussed in section 12.3.3, page 184. The location suggests that the tibia was processed in-situ, due to its association with most of the fragments from Individual 1.

### *12.4.6: Animal Activity*

There was a single occurrence of gnawing consistent with rodent activity. This occurred on an ulna recovered from the main cluster and coupled with the absence of any other animal activity suggests that the displacement of bones was not due to scavenging or animal agents. The presence of tufa across the assemblage may be obscuring modifications but more likely prevented access.

### *12.4.7: Invertebrate Activity*

There was limited evidence of invertebrate activity which occurred on fragments recovered from the main and southwest clusters. It is difficult to explore whether there is any significance to the location of invertebrate activity due to the limited sample. It may be possible that there is obfuscation of marks due to tufa build up, or that access was prevented.

### *12.4.8: Root and Weathering*

Evidence of weathering was limited and there was no root etching or embedding on the bones.

The spread of taphonomy for Individual 1 offers limited insights into deposition. While some inferences can be made, for example from the differential staining of the tibial fragments, for the most part taphonomic modifications can be seen across all areas of the cave. This may be a result of agents acting on bones prior to movement, or that similar processes are occurring across the whole cave. The spread of element groups offers more understanding, and we can begin to unpick sequences of movement. This will be explored in detail in section 18.2.2.

## 12.5: Individual 2 – Distribution of Fragments

Individual 2 was similarly distributed to Individual 1, with the highest concentration of fragments occurring to the back recess (figure 12.15) and two smaller clusters to the southeast and southwest of the main cluster. It is possible that the burial location for Individual 2 was also towards the back recess, however, there were much fewer fragments recovered. The following section explores movement according to skeletal element and whether insight can be gained into deposition.

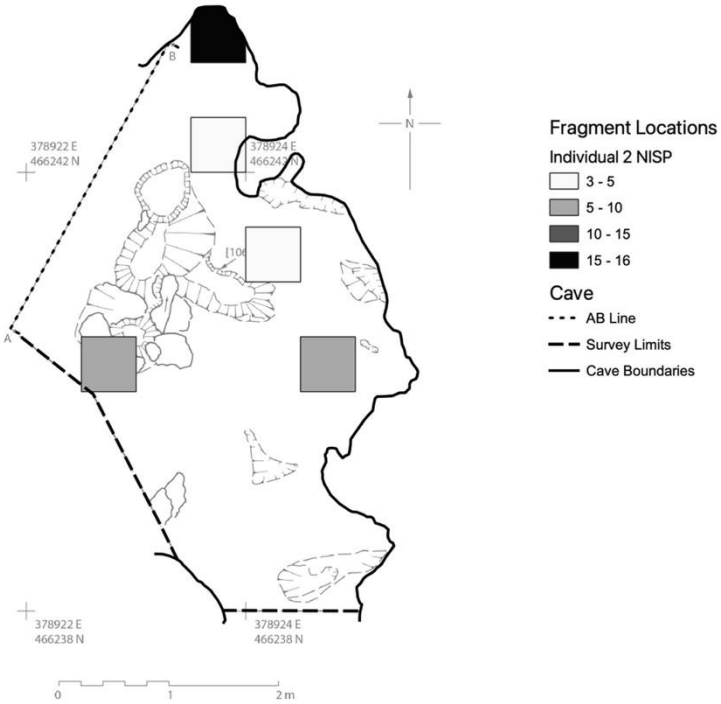


Figure 12.15: Distribution of fragments from Individual 2 according to NISP counts.

## 12.6: Individual 2 – Element Distribution

There was displacement of all element groups for Individual 2 (figure 12.16).

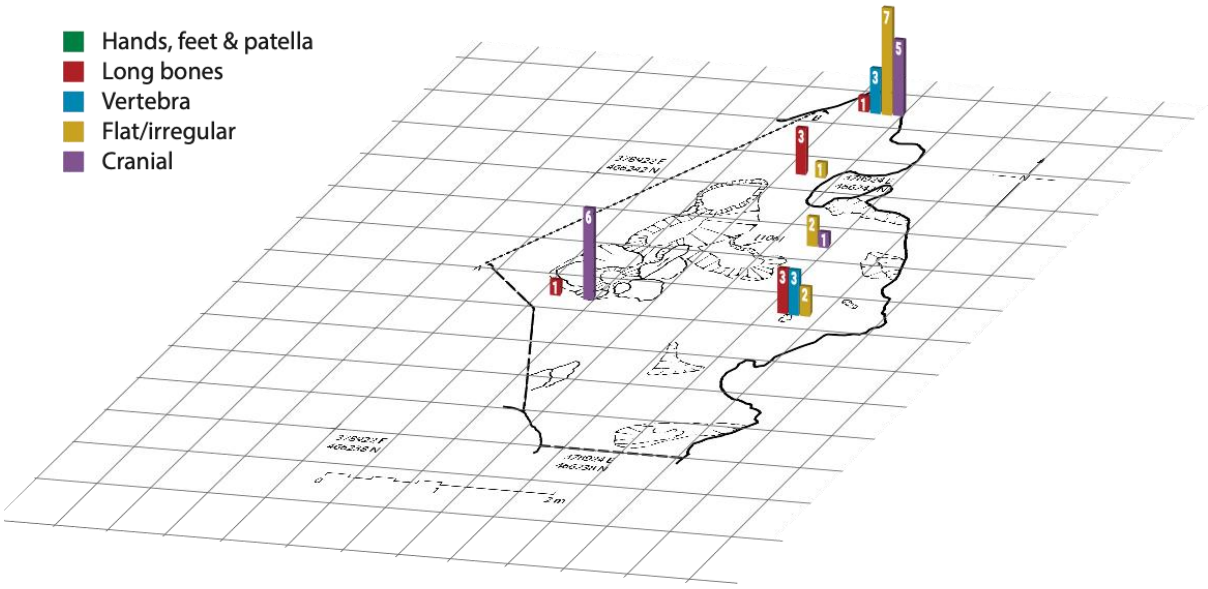


Figure 12.16: Distribution of fragments according to element group - Individual 2.

The furthest movement for fragments of Individual 2 was 2.88 m between the main cluster and the southwest cluster. This was the least dispersed Individual of the assemblage along with Individual 3.

### *12.6.1: Crania*

Cranial elements were found in the southwest and main cluster. The right zygomatic was found northwest of the southeast cluster, this was the only cranial fragment in that location associated to Individual 2, however, 11 fragments of cranium were recovered from this location that were unidentifiable to individual or element. It is possible that some of these fragments originated from Individual 2. The mandible, frontal and occipital bones were recovered in the southwest cluster and both temporal bones were recovered from the main cluster along with a fragment of the left maxilla and sphenoid (figure 12.17).

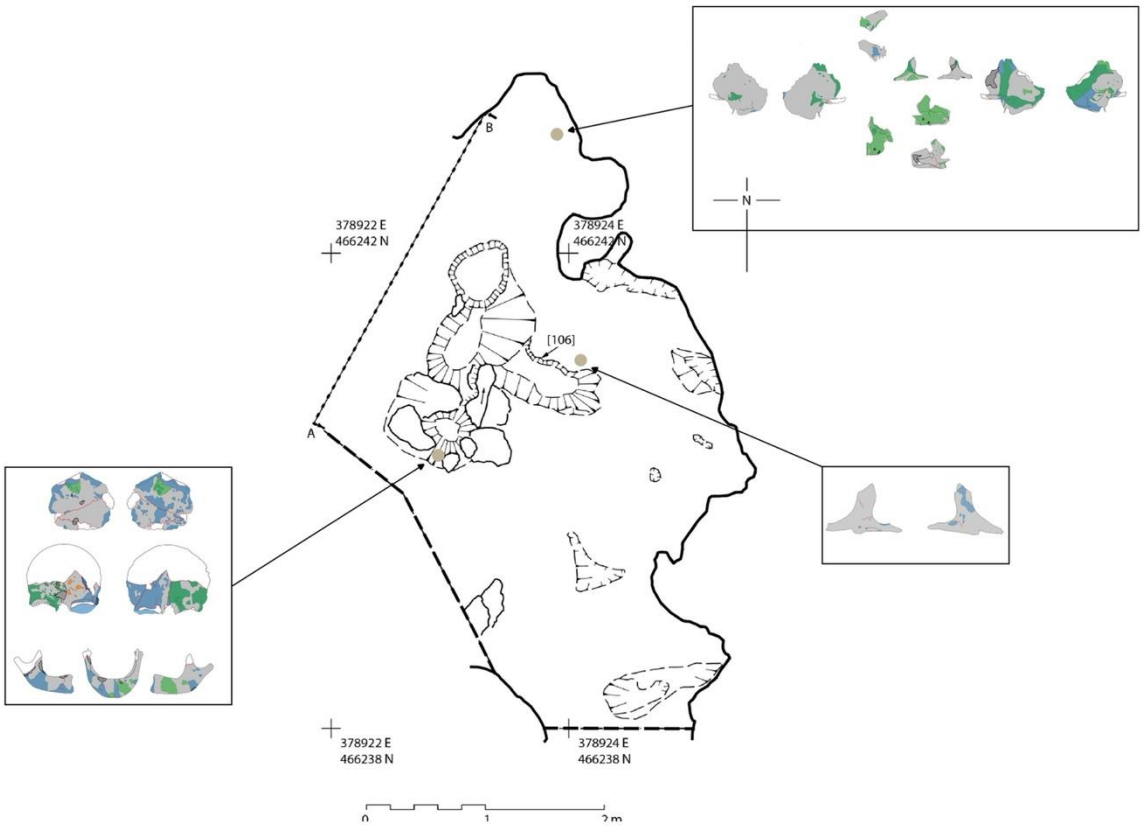


Figure 12.17: Distribution of cranial fragments - Individual 2.

It is likely that the cranium and mandible had separated prior to movement, particularly due to the mandible being recovered away from its articulating elements. Fusion of the cranial plates begins at approximately one year old and continues into the second year (Scheuer, Black and Schaefer, 2008). Due to the estimated age of Individual 2 of two to three years, the skull would have been fragile and possibly still in the early stages of fusion. The dispersal of the fragments indicate that the cranium had disarticulated prior to movement.

### *12.6.2: Vertebra*

The vertebrae were recovered from the main cluster and the southeast cluster. Only six vertebrae were recovered in total, four thoracic and two lumbar. These were evenly distributed between the cluster and offer little insight into deposition position.

### *12.6.3: Long Bones*

The long bones were spread throughout the cave. The left humerus was recovered from the main cluster, both femurs were recovered just south of the main cluster, the right ulna was

recovered from the southwest cluster and the left tibia and fibula were recovered from the southeast cluster (figure 12.18).

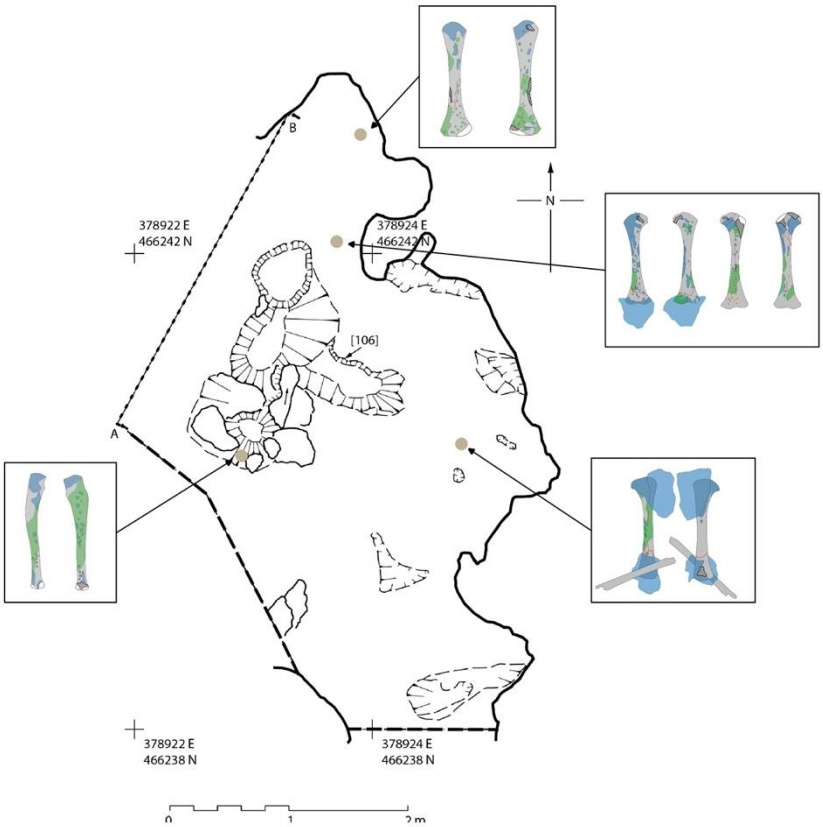


Figure 12.18: Distribution of long bone fragments - Individual 2.

The tibia and fibula were adhered in almost anatomical position by tufa (see section 11.2.5, figure 11.20). The tibia was fractured post-mortem and both fragments were located together. This indicates that the lower left limbs were likely articulated prior to movement. The fibula was at a slight angle, indicating that at the point of the tufa build up it had disarticulated from the tibia but not moved a significant degree. The post-mortem break most probably occurred after movement. Similarly, the right femur was in two fragments, in the same location, suggesting that the break occurred after movement.

The locations of the long bones offer insight into the possible burial position of Individual 2, assuming that the main cluster is the point of deposition. As discussed in section 11.2.3, there is evidence to suggest that the body was placed in a supine position. If the head was placed to towards the back recess, with the body laid out supine, and the left side of the body running

parallel to the back wall of the cave (figure 12.19), this would explain the movement of the lower limbs downward, to the southeast, and the right upper limb movement southwest.

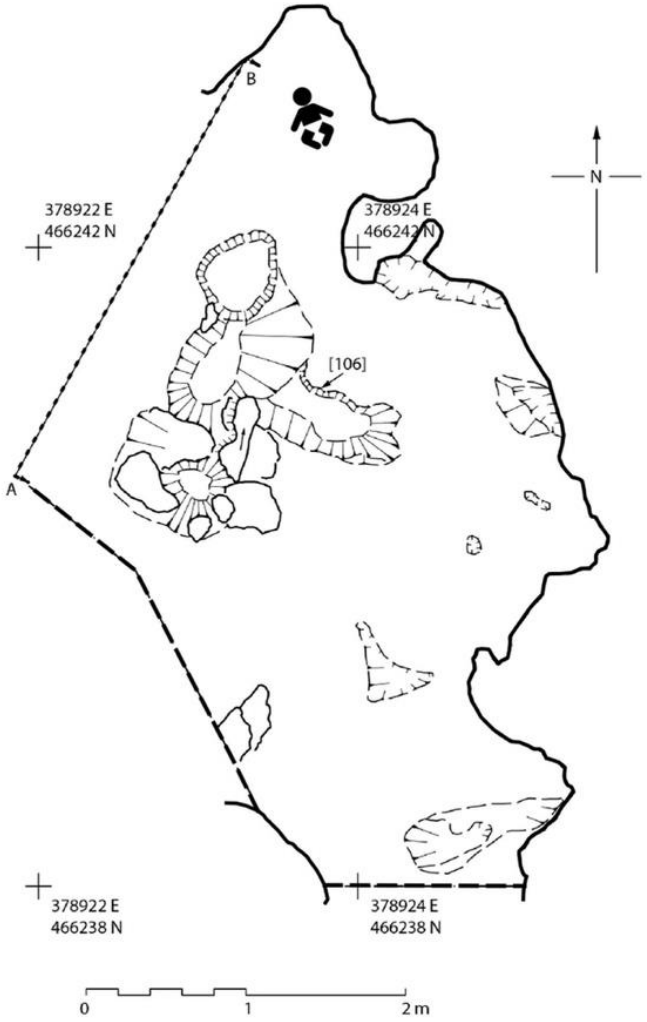


Figure 12.19: Possible body position of Individual 2.

While this is posited with caution, particularly as the main cluster may not be the original point of burial, the pattern of movement in the long bones of Individual 2 is interesting. This may also offer insight into the cranial movement. If the excluded cranial fragments belong to a different individual, then most of the cranial movement has occurred to the southwest, consistent with the positioning described above.

### *12.6.4: Flat/Irregular*

Due to placement issues only the first rib was recorded in GIS for Individual 2. The find locations for the remaining ribs were known and all were recovered from the main cluster except for two. One was recovered to the south of the main cluster and the other southeast to this with the right ilium. The left scapula and first rib were recovered from the southeast cluster (figure 12.20).

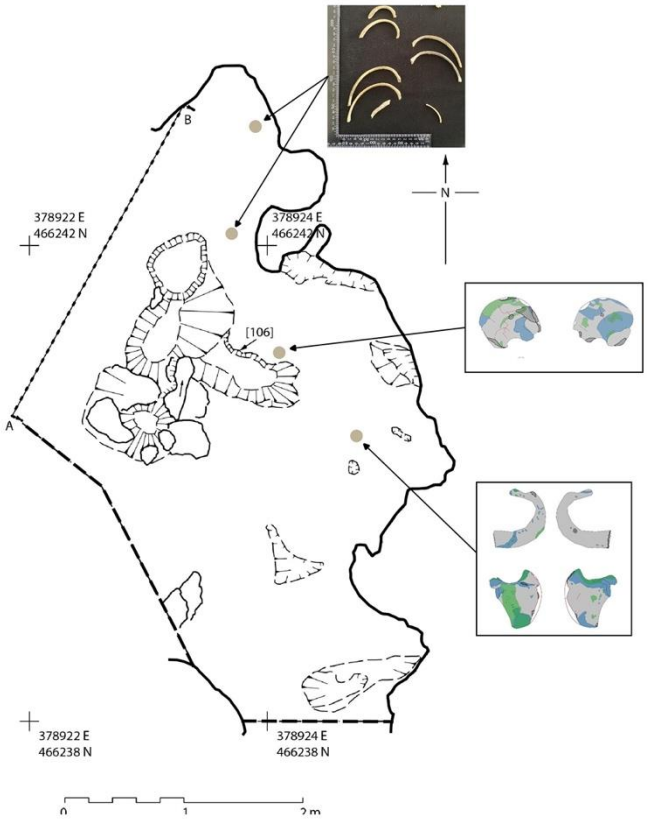


Figure 12.20: Distribution of irregular and flat fragments - Individual 2.

The ilium was recovered from the same location as both femurs, indicating the possibility that the lower portion of the body moved together. While the recovery of the left scapula and first rib from the southeast contradicts the patterns described above, the scapula is quick to disarticulate (Duday, 2009) and could therefore have been subjected to displacement earlier on in the sequence.

## 12.7: Individual 2 – Taphonomic Distribution

### *12.7.1: Fracturing*

Fracturing occurred on fragments recovered from all areas of the cave. Peri-mortem fractures only occurred in the main cluster and just to the south (figure 12.21). This was consistent with the peri-mortem crushing that occurred to the humerus and femur.

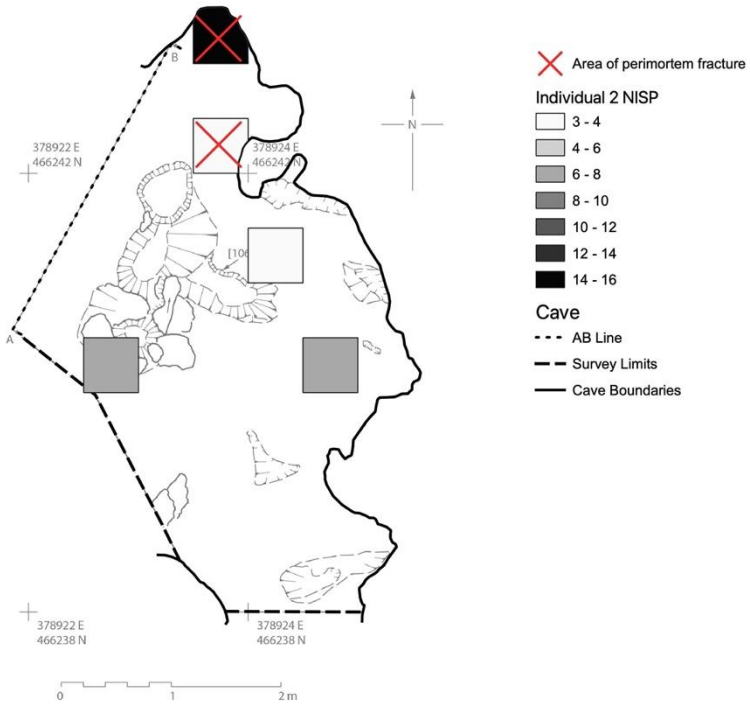


Figure 12.21: Distribution of fragments with peri-mortem fracture - Individual 2.

There was no significance to the distribution of incomplete fractures and cracking. This occurred across all areas where fragments of Individual 2 were recovered.

### *12.7.2: Destruction*

Destruction occurred in all areas of the cave where fragments of Individual 2 were recovered. Crushing occurred in the main cluster and to the southeast where the ilium was recovered (figure 12.22). While the femur had no area of crush damage, it did have spiral fractures consistent with a crushing force applied at a point when the bone retained some collagen. This is reflected in the peri-mortem fractures discussed above.

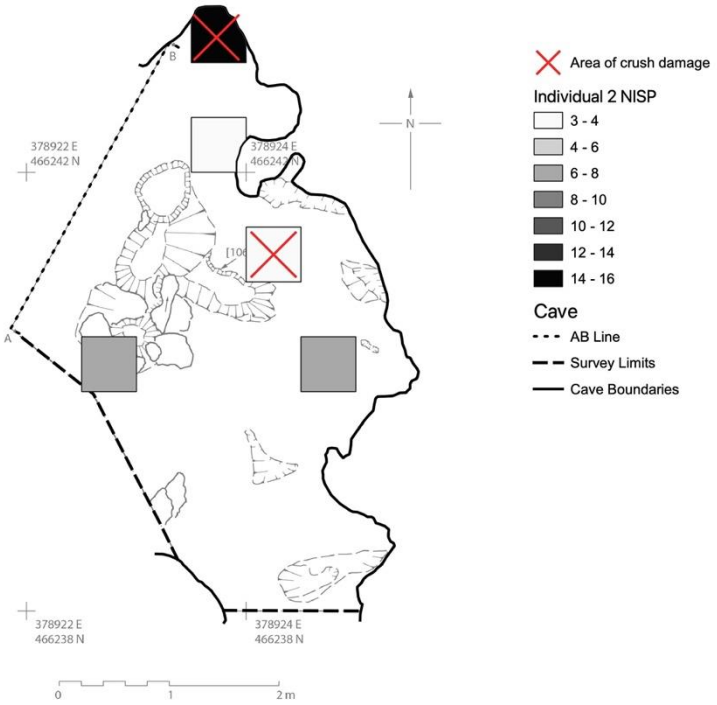


Figure 12.22: Distribution of fragments with evidence of crushing - Individual 2.

Fragments with peri-mortem fracturing and crushing appear to all have been recovered from along the perimeter of the cave. This could be indicative of rock fall occurring from the overhang of the shelter. Individual 2 is less dispersed than Individual 1, where the origin of crush damage may have been obscured through movement. All other damage classifications were found in all areas where fragments of Individual 2 were recovered, which is consistent with the burial environment.

### *12.7.3: Tufa Deposits*

Deposits occurred in all areas of the cave where fragments of Individual 2 were recovered. Embedded fragments were also found in all areas except for one area above the southeast cluster. Only three fragments were recovered from that area, which may account for the absence of embedding in this area. The spread of tufa is consistent with its presence throughout the cave.

*12.7.4: Staining*

Staining occurred in all areas of the cave where fragments of Individual 2 were recovered. Staining classified as either 'dark spotted' or 'dark matt' only occurred along the eastern border of the cave (figure 12.23).


Figure 12.23: Distribution of fragments with dark staining - Individual 2.

Staining was only analysed macroscopically, not tested to verify the cause, and was consistent with manganese staining (Waters and Lowe, 2013). The pattern of dark staining is consistent with Individual 1 and indicates an area of active elements, such as manganese, occurring in this location.

When the spatial distribution of staining is looked at in combination with body level changes, the position of Individual 2 argued above (figure 12.19) is supported further. If the body was positioned with its left side to the wall, parallel to where staining was strongest, then it could cause the bias in staining seen on the left-sided fragments discussed in section 11.2.6.

### *12.7.5: Invertebrate Activity*

Invertebrate activity was recorded on fragments recovered from the southwest, the southeast and just to the south of the main cluster (figure 12.24).

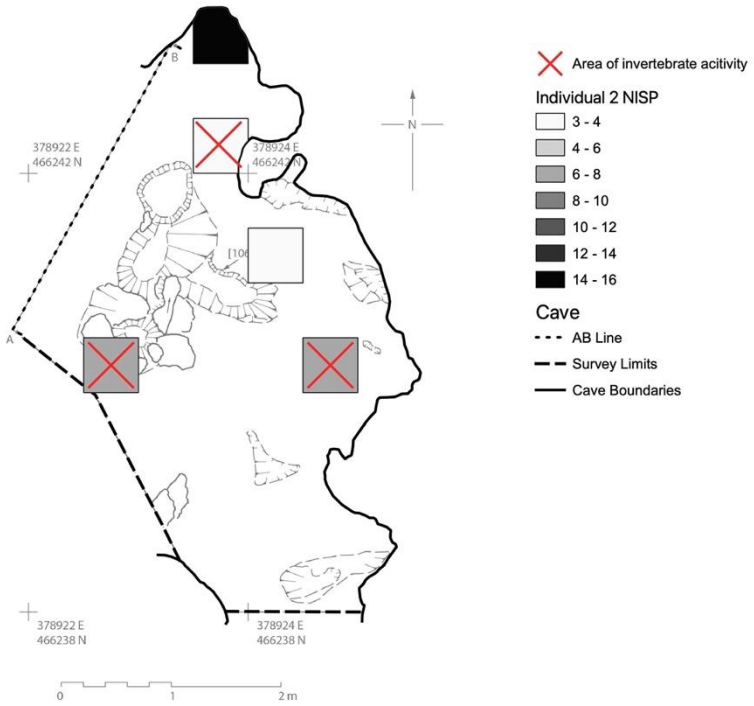


Figure 12.24: Distribution of fragments with invertebrate modifications - Individual 2.

While invertebrate activity is dispersed across most areas where fragments of Individual 2 were recovered, only three fragments in total exhibited modifications. It is likely that the tufa acted as a preservative, protecting cortical surfaces from modification.

### *12.7.6: Processing Modifications, Animal Activity, Root, and Weathering*

There was no evidence of large animal activity, deliberate processing or root action on fragments recovered from Individual 2 and evidence of weathering was minimal (see section 11.2.8).

Analysis of movement according to element group has offered insight into the potential position of deposition for Individual 2. A full understanding of deposition is difficult, however,

due to incomplete recovery. The spread of taphonomy for Individual 2 offers limited insights into deposition. While some inferences can be made, for example dark staining spread across the cave boundaries, for the most part taphonomic modifications can be seen across all areas of the cave. This may be a result of agents acting on bones prior to movement, or that similar processes are occurring across the whole cave.

## 12.8: Individual 3 – Distribution of Fragments

While fragments for Individual 3 were found in some of the same locations as Individuals 1 and 2, the main concentration was in the southeast cluster (figure 12.25). This appears to be inconsistent with archive reports that state that the infants (originally described as two, rather than three) were "recovered from a natural cavity within the far wall, to the west of the recess that contained some of the skeletal elements of the adult male" (Lord, 2004 cited in Leach, 2006, p. 165).

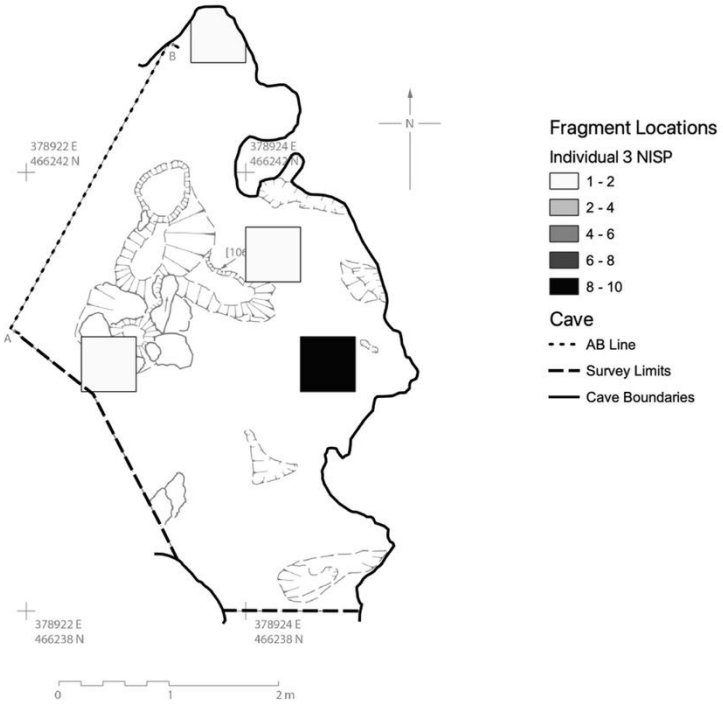


Figure 12.25: Distribution of fragments from Individual 3 according to NISP counts.

Individual 3 had the lowest representation of elements (total representation of 5.22%, comprised of 13 skeletal elements from 15 fragments). The NISP counts for the same grid square for Individuals 1 and 2 were 24 and eight respectively. It is possible that, rather than being an indication of a different burial position, it is an indication of excavation and destructive biases.

## 12.9: Individual 3 – Element Distribution

There was displacement of cranial fragments and flat/irregular bones for Individual 3 (figure 12.26). Vertebra and long bones were only recovered in one area (southwest and southeast clusters respectively).

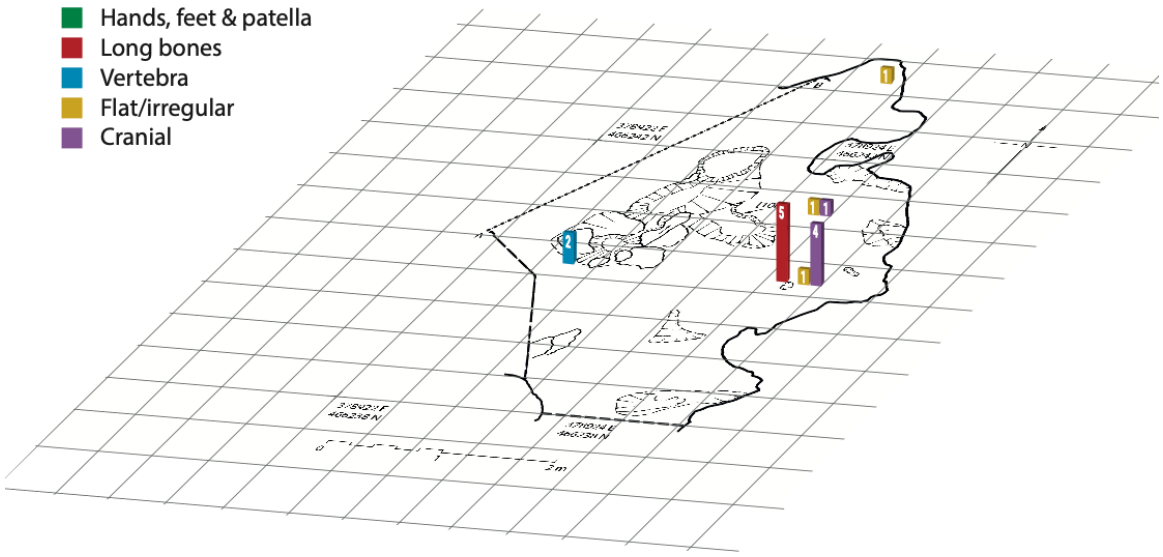


Figure 12.26: Distribution of fragments according to element group - Individual 3

The following section explores the spread of each element group; however, analysis is conducted with the understanding that preservation and recovery biases will affect interpretations.

### *12.9.1: Crania*

All cranial elements were recovered from the southeast cluster. These consisted of the squamous portion of the occipital and the right *pars lateralis* (figure 12.27). A single tooth, consistent with the age at death estimation of Individual 3 was also recovered from here. Several juvenile cranial fragments were also recovered from this area and are possibly associated to Individual 3.

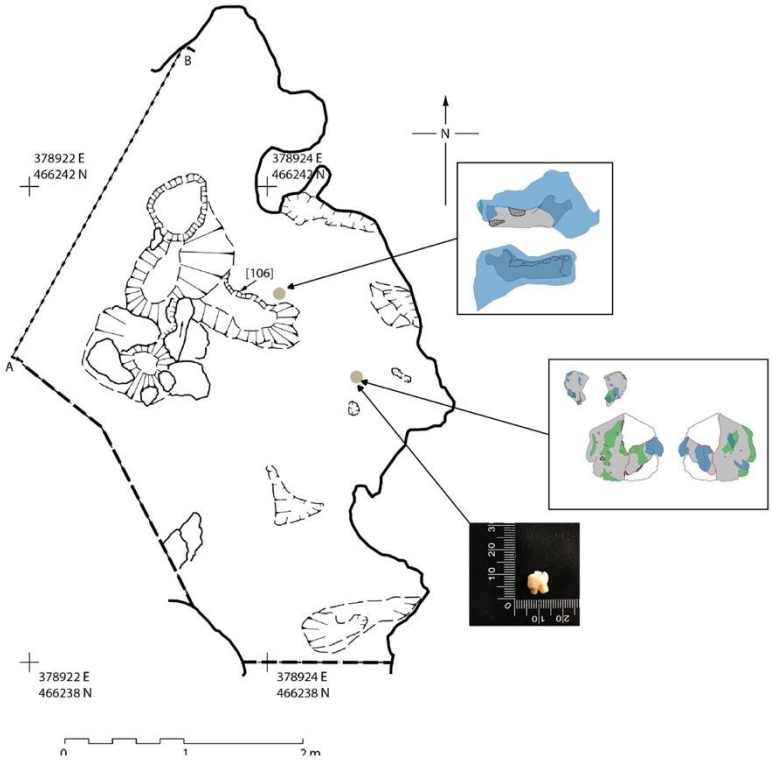


Figure 12.27: Distribution of cranial fragments - Individual 3.

The mandible that was embedded in tufa was recovered to the northwest of the occipital fragments and loose tooth.

### *12.9.2: Vertebra*

Two vertebral arches were recovered from the southwest cluster, no other vertebral fragments were associated to Individual 3.

### *12.9.3: Long Bones*

All long bones associated with Individual 3 were recovered from the southeast cluster. The left tibia was in two fragments, suggesting either that the bone fractured after movement, or may be indicative of no movement. The recovery of the long bones alongside most of the cranial fragments is the opposite pattern to Individual 2, which saw dispersal of the long bones away from the cranial fragments.

### *12.9.4: Flat/Irregular*

Flat and irregular bones were the most dispersed for individual 3. The left ilium was recovered in the main cluster, the left scapula was recovered with the mandible and the right first rib was recovered from the southeast cluster (figure 12.28).

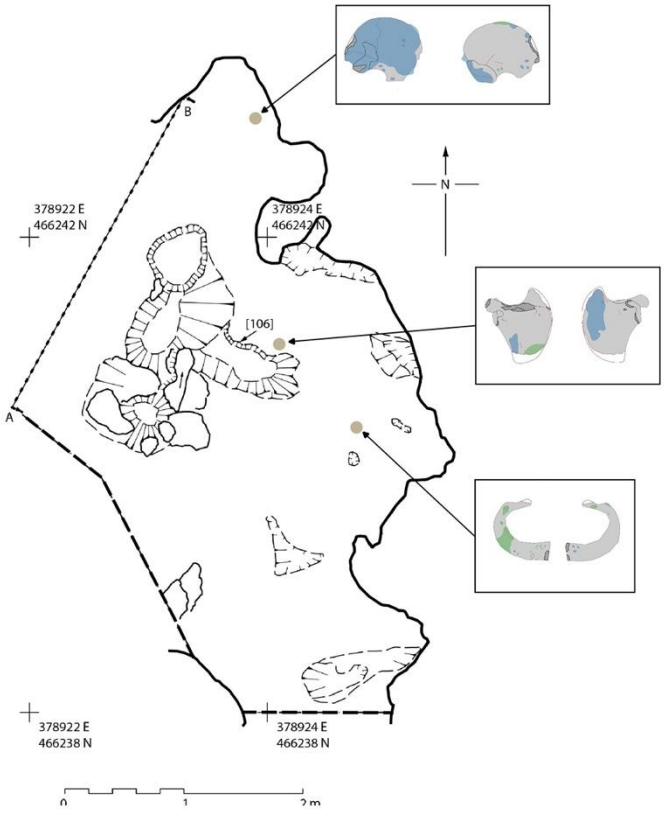


Figure 12.28: Distribution of irregular/flat fragments - Individual 3.

While discussed above that the limited recovery may be obscuring the original point of deposition, when the distribution of elements is examined in detail, it suggests that the southeast cluster was the location of burial.

## 12.10: Individual 3 – Taphonomic Distribution

### *12.10.1: Fracturing*

Fracturing, including incomplete cracking, occurred on fragments recovered from all areas of the cave except for the vertebral arches recovered from the southwest cluster. Associated fragments of the left tibia were found in the same location, indicating fracture sequence. Otherwise, there was no significance to the distribution of fractures for Individual 3.

### *12.10.2: Destruction*

Destruction occurred in all areas of the cave where fragments of Individual 3 were recovered. Crushing occurred in the southeast cluster and on the scapula recovered just above this (figure 12.29).

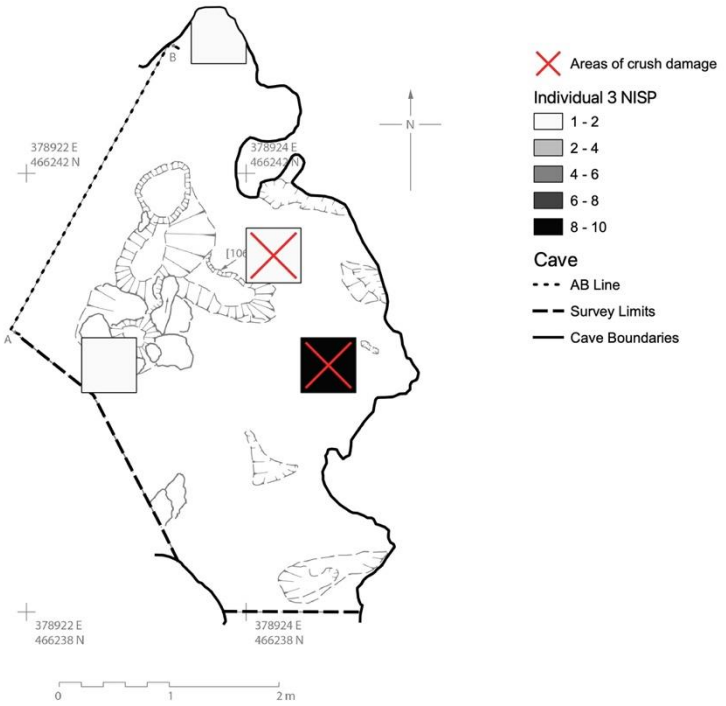


Figure 12.29: Distribution of fragments with evidence of crushing - Individual 3.

Crush damage only occurred to the east border of the cave, this is similar to Individual 2. However, it is possible that, due to the limited recovery, the true distribution is masked.

### *12.10.3: Tufa Deposits*

Deposits occurred in all areas of the cave where fragments of Individual 3 were recovered. Embedded fragments were only recovered from the eastern cave border (figure 12.30).


Figure 12.30: Distribution of fragments with tufa embedding - Individual 3.

While this could be interpreted as areas of more prolific tufa formation, it is likely that the distribution is skewed by recovery. Only two fragments were recovered from the southwest cluster. The distribution of embedding seen on Individuals 1 and 2 suggest that tufa formation was occurring throughout the cave, and earlier reports support this (Pentecost *et al.*, 1990).

### *12.10.4: Staining*

Staining occurred along the east border of the cave, staining classified as either ‘dark spotted’ or ‘dark matt’ was similarly distributed (figure 12.31).


Figure 12.31: Distribution of fragments with staining - Individual 3.

There was an absence of staining found on the vertebra recovered from the southwest cluster. The pattern of dark staining is consistent with the findings for Individuals 1 and 2, further supporting that there were certain staining agents acting along the border of the cave.

### *12.10.5: Invertebrate Activity*

Invertebrate activity was recorded on a single fragment recovered from the southeast cluster. There was limited evidence of invertebrate activity and the presence on a single element offers little insight into movement. It is likely that tufa acted as a protective agent from modification.

### *12.10.6: Processing Modifications, Animal Activity, Root, and Weathering*

There was no evidence of animal activity, deliberate processing or root action on fragments recovered from Individual 3 and evidence of weathering was minimal (see section 11.3.8).

A full understanding of deposition is difficult due to limited recovery; however, the accumulation of the long bones and cranial elements in the southeast cluster point to a possible deposition location. The spread of taphonomy for Individual 3 also offers limited insights into deposition. While some inferences can be made, for example dark staining spread across the cave boundaries, for the most part taphonomic modifications can be seen across all areas of the cave where fragments of Individual 3 were found.

## 12.11: Individual 4 – Distribution of Fragments

The concentration of fragments for Individual 4 was recovered to the southwest of the recess (figure 12.32), this is consistent with the archive reports.

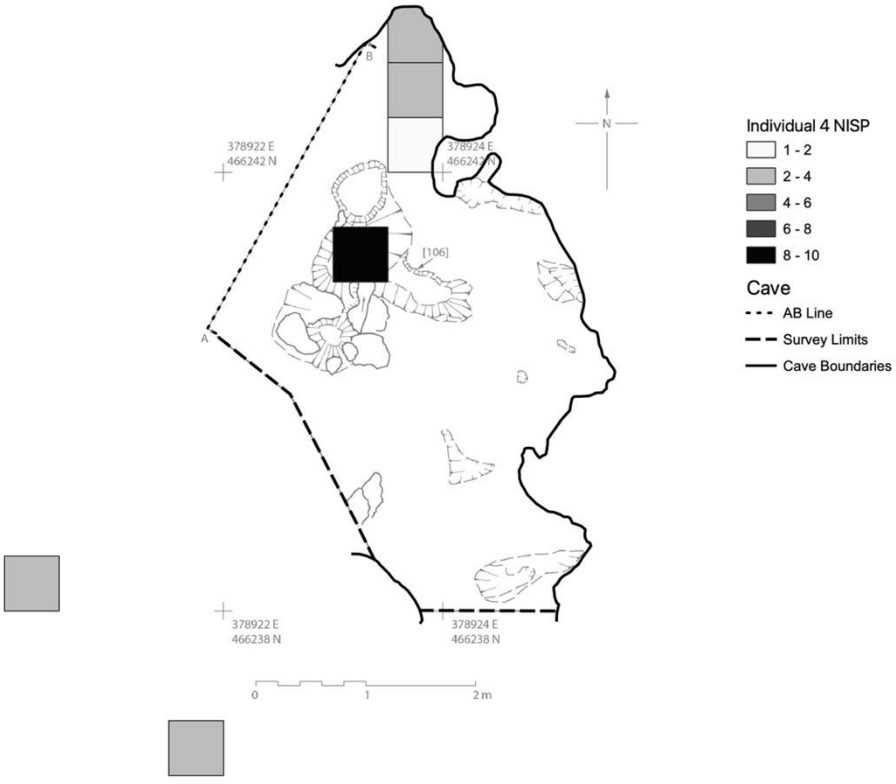


Figure 12.32: Distribution of fragments from Individual 4 according to NISP counts.

Again, the distribution of elements may be a result of destruction and recovery bias, rather than an indication that the body was placed away from the adult and older infant.

## 12.12: Individual 4 – Element Distribution

Fragments recovered from Individual 4 were dispersed the furthest (figure 12.33). Three cranial fragments were found 7.05 m southwest of the main cluster and 4.88 m from the southwest cluster.

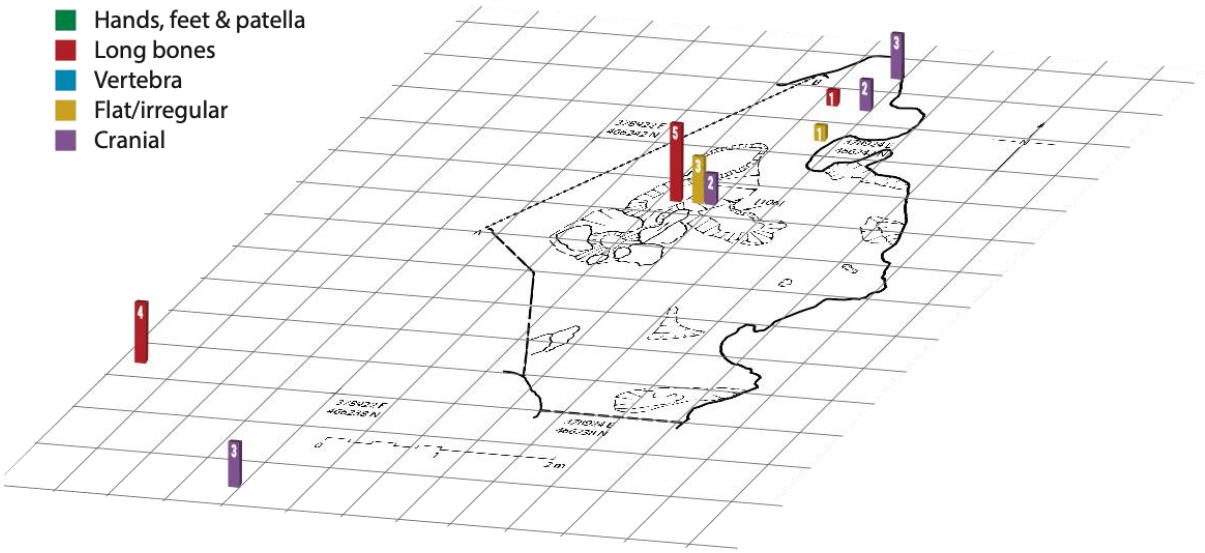


Figure 12.33: Distribution of fragments according to element group - Individual 4

Individual 4 was a neonate, estimated at around 38-40 foetal weeks. The bones of individual 4 are much smaller and less dense than the other individuals in the Cave Ha assemblage, particularly those of the adult. The literature is mixed when discussing transport of juvenile bones and mainly focuses on faunal remains rather than human. Bone transport is variable and affected by myriad characteristics (Evans, 2013). There is evidence, however, to suggest that smaller, less dense juvenile bones have increased transport potential (Boaz and Behrensmeyer, 1976; Buckberry, 2000; González *et al.*, 2012; Evans, 2013). This would explain the increased dispersal of fragments.

### *12.12.1: Crania*

Cranial fragments for Individual 4 were the most dispersed and were distributed to the southwest of the main cluster. The parietals and an unidentified fragment were recovered from the main cluster, a fragment of occipital and an unidentified fragment were found just

south of these, the right frontal bone and an unidentified cranial fragment were recovered from the southwest cluster, and the left frontal bone along with both temporals were recovered the furthest southwest (figure 12.34).

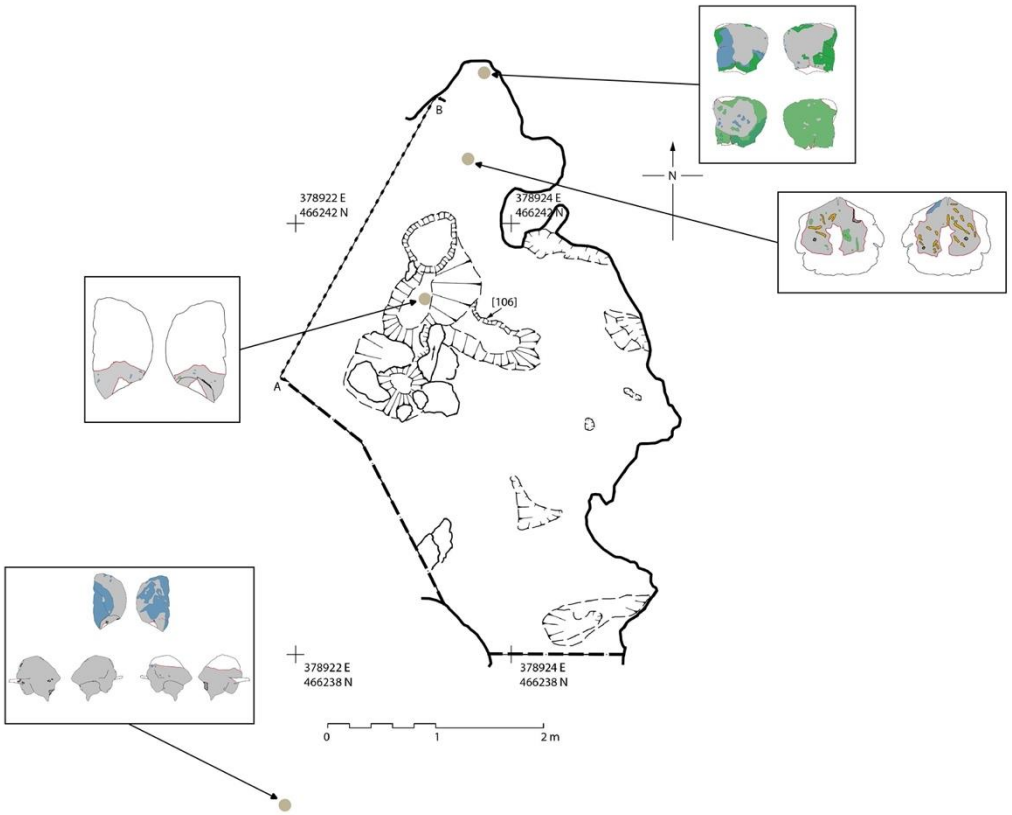


Figure 12.34: Distribution of cranial fragments - Individual 4.

The cranial vault is unfused in neonates and is unilaminar until approximately four years (Jin, Sim and Kim, 2016). The fragility of the bones makes them more susceptible to fragmentation and possible movement (Boaz and Behrensmeyer, 1976; Buckberry, 2000; González *et al.*, 2012; Evans, 2013) and would explain the extent of the dispersal.

### *12.12.2: Long Bones*

Most of the long bones associated to Individual 4 were recovered from the southwest cluster, the radii and tibiae were located 4.25 m southwest of these, and a single, left ulna was recovered just below the main cluster (figure 12.35).

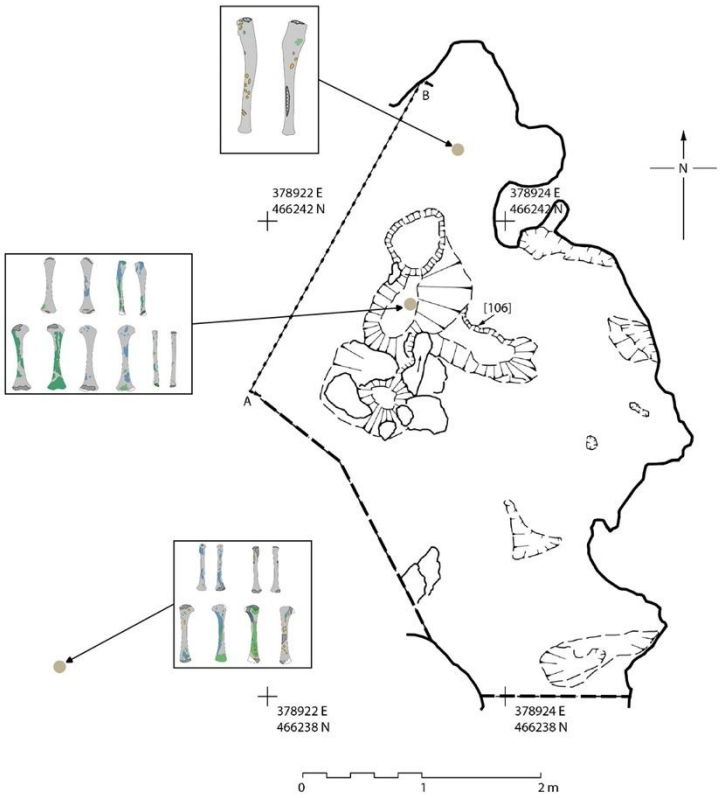


Figure 12.35: Distribution of long bones - Individual 4.

The distribution of long bones associated to Individual 4 offers little insight into deposition. While most are in the southwest cluster, potentially indicating burial location, a number have moved away from there.

### *12.12.3: Flat/Irregular*

The left scapula along with two fragments of rib were recovered from the southwest cluster, the right scapula was recovered to the south of the left ulna (figure 12.36).

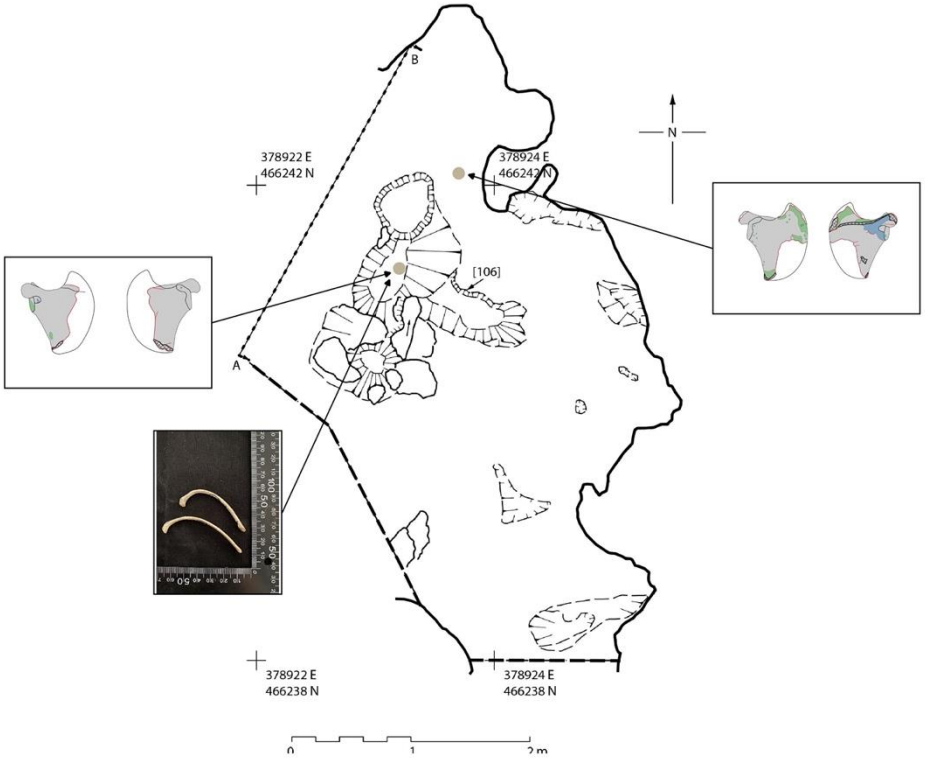


Figure 12.36: Distribution of flat/irregular bones - Individual 4.

The left scapula was recovered with right long bones, compared to the right scapula which was recovered with the left ulna. This suggests that movement did not occur when the upper limbs were articulated.

## 12.13: Individual 4 – Taphonomic Distribution

### *12.13.1: Fracturing*

Fracturing occurred on fragments recovered from all areas of the cave. Fractures consistent with peri-mortem breakage all occurred in the main cluster and were associated to the parietals that showed deformation. Incomplete cracking associated with crush damage was found to the south of the main cluster and in the southwest cluster (figure 12.37).

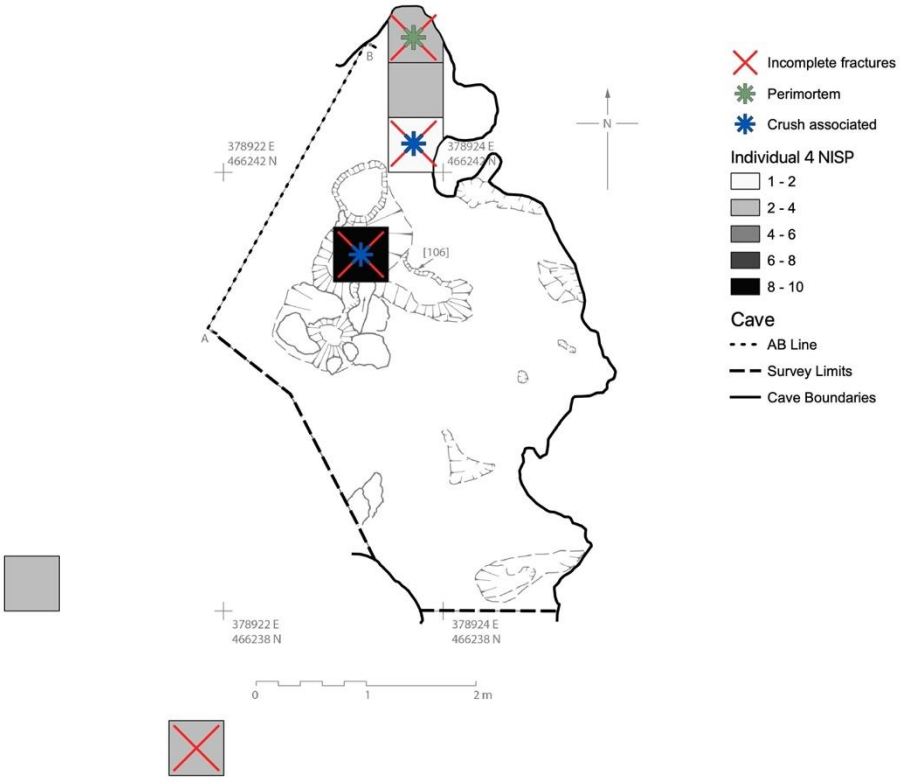


Figure 12.37: Distribution of fragments with incomplete or peri-mortem fractures - Individual 4.

There were three incomplete fractures recorded on fragments recovered from the furthest southwest. These were on cranial fragments and were consistent with post-mortem cracking.

### *12.13.2: Destruction*

Destruction occurred in all areas of the cave where fragments of Individual 4 were recovered, except for the main cluster. Crushing occurred on the scapula recovered to the south of the main cluster and on in the southeast cluster and on the right radius (figure 12.38).

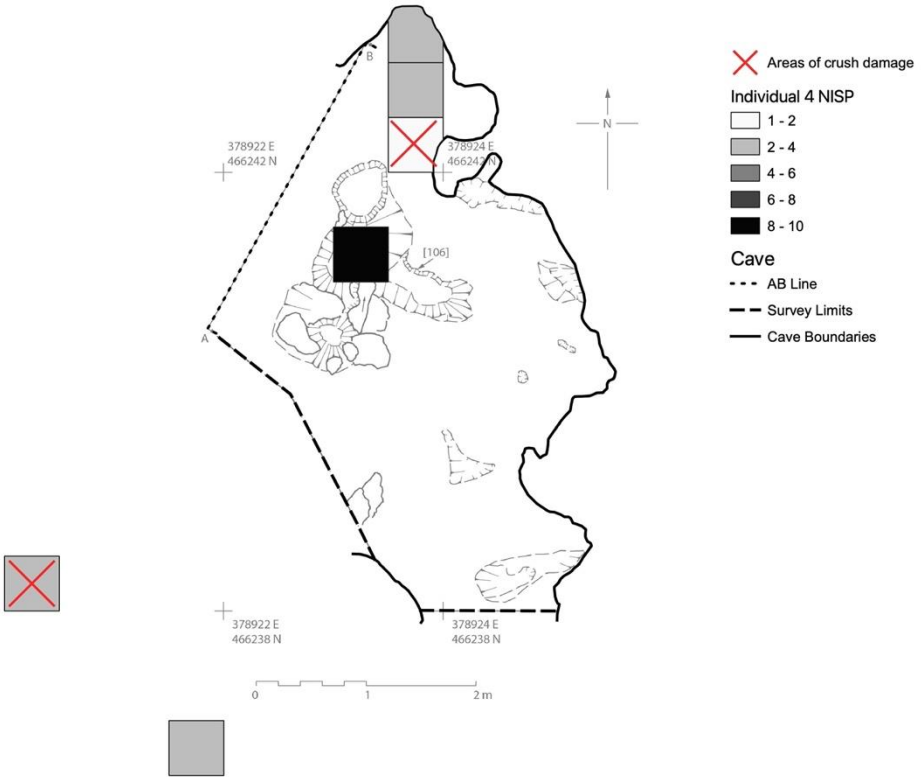


Figure 12.38: Distribution of fragments with peri-mortem crushing - Individual 4.

With exception of the crush damage recovered to the far southwest, all areas of peri-mortem crushing and fracturing occurred towards the top of the cave. This is consistent with the discussion above regarding areas of potential rock fall. The fragment to the far southwest (right radius) may be a result of movement occurring after damage.

### *12.13.3: Tufa Deposits*

Deposits occurred in all areas of the cave where fragments of Individual 4 were recovered. No fragments had embedding, and the distribution of tufa is consistent with formation across the cave. The cranial elements with higher frequencies of deposits discussed in section 11.4.5 were found in both in the main cluster and approximately six metres southwest of this, giving no indication of preferential tufa activity.

### *12.13.4: Staining*

Staining occurred in all areas of the cave where fragments of Individual 4 were recovered. Dark staining was similarly distributed which is the opposite finding for Individuals 1-3 (figure 12.39).


Figure 12.39: Distribution of fragments with dark staining - Individual 4.

While it could be an indication that dark staining occurred across the whole cave, factoring in the rest of the assemblage and the extent of dispersal of Individual 4, it is likely that the observed distribution is a result of movement after the point of staining.

### *12.13.5: Invertebrate Activity*

Invertebrate activity was recorded on fragments recovered from the southwest cluster, just south of the main cluster and to the southwest of the southwest cluster (figure 12.40).


Figure 12.40: Distribution of fragments with invertebrate modifications - Individual 4.

Like Individual 2 there were only three fragments that had modifications. The spread of invertebrate activity does not offer any significant information regarding the movement and deposition of Individual 4.

### *12.13.6: Processing Modifications, Animal Activity, Root, and Weathering*

There was no evidence of animal activity, deliberate processing or root action on fragments recovered from Individual 4 and evidence of weathering was minimal (see section 11.4.8).

A full understanding of deposition is difficult due to the extent that Individual 4 has been dispersed. The accumulation of long bones in the southwest cluster may be indicative of burial position, however a similar number of long bones were recovered away from here. The cranial material is the most dispersed and movement of fragments has also impacted assessments of taphonomy.

## 12.14: Spatial Summary of Cave Ha 3

Analysis of skeletal element distribution for Individuals 1 and 2 offer the most information regarding deposition and movement. Individuals 1 and 2 were likely deposited toward the back recess. It is important to note, however, that the nature of the archive records could be introducing bias due to some estimation of find locations. The limited recovery of Individual 3 hinders interpretation regarding location and fragments from Individual 4 were widely dispersed, masking any suggestion of burial location.

The spread of taphonomy offered some insight into processes. An area of dark staining across the east boundary of the cave has been highlighted, the same region is likely to be where peri-mortem crushing occurred. The distribution of post-mortem destruction is consistent with destructive processes occurring across the whole cave. Similarly, the distribution of tufa points to active formation within the whole area. There was active tufa formation before and after the Early Neolithic (Pentecost *et al.*, 1990) and since the current floor has maintained a flat surface, it was likely to have been flat at the point of deposition. Dispersion is therefore unlikely to be a result of rolling. The absence of animal activity discussed in chapter 11 also suggests movement through scavenging is unlikely. The geology of the cave and the climate make water transport likely. Research into the movement of bones in rainwater is scant, with research focusing on fluvial environments, however precipitation is known to cause sediment shifts in cave environments (González-Lemos, Jiménez-Sánchez and Stoll, 2015; Nicolosi *et al.*, 2023). Rainwater run-off from the walls of the rock shelter would explain patterns of dispersal in a southernly direction. This is reflected in the damage classified as “exposure of trabecular bone” which was found on fragments across the cave. This is consistent with damage from fluvial environments where thinning of the cortical surface exposes trabecular bone (Fernández-Jalvo and Andrews, 2003).

The analytical process used for Cave Ha 3 has been applied to Heaning Wood and is discussed in the following section. Section 18.2 explores the findings in more detail to construct possible burial narratives for each individual and the implications these have on site level interpretations.

# CHAPTER 13: HEANING WOOD – AN OVERVIEW

## 13.1: Site Stratigraphy and Original Excavations

Heaning Wood cave is a natural vertical shaft located in the limestone belt that extends westward from Yorkshire. The cave is in Heaning Wood, Great Urswick, Cumbria (NGR SD 2671 7483, site and monuments record: C 2366; figure 13.1).


Figure 13.1: Location of Heaning Wood Bone Cave

Access is from an artificially enlarged entrance within the ground surface (Holland, 1960). The expanded fault runs parallel to the hillside and widens into a main chamber with a secondary chute (figure 13.2).

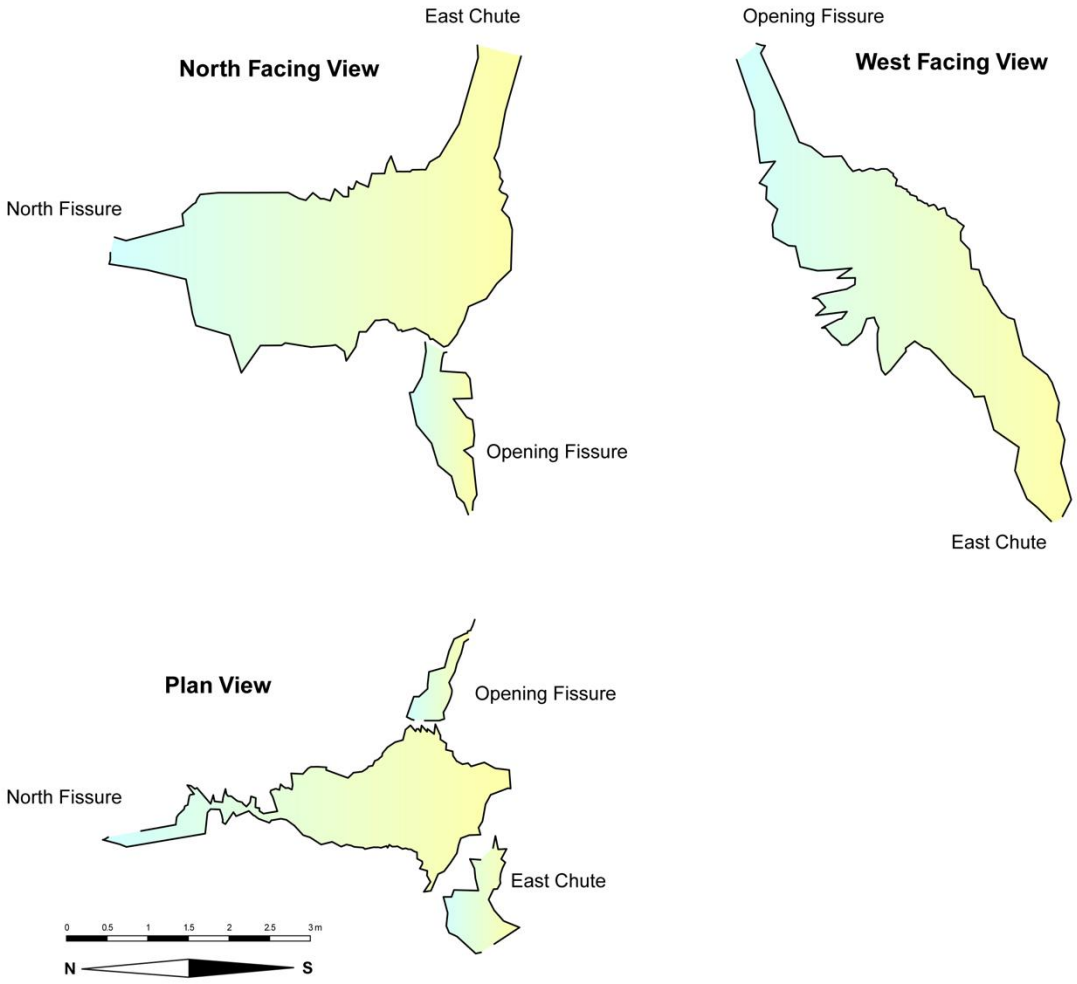


Figure 13.2: Plan, north-facing, and west-facing views of Heaning Wood Bone Cave

Originally excavated in 1958 through the north fissure, two human femurs were initially identified, alongside an abundance of faunal material including pig, sheep, horse, cow, deer, wolf, Celtic Ox, and boar (Holland, 1960). Further human remains were recovered, and the minimum number of individuals was described as four; “an old man, one middle-aged man and a woman and a child” (Holland, 1960, p. 42). Associated artefacts included a stone knife or “scraping tool” *(ibid, p.42),* a fragment of burial urn, and a bone pin or brooch. Initial interpretations based on the artefacts led to the inference that the remains dated to the “Middle Bronze Age: 1,000-1,700 B.C.” (*ibid, p.43*). Subsequent dating (C14), funded by the Research Committee of Cumberland and Westmorland Antiquarian and Archaeological Society (CWAAS), indicated Early Neolithic (animal) and Bronze Age (human). The findings

were reported as “unclear” due to the limited sampling, and further dating was advised (Smith, 2012, p. 6).

The assemblage formed a talus, believed to have accumulated through a shaft “at the apex of the rift” (Smith, 2012, p. 6). Further excavations were undertaken by Peter Redshaw in April 1974 and by Martin Stables between 2016 and 2019. The later excavations expanded the human, faunal and lithic material considerably. A chute, east to the main chamber, remains partially unexcavated. The top portion of the east chute has been excavated but access beyond this is difficult, although cavers who have managed to access it report that the area is clear of surface deposits (Martin Stables pers. comm.). It is considered that all bone and artefacts have been excavated. The human remains from the 1958 and 1974 excavations are currently held at the Dock Museum, Barrow-in-Furness. Material from subsequent excavations is held at the University of Central Lancashire. The assemblages have been combined to ensure that the following reports on the assemblage in its current entirety. Once complete, all remains will be held at the Dock Museum.

## 13.2: Radiocarbon (C-14) Dating

Eight bones and a shell bead were selected for radiocarbon dating as part of this project, based on the estimated number of individuals (table 13.1). Unfortunately, one individual (Individual G) was represented by so few elements that it was felt destructive testing could not be justified. A second bone from Individual D was tested as it consisted of elements excluded from the other three adults, based on duplication. It is, therefore, likely that Individual D has assigned fragments that belong to another individual. There was difficulty extracting collagen from one bone associated to Individual D; this was sent for further testing and returned a date that has a <5% likelihood of overlap with the other sample taken from Individual D. This indicates the likelihood of remains from at least one other adult at Heaning Wood.

Table 13.1: Radiocarbon dating results.

| Sample Nº | 14C Age | Error | $\delta^{15}N$ (‰ vs. air) | $\delta^{13}C$ (‰ vs. air) | Cal Years BC | Cal Years BP | Individual/Object | Period |
|---|---|---|---|---|---|---|---|---|
| HBC010 | 3705 | 20 | 10.6 | -21.0 | **2195-2025** | 4145-3980 | A | Early Bronze Age |
| HBC013 | 3730 | 20 | 10.7 | -21.0 | **2200-2035** | 4150-3985 | D | Early Bronze Age |
| HBC227 | 3660 | 20 | 10.6 | -21.2 | **2140-1960** | 4085-3900 | ?D | Early Bronze Age |
| HBC135 | 4910 | 25 | 9.6 | -21.3 | **3765-3640** | 5715-5590 | B | Early Neolithic |
| HNC229 | 4870 | 25 | 10.4 | -22.0 | **3705-3540** | 5655-5490 | C | Early Neolithic |
| HBC260 | 4885 | 25 | 9.9 | -21.6 | **3710-3635** | 5660-5585 | E | Early Neolithic |
| HBC297 | 4765 | 25 | 10.1 | -21.8 | **3635-3385** | 5585-5335 | H | Early Neolithic |
| HBC312 | 9720 | 40 | 12.7 | -19.3 | **9290-8930** | 11250-10880 | F | Mesolithic |
| HBC-HW1 | 9755 | 35 | / | / | **9115-8635** | 11065-10585 | Shell Bead | Mesolithic |

Radiocarbon dating showed results from three distinct periods, with long hiatuses. These spanned from the Early Mesolithic through to the Early Bronze Age. The significance of the earlier dates (Individual F and the shell bead) is discussed in detail in section 19.1.2.

Since the burials in Heaning Wood can be seen as distinct practices, rather than a continuing practice, the results section will report with this in mind. The Bronze Age Individuals (A and D) will be discussed first, followed by the Early Neolithic Individuals (B, C, E, and H), concluding with individual F (Mesolithic). Since Individual G was not dated it will be reported separately. An overview of taphonomy across the whole assemblage will be given to provide insight into geological processes within the cave, however, comparisons of taphonomy between individuals will be made within time-period groups when discussing burial practice.

To allow for consistency in reporting, a combined overview of the individuals found will be provided, as done for Cave Ha 3. It is important to note, however, that the assemblage demographics and bone representation indices (BRI) should not be interpreted as a group due to the distinct burial periods.

# CHAPTER 14: HEANING WOOD QUANTIFICATION

## 14.1: NISP AND MINI

A total of 363 fragments were identified as human from the material excavated between 2016 and 2019. An additional 61 human fragments were located at the Dock Museum. The final number of identified specimens (NISP) was 423 (appendix 5.1).

The total number of specimens (NSP) and animal fragments were not quantified due to the sheer volume. It was initially anticipated that these would be calculated by weight and size class but due to time constraints this was not completed. It is recommended that the faunal remains be examined within their own project, with the potential to combine results.

The minimum number of individuals (MNI) was estimated at eight. One middle adult, three young adults, two young children, one older infant and one neonate (table 14.1). Two fragments of maxilla (HBC510 and HBC511) were assigned to Individual D with tooth wear on the left premolars consistent to the wear on the mandible also assigned to D (HBC421). There was a degree of misalignment between the mandible and maxilla fragments, however fragmentation and taphonomic modifications meant there was insufficient evidence to say they were not associated. There was also a right calcaneus (HBC801) inconsistent in size to all individuals, despite not being a repeat element. These inconsistencies, coupled with two distinct dates taken from Individual D, strongly suggest that there was at least one other individual in the assemblage. There was no repetition of elements, or biological indicators, to firmly establish an MNI of nine, but the MNI reported here should be treated strictly as a minimum.

Table 14.1: Summary of Heaning Wood demographics

| **Individual** | **Age** | **Sex** | **Stature** | **Years BC** |
|---|---|---|---|---|
| A | 17-25 years | Male | 173.05 – 181.69 cm | 2195-2030 BC |
| D | 25-35 years | Male | Undetermined | 2200-2035 BC |
| B | 17-25 years | Male? | 150.25 – 156.79 cm | 3765-3640 BC |
| C | 25-33 years | Female | 149.91-163.25 cm | 3705-3540 BC |
| E | 2.5-3.5 years | Undetermined | Undetermined | 3710-3635 BC |
| H | 10-18 months | Undetermined | Undetermined | 3635-3385 BC |
| F | 2.5-3.5 years | Undetermined | Undetermined | 9290-8930 BC |
| G | 38-40 weeks | Undetermined | Undetermined | Untested |

## 14.2: Bone Representation Index

When all individuals are combined, elements from all areas of the body are represented. There were 120 fragments unassigned to individuals (appendix 5.2). Of the 120 unassigned fragments the majority were hands and feet (47.66%). This is due to difficulties in differentiating between them confidently enough to assign them to individuals. It was decided that assigning them to individuals may have skewed analysis and there were no taphonomic modifications that fell outside of the observed changes on the assigned fragments. When the bone representation indices (BRI) including the unassigned fragments are compared to the BRI excluding the unassigned fragments, the distribution of represented elements remains the same (figure 14.1). Long bones show the highest representation, followed by cranial elements. Flat/irregular elements were the lowest, with only a few ribs in the excluded fragments. Some bones, particularly when fragmented, are difficult to differentiate between animal and human (Adams and Crabtree, 2008, p.1), ribs are an example of this.

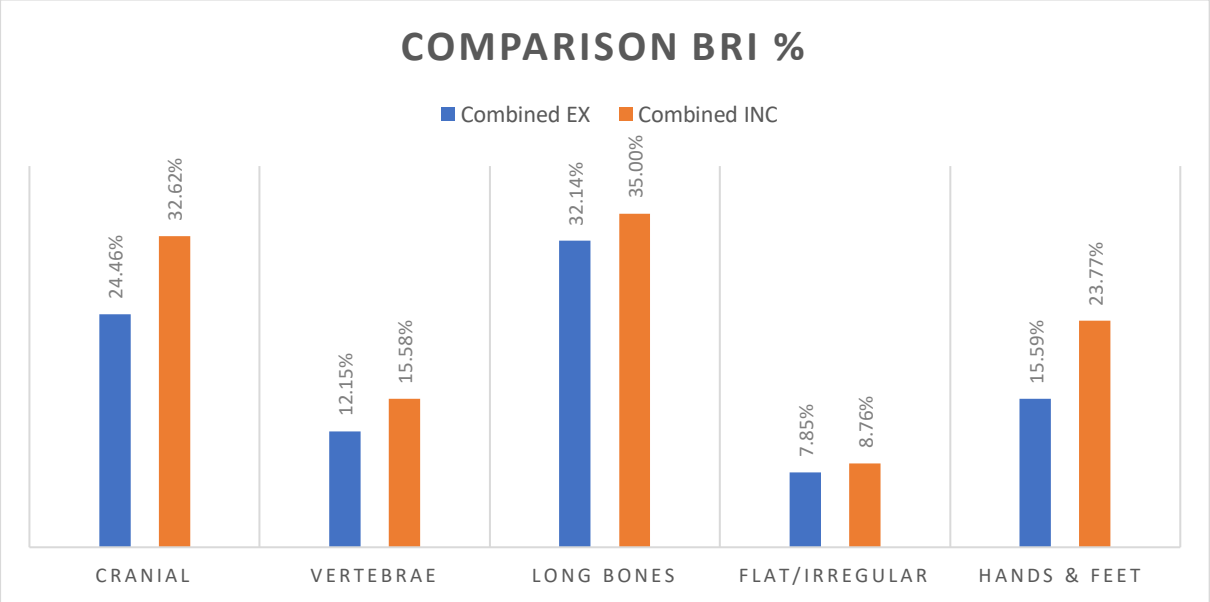


Figure 14.1: Total BRI % for grouped bones, excluding and including unassigned fragments,

Individual H (10-18 months) had the smallest number of skeletal elements (N=2), and Individual B (adult male[?], 17-25 years) the most (N=96). Individual C showed the highest

proportion of cranial elements, with 53.57% compared to the group total of 24.46% and Individuals F and H were only represented by cranial fragments (figure 14.2).

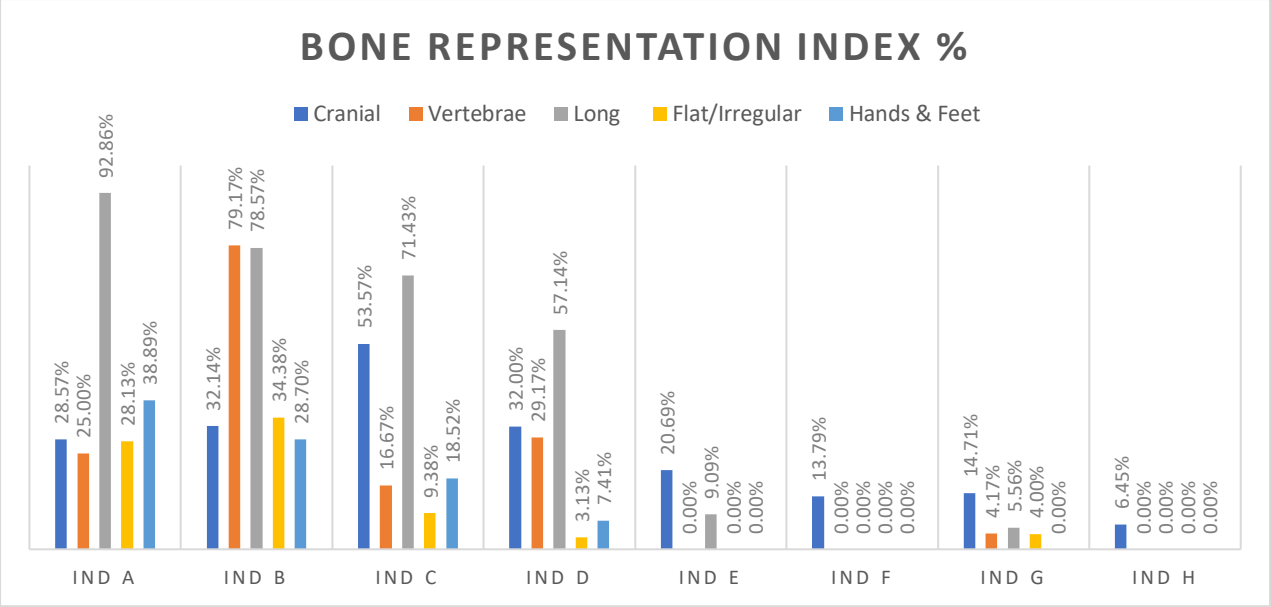


Figure 14.2: BRI % for grouped bones – excluding unidentified and unassigned fragments.

The presence of all element groups indicates that Individuals A to D were most likely deposited whole. An absence of smaller, quick to disarticulate, elements can be indicative of secondary burial (Robb, 2016), however, the representation profile of Individual G (a neonate) indicates that the level of recovery is good. This raises the possibility that Individuals E, F and H may be curated depositions. Care needs to be taken when discussing this, however, due to other potential variables impacting representation. The absence of other elements for the younger individuals could be due to destructive processes, rather than curated burial. The presence or absence of taphonomic modifications expected in relation to the burial environment may provide further insight into this and will be discussed at an individual level.

When grouped according to period, fragments associated with Early Bronze Age and Neolithic individuals remained consistent with long bones having the highest representation (figure 14.3).

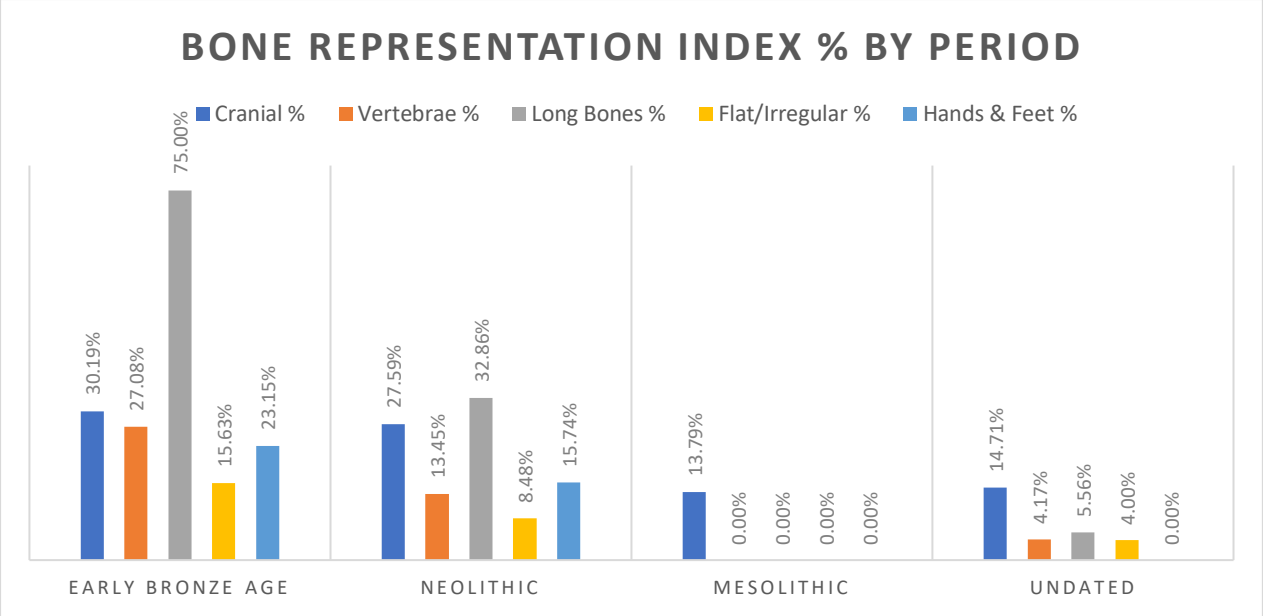


Figure 14.3: BRI % by period.

The Mesolithic individual was only represented by cranial elements. Recovery of Mesolithic burials is rare in Europe (Schulting, 2013; Orschiedt, 2018), however there is evidence of cranial only depositions as well as curation and secondary deposits (Orschiedt, 2012). The age of the bones, along with the estimated age at death (2.5-3.5 years) and the geology of Heaning Wood, it is possible that the rest of the body was subjected to destruction.

## 14.3: Preservation According to Anatomical Side

There was higher representation of left elements than right for all individuals, except for Individual A; 120 fragments were unassigned to an individual and 39 fragments were unable to be sided (table 14.2).

Table 14.2: Frequencies of fragments according to anatomical side.

| Side | A | B | C | D | E | F | G | H | Unassigned | Total |
|---|---|---|---|---|---|---|---|---|---|---|
| L | 31 | 30 | 25 | 13 | 6 | 6 | 5 | 1 | 26 | 143 |
| R | 32 | 30 | 14 | 10 | 5 | 1 | 2 | 1 | 22 | 117 |
| Unsided (u/s) | 11 | 23 | 6 | 10 | 0 | 0 | 4 | 0 | 33 | 87 |
| Unclassified | 14 | 17 | 4 | 0 | 0 | 1 | 0 | 0 | 39 | 77 |
| **Total** | **88** | **100** | **49** | **33** | **11** | **8** | **11** | **2** | **120** | **424** |

*teeth in sockets excluded and full skull counted as single fragment

Figure 14.4 shows the percentage split according to anatomical side. There is a slight bias toward left fragment preservation, however, 77 fragments were unclassified to side, which may potentially close this gap. The geology of Heaning Wood, with the talus deposit, suggests that the bodies were deposited through the opening fissure, rather than deliberately positioned. It would, therefore, be unlikely that any bias in preservation of side is a result of burial position.

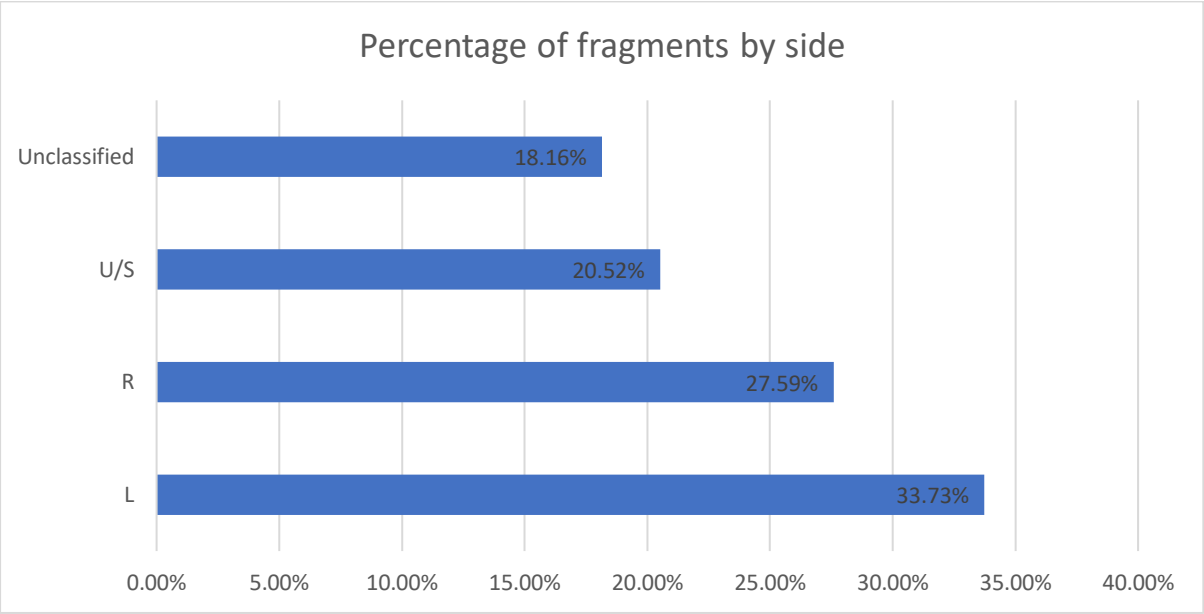


Figure 14.4: Percentage of fragments according to anatomical side.

The following section provides an overview of the demographic profiles, bone representation indices per individual will then be discussed in more detail, along with an exploration of taphonomy (chapter 16).

# CHAPTER 15: HEANING WOOD DEMOGRAPHICS

## 15.1: Bronze Age - Individual A

### *15.1.1: Age at Death Estimation*

Dental attrition was scored between stages two and three (Brothwell, 1981, p.69) for both mandibular and maxillary molars, providing an age estimation of 17-25 years (figure 15.1). The third molars had fully erupted.


Figure 15.1: Mandibular dentition for Individual A.

Assessment of the auricular surface was attempted (Buckberry and Chamberlain, 2002), specimen HBC438 was a portion of left pelvis, with some of the auricular surface intact. The surface was damaged making age estimation difficult. There was striation still evident, which is usually found in younger age groups.

Dental wear was consistent with a young adult, with some supporting evidence from the auricular surface.

### *15.1.2: Skeletal Sex and Stature*

There were limited metrics available due to post-mortem fracturing. Clavicular length (148.00 mm), radial head diameter (24.00 mm), and the transverse diameter of the sacrum (53.70 mm) all indicated male (Spradley and Jantz, 2011). Morphological assessments of the pelvis, supraorbital region and the mandible indicated male.

There were limited long bones available for stature estimation and fracturing to more commonly used long bones, such as the femur, prevented their use. HBC402 was a left ulna measuring 279.00 mm for the maximum length. This provided a stature estimation of 177.28 cm ± 4.32 (Trotter and Gleser, 1952; Trotter, 1970).

### *15.1.3: Paleopathology*

Individual A had evidence of cranial porotic hyperostosis, areas of new bone formation, to the parietals and supraorbital ridge (figure 15.2).

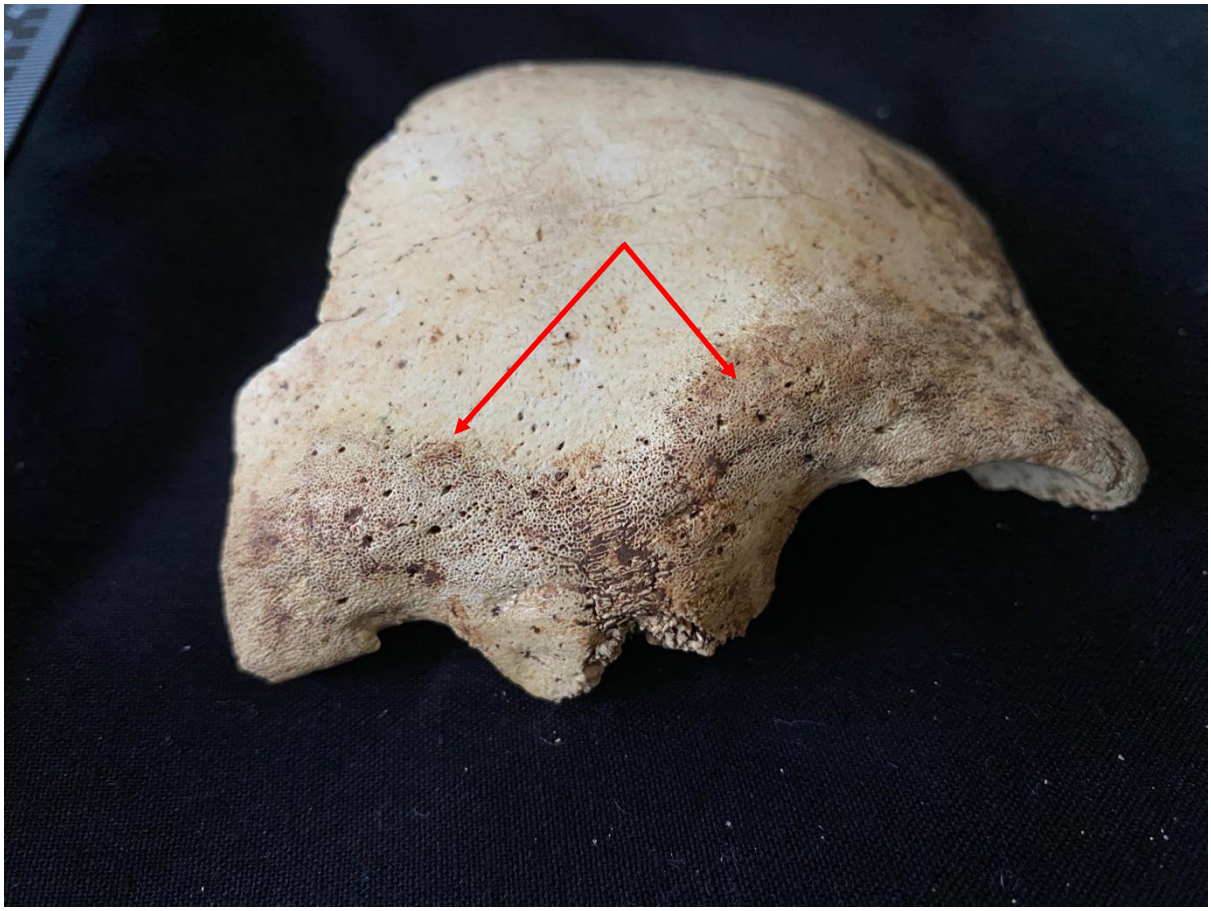

Figure 15.2: Frontal bone from Individual A showing area of porotic hyperostosis to the supraorbital ridge.

This may indicate anaemia, a result of "the body being stimulated to produce more red blood cells…to compensate for lack of iron" (Roberts and Manchester, 2010, p. 229). Similar changes can also occur due to vitamin C (scurvy) and vitamin D (rickets) deficiencies. Snoddy and colleagues (2018) developed diagnostic criteria to differentiate scurvy in the archaeological record, however assessment was difficult due to taphonomic destruction to the remaining bones. It is beyond the scope of this research to do a full assessment, however, there is evidence to suggest pathology in Individual A.

## 15.2: Bronze Age - Individual D

### *15.2.1: Age at Death Estimation*

Dental attrition was scored at stage three (Brothwell, 1981, p.69) for the left maxillary, first molar ($LM^1$) and between stages three and four for the mandibular molars (figure 15.3). While

the maxillary molar showed slightly less wear than the mandibular molars, greater weight was placed on the mandibular assessment due to the presence of all six molars. This provided an age estimation of 25-35 years. The first sacral body was fully fused, indicating an age older than 25 years.


Figure 15.3: Mandibular dentition for Individual D.

### *15.2.2: Skeletal Sex and Stature*

There were limited metrics available due to post-mortem fracturing. The transverse diameter of the sacrum (64.6 mm) and the maximum length of the calcaneus (83.16 mm) both indicated male (Spradley and Jantz, 2011). Morphological assessments of the mandible and the mastoid process of the temporal bone indicated male.

Fragmentation meant that stature estimation was not possible for Individual D.

## 15.3: Early Neolithic - Individual B

### *15.3.1: Age at Death Estimation*

Dental attrition was scored between stages two and three (Brothwell, 1981, p.69) for both mandibular and maxillary molars, providing an age estimation of 17-25 years. The third molars had fully erupted.

Specimen HBC226 was a fragmented sacrum with evidence of partial fusion of the first sacral body (figure 15.4). Full fusion of S1 and S2 is said to occur over the age of 25 years (Scheuer and Black, 2008) although variation has been found with some remaining unfused over the age of 32 years (Belcastro, Rastelli and Mariotti, 2008). There was a fragment of pubic symphysis; damage and taphonomic changes made assessment difficult but was tentatively assessed at stage 3 (Brooks and Suchey, 1990), giving an age estimation of 21-46 years.


Figure 15.4: Partial fusion of first and second sacral elements.

As there was damage to the pubic symphysis, greater weighting was given to fusion times and dental attrition, resulting in an age at death estimation of 17-25 years.

### *15.3.2: Skeletal Sex and Stature*

The skull and long bones associated to Individual B were small and gracile, despite being fully fused. Clavicular length (135.00 mm), radius maximum length (208.00 mm), femur maximum length (387.00mm) and the transverse diameter of the sacrum (45.9 mm) all indicated female (Spradley and Jantz, 2011). The mandible, however, had signs of sexual dimorphism, with gonial flaring. It is possible that Individual B was of small stature (see below), perhaps at the younger end of the age estimation, resulting in smaller metrics. Due to the morphology of the mandible Individual B was estimated to be a possible male.

HBC006/HBC030 was a left femur measuring 387.00 mm for the maximum length. This provided a stature estimation of 153.52 cm ± 3.27 (Trotter and Gleser, 1952; Trotter, 1970).

No pathology or non-metric traits were observed for Individual B.

## 15.4: Early Neolithic - Individual C

### *15.4.1: Age at Death Estimation*

Specimen HBC115 was a left clavicle with evidence of partial fusion of the medial end (figure 15.5). Full fusion of medial epiphyses is said to occur by 30 years old (Scheuer, Black and Schaefer, 2008), indicating that Individual C was likely under the age of 30 years at death. There was incomplete fusion of the sacrum (HBC255), however it was near complete.

Figure 15.5: Partial fusion of the medial epiphyseal flake of the clavical.

Dental attrition was scored at stage four for maxillary dentition and five for mandibular dentition (Brothwell, 1981, p.69), providing an age estimation of 25-35 years (Figure 15.6). The third molars had fully erupted. There was more dental attrition than would be expected on a younger adult, however the age estimation remains consistent with the fusion times described above. The final age at death estimation was 25-35 years.

Figure 15.6: Mandibular dentition for Individual C.

### *15.4.2: Skeletal Sex and Stature*

The skull and long bones associated to Individual C were small and gracile, despite being fully fused. Humeral breadth (57.63 mm) and calcaneal maximum length (71.10 mm) both indicate female (Spradley and Jantz, 2011). A partially intact cranium was associated to Individual C. Morphology of the supraorbital torus, supraorbital margins, mastoid processes, and nuchal crest were all scored between one and two (Buikstra and Ubelaker, 1994, p.20), giving a skeletal sex estimation of female. The morphology of the mandible and the sacrum were also assessed as female.

Due to a paucity of intact long bones, stature estimation was conducted using the upper breadth of a fragmented femur (VHA), as per Simmons, Jantz and Bass (1990). This provided a stature estimation of 156.58 cm ± 6.67.

No pathology or non-metric traits were observed for Individual C.

## 15.5: Early Neolithic - Individual E

### *15.5.1: Age at Death Estimation*

Individual E was estimated to be a young child aged 2.5-3.5 years.

Age at death estimation for individual E was conducted using the deciduous teeth present, analysis of the root development and adult tooth crowns visible in the crypt through x-ray (appendix 6.1). The left and right maxilla were fragmented with the portion towards the molar region remaining. An absence of deciduous teeth was not taken as an absence of development due to evidence of alveolar eruption. The dentition is summarised below, using Zsigmondy-Palmer notation (dentition marked in **bold** was assessed through x-ray).

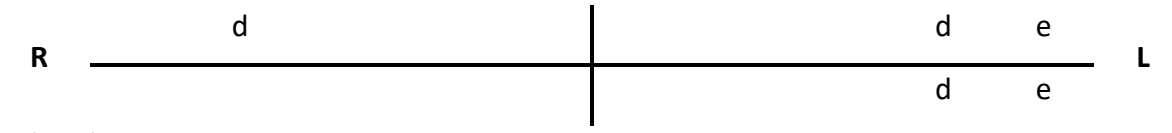


Deciduous dentition

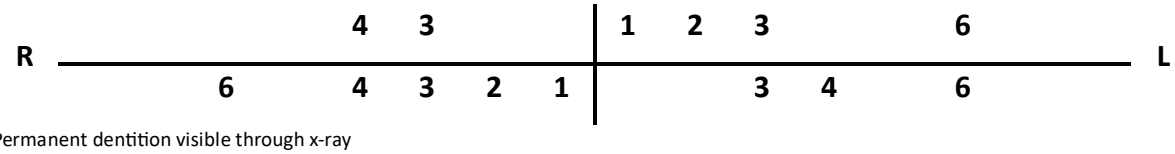


Permanent dentition visible through x-ray

Root formation for all deciduous teeth was assessed as stage $H_1$, except for ⌊e which was undetermined due to the roots being obscured. Root development of ⌈e gave a minimum age of 2.79 years (33 months) (Liversidge and Molleson, 2004). Development of adult dentition

was compared to the Atlas of Human Tooth Development and Eruption (AlQahtani, Hector and Liversidge, 2010), giving an age estimation of 2.5-3.5 years.

Maximum length of the clavicles (left = 63.2 mm, right = 63.8 mm) indicated an age of 1-3 years (Scheuer, Black and Schaefer, 2008). This supported the age ranges derived from dentition. Based on developmental markers and dentition a final age at death estimation of 2.5-3.5 years was assigned to individual E.

## 15.6: Early Neolithic - Individual H

### *15.6.1: Age at Death Estimation*

Individual H was estimated to be an older infant aged 10 – 18 months.

Age at death estimation for individual H was conducted using the deciduous teeth present, and adult tooth crown development from fragments of left and right maxilla. An absence of deciduous teeth was not taken as an absence of development due to evidence of alveolar eruption. The dentition is summarised below, using Zsigmondy-Palmer notation.

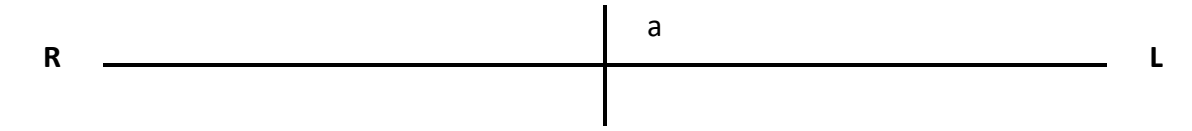


Deciduous dentition present in fractured maxilla

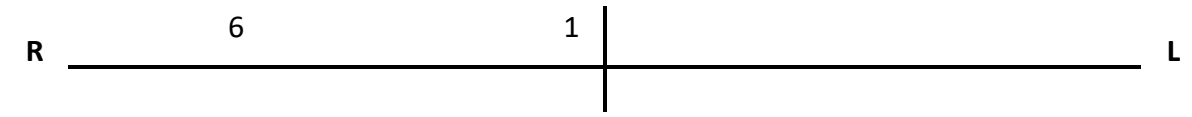


Adult dentition present in fractured maxilla, visible by sight.

Dental development was compared to the Atlas of Human Tooth Development and Eruption (AlQahtani, Hector and Liversidge, 2010), giving an age estimation of 18 months (1.5years). Complete eruption of the second, maxillary incisor indicated a minimum age of 10 months (1.13 ± 0.3 years) (Liversidge and Molleson, 2004).

No other elements were available for age estimation for Individual H.

## 15.7: Mesolithic - Individual F

### *15.7.1: Age at Death Estimation*

Individual F was estimated to be a young child aged 2.5-3.5 years.

Age at death estimation for individual F was conducted using the deciduous teeth present, analysis of the root development and adult tooth crowns visible in the crypt through x-ray (appendix 6.1). The right portion of mandible was absent. The right maxilla was fragmented, with the portion towards the molar region remaining. An absence of deciduous teeth was not taken as an absence of development due to evidence of alveolar eruption. The dentition is summarised below, using Zsigmondy-Palmer notation (dentition marked in **bold** was assessed through x-ray).

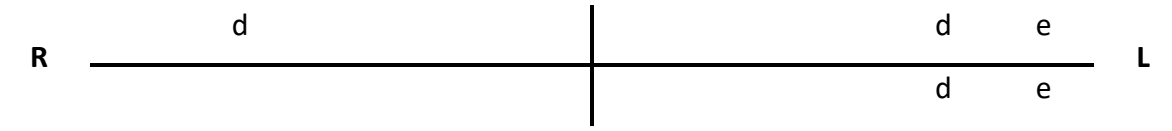


Deciduous dentition

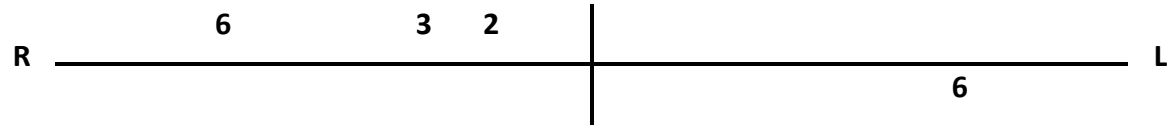


Adult dentition visible through x-ray (left maxilla was not x-rayed due to access issues)

Root formation for all deciduous teeth was assessed as stage G apart from ⌟d which was obscured on x-ray. This gave a minimum age of 2.14 years (26 months) (Liversidge and Molleson, 2004). Tooth development and emergence was compared to the Atlas of Human Tooth Development and Eruption (AlQahtani, Hector and Liversidge, 2010), giving an age estimation of 2.5 years.

With the absence of any other developmental markers the final age estimation was derived solely from dentition, giving a final estimation of 2.5-3.5 years for individual F.

## 15.8: Undated - Individual G

### *15.8.1: Age at Death Estimation*

Individual G was estimated to be a neonate aged 38-40 weeks; however, this is a very tentative assessment due to the presence of eight fragments. Of these eight fragments, the ilium, a left humerus, and the *pars basilaris* provided markers for age estimation.

Age at death was estimated using the maximum length (31.16 mm) and maximum width of the ilium (34.6 mm), the maximum length (15.5 mm), sagittal length (12.86 mm) and maximum width (14.7 mm) of the *pars basilaris*, and the maximum length of the humerus (66.00 mm). The ilium gave a wider age estimation of 40 weeks to 6 months (Fazekas and Kosa, 1978; Molleson and Cox, 1993). The *pars basilaris* and humerus gave an age estimation of 38-40 foetal weeks (Scheuer, Black and Schaefer, 2008).

The final age estimation for Individual G was 38-40 weeks. Due to an absence of any other indicators, it is not possible to determine whether Individual G had been carried to term. No other ontological assessments were possible and due to the limited number of fragments, they were not radiocarbon dated.

# CHAPTER 16 HEANING WOOD TAPHONOMY

## 16.1: Bronze Age - Individual A

### *16.1.1: Bone Representation*

All element groups were represented (figure 16.1) with near complete representation of all long bones (92.86%). Representation of the remaining element groups was similarly distributed, with vertebrae showing the lowest (25%).

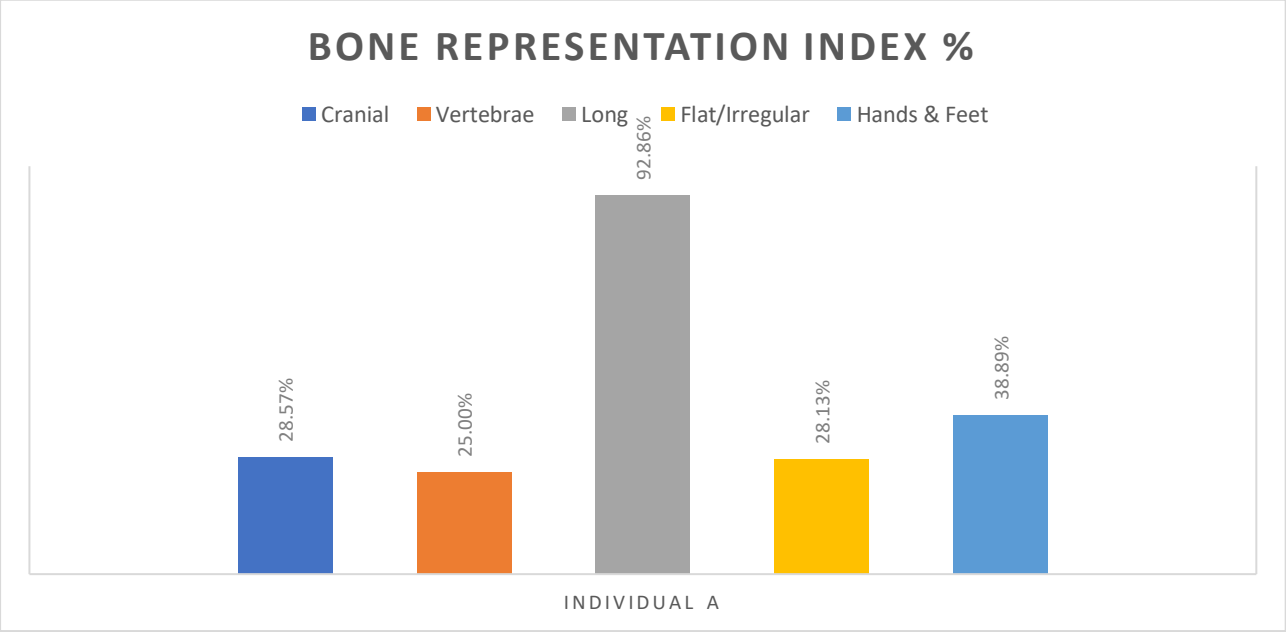


Figure 16.1: Bone representation for Individual A, Heaning Wood.

The high recovery of long bones, along with representation of all element groups, is consistent with expected destruction and recovery patterns of a whole-body deposition, primary deposition (Robb, 2016). There were slightly more right sided fragments than left (36.36% and 35.23% respectively), however the difference is marginal and is not considered to indicate burial position. There were 14 fragments where siding was not possible (15.91%), and the rest were unilateral elements (12.50%).

The following discusses frequencies of modifications, all tables for Individual A taphonomy can be found in appendix 7.1.

### *16.1.2: Whole Body Taphonomy*

All fragments from Individual A were altered by taphonomic processes (figure 16.2).

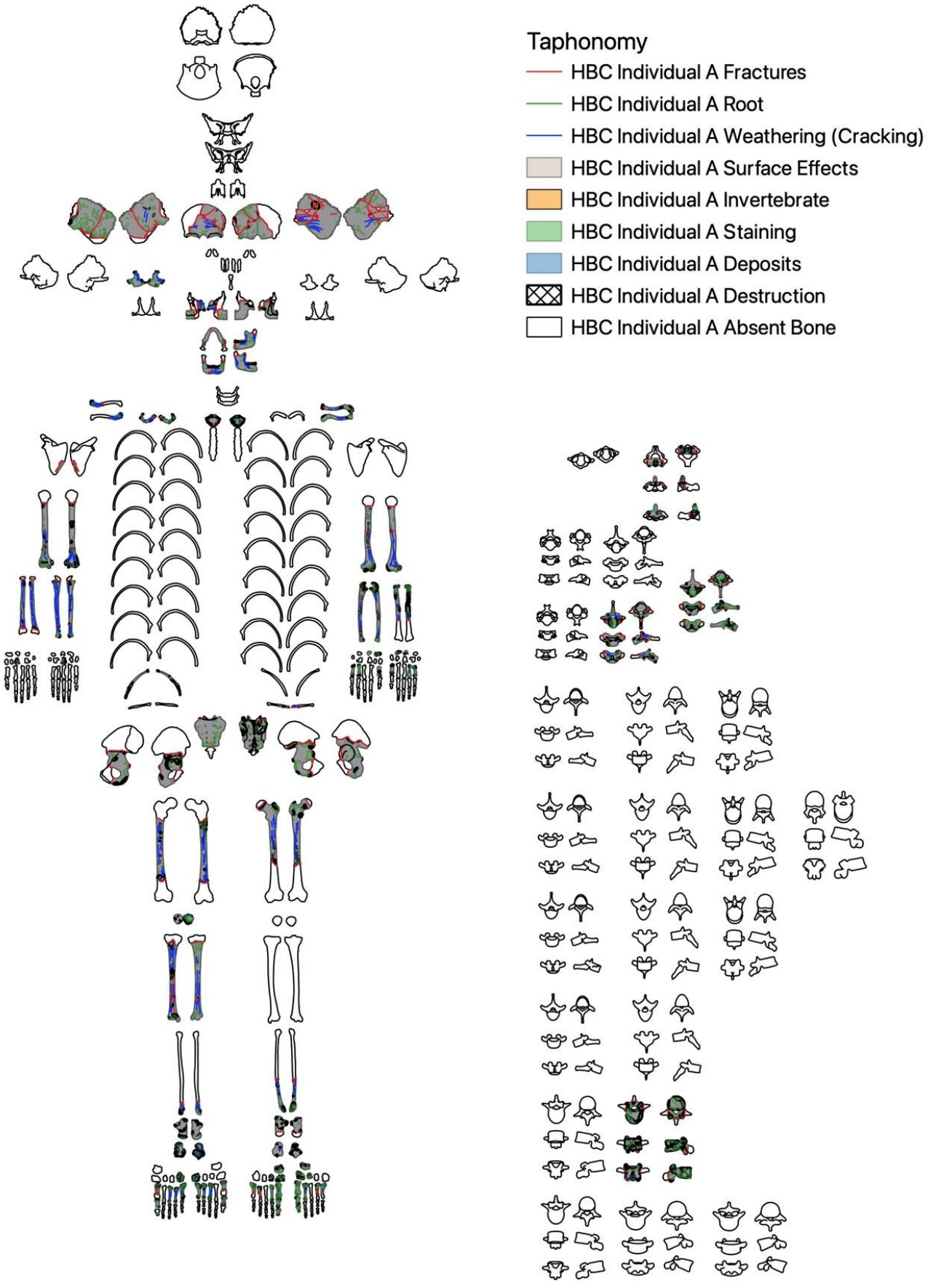


Figure 16.2: Distribution of all taphonomic modifications across Individual A.

Both left and right anatomical sides and all planes were affected by taphonomy. The left side of the body showed 42.98% of all taphonomic modifications, compared to 49.60% occurring on the right side of the body, the remaining 7.42% of modifications were on unilateral elements. This is reflective of the slightly higher proportion of right sided elements recovered.

When all taphonomic modifications were combined the posterior surface was the most affected by taphonomy (25.92%), with the anterior surface accounting for 21.66%. Superior surfaces were slightly more affected than the inferior surfaces (7.01% and 5.54% respectively). The combined lateral surfaces were more affected than medial (12.63% and 6.82% respectively). This difference may be due the presence of more lateral surfaces (for example on vertebrae), in addition to some lateral surfaces being more exposed, such as in the cranium. Most bones were assessed for their anterior or posterior surfaces which is reflected in the distributions.

### *16.1.3: Destruction*

All fragments associated to Individual A exhibited some form of destruction (figure 16.3). Most pairs of anatomical surfaces, for example dorsal and plantar/palmar, showed similar frequencies of destruction. Medial surfaces were again, less affected than lateral (2.05% and 7.11% respectively). The distribution of destruction according to side was reflective of the left and right fragments recovered, with slightly more right fragments showing destruction (39.02%) than lefts (34.12%).

When all sub-types of destruction were combined, the majority occurred to hands, feet, and patella. This is consistent with the understanding that small bones "…are more readily destroyed" (Robb, 2016, p.690). Only 24.33% of destruction occurred on long bones, despite having the highest representation.

Most of the destruction was classified as 'exposure of trabecular bone' (68.09%), followed by 18.64% classified as 'cortical removal without exposure'. Both types of destruction are consistent with the bones being in a cave environment for an extended period (Fernández-Jalvo and Andrews, 2016).

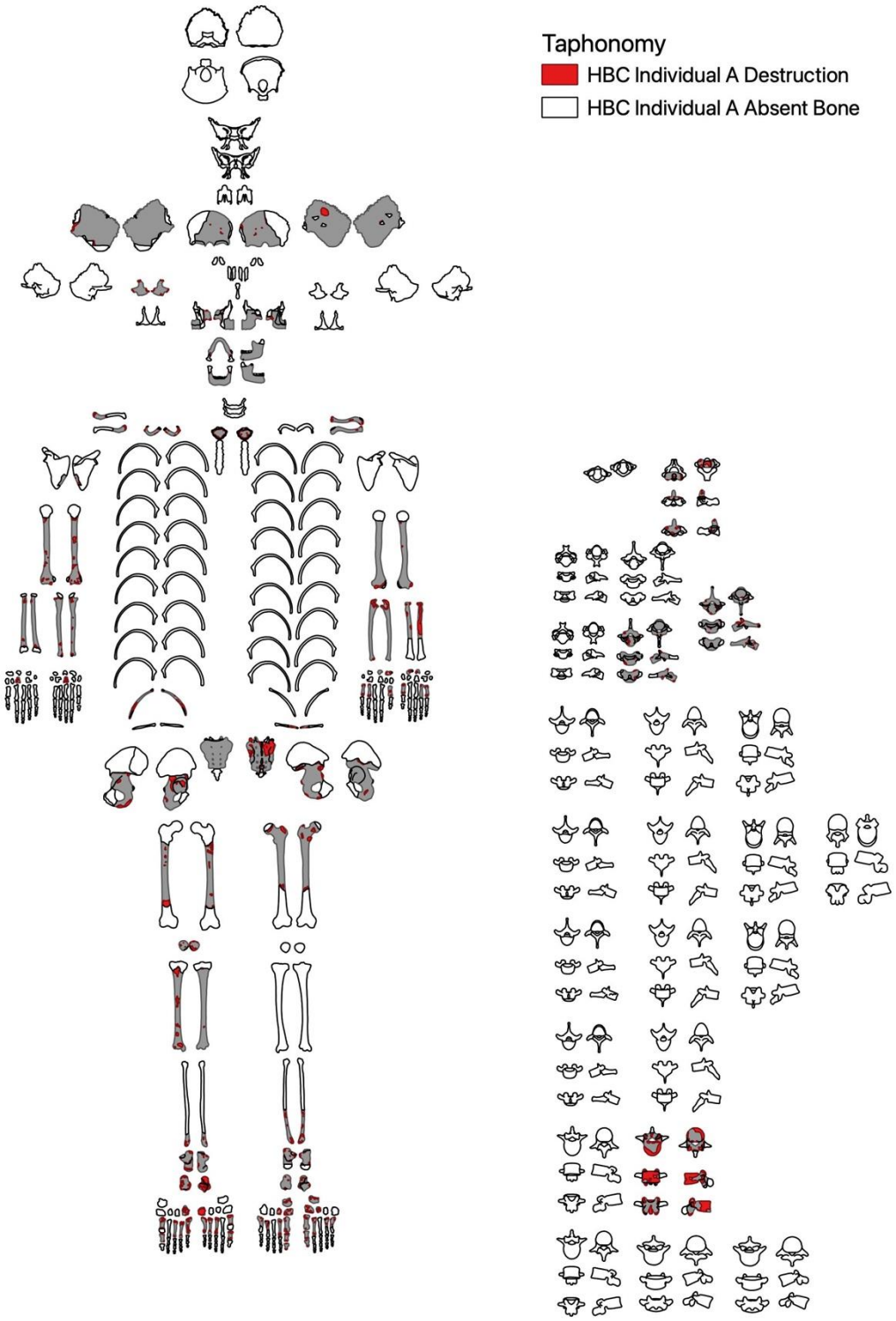


Figure 16.3: Distribution of destruction across Individual A.

Nine specimens from Individual A exhibited crush damage indicative of peri-mortem destruction (figure 16.4).

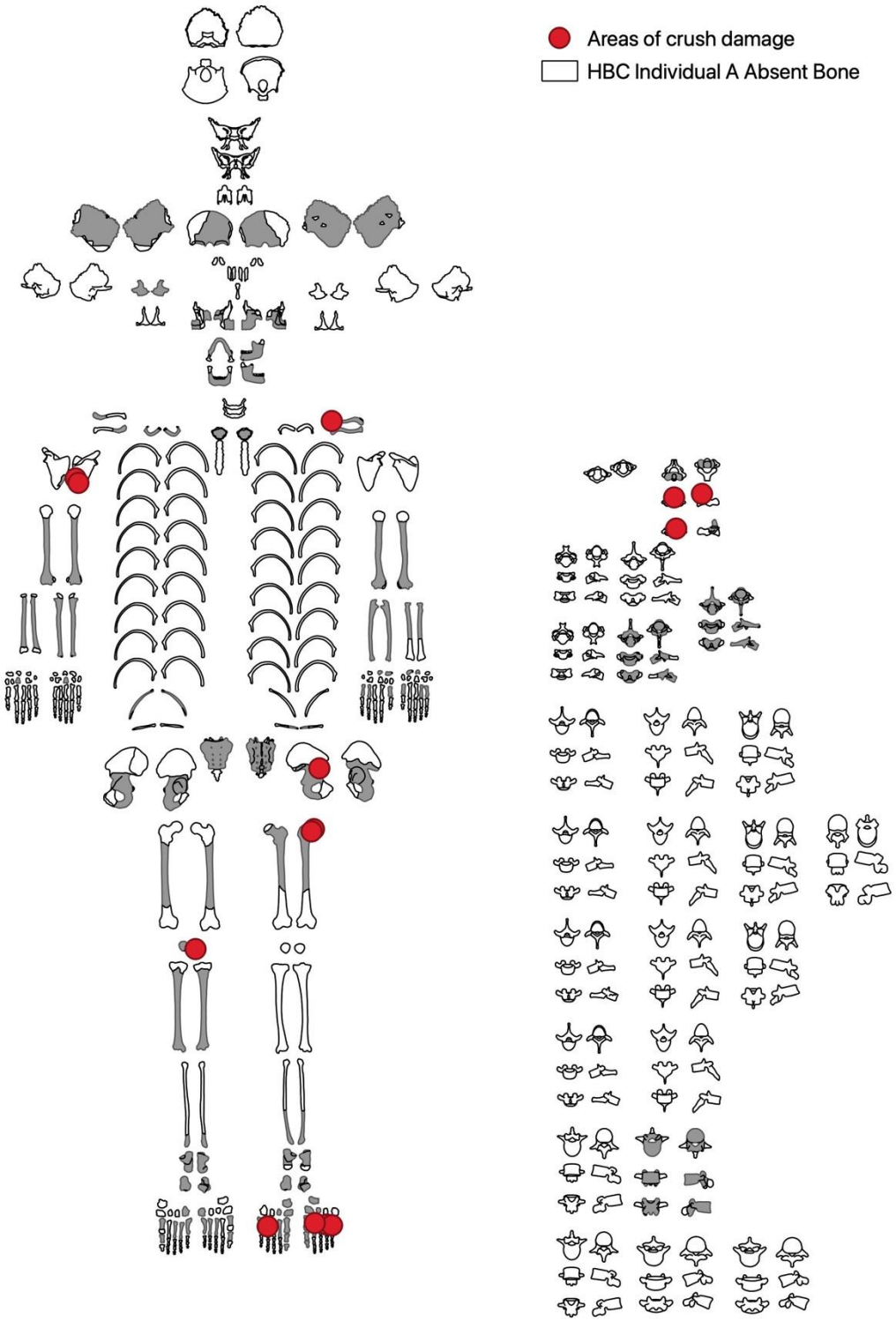


Figure 16.4: Distribution of crushing across Individual A.

Most of the crushing occurred on posterior surfaces (42.86%), compared to only 14.29% on anterior surfaces; this may be indicative of body position, with the back of the body exposed to falling sediment.

### *16.1.4: Fractures*

Incomplete and complete fractures were recorded in the same GIS layer. Fracturing occurred across most of Individual A, except for several hand and foot bones, the right zygomatic and the left ulna (figure 16.5). Complete fractures were evenly distributed across medial/lateral and dorsal/plantar surfaces. Marginally more fractures were recorded on posterior and superior surfaces than their counterparts, however, this is likely to be due to a lack of visibility of some fractures from certain views rather than a significant bias.

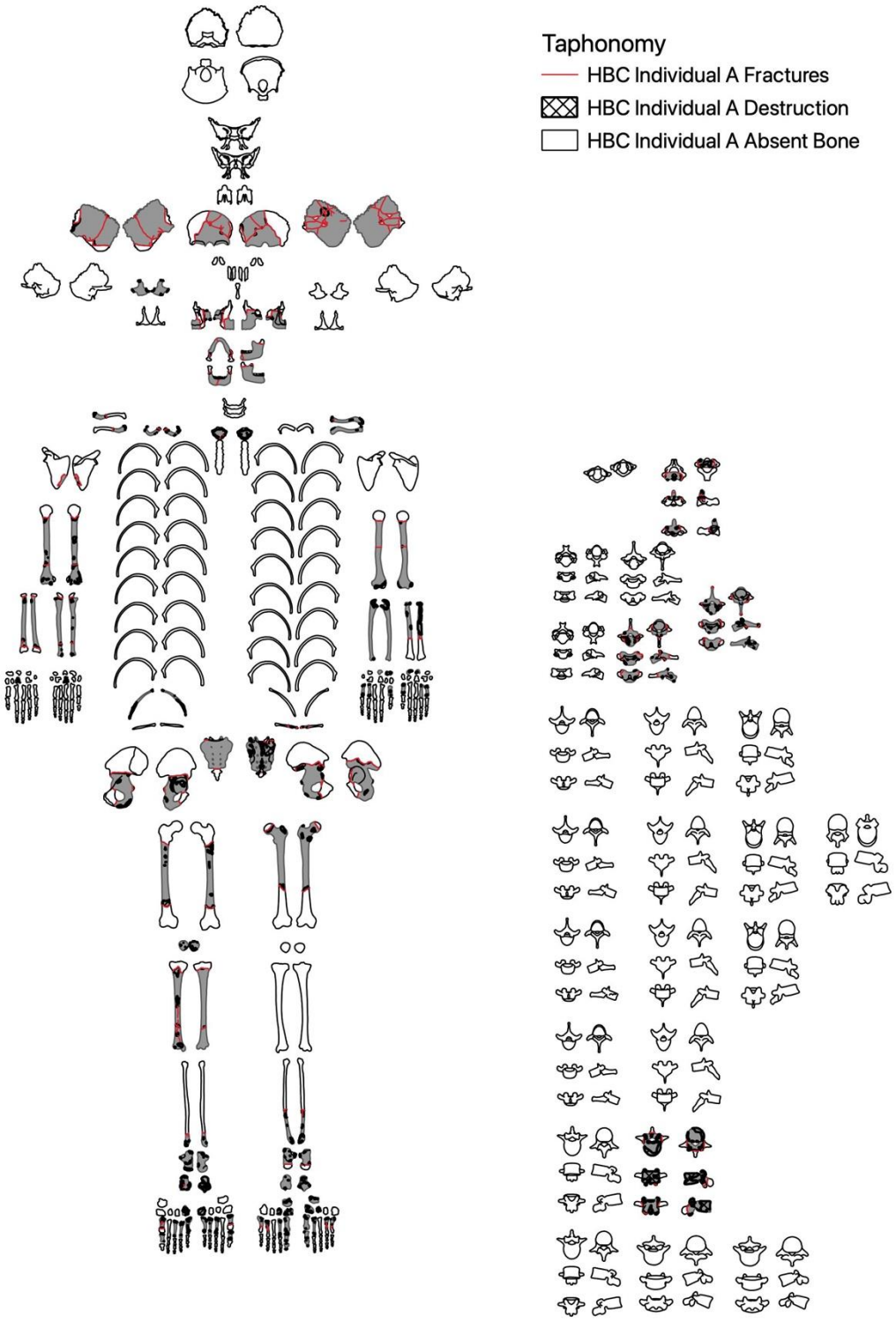


Figure 16.5: Distribution of fracturing across Individual A.

Of the fractures, 18.35% were classified as incomplete (recorded as cracking in QGIS). These usually originated from an area of damage or destruction. Analysis of areas of damage showed a bias towards the posterior surface, however, the distribution of incomplete fractures mainly occurred to the anterior surfaces (40.00%). The most common fracture classification was oblique dry (62.92%) with all fractures consistent with post-mortem breakage.

Most fractures (including incomplete cracking) occurred on the cranium (31.65%), perhaps due to fragility of isolated cranial elements. Hands and feet showed the fewest fractures (6.42%). Analysis of fracture patterns do not provide any clear indications of burial position.

### *16.1.5: Tufa Deposits*

There were fewer deposits on the Heaning Wood assemblage in comparison to Cave Ha 3. Some deposits were white, consistent with calcium carbonate, however there were a few deposits that were brown, soil-like build ups. This is consistent with the environment of Heaning Wood cave, which is predominantly an orange-brown silty clay, with some evidence of calcite formation (figure 16.6).


Figure 16.6: A) East view, across main chamber, B) West View, along fissure (photos by Martin Stables).

All the deposits on Individual A were classed as thin/flaked, with most occurring to anterior and posterior surfaces (23.11% and 20.89% respectively). There were very few deposits to medial surfaces (0.44%), while all lateral surfaces combined accounted for 10.22% of deposits, when the figure was adjusted to account for the increased number of lateral surfaces analysed, this dropped to 0.89%. More deposits occurred on the right elements (48.89%) than the left (21.33%), with the remaining 29.78% occurring on unilateral elements.

Hands, feet, and patella had the highest number of deposits (29.33%), with vertebra and long bones showing similar frequencies (28.00% and 24.44% respectively). The increase in deposits to the hands, feet, patella, and vertebra may be due to increased surface areas, in comparison to the long bones, which had a higher representation of elements.

Except for the plantar surface of the right talus (figure 16.7), all the deposits were small patches or dots (a full body image has been omitted for this reason).

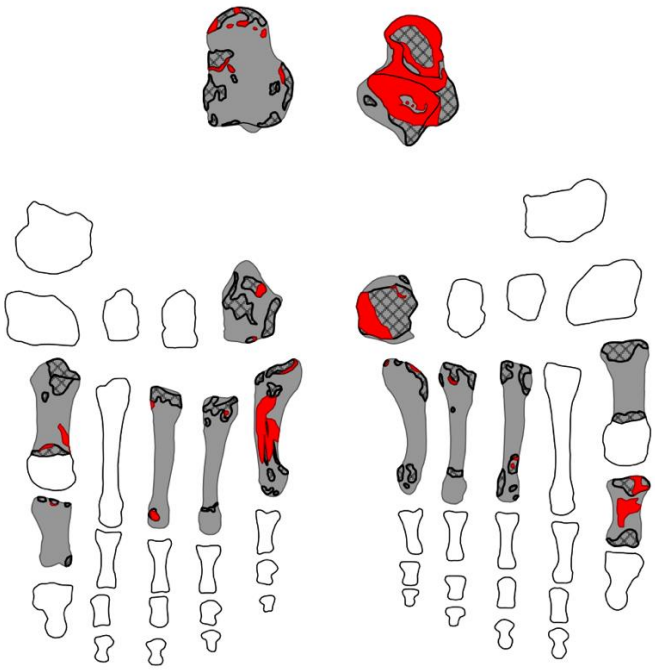

Figure 16.7: Right foot showing increased coverage of calcite deposits.

The distribution of deposits on the body does not provide any clear indication of burial position, although it could be possible that the increased number of deposits to right fragments is an indication that these fragments had greater exposure. Analysis of the spatial distributions of taphonomy and fragments may shed light on why there were significantly more deposits to the right elements. This will be explored in sections 17.4 to 17.6.

### *16.1.6: Staining*

All bones were pale with areas of light or dark soil staining, or patchy black-grey staining consistent with manganese staining (figure 16.8). There were occasionally small areas of orange-brown staining.

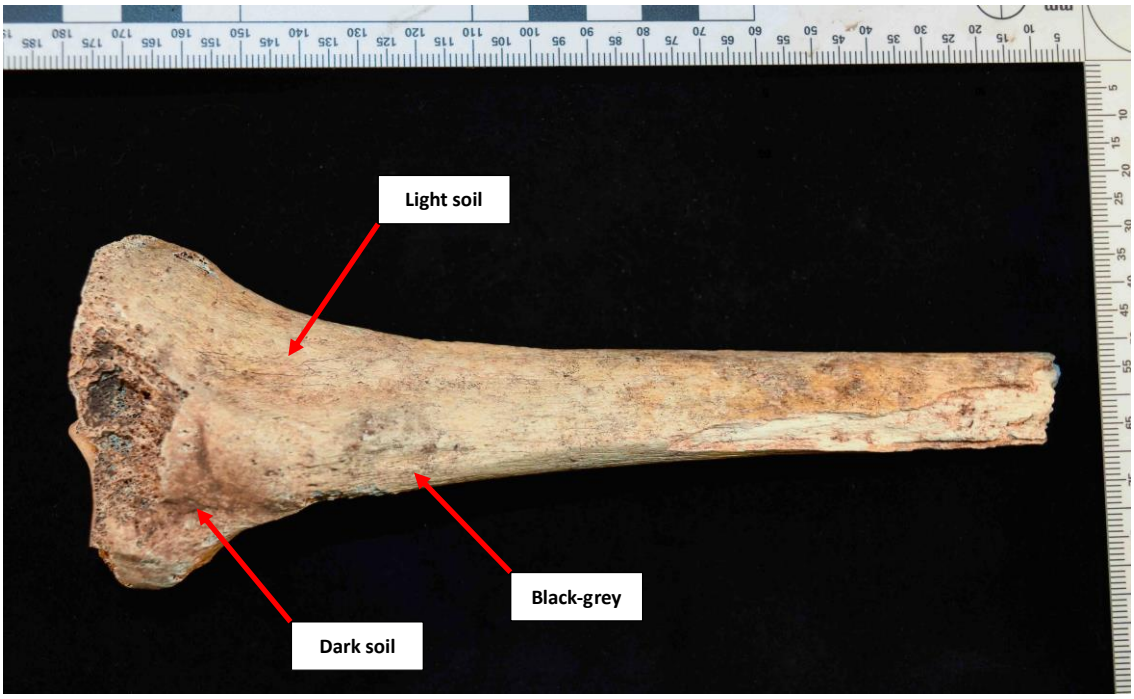


Figure 16.8: Tibia showing different stain types.

Staining occurred across all Individual A fragments (figure 16.9). Most staining was dark or light soil (42.84% and 20.79% respectively), with all stain types occurring mostly on the posterior (25.65%) and anterior (18.72%) surfaces. There is a slight difference in the amount of staining to the posterior surfaces in comparison to the anterior, possibly indicative of a bias in contact with surfaces. Staining was evenly distributed across left, right, and unilateral fragments.

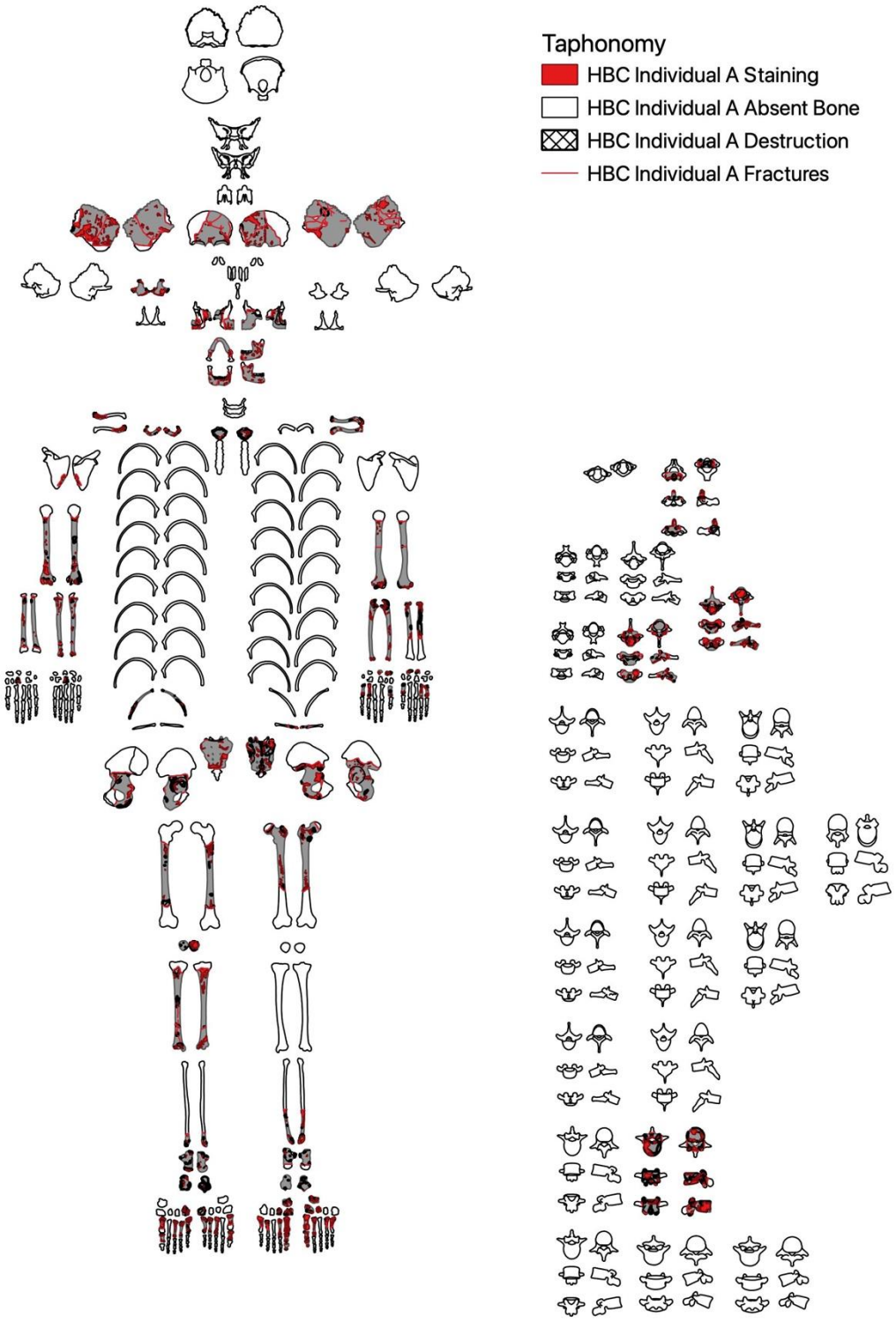


Figure 16.9: Distribution of staining across Individual A.

There were a few specimens where staining spanned across fractures. The staining on the right humerus, for example, spanned two fragments that were excavated at different times (figure 16.10). HBC010 was the distal portion and was recovered from layer four during the 2016-2019 excavations, the upper portion (HBC403) was recovered during the earlier excavations.

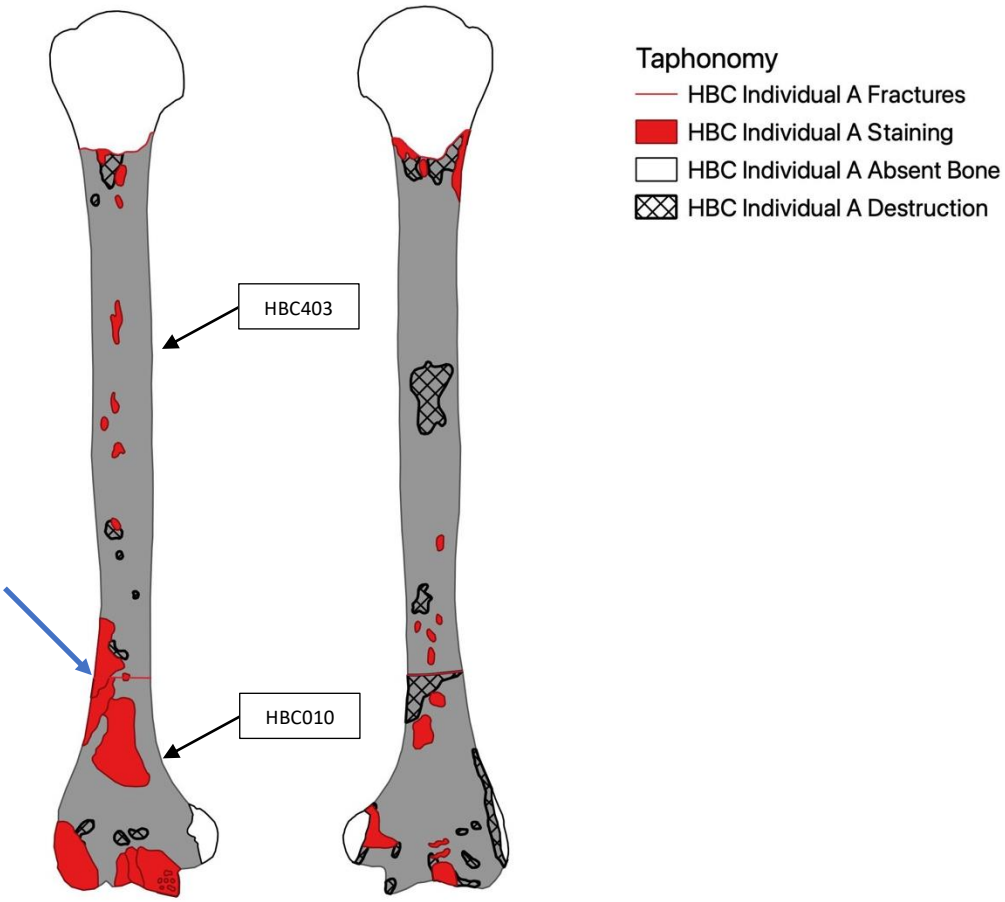


Figure 16.10: Staining spanning two fragments (blue arrow).

The spatial relationship of these fragments will be explored in section 17.5.3. The spread of staining across two fragments suggests that the fracture occurred late in the post-mortem period, after sufficient time had passed for the cortical surface to become stained.

Long bones had the highest frequency of staining (26.82%), consistent with the higher recovery rate of long bone elements. Flat/irregular bones showed the lowest (11.79%), perhaps due to irregularities in the bone reducing contact with cave surfaces. Some areas of

staining were modifying existing modifications (19.62% of all staining). This usually occurred in areas of destruction, with 63.30% classed as dark soil staining. This indicates that those areas of destruction were occurring prior to staining. On bones where there were patches of exposed trabecular bone there was often build-up of soil sediment, reflecting the humic condition of the cave (figure 16.11).


Figure 16.11: Soil embedded in exposed trabecular bone.

### *16.1.7: Large Animal and Invertebrate Activity*

There was no evidence of large animal activity across the human remains for Heaning Wood, despite Smith (2012, p. 6) describing "traces of butchery by humans in the caves and also carnivore damage". It is likely that this was describing the faunal remains that had undergone a different method of accumulation. There was a single portion of long bone shaft that had evidence of extensive gnawing, however damage prevented identification to species, however it was most likely faunal.

Eight bones from Individual A exhibited small areas of cortical removal consistent with invertebrate activity (figure 16.12). Similar modifications had previously been subjected to microscopy using a Leica M80 light microscope (Warburton, 2017).

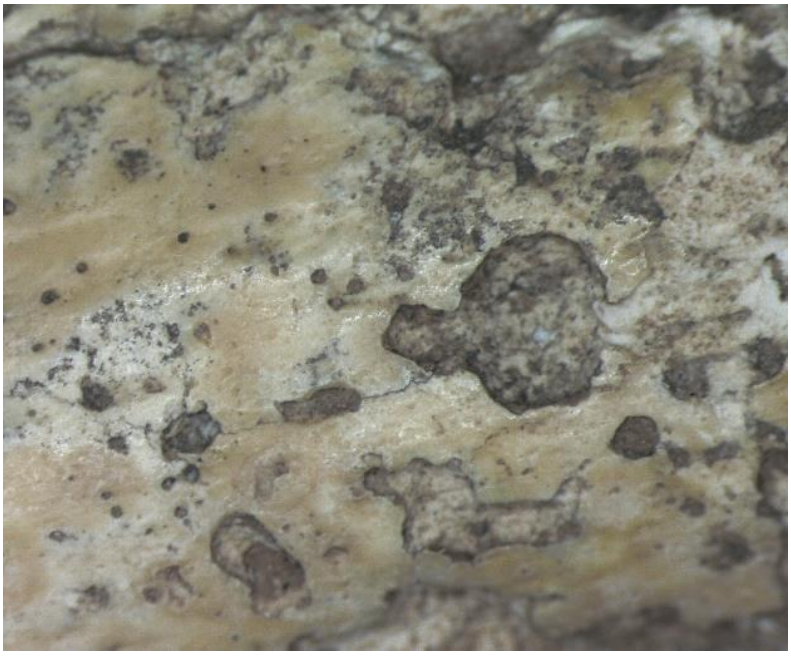

Figure 16.12: Example of circular areas of cortical removal consistent with invertebrate activity (taken from Warburton, 2017)

Pitting accounted for 87.21% of the invertebrate modifications on Individual A, with the majority occurring to left sided fragments (80.23%). The distribution according to anatomical side was mostly split evenly, with lateral sides showing the lowest (12.79%). Nearly all the modifications occurred on long bones (95.35%), with just four counts of invertebrate modification to cranial elements. All the modifications occurred on bones that were held in the Dock Museum collection. It is understood that these bones were collected from the top of the talus formation, and were, therefore, possibly more exposed than other bones accumulated deeper. The spatial distribution of these fragments will be explored in more detail in section 17.6.5.

### *16.1.8: Weathering and Surface Effects*

Evidence of weathering occurred to most of the body (figure 16.13) and was limited to linear cracking, usually in line with the bone grain, with some areas of delamination. Delamination was differentiated from more generic cortical removal due to cortical surface having the appearance of peeling, with a "fibrous texture" (Hawks *et al.*, 2017, *Supplementary file* 5, p.4).

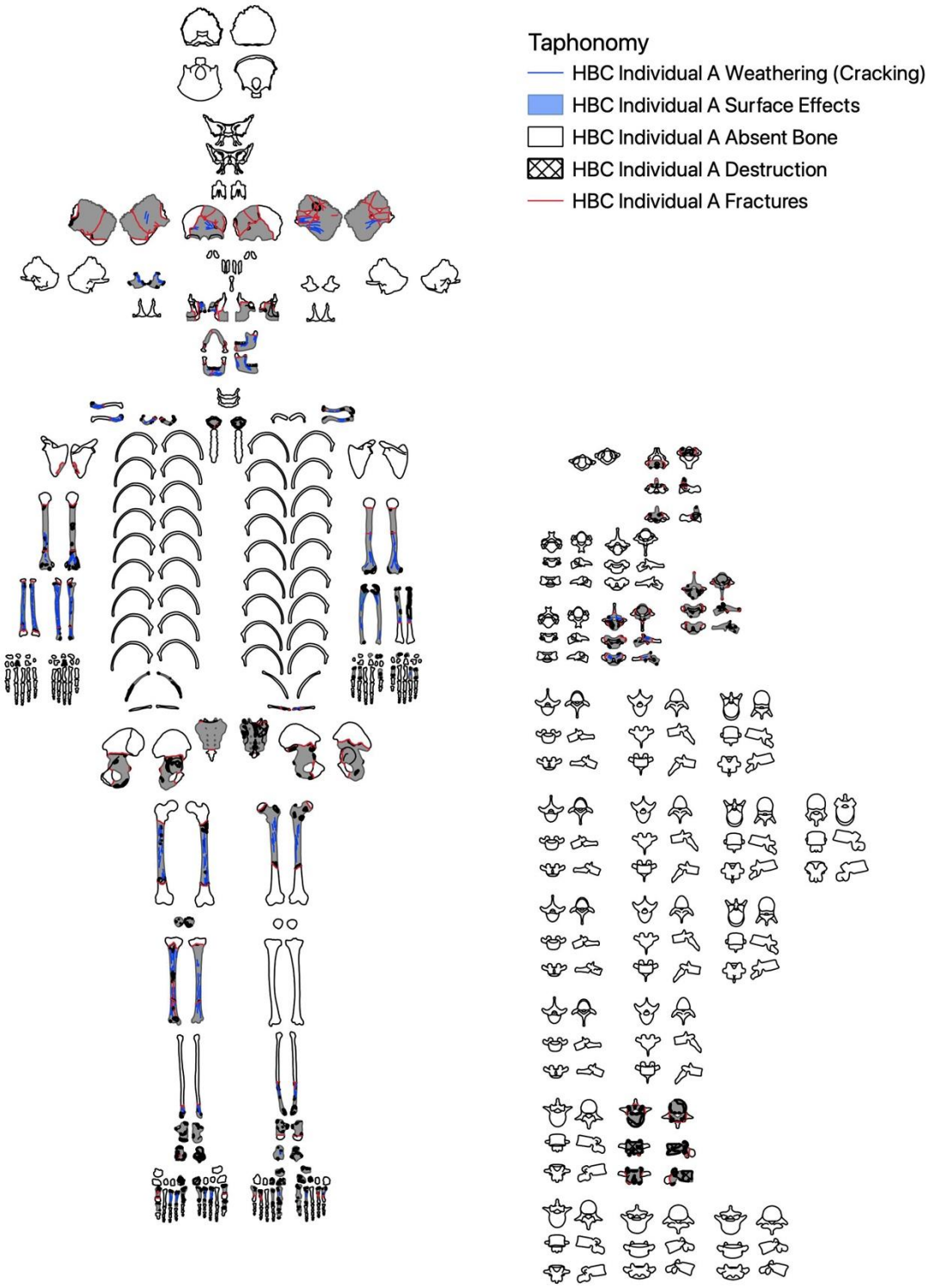


Figure 16.13: Distribution of weathering across Individual A.

There was no evidence of weathering affecting one surface over another, posterior and anterior surfaces were the most affected (30.72% and 27.78% respectively), which is in line with there being a higher proportion of those surfaces analysed. Right elements showed higher frequencies of weathering effects (58.50%) than left (27.78%) and unilateral (13.73%) elements. Although there were slightly more right fragments recovered than left, this does not explain the difference found here. Like the distribution of deposits, it is possible that the right fragments had more exposure to weathering effects within the cave.

Weathering predominantly affected long bones (63.40%), in line with the distribution of elements represented. Hands, feet, and patella were the least affected (6.54%). There was an absence of other weathering indicators such as bleaching, that would suggest the bones had been exposed to subaerial processes. The cracking and cortical peeling was consistent with slower weathering processes likely to occur in subterranean environments, such as wet/dry cycles.

All taphonomic changes to Individual A are consistent with a primary, whole-body burial, with an extended period in a cave environment. There was no clear suggestion of burial position, although some factors require further spatial analysis, such as side distribution of deposits and weathering, and destruction to posterior surfaces (see sections 17.4-17.6).

## 16.2: Bronze Age - Individual D

### *16.2.1: Bone Representation*

All element groups were represented (figure 16.14) with long bones having the highest representation (57.14%). Cranial and vertebrae were similarly represented (32.00% and 29.17% respectively), with flat/irregular showing the lowest (3.13%).

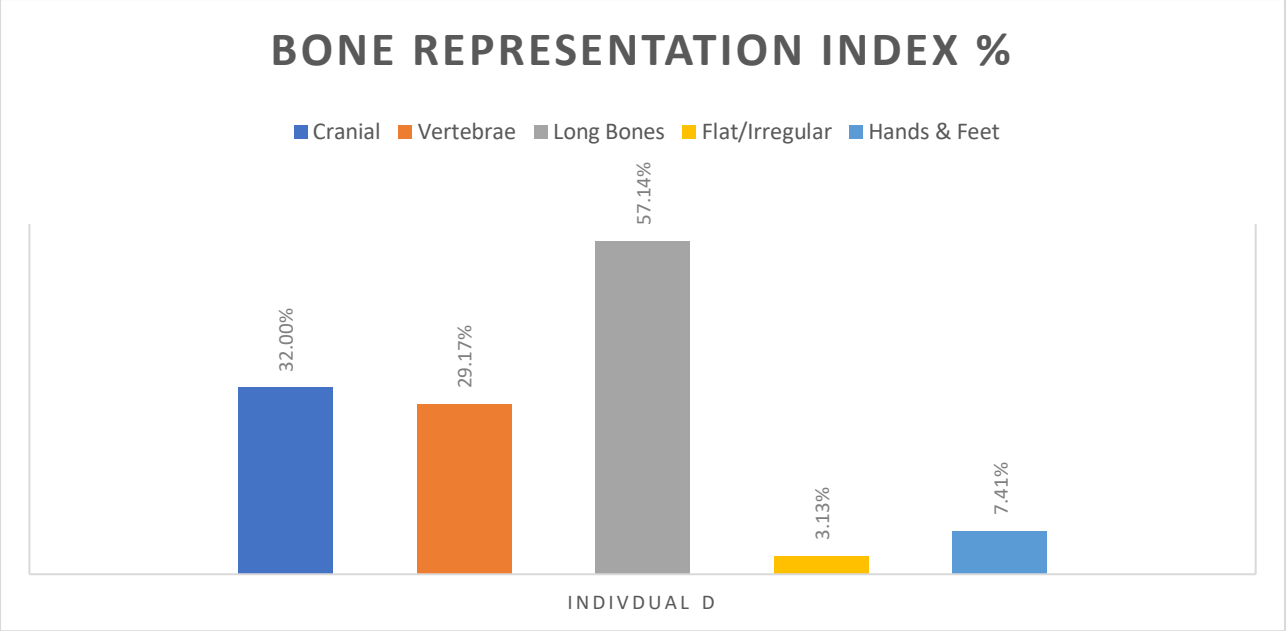


Figure 16.14: Bone representation for Individual D, Heaning Wood.

The high recovery of long bones, along with representation of all element groups, is consistent with expected destruction and recovery patterns of a whole-body, primary deposition (Robb, 2016). There were slightly more left sided fragments than right (39.39% and 30.30% respectively), however the difference is marginal and is not considered to indicate burial position. There were no fragments where siding was not possible, and the rest were unilateral elements (30.30%).

The following discusses frequencies of modifications; all tables for Individual D taphonomy can be found in appendix 7.2.

### *16.2.2: Whole Body Taphonomy*

All fragments from Individual D were altered by taphonomic processes (figure 16.15).

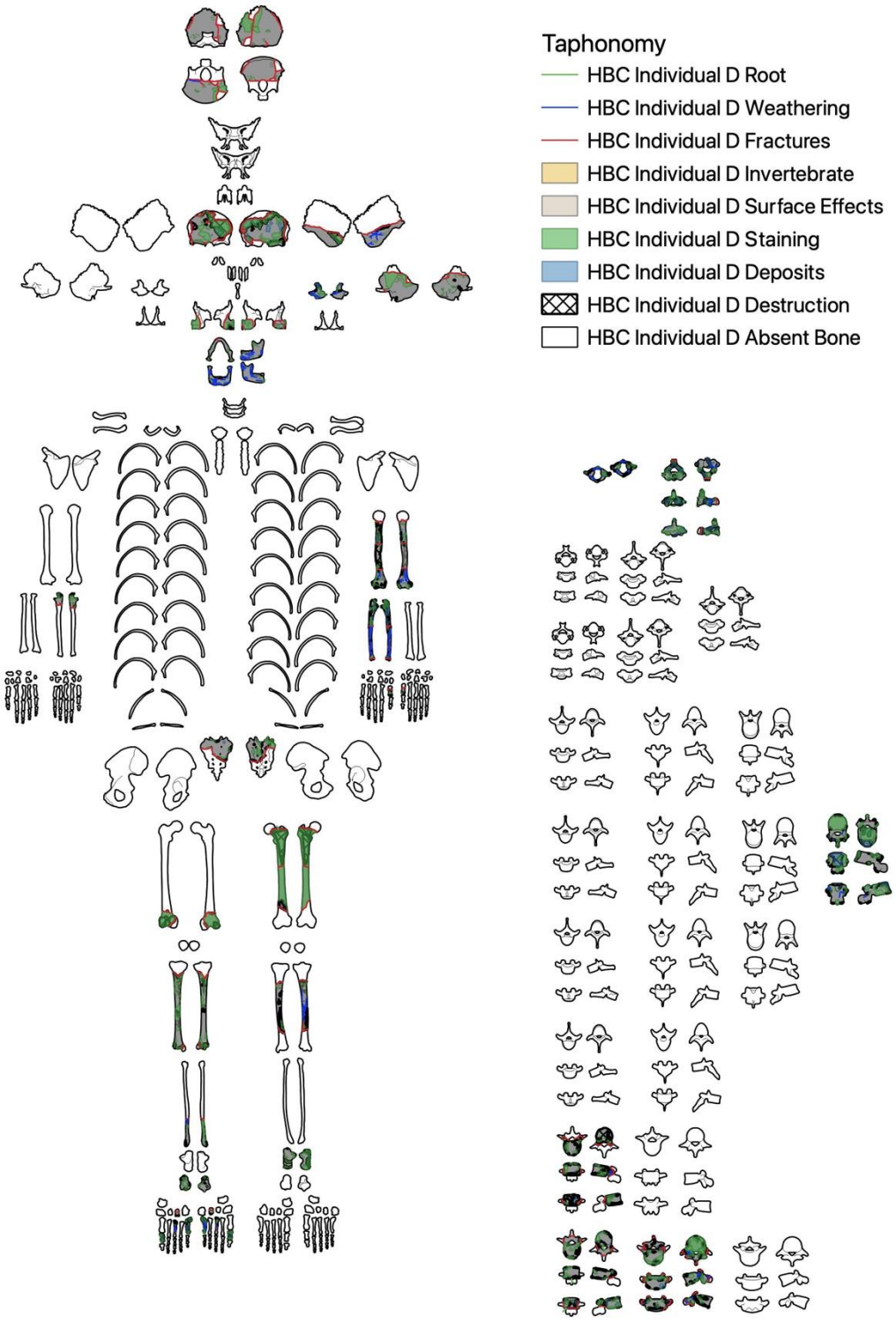


Figure 16.15: Distribution of all taphonomic modifications across Individual D.

Both left and right anatomical sides and all planes were affected by taphonomy. The left side of the body showed 25.95% of all taphonomic modifications, compared to 15.18% occurring on the right side of the body, the remaining 58.87% of modifications were on unilateral elements. This is reflective of the slightly higher proportion of left sided elements recovered, however unilateral elements are disproportionally affected; this is discussed in more detail in the section below (16.2.3: Destruction).

When all taphonomic modifications were combined the posterior surface was the most affected by taphonomy (22.14%), with the anterior surface accounting for 18.45%. Superior surfaces were slightly more affected than the inferior surfaces (11.90% and 10.24% respectively). The combined lateral surfaces were more affected than medial (19.40% and 7.98% respectively). This difference may be due the presence of more lateral surfaces (for example on vertebrae), in addition to some lateral surfaces being more exposed, such as in the cranium. Most bones were assessed for their anterior or posterior surfaces which is reflected in the distributions.

### *16.2.3: Destruction*

All fragments associated to Individual D exhibited some form of destruction (figure 16.16). Most pairs of anatomical surfaces, for example dorsal and plantar/palmar, showed similar frequencies of destruction. The distribution of destruction according to side was reflective of the left and right fragments recovered, however destruction to unilateral fragments was significantly higher (64.45%).

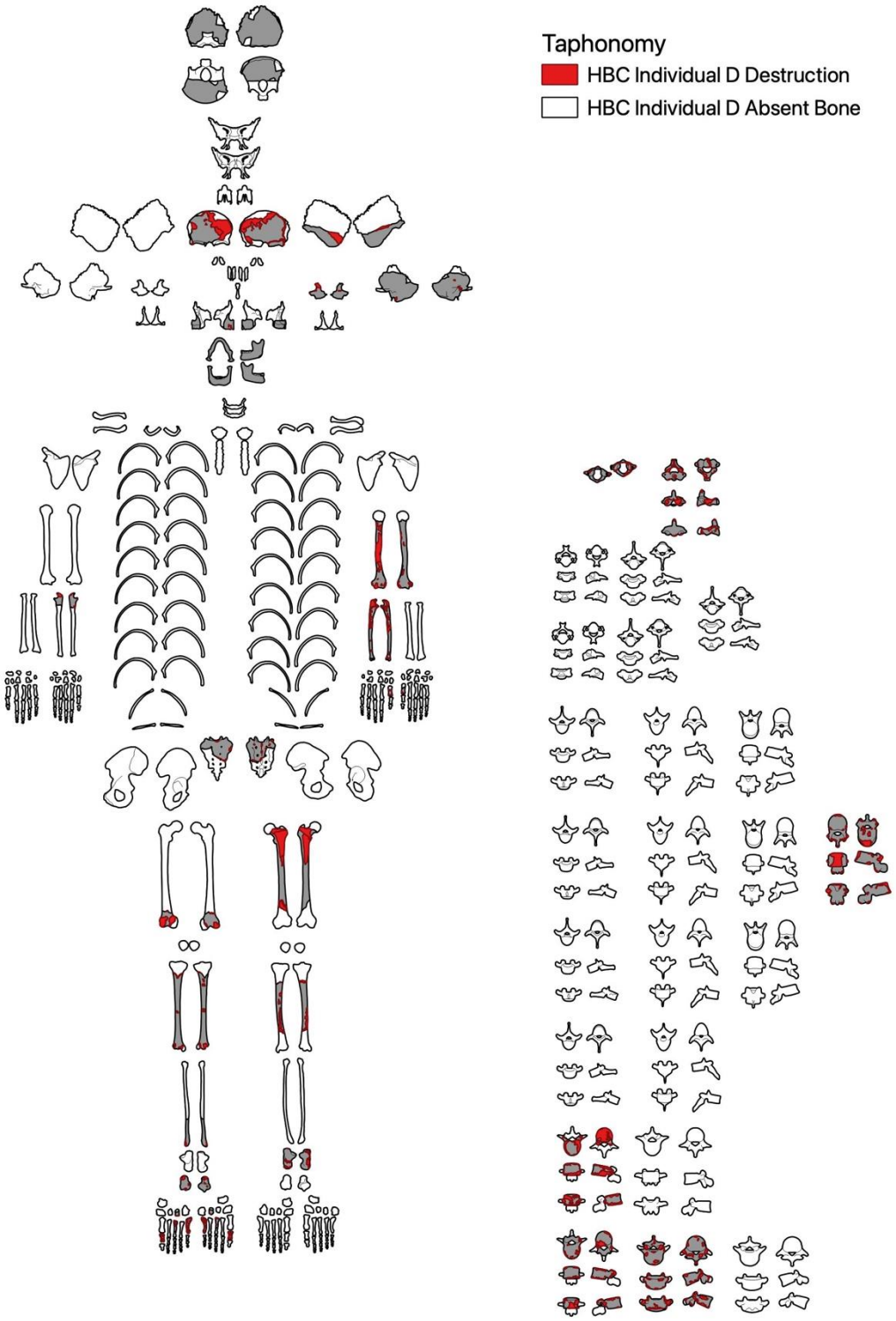


Figure 16.16: Distribution of destruction across Individual D.

When the frequencies were explored further, to look at both element type and side, vertebrae showed significantly higher occurrences of damage than any other element type. This is due to the increased recording of anatomical planes. When this was adjusted to only look at anterior and posterior views (in line with the predominant surfaces analysed in the rest of the body), damage fell within the expected distributions according to fragment representation (table 16.1).

Table 16.1: Adjusted and unadjusted frequencies of destruction.

| **Side** | **U/S** | **L** | **R** | **Total** |
|---|---|---|---|---|
| Destruction | 310 | 99 | 72 | 481 |
| Percentage | 64.45% | 20.58% | 14.97% | / |
| Destruction (adjusted) | 65 | 99 | 72 | 236 |
| Percentage (adjusted) | 27.54% | 41.95% | 30.51% | / |

Before adjusting, over half of destruction occurred on vertebrae (57.17%), when the frequencies were adjusted this dropped to 12.71%. Long bones then had the highest damage (40.68%), and the distribution was reflective of the bone representation indices.

Most of the destruction was classified as 'exposure of trabecular bone' (65.28%), followed by 'cortical removal without exposure' (23.91%). Both types of destruction are consistent with the bones being in a cave environment for an extended period. There were three counts of crush damage, however, crushing to left zygomatic had rough margins, with light edges and was not characteristic of the peri-mortem crushing discussed previously and is therefore likely to be post-mortem. This left one area or crushing on a left, first, metacarpal. There was no indication to suggest burial position from patterns of destruction.

### *16.2.4: Fractures*

Fracturing occurred across most of Individual D, except for the first cervical vertebra, the tarsals, and some metatarsals (figure 16.17). Complete fractures were evenly distributed across anatomical surfaces.

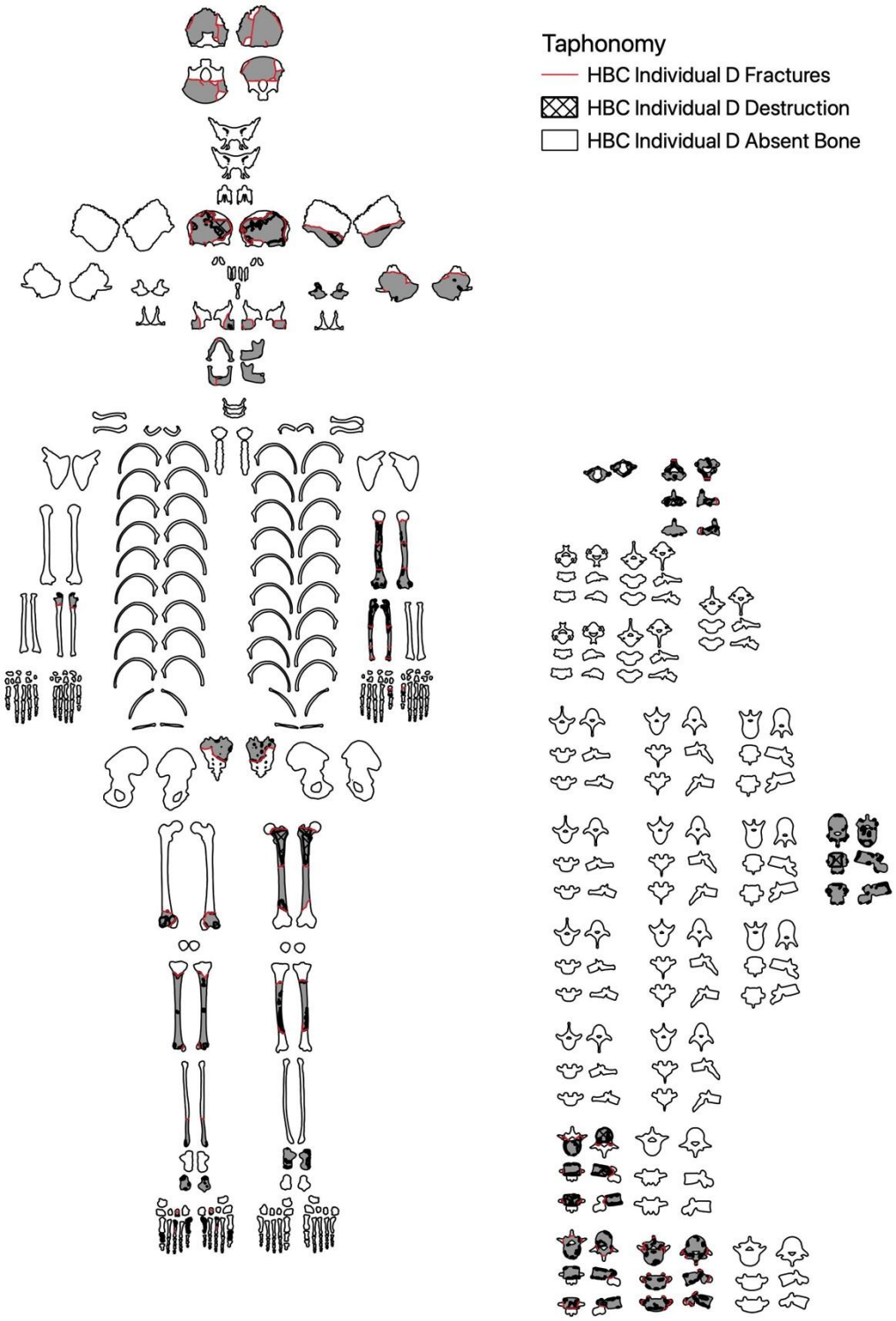


Figure 16.17: Distribution of fracturing across Individual D.

Of the fractures, 7.14% were classified as incomplete and all originated from existing complete fractures or destruction. The most common fracture classification was oblique dry (74.29%) with all fractures consistent with post-mortem breakage. There were more complete fractures to left fragments than right (25.71% and 15.00%) respectively. Again, unilateral fragments showed higher counts but once adjusted, the distribution was reflective of representation. The distribution of fractures did not indicate body position.

### *16.2.5: Tufa Deposits*

All deposits on Individual D were classified as 'thin/flaked', except for two patches recorded as 'thick/coated'. These occurred to the distal portion of the left humerus. Four of the deposits were classed as soil deposits, rather than white, calcite deposits. There was a complete absence of deposits to the lower limb bones (figure 16.18).

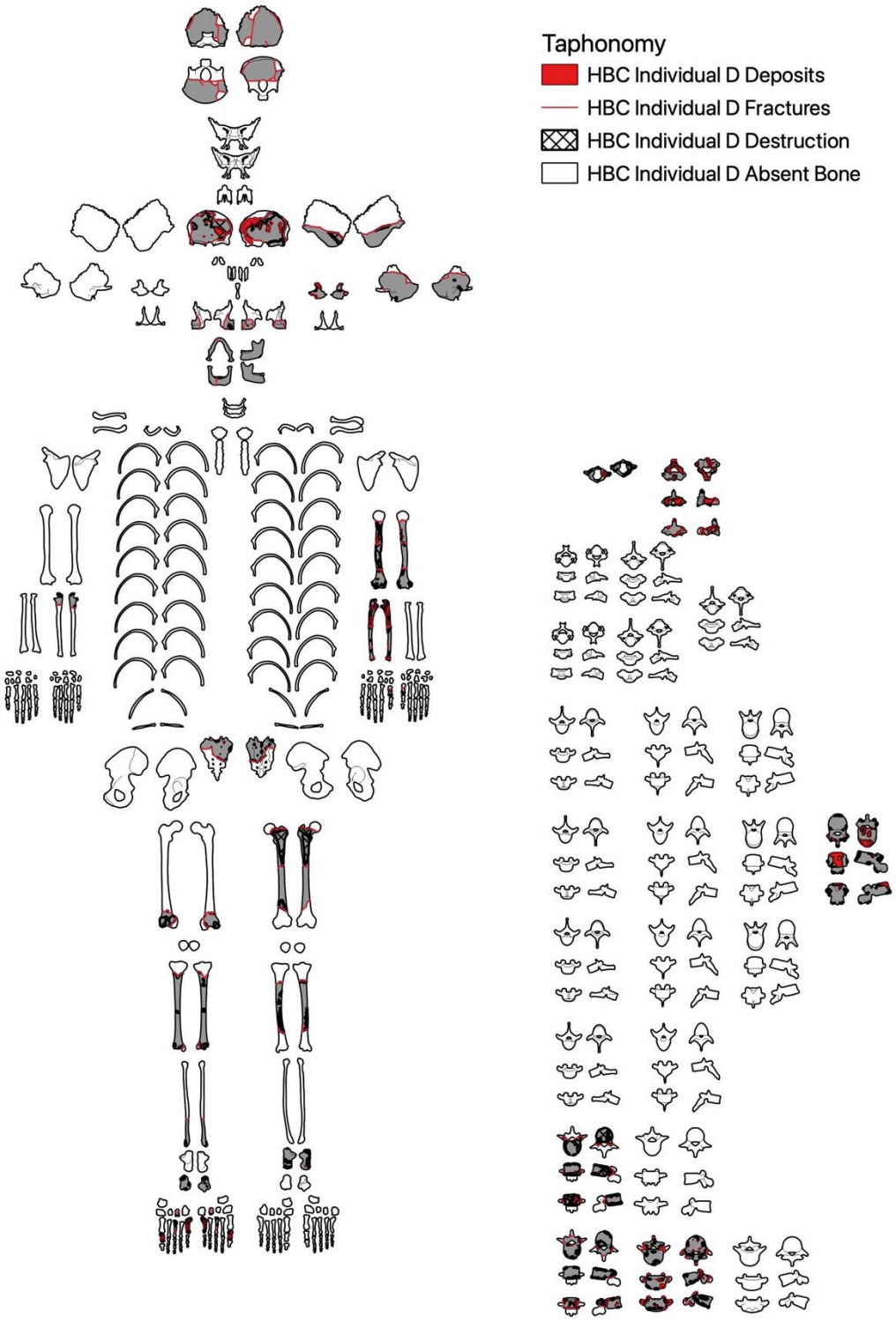


Figure 16.18: Distribution of deposits across Individual D.

The anterior and posterior surfaces had the most deposits (18.56% and 17.96% respectively), with all pairs of surfaces showing similar frequencies. After adjusting for vertebra, more deposits occurred on the left elements (45.68%) than the right (22.22%), with the remaining 32.10% occurring on unilateral elements.

Despite long bones having a higher representation, cranial elements had the highest frequency of deposits (35.80%, compared to 22.22%), this was due to the maxilla having several very small flecks. The left upper limb bones had fewer, but larger and thicker patches. This may be due to exposure or positioning in the cave, which is explored in section 17.9.4. The distribution of deposits across Individual D does not provide any clear indication of position.

### *16.2.6: Staining*

All bones were pale with areas of light or dark soil staining, or patchy black-grey staining consistent with manganese staining (figure 16.19), except both femurs.

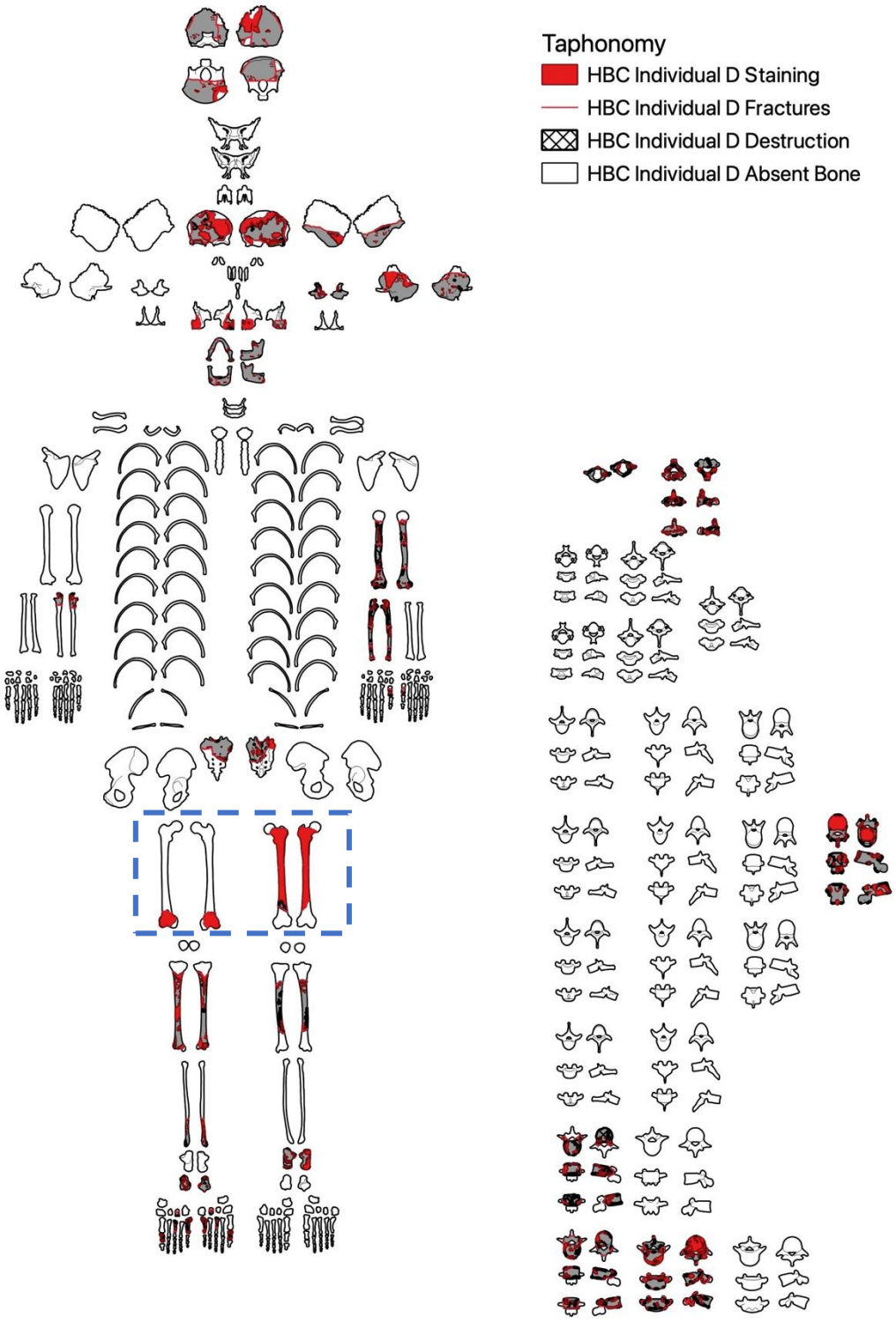


Figure 16.19: Distribution of staining across Individual D. Blue box indicates differential staining to femurs.

Fragments HBC807, HBC808, and HBC809 were all held at the Dock Museum and were collected by Peter Redshaw 1974. The cortices of these fragments were completely stained dark brown, consistent with soil staining (figure 16.20). It is unclear why the staining to these fragments appears advanced in comparison to the fragments excavated several decades later but may be the result of cleaning and preservatives applied to the 1958 specimens.


Figure 16.20: Darker staining to the Redshaw specimens.

The posterior and anterior surfaces showed similar frequencies of staining (21.10% and 19.83% respectively). There were, however, slight differences in the types of staining and how they were distributed. Most of the staining (52.83%) was classified as either light or dark soil, with the next most frequent stain type classified as dark spotted (33.99%), consistent with manganese. The posterior surfaces showed more dark soil staining than the anterior surfaces, conversely the anterior surfaces showed more dark spotted staining (table 16.2). This may be an indication of how the bones were laying in the cave, with posterior surfaces having greater exposure to the soil surface, and the anterior surfaces having greater exposure to areas of manganese.

Table 16.2: Staining frequencies according to classification and anatomical view for Individual D.

| Stain | Dark Soil | Light Soil | Light Brown/ Orange | Light Matt | Dark Matt | Light Spotted | Dark Spotted |
|---|---|---|---|---|---|---|---|
| Inf | 13 | 18 | 0 | 1 | 15 | 0 | 11 |
| Sup | 32 | 15 | 0 | 4 | 1 | 0 | 33 |
| LLat | 18 | 13 | 0 | 1 | 3 | 0 | 15 |
| RLat | 17 | 8 | 0 | 1 | 4 | 0 | 13 |
| Lat | 7 | 2 | 3 | 6 | 1 | 0 | 19 |
| Med | 28 | 2 | 0 | 3 | 0 | 0 | 43 |
| Palm | 0 | 0 | 0 | 3 | 0 | 0 | 0 |
| Plant | 18 | 7 | 0 | 0 | 2 | 4 | 0 |
| Dors | 7 | 12 | 0 | 3 | 2 | 7 | 2 |
| Post | 64 | 27 | 0 | 3 | 13 | 2 | 40 |
| Ant | 38 | 27 | 0 | 6 | 5 | 0 | 64 |

When all staining is combined, cranial elements have higher frequencies (43.65%) compared to long bones (31.75%), despite representation distribution. When distinct staining types are looked at, soil staining was as expected according to bone representation indices, however, dark spotted staining, was disproportionately found on cranial elements. This may indicate that cranial elements were in areas of greater manganese concentrations; this will be explored further in section 17.8.1.

### *16.2.7: Large Animal and Invertebrate Activity*

There was no evidence of carnivore or large animal activity on individual D. Only two fragments exhibited small areas of cortical removal consistent with invertebrate activity, both of which were tibial. Pitting accounted for all the invertebrate modifications, except for three patches of furrowing and one area where striations could be seen. The distribution according

to anatomical side was split evenly. All the modifications occurred on bones that were held in the Dock Museum collection. It is understood that these bones were collected from the top of the talus formation, and were, therefore, possibly more exposed than other bones accumulated deeper. The spatial distribution of these fragments will be explored in more detail in section 17.9.5.

### *16.2.8: Weathering and Surface Effects*

Just under half (48.48%) of the total fragments assigned to Individual D were affected by cracking (N=16) consistent with weathering (figure 16.21).


Figure 16.21: Example of linear cracking to a tibial diaphysis.

These were limited to linear cracking, usually in line with the bone grain, with some areas of delamination, and one area of patination (figure 16.22).

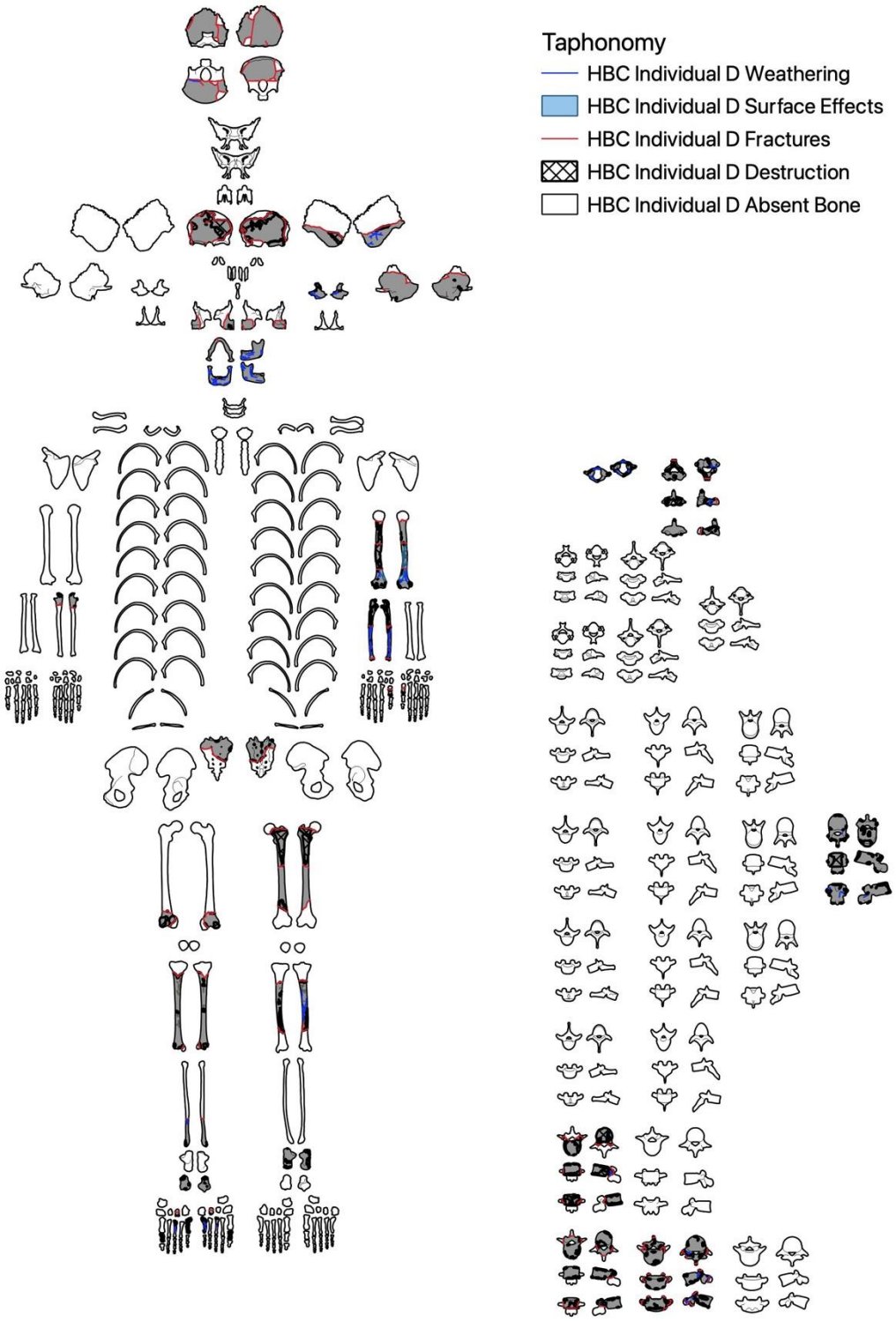


Figure 16.22: Distribution of weathering across Individual D.

Posterior surfaces had significantly more cracking than anterior (28.29% compared to 2.63%). This may be indicative of the posterior surface of bones having greater exposure. The remaining surfaces had similar frequencies of weathering; particularly once lateral surfaces were adjusted. Despite having lower representation than long bones, cranial elements showed the highest percentage of weathering (51.38%). A portion of mandible (HBC421) had more cracking than any other fragment, this may be an indication of greater exposure to mechanisms, such as wet/dry cycling, within the cave. The location of this fragment in comparison to others will be explored in section 17.9.6. The cracking to the mandible also impacted the distribution of cracking according to anatomical side, with unilateral elements showing the highest split (44.04%), despite left-sided fragments having a higher representation.

Surface effects were limited to delamination/peeling, which was only found on the left humerus. The left humerus consisted of two fragments, HBC011 and HBC401. Fragment HBC401 was recovered during the 1958 excavations, whereas HBC011 was recovered between 2016 and 2019. Despite being found at different times, the facture point crossed over the area of delamination, indicating that it occurred prior to breakage (figure 16.23).

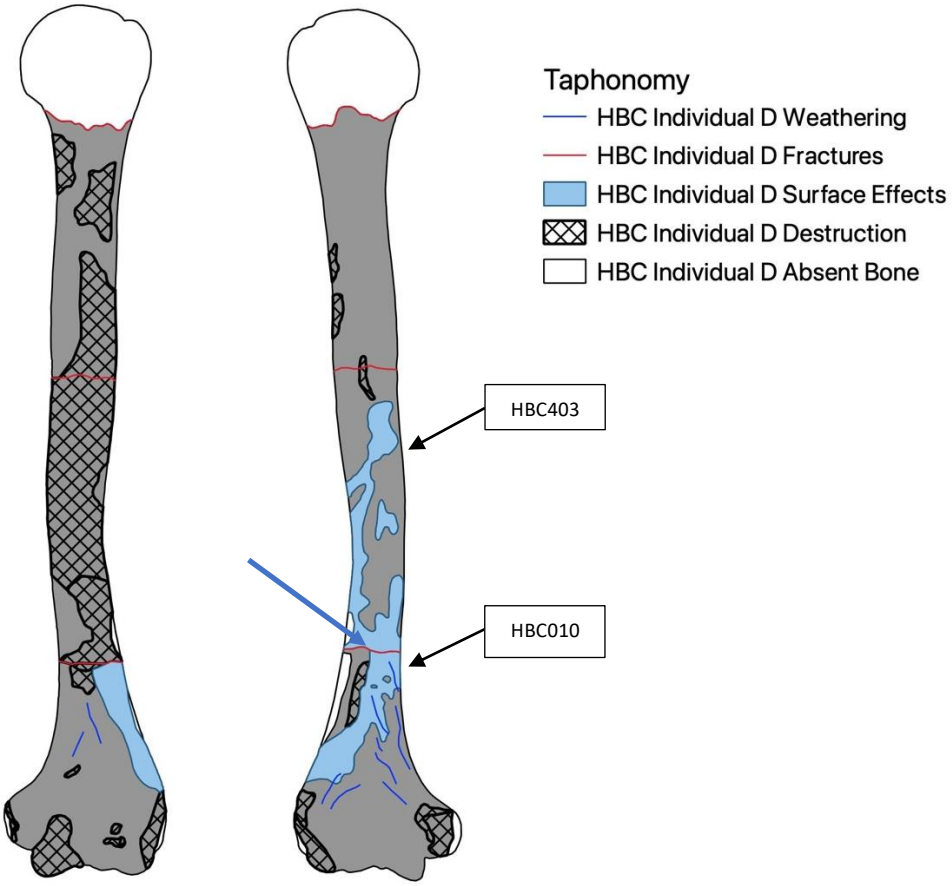


Figure 16.23: Delamination spanning two fragments, HBC011 and HBC401 (blue arrow).

All taphonomic changes to Individual D are consistent with a primary, whole-body burial, with an extended period in a cave environment. There are some areas such as soil staining and weathering that show a potential bias in modifications, analysis of fragment locations will help evaluate the significance of these.

## 16.3: Summary of Early Bronze Age Taphonomy

The taphonomic changes to the individuals dated to the Early Bronze Age provide no clear evidence of burial position or deposition narrative. There are some areas, such as weathering, staining, and deposits that may indicate differential exposure. The taphonomy is, however, generally homogenous, and consistent with deposition in a cave environment.

## 16.4: Early Neolithic - Individual B

### *16.4.1: Bone Representation*

All element groups were represented (figure 16.24) with vertebrae having the highest representation (79.17%), with a similarly high representation of long bones (78.57%). The remaining elements had similar distributions with hands and feet having the lowest (28.07%).

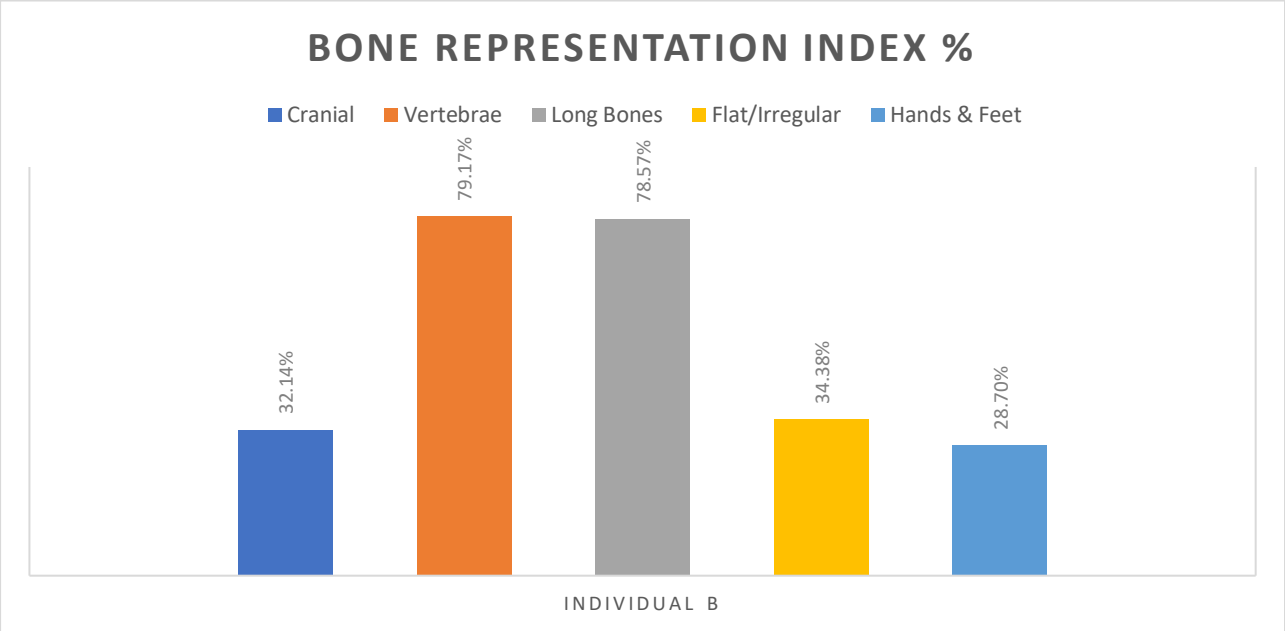


Figure 16.24: Bone representation for Individual B, Heaning Wood.

The high recovery of long bones, along with representation of all element groups, is consistent with expected destruction and recovery patterns of a whole-body deposition, primary deposition (Robb, 2016). The higher representation of vertebrae and hands and feet may be due to biases in individuation. Individual B was small in stature, which meant that bones with similar robusticity were easier to differentiate from the other adults in the assemblage.

There was an equal distribution of left and right sided fragments (31.25%) and 13 fragments that could not be sided (13.54%). The remaining fragments were from unilateral elements (23.96%).

The following discusses frequencies of modifications, all tables for Individual B taphonomy can be found in appendix 7.3.

### *16.4.2: Whole Body Taphonomy*

All fragments from Individual B were altered by taphonomic processes (figure 16.25).

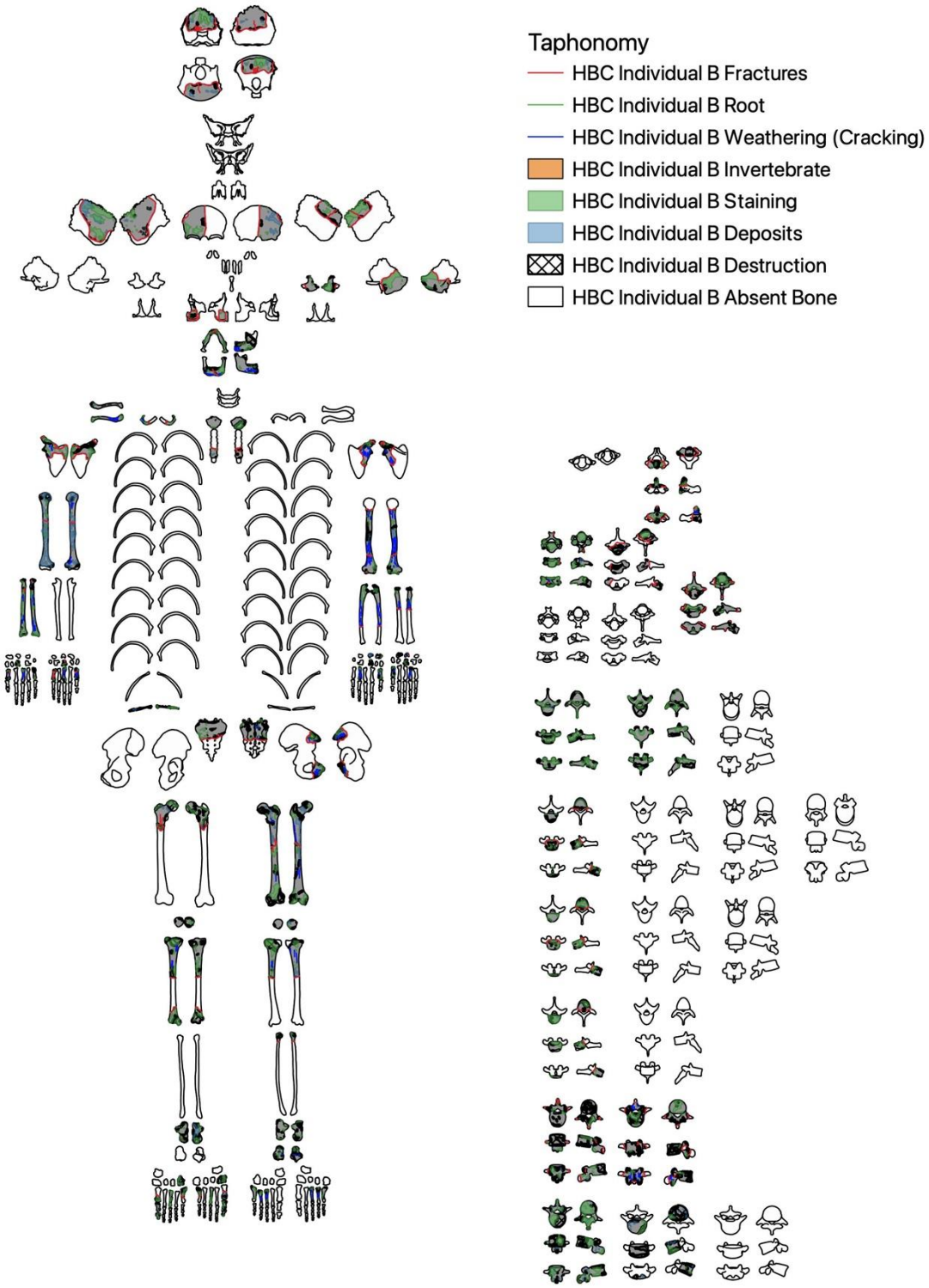


Figure 16.25: Distribution of all taphonomic modifications across Individual B.

Both left and right anatomical sides and all planes were affected by taphonomy. Left sided fragments showed 25.80% of all taphonomic modifications, compared to 25.22% occurring on

the right sided fragments, the remaining 48.98% of modifications were on unilateral elements. This is reflective of the BRI and the high proportion of vertebrae recovered.

When all taphonomic modifications were combined the posterior surface was the most affected by taphonomy (26.56%), with the anterior surface accounting for 25.14%. Superior surfaces were slightly more affected than the inferior surfaces (9.60% and 8.68% respectively). The combined lateral surfaces were more affected than medial (14.99% and 1.67% respectively). This difference may be due the presence of more lateral surfaces (for example on vertebrae), in addition to some lateral surfaces being more exposed, such as in the cranium. When this was adjusted, the medial and lateral surfaces were similarly affected (1.67% and 1.84% respectively). Most bones were assessed for their anterior or posterior surfaces which is reflected in the distributions.

### *16.4.3: Destruction*

All fragments associated to Individual B exhibited some form of destruction (figure 16.26). All pairs of anatomical surfaces showed similar frequencies of destruction, with most destruction occurring to posterior and anterior surfaces (24.55% and 21.28% respectively). The distribution of destruction according to side was reflective of the left and right fragments recovered, however destruction to unilateral fragments was significantly higher (56.42%), due to the number of vertebrae recovered. Hands, feet, and patella had higher frequencies of destruction compared to all other elements except vertebrae, despite having the lowest representation.

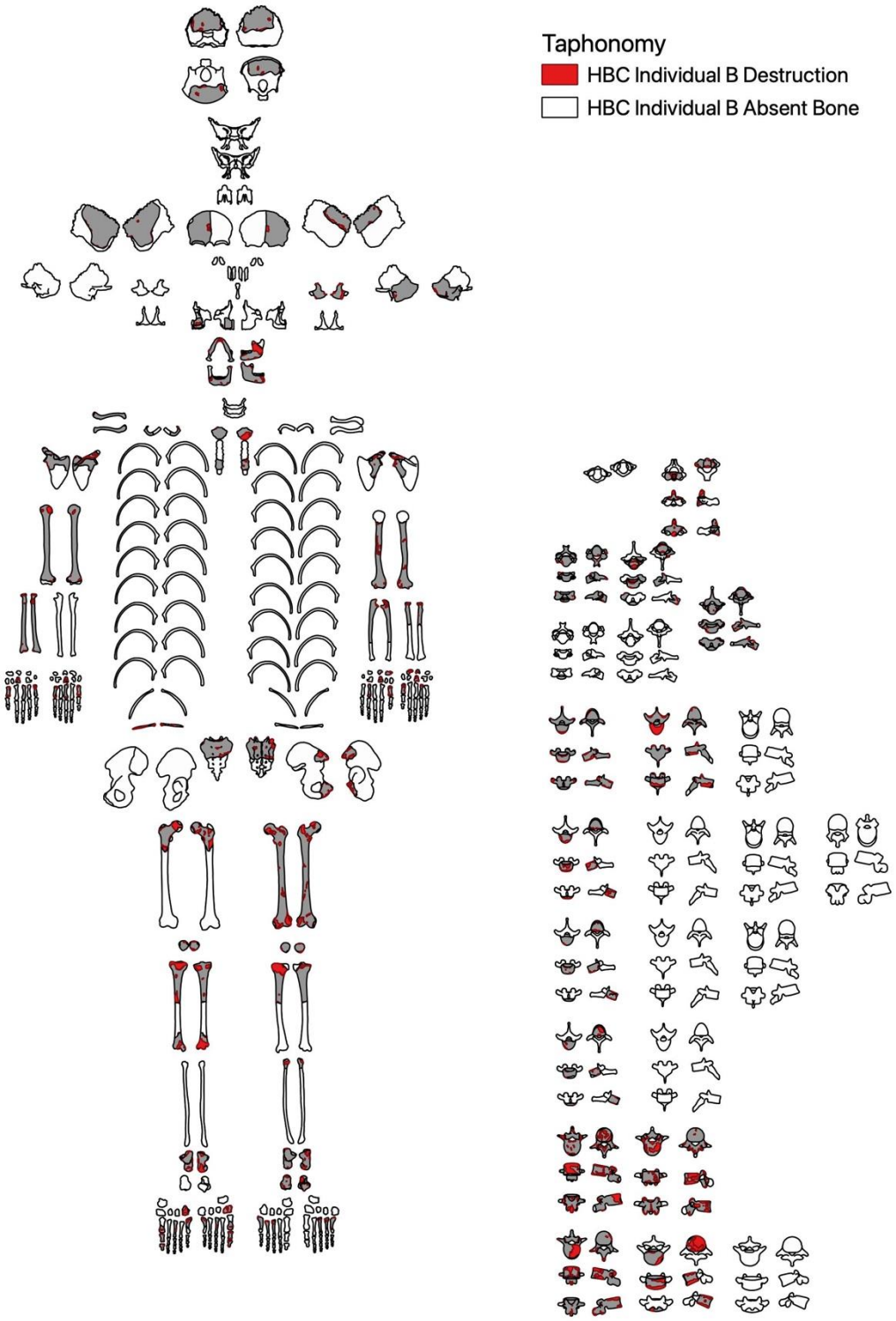


Figure 16.26: Distribution of destruction across Individual B.

There were nine areas of crushing, however only one had characteristics of peri-mortem damage. This occurred to the left lateral surface of the fourth thoracic vertebra. There did not appear to be any significance to where crushing occurred. The most frequent type of damage was classified as 'exposure of trabecular bone' (63.51%), consistent with extended periods in a cave environment.

### *16.4.4: Fractures*

Fracturing occurred across most of Individual B, except for some vertebrae, tarsals, the patella, and the manubrium (figure 16.27). Complete fractures were almost evenly distributed across anatomical surfaces, with anterior surfaces showing slightly more complete fractures than posterior (28.07% compared to 25.73%).

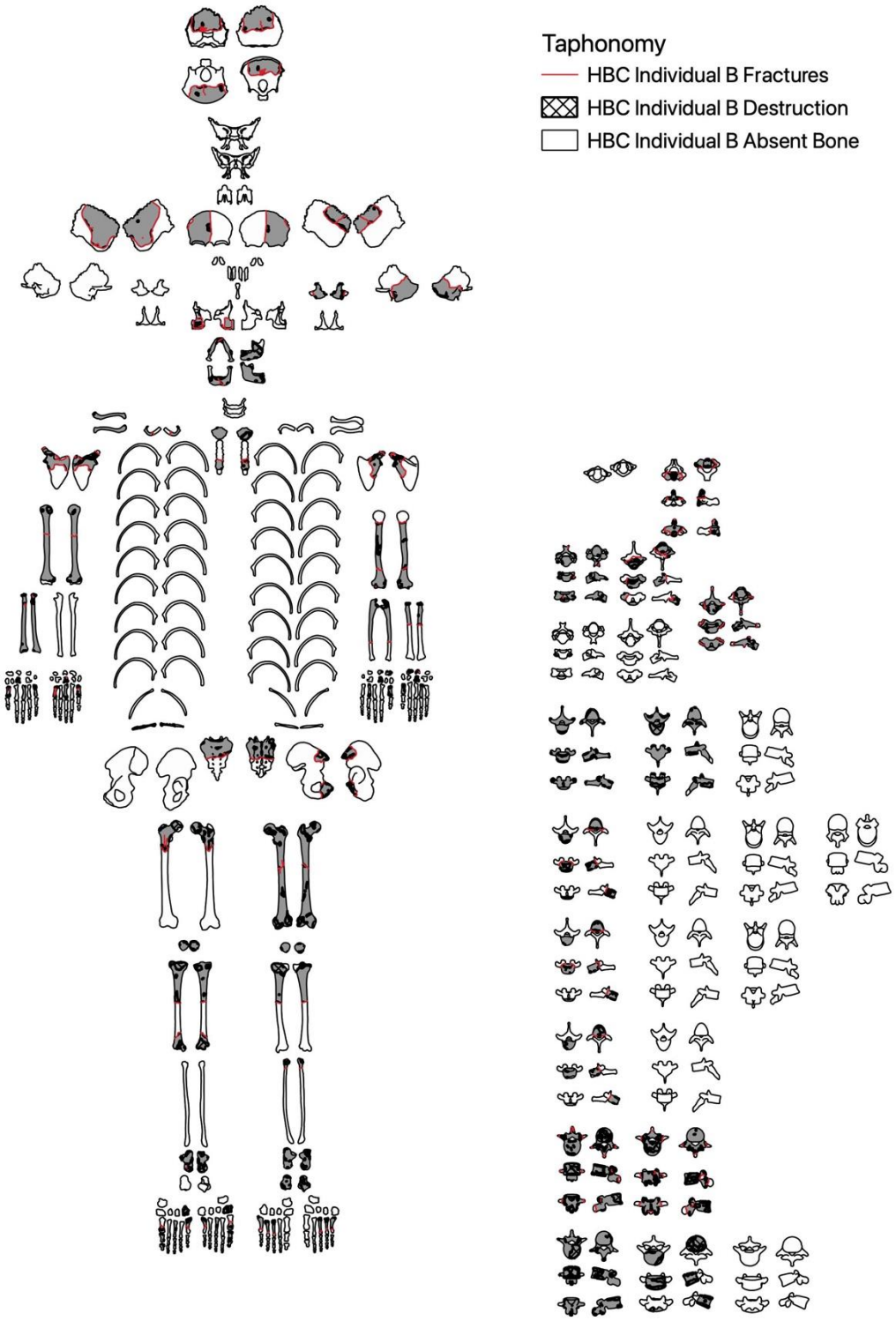


Figure 16.27: Distribution of fracturing across Individual B.

Of the fractures, 21.56% were classified as incomplete and all originated from existing complete fractures or destruction. The most common fracture classification was ‘oblique dry’ (65.60%) with all fractures consistent with post-mortem breakage. There were more complete fractures to right fragments than left (23.39% and 22.48% respectively). Again, unilateral fragments showed higher counts (54.13%) but was reflective of representation. The distribution of fractures did not indicate body position.

### *16.4.5: Tufa Deposits*

Individual B had deposits ranging from ‘thin/flaked’ to ‘embedded’. Embedded deposits were limited to the diaphysis of the right humerus (figure 16.28).


Figure 16.28: Build-up of calcite to the right humerus.

Not all fragments had deposits and the metatarsals and metacarpals were particularly unaffected (figure 16.29).

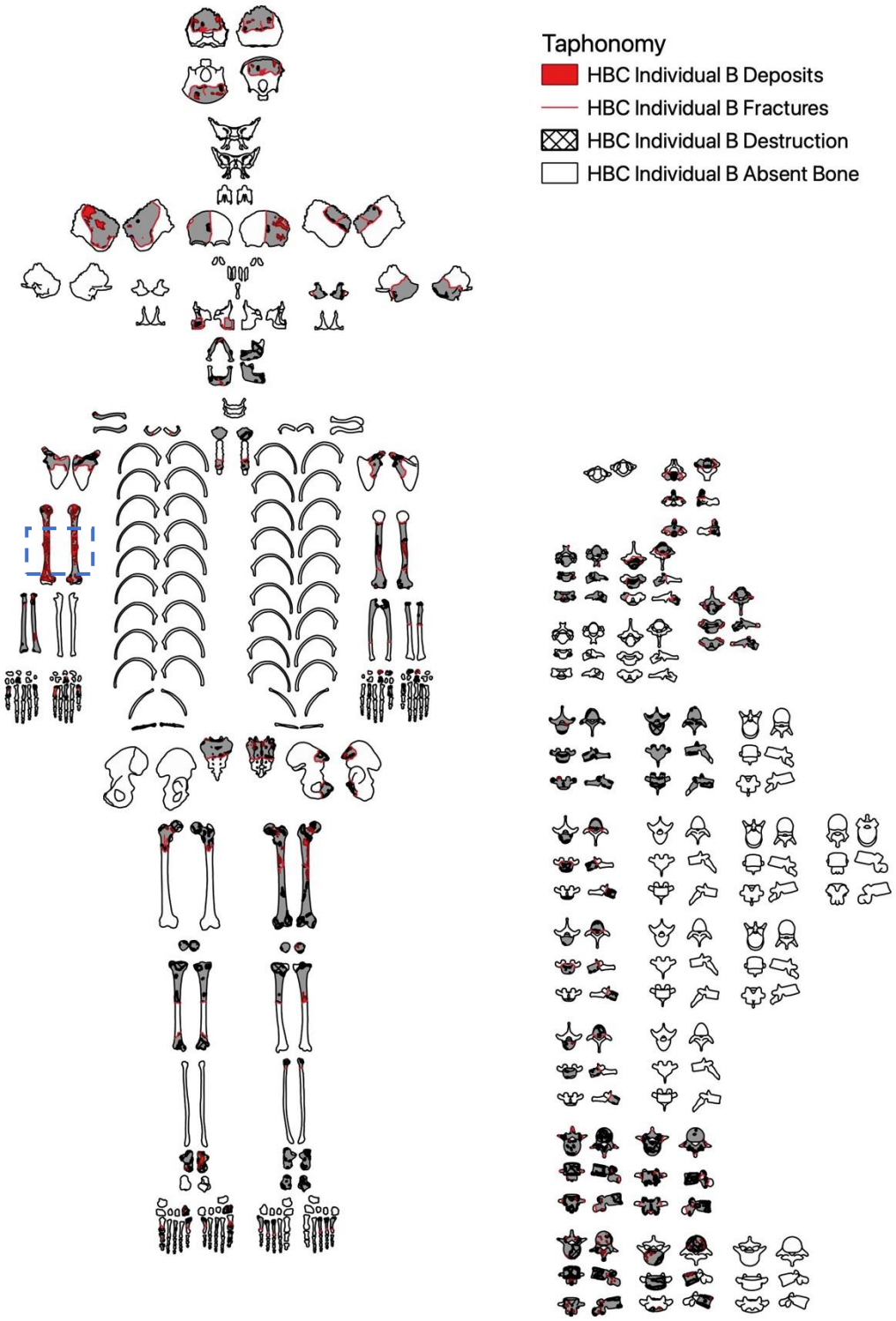


Figure 16.29: Distribution of deposits across Individual B (patches of embedded deposits marked with blue box).

The anterior and posterior surfaces had the most deposits, consistent with the proportion of those surfaces analysed. Posterior surfaces showed more deposits than anterior (38.43% compared to 25.62%). Similarly, inferior surfaces showed higher frequencies of deposits than superior (11.98% compared to 7.85%). Four deposits were classified as thick/coated, all of which occurred on the posterior surface. It is difficult to assess whether this has any particular significance due to the limited counts. The embedded deposits were found on both the anterior and posterior surface. The higher frequency of deposits on both the posterior and inferior surfaces, comparative to their counter parts, may be indicative of the back of the body having increased contact with areas of calcite formation.

Even without adjusting for the increased surfaces analysed on vertebrae, most deposits occurred to the long bones (43.39%) and vertebrae (26.86%). Right elements had higher frequencies of deposits (37.19%) than the left (21.90%), with the remaining 40.91% occurring on unilateral elements. This is despite there being an equal representation of left and right fragments and may be due to the right humerus having a greater build-up of deposits compared to the rest of the fragments (figure 16.30).

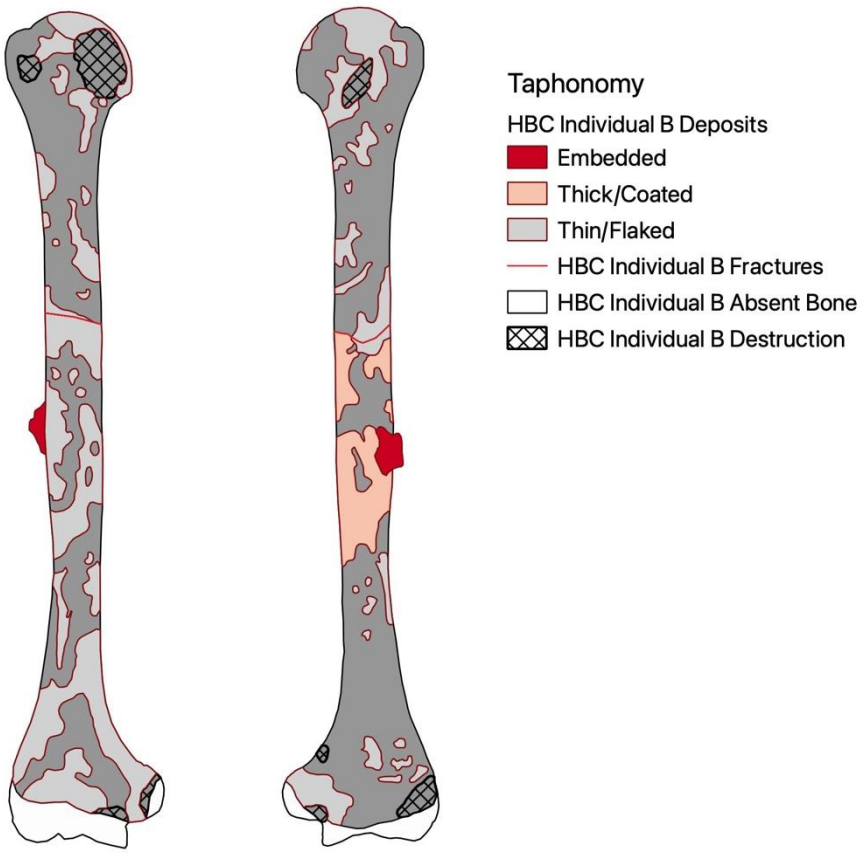


Figure 16.30: Build-up of deposit to the right humerus (HBC157/HBC158)

Spatial analysis may provide some indication as to whether this fragment was laying in an area with increased calcite and will be explored in section 17.12.3.

### *16.4.6: Staining*

All bones were pale with areas of light or dark soil staining, brown/orange staining, or mottled black-grey staining consistent with manganese staining (figure 16.31). Classifications of light or dark soil accounted for most staining (44.85% and 19.06%), with brown/orange staining accounting for only 2.16% of the total.

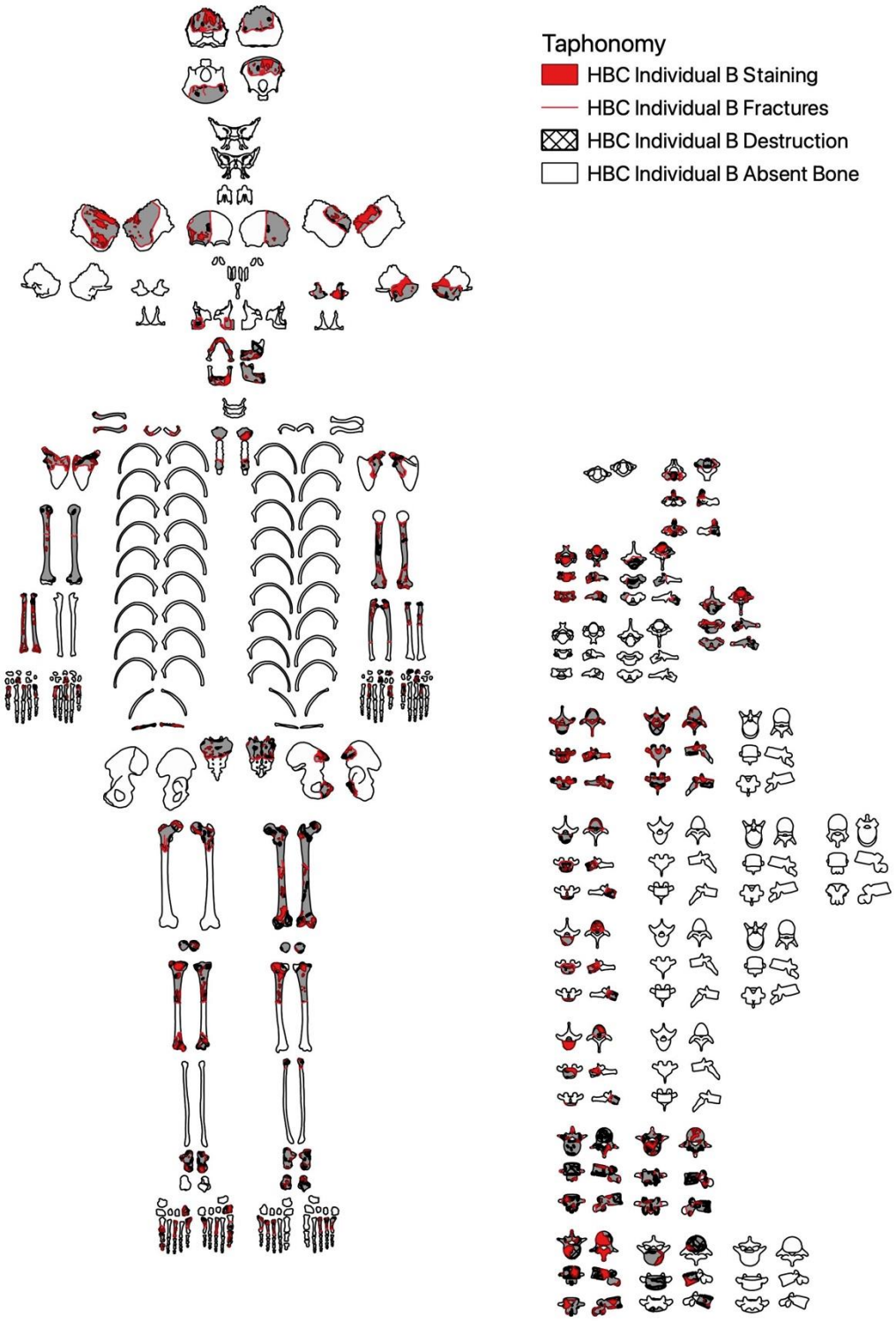


Figure 16.31: Distribution of staining across Individual B.

The posterior and anterior surfaces showed similar frequencies of total staining (23.89% and 27.95% respectively). There were, unlike individual D, no differences in the types of staining and how they were distributed.

When adjusted to only account for anterior and posterior views of vertebrae, long bones had the highest frequency of staining (20.08%), then cranial (16.52%), despite cranial elements having a relative low representation. Frequencies according to anatomical side were distributed in accordance with representation. While there is some indication of preferential staining to the cranial elements, which will be explored in the spatial analysis, there does not seem to be any significant indication of body position according to staining patterns.

Most staining was independent of any other modifications (86.66%), however, 13.34% were classed as modifying existing modifications ('modexmod'). Spotted, manganese staining showed the highest, with 28.06% of light and dark spotted staining overlaying existing changes. Soil staining showed a similar frequency with 24.45%. Usually this was over areas of pre-existing destruction or deposits, however 29.41% of deposits were also overlaying areas of destruction or staining. While this can help develop an understanding of timings regarding taphonomic agents, with both processes showing the potential to act before the other, it is likely that they occurred at a similar time. Destruction, however, was likely to occur earlier in the process.

### *16.4.7: Large Animal and Invertebrate Activity*

There was no evidence of carnivore or large animal activity on individual B. Only four bones from Individual B exhibited signs of invertebrate activity, the right parietal, sternum, third thoracic vertebra and right clavicle. A picture of the full body has been omitted due the small size of the pits making visibility difficult. Pitting accounted for all the invertebrate modifications, except for three patches of furrowing to the sternum and thoracic vertebra, these three modifications also accounted for the total representation to unilateral elements. The remaining invertebrate modifications were to right elements (88.46%). A concentrated area of pitting was recorded on the right parietal (figure 16.32), however the left parietal was partial and the equivalent portion was missing. This makes it difficult to ascertain whether there was preferential activity to the right or whether this is due to the fragments recovered.

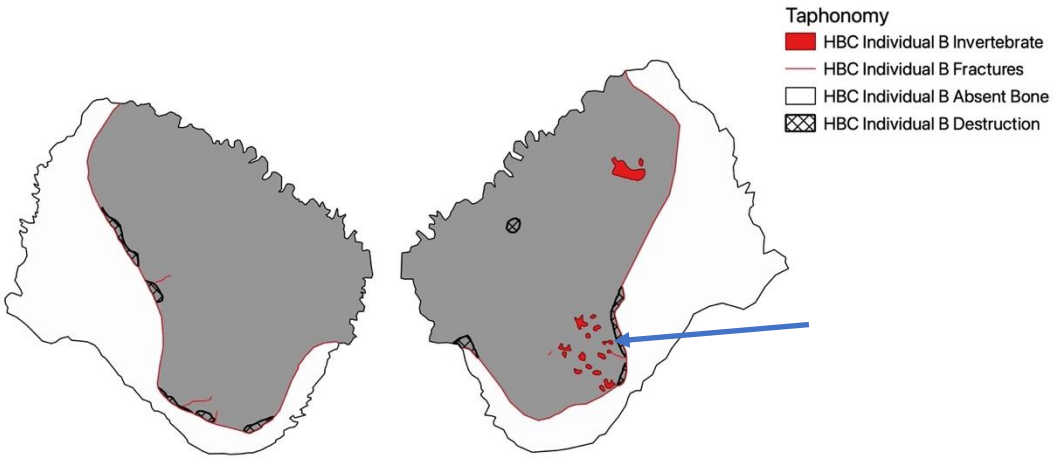


Figure 16.32: Area of focussed invertebrate pitting to the lateral, right parietal (blue arrow).

Contrary to individual D, none of the affected fragments were from the Dock Museum collection, the spatial distribution of these fragments will be explored in more detail in section 17.12.5.

### *16.4.8: Weathering and Surface Effects*

Just over a third (31.00%) of the total fragments assigned to Individual B were affected by cracking (N=31) consistent with weathering. These were limited to linear cracking, usually in line with the bone grain, with no areas of delamination or peeling (figure 16.33).

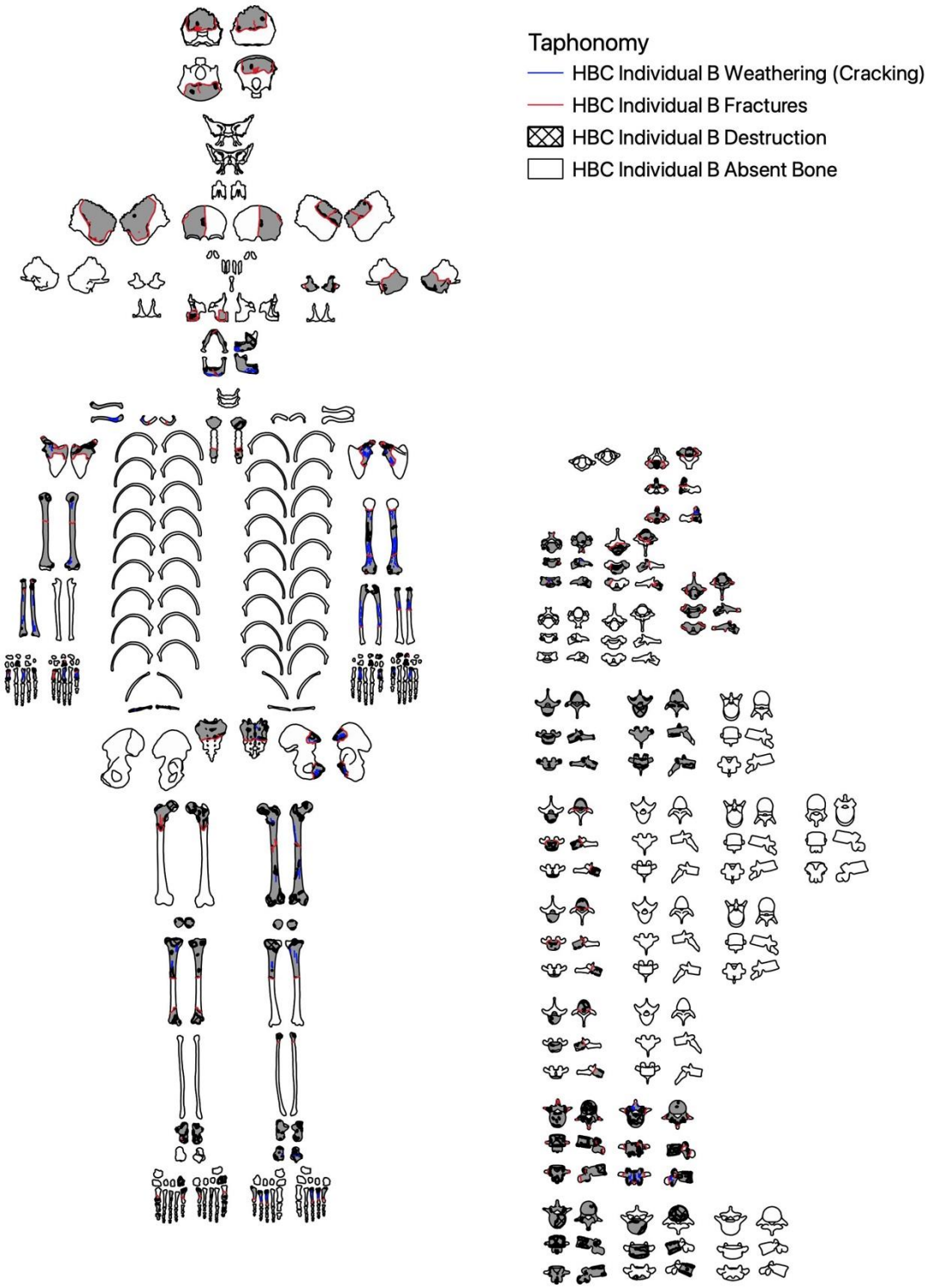


Figure 16.33: Distribution of weathering across Individual B.

The posterior surface had more cracking than the anterior (37.85% compared to 28.50%). Conversely, the superior surface showed 5.6% of cracking while the inferior surfaces had none. Increased cracking to the posterior surface may be indication of exposure. Deposits also showed higher frequencies to the posterior surfaces, and while in some cases this may provide protection, or obscure observations, most of the deposits on Individual B were thin/flaked, and therefore unlikely to prevent weathering processes.

Most of the cracking occurred to left elements (56.54%), however the left humerus had a high frequency of cracking compared to the right, which had large areas of deposits. While the deposits to the right humerus may be obscuring cracking, it may also have been sufficiently coated that the cortex was protected. All weathering to Individual B is minimal and consistent with wet/dry cycles within a cave environment. There was no evidence of subaerial exposure.

All taphonomic changes to Individual B are consistent with a primary, whole-body burial, with an extended period in a cave environment. Deposits and weathering potentially show a greater exposure of the posterior surface, analysis of fragments locations will help evaluate the significance of these.

## 16.5: Early Neolithic - Individual C

### *16.5.1: Bone Representation*

All element groups were represented (figure 16.34) with long bones having the highest representation (71.43%). Individual C had the highest representation of cranial elements (53.57%) for the entire assemblage due to the recovery of a partially intact cranium. Flat/irregular elements had the lowest representation (9.38%).

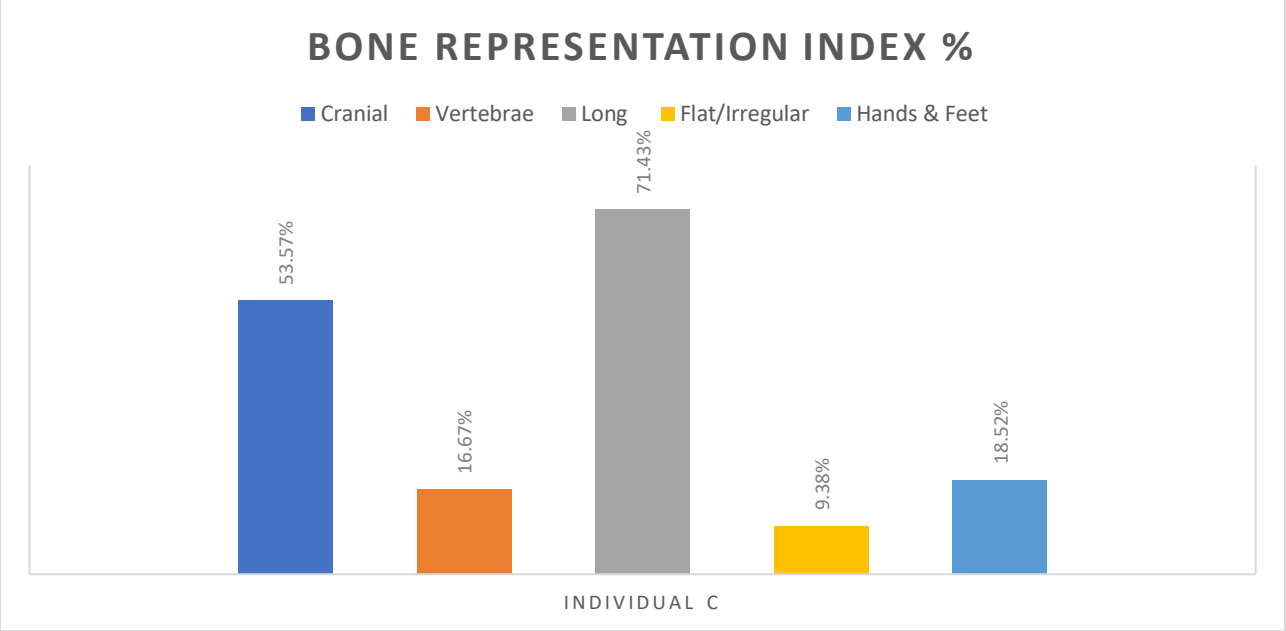


Figure 16.34: Bone representation for Individual C, Heaning Wood.

The high recovery of long bones, along with representation of all element groups, is consistent with expected destruction and recovery patterns of a whole-body deposition, primary deposition (Robb, 2016). There were more left sided fragments (46.67%) than right (31.67%). This was the highest difference for the adult individuals. A total of four fragments could not be sided (6.67%) and the remaining fragments were from unilateral elements (15%). Most elements had their corresponding sides, except for the feet, where there were more lefts than rights assigned. It is therefore unlikely that the preservation of side recovery was due to body position and rather, it is possible that some right pedal elements are within the excluded elements.

The skull associated with Individual C was recovered partially complete. This meant that some of the more complex bones in the facial region were obscured. The sphenoid, both palatines and the vomer were present but partially obscured. It was therefore decided that they would be excluded from recording in GIS to avoid skewing of taphonomy when analysing surfaces. These bones were recorded in the bone representation indices and the taphonomy that could be seen was consistent with the rest of the assemblage. There were no unique modifications that would alter interpretations.

The following discusses frequencies of modifications, all tables for Individual C taphonomy can be found in appendix 7.4.

### *16.5.2: Whole Body Taphonomy*

All fragments from Individual C were altered by taphonomic processes (figure 16.35).

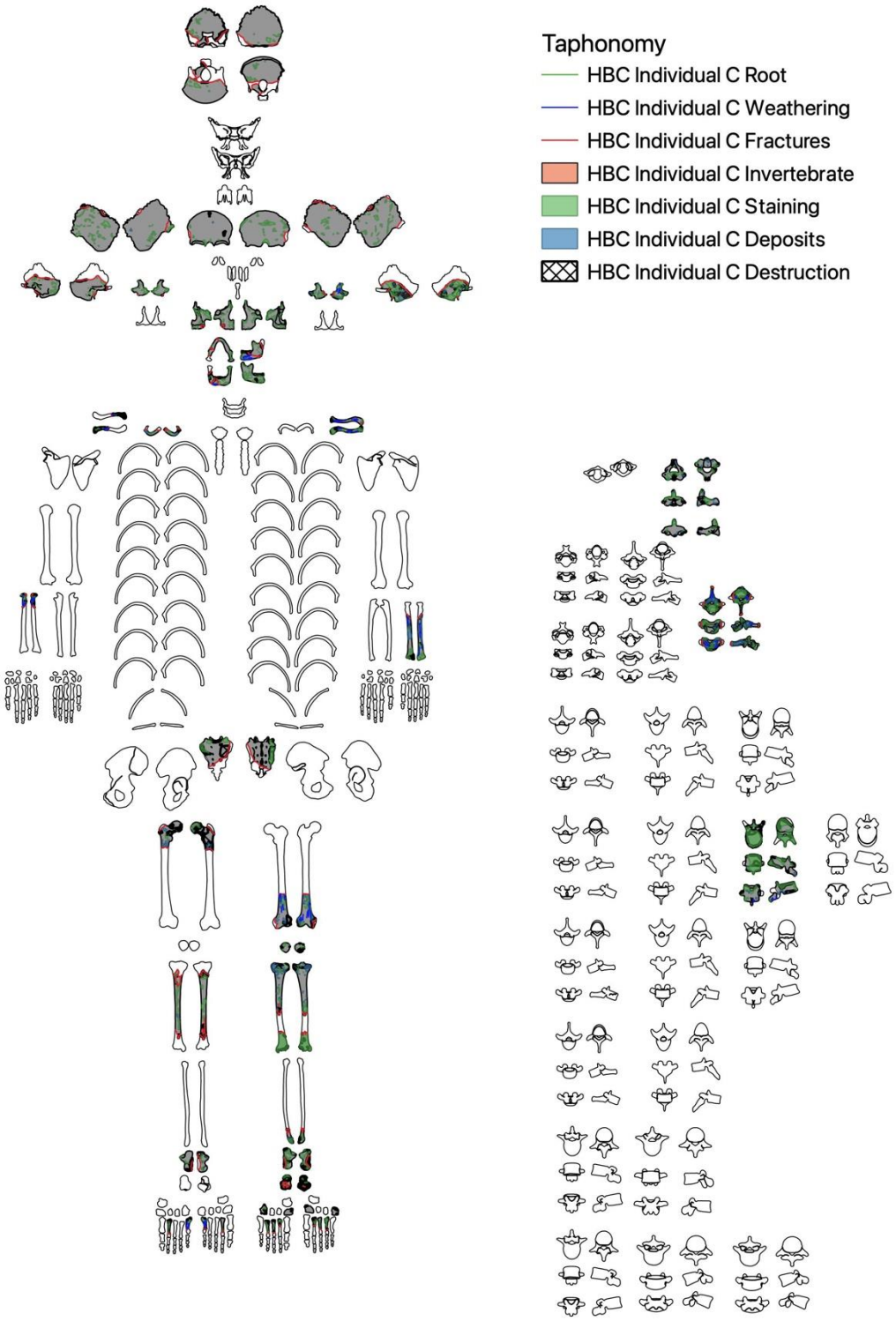


Figure 16.35: Distribution of all taphonomic modifications across Individual C.

Both left and right anatomical sides and all planes were affected by taphonomy. The left sided fragments showed 44.56% of all taphonomic modifications, compared to 27.16% occurring on right sided fragments, the remaining 28.28% of modifications were on unilateral elements. This is reflective of the BRI and the high proportion of left sided fragments recovered.

When all taphonomic modifications were combined the posterior surface was the most affected by taphonomy (23.20%), with the anterior surface accounting for 21.69%. Inferior surfaces were slightly more affected than the superior surfaces (9.10% and 8.11% respectively). The combined lateral surfaces were more affected than medial (17.07% and 10.22% respectively). This difference may be due the presence of more lateral surfaces (for example on vertebrae), in addition to some lateral surfaces being more exposed, such as in the cranium. When adjusted, the medial surfaces were slightly more affected than inferior (10.22% and 7.19% respectively). Most bones were assessed for their anterior or posterior surfaces which is reflected in the distributions.

### *16.5.3: Destruction*

All fragments associated to Individual C exhibited some form of destruction (figure 16.36). All pairs of anatomical surfaces showed similar frequencies of destruction, with most destruction occurring to posterior and anterior surfaces (20.87% and 21.16% respectively). Long bones showed the most destruction, which is consistent with representation. Most of the destruction (60.29%) was classified as 'exposure of trabecular bone' or 'cortical removal without exposure' (21.16%), both of which are consistent with damage occurring in cave environments (Fernández-Jalvo and Andrews, 2016).

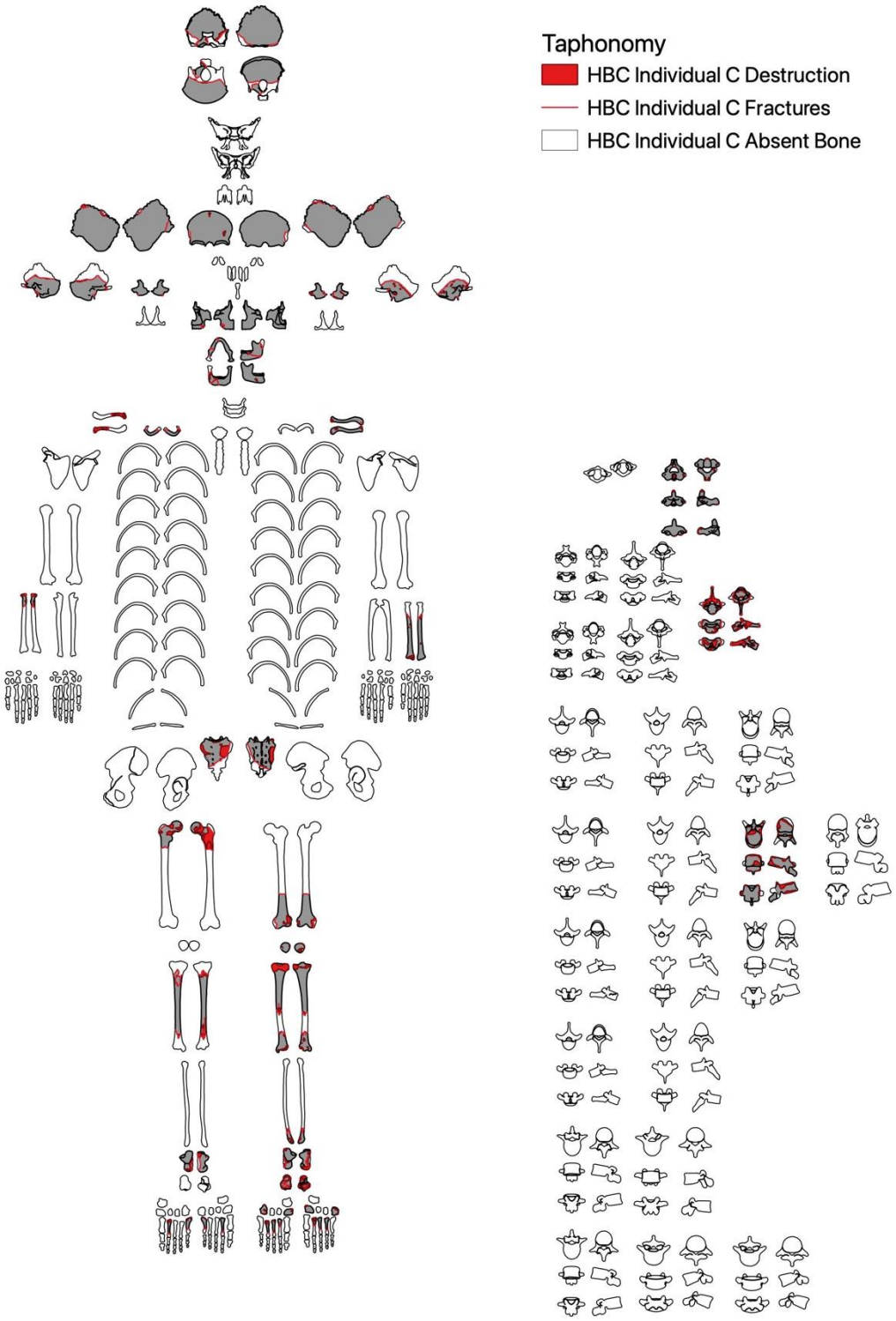


Figure 16.36: Distribution of destruction and fractures across Individual C.

There were two areas of peeling, both on the left tibia, on both the anterior and posterior views (figure 16.37). The peeling occurred next to fractures margins and appear to be where the cortex 'lifted' because of damage, rather than the delamination seen in Individuals A and D. It was therefore classified a destruction rather than weathering.


Figure 16.37: Area of cortical removal because of fracturing.

### *16.5.4: Fractures*

Fracturing occurred across all Individual C (see figure 16.36 above), except for some tarsals. Of the fractures, 18.18% were classified as incomplete and all originated from existing complete fractures or destruction. More complete fractures were recorded to the posterior surfaces (24.19%) than the anterior (17.74%). Superior surfaces had more complete fractures (12.10%) than inferior (7.26%). The most common fracture classification was 'oblique dry' (62.12%) with all fractures consistent with post-mortem breakage. There were more complete fractures to right fragments than left (45.45% and 33.33% respectively) and were reflective of representation.

While it is possible that the higher frequency of fractures to the posterior surface is reflective of positioning, the same bias was not seen in patterns of damage. If the bias was due to the body lying, or exposed, in a particular way, it would be expected that destruction would also be differentially distributed.

### *16.5.5: Tufa Deposits*

All the deposits on Individual C were classed as 'thin/flaked' and were found on most fragments (figure 16.38). There were minimal deposits found on cranial elements, except for the left temporal bone. The cranium was stored in the Dock Museum and was partially intact. The left temporal was found separate to this during the 2016-2019 excavations. The difference in deposits may be due to the left temporal remaining in the cave for longer than the rest of the cranium. The cranium had been treated with preservative, and therefore, some deposits may have been destroyed or masked.

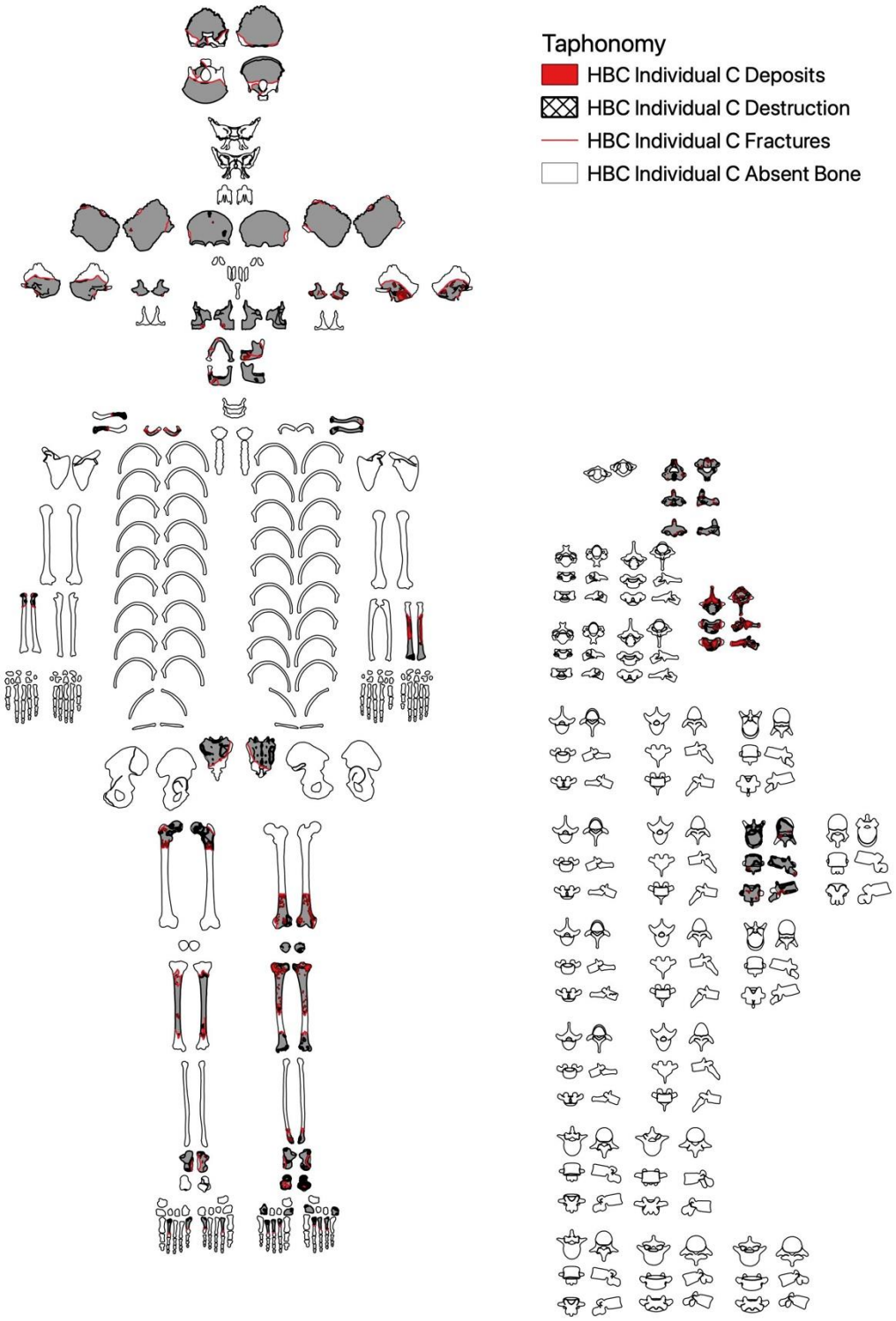


Figure 16.38: Distribution of deposits across Individual C.

Deposits were distributed according to side representation, with left sided fragments showing the highest frequencies (50.00%). The anterior surfaces had slightly more deposits than the posterior (33.20% and 26.64% respectively), whereas inferior surfaces had more than superior (11.48% and 6.56% respectively). This is possibly an indication of positioning. Deposits on long bones accounted for nearly half the total (45.49%), the left tibia and femur had multiple small flecks, compared to other fragments where the deposits consisted of larger patches.

Just under half of the deposits (47.13%) were overlying an existing modification. These were either on areas of staining or, more commonly destruction, indicating that destruction was likely occurring earlier. Where the deposits were modifying staining, it indicates that the staining was happening first. However, as will be discussed in the following section, some stains were over deposits, making the sequence of modification less clear cut.

### *16.5.6: Staining*

All bones were pale with areas of light or dark soil staining, patchy black-grey staining consistent with manganese staining, or light brown/orange (figure 16.39). The distal portion of the left tibia, fragment HBC800 (blue dashed box in figure 16.39) was stored with fragments HBC807, HBC808, and HBC809 (see page 270) and was similarly, completely stained dark brown. It is possible that these dark stained fragments were from the same individual, but the robustness of the tibia was more consistent with the smaller, gracile morphology of Individual C, than individual D.

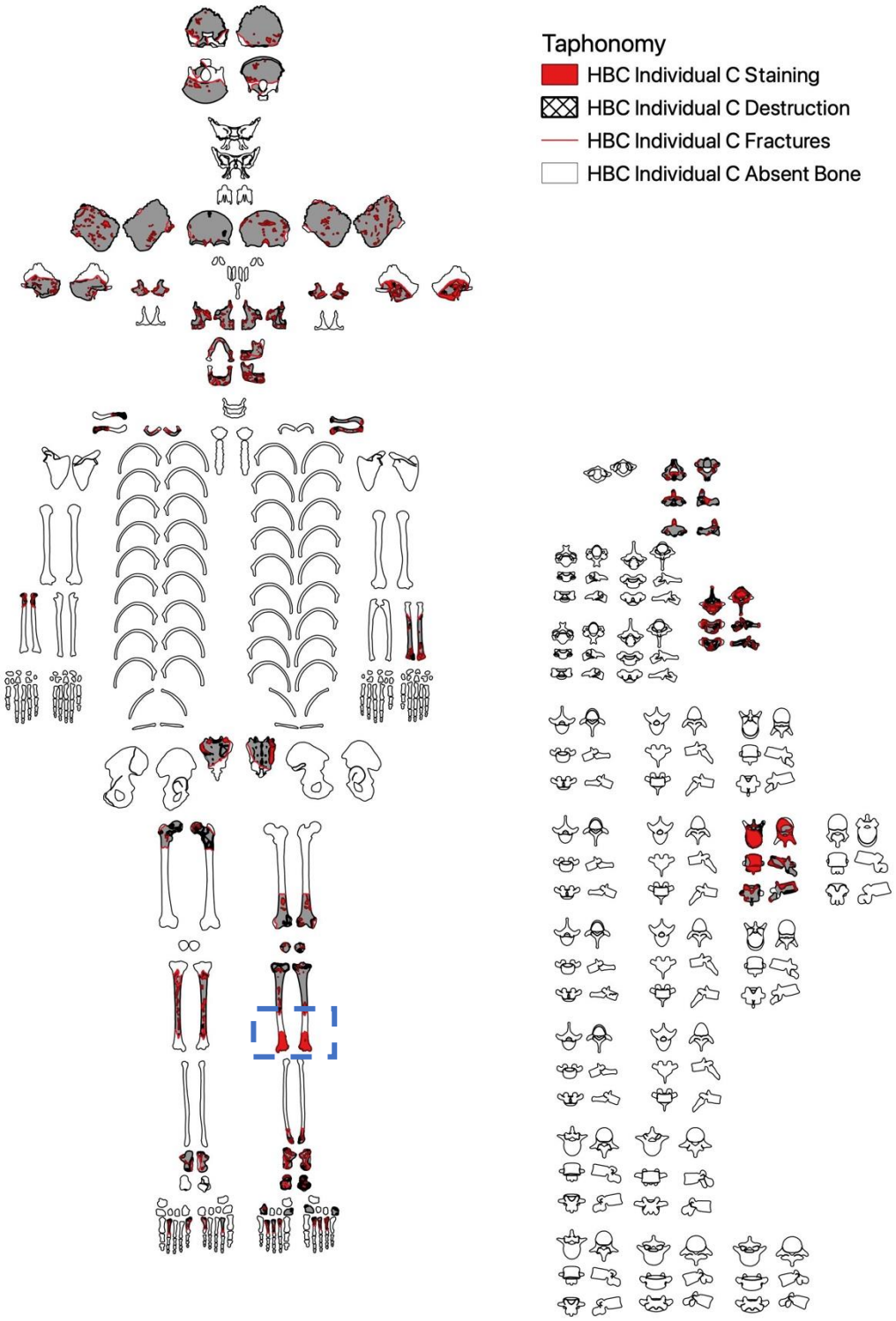


Figure 16.39: Distribution of staining across Individual C.

Classifications of light or dark soil accounted for most staining (62.11% total), with brown/orange staining accounting for the least (3.85%). Anterior and posterior surfaces had the highest frequencies (21.94% and 19.23% respectively) and there was no significant bias towards any view, even when staining was broken down into the different categories. The distribution of staining according to side was also reflective of recovery distributions, showing no indication of preferential staining.

There was a single area of light soil staining that crossed a fracture margin (figure 16.40). This was on the posterior (buccal) view of the mandible and shows that the staining occurred prior to the mandible fracturing.

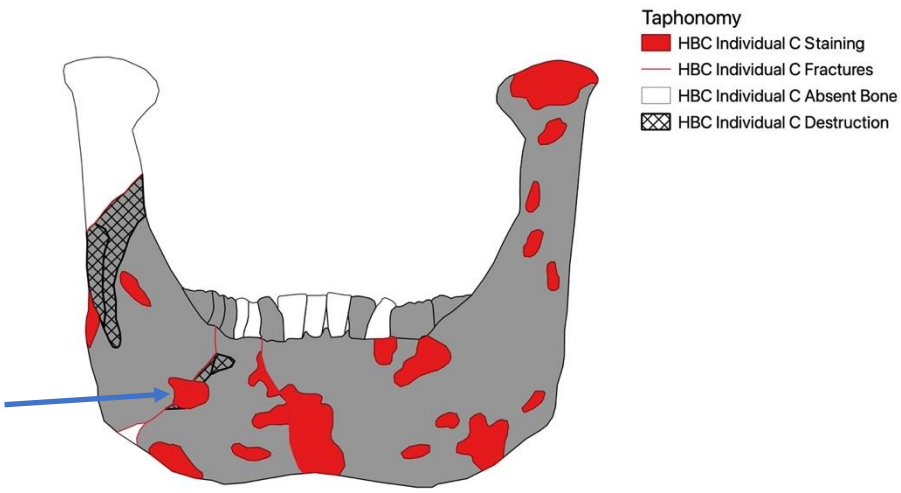


Figure 16.40: Staining crossing fracture margin (blue arrow).

Most stains were independent of other modifications, with only 14.39% of stains modifying existing changes. Most occurred over areas of damage, while others overlay deposits. As discussed in the previous section, there was less clarity over the sequence of staining and deposits, suggesting that both were occurring at a similar time. There was nothing in the distribution of staining to suggest body position.

### *16.5.7: Large Animal and Invertebrate Activity*

There was no evidence of carnivore or large animal activity on individual C. There was a single area of furrowing, consistent with invertebrate activity, to the lateral surface of the left temporal bone. The limited presence of modifications makes analysis difficult. The spatial distribution of affected fragments will be explored in section 17.15.5.

### *16.5.8: Weathering and Surface Effects*

Evidence of weathering was limited to linear cracking, usually in line with the bone grain, with no areas of delamination or peeling (figure 16.41). There was no cracking or signs of weathering to the intact cranium. It is possible that this is due to the preservative, or that it was recovered in the earlier excavations, and therefore had less time exposed to the cave environment.

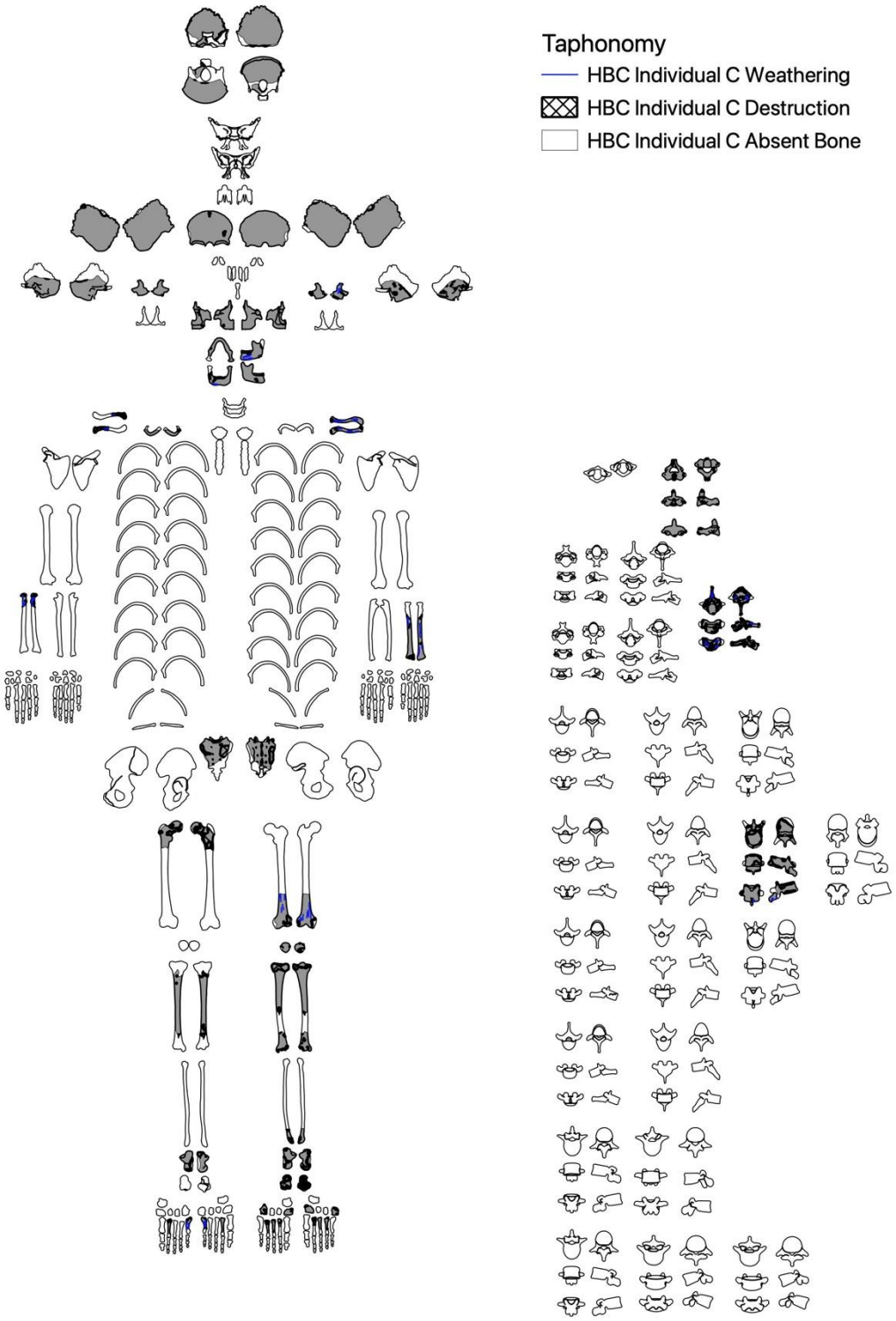


Figure 16.41: Distribution of weathering across Individual C.

Distribution according to side was in line with representation and long bones had the highest frequency with 53.16%. There was no cracking to medial surfaces, this may be because most of the medial surfaces recorded were in the skull. Most of the cranium was intact, therefore protecting the inner surfaces from exposure.

Posterior surfaces had more than twice the cracking than anterior surfaces (34.18% compared to 15.19%). All cracking found in the assemblage was a maximum score of 1 according to Behrensmeyer (1978), with an absence of evidence of subaerial exposure, such as bleaching. The weathering observed is consistent with expected wet/dry cycles (Hawks *et al.*, 2017; Pokines *et al.*, 2018), it is possible that the higher occurrence of cracking to posterior surfaces is indicative of greater exposure or increased contact with surfaces.

All taphonomic changes to Individual C are consistent with a primary, whole-body burial, with an extended period in a cave environment. Weathering potentially shows a greater exposure of the posterior surface; however, no other modifications show a clear bias in distribution.

## 16.6: Early Neolithic - Individual E

### *16.6.1: Bone Representation*

Only cranial and long bone elements were recovered from Individual E (figure 16.42), with cranial elements having the highest representation (20.69%). The distribution according to anatomical side was almost even, a total of eleven fragments were recovered, with six from the left (54.55%) and five from the right (45.45%).

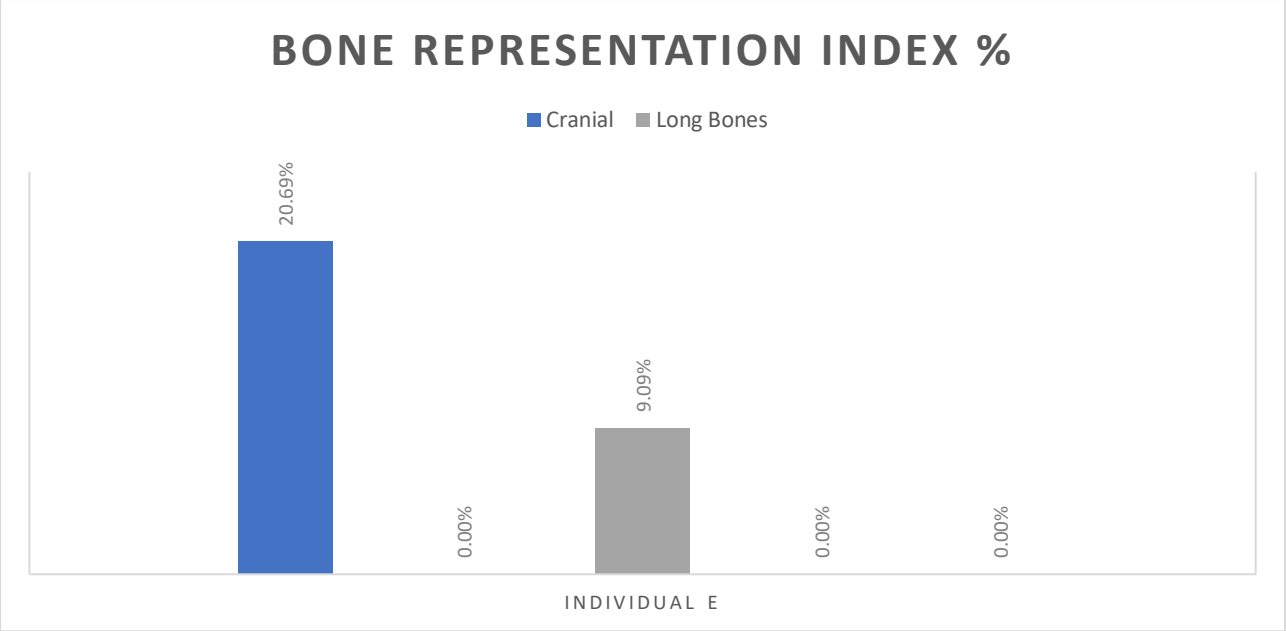


Figure 16.42: Bone representation for Individual E, Heaning Wood.

The long bones recovered for Individual E were the left and right clavicle. No other bones from appendicular portion of the skeleton were recovered. Early Neolithic cranial only depositions have been recovered from caves in Northwest England (Leach, 2006b, 2006a; Peterson, 2019), however care should be taken here to interpret this as a selective burial, due to the limited number of fragments recovered and the presence of the clavicles. The assemblage was commingled with a large proportion of faunal remains and multiple human internments, this may have led to a bias in recovery and destruction, particularly of more fragile juvenile bones.

The following discusses frequencies of modifications, all tables for Individual E taphonomy can be found in appendix 7.5.

### *16.6.2: Whole Body Taphonomy*

All fragments from Individual E were altered by taphonomic processes. Figure 16.43 shows the full body to provide an overall picture. When discussing each modification, a close-up of the recovered fragments will be used to increase clarity.

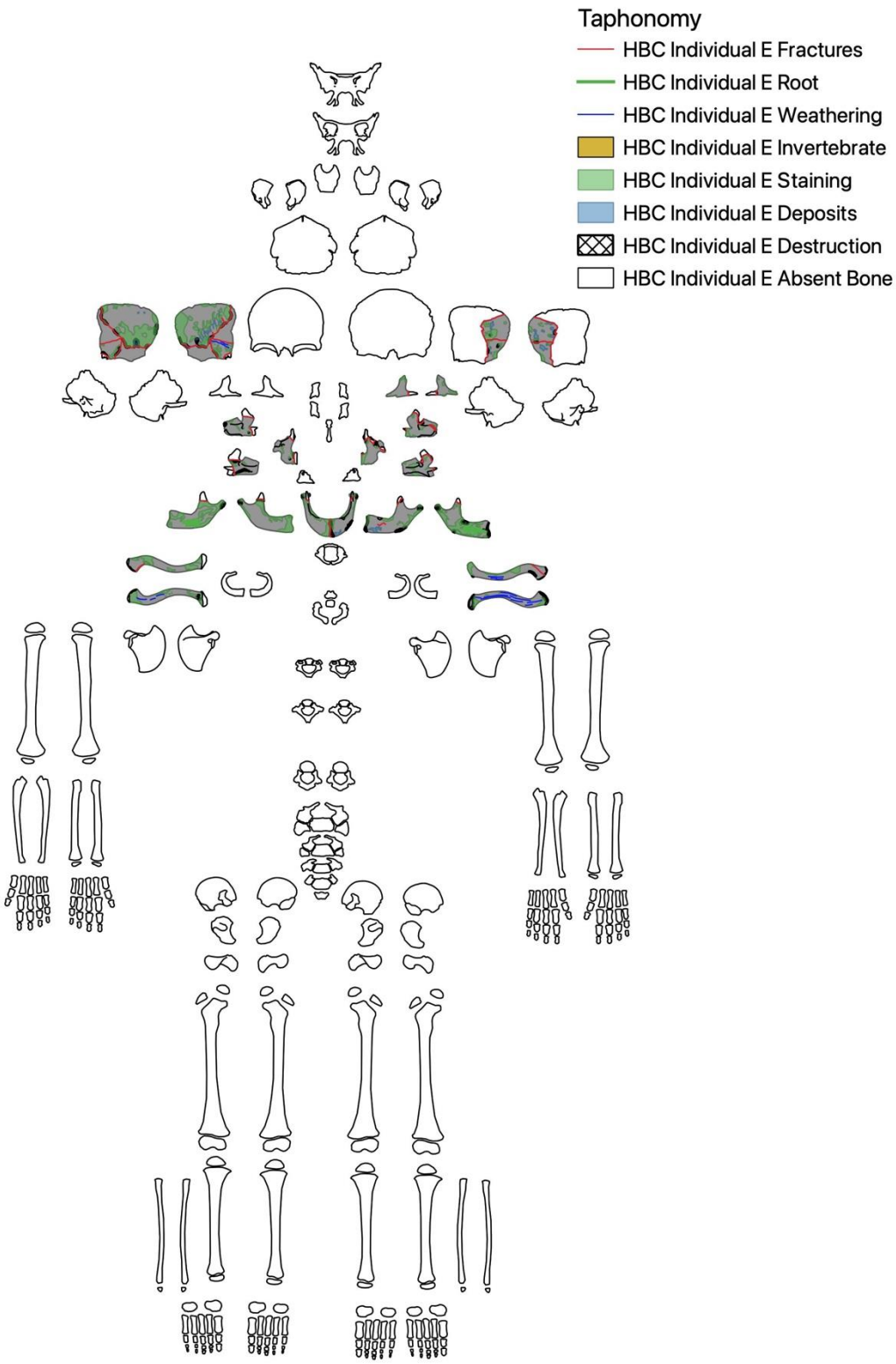


Figure 16.43: Distribution of all taphonomic modifications across Individual E.

Both left and right anatomical sides and all planes were affected by taphonomy. The left sided fragments showed 46.59% of all taphonomic modifications, compared to 53.41% occurring on right sided fragments. This is not reflective of the BRI, with several modifications showing higher frequencies on right sided fragments. This will be broken down and explored per separate modification.

While the anterior surfaces of the maxilla and mandible were recorded, due to the format of the infant templates, the corresponding posterior surfaces were not recorded. These fragments were also recorded for their lateral and medial surfaces (buccal/lingual for mandibular fragments). The anterior counts were therefore excluded from the figures reported to avoid the appearance that anterior surfaces were disproportionately affected compared to posterior surfaces.

When all taphonomic modifications were combined, lateral surfaces were the most affected (31.16%), with medial surfaces accounting for 23.44% of total modifications. The lingual surfaces on the mandible showed a similar bias. All medial and lateral surfaces recorded for Individual E were on cranial elements. The higher frequency of modifications to lateral surfaces may be due to the medial surfaces in the cranium being protected prior to fracturing. The Inferior surfaces of the clavicles were slightly more affected than the superior surfaces (7.12% and 4.45% respectively).

### *16.6.3: Destruction*

All fragments associated to Individual E exhibited some form of destruction (figure 16.44).

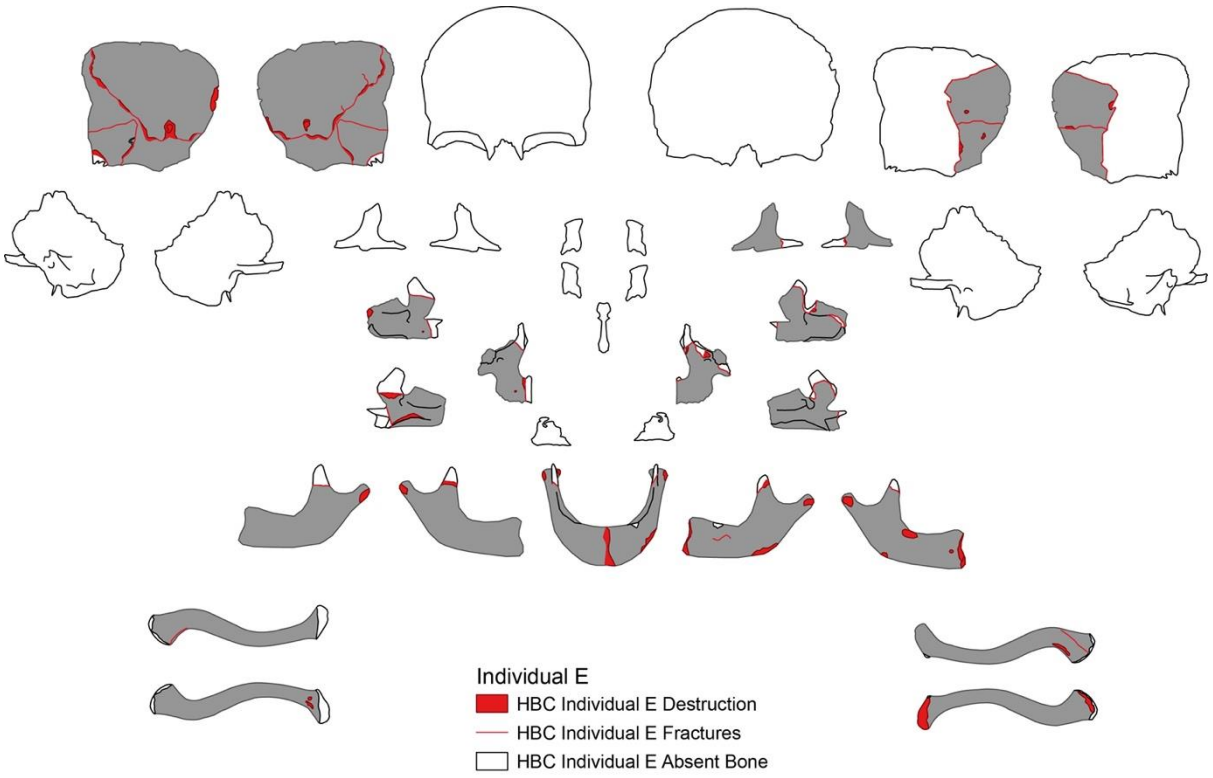


Figure 16.44: Distribution of destruction and fractures across Individual E.

'Exposure of trabecular bone' accounted for most of the damage (69.49%), with most damage occurring to lateral (28.81%) and right surfaces (54.24%). While the differences between damage to surfaces seems large, when the count is looked at the difference between lateral and medial surfaces is four, and five between left and rights. This is not sufficient to interpret as an indication of position.

### *16.6.4: Fractures*

Fracturing occurred to all fragments from Individual E (see figure 16.45 above). Of the fractures, 11.63% were classified as incomplete and occurred to both long bones and cranial elements. Complete fracturing was limited to cranial elements, with most identified as 'oblique dry'. All fractures were consistent with post-mortem fracturing. Slightly more fractures occurred on left elements (53.49%) than right (46.51%), however, the difference in counts is minimal, indicating no significant bias. Anatomical views also showed little differences.

*16.6.5: Tufa Deposits*

All the deposits on Individual E were classed as thin/flaked and were found only on the cranial elements (figure 16.45).

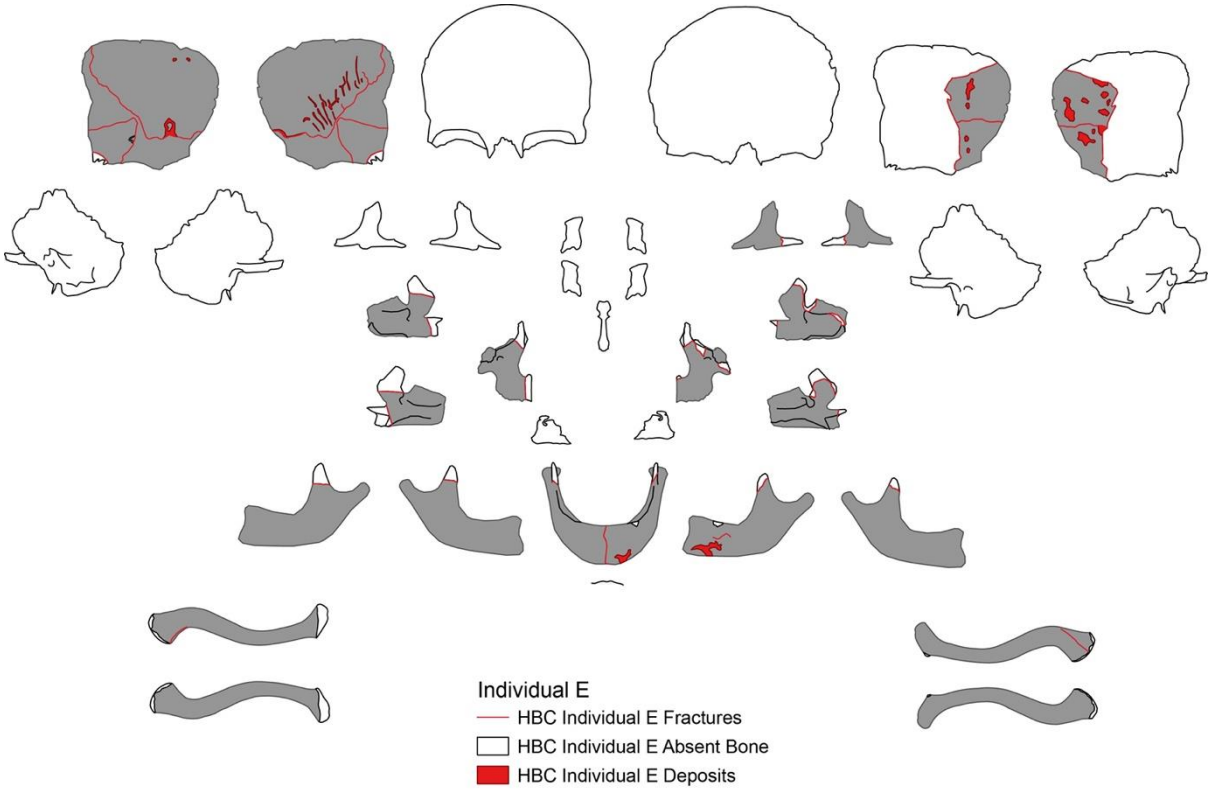


Figure 16.45: Distribution of deposits across Individual E.

Slightly more deposits occurred to right fragments than left (57.58% and 42.42% respectively) and lateral surfaces had higher frequencies than medial (57.58% compared to 36.36%). Once again, due to the small number of fragments and modifications the differences in count for both side and view was only five. This is insufficient to make an inference around bias or burial position.

Ten of the deposits were overlaying areas of staining, suggesting that they occurred later in the sequence.

*16.6.6: Staining*

Staining to fragments assigned to Individual E were consistent with staining seen across the assemblage, with soil staining accounting for half of all staining (figure 16.46).

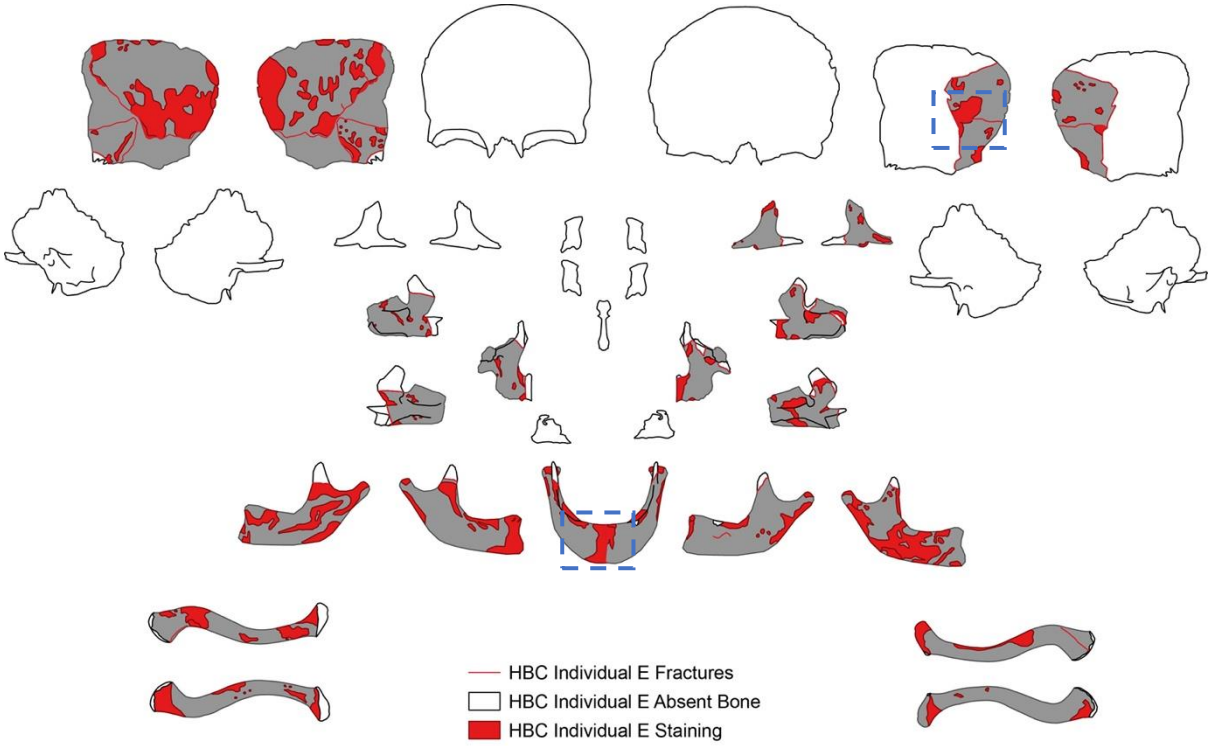


Figure 16.46: Distribution of staining across Individual E.

Lateral surfaces had higher frequencies of staining than medial (30.00% compared to 24.12%), with a count difference of ten. This may be a result of the lateral surfaces of the cranium having longer exposure prior to fracture, however, it is difficult to conclude when fragments are limited. Again, there were some areas where staining crossed fractures, indicating that staining occurred prior to breakage (blue boxes, figure 16.46).

Only 14 patches of staining (8.24%) were modifying existing modifications, all of which were areas of destruction. This suggests that destructive processes were occurring prior to some staining.

### *16.6.7: Large Animal and Invertebrate Activity*

The was a single furrow consistent with invertebrate activity on the medial surface of the right parietal. There was a complete absence of carnivore or other large animal activity.

### *16.6.8: Weathering and Surface Effects*

Evidence of weathering was limited to linear cracking, usually in line with the bone grain, with no areas of delamination or peeling (figure 16.47). There was limited cracking or signs of weathering to the cranial elements. Most of the weathering was to the inferior surface of the left clavicle.

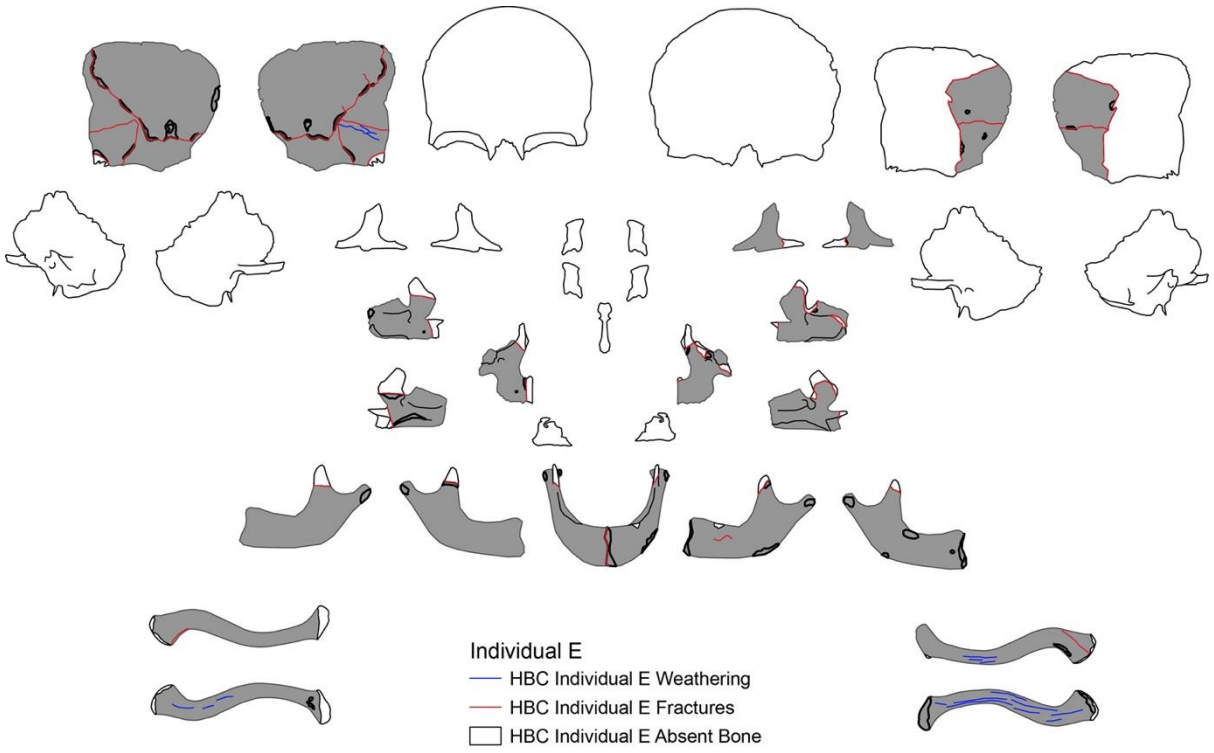


Figure 16.47: Distribution of weathering across Individual E.

Taphonomic analysis of Individual E was limited due to the number of fragments recovered. All changes were consistent with deposition in a cave environment, with no indication of prior burial or exposure elsewhere. On balance this suggests that individual E was unlikely to be a selective or secondary burial. There were no other indications of position or bias.

## 16.7: Early Neolithic - Individual H

### *16.7.1: Bone Representation*

Individual H was represented by just two fragments, a left and right maxilla (figure 16.48).

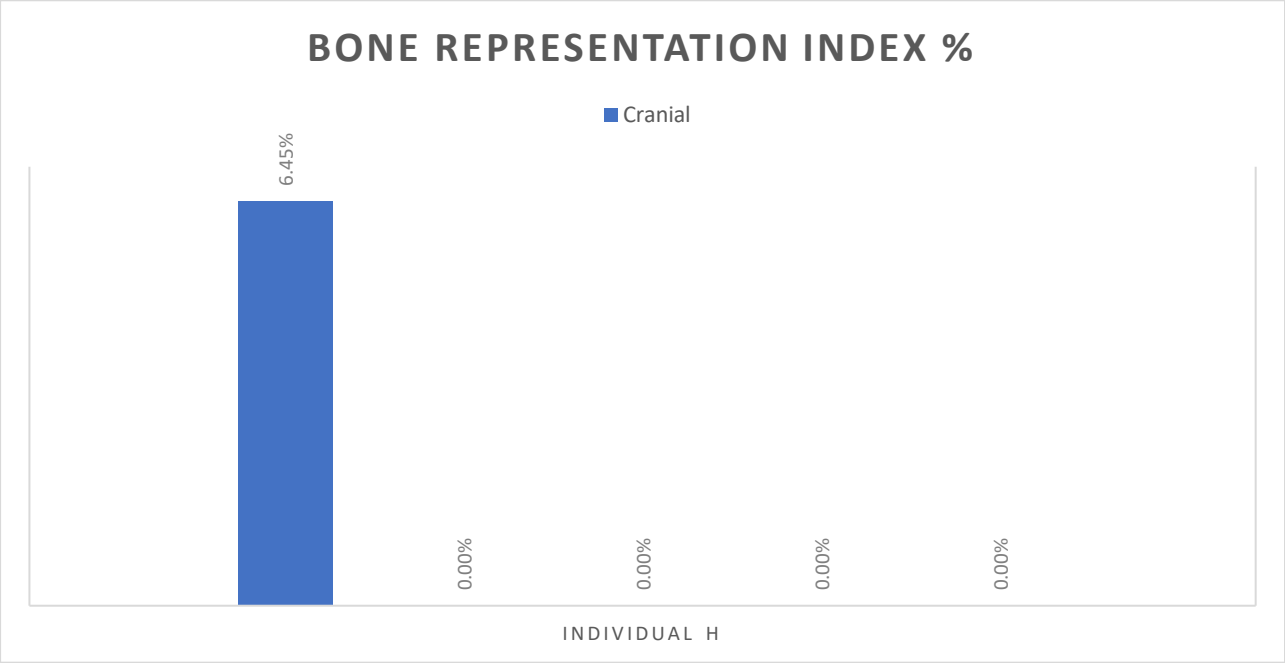


Figure 16.48: Bone representation for Individual H, Heaning Wood.

As discussed for Individual E, care should be taken interpreting this as a cranial only deposition.

### *16.7.2: Whole Body Taphonomy*

Due to the limited fragments taphonomic analysis was restricted. Figure 16.49 shows a close-up of all taphonomic modifications to the maxillae, followed by a qualitative discussion of modifications.

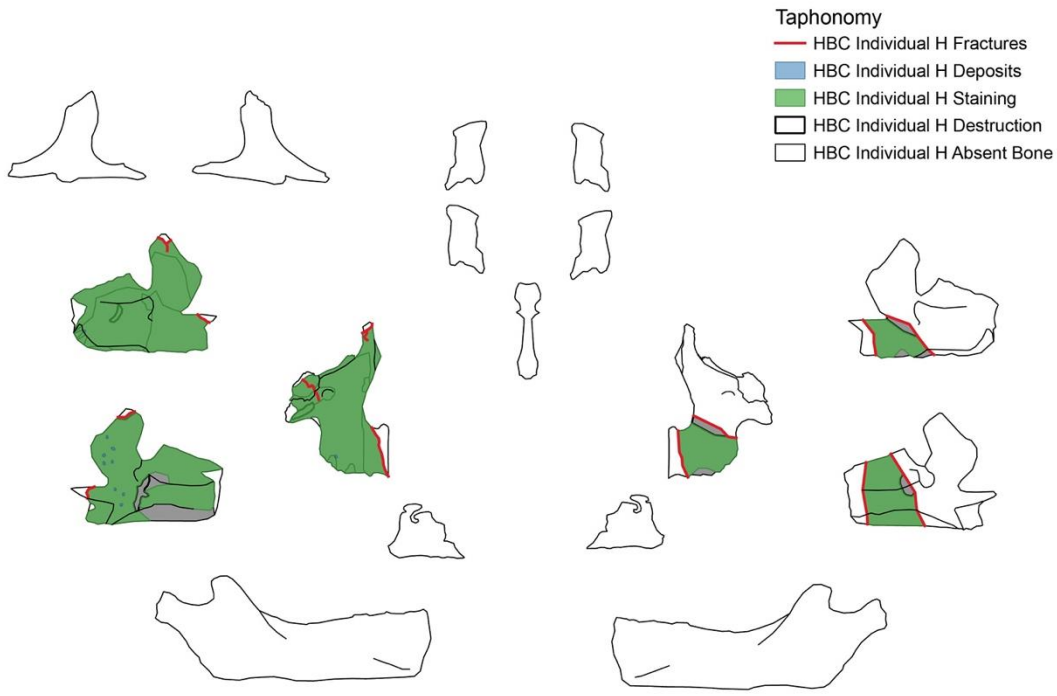


Figure 16.49: Distribution of all taphonomic modifications across Individual H.

All destruction was classified as 'exposure of trabecular bone', consistent with destructive processes within a cave environment. Fracturing was consistent with post-mortem breakage, with a couple of incomplete fractures to the right side. The fragments were soil stained, ranging from light to dark. There were a few small deposits to the right maxilla, with none observed to the left side. No large animal or invertebrate activity was observed and there was no cracking consistent with weathering effects.

The taphonomy on Individual H was consistent with an extended period in a cave environment. There was no evidence to suggest burial position, or that the fragments had been exposed to other environments outside of Heaning Wood. Due to the patterns of taphonomy, there is nothing to suggest that this was a secondary deposition, and it is therefore likely that individual H was not a curated burial. The absence of other elements, however, means that this cannot be completely ruled out.

## 16.8: Summary of Early Neolithic Taphonomy

The taphonomic changes to the individuals dated to the Early Neolithic provide no clear evidence of burial position or deposition narrative. While there are some areas of potential increased exposure, the taphonomy is generally homogenous, and consistent with deposition in a cave environment.

## 16.9: Mesolithic - Individual F

### *16.9.1: Bone Representation*

Individual F was the oldest burial in the assemblage, dating to 9290-8930 BC and was represented by just four fragments, all cranial (figure 16.50). There were two loose teeth that were possible matches.

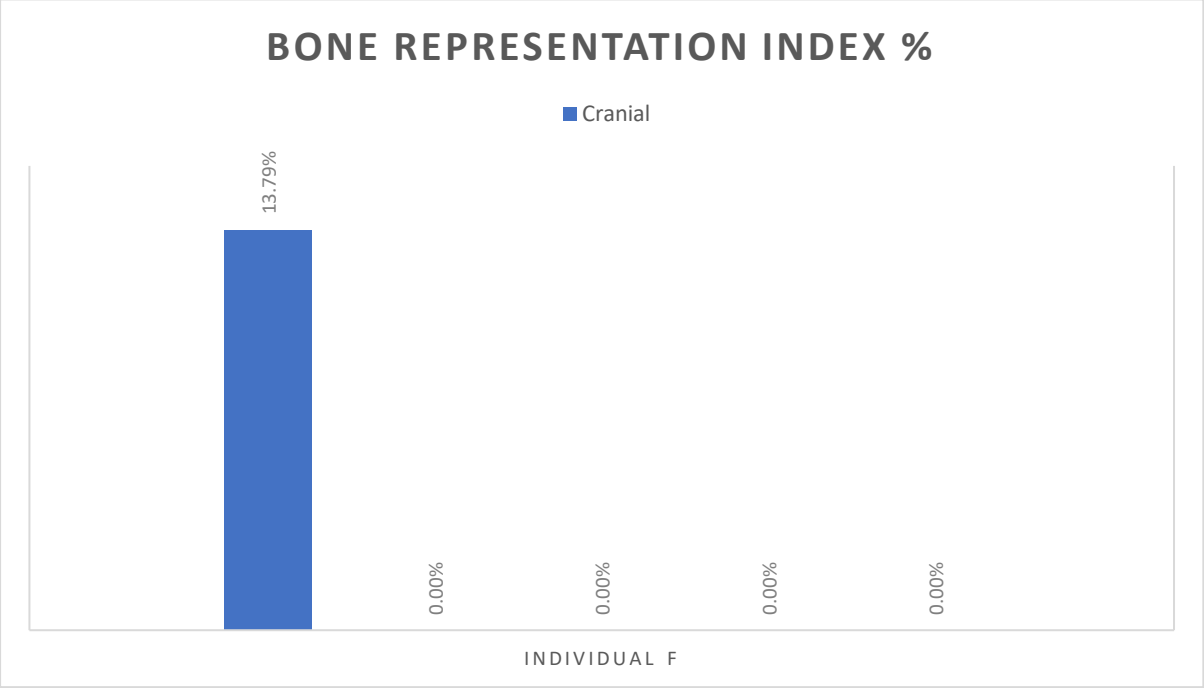


Figure 16.50: Bone representation for Individual F, Heaning Wood.

As discussed for Individual's E and H, care should be taken interpreting this as a cranial only deposition, particularly due to the burial phase. This is the earliest known deposition at Heaning Wood, therefore it would have potentially sat under a large accumulation of other

bone deposits. This, along with the length of time the remains were in the cave, and the fragility of juvenile remains, could have led to more advanced destruction.

### *16.9.2: Whole Body Taphonomy*

Due to the limited fragments taphonomic analysis was restricted. Figure 16.51 shows a close-up of all taphonomic modifications, followed by a qualitative discussion of modifications.

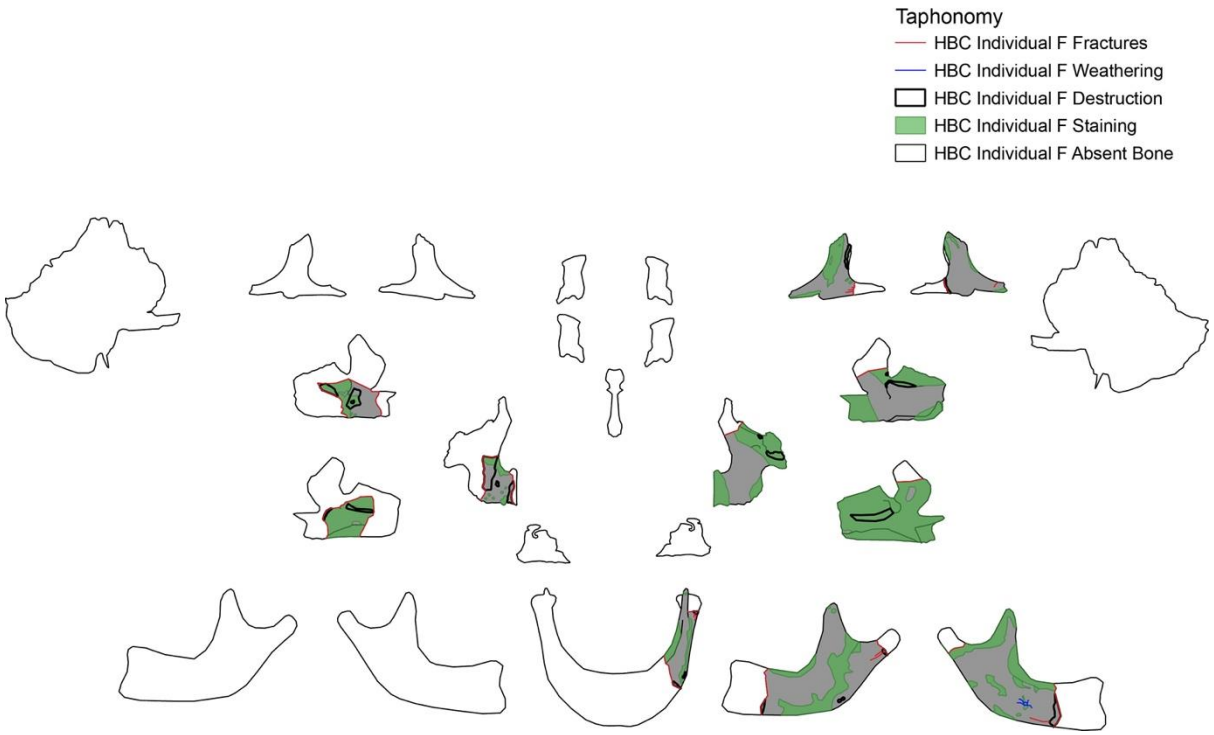


Figure 16.51: Distribution of all taphonomic modifications across Individual F.

All destruction was classified either as 'exposure of trabecular bone', or 'exposure of opposite bone surface' consistent with destructive processes within a cave environment. There was a single hole to the right maxilla, this had rough margins and was consistent with post-mortem damage. Fracturing was consistent with post-mortem breakage, with several incomplete fractures to left mandible and zygomatic. These originated from areas of destruction and complete fracture. All fragments were soil stained, ranging from light to dark, the mandible and right maxilla had some patches of mottled, black-grey staining consistent with manganese. There were no deposits observed. This may be due to Individual H being the earliest deposit, therefore protected from calcite build-up by other accumulated debris. No

large animal or invertebrate activity was observed. There was a single area of mosaic cracking to the lingual surface of the mandible, consistent with weathering effects.

The taphonomy on Individual F was consistent with an extended period in a cave environment. There was no evidence to suggest burial position, or that the fragments had been exposed to other environments outside of Heaning Wood. Due to the patterns of taphonomy, there is nothing to suggest that this was a secondary deposition, and it is therefore likely that individual F was not a curated burial.

## 16.10: Undated - Individual G

### *16.10.1: Bone Representation*

Individual G was estimated as the youngest age at death, at 38-40 weeks. There was representation from all areas of the body except for hands, feet, and patella (figure 16.52). The patella does not ossify until approximately a year and a half after birth, or later (Scheuer and Black, 2000), and while some ossification centres for the hands and feet are present at birth, many do not develop until later. This would explain the absence of elements from this category.

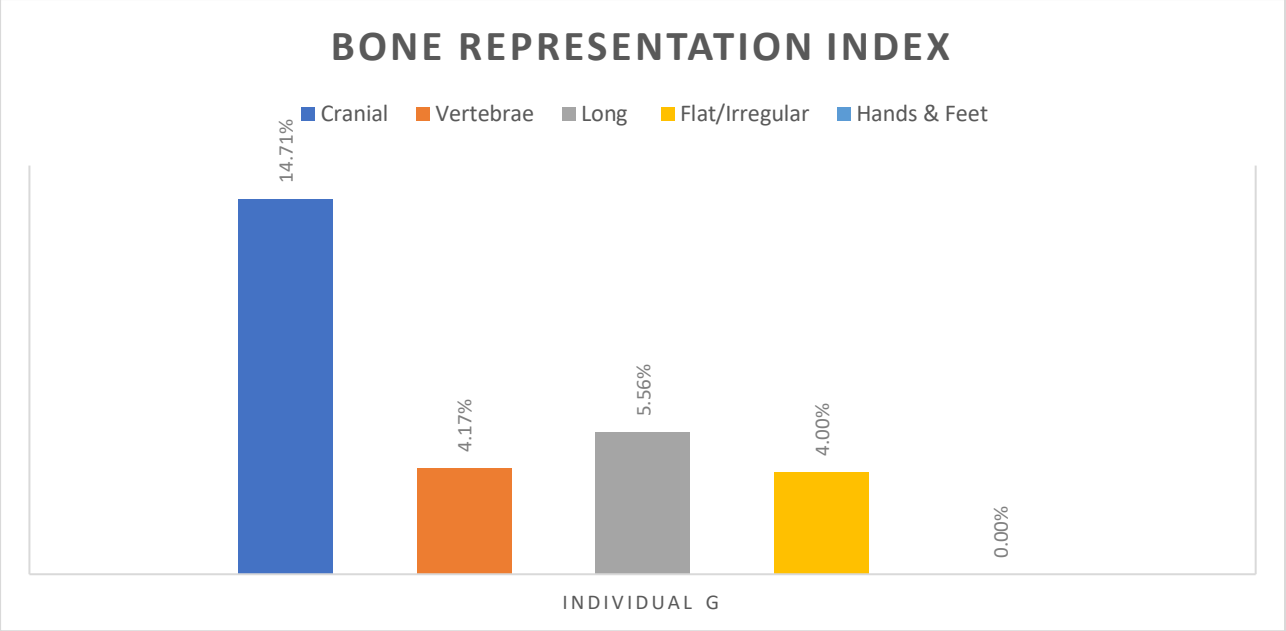


Figure 16.52: Bone representation for Individual G, Heaning Wood.

Individual G was mostly represented by cranial elements (14.71%) and out of a total of eleven fragments, five were left-sided (45.45%), two were right (18.18%), and four were unilateral (36.36%).

The following discusses frequencies of modifications, all tables for Individual G taphonomy can be found in appendix 7.6.

### *16.10.2: Whole Body Taphonomy*

All fragments from Individual G were altered by taphonomic processes (figure 16.53)

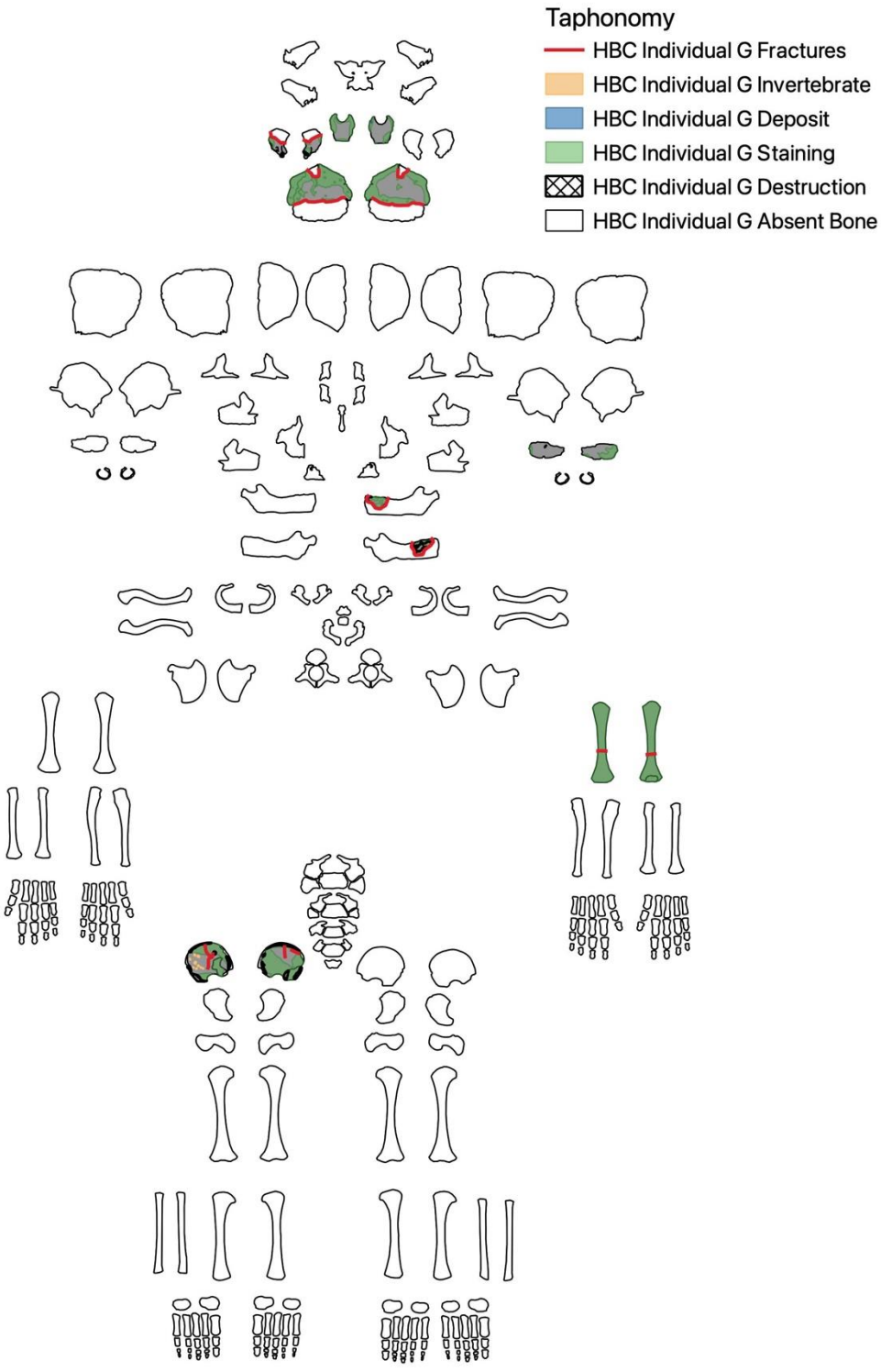


Figure 16.53: Distribution of all taphonomic modifications across Individual G.

*16.10.3: Destruction*

Destruction was limited to three fragments, the right *pars lateralis*, the ilium and a fragment of mandible (figure 16.54).

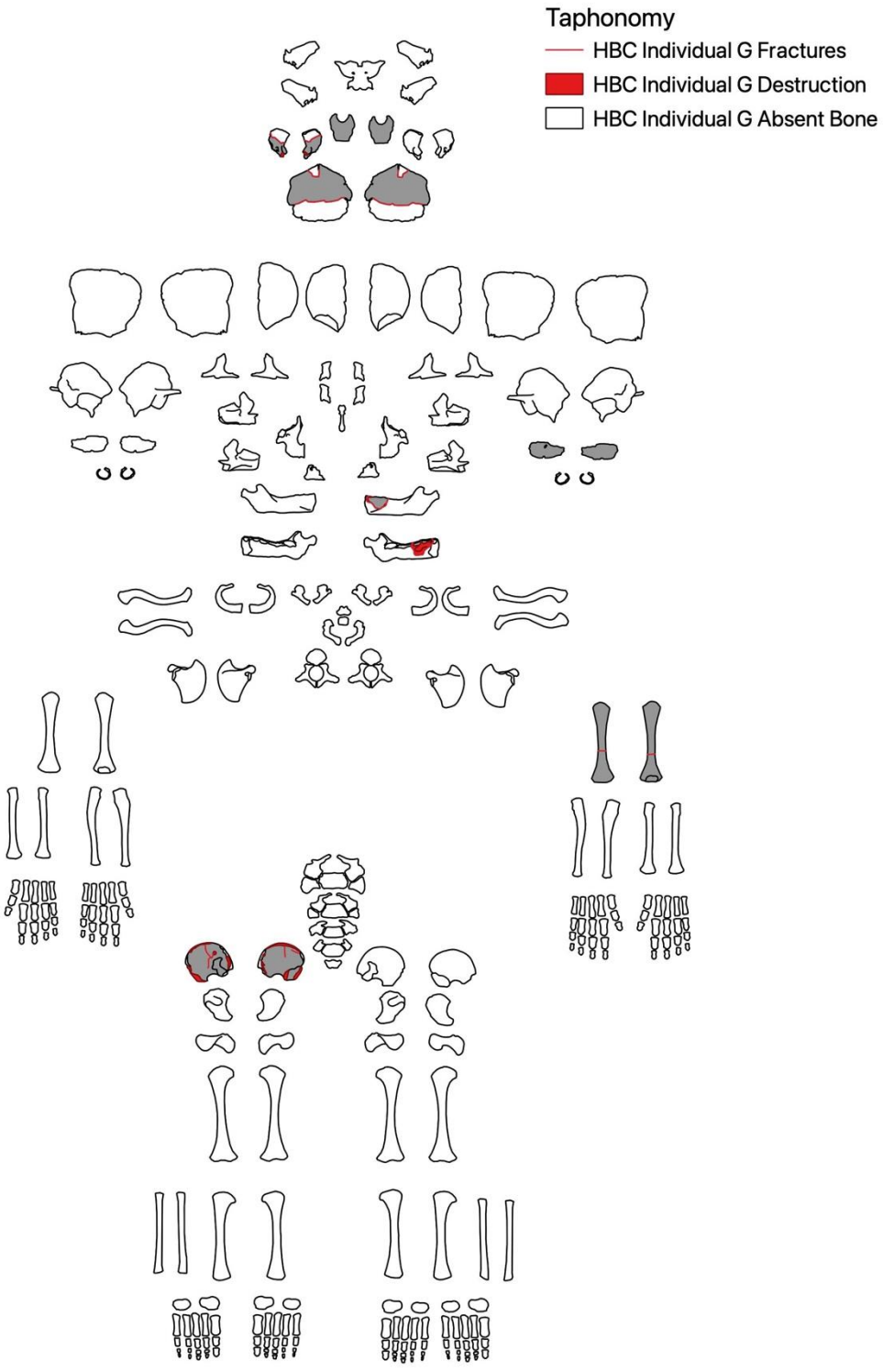


Figure 16.54: Distribution of all taphonomic modifications across Individual G.

Most of the destruction was classified as 'exposure of trabecular bone' (66.67%) which was evenly distributed across cranial and flat/irregular elements, despite flat/irregular having lower representation. The posterior surface was marginally more affected than anterior surfaces but the number of fragments limit interpretations. There was a single area of peri-mortem crushing on the anterior surface of the right ilium.

### *16.10.4: Fractures*

Fracturing occurred to all fragments except for the *pars basilaris* and the *pars petrous* (see figure 16.54, above). All fractures were consistent with post-mortem breakage, with 'transverse' and 'other (unclassified)' fracture types having the highest counts (28.57%). There were four incomplete fractures that all originated from an area of crush damaged located on the anterior surface of the ilium. Cranial elements had the highest fracture counts, most likely due to having a higher representation rather than bias in damage. Right fragments had more cracking than left (42.86% and 28.57% respectively), unilateral fragments accounted for 28.57% of fractures. Again, due to the limited number of fragments it is not possible to establish a clear bias.

### *16.10.5: Deposits*

There were only four patches of calcite deposits. Three were observed on the anterior surface of the right ilium and one on the posterior surface of the *pars basilaris*.

### *16.10.6: Staining*

All fragments associated to Individual G had patches of staining (figure 16.55). Cranial fragments had soil, mottled black-grey, and light brown/orange staining. Cranial staining accounted for 85.71% of all stains. The flat/irregular and long bones only had soil staining observed.

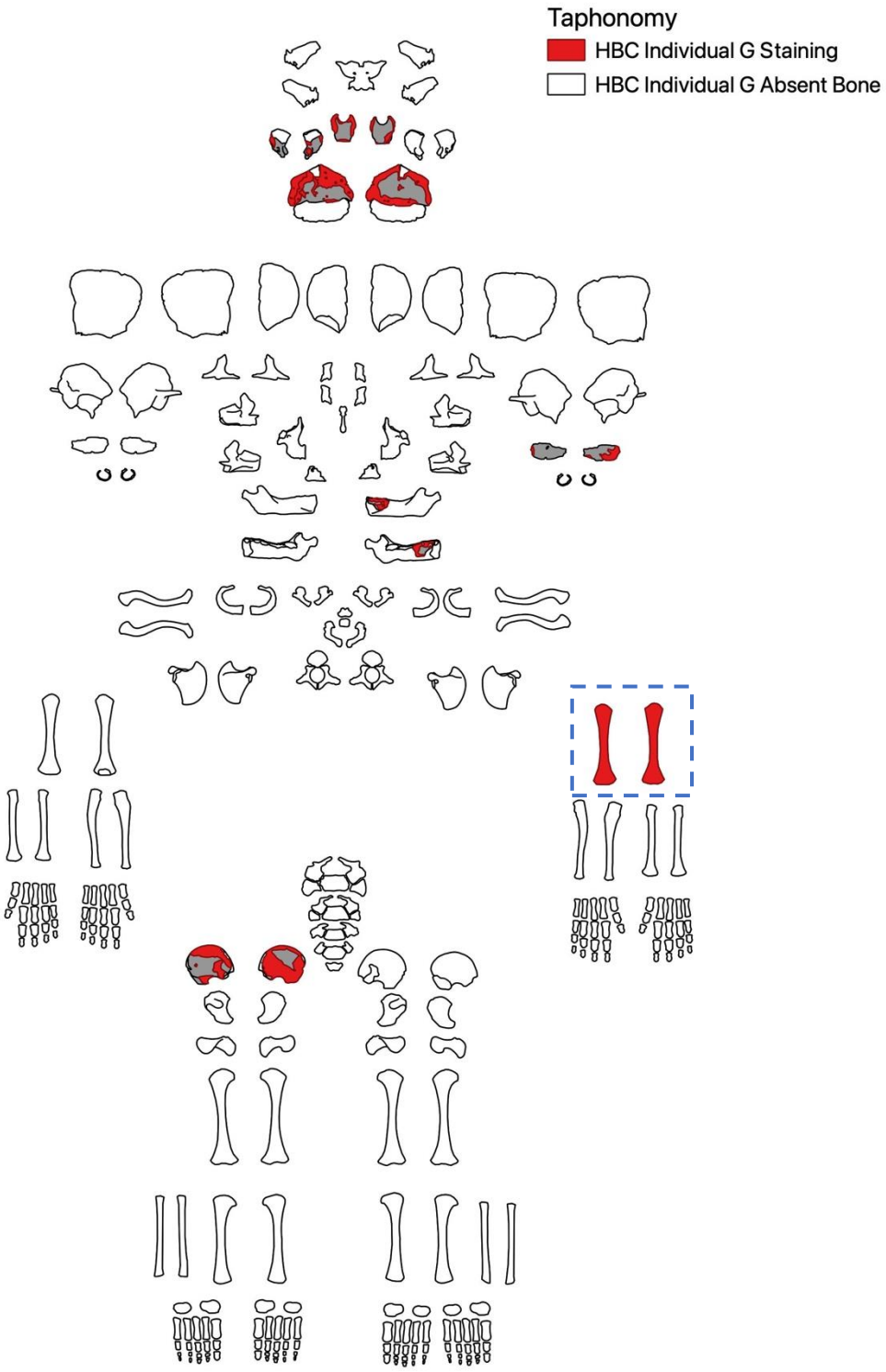


Figure 16.55: Distribution of staining across Individual G.

Fragment HBC804 (blue dashed box, figure 16.55) was a right humerus located in the Dock Museum collection. This was completely stained dark brown, similar to the distal tibia from Individual C and the femurs from Individual D (pages 270 and 300).

### *16.10.7: Large Animal and Invertebrate Activity*

Invertebrate activity was limited to the anterior surface of the right ilium. There was a complete absence of carnivore or other large animal activity.

### *16.10.8: Weathering and Surface Effects*

There was no evidence of cracking or surface effects consistent with weathering.

The taphonomy on Individual G was consistent with an extended period in a cave environment. There was no evidence to suggest burial position, or that the fragments had been exposed to other environments outside of Heaning Wood. Considering the age at death estimation (38-40 weeks), along with the deposition environment, the recovery of Individual G is reasonable. Dating was not possible for Individual G, and taphonomy does not give any indication of possible burial period.

## 16.11: Assemblage Taphonomy

The taphonomy across Heaning Wood is consistent with burial in a cave environment, with the deposits and staining all consistent with geological process found in the cave. There is no evidence on any of the bones to suggest that they were previously buried in another location, or that they had been exposed to processes such as carnivore excarnation, deliberate processing or subaerial exposure. Animal activity was limited to invertebrate modifications, which is consistent with the morphology of the cave, where access to larger animals would have been limited. Bone representation indicates whole body burials for all bodies, except for Individuals E, F and H, where the possibility of curated deposition is unlikely, but cannot be completely ruled out. The following section discusses how the taphonomy is spread spatially within the cave to further explore depositional narrative.

# CHAPTER 17: HEANING WOOD SPATIAL ANALYSIS

The spatial data for specimens recovered during the 2016-2019 excavations was confined to information about which layer each specimen came from. The excavation layers were approximately 0.125 m deep, with no information about where within each layer a fragment came from. Fragments that came from the West Fissure had more limited spatial data, with only an indication they originated from this area. The specimens held at the Dock Museum had little to no spatial information other than that they were likely to have been recovered from the top of the talus formation, towards the vertical opening. The following section has analysed distributions with this in mind. Diagrams have been created using layers. Where points are used, these are for illustrative purposes and not an indication of precise location; fragments may have been recovered from anywhere within that layer.

Fragments associated to individuals have been done with high confidence, however, there are limitations to individuating a commingled and fragmented assemblage which will be discussed in section 18.3.1. Analysis of movement according to individual has been done based on current individuation; should analysis highlight any incorrect associations these will be listed in the discussion.

## 17.1: Assemblage - Distribution of Fragments

Figure 17.1 shows the distribution of all the human remains recovered from Heaning Wood.

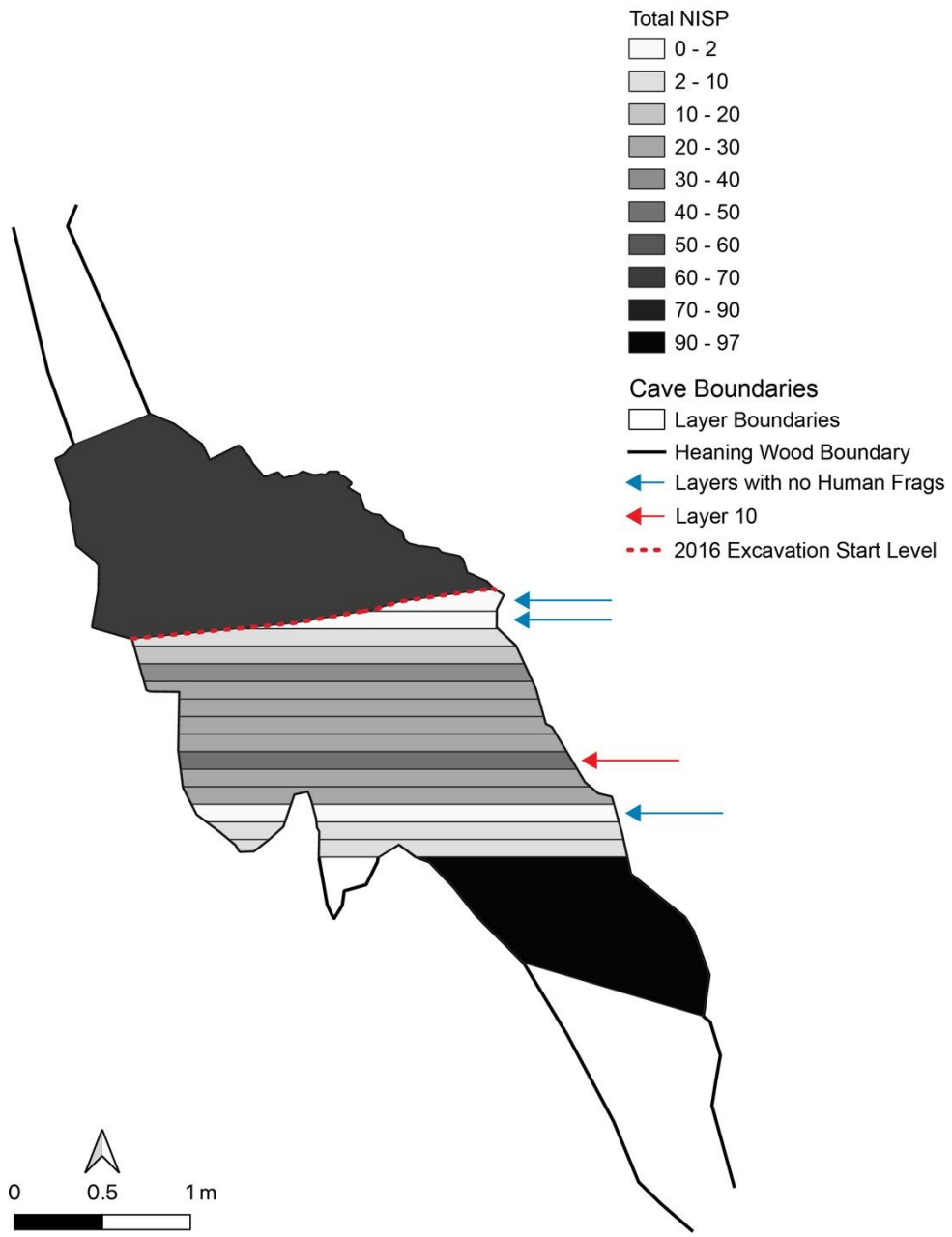


Figure 17.1: Distribution of fragments according to NISP counts.

Fragments were recovered from all layers except for layers one, two and thirteen (marked with blue arrows on figure 17.1). These contained faunal remains but no human specimens. The West Fissure and top area had the highest numbers of specimens; however, this would be expected due to the level of spatial detail, as these areas do not have layer sub-divisions. Layer ten (marked with the red arrow) also had a relatively high distribution of fragments (N = 49). This is consistent with a talus formation, with some later deposits spreading to lower layers through run off, the mechanism of which is illustrated in figure 17.2.

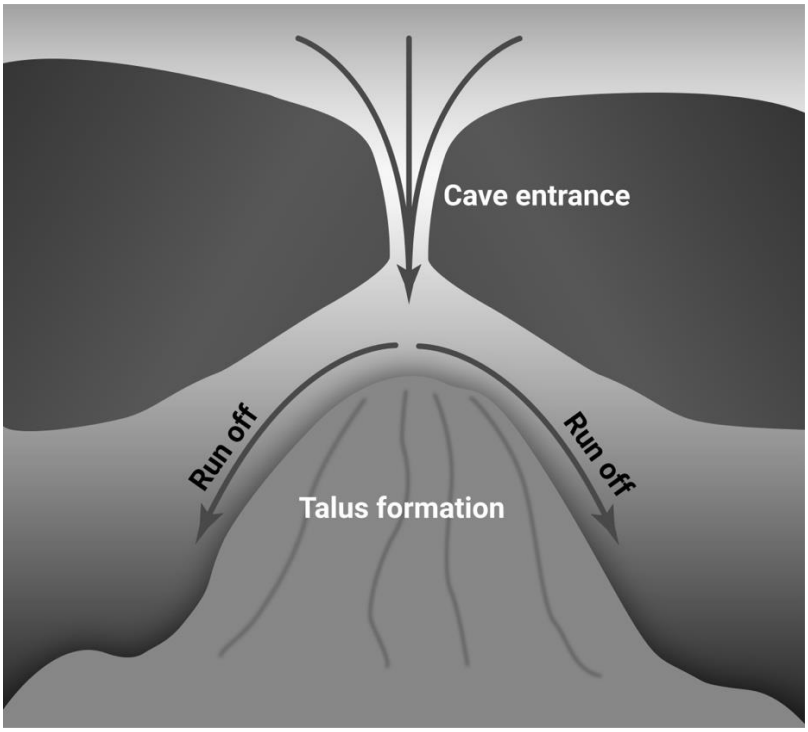


Figure 17.2: Illustration of talus formation with associated run off.

The following section explores the distribution of fragments according to burial period and the distribution of elements as an assemblage, before exploring spatial relationships of fragments and taphonomy by individual.

## 17.2: Distribution According to Burial Period

### *17.2.1: Dated Samples*

Figure 17.3 shows the eight fragments sampled for radiocarbon dating. As expected, the earlier dated fragments were lower in the cave. There was one sample that was initially associated with Individual D, where dating was difficult due to degradation (blue point, layer twelve, figure 17.3). It was suspected that this fragment was not from Individual D (see section 14.1, page 225), with a less than five percent chance of overlap. The modelled date placed the fragment from 2140-1965 years Cal BC, however despite the age, it was recovered below earlier burials, indicating that movement was occurring within the assemblage.

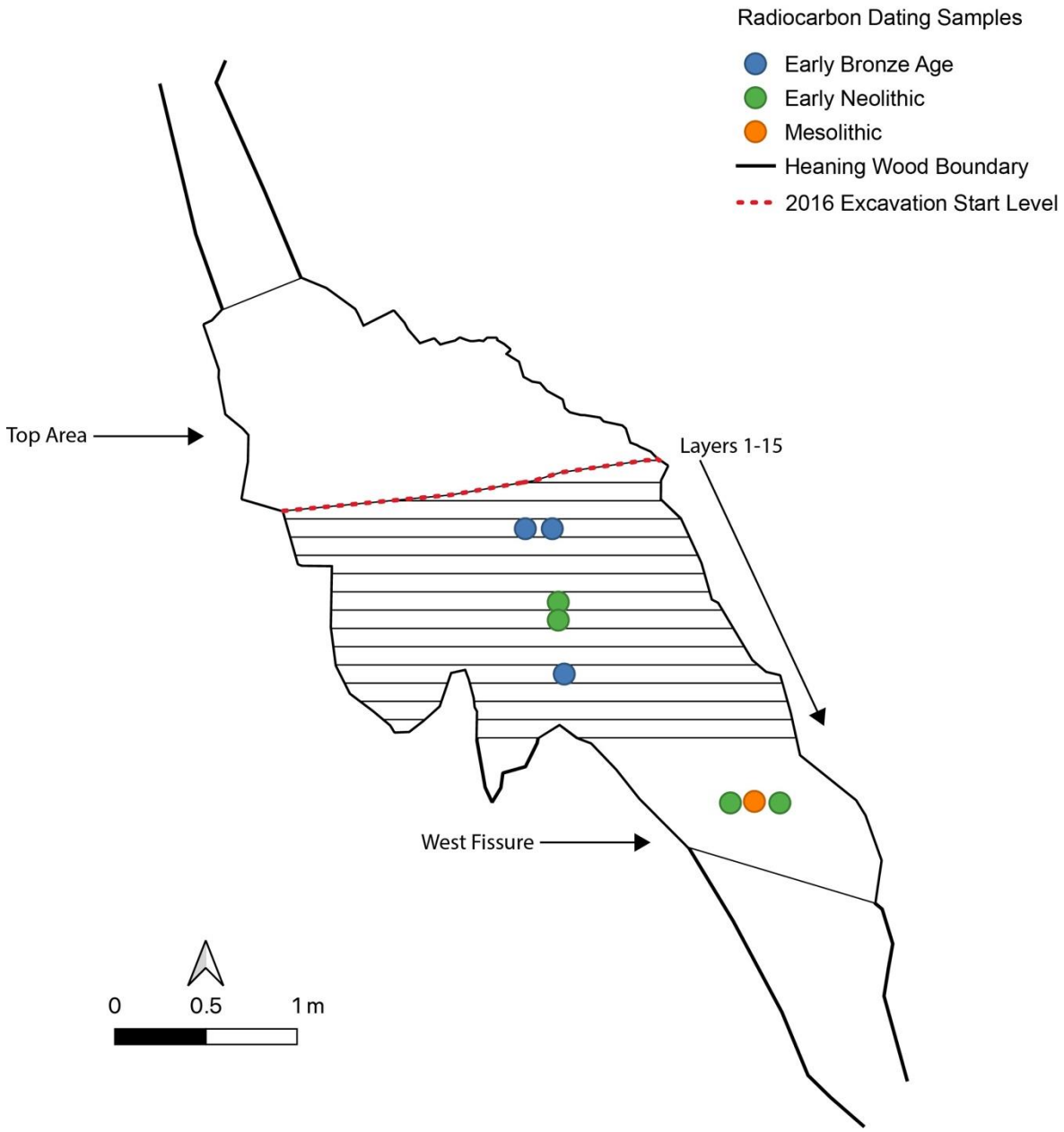


Figure 17.3: Distribution of radiocarbon dated samples.

### *17.2.2: Early Bronze Age Distribution*

Fragments assigned to Early Bronze Age individuals were found throughout the cave (figure 17.4) except for layers one to three, and thirteen to fifteen.

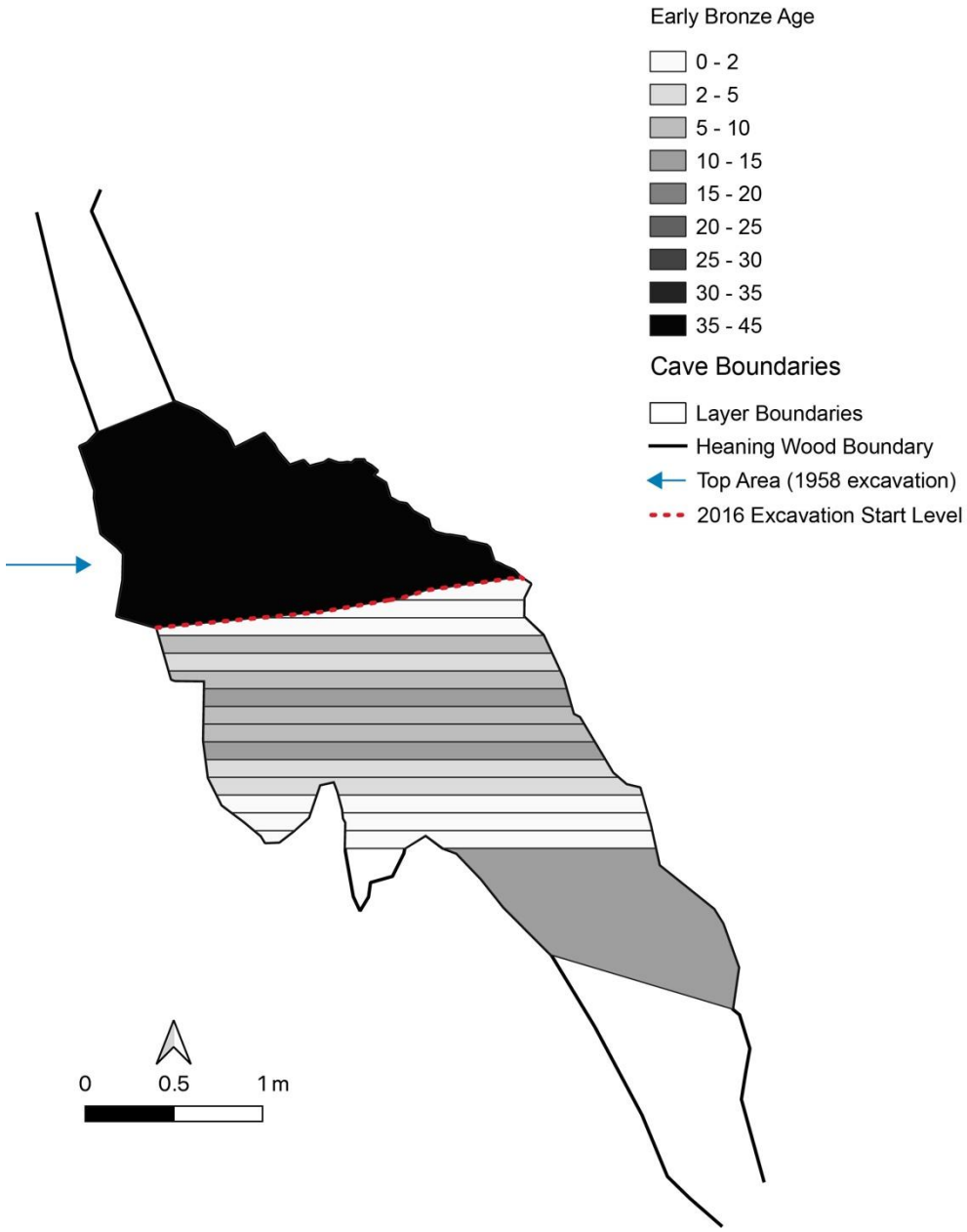


Figure 17.4: Distribution of fragments assigned to Early Bronze Age individuals.

The area associated with the 1958 and 1974 excavations had the highest concentrations of fragments (marked with a blue arrow). There were eleven fragments located in the West Fissure, compared to forty-four from the top layer. The higher concentrations towards the top of the chamber, with some accumulation lower down, are consistent with later depositions.

*17.2.3: Early Neolithic Distribution*

Fragments assigned to Early Neolithic individuals were found throughout the cave (figure 17.5) except for layers one to two, and thirteen to fifteen.

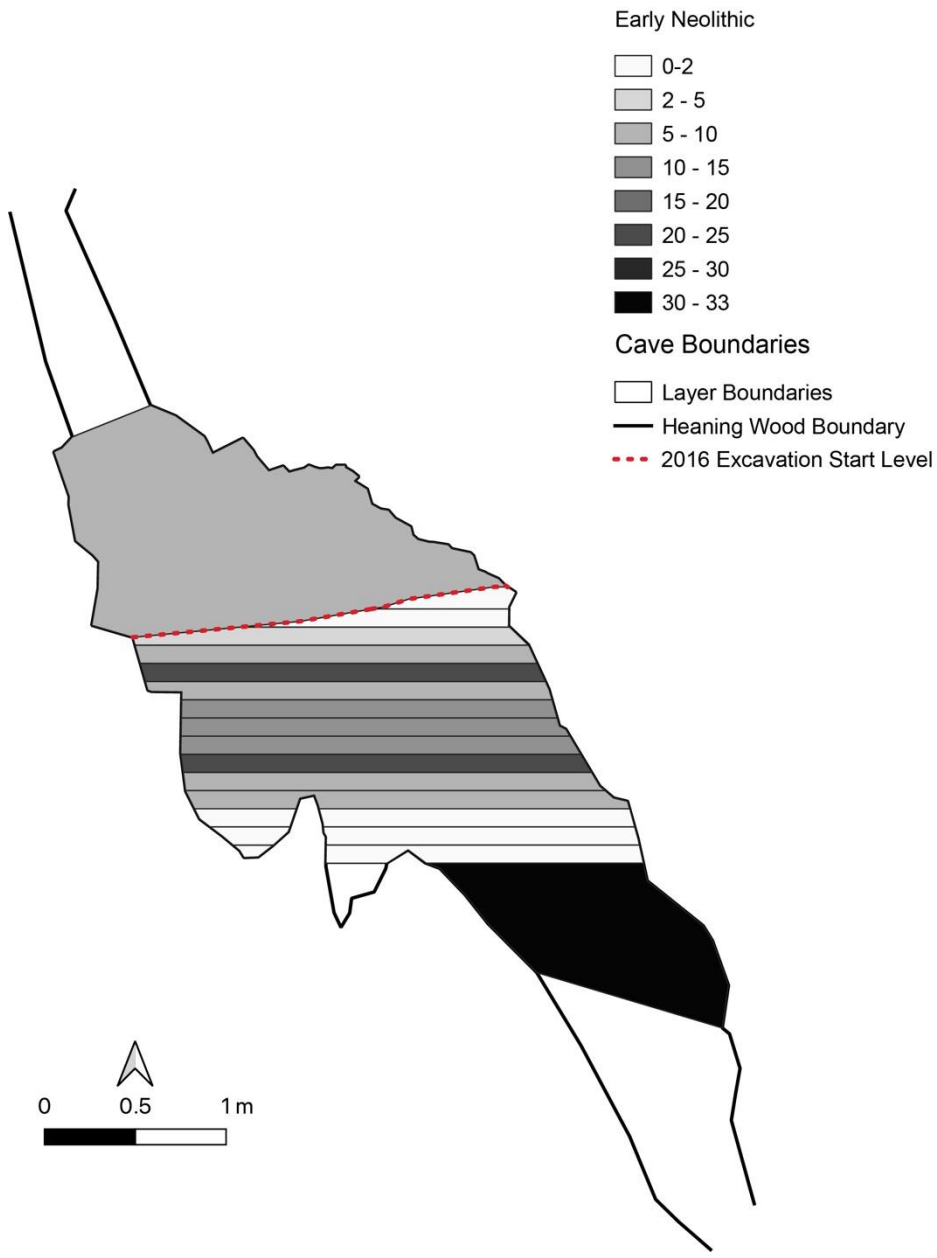


Figure 17.5: Distribution of fragments assigned to Early Neolithic individuals.

Layers five and ten had larger concentrations of fragments, with most fragments recovered from the West Fissure. The build-up of specimens lower in the cave, when compared to the distribution of the Early Bronze Age individuals is consistent with earlier deposition. Issues surrounding individuation will be discussed in more detail in section 18.3.1, however, it is

important to note that individuation may not be exact, and therefore some fragments shown here may belong to bodies from different time periods.

### *17.2.4: Mesolithic Distribution*

Fragments assigned to the Mesolithic individual were found in the bottom layers of the cave (figure 17.6). This is consistent with it being the earliest known deposition at the site.

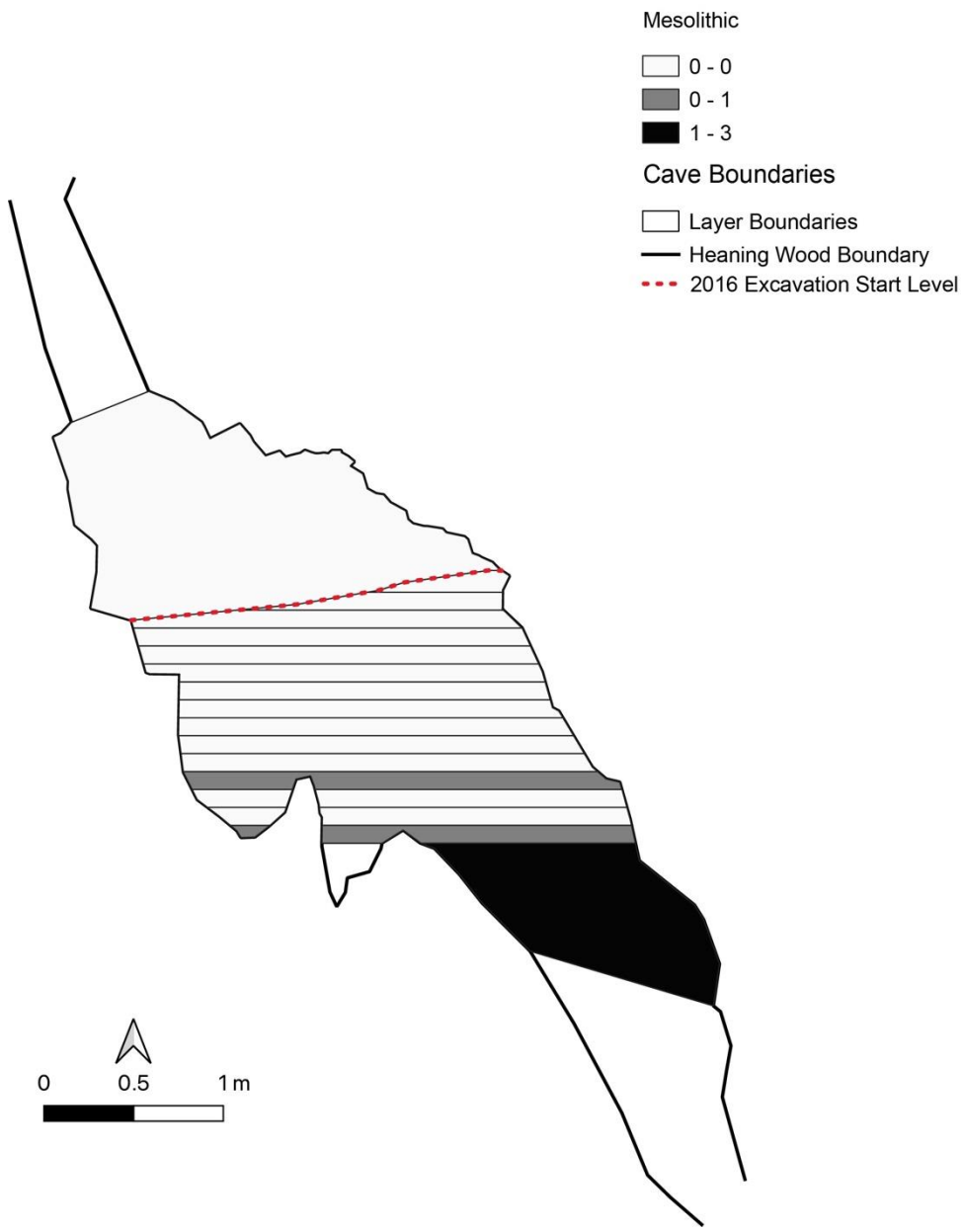


Figure 17.6: Distribution of fragments assigned to the Mesolithic individual.

There were only five fragments recovered for the Mesolithic individual, therefore care should be taking in interpreting distributions.

### *17.2.5: Unassigned Material Distribution*

Unassigned fragments were excavated from all layers of the cave (figure 17.7). Most fragments were found from the West Fissure but there was no clear pattern to suggest that unassigned specimens were associated to a particular period of deposition.

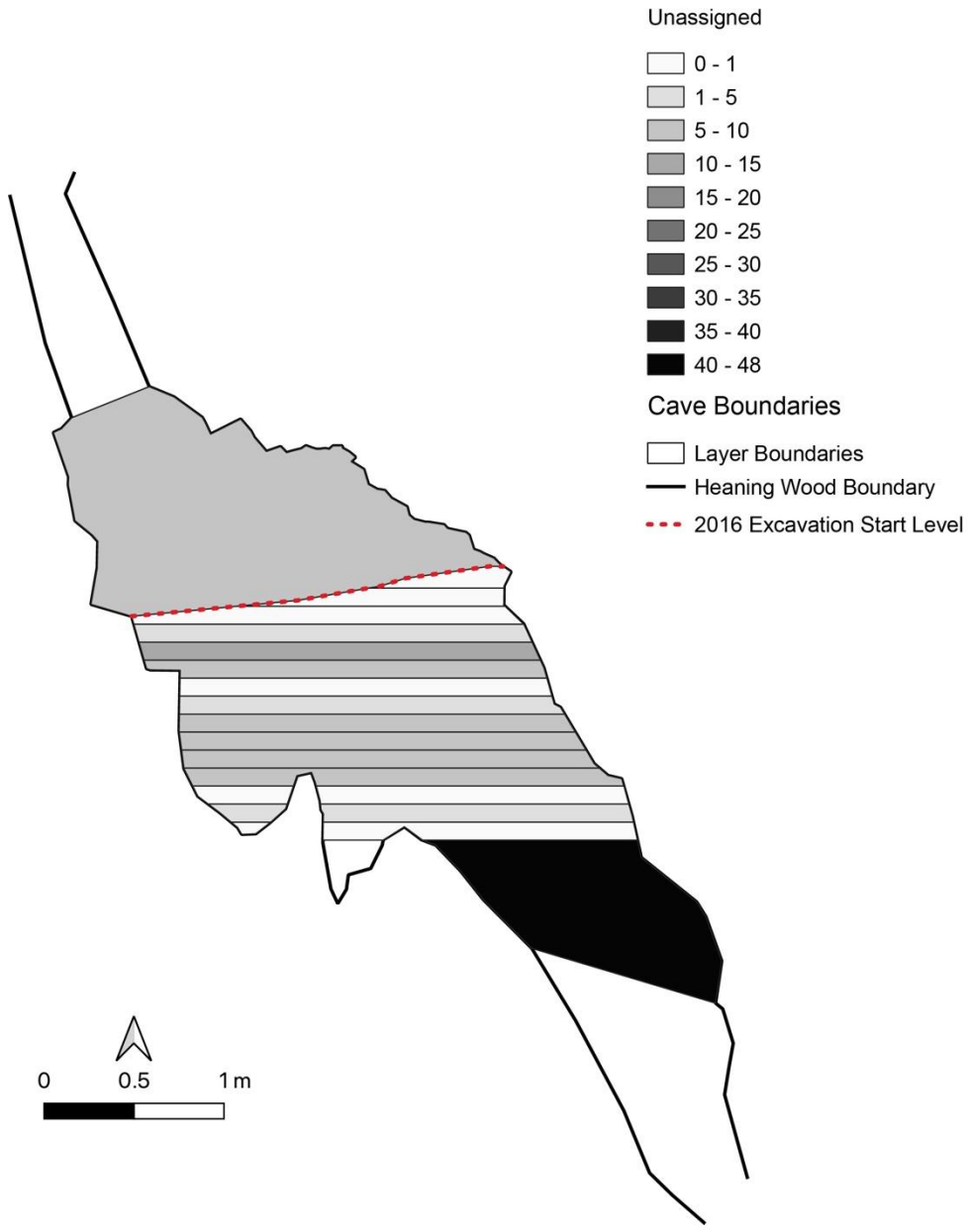


Figure 17.7: Distribution of unassigned fragments.

## 17.3: Assemblage - Element Distribution

The spatial distribution of fragments according to element group were looked at to explore the relationship between movement patterns, bone morphology and cave processes. When all fragments are grouped, cranial and flat/irregular specimens have greater concentrations towards the West Fissure (figure 17.8), suggesting greater movement potential. While sequences of disarticulation have been shown to vary depending on burial context, cranial elements have been shown to detach early in the sequence (Roksandic, 2002; Mickleburgh and Wescott, 2018). The rounded morphology of the cranium can lead to movement through rolling (Roksandic, 2002) and flat/irregular bones such as the sacrum, ribs and sternum may be more prone to movement due to lower bone density (Bello and Andrews, 2006). The characteristics of these elements, coupled with the talus formation, may have resulted in run off into the West Fissure.

The opposite was true for long bones which were concentrated towards the top of the cave. Long bones have been shown to retain articulations for longer (Roksandic, 2002) and have a higher density (Bello and Andrews, 2006), therefore may have been less affected by processes causing movement. Vertebrae and hands, feet and patellae had higher concentrations in the middle areas of the cave. The hands, feet, and patellae disarticulate early in the decomposition sequence (Bello and Andrews, 2006; Duday, 2009; Knüsel, 2014; Knüsel and Robb, 2016; Schotsmans *et al.*, 2022) and therefore may be prone to increased movement within the cave system.

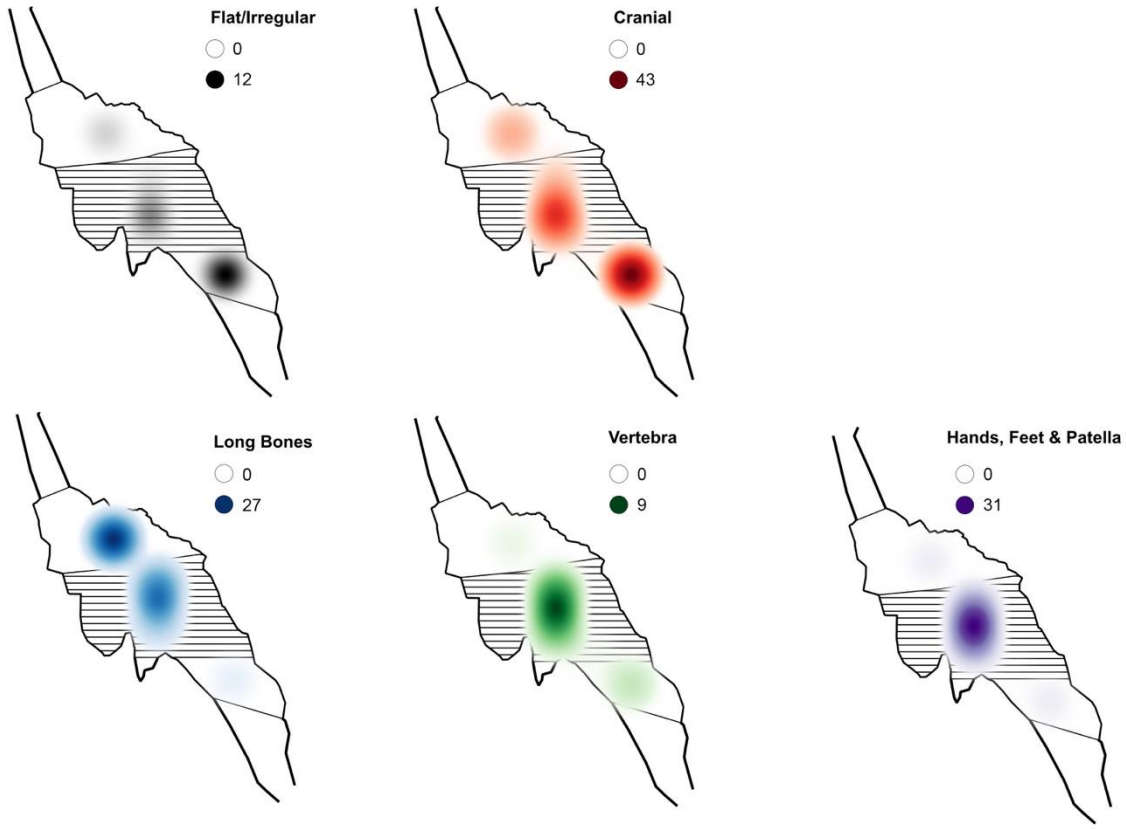


Figure 17.8: Concentration of fragments according to element group.

The next section will explore movement of skeletal elements per individual and the distribution of taphonomic modifications, with the view of highlighting potential agents for fragment movement and sequence of events post deposition.

## 17.4: Individual A (Early Bronze Age) – Distribution of Fragments

Fragments from Individual A were concentrated at the top of the cave, along with some distributed towards the middle layers and West Fissure (figure 17.9). The very lower levels (thirteen to fifteen) had no fragments associated with Individual A which is consistent with burial period.

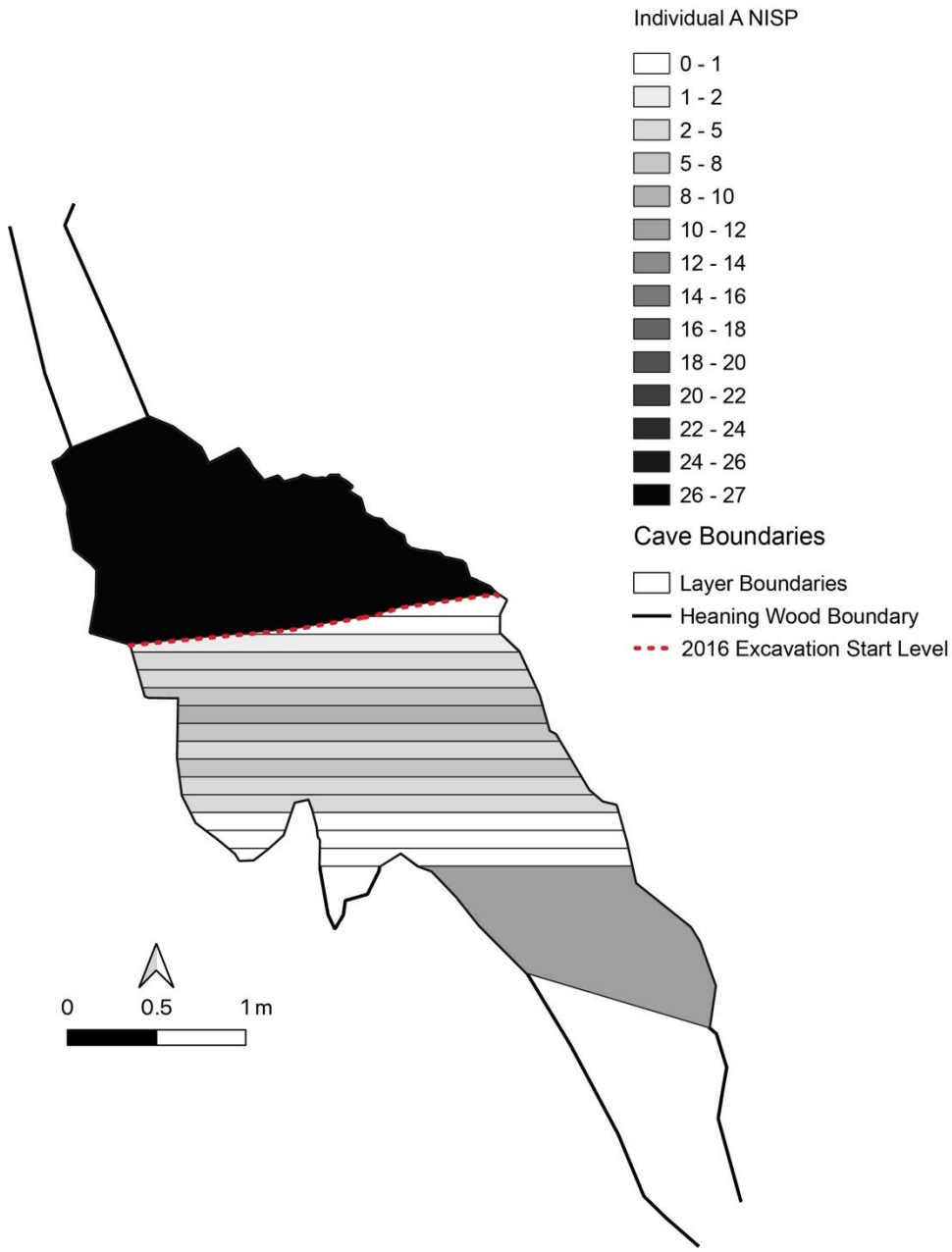


Figure 17.9: Distribution of fragments assigned to Individual A.

## 17.5: Individual A (Early Bronze Age) - Element Distribution

There was displacement of all element groups for Individual A (figure 17.10).

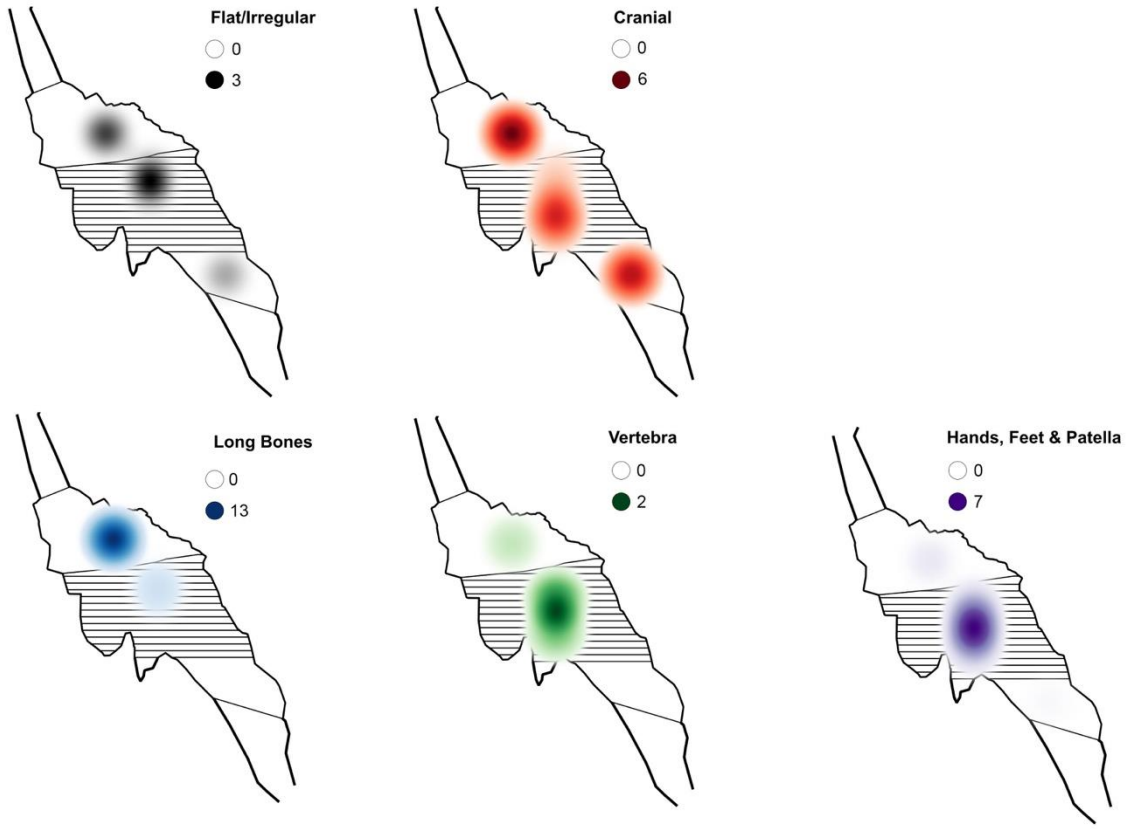


Figure 17.10: Concentration of fragments according to element group assigned to Individual A.

While cranial and flat/irregular fragments showed opposite concentrations than the whole assemblage, clustering in the top area, they were still the most dispersed element groups for Individual A. This is consistent with expectations of distributions according to burial period, with the body being introduced later in the accumulation process. Long bones have mostly remained in the top area, with other element groups showing dispersal in line with morphology and disarticulation sequences (Roksandic, 2002; Bello and Andrews, 2006; Duday, 2009; Knüsel, 2014; Knüsel and Robb, 2016; Schotsmans *et al.*, 2022).

### *17.5.1: Crania*

There were seventeen cranial fragments assigned to Individual A, including teeth. Layers eight, ten and eleven were limited to loose teeth. A fragment of cranium, thought to be occipital, was in layer twelve, and a right zygomatic and lower right molar were recovered from the West Fissure (figure 17.11).

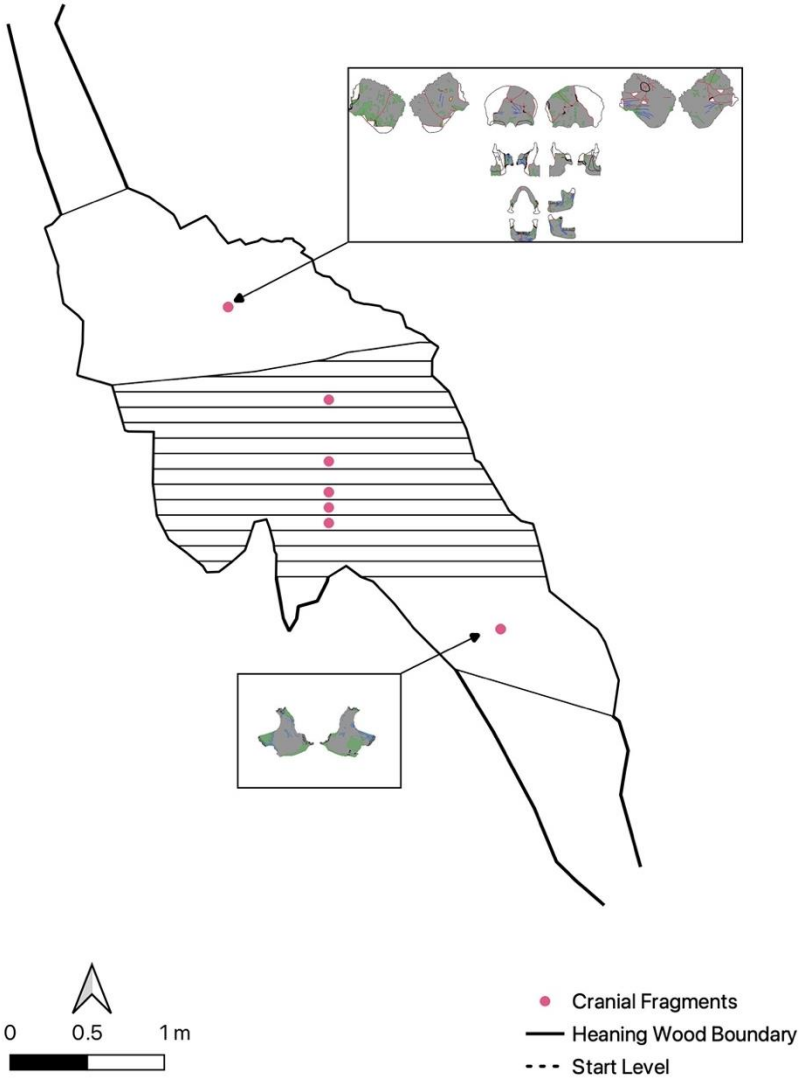


Figure 17.11: Distribution of cranial fragments assigned to Individual A.

The frontal, both parietals, the mandible, and maxillae were all located in the top area of the cave. The left mandibular condyle was recovered from layer four. The recovery of larger cranial and mandibular fragments from the top of the talus is consistent with a later deposition and supports individuation. There is a possibility that the loose teeth belong to other individuals in the assemblage but may have ended up lower in the cave due to their small size.

### *17.5.2: Vertebra*

Six vertebrae were assigned to Individual A; two were thoracic but unsequenced. The sixth cervical and third lumbar were found in level eleven. The seventh cervical vertebra was found with an un-sequenced thoracic in layer six. The axis (second cervical) was in the layer just

below this. The second un-sequenced thoracic vertebra was found in the top area of the cave (figure 17.12).

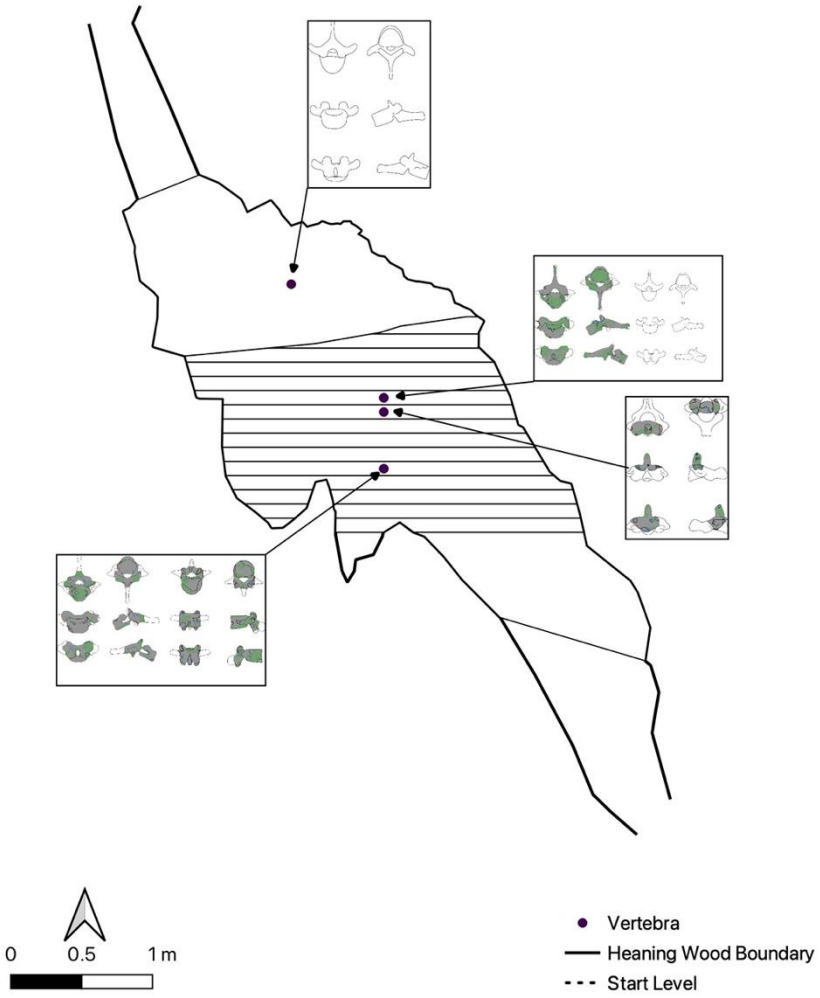


Figure 17.12: Distribution of vertebral fragments assigned to Individual A.

The axis was found away from most cranial fragments, however as discussed earlier detachment between the atlas and axis can occur early (Duday, 2009; Roksandic, Haglund, and Sorg, 2002), and therefore may have resulted in movement away from the cranium during, or after, decomposition.

*17.5.3: Long Bones*

Most of the long bones found in the top area (figure 17.13). The right humerus was fragmented into two, the distal portion was found in layer four (blue arrow), with the proximal portion in the top layer. A fragment of right clavicle and the distal portion of the left fibula were recovered away from the other long bones in layer six.

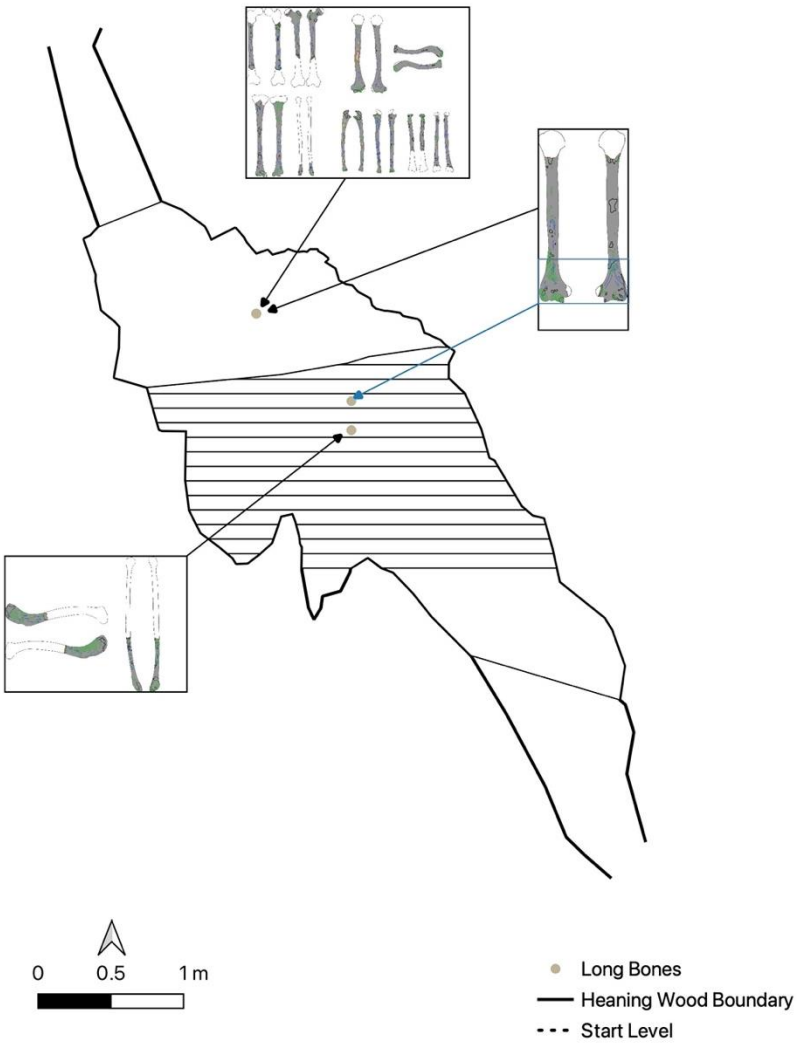


Figure 17.13: Distribution of long bone fragments assigned to Individual A.

While the location of the left fibula and right clavicle could indicate commingling, the dispersion of the right humerus shows that movement of associated fragments is occurring.

### *17.5.4: Flat/Irregular*

Fragments of flat/irregular elements were dispersed throughout the cave. The pelvis and sacrum were recovered in the top area (figure 17.14).

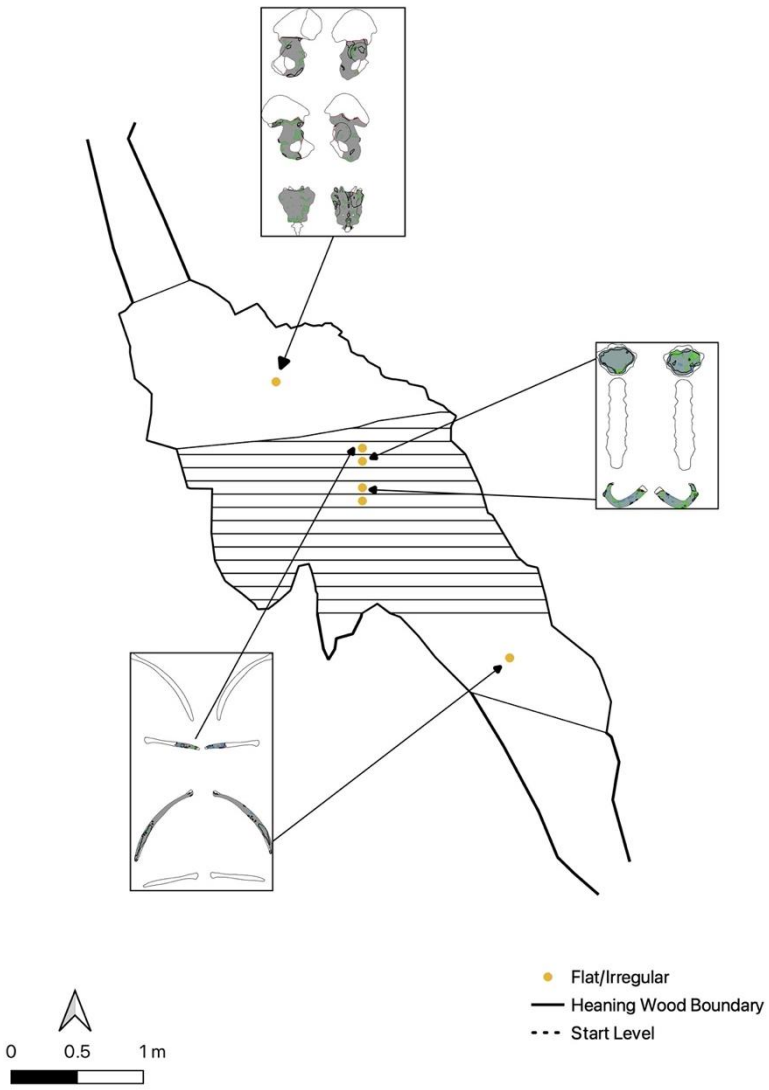


Figure 17.14: Distribution of long bone fragments assigned to Individual A.

Apart from the left fibula, all lower limbs and the pelvic girdle associated with Individual A were recovered in the top section of the cave. The eleventh rib was recovered from the West Fissure, significantly further away from the fragment of twelfth rib. This may be because of issues with individuation; however, it is possible that smaller fragments have ended up in the West Fissure because of run off from the main accumulation. The first rib was found in layer six, compared to the manubrium that was in layer four.

### *17.5.5: Hands, Feet & Patella*

Fragments of hands, feet and patella were the most dispersed element group for Individual A. It is particularly difficult to individuate elements such as phalanges and the level of dispersal could therefore be indicating that some of the fragments assigned to Individual A are incorrect. For this reason, figure 17.15 focuses on the location of the right talus in comparison to the associated left, both calcanei, and the right patella. There is high confidence in individuation of these fragments due to size, robusticity, and anatomical association. The right talus was recovered from layer eleven, showing a potential of up to 1.4 m of dispersal from its counterparts.

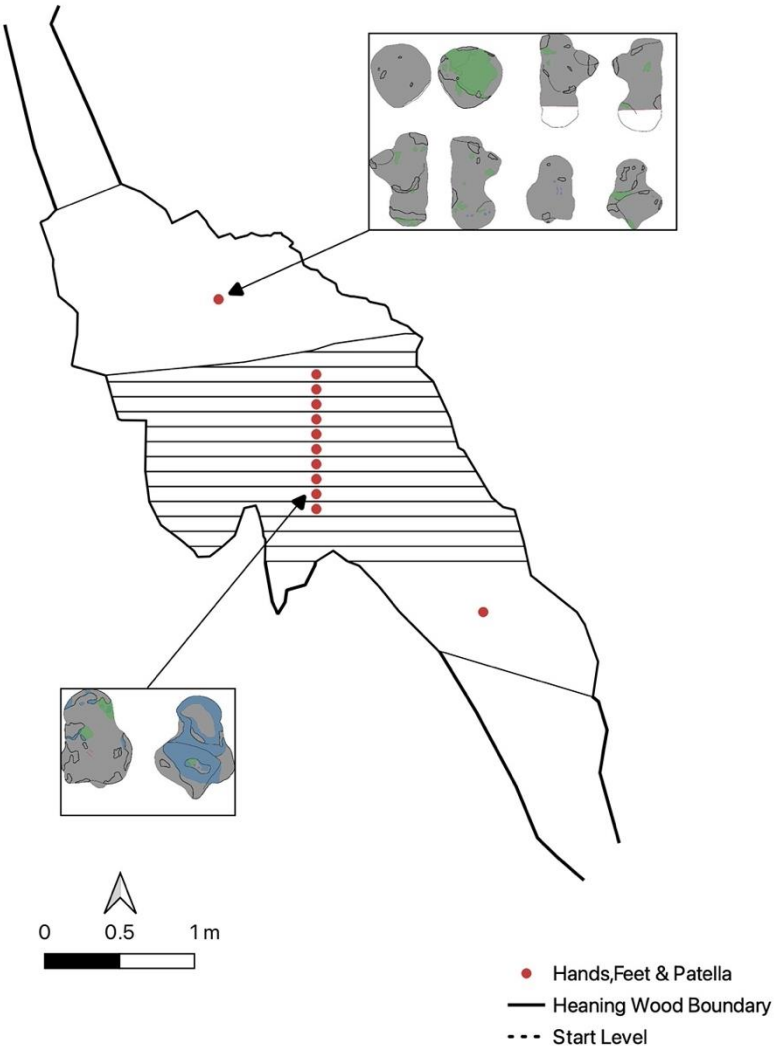


Figure 17.15: Distribution of hand, foot and patella fragments assigned to Individual A.

Detailed spatial analysis of fragments associated to Individual A show that most of the larger elements, such as the limb bones, cranium, pelvic girdle, patella, and tarsals, were all recovered higher up in the cave. This is consistent with a later deposition, with several anatomically associated bones remaining in the same area. There was some dispersal of fragments, particularly smaller fragments, hand and foot bones, and vertebrae. While individuation may skew data, there is high confidence in individuation of the larger fragments. The distal right humerus and right talus also show that movement has occurred.

## 17.6: Individual A (Early Bronze Age) - Taphonomic Distribution

### *17.6.1: Fracturing*

Four layers had specimens from Individual A with no fracturing, these were layers five, nine, twelve and the West Fissure. The fragments located in these layers were mainly hand and foot bones, in particular manual phalanges, and fracturing on fragments from other individuals was seen in these layers. It is therefore likely, that the absence of fracture is due to the element type, rather than an absence of mechanisms causing breakage.

Most incomplete cracking occurred on fragments recovered from the top area of the cave, this is consistent with the frequencies of specimens recovered from there. There does not seem to be any significant patterns relating to where in the cave fracturing was occurring.

### *17.6.2: Destruction*

Destruction occurred in all areas of the cave where fragments of Individual A were recovered. Damage classified as ‘exposure of trabecular bone’ occurred across all locations. ‘Cortical removal without exposure’ was absent from layers five, nine and twelve, again this may be due to the element type as seen in the distribution of fracturing rather than evidence of taphonomic agents. Crush damage was limited to the top area and layers seven, eight and ten. Due to the nature of the accumulation, it would be expected that crushing may be more prolific further down in the cave because of sediment build up, however most occurrences were in the top area and may be a result of infilling events from the entrance. There does not appear to be any significant area or bias to the spread of destruction and distribution reflects sediment abrasion and damage common in a cave environment (Fernández-Jalvo and Andrews, 2016).

### *17.6.3: Tufa Deposits*

Deposits occurred in all areas of the cave where fragments of Individual A were recovered. All deposits were classed as thin/flaked and no area seemed to have higher frequencies. During analysis of taphonomy at the body level there was a bias in deposits to right side. Right fragments were filtered and there was still no clear pattern. It is possible that some fragments were more exposed but due to the paucity of spatial information, analysis is limited.

### *17.6.4: Staining*

Staining occurred in all areas of the cave where fragments of Individual A were recovered, this was consistent even when stain type was broken down. The exception was 'light orange/brown', where only a single patch was found on a patella recovered from the top area of the cave. It is possible that this different stain type is related to the location, however, with only one data point it is not possible to draw any reliable conclusions.

### *17.6.5: Invertebrate Activity*

All invertebrate activity was found on bones in the top area of the cave for Individual A. Most invertebrate activity was seen on the long bones, which were mainly located in this area. When all invertebrate activity across the assemblage is examined, there were some modifications seen in layers nine onwards and most occur in the top layer (figure 17.16).

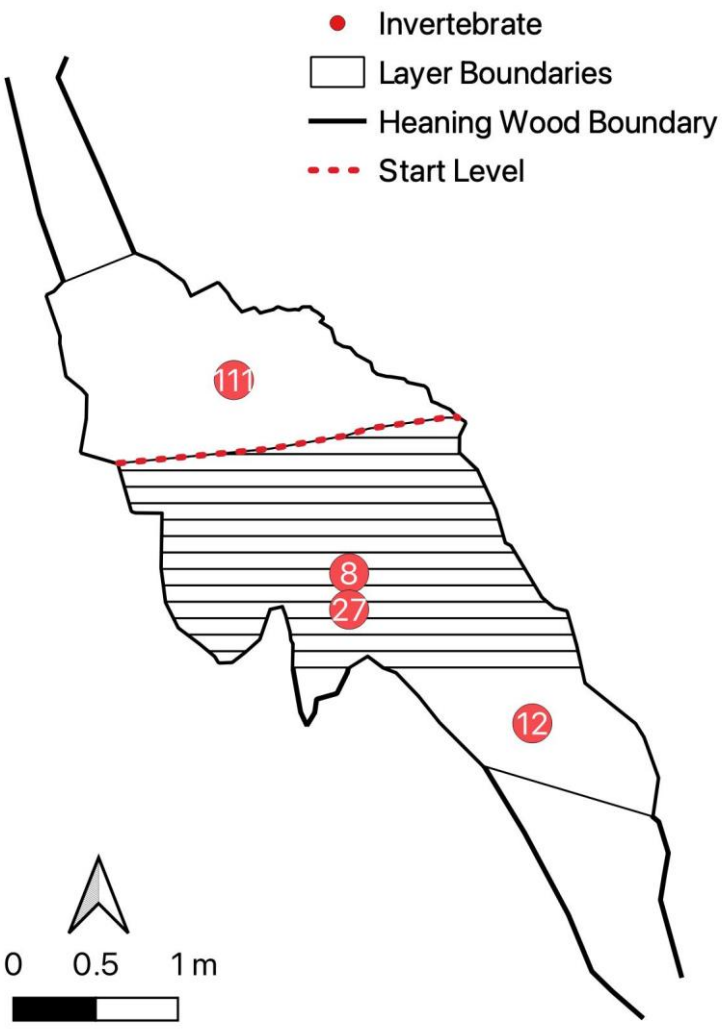


Figure 17.16: Frequency counts for invertebrate modifications across the whole assemblage

While there were a high number of fragments in the top area, there were more fragments located in the West Fissure when the assemblage is combined. This indicates that the distribution of invertebrate frequencies is not correlated to the number of fragments per layer. Terrell-Nield and Macdonald (1997) conducted experiments on the effect of decomposing animals on UK cave invertebrates. While they document invertebrate activity at all levels of the cave, including areas beyond light reach, the deeper parts of the cave saw insects playing "a lesser role" (Terrell-Nield and Macdonald, 1997, p. 62). The variability of temperature and air flow towards cave entrances impacted the type of invertebrates seen to colonise carcasses. Study into the invertebrates of Heaning Wood has not been conducted, however it is possible that the patterns seen here are due to varying species of invertebrates accessing remains in different layers. It is also possible that the fragments with invertebrate activity towards the

lower layers of the cave are a result of previously modified fragments moving within the cave system.

### *17.6.6: Root and Weathering*

Two occurrences of root embedding were found on fragments from Individual A, one on the sternum (HBC022), found in layer four and the other on the first metatarsal (HBC136) found in layer nine.

Weathering was found across the cave except for layers five, twelve and the West Fissure. The degree of weathering was minimal across the assemblage and consistent with changes expected from extended burial in a cave environment. There were six areas of delamination/peeling, across two fragments of bone, associated with Individual A. This was evidence of slightly more advanced weathering, and both fragments were recovered from the top area of the cave. This section will have seen more variability in temperature, humidity, and light levels, due to its proximity to the opening and may explain the increased signs of weathering.

The spread of taphonomy for Individual A offers limited insights into deposition. Poor spatial data is one of the main issues with analysing distribution of taphonomy, but movement of fragments across multiple layers also creates issues in understanding areas of taphonomic modifications.

## 17.7: Individual D (Early Bronze Age) - Distribution of Fragments

Fragments from Individual D were concentrated at the top of the cave, along with some distributed towards the middle layers (figure 17.17). The very lower levels (thirteen to fifteen) and West Fissure had no fragments associated with Individual D, which is consistent with burial period.

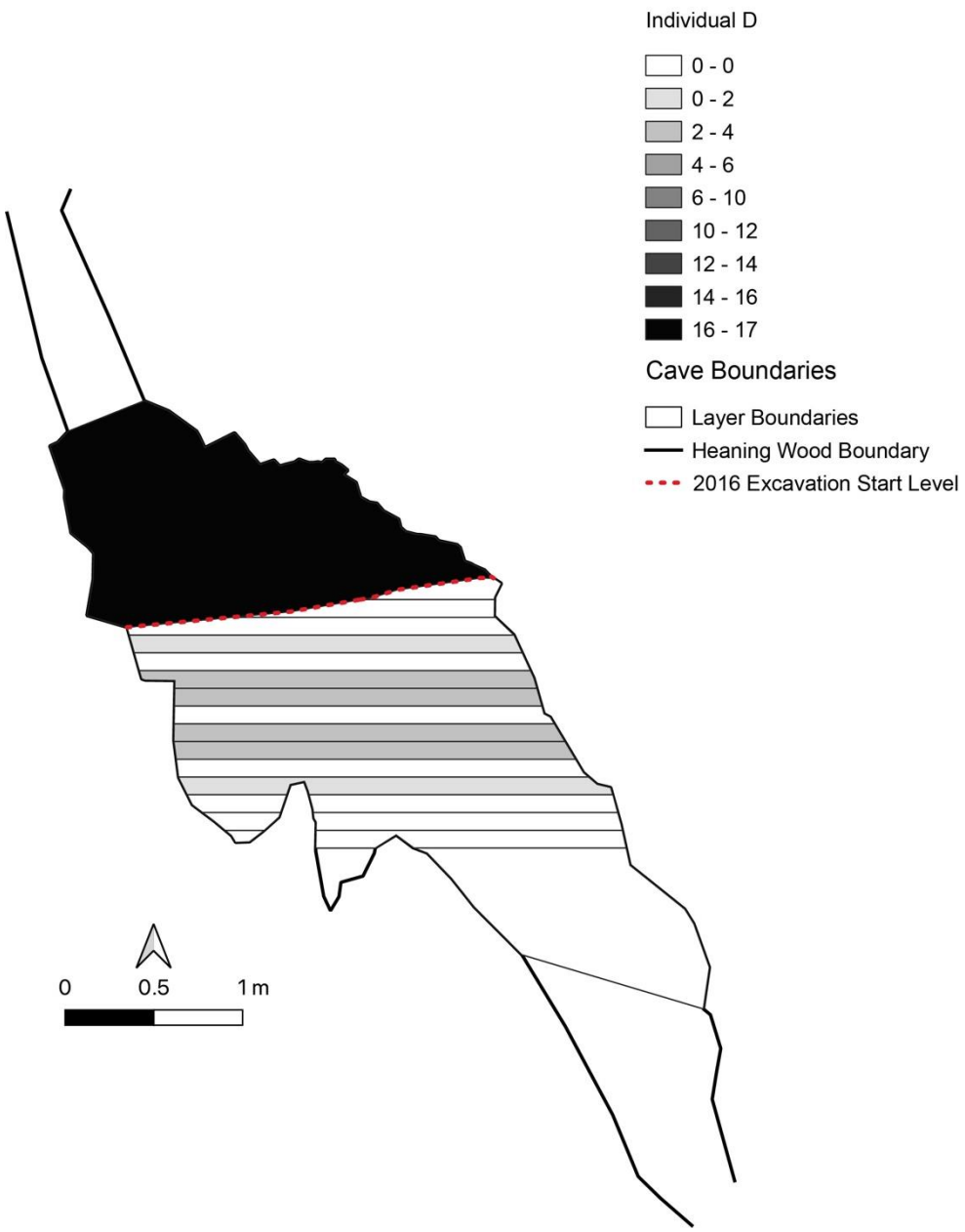


Figure 17.17: Distribution of fragments assigned to Individual D.

## 17.8: Individual D (Early Bronze Age) - Distribution of Elements

There was displacement of all element groups for Individual D, except for flat/irregular fragments (figure 17.18). There was limited dispersal for long bones, consistent with patterns of disarticulation described above.

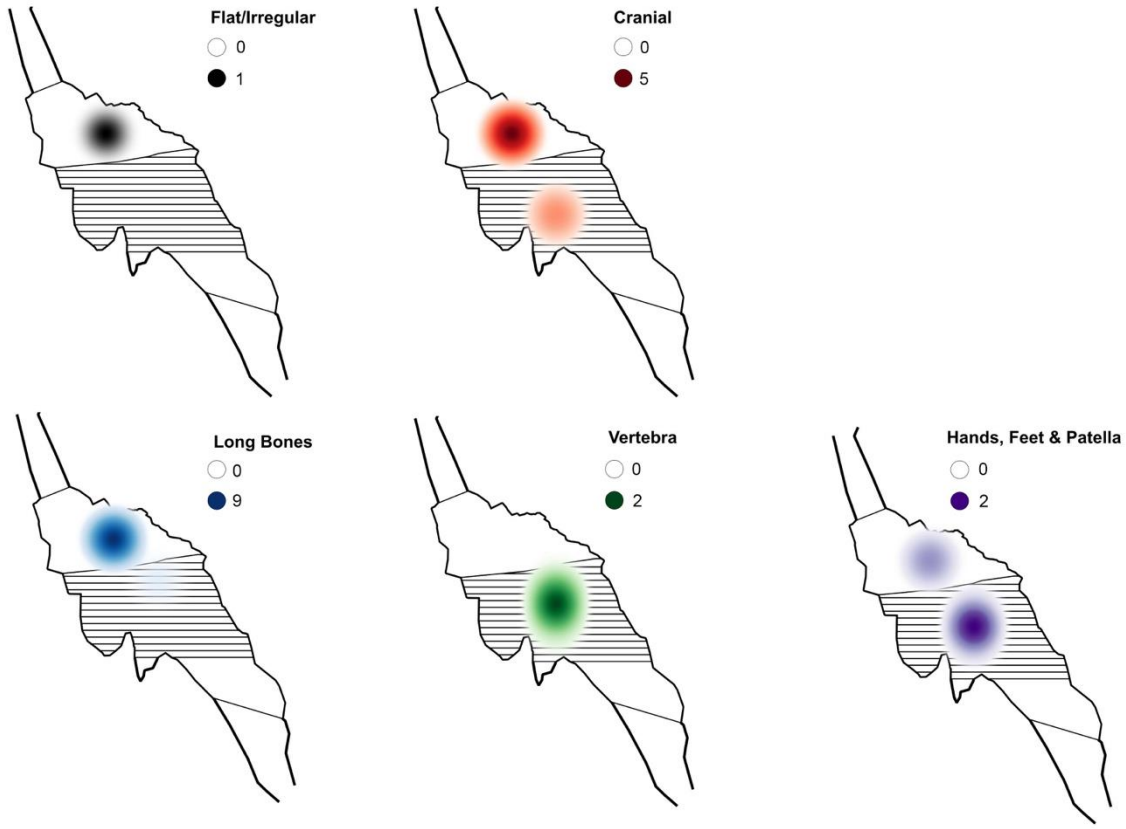


Figure 17.18: Concentration of fragments according to element group assigned to Individual D.

The element groups showed less spread than Individual A, with cranial, long bones and flat/irregular groups concentrated in the top layer. This is consistent with expectations of distributions according to burial period, with the body being introduced later in the accumulation process. The absence of movement for the flat/irregular bones is inconsistent with expected disarticulation patterns, however, only a single flat/irregular bone was associated to Individual D.

### *17.8.1: Crania*

All cranial fragments assigned to Individual D were excavated from the top area apart from the left zygomatic and frontal bone (figure 17.19). There was high confidence in the assignment of the frontal bone to Individual D due to ontological consistencies, and therefore the displacement is considered to be due to movement rather than individuation.


Figure 17.19: Distribution of cranial fragments assigned to Individual D.

Layer ten had a high number of fragments, consistent with the shape of the chamber and a talus formation. Since the spatial data is limited to layers, it is possible that the frontal bone ended up at a lower level in the assemblage due to run off from above.

### *17.8.2: Vertebra*

Seven vertebrae were assigned to Individual D, one thoracic was un-sequenced. The atlas and axis were five levels apart, with axis in layer four and the atlas in layer nine. These were both found away from the occipital fragments. The twelfth thoracic was found in the layer seven along with the first lumbar. It is possible these moved together, as they are anatomically associated, however care must be taken as they may not have been located together within

the same level. The un-sequenced thoracic and second lumbar vertebra were recovered from layer six and the fourth lumbar was the lowest, in layer ten (figure 17.20).

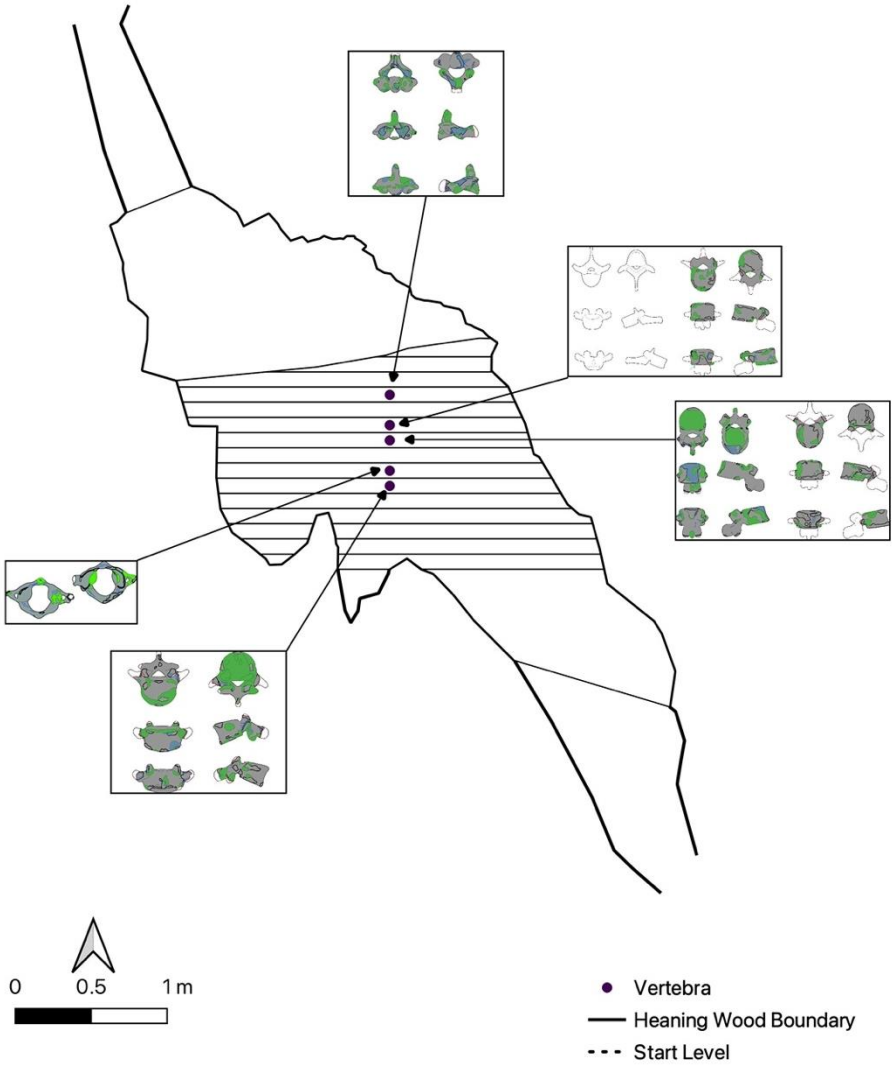


Figure 17.20: Distribution of vertebral fragments assigned to Individual D.

As with Individual A, vertebral fragments for Individual D were dispersed, although none were recovered from the lowest levels or West Fissure. This may be due to the difficulties in individuating vertebrae, however age and size indicators, along with reassociation meant these have been placed with high confidence.

*17.8.3: Long Bones*

All the long bones were found in the top area except for the distal portion of the left humerus, which was found in layer four (figure 17.21, blue arrow).

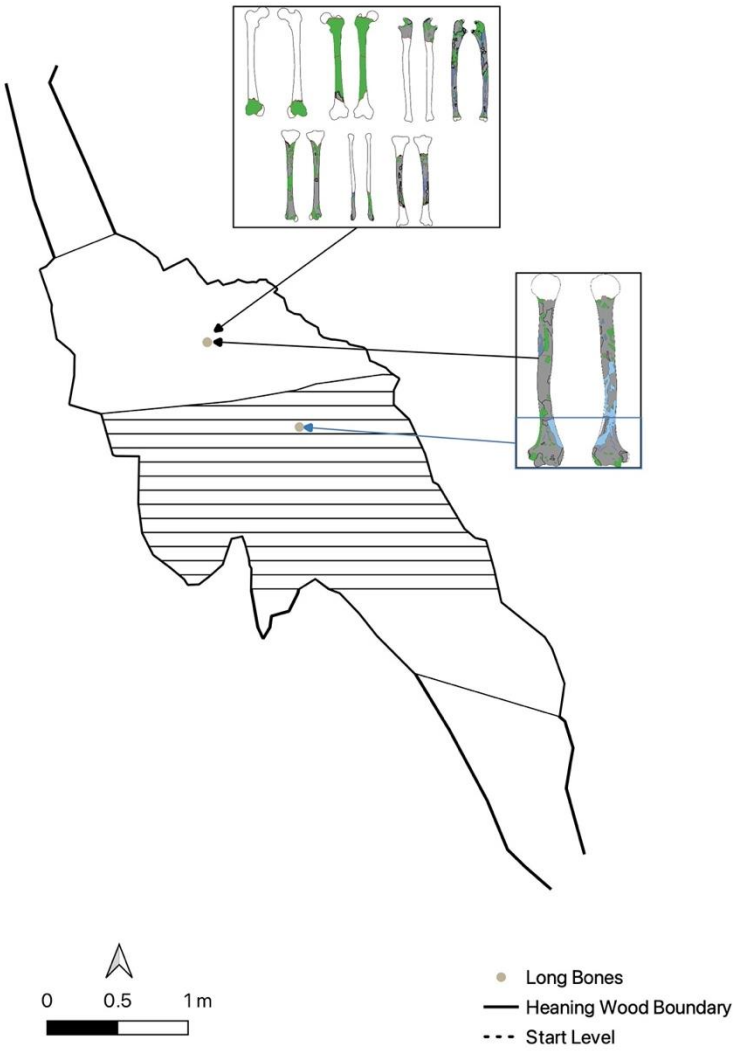


Figure 17.21: Distribution of long bone fragments assigned to Individual D.

The fracture and dispersal of the left humerus is the same as the right humerus seen in Individual A. The breakage point is a common fracture point in humeri (Galloway, 2014), demonstrating that similar mechanisms of destruction and movement acted on both individuals.

### *17.8.4: Flat/Irregular*

There was only one fragment classified as a flat/irregular element, the sacrum. This was in the top area of the cave, which is consistent with the later burial date of Individual D. It was excavated from the same area the long bones that have anatomical proximity.

### *17.8.5: Hands, Feet and Patella*

Fragments of hands, feet and patella were the most dispersed element group for Individual D. Again, this may be due to difficulties in individuation, and therefore evidence of commingling. The left calcaneus and right talus were found in the same layer as the lower limbs, which would be expected for a later deposition with little movement (figure 17.22).

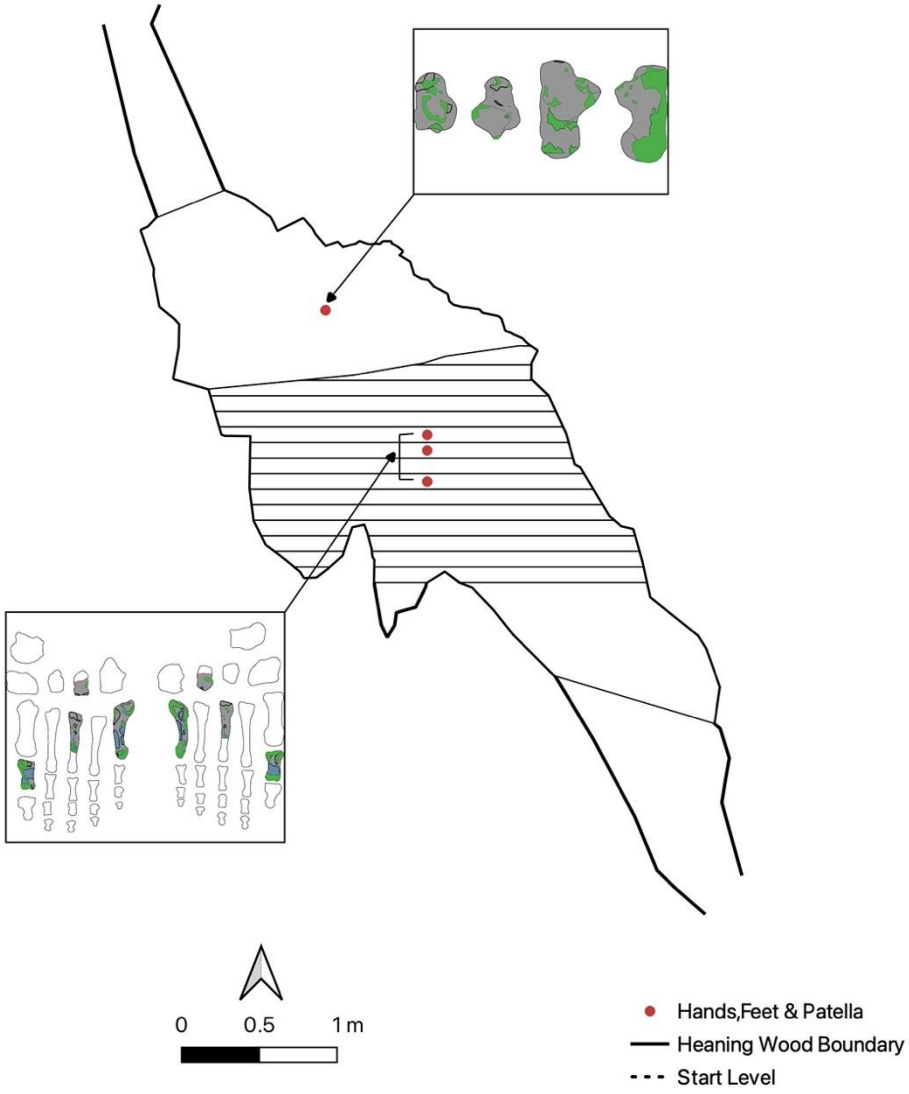


Figure 17.22: Distribution of hand, foot and patella fragments assigned to Individual D.

Detailed spatial analysis of fragments associated to Individual D show that most of the larger elements, such as the limb bones, cranium, sacrum, and tarsals, were all recovered higher up in the cave, consistent with later deposition. There was some dispersal of fragments, particularly smaller fragments, hand and foot bones, and vertebrae.

## 17.9: Individual D (Early Bronze Age) - Distribution of Taphonomy

### *17.9.1: Fracturing*

Fracturing occurred in all areas of the cave where fragments associated to Individual D were found. Incomplete cracking was limited to two layers, the top area and layer ten. Only 7.14% of fractures were incomplete for Individual D, which may be a result of the body being higher up, and therefore exposed to less pressure from overlaying sediment.

### *17.9.2: Destruction*

Destruction occurred in all areas of the cave where fragments of Individual D were recovered. There were higher frequencies of damage occurring in layers four, seven and nine, in comparison to the number of fragments from those layers. These layers contained several vertebrae, for which additional views were recorded in comparison to other elements. When the data was filtered to exclude the additional data, the frequency of damage was more reflective of the number of fragments in each layer (table 17.1).

Table 17.1: comparison of destruction counts per layer, including and excluding additional vertebral views.

| Layer | Total Fragments | N° Destruction | N° Destruction ex additional views |
|---|---|---|---|
| 0 | 17 | 92 | 92 |
| 4 | 2 | 90 | 54 |
| 6 | 3 | 44 | 14 |
| 7 | 3 | 102 | 35 |
| 9 | 3 | 48 | 23 |
| 10 | 4 | 105 | 64 |

Damage classified as ‘exposure of trabecular bone’ and ‘cortical removal without exposure’ occurred across all locations. Peri-mortem crush damage was limited to a single count in layer nine. This may have occurred lower down because of sediment build up, however there is

evidence for movement, and therefore difficult to infer mechanisms from the location of a single fragment. There does not appear to be any significant area or bias to the spread of destruction and distribution reflects sediment abrasion and damage common in a cave environment (Fernández-Jalvo and Andrews, 2016).

### *17.9.3: Tufa Deposits*

Deposits occurred in all areas of the cave where fragments of Individual D were recovered. All deposits were classed as 'thin/flaked', except for the 'thick/coated' patches to the distal humerus. Layer ten showed the highest frequencies of deposits, even when adjusted for additional vertebral sides (table 17.2).

Table 17.2: comparison of destruction counts per layer, including and excluding additional vertebral views.

| Layer | Total Fragments | N$^{o}$ Deposits | N$^{o}$ Deposits ex additional views |
|---|---|---|---|
| 0 | 17 | 19 | 19 |
| 4 | 2 | 49 | 27 |
| 6 | 3 | 12 | 4 |
| 7 | 3 | 25 | 6 |
| 9 | 3 | 12 | 10 |
| 10 | 4 | 50 | 35 |

There were fewer fragments in layers ten (n=4) and four (n=2), yet despite this they showed higher frequencies of deposits than the top area, where most fragments associated with Individual D were located. This suggests that calcite formation may have been more active in these layers and is supported by the thicker coating of tufa found on the distal humerus, which was located in Layer 4.

### *17.9.4: Staining*

Staining occurred in all areas of the cave where fragments of Individual D were recovered. This was consistent even when stain type was broken down. The top area had particularly high frequencies of staining in relation to the number of fragments; for example, dark spotted staining in this area was approximately ten times higher than in layer ten. This may be explained by the finding in section 16.2.6, where cranial elements had higher levels of staining consistent with manganese, since most of the cranial fragments were recovered from here. If

the increased staining was due to a concentration of the mineral it would be expected that all fragments recovered from that area, regardless of element group, would be similarly affected, which is not seen at the element level analysis.

### *17.9.5: Invertebrate Activity*

All invertebrate activity was found on bones in the top area of the cave for Individual D, adding support to invertebrate activity being more prolific towards the entrance of a cave. There was an absence of activity on fragments found further down.

### *17.9.6: Root and Weathering*

Three occurrences of root embedding were found on fragments from Individual D, one on the femur (HBC808) in the top area, and the others on lumber vertebrae (HBC071 and HBC166) found in layers six and ten. Root action would occur in areas where tree roots reach, however assessing the significance of root embedding is hindered by the limited samples and known movement of fragments.

Weathering was found throughout the cave, except for layer twelve. The degree of weathering was minimal across the assemblage and consistent with changes expected from extended burial in a cave environment (Pokines *et al.*, 2018). There were four areas of delamination/peeling, across the left humerus (HBC011 and HBC401). This was evidence of slightly more advanced weathering, with the distal portion recovered from layer four and the proximal portion from the top. As discussed for Individual A, there may be more variability in temperature, humidity, and light levels towards the top, increasing weathering. The patch of delamination spans the fracture margin, indicating that the increased exposure to the distal portion also occurred in the top area, prior to breakage and movement. The mandible also showed high frequencies of cracking in comparison to other fragments and was recovered from the top area of the cave.

The spread of taphonomy for Individual D offers limited insights into deposition. Areas of damage that cross fracture margins can offer insight into where some mechanisms were acting, however, movement of fragments across multiple layers provides challenges for the spatial understanding of taphonomy.

## 17.10: Individual B (Early Neolithic) - Distribution of Fragments

Fragments from Individual B were found throughout the cave with the highest concentrations occurring in layer ten and the West Fissure (figure 17.23).

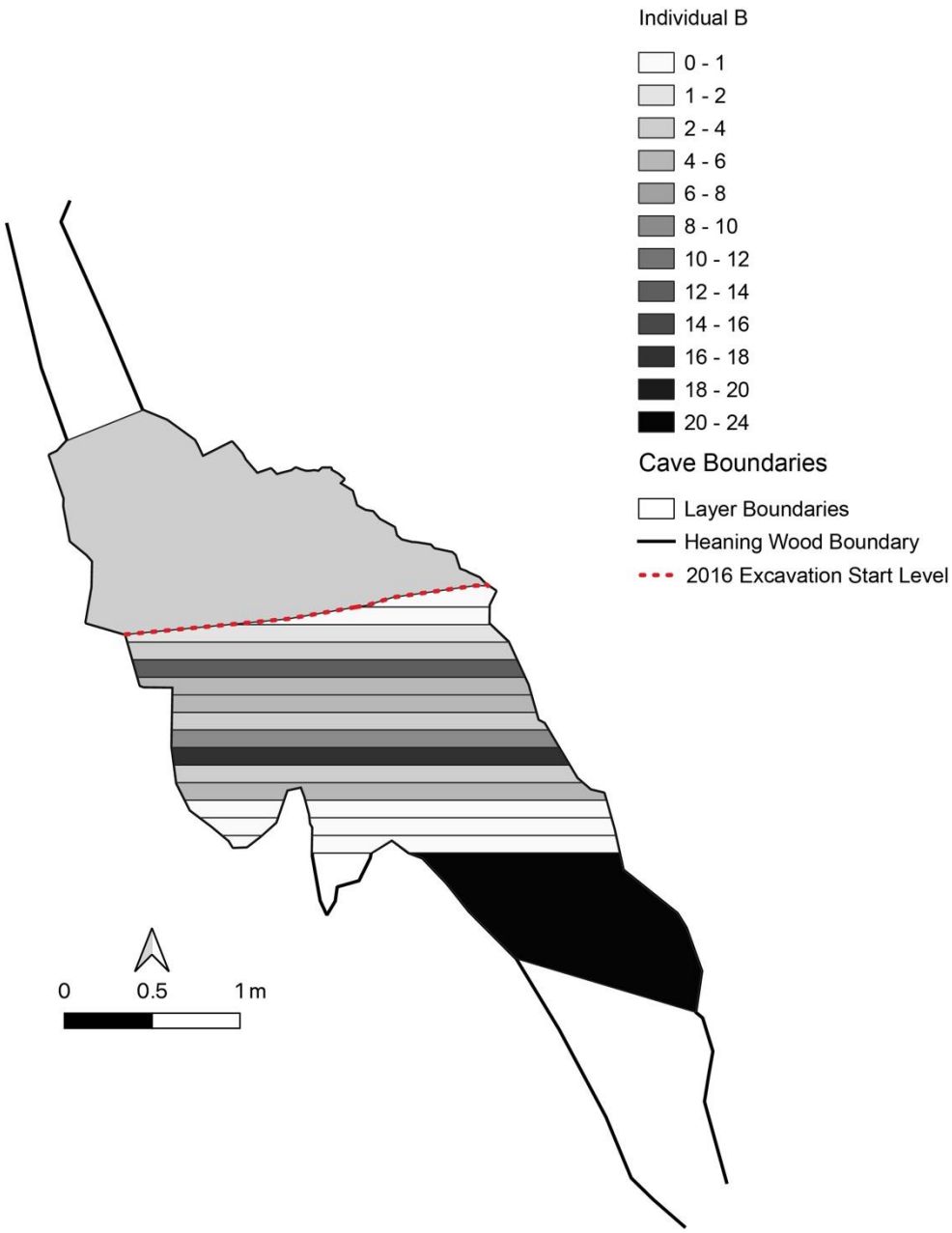


Figure 17.23: Distribution of fragments assigned to Individual B.

## 17.11: Individual B (Early Neolithic) - Distribution of Elements

The location of all element groups for Individual B is shown in figure 17.24.

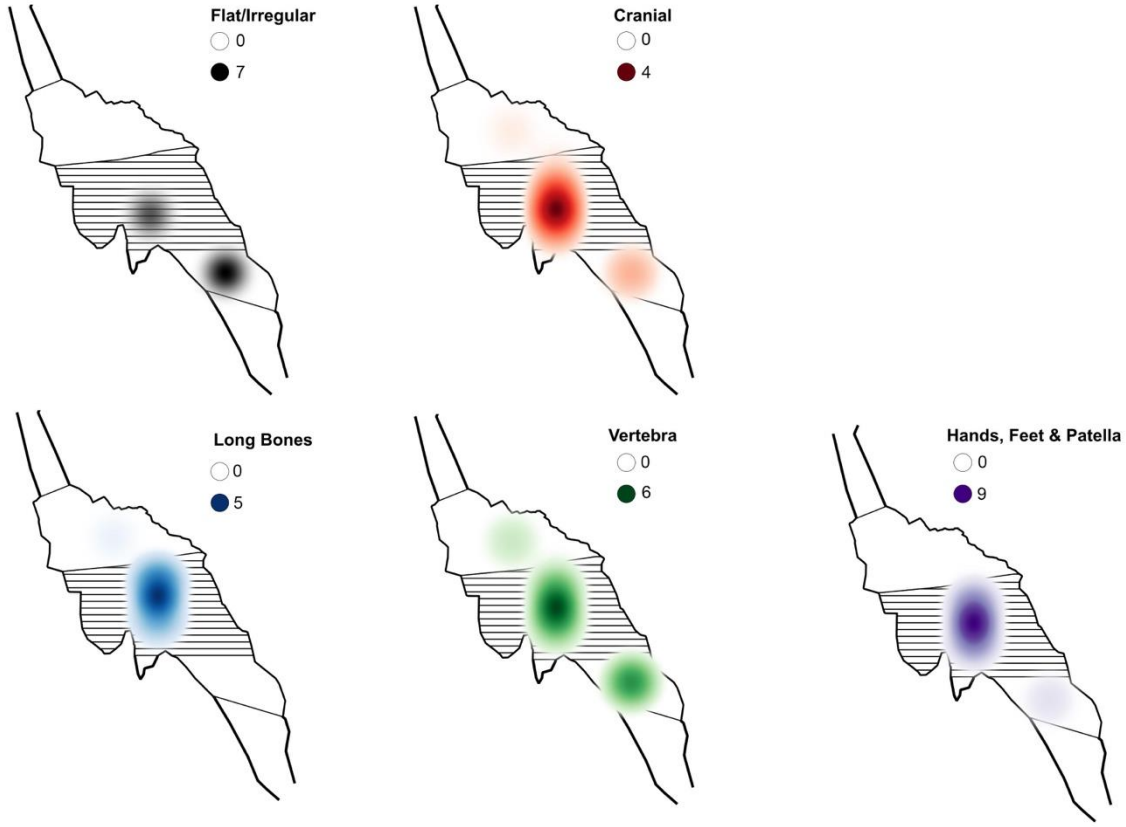


Figure 17.24: Concentration of fragments according to element group assigned to Individual B.

Fragments from all element groups were concentrated towards the middle section of the cave, around layer ten, except for flat/irregular fragments that were concentrated in the West Fissure.

### *17.11.1: Crania*

Cranial fragments were found dispersed throughout the cave (figure 17.25). Layers three, eight and the West Fissure contained teeth and small fragments of temporal and parietal bones. The occipital and the main portions of both parietals were found in layer twelve. These fragments refit, it is therefore possible that they moved together prior to breaking. The right portion of mandible was found in layer seven, with the corresponding left portion found in

layer nine. The maxilla was recovered from layer ten. The frontal bone was recovered from the top area during the earlier excavations.

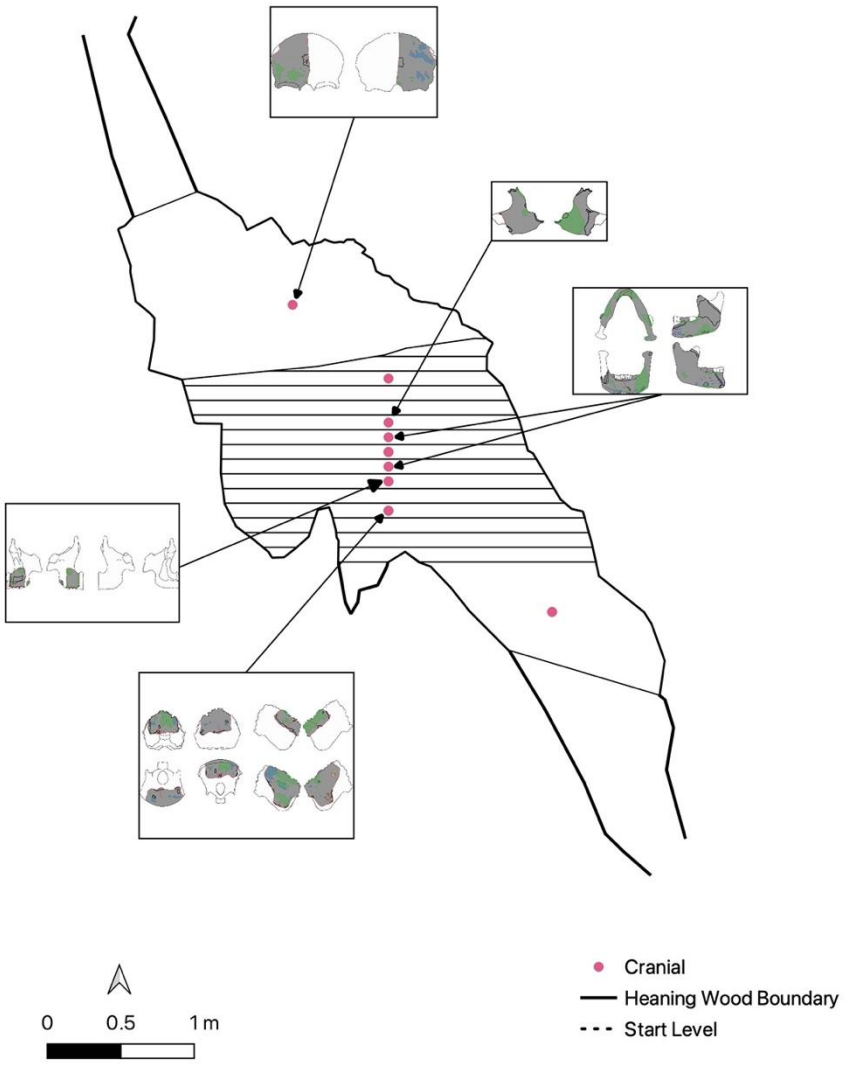


Figure 17.25: Distribution of cranial fragments assigned to Individual B.

The position of the occipital and parietals in layers below the mandible and maxilla may indicate rolling. The nature of the accumulation and geology of the cave would mean that upward movement is extremely unlikely. The frontal bone recovered from the top is apparently inconsistent with a later burial time, however spatial information in that section is limited. It is likely that the skull of Individual B was under fragments from Individuals A and D and once fragmented, rolled to lower layers of the cave.

*17.11.2: Vertebra*

Nineteen vertebrae were assigned to Individual B, with five un-sequenced. All the vertebrae were spread across multiple layers, with the West Fissure being the only area where sequential vertebrae were found (figure 17.26). The axis was six levels apart from the associated third cervical vertebra (blue bracket).

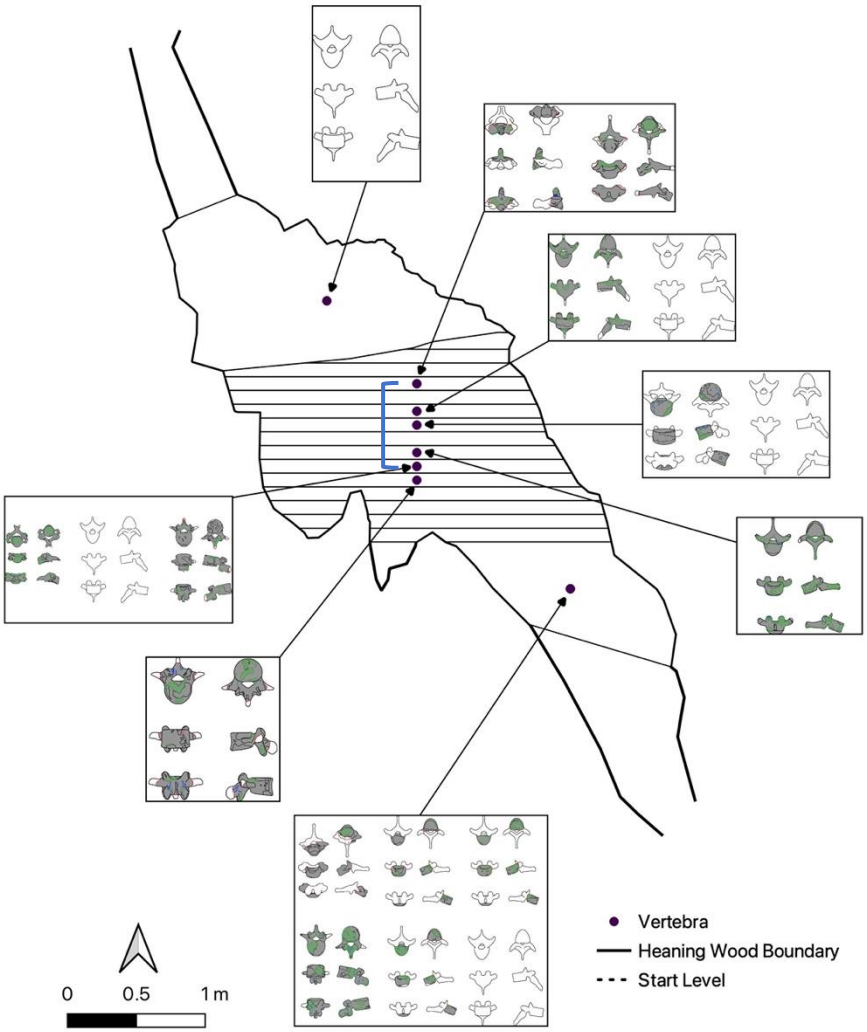


Figure 17.26: Distribution of vertebrae fragments assigned to Individual B.

The atlas was not recovered for Individual B and the axis was found in layer four, away from the occipital located in layer twelve. This further supports the possibility of the crania rolling from higher up in the chamber.

*17.11.3: Long Bones*

Long bones were distributed across the cave (figure 17.27). Layer five had the highest concentration with most of the lower limbs located here. The distal portion of the left femur was recovered from layer four (blue arrow). The distal portion of the right tibia (red box) was recovered from the top area of the cave during the earlier excavations. The distribution of all other fragments from layer four downwards suggests that this fragment is possibly not associated to Individual B. There was no direct refit and assignment was done through morphology, this will be discussed further in section 18.3.4, page 408.

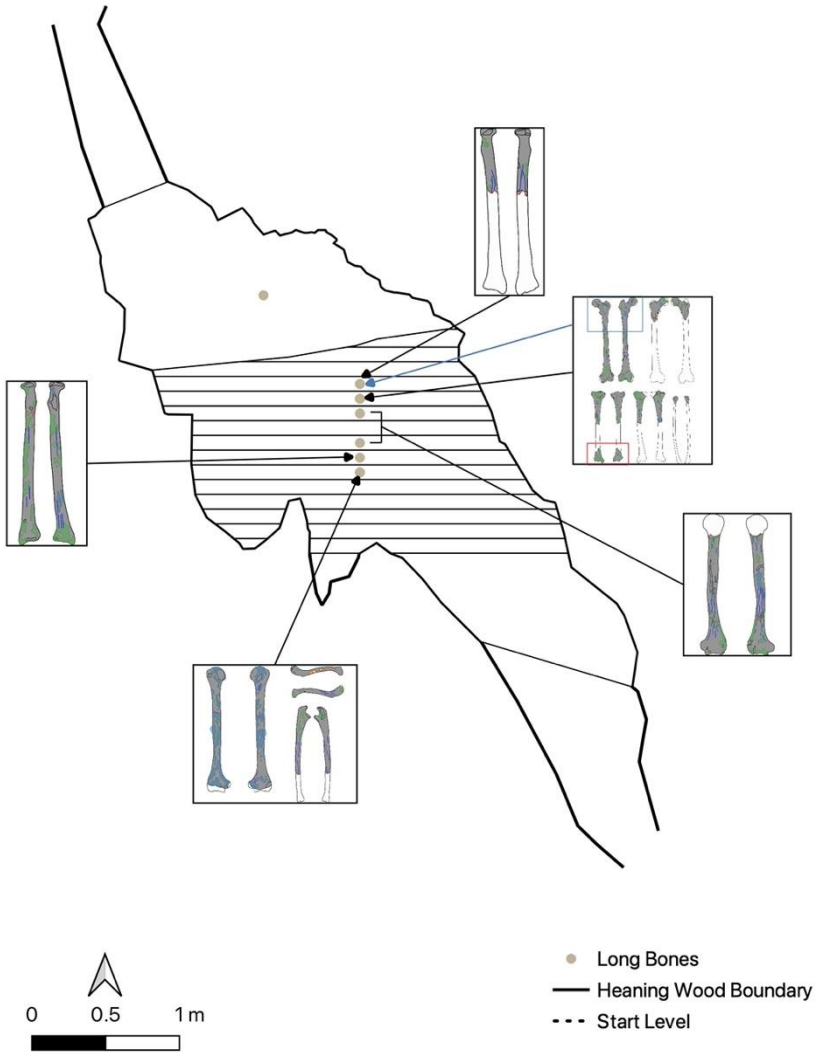


Figure 17.27: Distribution of vertebrae fragments assigned to Individual B

The upper limbs and right clavicle were recovered below the lower limbs. The left humerus was broken at the shaft, with the proximal shaft found in layer eight, below the distal portion. The right humerus was also broken however, both parts were recovered from the same layer. While this may suggest that no movement occurred, the fragments were not necessarily recovered together, as there is an absence of east-west spatial data.

### *17.11.4: Flat/Irregular*

Flat/irregular fragments were recovered from lower levels, starting from layer nine (figure 17.28). While the left scapula was recovered in layer nine, away from the left humerus (layers six and eight), the right scapula, right first rib and sternum were all recovered with anatomically associated elements such as the right humerus and clavicle in layer ten.


Figure 17.28: Distribution of flat/irregular fragments assigned to Individual B

The twelfth rib was recovered in the West Fissure with a few other rib fragments and a portion of left ilium. This is consistent with smaller fragments being dispersed across further distances, with some anatomically related elements retaining proximity.

### *17.11.5: Hands, Feet and Patella*

Fragments of hands, feet and patella were the most dispersed element group for Individual B. Again, this may be due to difficulties in individuation, and therefore evidence of commingling. Both calcanei were recovered from layer five, which is where all the lower limbs were found. The left talus was found in layer nine and both patellae were in layer ten (figure 17.29).

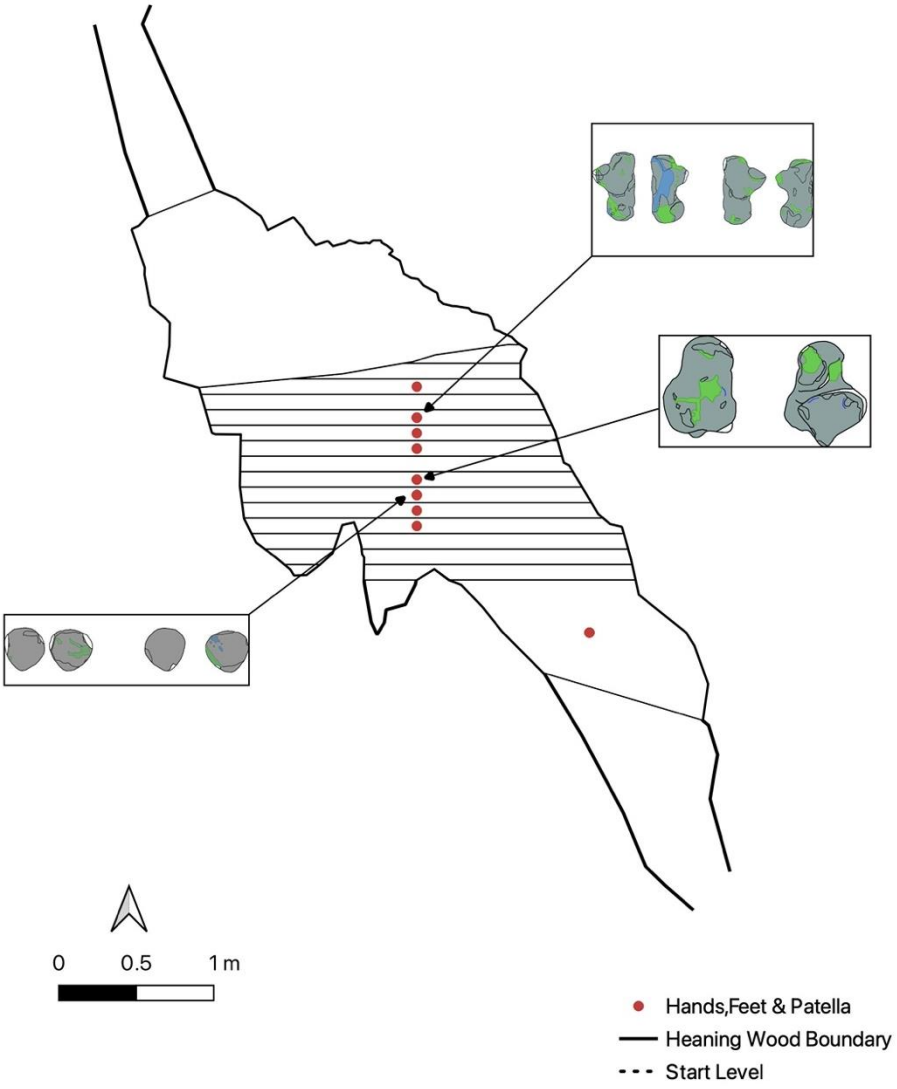


Figure 17.29: Distribution of hands, feet and patellae fragments assigned to Individual B

Detailed spatial analysis of fragments associated to Individual B show a concentration lower down in the cave compared to the Early Bronze Age individuals, consistent with an earlier deposition. There are some layers that contain associated bones, in layer five the lower limbs were recovered along with both calcanei and the right upper arm and thorax were found in layer ten. This suggests that certain sections of the body were moving together, however determining exact spatial relationships is difficult.

There was a paucity of fragments in the top area, except for the distal portion of the right tibia, a portion of frontal bone, and an un-sequenced vertebra, none of which have direct association with other fragments. The absence of any other fragments in this area, coupled with the timing of depositions could suggest that they do not belong to Individual B. As discussed in section 14.1, there is a high possibility of a fifth adult dating to the Early Bronze Age and these fragments may be associated to this body. If this is the case, then the concentration of lower limb bones across layers four and five may indicated the burial level for Individual B.

## 17.12: Individual B (Early Neolithic) - Distribution of Taphonomy

### *17.12.1: Fracturing*

Fracturing occurred in all areas of the cave where fragments associated to Individual B were found. Once additional surfaces recorded for vertebrae were removed, fractures per fragment found were highest in layers four, ten, eleven and twelve. Layer twelve had the highest frequencies of fractures with a ratio of 16:3 fractures to fragments, this may be a result of it being one of the lowest layers within the chamber, resulting in greater pressure from sediment build-up. Incomplete fractures showed a similar bias, with most (n=20) occurring in layer twelve.

### *17.12.2: Destruction*

Destruction occurred in all areas of the cave where fragments of Individual B were recovered, with both ‘exposure of trabecular bone’ and ‘cortical removal without exposure’ occurring in all levels. There was a single count of peri-mortem crush damage located in the West Fissure, the significance of this is unclear due to limited data.

When the data was filtered to exclude additional vertebral views, layer four had the highest frequencies of damage per fragment. There were only four fragments in this layer, two long bones and two vertebrae, high pattens of destruction may be indicative of an infilling event when the accumulation was at this level. This adds further support to the possibility that layer four was the point of deposition for Individual B.

### *17.12.3: Tufa Deposits*

Deposits occurred in all areas of the cave where fragments of Individual B were recovered, except for layer six. All deposits were classed as thin/flaked except for a fragment of right humerus (HBC158) where thick/coated and embedded deposits were recorded. All the thicker deposits occurred in layer ten, which was the layer that also had the highest frequencies of deposits per fragment count (35:4). This is consistent with Individual D which also showed highest frequencies in layer ten, indicating that calcite formation may have been more prolific in this section of the cave.

### *17.12.4: Staining*

Staining occurred in all areas of the cave where fragments of Individual B were recovered, except for layer three. Layer three had two fragments, on was a tooth which was excluded from taphonomic analysis and the other a left lunate (HBC002). When staining type was broken down, brown/orange staining was only present in layers four, nine and ten, with all other staining found across the cave.

Layers ten and twelve had the highest frequencies of staining per fragment count, which is in contradiction to Individual D where concentrations of staining were at the top. It is likely that staining was occurring throughout the cave system, in particular soil staining, however the movement of fragments is possibly obscuring patterns.

### *17.12.5: Invertebrate Activity*

All invertebrate activity was found on fragments in layers nine, ten, twelve and the West Fissure. The highest frequency of invertebrate damage was found in layer twelve. This is in contradiction to Individuals A and D, and concentrations may be the result of the distribution of Individuals, rather than areas of increased invertebrate activity. It is possible that

movement is skewing the results, however there were no counts of invertebrate activity for Individual B above layer nine, despite fragments being located there.

### *17.12.6: Root and Weathering*

Two occurrences of root embedding were found on fragments from Individual B, one on a fragment of right scapula (HBC165), found in layer ten, and the other on a fragment of sacrum (HBC226) found in layer twelve. Assessing the significance of root embedding is hindered by the limited samples and known movement of fragments.

Weathering was found from layer four down, fragments associated to Individual B in the top layer and layer three showed no cracking consistent with weathering. The degree of weathering was minimal across the assemblage, consistent with changes expected from extended burial in a cave environment, and concentrations reflected distributions of fragments.

Taphonomic processes are occurring throughout the cave, and it is difficult to know whether this is a result of fragments moving or that agents of taphonomy are present in all areas. Analysis shows some areas where mechanisms may be operating, such as calcite deposits in layer ten and increased destruction in layer four. The layers described for Heaning Wood are not contexts and should not considered to be fixed surfaces, however, concentrations of some fragments may suggest that layers four and five were an approximate deposition area for Individual B. Overall, the modifications occurring on Individual B are consistent with an extended burial within a cave environment, with episodes of sediment movement and infilling.

## 17.13: Individual C (Early Neolithic) - Distribution of Fragments

Fragments from Individual C were found throughout the cave with the highest concentrations occurring in layers five and eight (figure 17.30).


Figure 17.30: Distribution of fragments assigned to Individual C.

## 17.14: Individual C (Early Neolithic) - Distribution of Elements

There was displacement of all element groups for Individual C (figure 17.31).

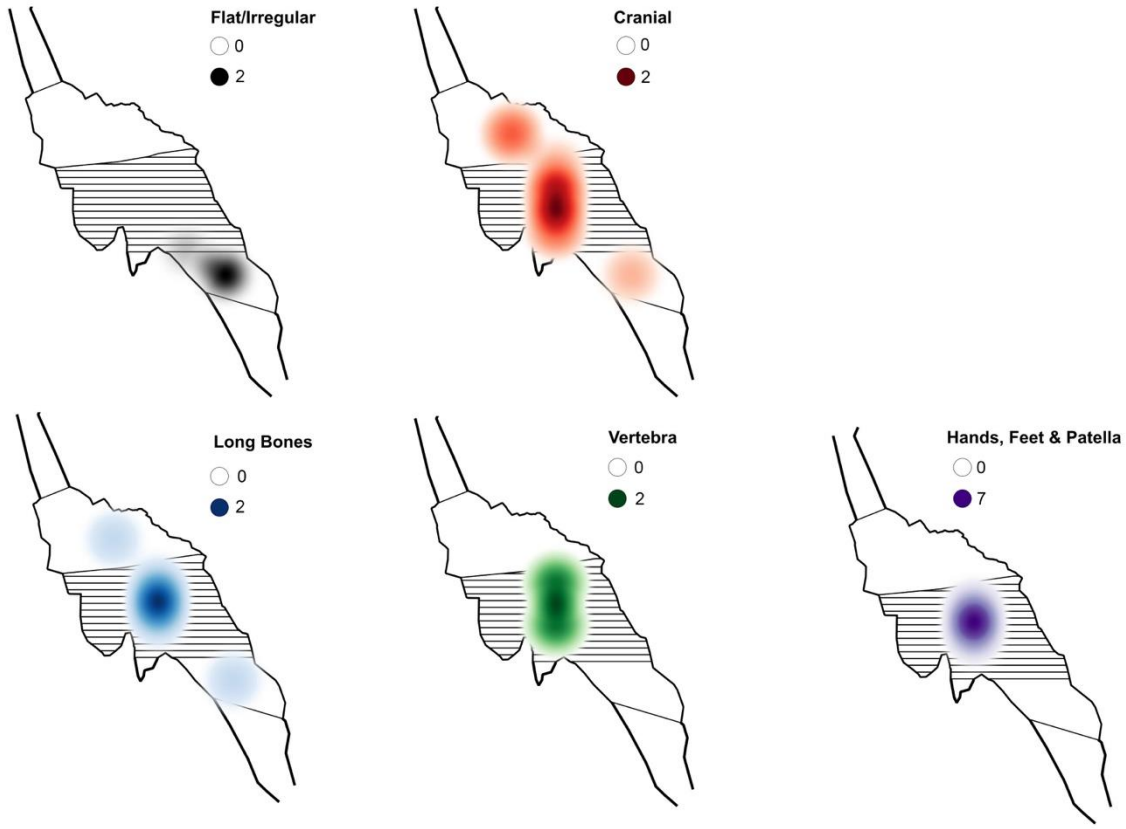


Figure 17.31: Concentration of fragments according to element group assigned to Individual C.

Fragments for all element groups were concentrated towards the middle section of the cave, cranial and long bone fragments were the most dispersed.

### *17.14.1: Crania*

Cranial fragments were found dispersed throughout the cave (figure 17.32), with an intact cranium recovered during the earlier excavations, and therefore likely to be from the top area of the cave. The left temporal and zygomatic were found in lower levels of the cave in levels eight and twelve. The mandible was fragmented and recovered from three different levels. The right portion was in the top area, with the left portion spread across layers six and eight.

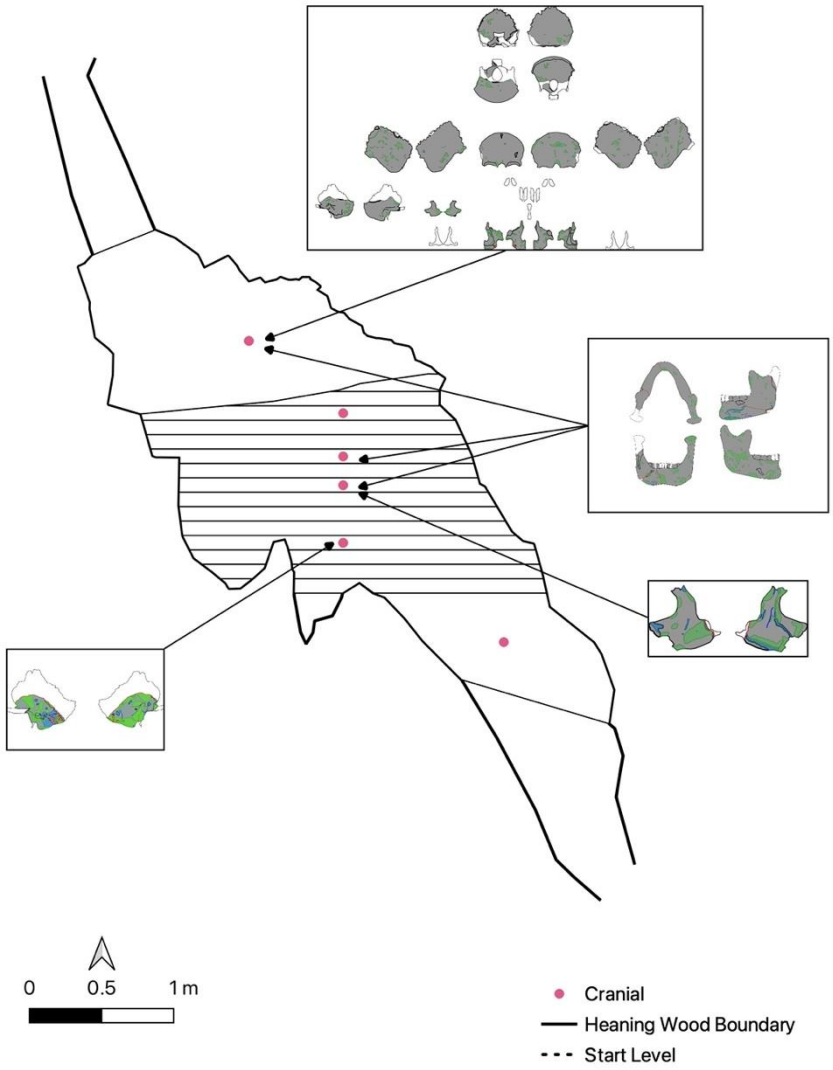


Figure 17.32: Distribution of cranial fragments assigned to Individual C.

The mandibular fragments refit, demonstrating the degree of movement occurring within Heaning Wood. It would be expected that Individual C, with an earlier deposition date than Individuals A and D, would have been recovered from lower down in the cave. The spatial information for the fragments excavated in 1958 is more limited than the later material, and the cranium could possibly have been located toward the bottom of this section. This indicates that there was a build-up of material between the deposition of Individuals B and C.

### *17.14.2: Vertebra*

Only four fragments of vertebrae were recovered. These were found in layers four and ten. An image has been omitted due to the limited distribution. The axis was recovered in layer ten,

around 1.25 m lower than the associated cranium. The dispersal of vertebrae is consistent with other adults in the assemblage, showing that there was increased movement of smaller fragments.

### *17.14.3: Long Bones*

Long bones were distributed across the cave (figure 17.33), unlike Individual B there were no areas where fragments were particularly concentrated.

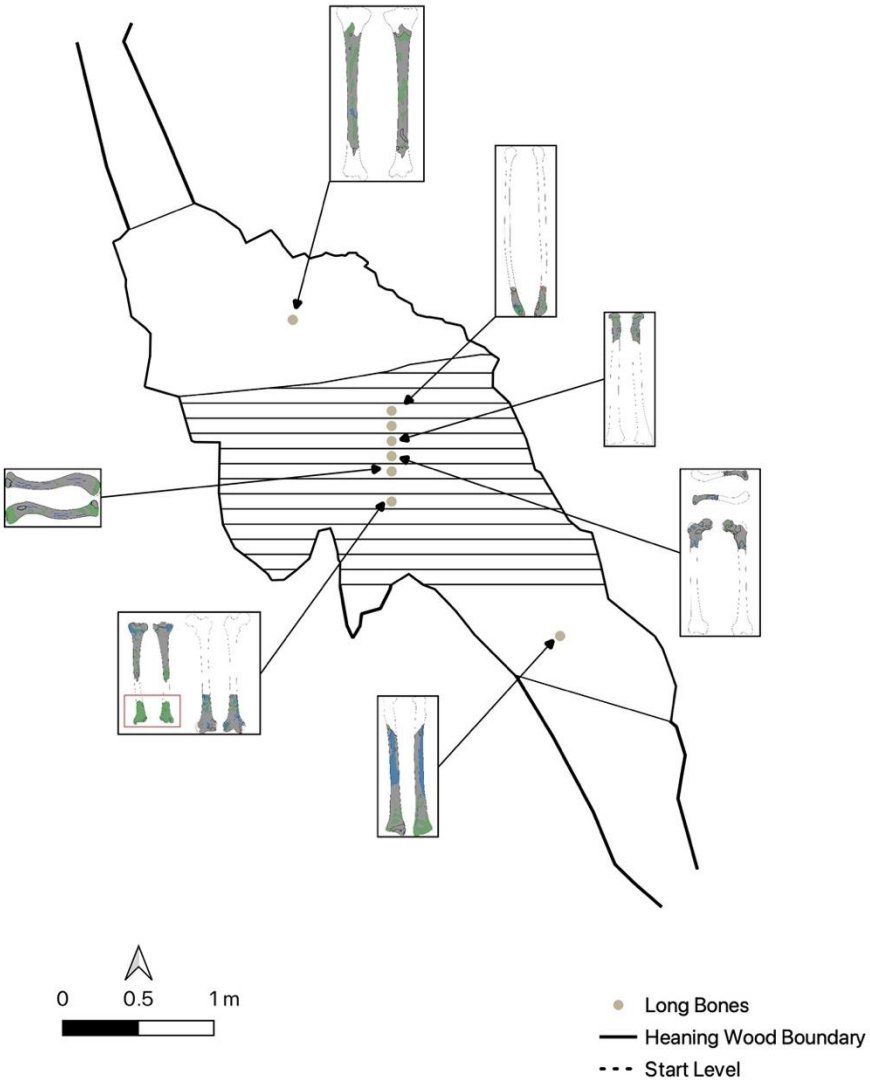


Figure 17.33: Distribution of long bones fragments assigned to Individual C.

The distal portion of the left tibia was recovered in the top area, away from the proximal end (highlighted in the red box).

### *17.14.4: Flat/Irregular*

Three fragments of flat/irregular bones were assigned to Individual C. The sacrum, a fragment of pelvis, and the right first rib. The sacrum was recovered in the bottom layer of the chamber, layer fifteen, with the remaining fragments located in the West Fissure. A picture has been omitted due to the limited dispersal. The sacrum was lowest fragment for Individual C and was recovered away from any elements with anatomical proximity, such as the femurs.

### *17.14.5: Hands, Feet and Patella*

Fragments of hands, feet and patella were one of the least dispersed element groups for Individual C, in direct contrast to dispersal patterns for other individuals in the assemblage. The left talus, cuboid, and medial cuneiform, along with the left patella, were all recovered from layer five (figure 17.34). Both calcanei were in the same layer as the right femur, layer seven.

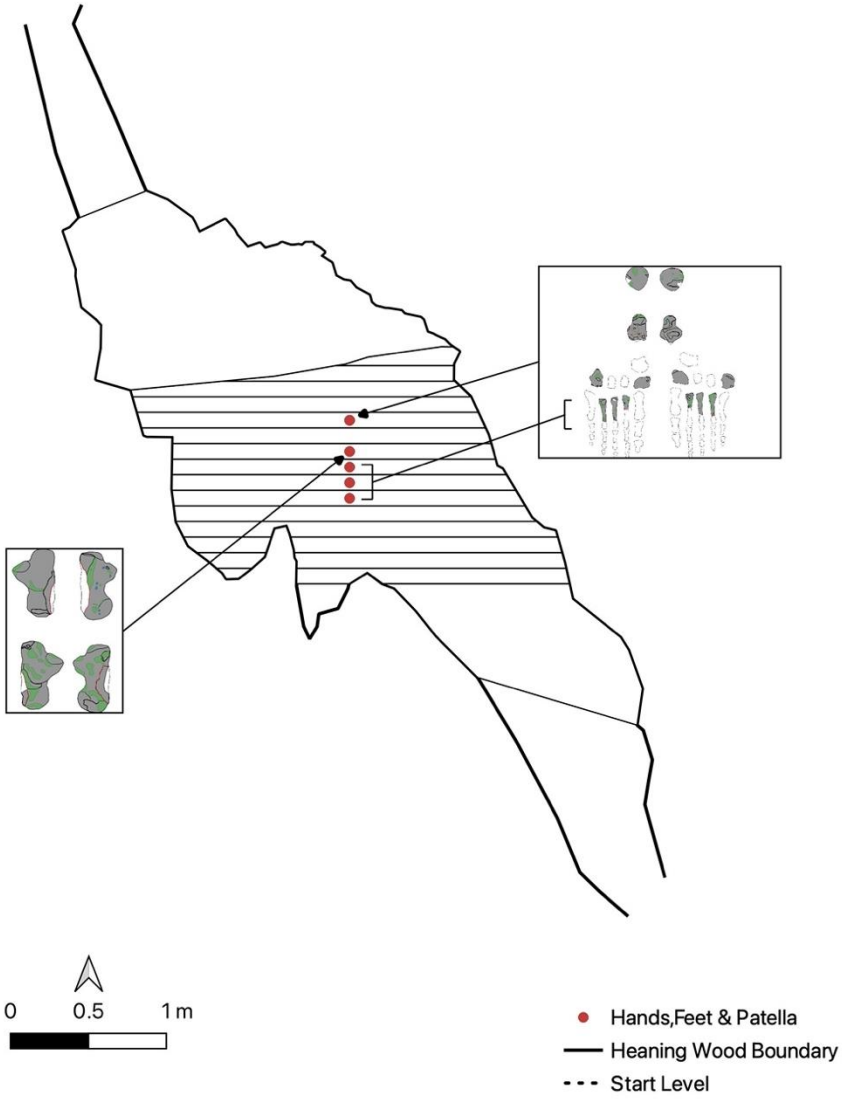


Figure 17.34: Distribution of hand, foot and patella fragments assigned to Individual C.

There is no clear evidence to show anatomically associated bones are moving together within the cave. The left foot may have moved or remained together in layer five but for all other element groups there is dispersion of fragments across the whole cave. There were few fragments located in the West Fissure, suggesting that run off from the talus was reduced for Individual C.

## 17.15: Individual C (Early Neolithic) - Distribution of Taphonomy

### *17.15.1: Fracturing*

Fracturing occurred in all areas of the cave where fragments associated to Individual C were found, except for layer fifteen. Once additional surfaces recorded for vertebrae were removed, fractures per fragment found were highest in the top layer with a ratio of 45:4 fractures to fragments. Incomplete fractures showed a similar bias with most (n=9) occurring at the top. This is the opposite pattern to Individual B where fracturing appeared to be more focused towards the lower levels of the cave.

### *17.15.2: Destruction*

Destruction occurred in all areas of the cave where fragments of Individual C were recovered, with 'exposure of trabecular bone' occurring in all levels. There were three counts of peri-mortem crush damage located at the top, and in layers five and seven. It is possible that where peri-mortem crushing is occurring indicates areas of rockfall within the cave, but movement of fragments may be obscuring significant areas.

When the data was filtered to exclude additional vertebral views, layer fifteen had the highest frequencies of damage per fragment, with a ratio of 13:1. Layer fifteen contained the sacrum (HBC255) and its irregular shape may make it more vulnerable to damage. Increased movement within the cave system may also be causing additional damage.

### *17.15.3: Tufa Deposits*

Deposits occurred in all areas of the cave where fragments of Individual C were recovered, except for layer five, and all deposits were classed as thin/flaked. Layer ten had the highest frequencies of deposits per fragment count (49:3). This is consistent with both Individuals D and B which also showed highest frequencies in layer ten, adding further weight to the inference that calcite formation was more prolific in this section of the cave.

### *17.15.4: Staining*

Staining occurred in all areas of the cave where fragments of Individual C were recovered. When staining type was broken down, brown/orange staining was only present in layer five

down, whereas soil and manganese staining were found across all layers. The top layer had the highest frequencies of staining to fragments, with a ratio of 86:1. This was where the intact skull had been found, and the staining patterns generally consisted of multiple small patches that had accumulated in fossae and grooves, whereas staining on other elements in other areas of the were larger patches, resulting in lower frequencies (figure 17.35).

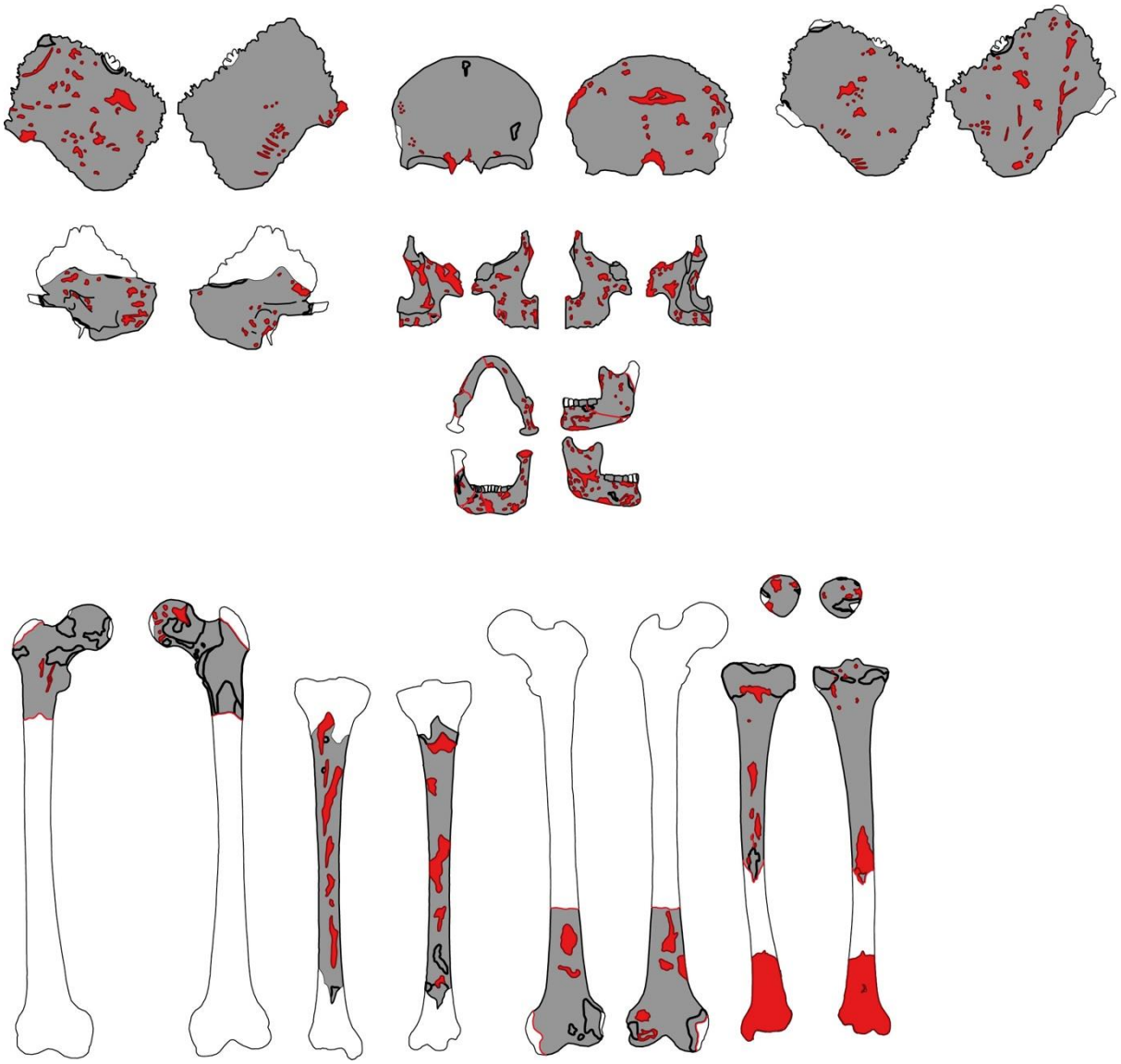

Figure 17.35: Distribution of staining across the skull versus long bones for Individual C.

Area analysis could be employed to gain further information around staining extent and will be discussed in section 18.4.1. The distribution of staining based on frequencies currently indicates it was occurring in all areas of the cave.

### *17.15.5: Invertebrate Activity*

Invertebrate activity was limited to layer twelve, with all activity occurring on the left temporal bone. The rest of the cranium was recovered in the top area, and it is likely that the temporal bone moved, there was a complete absence of invertebrate activity on the rest of the skull, suggesting that modifications occurred after movement, in the lower layer. This is in contradiction to other Individuals where invertebrate activity was predominately happening in the top area.

### *17.15.6: Root and Weathering*

Three occurrences of root embedding were found on fragments from Individual C, one on a fragment of right radius (HBC082) in layer six, one on a fragment of left tibia (HBC160) layer ten, and one on a fragment of sacrum (HBC255) in layer fifteen. Assessing the significance of root embedding is hindered by the limited samples and known movement of fragments. When all individuals are combined there are fragments with root embedding or etching across eight layers, with no apparent location significance (figure 17.36).

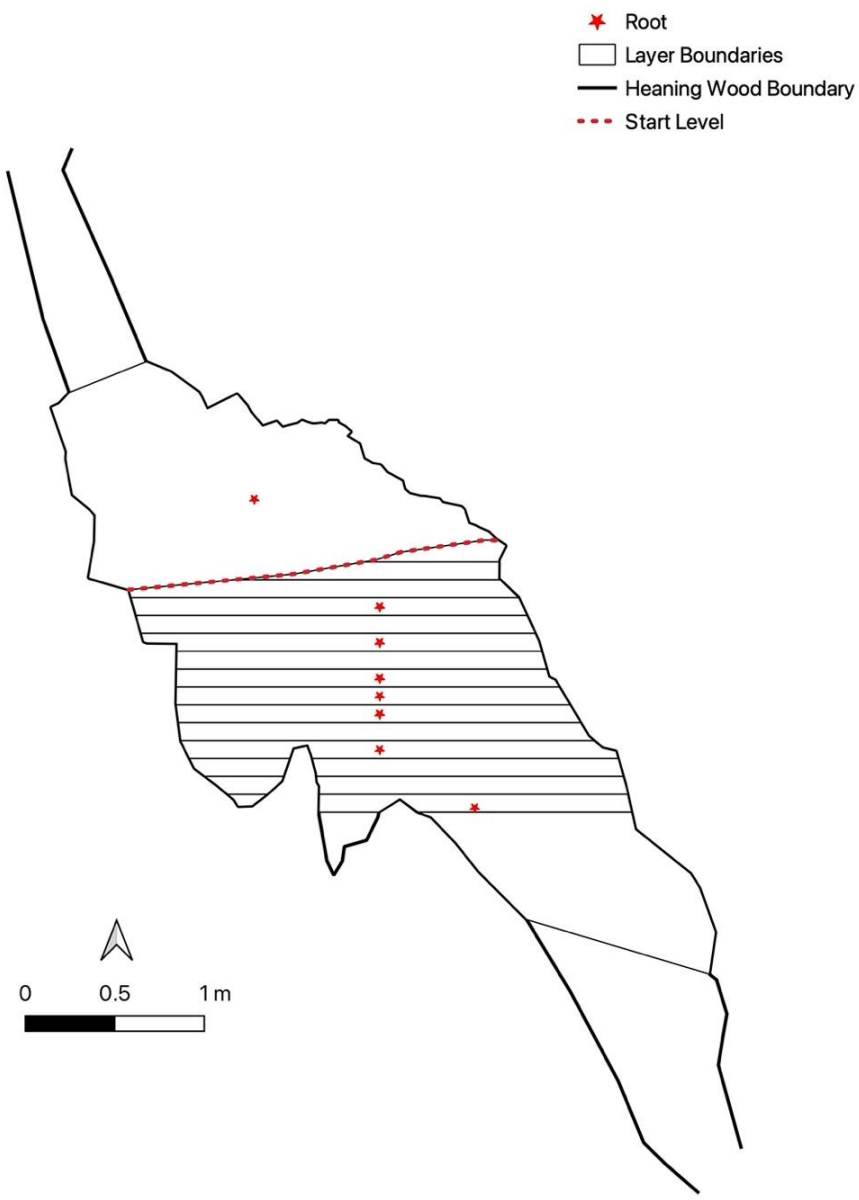


Figure 17.36: Distribution of root embedding for all individuals.

It is expected that root embedding occurs when fragments are at depths where tree roots reach, however movement of fragments may be obscuring patterns.

Weathering was found from layer four down. Fragments associated to Individual C in the top layer showed no cracking consistent with weathering. The fragments from the top layer were all recovered during the 1958 excavations, except for a distal portion of left tibia (HBC800), which was recovered in 1974. The 1958 fragments have been preserved with a clear substance, potentially masking some modifications such as cracking. The degree of

weathering for Individual C was minimal and concentrations reflected distributions of fragments.

Taphonomic processes on Individual C were occurring throughout the cave. Tufa deposits add further weight to layer ten being an area of calcite activity otherwise there are no clear indication of locations of geological processes. Modifications are consistent with movement and primary burial within a cave environment with no indications of exposure to processes outside of Heaning Wood.

## 17.16: Individual E (Early Neolithic) - Distribution of Fragments

There were eleven fragments assigned to Individual E, two clavicles and the rest were cranial. Layer eleven had the highest concentration of fragments and all other layers that contained fragments of Individual E only contained a single specimen (figure 17.37).


Figure 17.37: Distribution of fragments assigned to Individual E.

## 17.17: Individual E (Early Neolithic) - Distribution of Elements

Due to the limited number of fragments, figure 17.38 shows the distribution of all fragments and discusses them together.

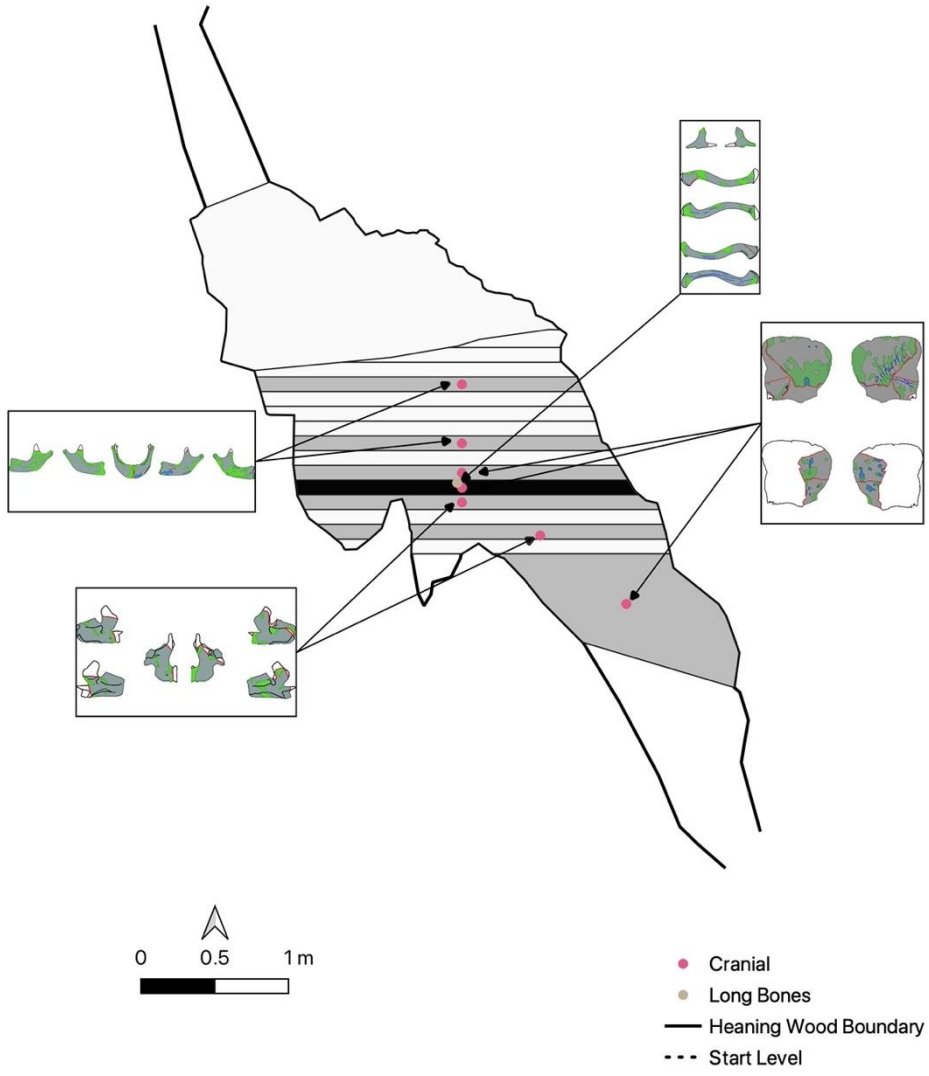


Figure 17.38: Distribution of cranial and long bone fragments assigned to Individual E.

The highest fragment was a portion of left mandible that was recovered in layer four. The corresponding right side was recovered four layers down in layer eight. The maxilla was similarly dispersed, with the right portion in layer twelve and the left in layer fourteen. There was a single fragment of right parietal in the West Fissure, but the remaining fragments were all located within the cave chamber. Due to the limited number of fragments recovered it is not possible to say whether this was due to reduced run off. The presence of associated fragments across multiple layers shows that movement was occurring.

## 17.18: Individual E (Early Neolithic) - Distribution of Taphonomy

Due to the limited number of fragments associated to Individual E, the distribution of taphonomy will be discussed together.

Layer eleven had the highest concentration of fragments (n=5). Other layers where Individual E was recovered only contained single fragments. This makes assessing the significance of where taphonomy is occurring difficult. Layers with single fragments are more likely to have fewer modifications, and an absence of taphonomy in a layer would not necessarily indicate an absence of the acting agent.

There are three exceptions to the expected pattern. The West Fissure and layer four had higher counts of destruction per fragment count (n=16 and n=15, respectively) compared to layer eleven (n=12). This follows a similar pattern to Individual B, adding evidence to the possibility that layer four was subjected to a period of infilling that caused increased destruction of fragments.

Deposits were highest in the West Fissure (n=18), whereas layer eleven only had eight counts across the five fragments. Layer ten, an area that for other individuals indicated potentially higher incidences of calcite formation, only had five patches of tufa on a single fragment.

Root etching was seen on two fragments from layers four and eight. There was an absence of root activity elsewhere, including the layer with multiple fragments.

While there were some differences to expected patterns based on fragment frequencies for destruction, deposits, and root action, the significance of these is difficult to assess due to the limited number for fragments. For Individual E the taphonomy is similar to the rest of the assemblage and is consistent with a primary and extended burial in a cave environment. There was no indication of burial position and limited information can be gained from spatial analysis of taphonomy.

## 17.19: Individual H (Early Neolithic) – All Distributions

Due to the limited fragments spatial analysis of Individual H is limited. Both fragments of maxilla were recovered from the West Fissure, providing little to no information about movement or taphonomy. There was an absence of weathering, root embedding and invertebrate activity to both fragments. All other taphonomy was similar to the rest of the assemblage and is consistent with primary and extended burial in a cave environment. There was no evidence of exposure to mechanisms other than those occurring in Heaning Wood.

## 17.20: Individual F (Mesolithic) - Distribution of Fragments

Due to the limited fragments spatial analysis was restricted of Individual F is limited. All fragments were cranial and were located from layer twelve down (figure 17.39).

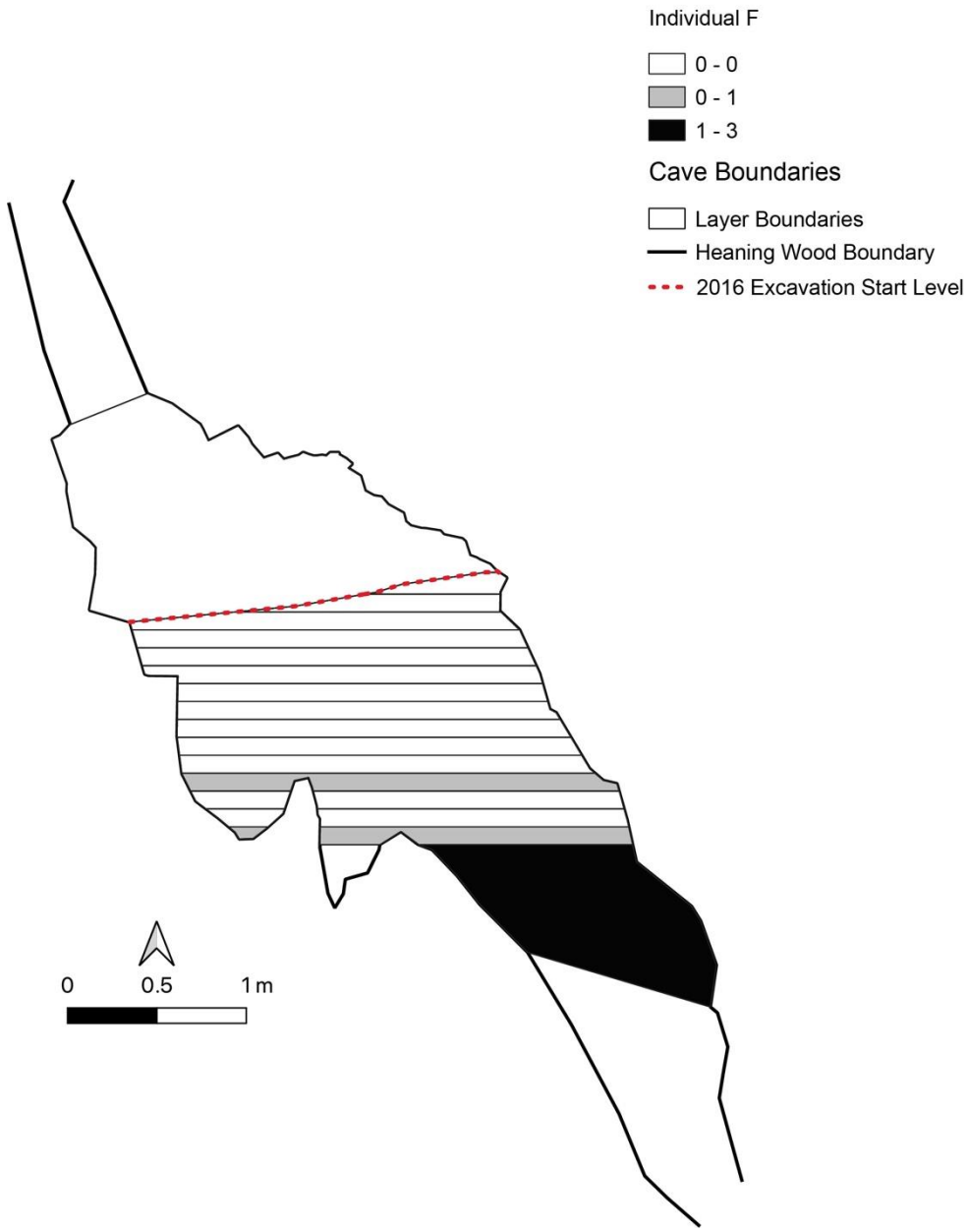


Figure 17.39: Distribution of fragments assigned to Individual F.

The distribution of fragments in the lower areas of the cave is consistent with the much earlier deposition period of Individual F. The three fragments located in the West Fissure were a molar tooth crown, a portion of maxilla and the left zygomatic. There were no direct associations to indicate movement patterns.

## 17.21: Individual F (Mesolithic) - Distribution of Taphonomy

There was an absence of root embedding, tufa deposits, and invertebrate activity to all fragments. There was a single area of mosaic cracking consistent with weathering processes to the left mandible, recovered from layer twelve. All other taphonomy was similar to the rest of the assemblage and was consistent with primary and extended burial in a cave environment. There was no evidence of exposure to mechanisms other than those occurring in Heaning Wood.

## 17.22: Individual G (Undated) - Distribution of Fragments

Fragments associated to Individual were distributed throughout the cave (figure 17.40).


Figure 17.40: Distribution of fragments assigned to Individual G.

## 17.22: Individual G (Undated) - Distribution of Elements

There were eleven fragments assigned to Individual G, most of which were cranial. Due to the limited number of fragments, figure 17.41 shows the distribution of all fragments and discusses them together.

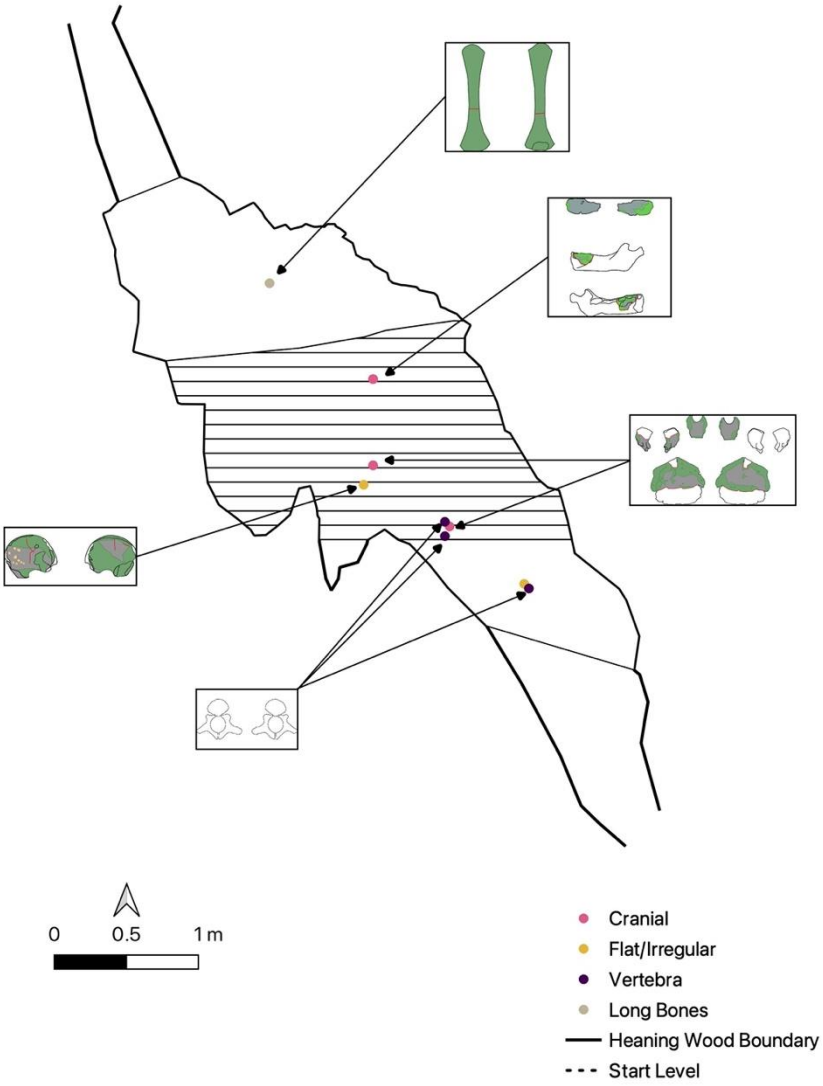


Figure 17.41: Distribution of all fragments assigned to Individual G.

In neonates the occipital bone comprises of four parts, the *pars basilaris*, two *pars lateralii,* and the *pars squama* (Scheuer and Black, 2000). Three of these parts were recovered for Individual G and were found split between layer ten and layer 14. There were three neural arches from unfused vertebrae, these were all recovered in the lowest levels and the West Fissure. A left humerus was found in the collection excavated in 1958 and is suspected to have been recovered from higher up in the cave.

There is no clear indication of burial period for Individual G based on fragment distribution. The presence of fragments higher up in the cave may indicate Early Bronze Age, however, other individuals with earlier dates have fragments originating in upper layers of the cave.

## 17.23: Individual G (Undated) - Distribution of Taphonomy

Due to the limited number of fragments associated to Individual G, the distribution of taphonomy will be discussed together. Interpretations of taphonomic spread are more difficult due to limited samples.

There were no signs of weathering or root action to any fragments from Individual G. Taphonomic modifications were absent from the fragments recovered from layer fifteen and the West Fissure, however these were fragments omitted from GIS recording due to issues with placement. This is, therefore, not an indication of an absence of taphonomic agents acting in these layers.

Layer ten had the highest frequencies of staining to fragments, with a ratio of 14:1, whereas layer twelve had higher counts of deposits. Invertebrate activity was limited to the right ilium (HBC235) recovered from layer twelve. This was also the fragment that had the only area of peri-mortem crush damage.

The taphonomy is similar to the rest of the assemblage and is consistent with a primary and extended burial in a cave environment. There was no indication of burial position and limited information can be gained from spatial analysis of taphonomy, however, there was no evidence of prior exposure outside of Heaning Wood.

## 17.24: Spatial Summary of Heaning Wood

Analysis of skeletal element distribution according to burial period follow expected patterns, with early burials concentrated further down the cave than later ones. Movement of fragments was seen for all individuals, except for Individual H, where only two fragments were recovered in the same layer. It is possible that apparent movement may be due to potential individuation errors, however there were some refitting fragments that were dispersed across multiple layers as evidence of movement.

There were no clear indications of burial position from fragment locations for most Individuals. There is some evidence to suggest that layers four and five may have been an approximate point of deposition for Individual B. Due to the nature of the spatial data the layers are not contexts, and therefore not considered to be a fixed surface, rather these should be thought of as areas of accumulation. This is also suggested based on the likelihood of fragments in the top area belonging to the unidentified fifth adult. This will be discussed further in section 18.3.4, pages 408-409, however, care should be taken interpreting this as fact. Similar movement patterns were seen for all the individuals, showing that the same mechanisms were acting on bodies.

The spread of taphonomy also offered insight into processes, however interpretations should be treated with care due to the evidence of extensive movement within the cave. Layer four showed increased levels of destruction for several of the individuals, indicating a possible period of sediment infilling when the talus was at this level.

The analysis of element and taphonomy distribution for the infants and neonate was limited due to so few fragments being recovered, and the absence of east-west coordinates for fragments from all individuals makes spatial interpretations difficult. Analysis shows that taphonomic agents were acting throughout the cave, was homogenous across the assemblage, and despite distinct burial periods, was consistent with primary depositions in a cave environment. There was no evidence of exposure to mechanisms other than those occurring in Heaning Wood.

# CHAPTER 18: DISCUSSION

## 18.1: Readdressing the research question

This research originally aimed to look at whether Geographical Information Systems (GIS), and more specifically the open-source software QGIS, could be used to refine and improve assessments of the minimum number of individuals (MNI) for fragmented assemblages. Early proposals suggested looking at case studies with previous publications, in this case Cave Ha 3 and other Yorkshire assemblages examined by Leach (2006a, 2006b), before applying the method to the Heaning Wood assemblage that was highly fragmented, commingled, and under-researched.

During the initial development of the method, photographs of fragments were georeferenced to templates to establish whether it was possible to record fragment outlines as vector polygons and digitally assess overlap (section 7.6.1). This failed due to the degree of biological variation in humans. Whole elements were not aligning to generic templates without distortion and distorting images would result in errors of overlap. Earlier work had managed to utilise GIS for MNI estimations by digitally re-drawing fragments, rather than using photographs (Parkinson, Plummer and Bose, 2014; Garcia Moreno *et al.*, 2015; Parkinson, 2018; Stavrova *et al.*, 2019; Parkinson *et al.*, 2022). The degree of manipulation needed to get fragments to sit on templates led to the method being rejected and it was felt that GIS would not offer a more precise MNI calculation than the zonation method (Knüsel and Outram, 2004).

The second part of the proposal was to extend the use of GIS from MNI estimations to look at taphonomy. The research question pivoted to make this the primary focus, with the aim of exploring whether GIS can be used to conduct multiscale analysis of taphonomic patterns at an element, body, and stratigraphic level. The aim was to reconstruct burial practices to develop understandings of the 'bigger picture' of Early Neolithic cave burials in North West England.

Four assemblages, dating to the Early Neolithic, were originally proposed: Cave Ha 3, Sewell's cave (cranial only), Lesser Kelco (cranial only), and Heaning Wood. Due to time limitations and

methodological problems with Sewell's cave and Lesser Kelco, analysis focused on Cave Ha 3 and Heaning Wood. The issues regarding Sewell's cave and Lesser Kelco are discussed in section 18.4.2. Cave Ha 3 was dated and reported on as part of Leach's work (Leach, 2006a, 2006b, 2008) and dates to the Early Neolithic. Dating work of Heaning Wood was completed part way through this project, and while half of the individuals returned dates from the Early Neolithic, two individuals dated to the Early Bronze age and one infant to the Early Mesolithic. A third Early Bronze Age date related to a metatarsal but was not assigned to an established individual. This is discussed in more depth in section 18.3.2. The earliest burial was significant as the date makes this the oldest known human burial from Northern Britain. The dates also changed the focus of the project slightly, in that discussions around depositions for Heaning Wood needed to reflect these distinct periods.

The following discussion looks at the key findings from both assemblages. Where possible burial narratives for individuals are provided, together with an overview of the temporal flow of taphonomic processes. The implications of these for the wider societal context of the burial period are then discussed. The use of GIS for this type of analysis, issues encountered, and refinements of the method will be considered before future research and applications of the method are proposed.

## 18.2: Cave Ha 3

### *18.2.1: Quantification and Individuation*

There was an MNI of four for Cave Ha 3, consisting of one mature adult male, two infants and a neonate. Two of the individuals, the adult male and the older infant, were radiocarbon dated, with the infant being re-dated by Brace and colleagues in 2019. The most recent dating places burials at Cave Ha 3 between 3660 Cal BC and 3113 Cal BC. Age, sex, and stature estimations were consistent with Leach's (2006a) original findings and are detailed in section 9.1, table 9.2. An additional adult ulna was in the collection. Original excavation reports indicated that this was found near Cave Ha 4 and that other bones could be seen (Leach, 2006a). During 2022 additional surveying of the Cave Ha complex was conducted. The previously excavated areas at Cave Ha 3 were re-excavated in the area of the rock-shelter and

Cave Ha 4 was mapped but not excavated due to licensing limitations. No other human remains were recovered. There were no other repetitions of elements for the Cave Ha 3 adult. With the level of preservation seen, this would have been expected if another body had been present. It is advised that a full excavation of Cave Ha 4 be conducted to establish if any other burials are present at the complex. Leach (2008) discusses the possibility of Cave Ha 3 representing 'odd ones out' due to potential facial disfigurement of the adult and smaller stature. If other burials are recovered from the Cave Ha complex this may add to the discussion.

The assemblage was commingled with faunal remains and, for the most part, disarticulated. Individuation therefore relied on size, robustness, and age. Individuation of Cave Ha 3 was facilitated by the age at death estimations and is reported with high confidence. Despite duplicates of elements for the younger individuals they were easy to place due to the lack of developmental crossover between ages. There were some cranial fragments that were difficult to assign to the middle two infants due to fragmentation. These were recorded separately for taphonomy but excluded from individual bone representation profiles. The exclusion of fragments will be discussed in more depth in section 18.4.2 which considers methodological issues.

All element groups were represented for all individuals except for an absence of vertebrae for the neonate and an absence of hands and feet for the infants. While the absence of smaller bones can be indicative of secondary burial, similar patterns can be seen in sequential depositions (Robb, 2016). Additionally, Cave Ha 3 had an abundance of tufa (calcite) formation that was active during the time of the burials (Pentecost *et al.*, 1990). This may have embedded much smaller elements seen in infants, rendering them unrecoverable or unrecognisable. There was retention of articulations seen in Individual 1 and 2, further supporting evidence for primary, whole-body burial. The following section outlines the key findings for each individual. Where possible schematics have been created to describe burial narrative.

*18.2.2: Individual 1*

Since Cave Ha 3 was a commingled burial, it is important to acknowledge the possibility of a composite burial. There have been burials in the Neolithic where different skeletal elements have been mixed to create a 'single' individual (Wysocki and Whittle, 2000; Fowler, 2010; Cummings, 2017, p.106; Lorentz, Casa and Miyauchi, 2021). Individual 1 appeared to have postcranial metrics that were more consistent with an adult female than an adult male, despite morphologically presenting as male. While it is important to mention this as a possibility it is considered unlikely due to several factors including:

- Sex estimation from postcranial measurements have been developed using more modern populations (e.g., Spradley and Jantz, 2011 used the Forensic Anthropology Data Bank, a collection of anthropological data of skeletons mainly born in the nineteenth century). These may not be applicable to the Early Neolithic where average heights were shorter (Roberts and Cox, 2003).
- There was evidence of possible "disfigurement" and "severe wear and tear" to the lower spine (Leach, 2008, p. 47); these may have contributed to the smaller stature.
- There were no repeat elements, except for the ulna associated to Cave Ha 4.
- There was evidence of articulated sections, such as the right foot, and all elements matched in size and morphology.
- There was an absence of evidence that the bones had been previously buried in another environment.

Individual 1 is therefore considered to be a primary, whole-body burial. Analysis of taphonomy at element and body level indicated that taphonomic processes were mostly homogenous, except for marrow extraction to one element. There were slightly more left sided fragments recovered than right, but the difference was not considered significant. Taphonomic modifications affected anatomical sides in line with representation. Analysis showed that the anterior surfaces were disproportionately affected by peri-mortem crush damage. These two factors suggest that the body was deposited in the supine position. Spatial analysis indicates that Individual 1 was deposited towards the back recess of the cave with movement of fragments spreading south-west, away from the overhang, and south-east along the cave wall.

The left tibia of Individual 1 was smashed with evidence of marrow extraction. There was no evidence of dismemberment using tools, however it is possible that this is due to a loss or destruction of the portion of bone that would exhibit these marks. It is likely though, that marrow extraction took place at a point when the tibia was either disarticulated or decomposed enough to allow manual removal. The right foot was embedded in tufa and several metatarsals retained anatomical proximity. As a minimum the foot was deposited whole and fleshed, or when there was still retention of articulations, supporting whole-body burial. Figure 18.1 describes the sequence of burial, as indicated by analysis of element, body and spatial distributions of taphonomic modifications. Some key moments of taphonomic modifications are highlighted, such as tufa adherence prior to the tibia smashing and embedding of the foot occurring after movement. It should be noted, however, that taphonomic processes were occurring across all time points and are not just limited to these incidents.

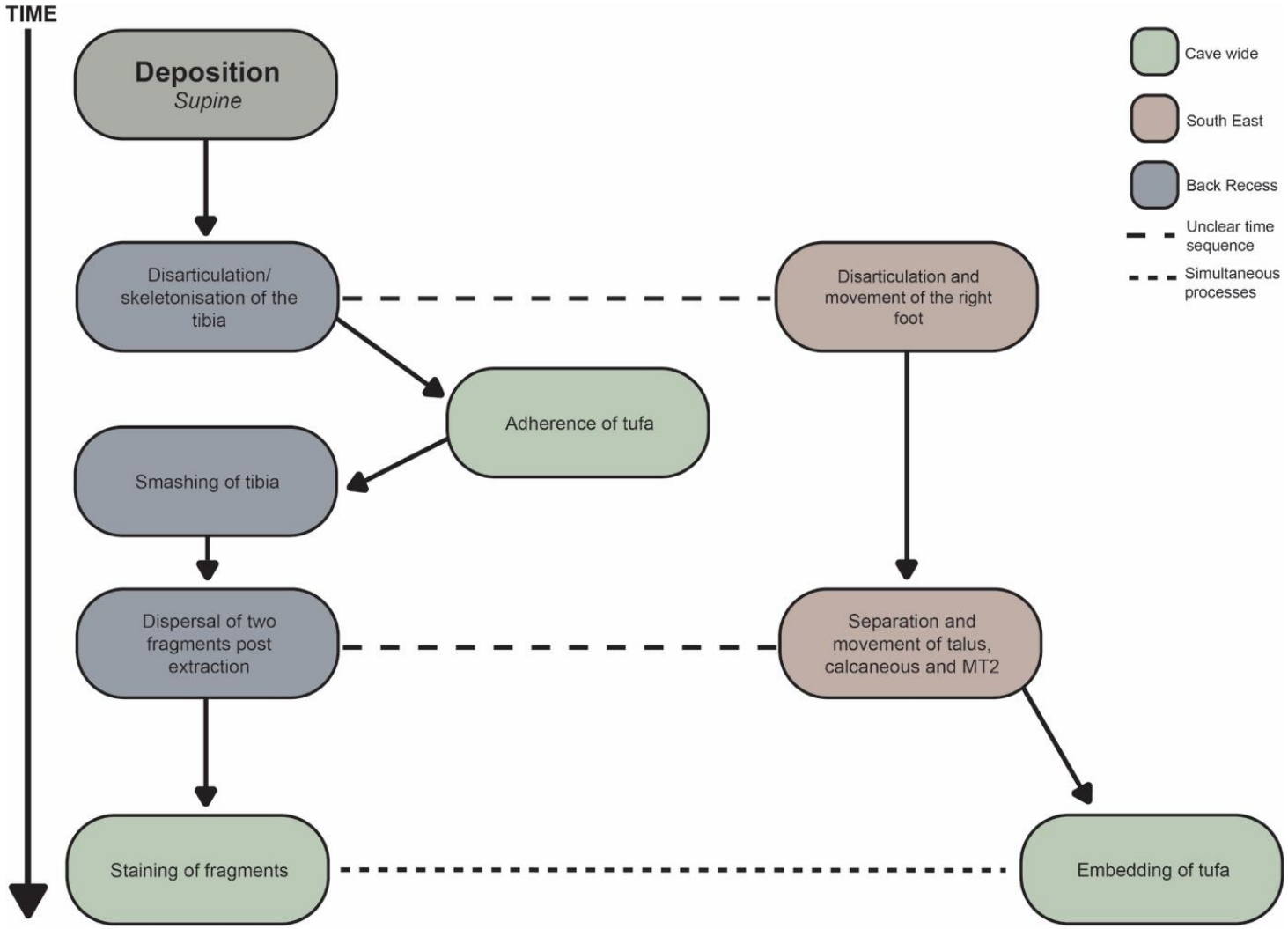


Figure 18.1: Sequence of events post deposition for Individual 1.

The sequences described above show that Individual 1 was subjected to extended burial rites with manipulation of the body after decomposition. This demonstrates an understanding of the body after death with specific rituals reserved for stages that would allow processing.

### *18.2.3: Individual 2*

Taphonomic processes were homogenous for Individual 2. There was representation of all element groups except for hands, feet, and patellae, indicating a whole-body burial. Several taphonomic processes showed biases towards surfaces. The posterior surfaces had higher frequencies of tufa with an absence of cortical removal. Anterior surfaces showed higher frequencies of invertebrate activity. While the evidence is less clear cut than for Individual 1, it is possible that these are indications of a supine burial. Analysis of the dispersal of fragments and taphonomy further supports this. There was a concentration of fragments towards the back recess of the cave, with left fragments moving along the east wall and right fragments spreading out to the west. Additionally, crushing and peri-mortem damage was seen to the lower limbs that had moved to the south-east, possibly indicating an incidence of rockfall. This is consistent with the geology of the cave, with these fragments located near the overhanging cave wall.

Figure 18.2 shows a possible sequence of events for Individual 2, highlighting key taphonomic processes. It should be noted that these are posited with caution as not all of Individual 2 was recovered and movement within the cave may have obscured other factors or possibilities.

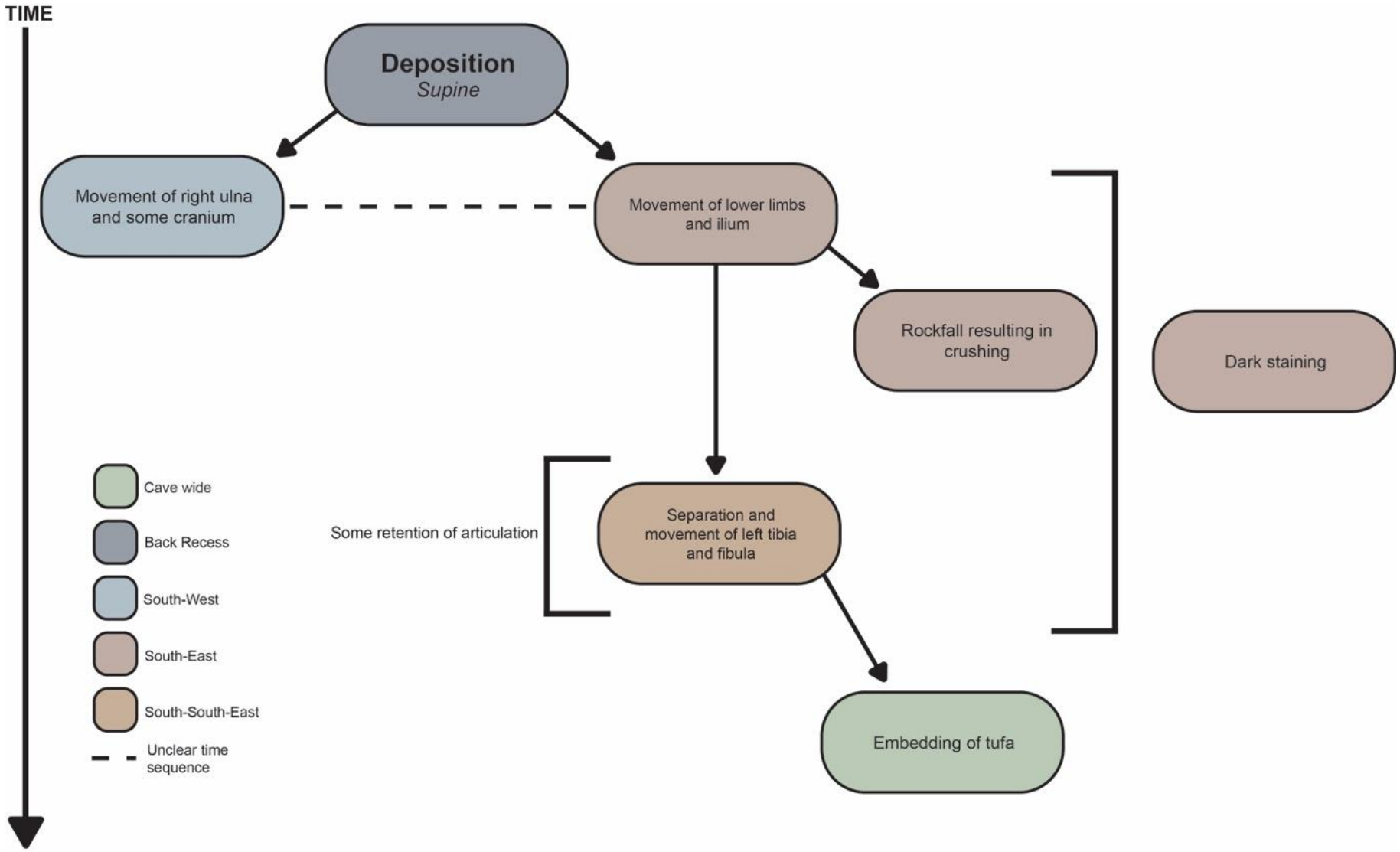


Figure 18.2: Sequence of events post deposition for Individual 2.

### *18.2.4: Individuals 3 and 4*

Analysis of Individuals 3 and 4 was limited due to the number of fragments recovered. The fragments for Individual 4 were also the most dispersed, with fragments recovered up to 7.05m away from the main cluster at the back recess. These factors masked any potential inference around burial position or taphonomic sequences.

### *18.2.5: Assemblage*

Even in excavations with excellent spatial data there will be issues in understanding taphonomy if movement has occurred prior to recovery. Cave environments can be subject to numerous processes that result in the dispersal of sediment including periods of rockfall, flooding, animal activity, human interference, successive depositions, and roof collapse (Andrews, 1990, p.91; Fernández-Jalvo and Andrews, 2016; Pokines *et al.*, 2018). There was dispersal of fragments for all individuals in Cave Ha 3, which in part hindered understanding, however it has been possible to understand some of the temporal sequences of taphonomy.

Individuals 1 and 2 highlighted possible locations of burials, as well as body positions and timing of taphonomic modifications. For the most part, processes were occurring simultaneously and across all areas of the cave, however, some processes can be pinpointed as occurring before others. Figure 18.3 shows an overview of when these were happening.

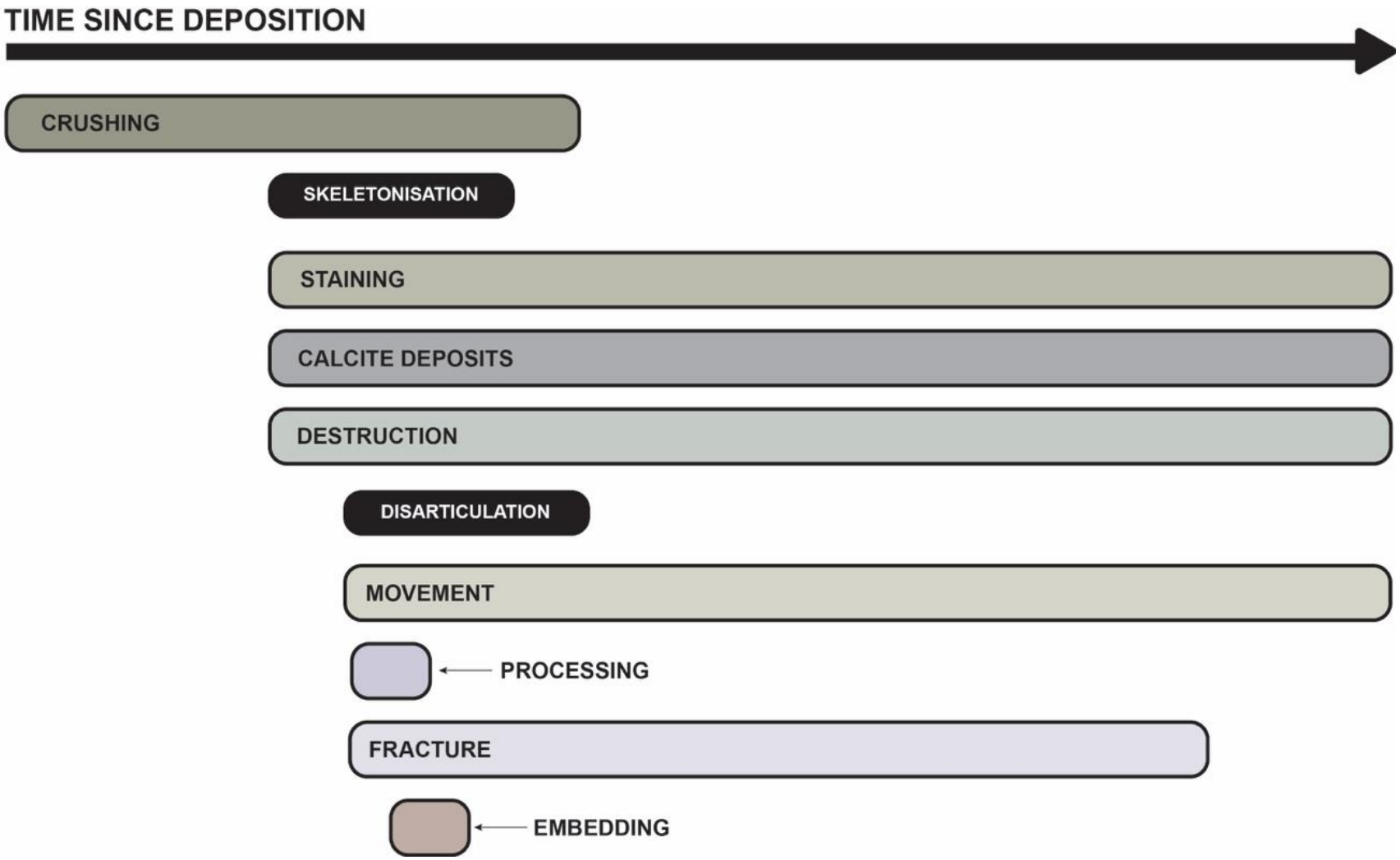


Figure 18.3: Sequence of taphonomic processes at Cave Ha 3

There was crossover of timing for all modifications, for example, staining occurred prior to and after disarticulation and movement. Similarly, deposits of tufa developed both before and after staining, movement, and fracture. Other processes can be picked out, such as the processing for marrow extraction, that had to have occurred after skeletonisation and tufa deposition due to an area of deposit spanning the fracture line. Section 12.14 discusses the possibility of movement because of heavy rainfall. The geology of the cave and the absence of evidence of other acting agents suggests that run-off of water and sediment may be a contributing factor to the movement of elements. This is a known cause of sediment movement in caves and rock shelters (González-Lemos, Jiménez-Sánchez and Stoll, 2015). There is also the possibility that human interference has played a role in the movement of specimens. Radiocarbon dating points to successive depositions, rather than a single burial event, and there is evidence that Individual 1 was returned to after deposition. The act of subsequently adding bodies and the processing of the tibia may have led to the movement of fragments and may offer insight into the wider burial practices. Leach (2008, p. 51) suggested that the deposition of bodies at Cave Ha 3 may have been a way to "separate these individuals from the collective dead" using the tufa as a way of immortalising them. If the purpose was immortalisation, then why smash the tibia? Leach (2008) offers a possible second explanation for the Cave Ha 3 burials, linking the depositions in tufa to ideas around ancestry, ritual, and spirituality, rather than separation. Schulting and colleagues (2015) propose that marrow extraction is often linked to speeding up decomposition, in a bid that the body joins the ancestors more quickly. Two different mechanisms, preservation and destruction, are being acted out on the body, and therefore seem to offer contradictory purposes. However, Whitely (2002, p. 122), argues that "…ethnographic evidence suggests that human bodies buried in unusual places of *[sic]* subjected to unusual treatment are more likely to be those of social outcasts (that is, of the unquiet dead) than those of ancestors". It could be considered that these are part of the same ideology and one of exclusion. Early Neolithic burials in caves are common however, which contradicts the idea that they are "unusual" places. The burials at Cave Ha 3 are consistent with varying practices seen across the area and in cave burials during the Early Neolithic.

Leach (2006a, 2006b, 2008) has provided discussion around the meaning of their burial. This research has been able to tease out more specific details around burial positions and

taphonomic sequences and adds quantitative support to previous research. The following section discusses the results for Heaning Wood before tackling more generic methodological issues encountered for both assemblages.

## 18.3: Heaning Wood

Analysis of Heaning Wood was less clear-cut than Cave Ha 3. The assemblage comprises three collections, excavated at different points, with differing levels of spatial information. The portions of the assemblage that were excavated in 1958 and 1974 are held at the Dock Museum, Barrow-in-Furness. These contain fragments that were significant, including a partially intact skull, several long bones, mandibles, and other cranial fragments that provided age and sex details. The largest portion of the assemblage, comprising 363 fragments of varying sizes, was recovered between 2016 and 2019. Analysis of the human remains from this collection was conducted in 2017 (Warburton, 2017, *unpublished*). Interpretations, including the final minimum number of individuals and ontological estimations, have been altered by the inclusion of material excavated after 2017 and combination with the material from the Dock Museum. The results presented here are considered comprehensive and include all identifiable human remains recovered to date. A survey of lower chutes by cavers indicated that it is unlikely that there any more remains left. The spatial data for the earlier excavations was limited and could only be interpreted to belonging to the 'top area' of the cave, meaning that the fragments could have originated from any area spanning metres in depth and width. Spatial data for the 2016 to 2019 excavations were better, but still limited to 0.125 m depths with no information of width distribution. Adding to the spatial difficulties was fragmentation and commingling, which created problems with individuation.

### *18.3.1: Individuation of Commingled and Fragmented Assemblages*

Unlike Cave Ha 3 where there were distinct ages to facilitate individuation, Heaning Wood was a larger assemblage with greater fragmentation and crossover of age estimations. Once development is complete, usually with the fusion of sternal end of the clavicle and the iliac crest (Ubelaker and Khosrowshahi, 2019), age estimations rely on degenerative changes in the skeleton. These methods have varying rates of success and often fail to consider taphonomic changes or the absence of key elements (Cappella *et al.*, 2017). For those methods that are

available the age estimations often span years, sometimes decades. For Heaning Wood, the estimations for the adults all fell within 17 and 35 years, with two at the lower end of the range and two at the upper end. This meant that individuation had to rely mostly on repetition of elements, size and morphological similarities, and refitting. Individuals B and C were more gracile in size, however, Individual B was consistent with a skeletal sex of male, whereas Individual C was consistent with female. This meant that some differentiation between fragments were facilitated, for example the sacra showed sexual dimorphism. Similarly, fragments from the larger, more robust adults (Individuals A and D) were easier to distinguish. It might have been possible to use spatial analysis to assist in individuation for Heaning Wood, for example, Tuller, Hofmeister and Daley (2008) applied spatial analysis to mass graves to assist in the reassociation of commingled remains. Their process, however, was facilitated by applying the method at the point of excavation, allowing for accurate recording of coordinates. Limited spatial data for Heaning Wood, coupled with evidence of refitting fragments moving across multiple layers, prevented such assessments. The exception to this is the frontal bone associated to Individual B, which is discussed in more detail in the following sections.

It may be possible for Ancient DNA (aDNA) and radiocarbon dating to facilitate MNI estimations and individuation (Alt *et al.*, 2016). However, the process is expensive and destructive, preventing the analysis of multiple fragments. Individuals A to H have been sampled for aDNA and the results are expected after the completion of this project. Due to the samples being limited to one fragment per individual it is not expected that this will change individuation. Radiocarbon dating was conducted and highlighted the possible presence of a fifth adult (see section 14.1, page 225). Eight samples were taken from seven of the individuals, excluding individual G due to limited fragments. At the time of sampling the fragments from the Dock Museum were not accessible and Individual D was suspected to be a composite individual made up of repeated elements that were not associated with the other three adults. For this reason, two fragments were selected from Individual D and the dates returned showed that there was less than a five percent probability the fragments were from the same period. This strongly suggests that the second sample originated from another adult within the assemblage. This is further supported by the presence of a calcaneus in the Dock Museum collection that does not match morphologically to the other adults. While an MNI of

nine was not possible to fully establish through individuation, the evidence suggests that there was at least one other body in Heaning Wood.

The individuation of Heaning Wood was done through a process of looking for repetition of elements (White, 1953), the zonation method (Dobney and Rielly, 1988; Knüsel and Outram, 2004) and manual refitting of fragments. The process was repeated each time new material was introduced, first when the new fragments were found after 2017 and again when the collection from the Dock Museum was accessed. Individuation is therefore comprehensive and reported with a high level of confidence. While the confidence is high for most of the assemblage, the frontal bone associated with Individual B raises some questions. Patterns of taphonomy highlight the possibility that this, and the distal portion of right tibia, which were not direct refits to other fragments, could possibly belong to the fifth adult. Similarly, the alignment of the maxilla for Individual D was off centre, however taphonomic modifications may have altered positioning. This is an example of where the detailed spatial analysis has provided insights into individuation and could be applied to commingled assemblages with better spatial data.

Due to difficulties in differentiating hand and foot bones and other elements that have fewer ontological differences such as vertebrae and ribs, a large proportion of fragments was excluded to prevent skewing of distribution data. These fragments were not looked at in depth because of time constraints, but a further development of this project could explore the relationship of unassigned fragments to others to see if patterns emerge, allowing for refinement of associations.

While the individuation is reported with high confidence, it is recognised that due to fragmentation, commingling, and close demographics of individuals, some errors may be present. All results and interpretations are made with this in mind, acknowledging that "ultimately, the capacity of archaeologists to infer past causes depends on the quality of the archaeological record" (Perreault, 2019, p. 2). The following section provides an overview of the findings for Heaning Wood, starting with the radiocarbon dating and its implications for how the site was used, before covering more micro-level details of the bodies and taphonomy.

### *18.3.2: Radiocarbon Dating: Changing the Narrative*

Early dating funded by the Cumberland and Westmorland Antiquarian and Archaeological Society (CWAAS) produced four radiocarbon dates placing human bones to the Early Bronze Age and butchered animal remains to the Early Neolithic (Smith, 2012). Further radiocarbon dating produced in parallel to this project returned dates ranging from the Early Mesolithic to the Early Bronze Age, with gaps between burial periods of thousands of years. Figure 18.4 shows dating in the context of the relevant periods (Jazwa, 2022).

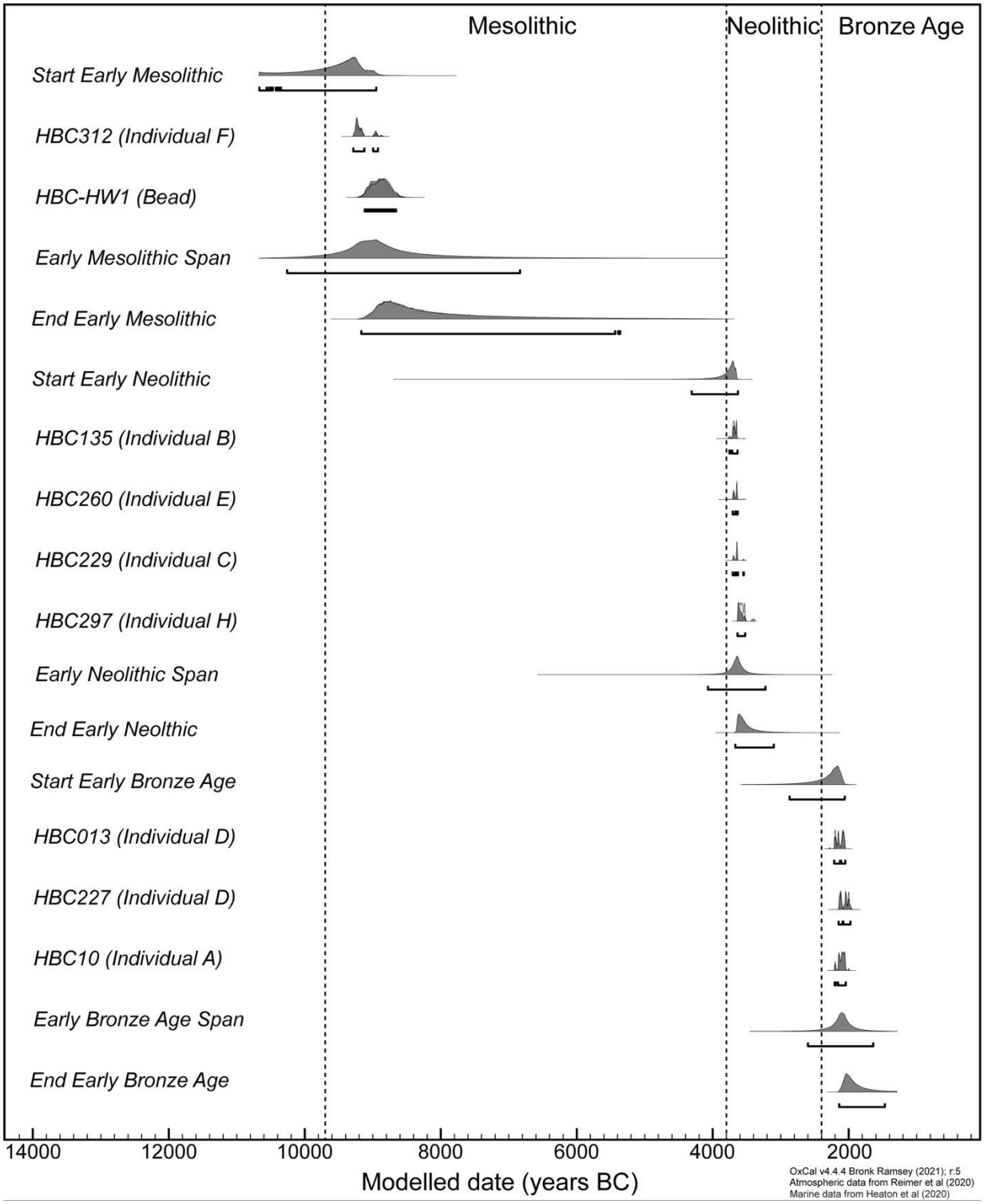


Figure 18.4: Radiocarbon modelled dates for Heaning Wood (Jazwa, 2022).

There are three distinct burial phases, and while it may be possible that destructive processes have masked potential continuity, it is unlikely due to the level of excavation, sieving and recovery conducted at Heaning Wood. This has implications for the discussion on whether cave burials were the continuation of Mesolithic practices, or the mirroring of Mesolithic

practices by Neolithic people (see section 2.2). The lack of crossover suggests distinct practices, and that it is unlikely to be a result of "long-term remembering" (Borić and Griffiths, 2015, p. 355) because of the number of years separating the events.

A large portion of the faunal remains are microfauna such as voles and amphibians and would be expected to be found in caves (Andrews, 1990, p.2). There was evidence of larger animal remains including pig, sheep, horse, cow, deer, Celtic ox, boar and wolf (Holland, 1960, p. 42). The morphology of the cave would not have allowed these larger animals to access the space unless they were introduced because of the opening acting as a faunal trap. Additionally, some of the bones had evidence of butchery (Smith, 2012) suggesting deliberate disposal. The evidence of butchery on some animal bones may indicate that the location was used for the deposition of domestic waste in addition to human remains and returns us to Bonsall and Tolan-Smith's (1997, p. 217) discussion around the use of caves as spaces for "the disposal of waste". There is no evidence of deliberate manipulation of the human specimens making it possible that Heaning Wood was a place of convenience for the disposal of the dead. Brück (2008), however, discusses Early Bronze Age burials where animal remains are incorporated in human burials, arguing that "humans and animals were treated in similar ways in the mortuary context" (Brück, 2004, p. 325). Cave burials in Central Europe dating to the Early Neolithic have also seen commingling of animal and human remains (Orschiedt, 2012). Rather than the inclusion of animals remains being an indication that the space was used for disposal, it may be that animal and human deaths were processed in similar ways.

Cave burials are seen during the Early Neolithic and Early Bronze Age across the UK (Chamberlain, 2013) and as such, the pattern seen here should not be unexpected (Peterson, 2022, personal communication, 12 December). The discussion around caves as spaces of spirituality versus convenience is not a new one. As described by Chamberlain (2013, p. 137) "…it is often difficult to elucidate patterns of usage from the cultural evidence preserved at specific cave sites…", with Heaning Wood offering no exception. While some of the animals may have been associated with the Early Bronze Age burials, a portion of the assemblage is likely to have accumulated much earlier than this. The cut-marked animal bones, larger faunal collection and artefacts need to be explored with reference to the associated burials to help

us to understand their connection, or lack of, with the human burials and their significance in relation to the period of burial.

Several artefacts were recovered in 1958, including lithics, pottery and a bone pin or brooch (Holland, 1960). Further artefacts were recovered from the 2016-2019 excavations, including periwinkle beads. A bead recovered from the later excavations was dated along with the human remains. Individual F and the bead returned dates from the Early Mesolithic (9290-8930 Cal BC and 9115-8635 Cal BC). The dates for these are significant, making Individual F the earliest known burial from Northwest England. Understanding of Mesolithic occupation of the UK is limited due to a paucity of "precise and reliable radiocarbon measurements" of Mesolithic artefacts (Conneller *et al.*, 2016, p. 1). The recovery of human remains with such an early date adds to our understanding about the occupation of Northern Britain in the Early Mesolithic and is discussed in section 19.1.2.

### *18.3.3: Bronze Age Burials*

Both individuals that dated to the Early Bronze Age (Individuals A and D) had elements represented from all element groups, with homogenous taphonomy consistent with whole-body burial and an extended period within a cave environment. There were no indications that the bones had been previously exposed to another environment. There were two areas of delamination on fragments from both bodies that indicated a slightly more advanced stage of weathering than the rest of the assemblage. This was not considered to be an indication of differential exposure, but rather that they were likely to have been deposited towards the top of the talus formation, closer to the entrance, and therefore more likely to be exposed to variations in temperature, humidity and light (Springer, 2005).

In the body-level analysis of taphonomy for individual D, the cranial elements appeared to have higher frequencies of dark spotted staining. When this was explored spatially, other fragments recovered from the same area did not share the same intensity of stain patterns. There are two possibilities for the differences found: it may be a result of the cranial fragments being in a different location within the same layer and therefore having greater exposure to the acting agent, or it may be that the cranial elements were more prone to staining due to

fossae within the cranial surface. Many of the staining patterns to the cranium were found in areas such as the meningeal grooves of the parietals (figure 18.5).

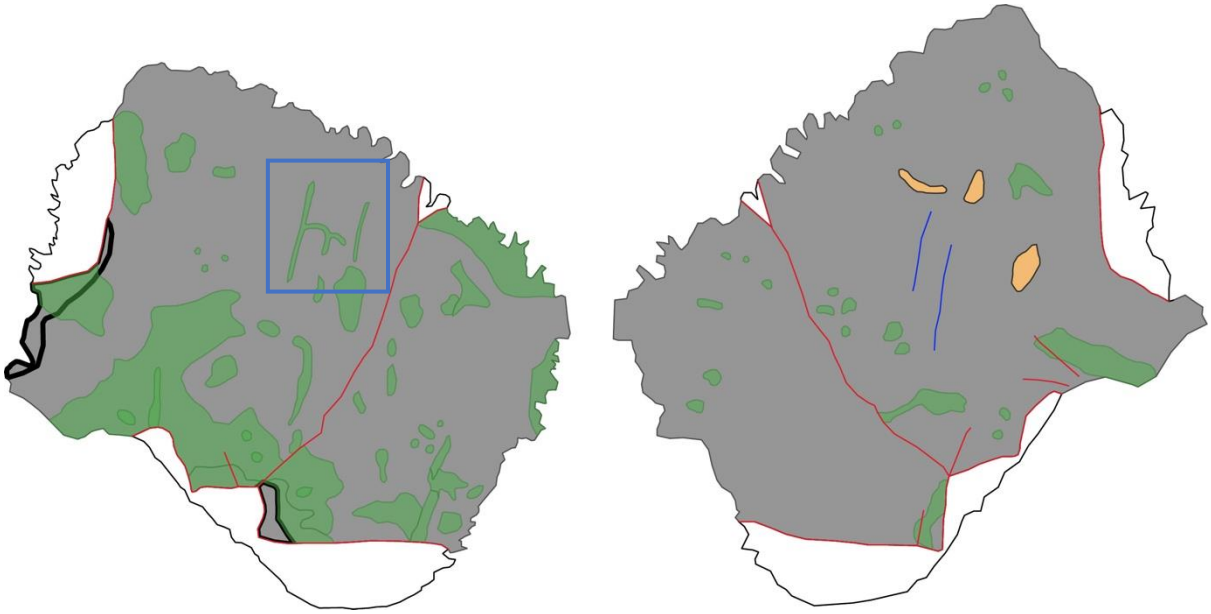

Figure 18.5: Example of staining following meningeal grooves in the parietal (blue box).

Unfortunately, due to the paucity of spatial data it was not possible to determine if it was due to location differences.

A left humerus belonging to Individual D was fractured at the distal end with the distal portion located in layer four, away from the proximal end in the top area. The exact same movement pattern and fracture occurred to the right humerus associated with Individual A. It was initially questioned whether this was an indication of incorrect assignment of the humeri, however the fracture is a common site in humeri (Galloway, 2014) and similar movement patterns were seen for both individuals. It is therefore considered that this is an indication that the same mechanisms of breakage and movement were acting on both individuals.

The distribution of invertebrate modifications showed higher frequencies in the top area of the cave. As discussed in section 17.6.5, page 344, research has shown variations in level and type of insect activity at different levels within a cave (Terrell-Nield and Macdonald, 1997; Moldovan, 2005). The fragments with invertebrate activity for Individuals A and D were all

from the Dock Museum collection. There have been cases of insect infestations in museum collections which can result in the destruction of collections including bone (Querner, 2015; Trematerra and Pinniger, 2018); however, activity was seen on fragments in other individuals that were not stored at the museum. It is therefore considered that these modifications were the result of insect activity within the cave rather than contamination at the museum. Further research for Heaning Wood could look at invertebrate activity at a microscopic and macroscopic level in conjunction with an entomological survey, providing important information about the impact of insect activity on bone survival in UK cave burials. Additionally, this might help shape spatial understanding. If modifications are found away from areas in the cave inhabited by particular invertebrates, then movement and original location of the fragments may be deduced.

There was no information to indicate burial position for either Individual A or D, and movement of fragments across several metres made analysis difficult. There was increased movement of smaller fragments and elements, with a concentration of fragments at the top, consistent with later deposition with run-off of fragments. Unfortunately, it is not possible to develop depositional narratives beyond a whole-body, primary burial, towards the top portion of the accumulated talus. Patterns of taphonomy across Individuals A and D suggest that mechanisms were acting simultaneously, with no clear evidence for one modification occurring before the other. The only exception to this was the area of delamination seen in the humerus of Individual D, which spanned a fracture margin. This indicated that the destruction happened prior to breakage and movement.

### *18.3.4: Neolithic Burials*

There were four individuals dated to the Early Neolithic: a young adult male, a middle adult female, a young child, and an older infant. The adults (Individuals B and C) had fragments representing all element groups. The young child (Individual E) was represented only by cranial elements and the clavicles. The older infant (Individual H) was represented only by the maxillae. The taphonomy was homogenous across all individuals and consistent with extended burial in a cave environment.

The element representation of Individuals E and H raises questions around whether these were curated burials. Cranial only burials dating to the Early Neolithic have been seen in caves with disarticulation and curation characterising Early Neolithic burials (Leach, 2006a, 2006b, 2008; Smith and Brickley, 2009, p.11; Cummings, 2017, p.136; Peterson, 2019, p.2). It is considered unlikely that Individual E and H were cranial only burials, despite their bone representation indices indicating otherwise. Robb (2016) modelled successive burials and argued that the loss of smaller, quick to disarticulate elements, is not always an indication of secondary burial or movement. The taphonomy on the fragments associated to Individuals E and H also indicated that they had not been exposed subaerially, to carnivore activity or manual processing. This, along with the increased fragility of infant remains (Scheuer and Black, 2000; Caruso *et al.*, 2021), means that it is possible that destructive processes are responsible for the loss of postcranial elements. There was excellent recovery seen at Heaning Wood, including the identification of neonatal fragments. It is possible that the survival of the neonatal fragments was due to them being a later deposition but without dating this cannot be determined. In the discussion around Sewell's cave, it was interpreted that the cranial elements had been moved as part of a "secondary burial rite" (Peterson, 2019, p. 121) despite showing an absence of carnivore modification and limited weathering. Peterson (2019, p.121) argues that if this is the case then the bodies were likely buried "during the earlier stages of the intermediary period". It is possible that Individuals E and H were treated similarly, with an initial burial in another location. Subsequent taphonomic changes may have masked evidence of an earlier burial location. On balance it is considered that the Early Neolithic burials at Heaning Wood were primary depositions, although curation of the infants cannot be completely ruled out. Either narrative fits the burial practices of the period and region since both curated and non-curated cave burials have been seen in North-West England (Leach, 2006a, 2006b; Peterson, 2019). Histological analysis discussed in relation to Early Bronze Age burials (Booth and Brück, 2020; Brück and Booth, 2022) may help determine whether there is a difference in the diagenesis of the infants and the adults. This could provide further evidence as to whether curation was being practised at Heaning Wood, but any differential diagenesis would need to account for structural differences between adult and juvenile bone (Scheuer and Black, 2000; Caruso *et al.*, 2021).

Taphonomic and spatial analysis of the younger individuals was limited due to the number of fragments recovered. Fragments for Individual E were recovered from layer four downwards. It is possible that this was the point of deposition, but care should be taken in determining this, since movement of fragments has been seen across the whole assemblage. There were insufficient fragments to pinpoint clusters of associated elements that would help support this interpretation. The fragments associated to individual H were both found in the West Fissure. With no other fragments to relate to it was not possible to create a depositional narrative.

There was less ambiguity around Individuals B and C regarding primary versus secondary burial. The bone representation indices and taphonomy were consistent with whole-body, primary burials. Posterior surfaces were more affected by weathering than anterior for fragments assigned to both Individuals B and C. This may be an indication of increased exposure, although none of the other modifications for Individual C showed a bias towards anatomical surface. There were higher frequencies of deposits on the posterior surfaces of Individual B, further supporting the possibility of positioning but the evidence is not clear enough to make a determination. There was evidence of staining occurring both before and after destruction, fracture, and calcite deposits. There was some indication that destruction pre-dated staining and deposits, although not in all cases. Determining the sequence of taphonomic changes was difficult for all the Early Neolithic bodies. There was a difference to deposits accumulated on fragments originating from the 1958 excavations compared to those recovered later. There appeared to be fewer deposits on the material from the Dock Museum possibly due to the shorter period in the cave. These had, however, been treated with a preservative which may have masked some changes.

Spatial analysis of taphonomy indicated that layer ten may have been an area of increased calcite accumulation. Both Individuals B and C showed the highest frequencies per fragment count for that layer. Most deposits were classed as ‘thin/flaked’ except for a fragment of right humerus (HBC158) which was also located in layer ten that has patches of ‘thick/coated’ calcite. Figure 18.6 shows an overview of layers that had higher frequencies of certain taphonomic modifications.

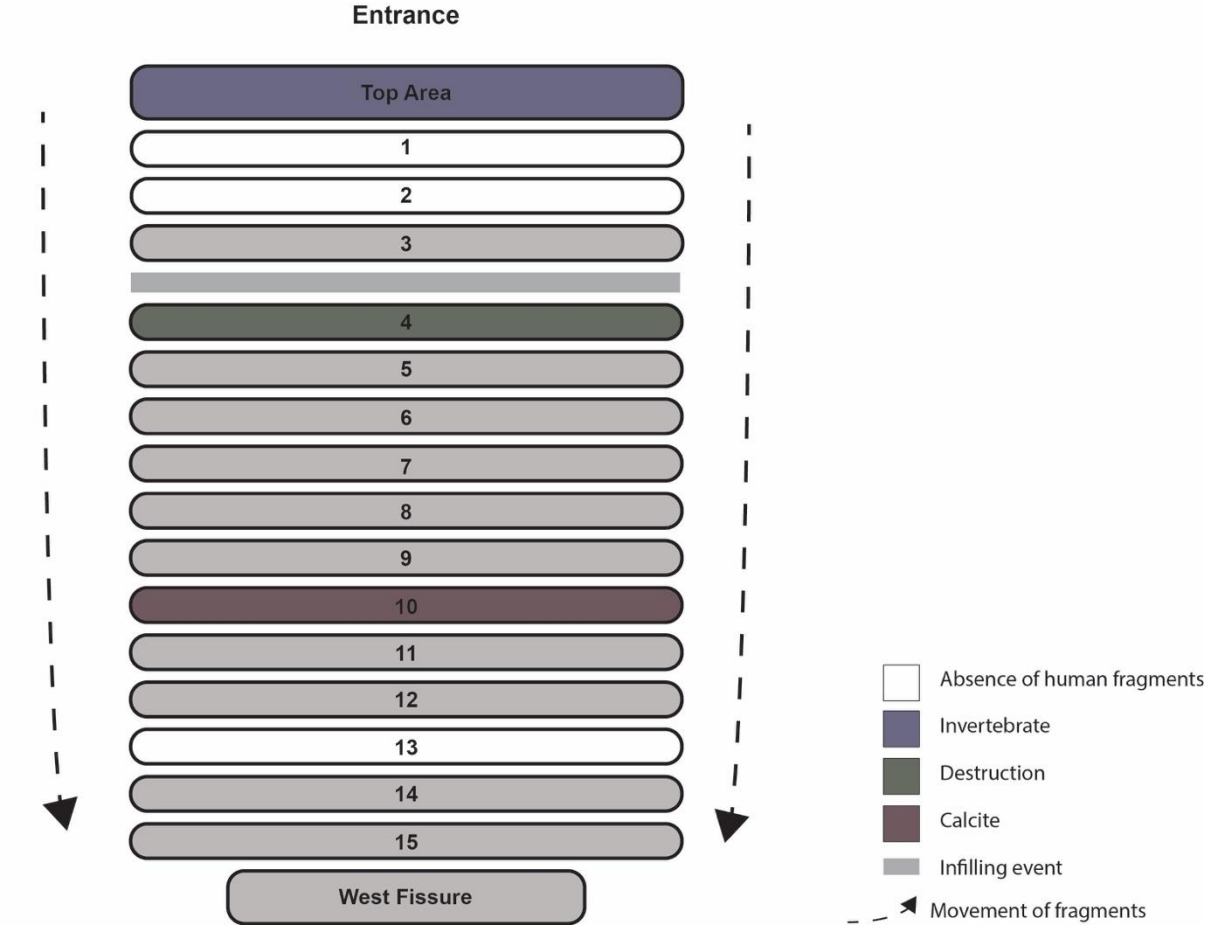


Figure 18.6: Layers with higher frequencies of modifications

As described in figure 18.6, layer four showed higher frequencies of destruction. This pattern was seen for Individuals B and E. There was a concentration of long bones for Individual B in layers four and five and these were fragments of elements that have anatomical proximity. In other individuals, particularly Individual C, there was a high degree of dispersal. Individual B did have dispersal of fragments across multiple layers but was the only burial to show a concentration of associated elements within one layer. There were two fragments for Individual B that were located above layer four, although it is possible that these fragments have been incorrectly associated. Individuation was done with high confidence but the frontal bone for Individual B was not a direct refit to other cranial elements. It was assigned due to it being adult, morphologically male, and a repeat of elements already assigned to the other adults. It is possible this fragment belongs to the fifth, unidentified adult. If this is the case, then layers four and five may indicate an approximate deposition point for individual B. Due to the nature of the spatial data the layers do not represent single events traditionally seen in

archaeological contexts. They therefore should not be thought of as fixed surfaces, rather the concentration of lower limbs seen in Individual B indicate an area of accumulation.

The increase of destruction at this level adds support to this and is possibly a point of infilling. There is an overlap to the radiocarbon dates for Individual C, but the overlap is small. Individual C is most likely a later deposition and fragments in higher levels would be consistent with burial sequences. Figure 18.7 proposes the sequence of depositions for the adult remains at Heaning Wood.

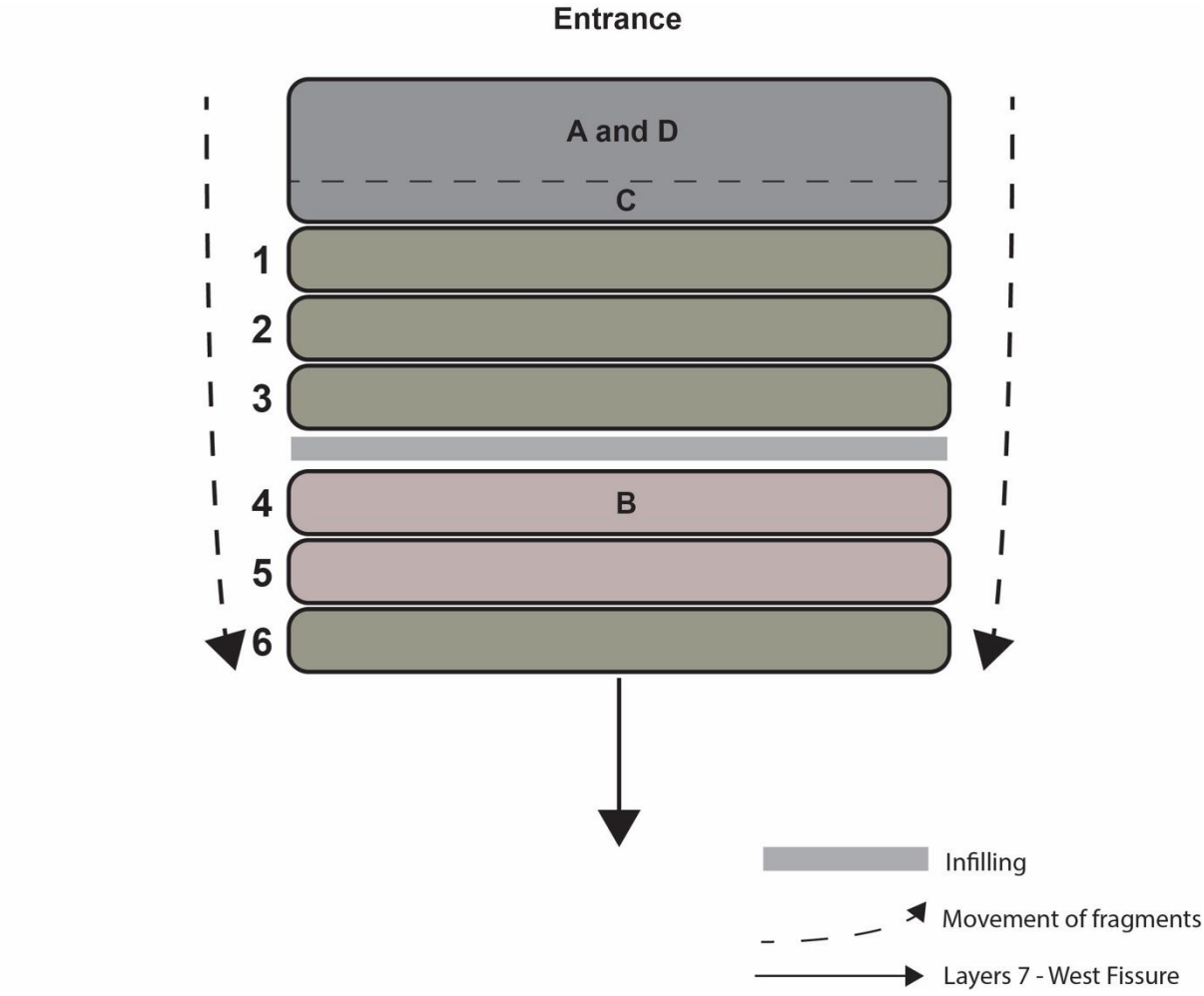


Figure 18.7: Sequence of depositions for Individuals A-D, Heaning Wood.

### *18.3.5: Mesolithic Burial*

Individual F was dated to 9290-8930 Cal BC and was represented solely by cranial fragments. Analysis of taphonomy was limited because of the number of fragments recovered. There was an absence of calcite deposits which may be due to the accumulation of material protecting the body from exposure. The taphonomy was consistent with an extended period within the cave environment, with nothing to indicate subaerial exposure. The questions around curated burials discussed above are also relevant here. The taphonomy suggests that there was no exposure outside Heaning Wood, but bone representation may be interpreted as evidence for curation. There was, however, no evidence of carnivore exposure or defleshing for Individual F and the bone representation indices (BRI) could be explained by destructive processes. The timing of the burial would place it further down in the talus. Such pressure, along with frequent infilling and successive internments, may have led to the destruction and loss of the rest of the skeleton. The presence of cracking and weathering does not preclude primary deposition in a cave.

### *18.3.6: Undated Burial*

Individual G was estimated to be 38-40 weeks at the time of death. It was decided that destructive analysis should not be conducted due to the limited fragments. The spatial distribution of fragments may indicate a later deposition, however fragments associated to Early Neolithic individuals were also found in the upper layers of the cave. Taphonomy and bone representation indices suggest a whole-body, primary burial.

The patterns of dispersal and taphonomy are consistent with the other burials at Heaning Wood. The representation of elements from all groups, except for hands, feet, and patellae, is different from the other infants in the assemblage. While both clavicles for Individual E were recovered, the infants were otherwise only represented by cranial fragments. Individual G shows that the level of recovery and identification was excellent and offers evidence for curated burials in the other individuals.

### *18.3.7: Assemblage*

Heaning Wood is a complex burial site. There are important implications for the dating, particularly the presence of Early Mesolithic remains. Movement and commingling have made

burial narratives difficult to construct. There is some evidence of a deposition level for Individual B, but this depends on queries around individuation. One of the key questions that remains is whether curation was happening with the Early Neolithic infants. Curation of the Mesolithic infant cannot be ruled out either, but the depth and length of time in the cave make it less likely. Table 18.1 outlines the evidence for and against curation.

Table 18.1: Evidence for and against curated burials at Heaning Wood.

| **Evidence For** | **Evidence Against** |
|---|---|
| BRI of Infants F and H limited to cranial only. | Depth and length of burial for Individual H. |
| BRI of Infant E limited to cranial and clavicles only. | Limited to infant remains*. |
| Individual G shows preservation, recovery, and recognition of small, juvenile remains. | No macroscopic evidence of exposure outside of Heaning Wood cave. |
| | Regular periods of infilling, including successive burials. |

*There is a possibility that differential treatment is occurring.

Clarity may be provided by histological techniques mentioned above (Booth, 2016; Booth and Madgwick, 2016; Booth and Brück, 2020; Brück and Booth, 2022) and will be discussed further in section 19.2.2. Before exploring implications for future research, Geographic Information Systems (GIS) as a tool for osteological analysis will be discussed.

## 18.4: Geographical Information Systems (GIS) as an Analytical Tool

The previous sections have offered an overview of the main findings associated with both caves, and have highlighted how in-depth analysis of taphonomy, even at the macroscopic level, can provide insight into burial narratives. Geographic Information Systems (GIS) have long since been used in archaeology for traditional spatial analysis as well as less conventional uses including skeletal analysis, dental topography, taphonomy, and bone histology (Zuccotti *et al.*, 1998; Ungar and Williamson, 2000; Marean *et al.*, 2001; Herrmann and Devlin, 2008; Rose *et al.*, 2012; Herrmann, Devlin and Stanton, 2014; Parkinson, Plummer and Bose, 2014; Garcia Moreno *et al.*, 2015; Parkinson, 2018; Stavrova *et al.*, 2019; Parkinson *et al.*, 2022). This study attempted to conduct human taphonomic analysis in a new way, using well-established software. This was neither a methodological project, nor a case study, rather a combination of the two. It aimed to offer quantitative and qualitative evidence for two cave assemblages, expanding the idea of treating bodies as a mappable space. The method has provided what it set out to do. It has offered insights that were previously unknown, for example burial positions in Cave Ha 3, and has shown the value in addressing the fragmented, commingled assemblages osteologists may want to shy away from. With the development of any method, however, there are inevitably areas where hindsight and retrospection lead to potential improvements. The following paragraphs provide an overview of how the method can be refined.

### *18.4.1: Templates and Recording Issues*

Although Marean and colleagues had kindly shared their templates from previous projects (Marean *et al.*, 2001), a non-standard template was needed to allow recording of multiple views. Additionally, infant templates were needed to reflect the different age estimations across both assemblages which meant that templates had to be created specifically for this project. Adult templates were relatively simple to produce, using a plastic skeletal model and photographing the required anatomical views. Issues arose with the development of infant and neonate templates. Cast models of infant skeletons are expensive and limited to specific ages, archaeological collections that have children of various ages are often fragmented, with access restricted, and photographs of child skeletons are limited. This is partly due to the limited recovery of infant remains in comparison to adults (Buckberry, 2000; Bello *et al.*, 2006;

Manifold, 2010), but perhaps also due to the sensitive nature of infant remains limiting images to academic and medical contexts. The templates for the infants were therefore developed using reference photographs from 'Juvenile Osteology: A Laboratory and Field Manual' (Scheuer, Black and Schaefer, 2008) and 'Developmental Juvenile Osteology' (Scheuer and Black, 2000). The illustrations in these volumes did not always provide multiple views, meaning anterior views had to be flipped to create an approximation of posterior views. Both the adult and juvenile templates were created without a coordinate reference system, nor to any scale. When photographs were tested to assess the use of GIS for MNI estimation it was found that, due to biological variations across humans, overlaying of fragments resulted in distortion. This was exacerbated by using cast materials and photographs that may have not retained consistency in angles, despite the use of strict photographing protocols. Since the project shifted its focus to taphonomy the decision was made to record modification manually. The size and scale of the templates in GIS was therefore not considered important and a representation was regarded as sufficient. The decision to draw the modifications and analyse them by frequency, however, introduced other biases.

Recording taphonomy as frequencies meant that some modifications, such as staining, ended up skewed. For example, spotted staining occasionally appeared more prolific than matte staining, despite covering less surface area. One alternative considered was the analysis of surface area. This would provide more detailed information on how affected a particular surface is. This relies on accurate drawings of modifications on templates that are to scale. This returns to the issue found when using photographs of fragments for MNI estimation. Since the templates are only an approximation, precise drawing of a modification to scale becomes difficult. Additionally, the templates would need to be redeveloped, so that they are to scale within GIS. To negate this issue an approach similar to Stavrova and colleagues (2019) and Parkinson, Plummer, and Bose (2014) could be employed. This involves recording the taphonomy as a single point on the template and would allow for cluster analysis and a more quantitative approach. This approach would be needed if the method were to be applied to microscopic taphonomy, the manual drawing of which would be incredibly difficult, if not impossible. For this research, however, part of the intention was to create a visualisation of taphonomy, which is often missing in more traditional recording methods. Lucas (2012) argues that maps should serve to reveal "assemblages that would be otherwise invisible to us" (cited

by Gillings, Hacıgüzeller and Lock, 2018, p. 14). The maps produced in this project gave life to taphonomy that is traditionally descriptive and are representations of what is visible.

Another issue was identified during the analysis stage. When developing templates, it was decided that multiple views of the vertebrae would be recorded due to their complex shape and concerns about missing important modifications. This resulted in skewing of data. Areas of the cave with vertebrae appeared to have more modifications, solely due to the increased number of surfaces recorded. Similarly, when exploring body level changes, the analysis of element group was affected. The data were adjusted within QGIS using the filter tool so that only anterior and posterior surfaces of vertebrae were included. This demonstrates the benefit of using a system that allows adjustments of data without having to re-record. Future applications of the method should consider the removal of some vertebral views. Research on the existing data could be conducted to see which views of the vertebra are most impacted by taphonomic changes and the templates changed to reflect this, however this may be site specific. A refinement of the templates is needed so that consistency of surfaces recorded is maintained throughout without having to manually adjust data at the analysis stage.

### *18.4.2: Placement of Fragments*

It was intended that two other assemblages would be included to augment the methodological portion of the research. Two assemblages were selected, Lesser Kelco and Sewell's cave, both from the Yorkshire Dales and cranial only depositions. All four assemblages had large numbers of cranial fragments that could not be identified, and the two cranial only assemblages proved difficult to both individuate and place within GIS. Lesser Kelco had a total of 46 fragments that could be placed, accounting for only 32.6% of the entire collection. This is before accounting for fragments that could be placed but not assigned to a specific individual. It was therefore considered to be unsuitable for this method. The placement of fragments and individuation for Sewell's cave was slightly better than Lesser Kelco (52.9% could be placed). Issues were encountered when it came to spatial data. Figure 18.8 shows the archive map, where the numbers relate to a finds list (figure 18.9).

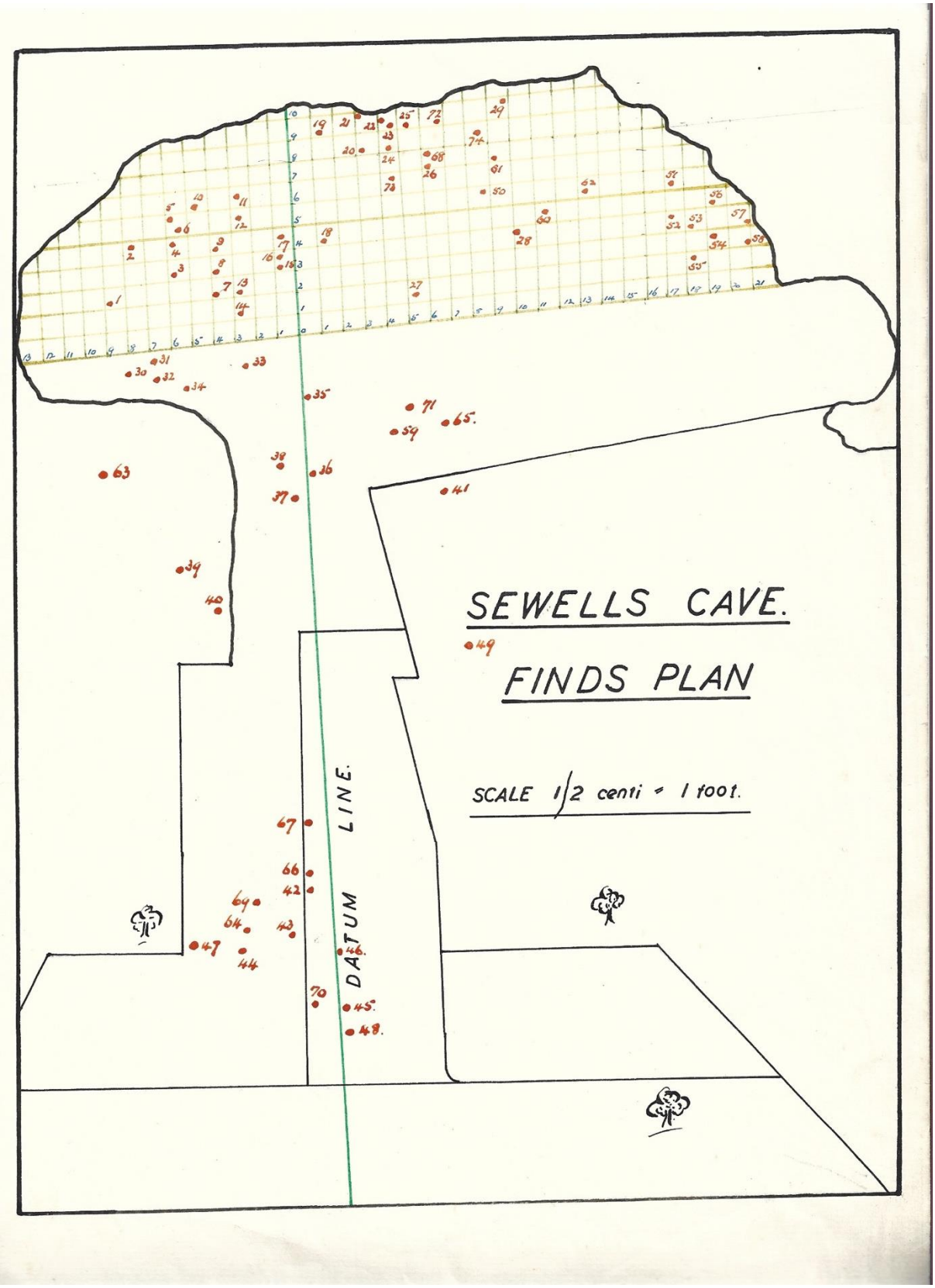


Figure 18.8: Archive map for Sewell's Cave {Citation}

| | Description | Ref.No. |
|---|---|---|
| 46. | Two fragments of iron wire found 3rd September 1933 at a depth of 2 feet | Iron 13 |
| 47. | Fragments of Neolithic Pottery found 27th August 1933 at a depth of 2 feet | |
| | A Trumpet Brooch, type R(ii)(Collingwood) Trumpet form head derived from pre-Roman type (Aylesford type) Central part of bow is a cushion or disc embraced by two members, each consisting of an acanthus. Foot circular with three moulds. Lower part of stem triangular section, rising to a low ridge down centre. Head loop and pin are missing Spring for pin present, period 100-150 AD North of England. Traces of the workshops where these were made are found at Brough-under-Stainmoor and Kirkby Thore in Westmorland. This is the best known type of Romano-British brooch. Examples were found at Elslack and other places in West Yorkshire found 27th August 1933 at a depth of 2 feet | Bronze Iron 1 |
| 48. | Tip of a knife found 10th September 1933 at a depth of 3 feet | Iron 5 |
| | Parts of Jaw and skull found 10th September 1933 at a depth of 1 foot 6 inches | |
| | A Bone toggle found 10th September 1933 at a depth of 1 foot 6 inches | Bone 5 |
| 49. | Fragments of Pottery found 29th November 1933 at a depth of 3 feet | |
| 50. | Fragments of Pottery found 11th February 1934 at a depth of 2 feet | |
| 51. | A piece of Flint found 11th March 1934 at a depth of 2 feet | |
| 52. | A Bronze Ring (plain) probably off harness trappings found on 11th March 1934 at a depth of 2 feet 6 inches | Bronze 7 |

Figure 18.9: Finds list for Sewell's Cave {Citation}

While it first appeared that there was sufficient spatial information there were ambiguities in the finds list, such as “parts of Jaw and skull found”. This meant that tying the location to the specific ‘jaw’ or ‘skull’ referenced was impossible. Sewell’s cave would have been limited to body level analysis, with near to half of the assemblage excluded, which led to the assemblage also being rejected for this analysis.

This method relies on the identification and placement of fragments. There were several fragments that could not be positioned for both Heaning Wood and Cave Ha 3. Despite this there were sufficient data to gain understanding around depositions. Working with old excavations and archive records can be frustrating, and it is tempting to reject a method completely when it is found to not fit all circumstances. Archaeological burials are nuanced, and a one size fits all approach is never going to work. While this method may not be suitable for all collections, the analysis of Heaning Wood and Cave Ha 3 has shown that there are benefits to in-depth analysis of older assemblages with patchy spatial recording and that it is possible to gain further understanding through such an approach.

# CHAPTER 19: CONCLUSION

## 19.1: The Bigger Picture: Heaning Wood and Cave Ha 3 in Context

### *19.1.1: Cave Morphology*

This study has shown that different processes were occurring at Heaning Wood and Cave Ha 3. Evidence from Cave Ha 3 indicates an extended, multistage burial rite. Manipulation of Individual 1 occurred at a specific point during decomposition when access to the tibia would have been facilitated by skeletonisation. The cave site is open, repeated visits to the bodies would have possible and the preservative properties of active tufa evident. The opposite is seen at Heaning Wood. This was also a site of successive burial, but lacks any evidence of extended, multistage rites. It is possible that there was another access point, but spatial analysis and the talus formation indicates that bodies were introduced from the vertical fissure. Repeated access to the bodies would have been difficult, if not impossible. If these were bodies subjected to extended practices this would have been the final point of deposition. There is no evidence, however, of previous exposure to other environments or deliberate manipulation.

Wysocki and Whittle (2000) argue that there was less of a concern in the Early Neolithic over preservation of the whole body, seen in the manipulation and circulation of remains. Disarticulation of bodies can be due to deliberate interference but natural, taphonomic factors can also be a driver (Beckett and Robb, 2006; Peterson, 2019, p.2). The preservative nature of caves is well discussed (Orschiedt, 2012; Schulting, 2016; Peterson, 2019, p.4) and Heaning Wood is an example of the cave acting on the body as the mechanism of transformation (Peterson, 2019, p.4) without complete destruction of the body.

The different morphologies of Heaning Wood and Cave Ha 3 are important. Cave Ha 3 offered a space that lent itself to extended burial rites and the preservative nature of Cave Ha 3 would have likely been evident (Leach, 2006a, 2006b, 2008). Tufa formation would have been active at the time (Pentecost *et al.*, 1990) and was understood in the Early Neolithic for its stone-like properties (Lewis *et al.*, 2019). This comprehension may have been the driver for deliberate

manipulation, preventing the tufa from retaining the full form. Here, both humans and natural processes are the agents of change.

### *19.1.2: Mesolithic Cave Burials*

Mesolithic burials are rare, both in the UK and Europe (Orschiedt, 2012; Hodgkins *et al.*, 2021). Of the cave burials that have been recovered, there has been evidence of cranial only and curated depositions. Ofnet, Hohlenstein-Stadel, Kaufertsberg, and Oberlarg are all described by Orschiedt (2012, p.215) as sites with "head burials". The dates are for these sites range from 6500-6000 Cal BC for Ofnet and Hohlenstein-Stadel, 6200-5900 Cal BC for Oberlarg and the Late Mesolithic horizon for Kaufertsberg. These all date later than the Heaning Wood Mesolithic infant with Hohlenstein-Stadel also showing evidence of violence. While there are some questions around curation possibilities for Individual F, it is not possible to determine when only one fragment is present. The fragment that survived would not typically be associated with blunt force trauma seen in interpersonal violence (Galloway and Wedel, 2014) and any evidence of deliberate detachment of the head would not be seen on the maxillae. Violence is not the only form of curated burials seen in the Early Mesolithic. Sites such as Blätterhöhle at Hagen and Margaux Cave, Belgium have shown both curation of bones and extended burial rites evidenced by cranial cut marks, absence of anatomical connections and individuals represented by single bones (Toussaint, 2011; Orschiedt, 2012). It is possible that Individual F fits the single bone, curated deposit narrative. The presence of one fragment with no evidence of exposure outside of Heaning Wood makes it difficult to interpret.

Individual F was estimated to be 2.5 – 3.5 years old. Hodgkins and colleagues (2021, p.6) argue that infant burials in the later Mesolithic were "treated similarly to adults in terms of burial rites" and were considered to have identity. It is possible that this also related to Early Mesolithic burials, however the difficulty lies in limited evidence and on occasion poor osteological information. The Mesolithic infant at Heaning Wood only accounts for one individual. The absence of other Mesolithic burials in the cave mean inferences around the treatment of different demographics is impossible. It may be tempting to stray into interpretations that place an emphasis on it being a young child, but this should be avoided without comparators. Shell beads were also recovered at Heaning Wood, with one dating to 9120-8630 Cal BC. Unfortunately, the lack of stratigraphic information meant that any possible

association to Individual F was lost. It is worth noting, however, that infant burials with artefacts have been found. An infant burial from Arma Veirana, North West Italy was recovered in a shallow grave in the cave floor. Several shell beads were associated to the burial and were not considered to be funeral specific but rather 'passed on' at the point of burial (Hodgkins et al., 2021; Gravel-Miguel et al., 2022). Gravel-Miguel and colleagues (2022) discuss the importance of such burial goods, highlighting the connection to personhood and social identity within the Early Mesolithic.

The little that is known about Mesolithic burials indicate that processes were varied and complex. Unfortunately, the discovery of Individual F at Heaning Wood has not added much to the understanding due to being represented by a single fragment. Limited spatial data has also hindered interpretations. It is significant, however, in that it adds evidence to Early Mesolithic occupation in the North of England and is currently the earliest human burial from the area. Discussions around the reoccupation of Britain after the last Ice Age previously focussed on archaeological evidence from the south (Evison, 1999). Recent research into the changes in climate have shown that areas around North Yorkshire and the Pennines would have been "key arterial communication routes" (Hudson *et al.*, 2023, p. 418) and one of the most important British Early Mesolithic occupation sites, Star Carr, is also located near to the region to the South East of the North York Moors National Park (Milner, Conneller and Taylor, 2018). Despite this, burials dating to the Mesolithic are rare. Meiklejohn, Chamberlain and Schulting (2011) described eighteen sites with human remains dating to the Mesolithic, with an absence of any sites located in the North of England. In 2013 a portion of femur found in Kent's Bank Cavern was dated to 9100 ± 35 $^{14}$C a BP (Smith, Wilkinson and O'Regan, 2013). At the time this made it the earliest known human burial from the North and was considered to be contemporary with remains such as those found at Aveline's Hole, in the South West of Britain. Individual F pre-dates Kent's Bank Cavern and provides further support for the reoccupation of Britain occurring in the North West, simultaneously with occupation in the South.

### *19.1.3: Neolithic Cave Burials*

Cave burial rites in the North of England show varying practices, often with secondary, or multi-stage funerals (Peterson, 2019, p.125). Sewell's cave and Lesser Kelco Cave (North

Yorkshire) are two examples of curated burials, where crania were selected. These caves were proposed for analysis, but due to methodological and time issues were excluded (see section 18.4.2). The Early Neolithic burials at Heaning Wood appear to be primary, whole-body, successive inhumations. Heaning Wood is not the only example of primary cave burials, however, primary burial is considered rare (Peterson, 2019, p154). The morphology of Heaning Wood makes the cave unlikely to be a place where there was intention of returning to the deposited bodies. It is possible that some curation was occurring, as discussed in relation to the juvenile remains. If this is the case, then it challenges whether there are different practices taking place within the same cave and whether demographics impact the type of rite practised. Thompson and colleagues (2020) suggest that younger burials would occasionally inform subsequent burials of older individuals. It is possible that this is occurring at Heaning Wood, however, their findings were specific to the European Late Neolithic. It may also be that the infant remains at Heaning Wood, if secondary internments, were introduced as part of the burial rites of the adult remains. Heaning Wood has proved to be a difficult assemblage to understand. The combination of poor spatial data along with movement of fragments across several metres masked possible associations. Peterson (2019, p.154) highlights several caves where burial rites are unclear and it may be that Heaning Wood remains such a site.

### *19.1.4: Bronze Age Cave Burials*

Orschiedt (2012) describes a reluctance to acknowledge cave remains dating to the Bronze Age and beyond as burials. It is evident, however, that caves were being used as burial sites, both in the UK and beyond (Leach, 2006a, 2006b; Orschiedt, 2012; Dowd, 2015, p.125; Peterson, 2019). While Leach (2006a, 2006b) warns against an overemphasis on cave burials from this period due to incorrect dating by artefact association, her work on Yorkshire cave burials reports five sites with radiocarbon dates to the Late Neolithic/Early Bronze Age, with some dates falling within what would be considered the transition phase. Leach (2006b, p. 388) describes cave burials in Yorkshire, and more widely, as a continuous practice "without significant chronological hiatus of activities" between the Early and Middle Neolithic, until a gap occurs in the practice. Cave burials are then resumed during the Late Neolithic and Early Bronze Age (Chamberlain, 1996), with this pattern reflected at Heaning Wood. There are distinct gaps in burials that cannot be explained by destruction of remains which suggests that

the Early Bronze Age burials here were not a case of continuing Neolithic or even Mesolithic practice. It is important, however, to consider that the spike in Early Neolithic cave burials is often related to sites with single radiocarbon dates and it is possible that these are successive burials dating to more than one period. More comprehensive dating such as that conducted at Heaning Wood would help work towards a better understanding of these patterns.

Bronze Age burials have been described as complex and varied (Brück, 2004) with practices often involving enclosure, wrapping, re-use of space, defleshing and excarnation (Brück, 2004; Booth and Brück, 2020; Brück and Booth, 2022). The Early Bronze Age burials at Heaning Wood do not offer clear narratives due to the limited spatial data. They do, however, fall within what would have been expected for burial practices within the period. Single inhumation and cremation with a shift to focusing on the individual are often claimed to be typical of Bronze Age burials (Brück, 2004; Teather and Chamberlain, 2016), although occurrences of curation and commingled burials are not unusual. Booth and Brück (2020) describe evidence of curated burials with fragments of older remains being reintroduced into newer burials. These curated bones typically originated from two generations before and likely come from individuals who were within living memory of the society doing the curation. There is nothing to suggest that this was practiced at Heaning Wood due to the length of time between dates. There was an absence of evidence of the bones being exposed to any other environment than the cave and re-use of the site and commingling of bodies counter the emphasis placed on individualism.

## 19.2: Where Next? Implications for Future Research

Insights into the burials at Cave Ha 3 have been more forthcoming than those at Heaning Wood. Poor spatial recording, movement, and comingling created difficulties in understanding taphonomic and burial sequences. The method applied has, however, highlighted new information. The burial positions of two of Cave Ha 3's burials are now better understood. Visualisations of taphonomy have been created and are held in an open access format. The maps produced give life to taphonomy that is traditionally descriptive or codes on a spreadsheet. The taphonomy analysed is not exhaustive and is limited to macroscopic analysis. An extension to this method would be to explore what cannot be seen on the surface. The mapping of histological and microscopic changes, embedded within the layers of

macroscopic modifications, would further enhance the taphonomic analysis and interpretations. Deeper analyses at body and stratigraphic levels will shape our understanding of patterns of destruction in cave burials.

### *19.2.1: Alternative Visualisations*

Due to time constraints alternative versions of visualisations were not included in the main analysis. It is possible to express the distribution of fragments using the body rather than a traditional map. This works particularly well for Heaning Wood due to the spatial data representing depths. Figures 19.1 and 19.2 show an alternative way of representing the spread of fragments across the cave for Individuals A and B.

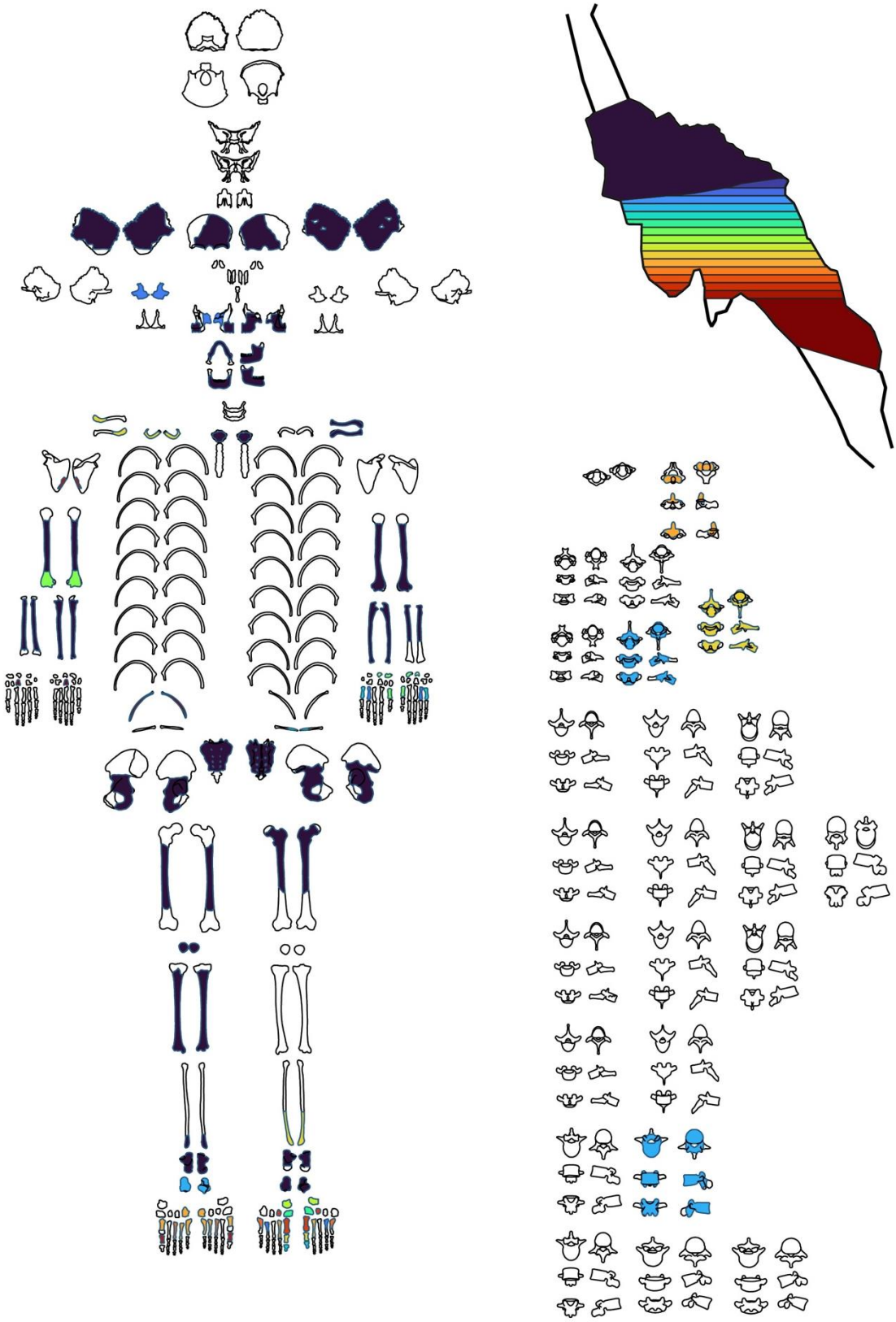

Figure 19.1: Distribution of fragments from Individual A according to depth.

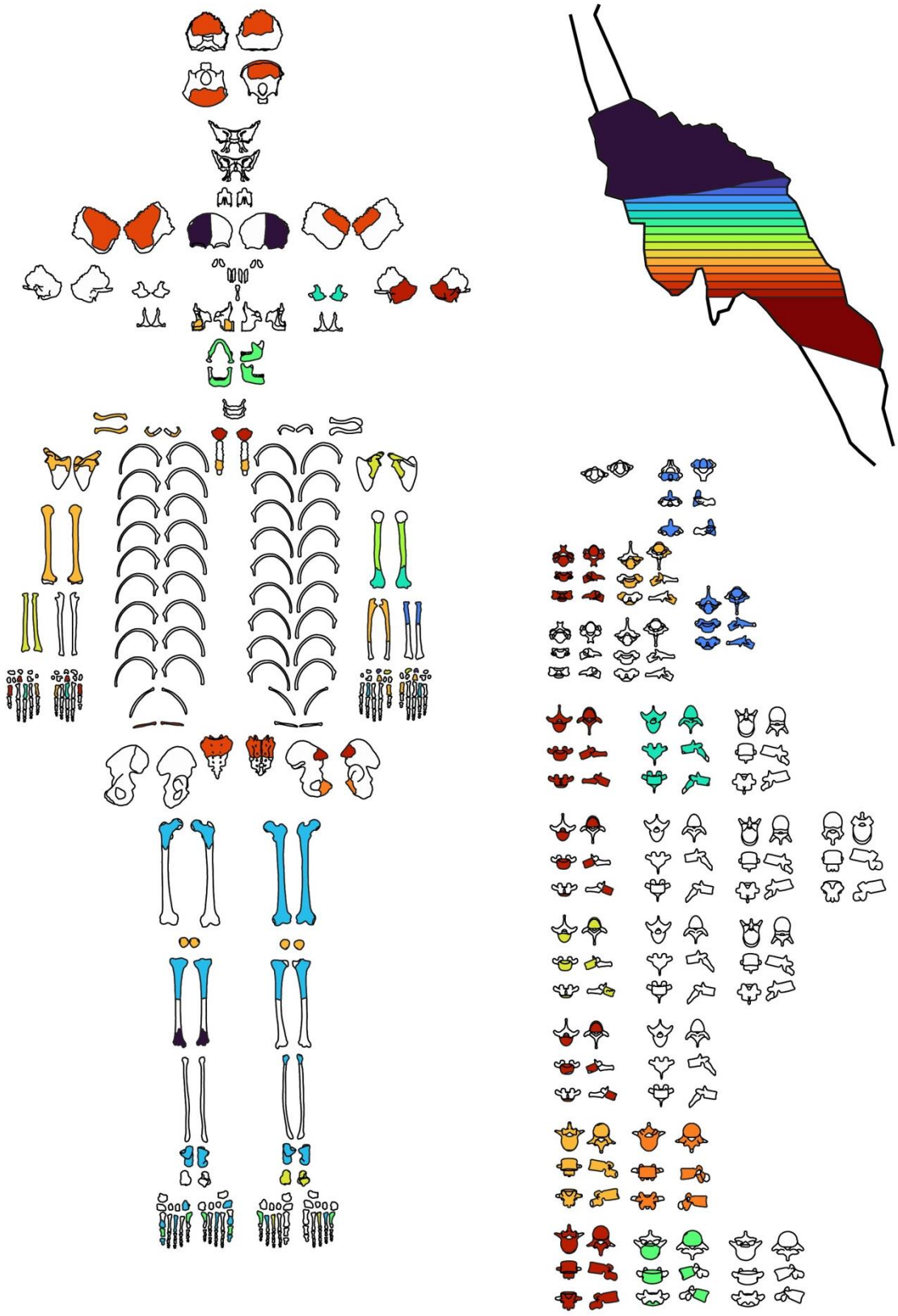

Figure 19.2: Distribution of fragments from Individual B according to depth.

From these images it is possible to see the concentration of Individual A towards the top of the cave and the increased dispersal of smaller elements such as the pedal bones. This can be compared to the increased spread of fragments from Individual B. This shows the diversity of using QGIS for such analyses.

The illustrations above work to overcome some of the data limitations encountered at Heaning Wood, providing a more accessible overview of the movement of fragments. The lack of contexts, resulting in flat spits, simplify the complex 3D nature of the site. Data visualisations that employ 3D techniques, such as those discussed by Randolph-Quinney, Haines and Kruger (2018) and Dell'Unto and Landeschi (2022) would extend possible analyses of the taphonomic data. High quality recording is, however, required for such techniques. With full 3D spatial recording it would be possible to combine the elements and body level taphonomy with the spatial maps to create a truly multiscale map.

### *19.2.2: Histological and Microscopic Analysis*

There has been some suggestion that bone histology can indicate whether there has been processing of a body, in the form of multi-stage rites. If microbial destruction of bone originates from bacteria in the gut, then it is posited that processing of bodies will reduce exposure to internal bacteria and therefore lower levels of histotaphonomic damage will be seen (Mavroudas *et al.*, 2023). Analysis of bone histology may then offer the potential to answer some of the questions around primary and secondary burials raised by the Early Neolithic individuals at Heaning Wood (Booth, 2016; Booth and Madgwick, 2016; Booth and Brück, 2020; Bricking, Hayes and Madgwick, 2022; Brück and Booth, 2022). The method may not be as clear-cut as first anticipated, however, and there appears to be a lack of clarity as to the origin and timings of bacterial attack (Mavroudas *et al.*, 2023). Mavroudas and colleagues (2023) suggest that the sensitivity of scoring systems of histological changes may be too coarse and highlight the need to look at archaeological samples within the context of the burial environment. Heaning Wood would offer an opportunity to look at diagenesis of bones buried in cave environments and to explore the relationship between macroscopic, microscopic, and histological changes. These data could then be used as a comparator for other burials across different environments.

### *19.2.3: Biochemical Analysis*

Analysis of the deposits and staining was limited to visual appearance. The deposits on Heaning Wood were variable, with some having the appearance of soil build up, rather than the lighter deposits consistent with tufa. These were noted within GIS but not coded for separately as they had not been chemically tested. The staining was interpreted from macroscopic analysis with black-mottled staining interpreted as manganese, but it is emphasised that this is not definitive. Research into the biochemistry of the modifications would help differentiate processes, particularly regarding staining and deposits. Biochemical analysis could then be linked to patterns of diagenesis as well as explored spatially to see if any further insights into burial practices, cave taphonomy and diagenesis can be made.

### *19.2.4: Ancient DNA and Isotope Analysis*

Ancient DNA and isotope analysis of the remains can go further than understanding the burials and start to explore the lives of those buried at Cave Ha 3 and Heaning Wood. Isotopic analysis can provide insight into diet, nutrition and disease as well as revealing "information about place of residence and migration" (Katzenberg and Waters-Rist, 2018, p. 469). Ancient DNA can provide anthropological information such as genetic sex, as well as information on migration and population origins (Nieves-Colón and Stone, 2018). Testing has already been conducted on two of the individuals from Cave Ha 3 (Booth, 2019) and samples have been taken from the Heaning Wood assemblage. These results will be added to an already growing data set of genetic information on Mesolithic and Neolithic burials in Britain (Brace *et al.*, 2019).

### *19.2.5: Excavation and Faunal and Artefact Analysis*

Further excavation of Cave Ha 4 is needed to establish the origin of the adult ulna currently held in the Cave Ha 3 collection. To reach the full potential of using GIS as a tool for taphonomic and osteological analysis, proper in-situ recording of all fragments recovered is needed. X, Y and Z coordinates of bone locations, along with measurements of fragments, will allow the coalescence of taphonomic data with spatial. Additionally, where funding and resources allow, the 3D recording of bone fragments, both in-situ and post excavation, has the potential to enhance the method further. Such 3D recording is discussed in detail by Dell'Unto and Landeschi (2022).

Additionally, full analysis of the Heaning Wood faunal material and artefacts, including spatial relationships with the human material, would help further our understanding of human-animal social relationships in prehistory.

## 19.3 Conclusion

This research aimed to assess whether Geographic Information Systems (GIS) can be used to explore the taphonomy of fragmented and commingled cave burials from the Early Neolithic. By applying digital methods to the macroscopic taphonomic analysis of two case studies it has been possible to understand burial narratives, demonstrating that GIS is an appropriate tool for taphonomic analysis.

The method has highlighted potential burial positions for Cave Ha 3, providing new information about a site that has previously been well-analysed. It has also helped to unravel the burials at Heaning Wood, despite missing key spatial information.

The thesis provides the most comprehensive analysis of Heaning Wood to date, combining material from three different excavations. Radiocarbon dating showed successive use over several periods with long hiatuses, as well as uncovering the oldest human burial in the North of Britain. The dating of four individuals to the Early Neolithic changes previous discourse around the absence of Early Neolithic cave burials along the south coast of Cumbria. The Early Mesolithic date also provides support for the reoccupation of Britain occurring in the North West, simultaneous with occupation in the South, challenging more traditional narratives.

This thesis has highlighted opportunities for future research that will further our understanding of cave burials in the region, as well as offering a method of taphonomic analysis that goes beyond traditional recording systems of presence and absence. The quality of the spatial data for Heaning Wood and Cave Ha 3 meant that the method did not reach its full potential. With more detailed recording at the point of excavation it would be possible to combine taphonomic analyses with the spatial. It is recommended that future excavations record, at a minimum, the X, Y and Z coordinates, along with the related measurements of the

fragment. As discussed in section 19.2.5, where possible 3D recording can also be implemented. This would allow for true multiscale maps, where the user can move from a geographical overview into individual fragments and the recorded taphonomic modifications.

# REFERENCES


Abe, Y. *et al.* (2002) 'The analysis of cutmarks on archaeofauna: a review and critique of quantification procedures, and a new image-analysis GIS approach.', *American Antiquity*, 67(4), pp. 643–663.

Adams, B.J. and Crabtree, P.J. (2008) *Comparative Skeletal Anatomy. A Photographic Atlas for Medical Examiners, Coroners, Forensic Anthropologists, and Archaeologists, Totowa (NJ): Humana Press.* Totowa (NJ): Humana Press.

Adams, B.J. and Königsberg, L.W. (2004) 'Estimation of the most likely number of individuals from commingled human skeletal remains', *American Journal of Physical Anthropology*, 125(2), pp. 138–151. Available at: https://doi.org/10.1002/ajpa.10381.

Aldenderfer, M. (1996) 'Introduction', in M. Aldenderfer and H.D.G. Maschner (eds) *Anthropology, Space and Geographic Information Systems*. New York Oxford: Oxford University Press, pp. 3–18.

AlQahtani, S.J., Hector, M.P. and Liversidge, H.M. (2010) 'Brief communication: The London atlas of human tooth development and eruption', *American Journal of Physical Anthropology*, 142(3), pp. 481–490. Available at: https://doi.org/10.1002/ajpa.21258.

Alt, K.W. *et al.* (2016) 'A Community in Life and Death: The Late Neolithic Megalithic Tomb at Alto de Reinoso (Burgos, Spain)', *PLOS ONE*. Edited by S.E. Halcrow, 11(1), p. e0146176. Available at: https://doi.org/10.1371/journal.pone.0146176.

Andrews, P. (1990) *Owls, Caves and Fossils*. The University of Chicago Press.

Andrews, P. (1995) 'Experiments in taphonomy', *Journal of Archaeological Science*, 22(2), pp. 147–153. Available at: https://doi.org/10.1006/jasc.1995.0016.

Ashbee, P. (1966) 'I.—The Fussell's Lodge Long Barrow Excavations 1957', *Archaeologia*, 100, pp. 1–80. Available at: https://doi.org/10.1017/S0261340900013709.

Badiella, C.M. (2020) 'Experiencing the limits', *Scripta Instituti Donneriani Aboensis*, 29, pp. 147–168. Available at: https://doi.org/10.30674/scripta.85214.

Barnatt, J. and Edmonds, M. (2002) 'Places apart? Caves and monuments in Neolithic and earlier Bronze Age Britain', *Cambridge Archaeological Journal*, 12(1), pp. 113–129. Available at: https://doi.org/10.1017/S0959774302000069.

Barrett, L. *et al.* (2004) 'Habitual cave use and thermoregulation in chacma baboons (Papio hamadryas ursinus)', *Journal of Human Evolution*, 46(2), pp. 215–222. Available at: https://doi.org/10.1016/j.jhevol.2003.11.005.

Barton, N. *et al.* (2008) 'Human burial evidence from Hattab II Cave and the question of continuity in late Pleistocene-Holocene mortuary practices in northwest Africa', *Cambridge Archaeological Journal*, 18(2), pp. 195–214. Available at: https://doi.org/10.1017/S0959774308000255.

Bayliss, A. *et al.* (2011) 'Neolithic narratives: British and Irish enclosures in their timescapes', in Alasdair Whittle, F. Healy, and Alex Bayliss (eds) *Gathering Time. Dating the Early Neolithic Enclosures of Southern Britain and Ireland. Volume 2*. Oxford, UK: Oxbow Books, pp. 682–847.

Beckett, J. and Robb, J. (2006) 'Neolithic burial taphonomy, ritual and interpretation in Britain and Ireland: a review.', in R.L. Gowland and C.J. Knüsel (eds) *The Social Archaeology of Funerary Remains*. Oxford: Oxbow Books, pp. 57–80.

Beckett, J.F. (2011) 'Interactions with the Dead: A Taphonomic Analysis of Burial Practices in Three Megalithic Tombs in County Clare, Ireland', *European Journal of Archaeology*, 14(3), pp. 394–418. Available at: https://doi.org/10.1179/146195711798356719.

Behrensmeyer, A.K. (1978) 'Taphonomic and Ecologic Information from Bone Weathering', *Paleobiology*, 4(2), pp. 150–162.

Belcastro, M.G., Rastelli, E. and Mariotti, V. (2008) 'Variation of the degree of sacral vertebral body fusion in adulthood in two European modern skeletal collections', *American Journal of Physical Anthropology*, 135(2), pp. 149–160. Available at: https://doi.org/10.1002/ajpa.20716.

Bello, S.M. *et al.* (2006) 'Age and sex bias in the reconstruction of past population structures', *American Journal of Physical Anthropology*, 129(1), pp. 24–38. Available at: https://doi.org/10.1002/ajpa.20243.

Bello, S.M. *et al.* (2015) 'Upper Palaeolithic ritualistic cannibalism at Gough's Cave (Somerset,UK): THE human remains from head to toe', *Journal of Human Evolution*, 82, pp. 170–189. Available at: https://doi.org/10.1016/j.jhevol.2015.02.016.

Bello, S.M. *et al.* (2016) 'Cannibalism versus funerary defleshing and disarticulation after a period of decay: comparisons of bone modifications from four prehistoric sites', *American Journal of Physical Anthropology*, 161(4), pp. 722–743. Available at: https://doi.org/10.1002/ajpa.23079.

Bello, S.M. *et al.* (2017) 'An Upper Palaeolithic engraved human bone associated with ritualistic cannibalism', *PLoS ONE*, 12(8), pp. 0–12. Available at: https://doi.org/10.1371/journal.pone.0182127.

Bello, S.M. and Andrews, P. (2006) 'The intrinsic pattern of preservation of human skeletons and its influence on the interpretation of funerary behaviour', in R. Gowland and C.J. Knüsel (eds) *Social Archaeology of Funerary Remains*. Oxbow Books, pp. 1–13.

Bello, S.M., Parfitt, S.A. and Stringer, C.B. (2011) 'Earliest directly-dated human skull-cups', *PLoS ONE*, 6(2). Available at: https://doi.org/10.1371/journal.pone.0017026.

Bennett, J.L. (1999) 'Thermal alteration of buried bone', *Journal of Archaeological Science*, 26(1), pp. 1–8. Available at: https://doi.org/10.1006/jasc.1998.0283.

Berger, L.R. *et al.* (2015) 'Homo naledi, a new species of the genus Homo from the Dinaledi Chamber, South Africa', *eLife*, 4(September2015), pp. 1–35. Available at: https://doi.org/10.7554/eLife.09560.

Bertsatos, A. and Chovalopoulou, M.E. (2020) 'Advances in Osteometric Sorting: Utilizing Diaphyseal CSG Properties for Lower Limb Skeletal Pair-Matching', *Journal of Forensic Sciences*, 65(5), pp. 1400–1405. Available at: https://doi.org/10.1111/1556-4029.14480.

Bidmos, M. and Asala, S. (2005) 'Calcaneal measurement in estimation of stature of South African blacks', *American Journal of Physical Anthropology*, 126(3), pp. 335–342. Available at: https://doi.org/10.1002/ajpa.20063.

Bidmos, M.A. (2008) 'Estimation of stature using fragmentary femora in indigenous South Africans', *International Journal of Legal Medicine*, 122(4), pp. 293–299. Available at: https://doi.org/10.1007/s00414-007-0206-2.

Binford, L.R. (1978) 'Dimensional Analysis of Behavior and Site Structure: Learning from an Eskimo Hunting Stand', *American Antiquity*, 43(3), pp. 330–361. Available at: https://doi.org/10.2307/279390.

Binford, L.R. (1981) *Bones: Ancient Men and Modern Myths*. London: Academic Press.

Binford, L.R. (1985) 'Human ancestors: Changing views of their behavior', *Journal of Anthropological Archaeology*, 4(4), pp. 292–327. Available at: https://doi.org/10.1016/0278-4165(85)90009-1.

Blumenschine, R.J. (1988) 'An experimental model of the timing of hominid and carnivore influence on archaeological bone assemblages', *Journal of Archaeological Science*, 15(5), pp. 483–502. Available at: https://doi.org/10.1016/0305-4403(88)90078-7.

Boaz, N.T. and Behrensmeyer, A.K. (1976) 'Hominid taphonomy: Transport of human skeletal parts in an artificial fluviatile environment', *American Journal of Physical Anthropology*, 45(1), pp. 53–60. Available at: https://doi.org/10.1002/ajpa.1330450107.

Bocquet-Appel, J.P. *et al.* (2009) 'Detection of diffusion and contact zones of early farming in Europe from the space-time distribution of 14C dates', *Journal of Archaeological Science*, 36(3), pp. 807–820. Available at: https://doi.org/10.1016/j.jas.2008.11.004.

Bombieri, G. *et al.* (2018) 'Patterns of wild carnivore attacks on humans in urban areas', *Scientific Reports*, 8(1), pp. 1–9. Available at: https://doi.org/10.1038/s41598-018-36034-7.

Bombieri, G. *et al.* (2019) 'Brown bear attacks on humans: a worldwide perspective', *Scientific Reports*, 9(1), pp. 1–10. Available at: https://doi.org/10.1038/s41598-019-44341-w.

Bonsall, C.T. and Tolan-Smith, C. (1997) *The human use of caves*, *BAR International Series*, p. 219.

Booth, T.J. (2016) 'An Investigation into the Relationship Between Funerary Treatment and Bacterial Bioerosion in European Archaeological Human Bone: Funerary treatment and

bacterial bioerosion in human bone', *Archaeometry*, 58(3), pp. 484–499. Available at: https://doi.org/10.1111/arcm.12190.

Booth, T.J. (2019) 'British Prehistory in Microcosm: Human Ancient DNA from the Craven Caves', *Prehistoric Yorkshire*, 56, pp. 6–16.

Booth, T.J. and Brück, J. (2020) 'Death is not the end: radiocarbon and histo-taphonomic evidence for the curation and excarnation of human remains in Bronze Age Britain', *Antiquity*, 94(377), pp. 1186–1203. Available at: https://doi.org/10.15184/aqy.2020.152.

Booth, T.J. and Madgwick, R. (2016) 'New evidence for diverse secondary burial practices in Iron Age Britain: A histological case study', *Journal of Archaeological Science*, 67, pp. 14–24. Available at: https://doi.org/10.1016/j.jas.2016.01.010.

Borić, D. and Griffiths, S. (2015) 'The Living and The Dead, Memory and Transition: Bayesian Modelling of Mesolithic and Neolithic Deposits from Vlasac, the Danube Gorges', *Oxford Journal of Archaeology*, 34(4), pp. 343–364. Available at: https://doi.org/10.1111/ojoa.12063.

Brace, S. *et al.* (2019) 'Ancient genomes indicate population replacement in Early Neolithic Britain', *Nature Ecology & Evolution*, 3(5), pp. 765–771. Available at: https://doi.org/10.1038/s41559-019-0871-9.

Brain, C.K. (1981) *The Hunters or the Hunted? An Introduction to African Cave Taphonomy*. Chicago: The University of Chicago Press.

Bramanti, B. *et al.* (2009) 'Genetic Discontinuity Between Local Hunter-Gatherers and Central Europe's First Farmers', *Science*, 326(5949), pp. 137–140. Available at: https://doi.org/10.1126/science.1176869.

Bricking, A., Hayes, A. and Madgwick, R. (2022) 'An interim report on the histological analysis of human bones from Fishmonger's Swallet, Gloucestershire', *Proceedings of the University of Bristol Speleological Society*, 29(1), pp. 67–86.

Brickley, M. and McKinley, J.I. (2004) 'Guidelines to the Standards for Recording Human Remains', (7).

Brooks, S. and Suchey, J.M. (1990) 'Skeletal age determination based on the os pubis: a comparison of the Acsádi-Nemeskéri and Suchey-Brooks methods.', *Human Evolution*, 5, pp. 227–238.

Brothwell, D.R. (1981) *Digging Up Bones*. London: Natural History Museum Publications.

Brouwer Burg, M. (2017) 'It must be right, GIS told me so! Questioning the infallibility of GIS as a methodological tool', *Journal of Archaeological Science*, 84, pp. 115–120. Available at: https://doi.org/10.1016/j.jas.2017.05.010.

Brück, J. (2004) 'Material metaphors: The relational construction of identity in Early Bronze Age burials in Ireland and Britain', *Journal of Social Archaeology*, 4(3), pp. 307–333. Available at: https://doi.org/10.1177/1469605304046417.

Brück, J. and Booth, T.J. (2022) 'The Ambivalent Dead: Curation, Excarnation and Complex Post-mortem Trajectories in Middle and Late Bronze Age Britain', *Proceedings of the Prehistoric Society*, 88, pp. 193–220. Available at: https://doi.org/10.1017/ppr.2022.8.

Bruzek, J. (2002) 'A method for visual determination of sex, using the human hip bone', *American Journal of Physical Anthropology*, 117(2), pp. 157–168. Available at: https://doi.org/10.1002/ajpa.10012.

Buckberry, J. (2000) 'Missing, Presumed Buried? Bone Diagenesis and the Under-Representation of Anglo-Saxon Children.', *Assemblage*, 5. Available at: http://core.kmi.open.ac.uk/download/pdf/135012.pdf.

Buckberry, J. and Chamberlain, A.T. (2002) 'Age estimation from the auricular surface of the ilium: a revised method.', *American Journal of Physical Anthropology*, 119(3), pp. 231–239.

Buikstra, J.E. and Ubelaker, D.H. (1994) 'Standards for data collection from human skeletal remains.', in *Arkansas archaeological survey research series*.

Bunn, H.T. (1981) 'Archaeological evidence for meat-eating by Plio-Pleistocene hominids from Koobi Fora and Olduvai Gorge', *Nature*, 291(5816), pp. 574–577. Available at: https://doi.org/10.1038/291574a0.

Bunn, H.T. (1983) 'Comparative analsysis of modern bone assemblages from a San huntergatherer camp in the Kalahari Desert, Botswana, and from a spotted hyene den near Nairobi, Kenya', in J. Clutton-Brock (ed.) *Animals and archaeology. 1. Hunters and their prey*. Oxford: BAR International Series, pp. 143–148.

Bunn, H.T. (1986) 'Patterns of skeletal representation and hominid subsistence activities at Olduvai Gorge, Tanzania, and Koobi Fora, Kenya', *Journal of Human Evolution*, 15(8), pp. 673–690. Available at: https://doi.org/10.1016/S0047-2484(86)80004-5.

Cannon, M.D. (2013) 'NISP, Bone Fragmentation, and the Measurement of Taxonomic Abundance', *Journal of Archaeological Method and Theory*, 20(3), pp. 397–419. Available at: https://doi.org/10.1007/s10816-012-9166-z.

Cappella, A. *et al.* (2017) 'The Issue of Age Estimation in a Modern Skeletal Population: Are Even the More Modern Current Aging Methods Satisfactory for the Elderly?', *Journal of Forensic Sciences*, 62(1), pp. 12–17. Available at: https://doi.org/10.1111/1556-4029.13220.

Caruso, V. *et al.* (2021) 'Diagenesis of juvenile skeletal remains: A multimodal and multiscale approach to examine the post-mortem decay of children's bones', *Journal of Archaeological Science*, 135, p. 105477. Available at: https://doi.org/10.1016/j.jas.2021.105477.

Castaños, J. *et al.* (2019) 'A large mammal assemblage during MIS 5c: Artazu VII (Arrasate, northern Iberian Peninsula)', *Historical Biology*, 31(6), pp. 731–747. Available at: https://doi.org/10.1080/08912963.2017.1389923.

Casteel, R. and Grayson, D. (1977) 'Terminological problems in quantitative faunal analysis', *World Archaeology*, 9, pp. 235–242.

Casteel, R.W. (1977) ‘Characterization of faunal assemblages and the minimum number of individuals determined from paired elements: Continuing problem in archaeology’, *Journal of Archaeological Science*, 4(2), pp. 125–134. Available at: https://doi.org/10.1016/0305-4403(77)90059-0.

Chamberlain, A.T. (1996) ‘More dating evidence for human remains in British caves’, *Antiquity*, 70(270), pp. 950–953. Available at: https://doi.org/10.1017/S0003598X00084222.

Chamberlain, A.T. (2013) ‘Caves and the Funerary Landscape of Prehistoric Britain.’, in H. Moyes (ed.) *Sacred Darkness: A Global Perspective on the Ritual Use of Caves*. University Press of Colorado, pp. 135–143. Available at: https://ebookcentral.proquest.com/lib/uclan-ebooks/detail.action?docID=3039789. (Accessed: 21 June 2023).

Channarayapatna, S. *et al.* (2018) ‘Application du SIG pour l’étude de la distribution de divers agents taphonomiques et leurs effets sur les restes fauniques du niveau 3 colluvium d’isernia la pineta: données préliminaires’, *Quaternaire*, 29(1), pp. 31–38.

Clark, K.M. (2015) ‘Dogs and Wolves in the Neolithic of Britain’, in D. Serjeantson and D. Field (eds) *Animals in the Neolithic of Britain and Europe*. Havertown: Oxford Books, Limited, pp. 32–41. Available at: https://doi.org/10.2307/j.ctt1w1vjbn.11.

Coard, R. (1999) ‘One bone, two bones, wet bones, dry bones: Transport potentials under experimental conditions’, *Journal of Archaeological Science*, 26(11), pp. 1369–1375. Available at: https://doi.org/10.1006/jasc.1999.0438.

Coard, R. and Dennell, R.W. (1995) ‘Taphonomy of Some Articulated Skeletal Remains: Transport Potential in an Artificial Environment’, *Journal of Archaeological Science*, 22(3), pp. 441–448. Available at: https://doi.org/10.1006/jasc.1995.0043.

Conneller, C. *et al.* (2016) ‘The Resettlement of the British Landscape: Towards a chronology of Early Mesolithic lithic assemblage types.’, *Internet Archaeology* [Preprint], (42). Available at: https://doi.org/10.11141/ia.42.12.

Cox, S.L. *et al.* (2019) ‘Genetic contributions to variation in human stature in prehistoric Europe’, *Proceedings of the National Academy of Sciences*, 116(43), pp. 21484–21492. Available at: https://doi.org/10.1073/pnas.1910606116.

Cruz-Uribe, K. (1991) ‘Distinguishing hyena from hominid bone accumulations’, *Journal of Field Archaeology*, 18(4), pp. 467–486. Available at: https://doi.org/10.1179/009346991791549068.

Cummings, V. (2017) *The Neolithic of Britain and Ireland*. London and New York: Routledge (Routledge Archaeology of Northern Europe). Available at: https://doi.org/10.4324/9781315718866.

Cummings, V. and Whittle, A. (2004) ‘Stones that float to the sky: seeing place, myth and history’, *Places of Special Virtue. Megaliths in the Neolithic landscapes of Wales*, pp. 69–91.

Dabkowski, J. (2014) 'High potential of calcareous tufas for integrative multidisciplinary studies and prospects for archaeology in Europe', *Journal of Archaeological Science*, 52(December 2014), pp. 72–83. Available at: https://doi.org/10.1016/j.jas.2014.07.013.

Davies, P. and Robb, J.G. (2002) 'The appropriation of the material of places in the landscape: The case of tufa and springs', *Landscape Research*, 27(2), pp. 181–185. Available at: https://doi.org/10.1080/01426390220128659.

De Groote, I. and Humphrey, L.T. (2011) 'Body mass and stature estimation based on the first metatarsal in humans', *American Journal of Physical Anthropology*, 144(4), pp. 625–632. Available at: https://doi.org/10.1002/ajpa.21458.

Dell'Unto, N. and Landeschi, G., 2022. *Archaeological 3D GIS*. Taylor & Francis.

Dirks, P.H.G.M. *et al.* (2015) 'Geological and taphonomic context for the new hominin species Homo naledi from the Dinaledi Chamber, South Africa', *eLife*, 4(September2015), pp. 1–37. Available at: https://doi.org/10.7554/eLife.09561.

Dobney, K. and Rielly, K. (1988) 'A method for recording archaeological animal bones: the use of diagnostic zones', *CIRCAEA - Bulletin of the Association for Environmental Archaeology*, pp. 79–96.

Dodson, P. and Wexlar, D. (1979) 'Taphonomic investigations of owl pellets', *Paleobiology*, 5(3), pp. 275–284. Available at: https://doi.org/10.1017/S0094837300006564.

Domínguez-Rodrigo, M. (2012) 'Critical review of the MNI (minimum number of individuals) as a zooarchaeological unit of quantification', *Archaeological and Anthropological Sciences*, 4(1), pp. 47–59. Available at: https://doi.org/10.1007/s12520-011-0082-z.

Dowd, M. (2015) *The Archaeology of Caves in Ireland*. Oxbow Books, Limited.

Dowd, M.A. (2008) 'The use of caves for funerary and ritual practices in Neolithic Ireland', *Antiquity*, 82(316), pp. 305–317. Available at: https://doi.org/10.1017/S0003598X00096824.

Duday, H. (2009) 'L'Archéothanatologie ou l'archéologie de la mort (Archaeothantology or the Archaeology of Death).', in R. Gowland and C. Knüsel (eds), C. Knüsel (tran.) *Social Archaeology of Funerary Remains*. Oxford, UK: Oxbow Books, pp. 30–56.

Efremov, I.A. (1940) 'Taphonomy: a new branch of paleontology.', *Pan-American Geologist*, 74, pp. 81–93.

Eickhoff, S. and Herrmann, B. (1985) 'Surface marks on bones from a neolithic collective grave (odagsen, lower saxony). A study on differential diagnosis', *Journal of Human Evolution*, 14(3), pp. 263–274. Available at: https://doi.org/10.1016/S0047-2484(85)80067-1.

Evans, T. (2013) 'Fluvial Taphonomy', in James.T. Pokines and S. Symes (eds) *Manual of Forensic Taphonomy*. 1st edn. CRC Press, pp. 115–141.

Evans, T. (2021) ‘Fluvial Taphonomy’, in James.T. Pokines and S. Symes (eds) *Manual of Forensic Taphonomy*. 2nd edn. CRC Press, pp. 163–191.

Evison, M.P. (1999) ‘Perspectives on the Holocene in Britain: human DNA.’, *Journal of Quaternary Science*, 14(6), pp. 615–623.

Fancourt, H.S.M. *et al.* (2021) ‘Next-generation osteometric sorting: Using 3D shape, elliptical Fourier analysis, and Hausdorff distance to optimize osteological pair-matching’, *Journal of Forensic Sciences*, (November 2020), pp. 1–16. Available at: https://doi.org/10.1111/1556-4029.14681.

Fernández-Jalvo, Y. *et al.* (1996) ‘Evidence of early cannibalism.’, *Science*, 271(5247), pp. 277–278. Available at: https://doi.org/10.1126/science.271.5247.277.

Fernández-Jalvo, Y. *et al.* (1999) ‘Human cannibalism in the Early Pleistocene of Europe (Gran Dolina, Sierra de Atapuerca, Burgos, Spain)’, *Journal of Human Evolution*, 37(3–4), pp. 591–622. Available at: https://doi.org/10.1006/jhev.1999.0324.

Fernández-Jalvo, Y. and Andrews, P. (2003) ‘Experimental Effects of Water Abrasion on Bone Fragments’, *Journal of Taphonomy*, 1(3), pp. 147–163.

Fernández-Jalvo, Y. and Andrews, P. (2016) *Atlas of taphonomic identifications: 1001+ images of fossil and recent mammal bone modification.* Springer (Vertebrate Paleobiology and Paleoanthropology Series). Available at: https://doi.org/10.1007/978-94-017-7432-1.

Fowler, C. (2010) ‘Pattern and diversity in the Early Neolithic mortuary practices of Britain and Ireland: Contextualising the treatment of the dead’, *Documenta Prehistorica*, 37(1), pp. 1–22. Available at: https://doi.org/10.4312/dp.37.1.

Freikman, M. (2017) ‘Into the darkness: Deep caves in the ancient near East’, *Journal of Landscape Ecology(Czech Republic)*, 10(3), pp. 81–99. Available at: https://doi.org/10.1515/jlecol-2017-0027.

Galloway, A. (2014) ‘The Upper Extremity’, in V.L. Wedel and A. Galloway (eds) *Broken bones: Anthropological analysis of blunt force trauma*. 2nd edn. Springfield, Illinois: Charles C Thomas Publisher LTD, pp. 47–58.

Galloway, A. and Wedel, V.L. (2014) ‘Bones of the Skull, the Dentition, and Osseous Structures of the Throat.’, in V.L. Wedel and A. Galloway (eds) *Broken bones: Anthropological analysis of blunt force trauma*. 2nd edn. Springfield, Illinois: Charles C Thomas Publisher LTD, pp. 47–58.

Galloway, A., Zephro, L. and Wedel, V.L. (2014) ‘Diagnostic Criteria for the Determination of Timing and Fracture Mechanism’, in V.L. Wedel and A. Galloway (eds) *Broken bones: Anthropological analysis of blunt force trauma*. 2nd edn. Springfield, Illinois: Charles C Thomas Publisher LTD, pp. 47–58.

Garcia Moreno, A. *et al.* (2015) ‘Counting sheep without falling asleep: using GIS to calculate the Minimum Number of Elements (MNE) and other archaeozoological measures at

Schöningen 13II-4 “Spear Horizon”’, *CAA2014. 21st Century Archaeology. Concepts, methods and tools. Proceedings of the 42nd Annual Conference on Computer Applications and Quantitative Methods in Archaeology*, pp. 407–412.

García-Sagastibelza, A. *et al.* (2020) ‘The funerary use of caves during the holocene in the Atlantic Western Pyrenees: New information from Atxuri-I and Txotxinkoba caves (Biscay, Northern Iberian peninsula)’, *Quaternary International* [Preprint]. Available at: https://doi.org/10.1016/j.quaint.2020.09.029.

Garrow, D. *et al.* (2017) ‘Stepping Stones to the Neolithic? Radiocarbon Dating the Early Neolithic on Islands Within the “Western Seaways” of Britain’, *Proceedings of the Prehistoric Society*, 83(September 2017), pp. 97–135. Available at: https://doi.org/10.1017/ppr.2017.4.

Gibbon, R.J. *et al.* (2014) ‘Cosmogenic nuclide burial dating of hominin-bearing Pleistocene cave deposits at Swartkrans, South Africa’, *Quaternary Geochronology*, 24, pp. 10–15. Available at: https://doi.org/10.1016/j.quageo.2014.07.004.

Gillings, M. (2017) ‘Mapping liminality: Critical frameworks for the GIS-based modelling of visibility’, *Journal of Archaeological Science*, 84, pp. 121–128. Available at: https://doi.org/10.1016/j.jas.2017.05.004.

Gillings, M., Hacıgüzeller, P. and Lock, G. (2018) ‘On maps and mapping’, in M. Gillings, P. Hacıgüzeller, and G. Lock (eds) *Re-Mapping Archaeology: Critical Perspectives, Alternative Mappings.* Milton: Taylor & Francis Group, pp. 1–16.

Giovas, C.M. (2009) ‘The shell game: analytic problems in archaeological mollusc quantification’, *Journal of Archaeological Science*, 36(7), pp. 1557–1564. Available at: https://doi.org/10.1016/j.jas.2009.03.017.

González, M.E. *et al.* (2012) ‘Differential Bone Survivorship and Ontogenetic Development in Guanaco ( *Lama guanicoe* ): Differential Bone Survivorship and Ontogenetic Development’, *International Journal of Osteoarchaeology*, 22(5), pp. 523–536. Available at: https://doi.org/10.1002/oa.1271.

González-Lemos, S., Jiménez-Sánchez, M. and Stoll, H.M. (2015) ‘Sediment transport during recent cave flooding events and characterization of speleothem archives of past flooding’, *Geomorphology*, 228, pp. 87–100. Available at: https://doi.org/10.1016/j.geomorph.2014.08.029.

Grayson, D.K. (1984) *Quantitative Zooarchaeology: Topics in the Analysis of Archaeological Faunas.* Orlando, Florida: Academic Press, Inc.

Griffiths, S. (2014) ‘A Bayesian Radiocarbon Chronology of the Early Neolithic of Yorkshire and Humberside’, *Archaeological journal*, 171(1), pp. 2–29. Available at: https://doi.org/10.1080/00665983.2014.11078260.

Gümrükçü, M. and Pante, M.C. (2018) ‘Assessing the effects of fluvial abrasion on bone surface modifications using high-resolution 3-D scanning’, *Journal of Archaeological Science: Reports*, 21(July), pp. 208–221. Available at: https://doi.org/10.1016/j.jasrep.2018.06.037.

Günther, T. and Jakobsson, M. (2016) 'Genes mirror migrations and cultures in prehistoric Europe — a population genomic perspective', *Current Opinion in Genetics & Development*, 41, pp. 115–123. Available at: https://doi.org/10.1016/j.gde.2016.09.004.

Haglund, William.D. (1997) 'Scattered Skeletal Human Remains: Search Strategy Considerations for Locating Missing Teeth.', in William.D. Haglund and Marcella.H. Sorg (eds) *Forensic Taphonomy: The Postmortem Fate of Human Remains*, pp. 383–394.

Harcourt, R.A. (1974) 'The dog in prehistoric and early historic britain', *Journal of Archaeological Science*, 1(2), pp. 151–175. Available at: https://doi.org/10.1016/0305-4403(74)90040-5.

Harris, J.A. *et al.* (2017) 'The trajectory of bone surface modification studies in paleoanthropology and a new Bayesian solution to the identification controversy', *Journal of Human Evolution*, 110, pp. 69–81. Available at: https://doi.org/10.1016/j.jhevol.2017.06.011.

Hartnett, K.M. (2010) 'Analysis of Age-at-Death Estimation Using Data from a New, Modern Autopsy Sample-Part II: Sternal End of the Fourth Rib', *Journal of Forensic Sciences*, 55(5), pp. 1152–1156. Available at: https://doi.org/10.1111/j.1556-4029.2010.01415.x.

Hawks, J. *et al.* (2017) 'New fossil remains of Homo naledi from the Lesedi Chamber, South Africa', *eLife*, 6, p. e24232. Available at: https://doi.org/10.7554/eLife.24232.

Hellewell, E. and Milner, N. (2011) 'Burial practices at the Mesolithic-Neolithic transition in Britain: Change or continuity?', *Documenta Praehistorica*, 38(1), pp. 61–68. Available at: https://doi.org/10.4312/dp.38.5.

Hensey, R. (2016) 'Past dark: a short introduction to the human relationship with darkness over time', in M. Dowd and R. Hensey (eds) *The Archaeology of Darkness*. Oxbow Books, Limited, pp. 1–10.

Herrmann, N. (2002) 'GIS applied to bioarchaeology: An example from the Río Talgua Caves in Northeast Honduras', *Journal of Cave and Karst Studies*, 64(1), pp. 17–22.

Herrmann, N.P. and Devlin, J.B. (2008) 'Assessment of commingled human remains using a GIS-based approach', in B. Adams and J. Byrd (eds) *Recovery, Analysis, and Identification of Commingled Human Remains*. Totowa, NJ: Humana Press, pp. 257–269. Available at: https://doi.org/10.1007/978-1-59745-316-5_13.

Herrmann, N.P., Devlin, J.B. and Stanton, J.C. (2014) 'Assessment of Commingled Human Remains Using a GIS-Based and Osteological Landmark Approach', in B.J. Adams and J.E. Byrd (eds) *Commingled Human Remains: Methods in Recovery, Analysis, and Identification*. Oxford: Academic Press, pp. 221–237. Available at: https://doi.org/10.1016/B978-0-12-405889-7.00010-1.

Hodgkins, J. *et al.* (2021) 'An infant burial from Arma Veirana in northwestern Italy provides insights into funerary practices and female personhood in early Mesolithic Europe',

*Scientific Reports*, 11(1), p. 23735. Available at: https://doi.org/10.1038/s41598-021-02804-z.

Holland, E.G. (1960) *Underground in Furness: A Guide to the Geology, Mines, Potholes and Caves.* Clapham, via Lancaster: The Dalesman Publishing Company.

Holland, T.D. (1992) 'Estimation of Adult Stature from Fragmentary Tibias', *Journal of Forensic Sciences*, 37(5), p. 13309J. Available at: https://doi.org/10.1520/JFS13309J.

Hudson, S.M. *et al.* (2023) 'Lateglacial and Early Holocene palaeoenvironmental change and human activity at Killerby Quarry, North Yorkshire, UK', *Journal of Quaternary Science*, 38(3), pp. 403–422. Available at: https://doi.org/10.1002/jqs.3488.

Hughes, T.M. (1874) 'Exploration of Cave Ha near Giggleswick, Settle, Yorkshire.', *Journal of the Royal Anthropological Institute*, 1, pp. 383–387.

Hunter, G.J. (2005) 'Managing uncertainty in GIS. Geographical information systems, 2(part 3), pp.633-641.', in P.A. Longley et al. (eds) *New Developments in Geographical Information Systems: Principles, Techniques, Management and Applications*. 2nd edn. John Wiley & Sons, Ltd, pp. 633–641. Available at: https://www.geos.ed.ac.uk/~gisteac/gis_book_abridged/ (Accessed: 12 July 2023).

İşcan, M.Y., Loth, S.R. and Wright, R.K. (1984) 'Metamorphosis at the sternal rib end: A new method to estimate age at death in white males', *American Journal of Physical Anthropology*, 65(2), pp. 147–156. Available at: https://doi.org/10.1002/ajpa.1330650206.

Ishihara-Brito, R. and Guerra, J. (2012) 'Windows of the Earth: An Ethnoarchaeological Study on Cave Use in Suchitepéquez and Sololá, Guatemala.', in J.E. Brady (ed.) *Heart of Earth: Studies in Maya Ritual Cave Use*. Association for Mexican Cave Studies, pp. 51–60.

Jazwa, C.S. (2022) 'Heaning Wood Radiocarbon Modelled Dates', *Private Correspondence.* The University of Nevada, Reno. *Unpublished.*

Jilala, W. *et al.* (2021) 'Sexing contemporary Tanzanian skeletonized remains using skull morphology: A test of the walker sex assessment method', *Forensic Science International: Reports*, 3, p. 100195. Available at: https://doi.org/10.1016/j.fsir.2021.100195.

Jin, S.-W., Sim, K.-B. and Kim, S.-D. (2016) 'Development and Growth of the Normal Cranial Vault : An Embryologic Review', *Journal of Korean Neurosurgical Society*, 59(3), p. 192. Available at: https://doi.org/10.3340/jkns.2016.59.3.192.

Karell, M.A. *et al.* (2016) 'A novel method for pair-matching using three-dimensional digital models of bone: mesh-to-mesh value comparison', *International Journal of Legal Medicine*, 130(5), pp. 1315–1322. Available at: https://doi.org/10.1007/s00414-016-1334-3.

Katsianis, M. *et al.* (2008) 'A 3D digital workflow for archaeological intra-site research using GIS', *Journal of Archaeological Science*, 35(3), pp. 655–667. Available at: https://doi.org/10.1016/j.jas.2007.06.002.

Katzenberg, M.A. and Waters-Rist, A.L. (2018) 'Stable Isotope Analysis: A tool for Studying Past Diet, Demography and Life History.', in M.A. Katzenberg and A.L. Grauer (eds) *Biological Anthropology of the Human Skeleton*. 3rd edn. John Wiley & Sons, Ltd, pp. 467–504.

Klales, A.R., Ousley, S.D. and Vollner, J.M. (2012) 'A revised method of sexing the human innominate using Phenice's nonmetric traits and statistical methods', *American Journal of Physical Anthropology*, 149(1), pp. 104–114. Available at: https://doi.org/10.1002/ajpa.22102.

Klein, R.G. and Cruz-Uribe, K. (1984) *The Analysis of Animal Bones from Archaeological Sites*. Edited by K. Butzer and L. Freeman. Chicago; London: The University of Chicago Press (Prehistoric Archeology and Ecology Series). Available at: https://doi.org/10.2307/281106.

Knüsel, C.J. (2014) 'Crouching in fear: Terms of engagement for funerary remains The recording example can be found at http://jsa.sagepub.com/', *Journal of Social Archaeology*, 14(1), pp. 26–58. Available at: https://doi.org/10.1177/1469605313518869.

Knüsel, C.J. and Outram, A.K. (2004) 'Fragmentation: The zonation method applied to fragmented human remains from archaeological and forensic contexts', *Environmental Archaeology*, 9(1), pp. 85–97. Available at: https://doi.org/10.1179/env.2004.9.1.85.

Knüsel, C.J. and Robb, J. (2016) 'Funerary taphonomy: An overview of goals and methods', *Journal of Archaeological Science: Reports*, 10, pp. 655–673. Available at: https://doi.org/10.1016/j.jasrep.2016.05.031.

Kos, A.M. (2003) 'Pre-burial taphonomic characterisation of a vertebrate assemblage from a pitfall cave fossil deposit in southeastern Australia', *Journal of Archaeological Science*, 30(6), pp. 769–779. Available at: https://doi.org/10.1016/S0305-4403(02)00251-0.

L'Abbe, E.N. *et al.* (2015) 'Evidence of fatal skeletal injuries on Malapa Hominins 1 and 2', *Scientific Reports*, 5(October). Available at: https://doi.org/10.1038/srep15120.

Lam, Y.M. (1992) 'Variability in the behaviour of spotted hyaenas as taphonomic agents', *Journal of Archaeological Science*, 19(4), pp. 389–406. Available at: https://doi.org/10.1016/0305-4403(92)90057-A.

Lambacher, N. *et al.* (2016) 'Evaluating three methods to estimate the number of individuals from a commingled context', *Journal of Archaeological Science: Reports*, 10, pp. 674–683. Available at: https://doi.org/10.1016/j.jasrep.2016.07.008.

Lamer, M., Spake, L. and Cardoso, H.F.V. (2021) 'Testing the cross-applicability of juvenile sex estimation from diaphyseal dimensions', *Forensic Science International*, 321, p. 110739. Available at: https://doi.org/10.1016/j.forsciint.2021.110739.

Lamerton, P. *et al.* (2021) 'Post-mortem movement and skeletal disarticulation after death', *Australian Journal of Forensic Sciences*, pp. 1–19. Available at: https://doi.org/10.1080/00450618.2021.1998628.

Landeschi, G. *et al.* (2019) 'Re-enacting the sequence: combined digital methods to study a prehistoric cave', *Archaeological and Anthropological Sciences*, 11(6), pp. 2805–2819. Available at: https://doi.org/10.1007/s12520-018-0724-5.

Lara, M. *et al.* (2017) 'Archaeological recognition of mortuary behavior in Callao Cave, northern Luzon, Philippines through taphonomic analysis of isolated human remains', *Archaeological and Anthropological Sciences*, 9(6), pp. 1169–1186. Available at: https://doi.org/10.1007/s12520-015-0307-7.

Leach, S. (2006a) *Going Underground: An anthropological and taphonomic study of human skeletal remains from caves and rock shelters in Yorkshire. Volume I of II*. Ph.D. Thesis. University of Southampton.

Leach, S. (2006b) *Going Underground: An anthropological and taphonomic study of human skeletal remains from caves and rock shelters in Yorkshire. Volume II of II*. Ph.D. Thesis. University of Southampton.

Leach, S. (2008) 'Odd one out? Earlier Neolithic deposition of human remains in caves and rock shelters in the Yorkshire Dales', in E. Murphy (ed.) *Deviant Burial in the Archaeological Record*. Oxford: Oxbow, pp. 35–56.

Leach, S. (2015) 'Going Underground: an anthropological and taphonomic study of human skeletal remains from caves and rock shelters in Yorkshire (2 vols).', *Leeds: Yorkshire Archaeological Society* [Preprint].

Lewin, J. and Woodward, J. (2009) 'Karst Geomorphology and Environmental Change', in Lewin, J. and Woodward, J., *The Physical Geography of the Mediterranean*. Oxford University Press. Available at: https://doi.org/10.1093/oso/9780199268030.003.0022.

Lewis, J. *et al.* (2019) 'Making a significant place: excavations at the Late Mesolithic site of Langley's Lane, Midsomer Norton, Bath and North-East Somerset', *Archaeological journal*, 176(1), pp. 1–50. Available at: https://doi.org/10.1080/00665983.2019.1551507.

Lewis, M.E. and Flavel, A. (2006) 'Age Assessment of Child Skeletal Remains in Forensic Contexts', in A. Schmitt, E. Cunha, and J. Pinheiro (eds) *Forensic Anthropology and Medicine*. Totowa, NJ: Humana Press, pp. 243–257. Available at: https://doi.org/10.1007/978-1-59745-099-7_10.

Lewis-Williams, D.J. and Clottes, J. (1998) 'The Mind in the Cave the Cave in the Mind: Altered Consciousness in the Upper Paleolithic', *Anthropology of Consciousness*, 9(1), pp. 13–21. Available at: https://doi.org/10.1525/ac.1998.9.1.13.

Liversidge, H.M. and Molleson, T. (2004) 'Variation in crown and root formation and eruption of human deciduous teeth', *American Journal of Physical Anthropology*, 123(2), pp. 172–180. Available at: https://doi.org/10.1002/ajpa.10318.

López-González, F., Grandal-d'Anglade, A. and Vidal-Romaní, J.R. (2006) 'Deciphering bone depositional sequences in caves through the study of manganese coatings', *Journal of*

*Archaeological Science*, 33(5), pp. 707–717. Available at: https://doi.org/10.1016/j.jas.2005.10.006.

Lord, T. (2004) '2004 Site Archival Notes, Lord Cave Archive. Unpublished'. Unpublished.

Lord, T. and Howard, J. (2013) 'Cave Archaeology', in T. Waltham and D. Lowe (eds) *Caves and Karst of the Yorkshire Dales: Volume 1*. British Cave Research Association, pp. 239–251.

Lord, T.C. *et al.* (2007) 'People and large carnivores as biostratinomic agents in Lateglacial cave assemblages', *Journal of Quaternary Science*, 22(7), pp. 681–694. Available at: https://doi.org/10.1002/jqs.1101.

Lorentz, K.O., Casa, B. and Miyauchi, Y. (2021) 'Disposed young: Nonadult element representation and bone positioning in complex mortuary programmes in Chalcolithic Cyprus', *International Journal of Osteoarchaeology*, 31(5), pp. 727–741. Available at: https://doi.org/10.1002/oa.2985.

Lovejoy, C.O. *et al.* (1985) 'Chronological metamorphosis of the auricular surface of the ilium: a new method for the determination of adult skeletal age at death.', *American Journal of Physical Anthropology*, 68(1), pp. 15–28.

Lovejoy, C.O. (1985) 'Dental Wear in the Libben Population: Its Functional Pattern and Role in the Determination of Adult Skeletal Age at Death', *American Journal of Physical Anthropology*, 68, pp. 47–56.

Lucas, G. (2012) *Understanding the Archaeological Record.* New York: Cambridge University Press.

Lyman, R. (1994a) 'Quantitative Units and Terminology in Zooarchaeology', *American Antiquity*, 59(1), pp. 36–71. Available at: https://doi.org/10.2307/3085500.

Lyman, R. (1994b) *Vertebrate Taphonomy*. Cambridge: Cambridge University Press. (Cambridge Manuals in Archaeology).

Lyman, R. (2008a) 'Estimating Taxonomic Abundances: NISP and MNI', in *Quantitative Paleozoology*. Cambridge University Press.

Lyman, R. (2008b) 'Tallying for Taphonomy: Weathering, Burning, Corrosion, and Butchering', in *Quantitative Paleozoology*. Cambridge: Cambridge University Press.

Lyman, R. (2010) 'What Taphonomy Is, What it Isn't, and Why Taphonomists Should Care about the Difference', *Journal of taphonomy*, 8(1), pp. 1–16.

Lyman, R. (2018) 'Observations on the history of zooarchaeological quantitative units: Why NISP, then MNI, then NISP again?', *Journal of Archaeological Science: Reports*, 18(January), pp. 43–50. Available at: https://doi.org/10.1016/j.jasrep.2017.12.051.

Lyman, R. (2019) 'A Critical Review of Four Efforts to Resurrect MNI in Zooarchaeology', *Journal of Archaeological Method and Theory*, 26(1), pp. 52–87. Available at: https://doi.org/10.1007/s10816-018-9365-3.

Lyman, R. and Fox, G.L. (1989) ‘A critical evaluation of bone weathering as an indication of bone assemblage formation’, *Journal of Archaeological Science*, 16, pp. 293–317.

Lyman, R.L. and O’Brien, M.J. (1987) ‘Plow-zone Zooarchaeology: Fragmentation and Identifiability’, *Journal of Field Archaeology*, 14(4), pp. 493–500.

Mack, J.E. *et al.* (2016) ‘Applying Zooarchaeological Methods to Interpret Mortuary Behaviour and Taphonomy in Commingled Burials: The Case Study of the Late Neolithic Site of Bolores, Portugal’, *International Journal of Osteoarchaeology*, 26(3), pp. 524–536. Available at: https://doi.org/10.1002/oa.2443.

Madgwick, R. and Mulville, J. (2015) ‘Reconstructing depositional histories through bone taphonomy: Extending the potential of faunal data’, *Journal of Archaeological Science*, 53, pp. 255–263. Available at: https://doi.org/10.1016/j.jas.2014.10.015.

Mahler, R. (2022) ‘A formalized approach to choosing the best methods for reconstructing stature in the case of poorly preserved skeletal series’, *Archaeometry*, 64(1), pp. 265–280. Available at: https://doi.org/10.1111/arcm.12700.

Mainland, I. *et al.* (2014) ‘“SmartFauna”: a microscale GIS-based multi-dimensional approach to faunal deposition at the Ness of Brodgar, Orkney’, *Journal of Archaeological Science*, 41, pp. 868–878. Available at: https://doi.org/10.1016/j.jas.2013.10.019.

Manifold, B.M. (2010) ‘The Representation of Non-adult Skeletal Elements Recovered from British Archaeological Sites’, *Childhood in the Past*, 3(1), pp. 43–62. Available at: https://doi.org/10.1179/cip.2010.3.1.43.

Marean, C.W. (1991) ‘Measuring the post-depositional destruction of bone in archaeological assemblages’, *Journal of Archaeological Science*, 18(6), pp. 677–694. Available at: https://doi.org/10.1016/0305-4403(91)90029-O.

Marean, C.W. *et al.* (2001) ‘Estimating the Minimum Number of Skeletal Elements (MNE) in Zooarchaeology: A Review and a New Image-Analysis GIS Approach’, *American Antiquity*, 66(2), pp. 333–348.

Marean, C.W. and Spencer, L.M. (1991) ‘Impact of Carnivore Ravaging on Zooarchaeological Measures of Element Abundance’, *American Antiquity*, 56(4), pp. 645–658. Available at: https://doi.org/10.2307/281542.

Marginedas, F. *et al.* (2020) ‘Making skull cups: Butchering traces on cannibalised human skulls from five European archaeological sites’, *Journal of Archaeological Science*, 114(December 2019). Available at: https://doi.org/10.1016/j.jas.2020.105076.

Marín-Arroyo, A.B.M. (2009) ‘Assessing What Lies Beneath the Spatial Distribution of a Zooarchaeological Record: The Use of GIS and Spatial Correlations at El Mirón Cave (Spain).’, *Archaeometry*, 51(3), pp. 506–524. Available at: https://doi.org/10.1111/j.1475-4754.2008.00411.x.

Márquez-Grant, N. *et al.* (2016) 'Physical Anthropology and Osteoarchaeology in Europe: History, Current Trends and Challenges', *International Journal of Osteoarchaeology*, 26(6), pp. 1078–1088. Available at: https://doi.org/10.1002/oa.2520.

Marshall, F. and Pilgram, T. (1993) 'NISP vs. MNI in Quantification of Body-Part Representation', *American Antiquity*, 58(2), pp. 261–269.

Mavroudas, S.R. *et al.* (2023) 'Experimental investigation of histotaphonomic changes in human bone from whole-body donors demonstrates limited effects of early post-mortem change in bone', *Journal of Archaeological Science*, 154, p. 105789. Available at: https://doi.org/10.1016/j.jas.2023.105789.

McKern, T.W. and Stewart, T.D. (1957) 'Skeletal age changes in young American males: analysed from the standpoint of age identification.', *Headquarters, Quartermaster Research & Development Command.* [Preprint].

McKinley, J.I. and Smith, M. (2017) 'Compiling a skeletal inventory: disarticulated and commingled remains', in P.D. Mitchell and M. Brickley (eds) *Updated Guidelines to the Standards for Recording Human Remains*. Chartered Institute for Archaeologists, pp. 20–24.

Meiklejohn, C. *et al.* (2005) 'Spatial Relationships, Dating and Taphonomy of the Human Bone from the Mesolithic site of Cnoc Coig, Oronsay, Argyll, Scotland', *Proceedings of the Prehistoric Society*, 71, pp. 85–105. Available at: https://doi.org/10.1017/S0079497X00000967.

Meiklejohn, C., Chamberlain, A.T. and Schulting, R.J. (2011) 'Radiocarbon dating of Mesolithic human remains in Great Britain.', *Mesolithic Miscellany*, 21(2), pp. 20–58.

Meindl, R.S. and Lovejoy, C.O. (1985) 'Ectocranial suture closure: A revised method for the determination of skeletal age at death based on the lateral-anterior sutures.', *American Journal of Physical Anthropology*, 68(1), pp. 57–66.

Mickleburgh, H.L. and Wescott, D.J. (2018) 'Controlled experimental observations on joint disarticulation and bone displacement of a human body in an open pit: Implications for funerary archaeology', *Journal of Archaeological Science: Reports*, 20, pp. 158–167. Available at: https://doi.org/10.1016/j.jasrep.2018.04.022.

Milner, N., Conneller, C. and Taylor, B. (eds) (2018) 'Introduction', in *Star Carr Volume I*. White Rose University Press, pp. 3–9. Available at: https://doi.org/10.22599/book1.a.

Mitchell, P.D. and Brickley, M. (2017) *Updated Guidelines to the Standards for Recording Human Remains*, *Updated Guidlines to the Standards for Recording Human Remains*. Chartered Institute for Archaeologists, p. 32.

Mlekuž, D. (2012) 'Notes from the Underground: Caves and People in the Mesolithic and Neolithic Karst', in K.A. Bergsvik and R. Skeates (eds) *Caves in Context: The Cultural Significance of Caves and Rockshelters in Europe*. Oxbow Books, pp. 199–211. Available at: https://doi.org/10.2307/j.ctvh1djk4.18.

Moldovan, O. (2005) ‘Beetles’, in D. Culver and W. White (eds) *Encyclopedia of Caves*. San Diego, California: Elsevier Academic Press, pp. 45–50.

Moraitis, K. and Spiliopoulou, C. (2006) ‘Identification and differential diagnosis of perimortem blunt force trauma in tubular long bones’, *Forensic Science, Medicine, and Pathology*, 2(4), pp. 221–229. Available at: https://doi.org/10.1385/FSMP:2:4:221.

Morales-Pérez, J.V. *et al.* (2017) ‘Funerary practices or food delicatessen? Human remains with anthropic marks from the Western Mediterranean Mesolithic’, *Journal of Anthropological Archaeology*, 45, pp. 115–130. Available at: https://doi.org/10.1016/j.jaa.2016.11.002.

Morin, E. *et al.* (2017a) ‘Problems of Identification and Quantification in Archaeozoological Analysis, Part I: Insights from a Blind Test’, *Journal of Archaeological Method and Theory*, 24(3), pp. 886–937. Available at: https://doi.org/10.1007/s10816-016-9300-4.

Morin, E. *et al.* (2017b) ‘Problems of Identification and Quantification in Archaeozoological Analysis, Part II: Presentation of an Alternative Counting Method’, *Journal of Archaeological Method and Theory*, 24(3), pp. 938–973. Available at: https://doi.org/10.1007/s10816-016-9301-3.

Morin, E. *et al.* (2019) ‘The Number of Distinct Elements: Extending a landmark-based counting unit to other taxa’, *Journal of Archaeological Science: Reports*, 24(January), pp. 773–784. Available at: https://doi.org/10.1016/j.jasrep.2019.01.007.

Morlan, R.E. (1994) ‘Bison bone fragmentation and survivorship: A comparative method’, *Journal of Archaeological Science*, 21(6), pp. 797–807. Available at: https://doi.org/10.1006/jasc.1994.1077.

Murphy, P.J. and Hodgson, D.G. (2017) ‘Revisiting the “reefs” of Black Reef Cave, Ribblehead, North Yorkshire (UK), with some observations on cave-divers’ “chert”’, *Cave and Karst Science*, 44(1), pp. 43–45.

Murray, S. and Kunz, T. (2005) ‘Bats’, in D. Culver and W. White (eds) *Encyclopedia of Caves*. San Diego, California: Elsevier Academic Press, pp. 45–50.

Nardini, A. and Salvadori, F. (2003) ‘A GIS Platform Dedicated to the Production of Distribution Models of Archaeozoological Remains’, *Archaeofauna*, 12, pp. 127–141.

Nawrocki, Stephen.P. *et al.* (1997) ‘Fluvial Transport of Human Crania’, in William.D. Haglund and Marcella.H. Sorg (eds) *Forensic Taphonomy:The Postmortem Fate of Human Remains*. Boca Raton: CRC Press, pp. 599–622.

Nicolosi, T. *et al.* (2023) ‘On the traces of lost identities: chronological, anthropological and taphonomic analyses of the Late Neolithic/Early Eneolithic fragmented and commingled human remains from the Farneto rock shelter (Bologna, northern Italy)’, *Archaeological and Anthropological Sciences*, 15(3), p. 36. Available at: https://doi.org/10.1007/s12520-023-01727-2.

Niel, M., Chaumoître, K. and Adalian, P. (2022) 'Age-at-Death Estimation of Fetuses and Infants in Forensic Anthropology: A New "Coupling" Method to Detect Biases Due to Altered Growth Trajectories', *Biology*, 11(2), p. 200. Available at: https://doi.org/10.3390/biology11020200.

Nieves-Colón, M.A. and Stone, A.C. (2018) 'Ancient DNA Analysis of Archaeological Remains', in M.A. Katzenberg and A.L. Grauer (eds) *Biological Anthropology of the Human Skeleton*. 3rd edn. John Wiley & Sons, Ltd, pp. 515–544.

Nigro, J.D. *et al.* (2003) 'Developing a Geographic Information System (GIS) for mapping and analysing fossil deposits at Swartkrans, Gauteng Province, South Africa', *Journal of Archaeological Science*, 30(3), pp. 317–324. Available at: https://doi.org/10.1006/jasc.2002.0839.

Nikita, E., Karligkioti, A. and Lee, H. (2019) *Excavation and study of commingled human skeletal remains*, p. 46.

Orschiedt, J. (2012) 'Cave Burials in Prehistoric Central Europe', in K.A. Bergsvik and R. Skeates (eds) *Caves in Context: The cultural Significance of Caves and Rockshelters in Europe.* Oxford, UK: Oxbow Books.

Orschiedt, J. (2018) 'The Late Upper Palaeolithic and earliest Mesolithic evidence of burials in Europe', *Philosophical Transactions of the Royal Society B: Biological Sciences*, 373(1754), p. 20170264. Available at: https://doi.org/10.1098/rstb.2017.0264.

Osterholtz, A.J. (2019) 'Advances in Documentation of Commingled and Fragmentary Remains', *Advances in Archaeological Practice*, 7(1), pp. 77–86. Available at: https://doi.org/10.1017/aap.2018.35.

Outram, A.K. (2001) 'A new approach to identifying bone marrow and grease exploitation: Why the "Indeterminate" fragments should not be ignored', *Journal of Archaeological Science*, 28(4), pp. 401–410. Available at: https://doi.org/10.1006/jasc.2000.0619.

Outram, A.K. *et al.* (2005) 'Understanding complex fragmented assemblages of human and animal remains: A fully integrated approach', *Journal of Archaeological Science*, 32(12), pp. 1699–1710. Available at: https://doi.org/10.1016/j.jas.2005.05.008.

Pailler, Y. and Sheridan, A. (2009) 'Everything you always wanted to know about... la néolithisation de la Grande-Bretagne et de l'Irlande', *Bulletin de la Société préhistorique française*, 106(1), pp. 25–56. Available at: https://doi.org/10.1207/s15327965pli0404_19.

Palmiotto, A., Brown, C. and LeGarde, C. (2019) 'Estimating the Number of Individuals in a Large Commingled Assemblage', *Forensic Anthropology*, 2(2), pp. 129–138. Available at: https://doi.org/10.5744/fa.2019.1002.

Parker Pearson, M. (2000) 'Ancestors, bones and stones in Neolithic and Early Bronze Age Britain and Ireland', in A. Ritchie (ed.) *Neolithic Orkney in its European Context*. Cambridge: McDonald Institute for Archaeological Research, pp. 203–14.

Parker Pearson, M. and Ramilisonina (1998) ‘Stonehenge for the ancestors: the stones pass on the message’, *Antiquity*, 72, pp. 308–326.

Parkinson, J.A. (2013) *A GIS image analysis approach to documenting Oldowan hominin carcass acquisition: Evidence from Kanjera South, FLK Zinj, and neotaphonomic models of carnivore bone destruction*. City University of New York.

Parkinson, J.A. (2018) ‘Revisiting the hunting-versus-scavenging debate at FLK Zinj: A GIS spatial analysis of bone surface modifications produced by hominins and carnivores in the FLK 22 assemblage, Olduvai Gorge, Tanzania’, *Palaeogeography, Palaeoclimatology, Palaeoecology*, 511(June), pp. 29–51. Available at: https://doi.org/10.1016/j.palaeo.2018.06.044.

Parkinson, J.A. *et al.* (2022) ‘Meat on the menu: GIS spatial distribution analysis of bone surface damage indicates that Oldowan hominins at Kanjera South, Kenya had early access to carcasses’, *Quaternary Science Reviews*, 277, p. 107314. Available at: https://doi.org/10.1016/j.quascirev.2021.107314.

Parkinson, J.A., Plummer, T.W. and Bose, R. (2014) ‘A GIS-based approach to documenting large canid damage to bones’, *Palaeogeography, Palaeoclimatology, Palaeoecology*, 409, pp. 57–71. Available at: https://doi.org/10.1016/j.palaeo.2014.04.019.

Pelletier, M. *et al.* (2020) ‘Identifying the accidental-natural mortality of leporids in the archaeological record: insights from a taphonomical analysis of a pitfall without evidence of human presence’, *Journal of Quaternary Science*, 35(5), pp. 677–694. Available at: https://doi.org/10.1002/jqs.3203.

Pentecost, A. *et al.* (1990) ‘Some Radiocarbon Dates for Tufas of the Craven District of Yorkshire.’, *Radiocarbon*, 32(1), pp. 93–97.

Pentecost, A. (2013) ‘Travertine and Tufa’, in T. Waltham and D. Lowe (eds) *Caves and Karst of the Yorkshire Dales*. British Cave Research Association, pp. 111–116.

Perreault, C. (2019) *The Quality of the Archaeological Record*. Chicago; London: The University of Chicago Press.

Peterson, R. (2019) *Neolithic cave burials: Agency, structure and environment.* Manchester University Press.

Peterson, R. (2022), Email to Keziah Warburton, 12 December.

Pickering, T.R. (2002) ‘Reconsideration of Criteria for Differentiating Faunal Assemblages Accumulated by Hyenas and Hominids’, *International Journal of Osteoarchaeology*, 12(2), pp. 127–141. Available at: https://doi.org/10.1002/oa.594.

Pobiner, B.L. and Braun, D.R. (2005) ‘Strengthening the inferential link between cutmark frequency data and Oldowan hominid behavior: results from modern butchery experiments’, *Journal of Taphonomy*, 3, pp. 107–119.

Pokines, J. *et al.* (2011) 'The functioning of a natural faunal trap in a semi-arid environment: preliminary investigations of WZM-1, a limestone sinkhole site near Wadi Zarqa Ma'in, Hashemite Kingdom of Jordan', *Journal of taphonomy*, 9(2), pp. 89–115.

Pokines, J. *et al.* (2013) 'Taphonomic Bone Staining and Color Changes in Forensic Contexts', in J.T. Pokines and S. Symes (eds) *Manual of Forensic Taphonomy*. CRC Press, pp. 315–340. Available at: https://doi.org/10.1201/b15424-13.

Pokines, J.T. (2013a) 'Faunal Dispersal, Reconcentration, and Gnawing Damage to Bone in Terrestrial Environments', in J. Pokines and S. Symes (eds) *Manual of Forensic Taphonomy*. CRC Press, pp. 201–248.

Pokines, J.T. (2013b) 'Introduction', in J.T. Pokines and S. Symes (eds) *Manual of Forensic Taphonomy*. CRC Press, pp. 1–18.

Pokines, J.T. *et al.* (2018) 'The effects of repeated wet-dry cycles as a component of bone weathering', *Journal of Archaeological Science: Reports*, 17(November 2017), pp. 433–441. Available at: https://doi.org/10.1016/j.jasrep.2017.11.025.

Pokines, J.T. and Baker, J.E. (2014) 'Effects of burial environment on osseous remains.', in J.T Pokines and S.A. Symes (eds) *Manual of Forensic Taphonomy*. Boca Raton, Fl: CRC Press, pp. 73–114.

Pollard, J., Serjeantson, D. and Field, D. (2015) 'A Community of Beings Animals and People in the Neolithic of Southern Britain', in D. Serjeantson and D. Field (eds) *Animals in the Neolithic of Britain and Europe*. Havertown: Oxford Books, Limited, pp. 135–148. Available at: http://www.jstor.org/stable/j.ctt1w1vjbn.17.

Posth, C. *et al.* (2016) 'Pleistocene Mitochondrial Genomes Suggest a Single Major Dispersal of Non-Africans and a Late Glacial Population Turnover in Europe', *Current Biology*, 26(6), pp. 827–833. Available at: https://doi.org/10.1016/j.cub.2016.01.037.

Pu, F. *et al.* (2011) 'Effect of different labor forces on fetal skull molding', *Medical Engineering & Physics*, 33(5), pp. 620–625. Available at: https://doi.org/10.1016/j.medengphy.2010.12.018.

Querner, P. (2015) 'Insect Pests and Integrated Pest Management in Museums, Libraries and Historic Buildings', *Insects*, 6(2), pp. 595–607. Available at: https://doi.org/10.3390/insects6020595.

Randolph-Quinney, P.S. *et al.* (2016) 'Response to Thackeray (2016) – The possibility of lichen growth on bones of Homo naledi: Were they exposed to light?', *South African Journal of Science*, 112(9). Available at: https://doi.org/10.17159/sajs.2016/a0177.

Randolph-Quinney, P.S., Haines, S.D. and Kruger, A. (2018) 'The use of three-dimensional scanning and surface capture methods in recording forensic taphonomic traces: issues of technology, visualisation, and validation', in Barone, P.M. and Groen, W.J.M (eds) *Multidisciplinary approaches to forensic archaeology: topics discussed during the European Meetings on Forensic Archaeology (EMFA)*. Springer International Publishing, pp. 115-130.

Rellini, I. *et al.* (2020) 'Micromorphological investigations at Scaloria Cave (Puglia, South-east Italy): new evidences of multifunctional use of the space during the Neolithic', *Archaeological and Anthropological Sciences*, 12(1). Available at: https://doi.org/10.1007/s12520-019-01005-0.

Rivals, F. *et al.* (2022) 'Diet and ecological niches of the Late Pleistocene hyenas Crocuta spelaea and C. ultima ussurica based on a study of tooth microwear', *Palaeogeography, Palaeoclimatology, Palaeoecology*, 601, p. 111125. Available at: https://doi.org/10.1016/j.palaeo.2022.111125.

Robb, J. *et al.* (2015) 'Cleaning the dead: Neolithic ritual processing of human bone at Scaloria Cave, Italy', *Antiquity*, 89(343), pp. 39–54. Available at: https://doi.org/10.15184/aqy.2014.35.

Robb, J. (2016) 'What can we really say about skeletal part representation, MNI and funerary ritual? A simulation approach', *Journal of Archaeological Science: Reports*, 10, pp. 684–692. Available at: https://doi.org/10.1016/j.jasrep.2016.05.033.

Robb, J. (2020) 'Art (Pre)History: Ritual, Narrative and Visual Culture in Neolithic and Bronze Age Europe', *Journal of Archaeological Method and Theory*, 27(3), pp. 454–480. Available at: https://doi.org/10.1007/s10816-020-09471-w.

Roberts, C. and Cox, M. (2003) *Health and Disease in Britain: from Prehistory to the Present Day*. Sutton Publishing Limited.

Roberts, C. and Manchester, K. (2010) *The archaeology of disease.* Third. Gloucestershire: The History Press.

Robinson, D.W. *et al.* (2020) 'Datura quids at Pinwheel Cave, California, provide unambiguous confirmation of the ingestion of hallucinogens at a rock art site', *Proceedings of the National Academy of Sciences of the United States of America*, 117(49), pp. 31026–31037. Available at: https://doi.org/10.1073/pnas.2014529117.

Roksandic, M. (2002) 'Position of skeletal remains as a key to understanding mortuary behavior.', in William.D. Haglund and Marcella.H. Sorg (eds) *Advances in forensic taphonomy: method, theory, and archaeological perspectives*. Boca Raton: Taylor & Francis Group, pp. 99–117.

Rose, D.C. *et al.* (2012) 'Technical note: The use of geographical information systems software for the spatial analysis of bone microstructure', *American Journal of Physical Anthropology*, 148(4), pp. 648–654. Available at: https://doi.org/10.1002/ajpa.22099.

Rougier, H. and Trinkaus, E. (2013) 'The Human Cranium from the Peştera cu Oase, Oase 2', in E. Trinkaus, S. Constantin, and J. Zilhão (eds) *Life and Death at the Peştera cu Oase: A Setting for Modern Human Emergence in Europe.* Oxford University Press, pp. 257–320.

Saladié, P. and Rodríguez-Hidalgo, A. (2017) 'Archaeological Evidence for Cannibalism in Prehistoric Western Europe: from Homo antecessor to the Bronze Age', *Journal of*

*Archaeological Method and Theory*, 24(4), pp. 1034–1071. Available at: https://doi.org/10.1007/s10816-016-9306-y.

Santana, J. *et al.* (2019) 'Aggressive or funerary cannibalism? Skull-cup and human bone manipulation in Cueva de El Toro (Early Neolithic, southern Iberia)', *American Journal of Physical Anthropology*, 169(1), pp. 31–54. Available at: https://doi.org/10.1002/ajpa.23805.

Sauqué, V. *et al.* (2018) 'Los Batanes: A trap for the Pyrenean wild goat during the Late Pleistocene (Spain)', *Quaternary International*, 481, pp. 75–90. Available at: https://doi.org/10.1016/j.quaint.2017.09.011.

Scheuer, L. and Black, S. (2000) *Developmental Juvenile Osteology*. Oxford, UK: Elsevier.

Scheuer, L., Black, S. and Schaefer, M.C. (2008) *Juvenile Osteology: A Laboratory and Field Manual*. London: Academic Press.

Schotsmans, E.M.J. *et al.* (2022) 'From Flesh to Bone', in Knüsel, C. J. and Schotsmans, E. M. J., *The Routledge Handbook of Archaeothanatology*. 1st edn. London: Routledge, pp. 500–541. Available at: https://doi.org/10.4324/9781351030625-32.

Schulting, R. *et al.* (2013) 'Mesolithic and neolithic human remains from Foxhole Cave, Gower, South Wales', *Antiquaries Journal*, 93, pp. 1–23. Available at: https://doi.org/10.1017/S000358151300019X.

Schulting, R. (2013) '"Tilbury Man": A Mesolithic Skeleton from the Lower Thames', *Proceedings of the Prehistoric Society*, 79, pp. 19–37. Available at: https://doi.org/10.1017/ppr.2013.12.

Schulting, R.J. (2007) 'Non-monumental burial in Britain: A (largely) cavernous view', *Bericht der Romisch-Germanischen Kommission*, 88(January 2007), pp. 581–603.

Schulting, R.J. *et al.* (2015) 'A Cut-marked and Fractured Mesolithic Human Bone from Kent's Cavern, Devon, UK: Kent's Cavern Mesolithic Cut-marked Ulna', *International Journal of Osteoarchaeology*, 25(1), pp. 31–44. Available at: https://doi.org/10.1002/oa.2261.

Schulting, R.J. (2016) 'Holes in the world: the use of caves for burial in the Mesolithic.', *Mesolithic Burials–Rites, Symbols and Social Organisation of Early Postglacial Communities*, pp. 555-568.

Schulting, R.J. (2020) 'Claddedigaethau mewn ogofâu: prehistoric human remains (mainly) from the caves of Wales', *Proceedings of the University of Bristol Spelaeological Society*, 28(2), pp. 185–219.

Schulting, R.J., Chapman, M. and Chapman, E.J. (2013) 'AMS 14C dating and stable isotope (carbon, nitrogen) analysis of an earlier Neolithic human skeletal assemblage from Hay Wood Cave, Mendip, Somerset.', *Proceedings of the University of Bristol Speleological Society*, 26(1), pp. 9–26.

Scott, D.D. and Connor, M. (1997) 'Context Delicti: Archaeological Context in Forensic Work', in W. Hagland and M. Sorg (eds) *Forensic Taphonomy:The Postmortem Fate of Human Remains*. CRC Press LLC.

Serjeantson, D. (2014) 'Survey of animal remains from southern Britain finds no evidence for continuity from the Mesolithic period', *Environmental Archaeology*, 19(3), pp. 256–262. Available at: https://doi.org/10.1179/1749631414Y.0000000020.

Sheridan, A. (2004) 'Neolithic connections along and across the Irish Sea', in V. Cummings and C. Fowler (eds) *The Neolithic of the Irish Sea: Materiality and traditions of practice*. Oxbow Books, pp. 9–21. Available at: https://doi.org/10.2307/j.ctvh1dq1n.7.

Sheridan, A. (2007) 'From Picardie to Pickering and Pencraig Hill? New information on the "Carinated Bowl Neolithic" in northern Britain.', in A. Whittle and V. Cummings (eds) *Going Over: The Mesolithic–Neolithic Transition in North-West Europe.* Oxford: British Academy and Oxford University Press., pp. 441–492.

Sheridan, A. (2010) 'The Neolithization of Britain and Ireland: The "Big Picture"', in B. Finlayson and G. Warren (eds) *Landscapes in transition*. Oxbow Books.

Sheridan, A. and Pétrequin, P. (2014) 'Constructing a Narrative for the Neolithic of Britain and Ireland: The Use of "Hard Science" and Archaeological Reasoning', in A. Whittle and P. Bickle (eds) *Early Farmers: The View of Archaeology and Science (Proceedings of the British Academy 198)*. Oxford: Oxford University Press, pp. 369–390. Available at: https://doi.org/10.5871/bacad/9780197265758.003.0019.

Shipman, P. (1981) 'Applications of Scanning Electron Microscopy to Taphonomic Problems', *Annals of the New York Academy of Sciences*, 376(1), pp. 357–385. Available at: https://doi.org/10.1111/j.1749-6632.1981.tb28179.x.

Silvestri, L. *et al.* (2020) 'Grotta Mora Cavorso: Physical, material and symbolic boundaries of life and death practices in a Neolithic cave of central Italy', *Quaternary International*, 539(September 2018), pp. 29–38. Available at: https://doi.org/10.1016/j.quaint.2018.09.050.

Simmons, T., Jantz, R.L. and Bass, W.M. (1990) 'Stature Estimation from Fragmentary Femora: A Revision of the Steele Method', *Journal of Forensic Sciences*, 35(3), p. 12868J. Available at: https://doi.org/10.1520/JFS12868J.

Smith, D.E. *et al.* (2011) 'The early Holocene sea level rise', *Quaternary Science Reviews*, 30(15–16), pp. 1846–1860. Available at: https://doi.org/10.1016/j.quascirev.2011.04.019.

Smith, I.R. (2012) 'Radio-carbon Dating of Bones from Caves in Furness.', *Cumberland and Westmorland Antiquarian and Archaeological Society Newsletter*, 70(6).

Smith, I.R., Wilkinson, D.M. and O'Regan, H.J. (2013) 'New Lateglacial fauna and early Mesolithic human remains from Northern England.', *Journal of Quaternary Science*, 28(6), pp. 542–544. Available at: https://doi.org/10.1002/jqs.2655.

Smith, M. (2006) 'Bones chewed by canids as evidence for human excarnation: A British case study', *Antiquity*, 80(309), pp. 671–685. Available at: https://doi.org/10.1017/S0003598X00094126.

Smith, M. and Brickley, M. (2009) *People of the long barrows: life, death and burial in the Earlier Neolithic*. Gloucestershire: The History Press.

Snoddy, A.M.E. *et al.* (2018) 'Macroscopic features of scurvy in human skeletal remains: A literature synthesis and diagnostic guide', *American Journal of Physical Anthropology*, 167(4), pp. 876–895. Available at: https://doi.org/10.1002/ajpa.23699.

Snodgrass, J.J. (2004) 'Sex Differences and Aging of the Vertebral Column', *Journal of Forensic Sciences*, 49(3), pp. 1–6. Available at: https://doi.org/10.1520/JFS2003198.

Snoeck, C., Lee-Thorp, J.A. and Schulting, R.J. (2014) 'From bone to ash: Compositional and structural changes in burned modern and archaeological bone', *Palaeogeography, Palaeoclimatology, Palaeoecology*, 416, pp. 55–68. Available at: https://doi.org/10.1016/j.palaeo.2014.08.002.

Sorg, Marcella.H. and Haglund, William.D. (2002) 'Advancing Forensic Taphonomy: Purpose, Theory, and Process', in William.D. Haglund and Marcella.H. Sorg (eds) *Advances in Forensic Taphonomy. Method, Theory, and Archaeologial Perspectives*. Boca Raton, Fl: CRC Press, pp. 3–30.

Spradley, M.K. and Jantz, R.L. (2011) 'Sex Estimation in Forensic Anthropology: Skull Versus Postcranial Elements', *Journal of Forensic Sciences*, 56(2), pp. 289–296. Available at: https://doi.org/10.1111/j.1556-4029.2010.01635.x.

Springer, G. (2005) 'Clastic Sediments in Caves', in D. Culver and W. White (eds) *Encyclopedia of Caves*. San Diego, California: Elsevier Academic Press, pp. 102–107.

Stavrova, T. *et al.* (2019) 'A GIS based approach to long bone breakage patterns derived from marrow extraction', *PLoS ONE*, 14(5), pp. 1–26. Available at: https://doi.org/10.1371/journal.pone.0216733.

Steele, D.G. and McKern, T.W. (1969) 'A method for assessment of maximum long bone length and living stature from fragmentary long bones', *American Journal of Physical Anthropology*, 31(2), pp. 215–227. Available at: https://doi.org/10.1002/ajpa.1330310211.

Stiner, M.C. (1994) *Honor among thieves: A Zooarchaeological study of neandertal ecology.* Princeton: Princeton University Press.

Stiner, M.C. (2004) 'Comparative ecology and taphonomy of spotted hyenas, humans, and wolves in Pleistocene Italy', *Revue de Paléobiologie, Gèneve*, 23(2), pp. 771–785.

Straus, L. (1990) 'Underground Archaeology: Perspectives on Caves and Rockshelters', in *Archaeological Method and Theory*. Springer, pp. 255–304.

Straus, L. (1997) 'Convenient cavities: some human uses of caves and rockshelters', *BAR International Series*, 667, pp. 1–8.

Stull, K.E. *et al.* (2020) 'Subadult sex estimation and KidStats', in *Sex Estimation of the Human Skeleton*. Academic Press, pp. 219–242.

Stull, K.E., L'Abbé, E.N. and Ousley, S.D. (2017) 'Subadult sex estimation from diaphyseal dimensions: STULL ET AL .', *American Journal of Physical Anthropology*, 163(1), pp. 64–74. Available at: https://doi.org/10.1002/ajpa.23185.

Sutton, T. *et al.* (2023) '17.3. Georeferencer - QGIS User Guide'. Available at: https://docs.qgis.org/3.28/en/docs/user_manual/working_with_raster/georeferencer.html (Accessed: 12 July 2023).

Sykes, N. (2017) 'Fair game: exploring the dynamics, perception and environmental impact of "surplus" wild foods in England 10kya–present', *World Archaeology*, 49(1), pp. 61–72. Available at: https://doi.org/10.1080/00438243.2016.1269666.

Symes, S., L'Abbé, E., Stull, K., *et al.* (2013) 'Taphonomy and the Timing of Bone Fractures in Trauma Analysis', in James.T. Pokines and S. Symes (eds) *Manual of Forensic Taphonomy*. CRC Press, pp. 341–362.

Symes, S., L'Abbé, E., Pokines, J., *et al.* (2013) 'Thermal Alteration to Bone', in J.T. Pokines and S. Symes (eds) *Manual of Forensic Taphonomy*. CRC Press, pp. 367–402.

Teather, A. and Chamberlain, A. (2016) 'Dying Embers: Fire-lighting Technology and Mortuary Practice in Early Bronze Age Britain', *Archaeological Journal*, 173(2), pp. 188–205. Available at: https://doi.org/10.1080/00665983.2016.1177258.

Terrell-Nield, C. and Macdonald, J. (1997) 'The effects of decomposing animal remains on cave invertebrate communities.', *Cave and Karst Science*, 24(2), pp. 53–63.

Thomas, J. (2000) 'Death , Identity and the Body in Neolithic Britain', *The Journal of the Royal Anthropological Institute*, 6(4), pp. 653–668.

Thomas, J. (2003) 'Thoughts on the "repacked" Neolithic revolution. Antiquity, 77(295), pp.67-74.', *Antiquity*, 77(295), pp. 67–74.

Thomas, J. (2004) 'Current debates on the Mesolithic-Neolithic transition in Britain and Ireland', *Documenta Praehistorica*, 31(January), pp. 113–130. Available at: https://doi.org/10.4312/dp.31.8.

Thomas, J. (2013) *The Birth of Neolithic Britain*. 1st edn. Oxford: Oxford University Press.

Thompson, J.E. *et al.* (2020) 'Placing and remembering the dead in late Neolithic Malta: bioarchaeological and spatial analysis of the Xagħra Circle Hypogeum, Gozo', *World Archaeology*, 52(1), pp. 71–89. Available at: https://doi.org/10.1080/00438243.2019.1745680.

Todd, T.W. (1920) 'Age changes in the pubic bone in the male white pubis.', *American Journal of Physical Anthropology*, 3(3), pp. 285–334.

Tomé, T., Díaz-Zorita Bonilla, M. and Silva, A.M. (eds) (2017) *Current approaches to collective burials in the late European prehistory*. *UISPP World Congress*, Oxford: Archaeopress Publishing Ltd (Proceedings of the XVII UISPP World Congress (1–7 September 2014, Burgos, Spain), volume 14 = session A25b).

Tomkins, p (2012) 'Landscapes of Ritual, Identity, and Memory: Reconsidering Neolithic and Bronze Age Cave Use in Crete, Greece', in H. Moyes (ed.) *Sacred Darkness : A Global Perspective on the Ritual Use of Caves*. Boulder: University Press of Colorado, pp. 104–134.

Toussaint, M. (2011) 'Intentional cutmarks on an early mesolithic human calvaria from Margaux Cave (Dinant, Belgium)', *American Journal of Physical Anthropology*, 144(1), pp. 100–107. Available at: https://doi.org/10.1002/ajpa.21375.

Trematerra, P. and Pinniger, D. (2018) 'Museum Pests–Cultural Heritage Pests', in C.G. Athanassiou and F.H. Arthur (eds) *Recent Advances in Stored Product Protection*. Berlin, Heidelberg: Springer Berlin Heidelberg, pp. 229–260. Available at: https://doi.org/10.1007/978-3-662-56125-6_11.

Trotter, M. (1970) 'Estimation of stature from intact limb long bones.', in T.D. Stewart (ed.) *Personal Identification in Mass Disasters*. Smithsonian Institution: Washington., pp. 71–83.

Trotter, M. and Gleser, G. (1952) 'Estimation of stature from long bones of American Whites and Negroes.', *American Journal of Physical Anthropology*, 10, pp. 463–514.

Tuller, H., Hofmeister, U. and Daley (2008) 'Spatial Analysis of Mass Grave Mapping Data to Assist in the Reassociation of Disarticulated and Commingled Human Remains Recovery, Analysis, and Identification of Commingled Human Remains', in B. Adams and J.E. Byrd (eds) *Recovery, Analysis, and Identification of Commingled Human Remains*. Totowa, NJ: Humana Press, pp. 7–30.

Turner, A., Gonzalez, S. and Ohman, J.C. (2002) 'Prehistoric human and ungulate remains from Preston Docks, Lancashire, UK: Problems of river finds', *Journal of Archaeological Science*, 29(4), pp. 423–433. Available at: https://doi.org/10.1006/jasc.2002.0730.

Ubelaker, D.H. (1989) *Human skeletal remains.* Washington, DC: Taraxxacum Press.

Ubelaker, D.H. (2014) 'Commingling Analysis: Historical and Methodological Perspectives', in B.J. Adams and J.E. Byrd (eds) *Commingled Human Remains: Methods in Recovery, Analysis, and Identification*. Academic Press, pp. 1–6. Available at: https://doi.org/10.1016/C2012-0-02768-8.

Ubelaker, D.H. and Khosrowshahi, H. (2019) 'Estimation of age in forensic anthropology: historical perspective and recent methodological advances', *Forensic Sciences Research*, 4(1), pp. 1–9. Available at: https://doi.org/10.1080/20961790.2018.1549711.

Ungar, P. and Williamson, M. (2000) 'Exploring the Effects of Toothwear on Functional Morphology: A Preliminary Study Using Dental Topographic Analysis.', *Palaeontologia Electronica*, 3(1), pp. 1–18.

Ustinova, Y. (2009) ‘Caves and the Ancient Greek Mind: Descending Underground in the Search for the Ultimate Truth’, in. Oxford: Oxford University Press. Available at: https://doi.org/10.1093/acprof:oso/9780199548569.001.0001.

Val, A., Taru, P. and Steininger, C. (2014) ‘New taphonomic analysis of large-bodied primate assemblage from Cooper’s D, Bloubank Valley, South Africa.’, *South African Archaeological Bulletin*, 69(199), pp. 49–58.

Verhagen, P. (2018) ‘Spatial Analysis in Archaeology: Moving into New Territories’, in C. Siart, M. Forbriger, and O. Bubenzer (eds) *Digital Geoarchaeology*. Cham: Springer International Publishing (Natural Science in Archaeology), pp. 11–25. Available at: https://doi.org/10.1007/978-3-319-25316-9_2.

Villa, P. *et al.* (1986) ‘Cannibalism in the neolithic’, *Science*, 233(4762), pp. 431–437. Available at: https://doi.org/10.1126/science.233.4762.431.

Villa, P. and Mahieu, E. (1991) ‘Breakage patterns of human long bones’, *Journal of Human Evolution*, 21(1), pp. 27–48. Available at: https://doi.org/10.1016/0047-2484(91)90034-S.

Villotte, S. *et al.* (2020) ‘Disentangling Cro-Magnon: The adult upper limb skeleton’, *Journal of Archaeological Science: Reports*, 33(July), pp. 102475–102475. Available at: https://doi.org/10.1016/j.jasrep.2020.102475.

Walker, P.L. (2005) ‘Greater sciatic notch morphology: Sex, age, and population differences’, *American Journal of Physical Anthropology*, 127(4), pp. 385–391. Available at: https://doi.org/10.1002/ajpa.10422.

Waltham, T. and Lowe, D. (2013) ‘The Yorkshire Dales’, in T. Waltham and D. Lowe (eds) *Caves and Karst of the Yorkshire Dales: Volume 1*. British Cave Research Association, pp. 1–10.

Waltham, T. and Murphy, P. (2013) ‘Cave geomorphology’, in T. Waltham and D. Lowe (eds) *Caves and Karst of the Yorkshire Dales: Volume 1*. British Cave Research Association, pp. 117–146.

Warburton, K.C. (2017) *An Osteoarchaeological and Taphonomic Analysis of Neolithic and Bronze Age Human Skeletal Remains from Heaning Wood Bone Cave, Great Urswick, Cumbria*. Unpublished Thesis. University of Central Lancashire.

Waters, C. and Lowe, D. (2013) ‘Geology of the limestones’, in T. Waltham and D. Lowe (eds) *Caves and Karst of the Yorkshire Dales: Volume 1*. British Cave Research Association, pp. 11–28.

Watson, J.P.N. (1979) ‘The estimation of the relative frequencies of mammalian species: Khirokitia 1972’, *Journal of Archaeological Science*, 6(2), pp. 127–137. Available at: https://doi.org/10.1016/0305-4403(79)90058-X.

White, T.D., Black, M.T. and Folkens, P.A. (2011) ‘Human osteology.’ Academic Press.

White, T.D. and Folkens, P.A. (2005) *The human bone manual.* Elsevier.

White, T.E. (1953) ‘A Method of Calculating the Dietary Percentage of Various Food Animals Utilized by Aboriginal Peoples’, *American Antiquity*, 18(4), pp. 396–398. Available at: https://doi.org/10.2307/277116.

White, W.B. (2007) 'Cave sediments and paleoclimate', Journal of Cave and Karst Studies, 69(1), pp.76-93.

Whitehouse, N.J. *et al.* (2014) ‘Neolithic agriculture on the European western frontier: The boom and bust of early farming in Ireland’, *Journal of Archaeological Science*, 51, pp. 181–205. Available at: https://doi.org/10.1016/j.jas.2013.08.009.

Whitehouse, R. (2015) ‘Water turned to stone Stalagmites and stalactites in cult caves in prehistoric Italy’, *Accordia Research Papers*, 14, pp. 49–62.

Whitehouse, R. (2016) ‘Between symbol and senses: the role of darkness in prehistoric Italy’, in M. Dowd and R. Hensey (eds) *The Archaeology of Darkness*. Oxford Books, Limited, pp. 25–38.

Whitley, J. (2002) ‘Too many ancestors’, *Antiquity*, 76(291), pp. 119–126. Available at: https://doi.org/10.1017/S0003598X00089870.

Whittle, A. *et al.* (2007) ‘Building for the dead: Events, processes and changing worldviews from the thirty-eighth to the thirty-fourth centuries cal. bc in Southern Britain’, *Cambridge Archaeological Journal*, 17(SUPPL.1), pp. 123–147. Available at: https://doi.org/10.1017/S0959774307000200.

Whittle, A. (2007) ‘The temporality of transformation: dating the early development of the southern British Neolithic’, in A. Whittle and V. Cummings (eds) *Going Over: The Mesolithic-Neolithic Transition in North-West Europe.* British Academy.

Whittle, A. and Bayliss, A. (2007) ‘The times of their lives: From chronological precision to kinds of history and change’, *Cambridge Archaeological Journal*, 17(1), pp. 21–28. Available at: https://doi.org/10.1017/S0959774307000030.

Whittle, A., Bayliss, A. and Healy, F. (2011) ‘Gathering time: the social dynamics of change’, in Whittle, A., F. Healy, and Alex Bayliss (eds) *Gathering Time. Dating the Early Neolithic Enclosures of Southern Britain and Ireland. Volume 2*. Oxford, UK: Oxbow Books, pp. 848–914.

Whittle, A., Bayliss, A. and Wysocki, M. (2007) ‘Once in a lifetime: The date of the wayland’s smithy long barrow’, *Cambridge Archaeological Journal*, 17(SUPPL.1), pp. 103–121. Available at: https://doi.org/10.1017/S0959774307000194.

Whittle, A., Healy, F. and Bayliss, A. (2011a) ‘Gathering time: causewayed enclosures and the early Neolithic of southern Britain and Ireland’, in A. Whittle, F. Healy, and A. Bayliss (eds) *Gathering Time. Dating the Early Neolithic Enclosures of Southern Britain and Ireland. Volume 1*. Oxford, UK: Oxbow Books, pp. 1–16.

Whittle, A., Healy, F. and Bayliss, A., (2011b). *Gathering time: dating the early Neolithic enclosures of southern Britain and Ireland*. Oxbow Books.

Wilbur, A.K. (1998) 'The utility of hand and foot bones for the determination of sex and the estimation of stature in a prehistoric population from west-central Illinois', *Int. J. Osteoarchaeol.*, p. 12.

Wilson, A. *et al.* (2020) 'Quantifying human post-mortem movement resultant from decomposition processes', *Forensic Science International: Synergy*, 2, pp. 248–261. Available at: https://doi.org/10.1016/j.fsisyn.2020.07.003.

Wysocki, M., Bayliss, A. and Whittle, A. (2007) 'Serious mortality: The date of the fussell's lodge long barrow', *Cambridge Archaeological Journal*, 17(SUPPL.1), pp. 65–84. Available at: https://doi.org/10.1017/S0959774307000170.

Wysocki, M. and Whittle, A. (2000) 'Diversity, lifestyles and rites: New biological and archaeological evidence from British Earlier Neolithic mortuary assemblages', *Antiquity*, 74(285), pp. 591–601. Available at: https://doi.org/10.1017/S0003598X00059950.

Zanetti, N.I., Visciarelli, E.C. and Centeno, N.D. (2014) 'Taphonomic marks on pig tissue due to cadaveric coleoptera activity under controlled conditions.', *Journal of Forensic Sciences*, 59(4), pp. 997–1001.

Zephro, L. and Galloway, A. (2014) 'The biomechanics of fracture production', in V.L. Wedel and A. Galloway (eds) *Broken bones: Anthropological analysis of blunt force trauma*. 2nd edn. Springfield, Illinois: Charles C Thomas Publisher LTD, pp. 33–45.

Zuccotti, L.F. *et al.* (1998) 'Technical note: Modeling primate occlusal topography using geographic information systems technology', *American Journal of Physical Anthropology*, 107(1), pp. 137–142. Available at: https://doi.org/10.1002/(SICI)1096-8644(199809)107:1<137::AID-AJPA11>3.0.CO;2-1.

# APPENDICES

Due to the size of some spreadsheets several are listed as a hyperlink. Clicking the link will automatically download the relevant Excel file.

The following lists all links in an index for quick reference:
https://kcw.q-ten.net/appendix/

# APPENDIX ONE: METHODOLOGY

## 1.1: Bone Names and Associated Codes

Table 1.1: List of skeletal elements and codes

| Element | Element ID |
|---|---|
| **Cranial** | |
| Cranium | CR |
| Fragment | $CR_{fg}$ |
| Frontal | CRF |
| Parietal | CRP |
| Sphenoid | CRS |
| Zygomatic | CRZ |
| Temporal | CRT |
| Petrous only | $CRT_P$ |
| Maxilla | CRM |
| Nasal | CRN |
| Lacrimal | CRL |
| Occipital | CRO |
| Ethmoid | CRE |
| Palatine | CRPa |
| Vomer | CRV |
| Inferior Nasal Concha | CRInc |
| Mandible | MB |
| Incus | IN |
| Malleus | ML |
| Stapes | SP |
| **Post Cranial** | |
| Hyoid | HY |
| Sternum | ST |
| Clavicle | CL |
| Rib 1 | R1 |
| Rib 2 | R2 |
| Rib 3 | R3 |
| Rib 4 | R4 |

| | |
|---|---|
| Rib 5 | R5 |
| Rib 6 | R6 |
| Rib 7 | R7 |
| Rib 8 | R8 |
| Rib 9 | R9 |
| Rib 10 | R10 |
| Rib 11 | R11 |
| Rib 12 | R12 |
| Rib head | RH |
| Rib end | RE |
| Scapula | SC |
| Humerus | HU |
| Radius | RA |
| Ulna | UL |
| Femur | FE |
| Patella | PA |
| Tibia | TI |
| Fibula | FI |
| Pelvis | PE |
| Scaphoid | SD |
| Lunate | LU |
| Triquetral | TQ |
| Pisiform | PI |
| Trapezium | TZM |
| Trapezoid | TZD |
| Capitate | CA |
| Hamate | HA |
| MC1 | 1MC |
| MC2 | 2MC |
| MC3 | 3MC |
| MC4 | 4MC |
| MC5 | 5MC |
| Manual Phalanges | MPH |

| | |
|---|---|
| Calcaneus | CL |
| Talus | TL |
| Navicular | NA |
| Cuboid | CU |
| Medial Cuneiform | MCU |
| Intermediate Cuneiform | ICU |
| Lateral Cuneiform | LCU |
| MT1 | 1MT |
| MT2 | 2MT |
| MT3 | 3MT |
| MT4 | 4MT |
| MT5 | 5MT |
| Pedal Phalanges | PPH |
| C1 | 1C |
| C2 | 2C |
| C7 | 7C |
| T1 | 1T |
| T10 | 10T |
| T11 | 11T |
| T12 | 12T |
| Cervical | CV |
| Thoracic | TV |
| Lumbar | LV |
| Sacrum | SM |
| Coccyx | CX |
| Juvenile (variants) | |
| Ilium | $PE_{IL}$ |
| Ischium | $PE_{IC}$ |
| Pubis | $PE_{p}$ |

## 1.2: QGIS Codes

### *1.2.1: Field Attributes for GIS*

Table 1.2: Field names for GIS

| ALL | ID | Bone Code | Specimen | Bone ID | Side | Position | Position2 | View | Layer | Element | | | | | | | | | | |
|---|---|---|---|---|---|---|---|---|---|---|---|---|---|---|---|---|---|---|---|---|
| **Deposits** | *ID* | *Bone Code* | *Specimen* | *Bone ID* | *Side* | *Position* | *Position2* | *View* | *Position2* | *View* | Deposit | Depos Desc | ModExMod | Notes | | | | | | |
| **Staining** | *ID* | *Bone Code* | *Specimen* | *Bone ID* | *Side* | *Position* | *Position2* | *View* | *Position2* | *View* | Stain | Stain Desc | Tidemark | ModExMod | Notes | | | | | |
| **Destruction** | *ID* | *Bone Code* | *Specimen* | *Bone ID* | *Side* | *Position* | *Position2* | *View* | *Position2* | *View* | Destruc | Dest Desc | Timing | Time Desc | Notes | | | | | |
| **Fractures** | *ID* | *Bone Code* | *Specimen* | *Bone ID* | *Side* | *Position* | *Position2* | *View* | *Position2* | *View* | Fracture | Frac Desc | Timing | Time Desc | Cracking | Crack Type | Crack Desc | Depth | Depth Desc | Notes |
| **Absent Bone** | *ID* | *Bone Code* | *Specimen* | *Bone ID* | *Side* | *Position* | *Position2* | *View* | *Position2* | *View* | Destruc | Dest Desc | | | | | | | | |
| **Animal Modifications** | *ID* | *Bone Code* | *Specimen* | *Bone ID* | *Side* | *Position* | *Position2* | *View* | *Position2* | *View* | Animal | Animal Des | Mark Type | Mark Desc | Notes | | | | | |
| **Processing Modifications** | *ID* | *Bone Code* | *Specimen* | *Bone ID* | *Side* | *Position* | *Position2* | *View* | *Position2* | *View* | Modif | Modif Desc | Notes | | | | | | | |
| **Weathering (cracking)** | *ID* | *Bone Code* | *Specimen* | *Bone ID* | *Side* | *Position* | *Position2* | *View* | *Position2* | *View* | Cracking | Crack Desc | Crack Type | Type Desc | Depth | Depth Desc | Notes | | | |
| **Surface Effects** | *ID* | *Bone Code* | *Specimen* | *Bone ID* | *Side* | *Position* | *Position2* | *View* | *Position2* | *View* | Surf Eff | Sur Ef Des | Notes | | | | | | | |
| **Root** | *ID* | *Bone Code* | *Specimen* | *Bone ID* | *Side* | *Position* | *Position2* | *View* | *Position2* | *View* | Root Type | Root Desc | Notes | | | | | | | |
| **Invertebrate** | *ID* | *Bone Code* | *Specimen* | *Bone ID* | *Side* | *Position* | *Position2* | *View* | *Position2* | *View* | Cort Remv | Remv Desc | Spread | Spread Desc | Location | Loc Desc | Notes | | | |

| Key |
|---|
| Integer |
| String |
| Y/N |

### *1.2.2: Taphonomy Codes for GIS*

Table 1.3: GIS codes for taphonomy subcategories

| Classification | Sub Classification | Code | Description |
|---|---|---|---|
| **Destruction /Damage** | **Fracture Type** | 1 | Transverse |
| | | 2 | Step/Columnar |
| | | 3 | Oblique dry |
| | | 4 | Y-shaped |
| | | 5 | Flaked |
| | | 6 | Longitudinal |
| | | 7 | Other |
| | | 8 | Spiral |
| | | 9 | Comminuted |
| | | 10 | Butterfly |
| | | 11 | Segmental |
| | | 12 | Greenstick |
| | | 13 | V-Shaped |
| | | 14 | Oblique |
| | **Fracture Timing** | 1 | Peri |
| | | 2 | Post |
| | | 3 | Ante |
| | **Cracking** | Y | Present |
| | | N | Absent |
| | **Crack Type** | 1 | Transverse |
| | | 2 | Longitudinal |
| | | 3 | Bone Grain |
| | | 4 | Other |
| | | 5 | Spiral |
| | **Crack Depth** | 1 | Superficial |
| | | 2 | Deep |
| | **Destruction** | 1 | Bone Absent |
| | | 2 | Exposure of trabecular bone |
| | | 3 | Cortical removal no exposure |
| | | 4 | Crush |

| | | | |
|---|---|---|---|
| | | 5 | Exposure of internal surface of opposite bone |
| | | 6 | Depression |
| | | 7 | Hole |
| | | 8 | Peeling |
| | | 9 | Porosity |
| | | 10 | Recent edgewear |
| **Deposits** | **Tufa/Calcite** | 1 | Thin/Flaked |
| | | 2 | Thick/Coated |
| | | 3 | Embedded |
| **Staining** | **Manganese** | 1 | Light Spotted |
| | | 2 | Dark Spotted |
| | | 3 | Light Matt |
| | | 4 | Dark Matt |
| | **Other** | 5 | Light Brown/Orange |
| | | 6 | Dark Brown/Orange |
| | **Soil** | 7 | Light Soil |
| | | 8 | Dark Soil |
| | **Tidemark** | Y | Present |
| | | N | Absent |
| **Animal** | **Animal** | 1 | Rodent |
| | | 2 | Carnivore |
| | | 3 | Other |
| | **Animal Mark** | 1 | Bone Cylinder |
| | | 2 | Tooth Pit |
| | | 3 | Tooth Score |
| | | 4 | Scalloped End |
| | | 5 | Gastric Corrosion |
| **Invertebrate** | **Cortical Removal** | 1 | Furrow |
| | | 2 | Gouge |
| | | 3 | Striation |
| | | 4 | Pitting |
| | **Spread** | 1 | Focussed |
| | | 2 | Multifocal |

| | | | |
|---|---|---|---|
| | | 3 | Diffuse |
| | | 4 | Singular |
| | **Location** | 1 | Random/Diffuse |
| | | 2 | Adjacent to joint |
| | | 3 | Distal to joint |
| **Butchery** | **Processing modifications** | 1 | Cut mark |
| | | 2 | Peeling/shaved |
| | | 3 | Point insertions/notched defects |
| | | 4 | Slot fractures |
| | | 5 | Chop marks/scoop defects |
| **Root** | | 1 | Embedding |
| | | 2 | Etching |
| **Weathering** | **Cracking** | 1 | Linear |
| | | 2 | Patination (Mosaic cracking) |
| | **Crack Type** | 1 | Transverse |
| | | 2 | Longitudinal |
| | | 3 | Bone Grain |
| | | 4 | Other |
| | **Crack Depth** | 1 | Superficial |
| | | 2 | Deep |
| | **Surface Effects** | 1 | Delamination/Peeling |
| | | 2 | Bleaching |

## 1.3: Cave Ha 3 Discrepancies

Table 1.4: Cave Ha 3 discrepancies to Leach (2006a)

| Bag Information | SL Specimen No | KW Specimen No | (KW) NISP | (KW) Element | (KW) Side | Discrepency Information |
|---|---|---|---|---|---|---|
| CH3.73.53 | CH3.100 | CH161 | 1 | MCU | L | Listed as right |
| CH3.73.43 | CH3.101 | CH164 | 1 | CU | L | Listed as right |
| CH3.37.470 | CH3.105 | CH034 | 1 | $CR_f$ | L | Listed as CRfg |
| CH3.63.87 | CH3.12 | CH055 | 1 | TV(6) | | Listed as TV5 |
| CH3.72 | | CH120 | 1 | CV1 | | Listed as CH3.63 find information and not as C1 |
| CH3.63.88 | CH3.13 | CH053 | 1 | TV(5) | | Listed as TV6 |
| CH3.73.440 | CH3.14 | CH171 | 1 | TV | u/s | Listed as TV7 |
| CH3.73.440 | CH3.15 | CH172 | 1 | TV | u/s | Listed as TV8 |
| CH3.65.65 | CH3.57 | CH089 | 1 | LU | L | Listed as scaphoid |
| CH3.65.66 | CH3.58 | CH122 | 1 | HA | L | Listed as right lunate |
| CH3.65.64 | CH3.63 | CH088 | 1 | LU | R | Listed as trapezoid |
| CH3.65.463 | CH3.64 | CH091 | 1 | TZD | L | Listed as left lunate |
| CH3.73.73 | CH3.74 | CH152 | 1 | PA | R | Listed as left |
| CH3.67.81 | CH3.75 | CH084 | 1 | PA | L | Listed as right |
| CH3.63.94 | CH3.9 | CH057 | 1 | LV(5) | | Listed as TV2 |
| CH3.73.52 | CH3.93 | CH163 | 1 | PPH | R | Listed as 4 in total |
| CH3.73.55 | CH3.95 | CH156 | 1 | PPH | L | Listed as one of the Rights - CH3.93 |
| CH3.13.116 | CH3.129 | CH010 | 1 | UL | R | Listed as CH3.73 find code |
| CH3.70.430 | | CH090 | 1 | SD | L | Not listed on SL database |
| CH3.65 | | CH092 | 1 | TZM | L | Not listed on SL database |
| CH3.42.488 | | CH099 | 1 | FE | R | Not listed on SL database |
| CH3.63.492 | | CH143 | 1 | LV | | Not listed on SL but CH3.63.94 was listed as TV |
| CH3.73.44 | | CH166 | 1 | NV | L | Not listed on SL database |
| CH3.73.67 | | CH189 | 1 | TI | L | Not listed on SL database |
| CH3.73.69 | | CH219 | 1 | TI | L | Not listed on SL database |
| CH3.73.68 | | CH220 | 1 | TI | L | Not listed on SL database |
| CH3.73.39 | | CH222 | 1 | TI | L | Not listed on SL database |
| CH3.76.241 | CH3.7 | | 1 | CV3 | | Missing |
| CH3.62.94 | CH3.21 | | 1 | LV | | Missing |
| CH3.65 | CH3.130 | | 1 | UL | R | Missing |

| Rib and Cranial Discrepencies |
|---|

| Ribs | U/S | L | R | Excluded | Total |
|---|---|---|---|---|---|
| KW | 4 | 11 | 11 | 12 | 38 |
| SL | 4 | 22 | 13 | 0 | 39 |

| Cranial Fragments | Unplaced | Placed | Excluded | | Total |
|---|---|---|---|---|---|
| KW | 27 | 22 | 3 | | 52 |
| SL | 37 | 0 | 0 | | 37 |

## 1.4: Osteology Observation Forms

### *1.4.1: Observational notes*

Specimen ID:_____

Site: Box Nº: Find Location: Find Nº:

Bone Code: Zones Present: Percent Complete: Bone Condition:

Entered on zonation form: ☐ Placeable on GIS: ☐ Taphonomy entered: ☐

Microscopy: ☐ X-Ray: ☐ CT: ☐

**Ontological Comments:**

Age:

**Metrics:**

**Taphonomic Observations:**

### *1.4.2: Adult Skeletal Sketch*

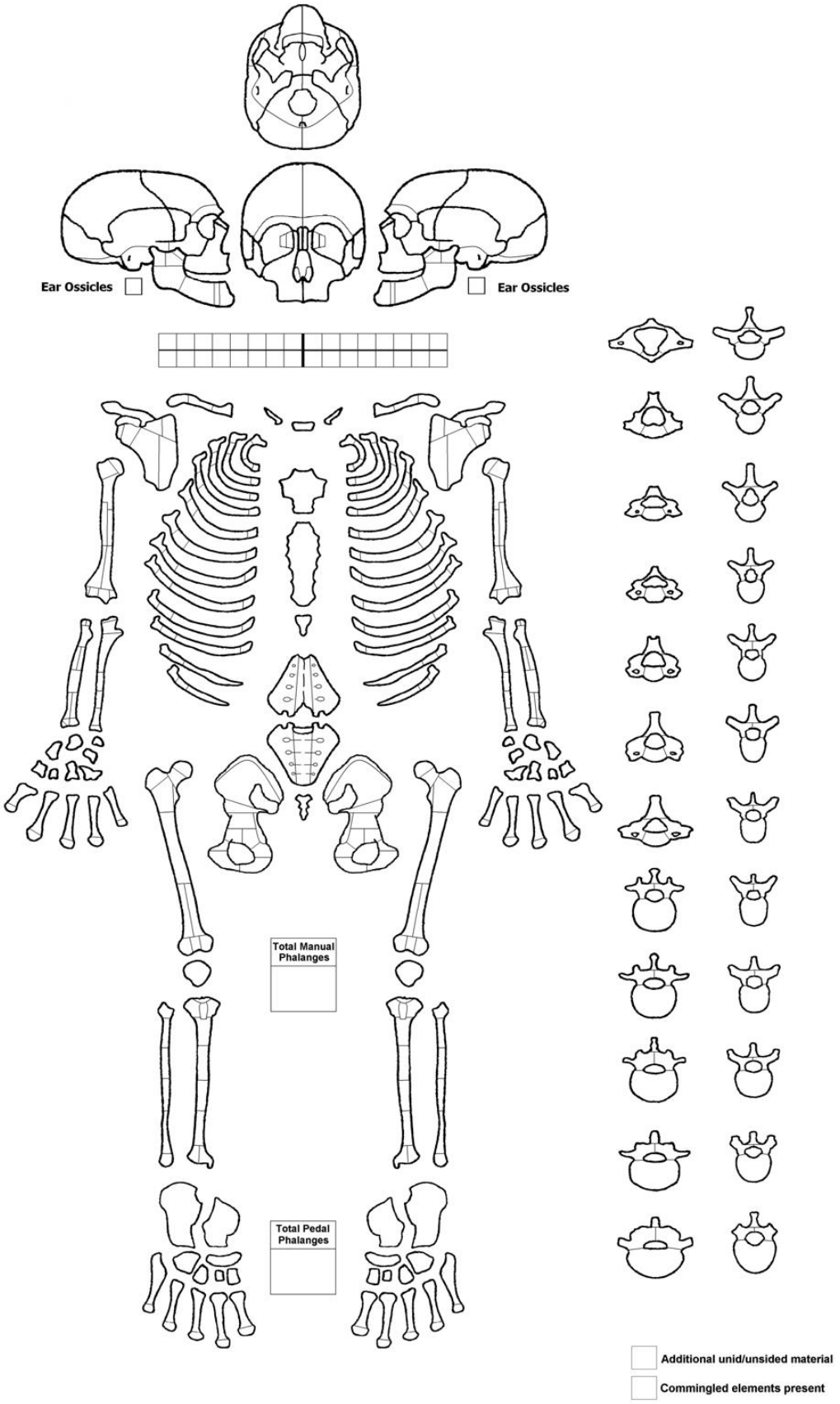


Figure 1.5: Adult sketch for initial observations

### *1.4.3: Infant Skeletal Sketch*

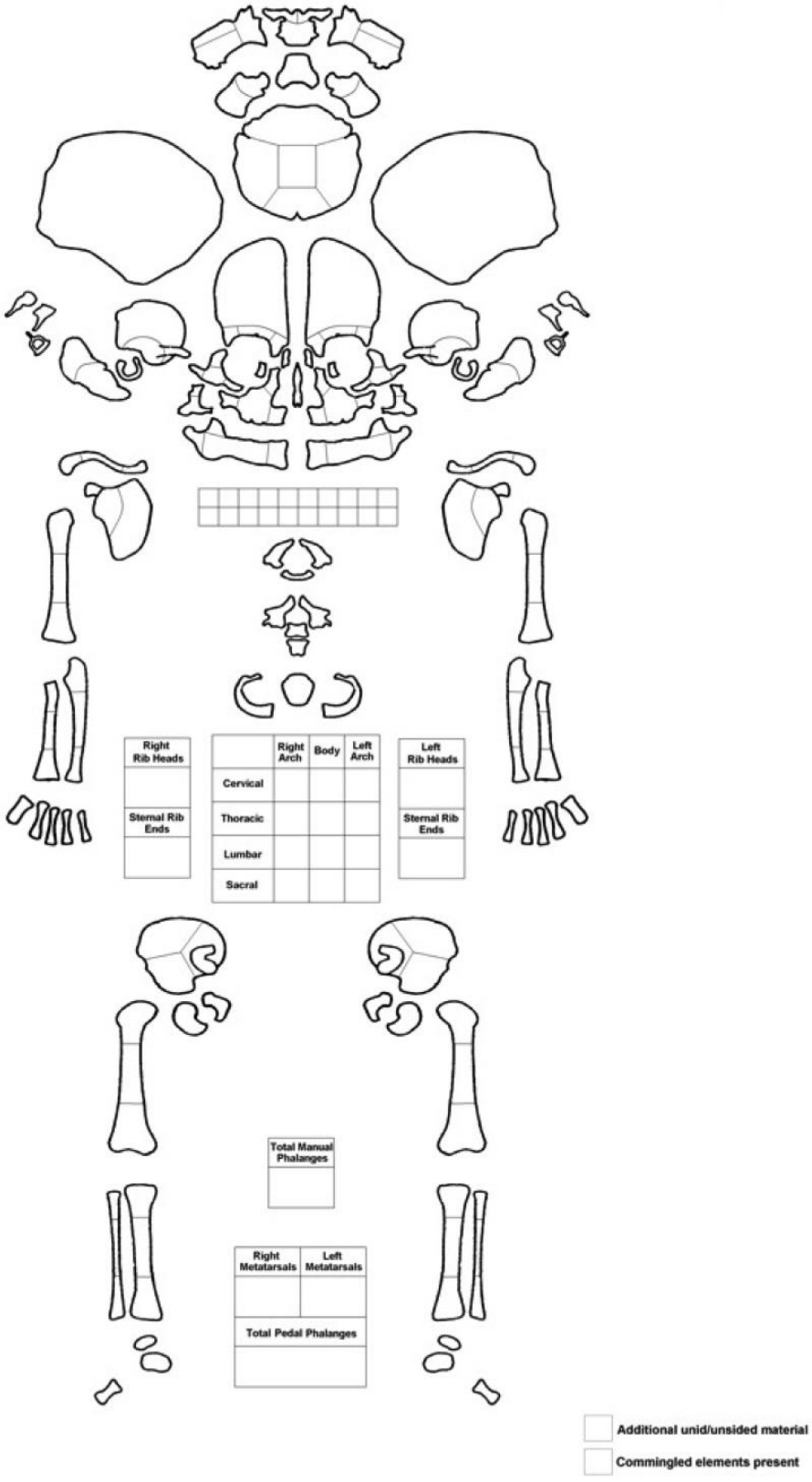


Figure 1.5: Adult sketch for initial observations

## 1.5: Skeletal Zones

### *1.5.1: Adult Zones*

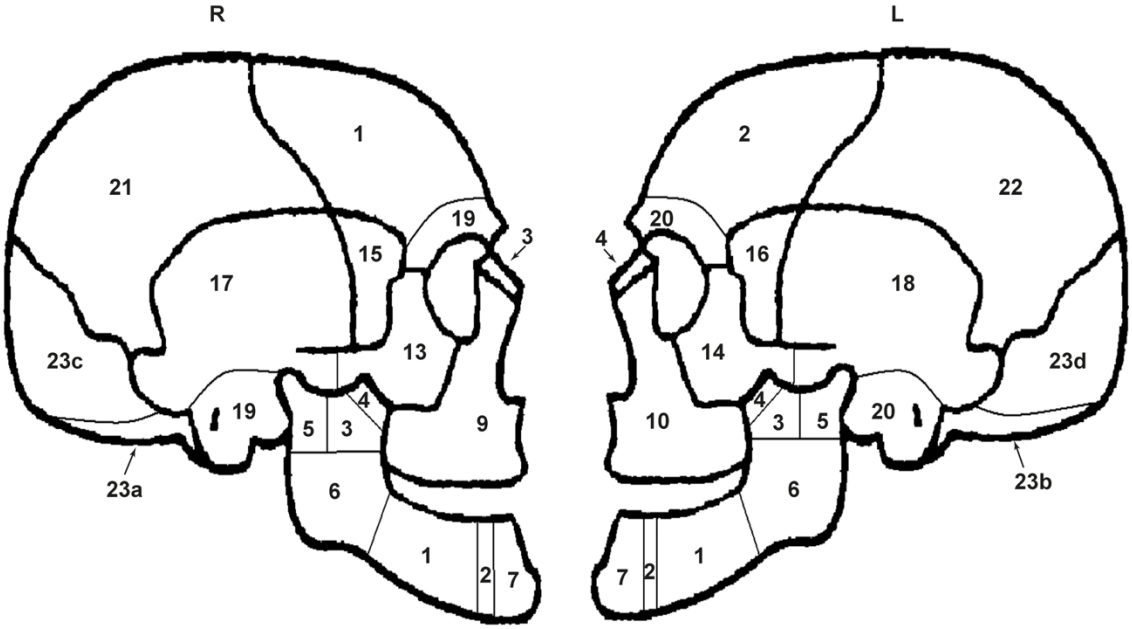


Figure 1.6: Cranial Zones (Lateral view)

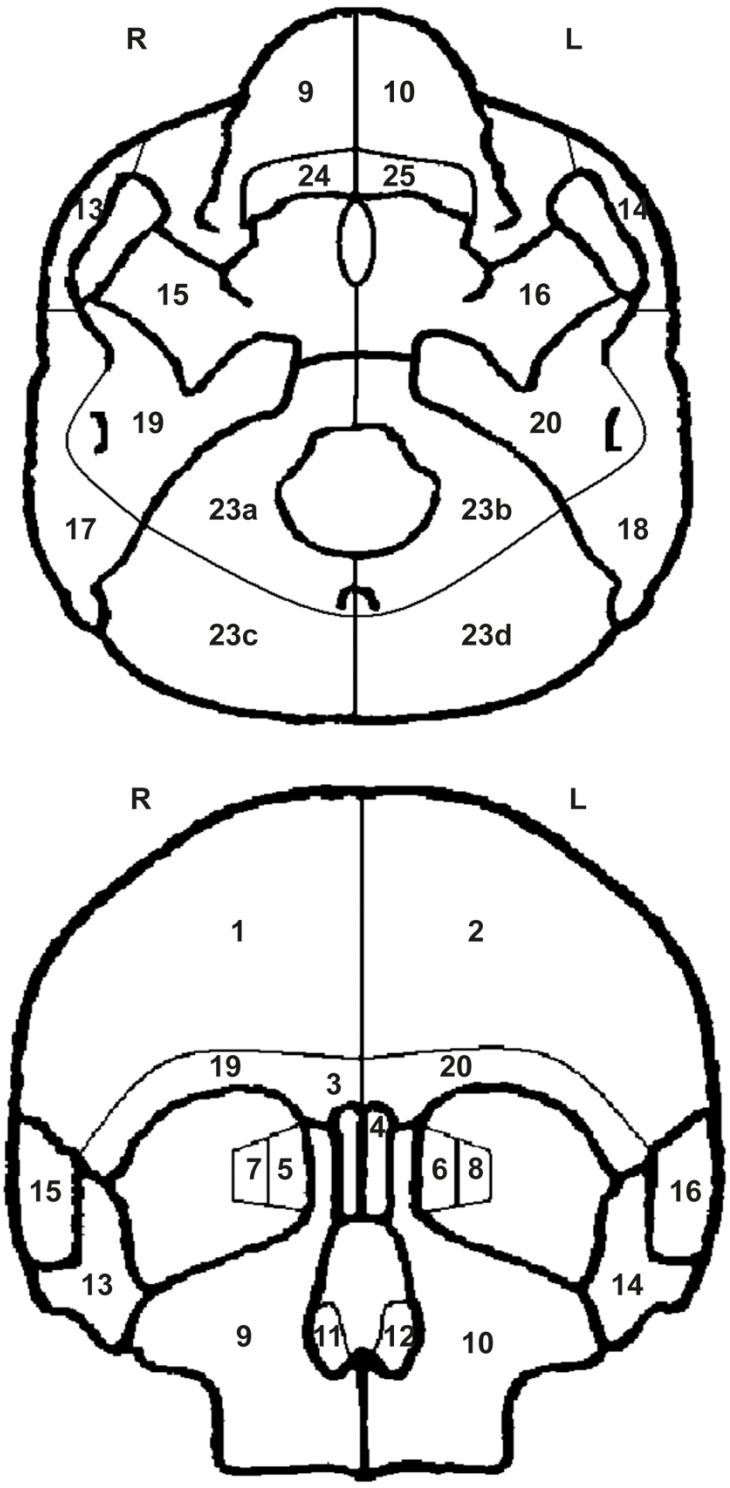


Figure 1.7: Cranial Zones (frontal and posterior view)

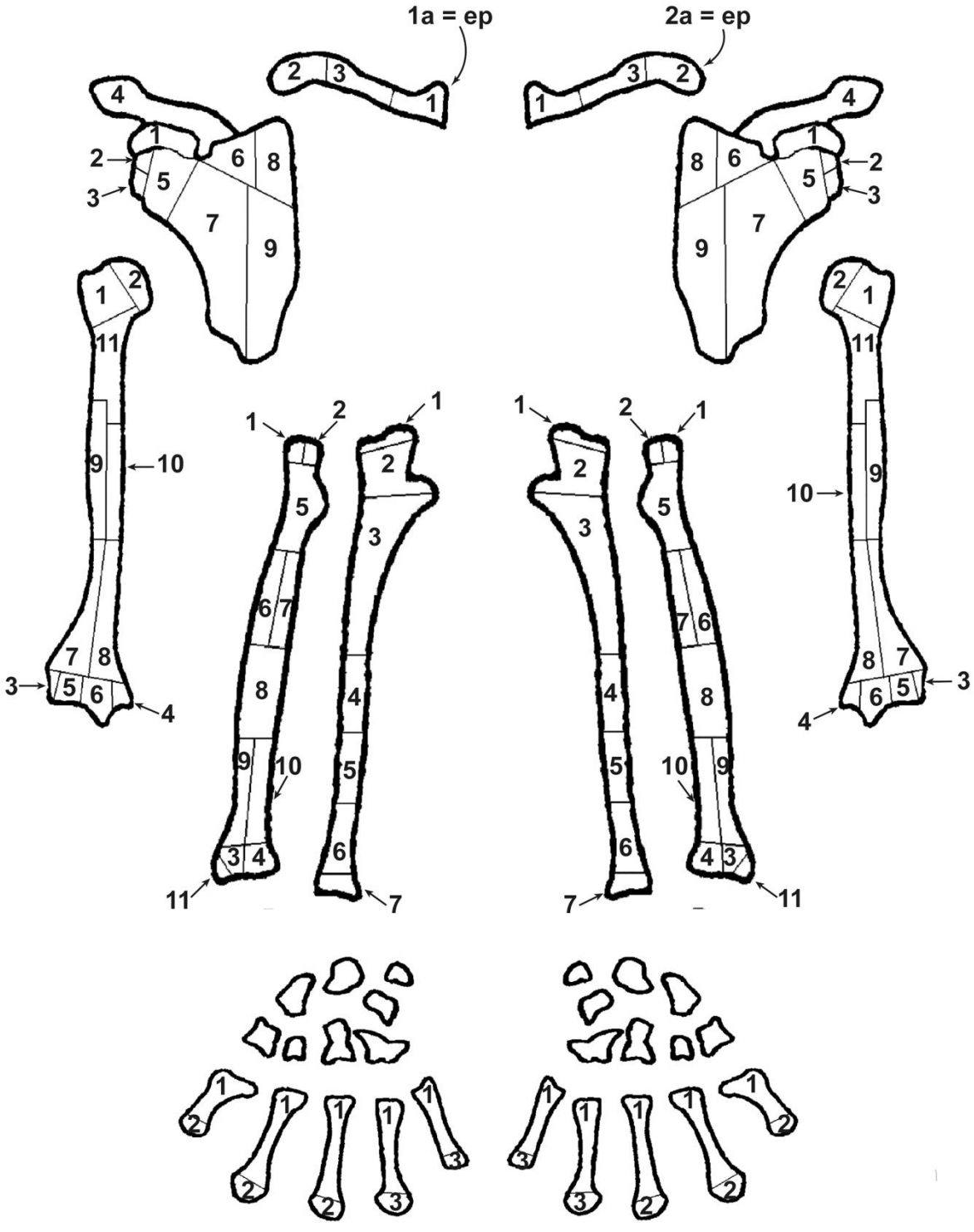


Figure 1.8: Upper Limb Zones

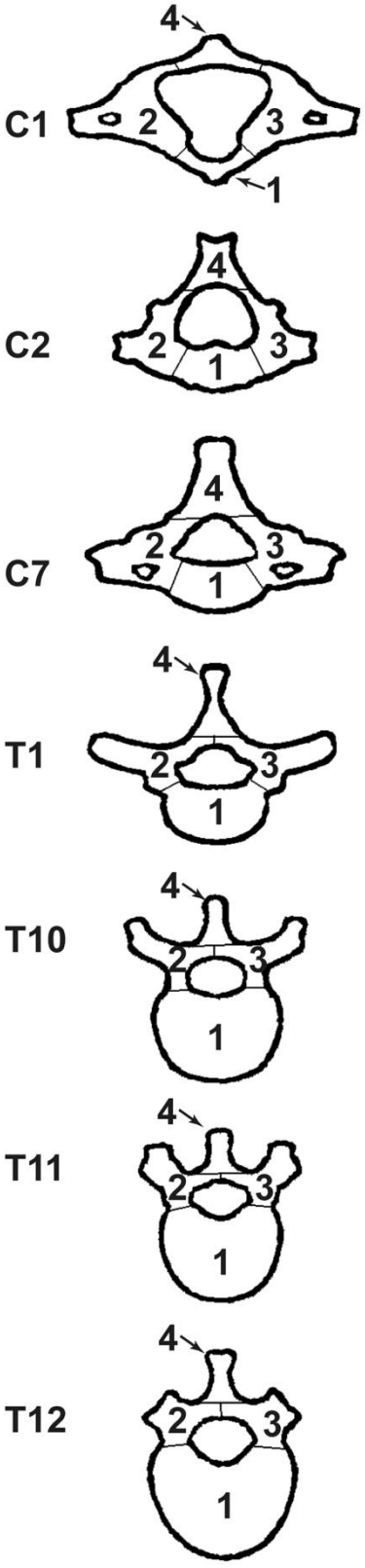


Figure 1.9: Vertebral Zones

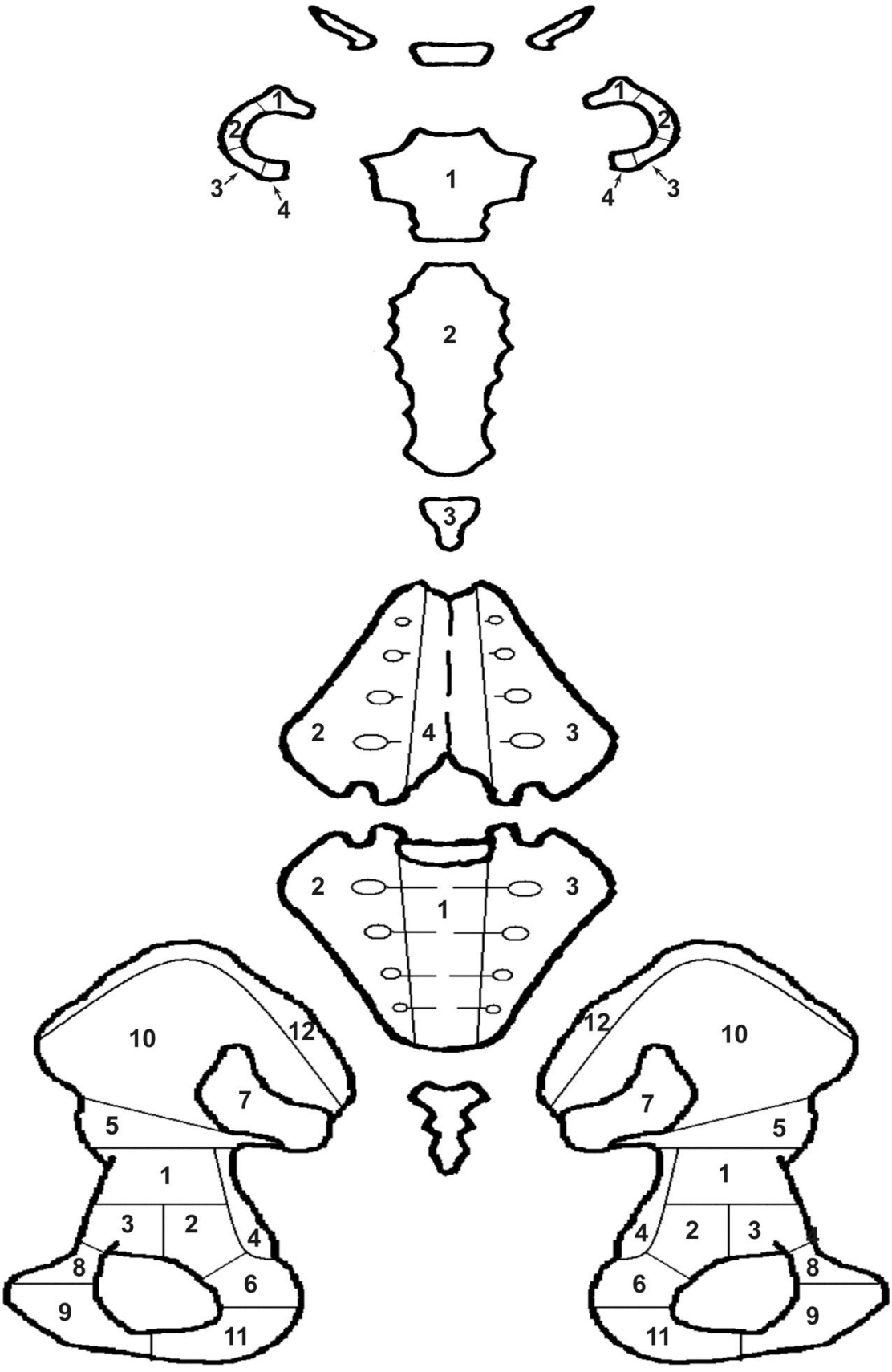


Figure 1.10: Axial Zones

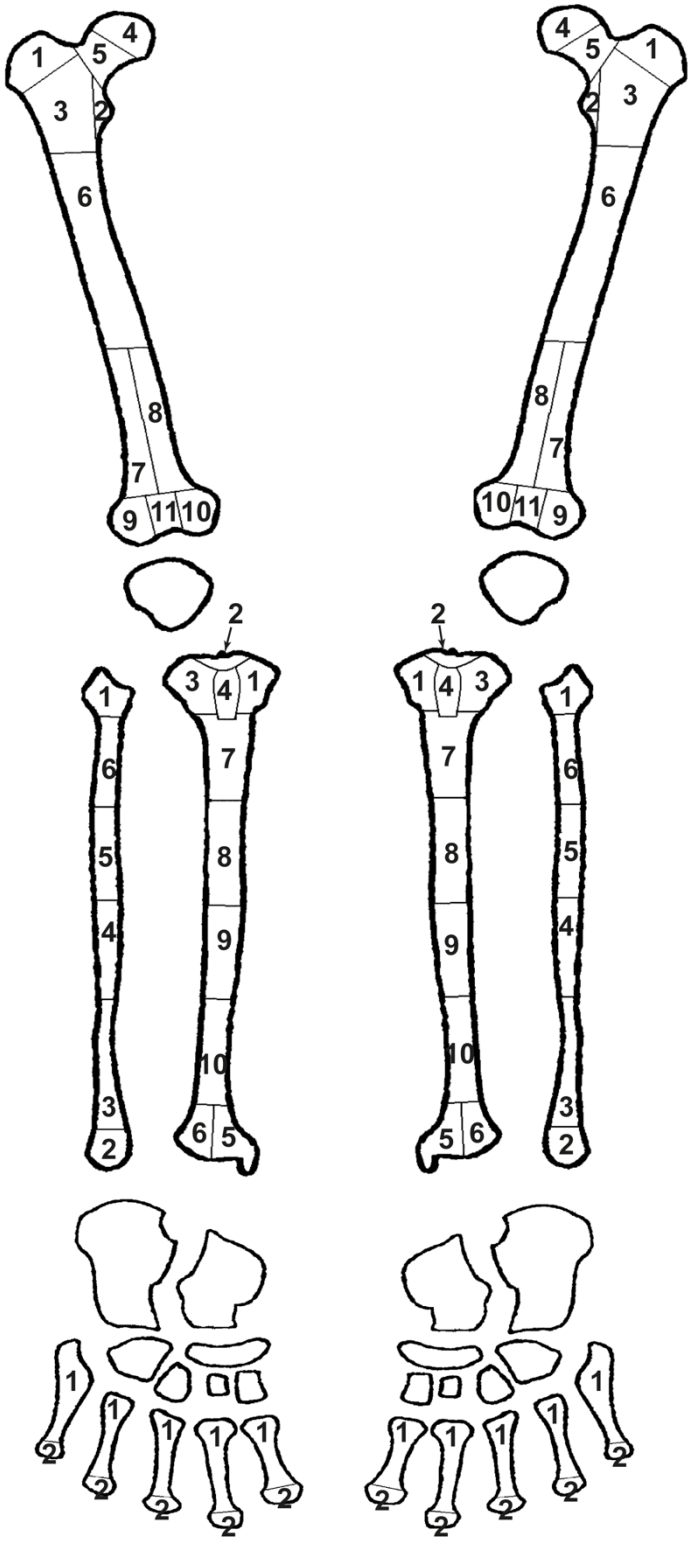


Figure 1.11: Lower Limb Zones

*1.5.2: Infant Zones*

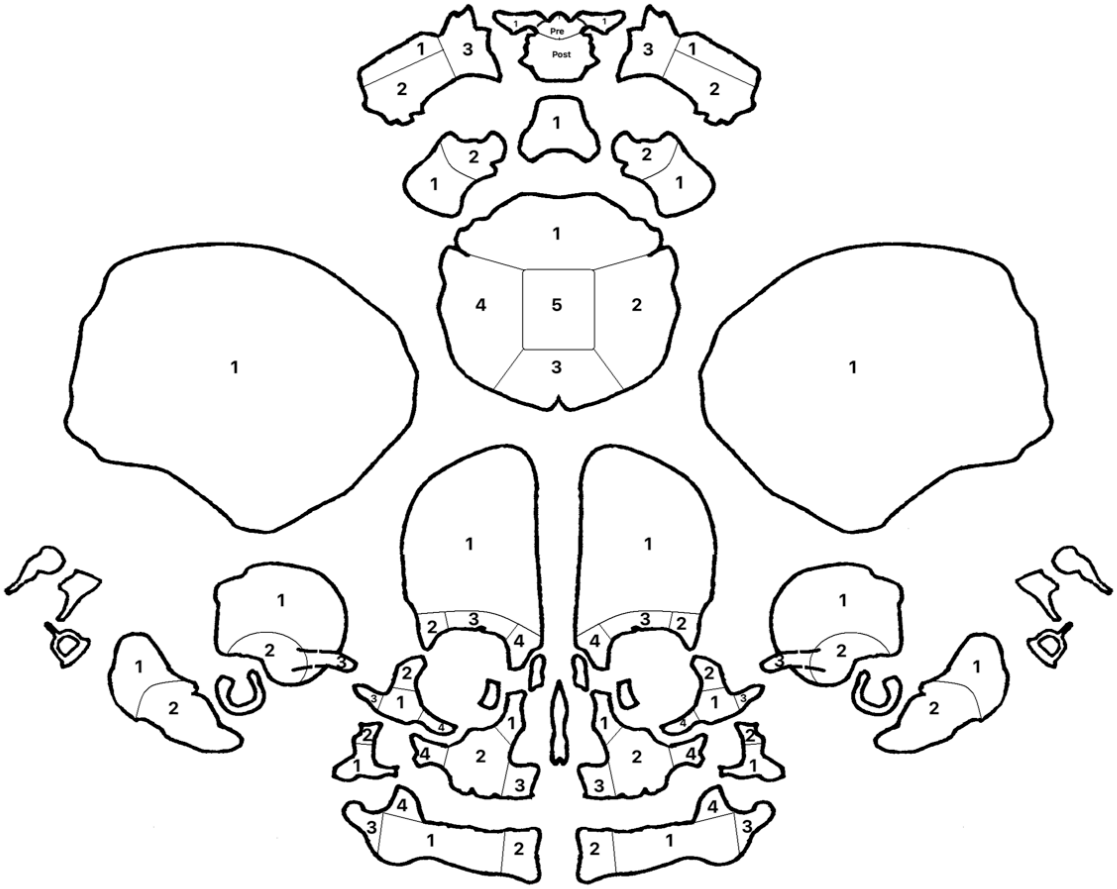


Figure 1.12: Infant Cranial Zones

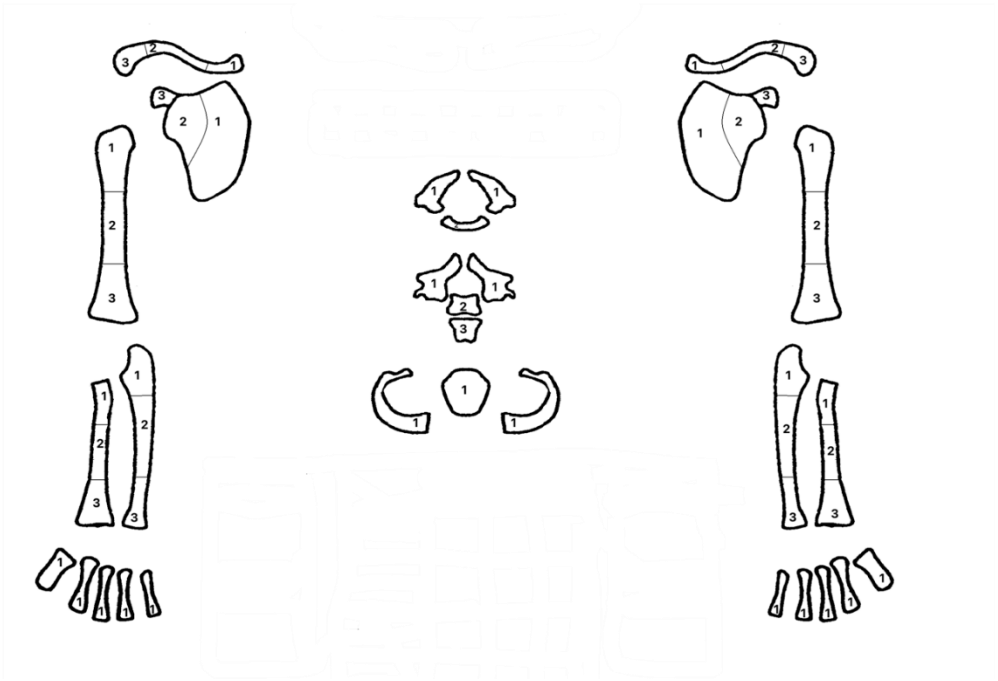

Figure 1.13: Infant Upper Limb Zones

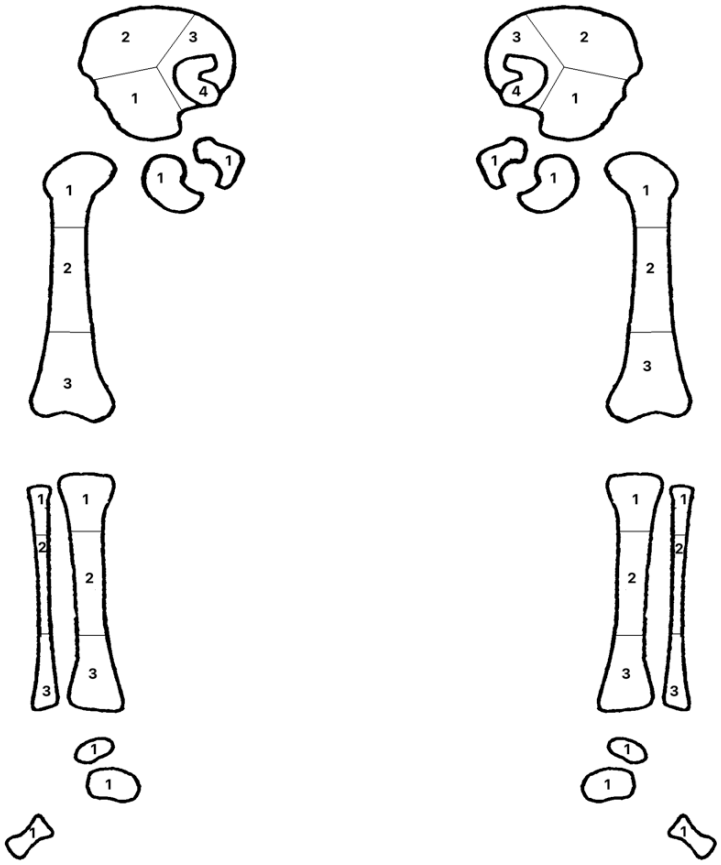

Figure 1.14: Infant Lower Limb Zones

## 1.6: Zonation Forms

Please click here https://kcw.q-ten.net/appendix/a1.6_zonation_forms.xlsx for the zonation forms. This link will automatically download the relevant appendix.

## 1.7: Example Dental Inventory Form

**Site**___ _____ **License no**_____ **BODY NO** | |

**Observer** _____ **Grave cut** _____ **BURIAL NO** | |

| | | | |
|---|---|---|---|
| \ | Tooth lost post mortem | **CR** | Caries |
| - | Tooth present but socket missing | **C** | Calculus |
| **X** | Tooth lost ante mortem | **A** | Abscess |
| **NP** | Tooth not present | **E** | Tooth erupting |
| **CA** | Congenital absence | **U** | Tooth unerupted |

### Presence

| Right | M3 | M2 | M1 | P4 | P3 | C | I2 | I1 | I1 | I2 | C | P3 | P4 | M1 | M2 | M3 | Left |
|---|---|---|---|---|---|---|---|---|---|---|---|---|---|---|---|---|---|
| *Max* | | | | | | | | | | | | | | | | | *Max* |
| *Mand* | | | | | | | | | | | | | | | | | *Mand* |
| Right | M3 | M2 | M1 | P4 | P3 | C | I2 | I1 | I1 | I2 | C | P3 | P4 | M1 | M2 | M3 | Left |

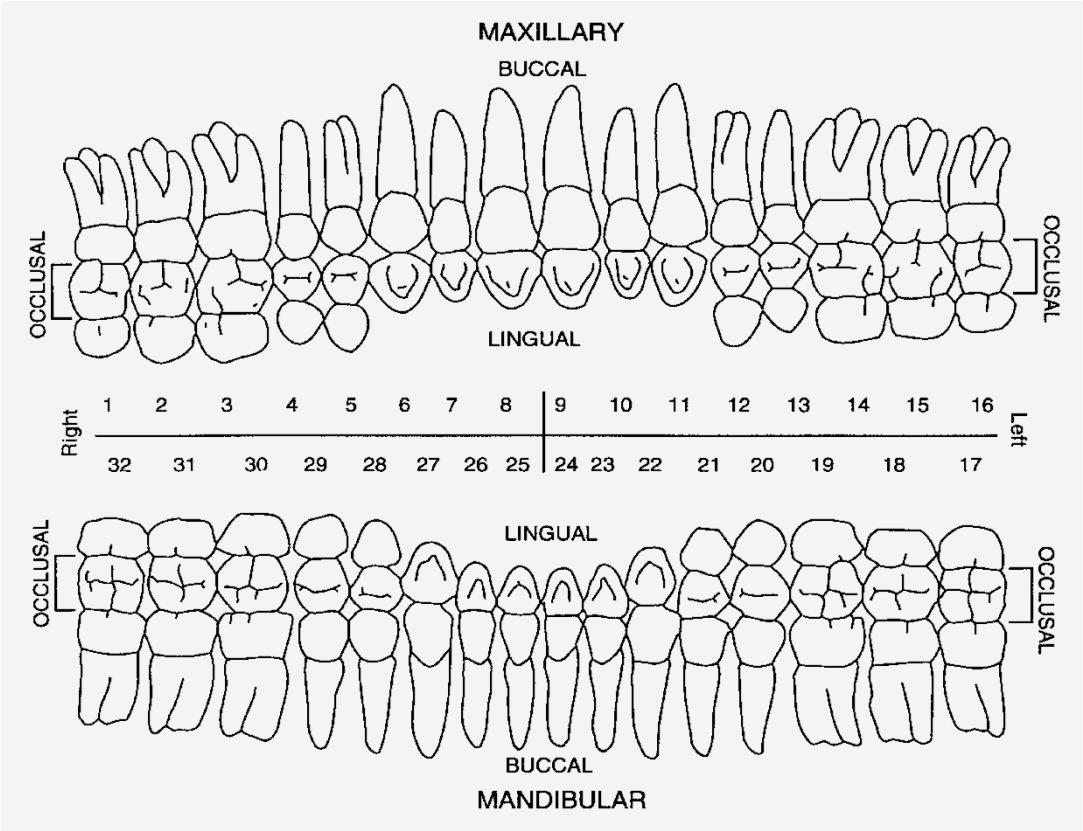

## Calculus

| Right | M3 | M2 | M1 | P4 | P3 | C | I2 | I1 | I1 | I2 | C | P3 | P4 | M1 | M2 | M3 | Left |
|---|---|---|---|---|---|---|---|---|---|---|---|---|---|---|---|---|---|
| *Max* | | | | | | | | | | | | | | | | | *Max* |
| *Mand* | | | | | | | | | | | | | | | | | *Mand* |
| Right | M3 | M2 | M1 | P4 | P3 | C | I2 | I1 | I1 | I2 | C | P3 | P4 | M1 | M2 | M3 | Left |

## Caries

| Right | M3 | M2 | M1 | P4 | P3 | C | I2 | I1 | I1 | I2 | C | P3 | P4 | M1 | M2 | M3 | Left |
|---|---|---|---|---|---|---|---|---|---|---|---|---|---|---|---|---|---|
| *Max* | | | | | | | | | | | | | | | | | *Max* |
| *Mand* | | | | | | | | | | | | | | | | | *Mand* |
| Right | M3 | M2 | M1 | P4 | P3 | C | I2 | I1 | I1 | I2 | C | P3 | P4 | M1 | M2 | M3 | Left |

## Hypoplasia

| Right | M3 | M2 | M1 | P4 | P3 | C | I2 | I1 | I1 | I2 | C | P3 | P4 | M1 | M2 | M3 | Left |
|---|---|---|---|---|---|---|---|---|---|---|---|---|---|---|---|---|---|
| *Max* | | | | | | | | | | | | | | | | | *Max* |
| *Mand* | | | | | | | | | | | | | | | | | *Mand* |
| Right | M3 | M2 | M1 | P4 | P3 | C | I2 | I1 | I1 | I2 | C | P3 | P4 | M1 | M2 | M3 | Left |

## Attrition

| Right | M3 | M2 | M1 | P4 | P3 | C | I2 | I1 | I1 | I2 | C | P3 | P4 | M1 | M2 | M3 | Left |
|---|---|---|---|---|---|---|---|---|---|---|---|---|---|---|---|---|---|
| *Max* | | | | | | | | | | | | | | | | | *Max* |
| *Mand* | | | | | | | | | | | | | | | | | *Mand* |
| Right | M3 | M2 | M1 | P4 | P3 | C | I2 | I1 | I1 | I2 | C | P3 | P4 | M1 | M2 | M3 | Left |

## Peridontitis

| Right | M3 | M2 | M1 | P4 | P3 | C | I2 | I1 | I1 | I2 | C | P3 | P4 | M1 | M2 | M3 | Left |
|---|---|---|---|---|---|---|---|---|---|---|---|---|---|---|---|---|---|
| *Max* | | | | | | | | | | | | | | | | | *Max* |
| *Mand* | | | | | | | | | | | | | | | | | *Mand* |
| Right | M3 | M2 | M1 | P4 | P3 | C | I2 | I1 | I1 | I2 | C | P3 | P4 | M1 | M2 | M3 | Left |

## 1.8: Gross Taphonomy

Please click here https://kcw.q-ten.net/appendix/a1.8_gross_taphonomy.xlsx for the gross taphonomy spreadsheets. This link will automatically download the relevant file.

## 1.9: Criteria for Taphonomy Observations

Table 1.5: Descriptive criteria for Taphonomy observations from Hawks et al., 2017

| Taphonomic Character | Descriptive Criteria |
|---|---|
| **General preservation** | This is an assessment of general bone quality and preservation, encoding information related to the degree of surface modification, surface erosion and cortical integrity. Criteria are modified from *Standards for Recording Human Remains* for skeletal inventories [1]. Four grades defined; (1) denotes slight to patchy surface erosion or modification; (2) more extensive surface erosion than grade 1 with deeper surface penetration; (3) most of bone surface affected by some degree of erosion - general morphology maintained but detail of parts of surface masked by erosive action; (4) majority of bone surface affected by erosive action - general profile maintained and depth of modification not uniform across whole surface. |
| **Mineral Staining** | Iron (red) staining. Denotes the presence of iron oxide staining on bone surfaces. Graded as (1) heavy indicating surface staining of more than 50% of the bone surface (may be continuous or discontinuous), or (2) patchy indicating discontinuous coverage over less than 50% of the surface. |
| | Manganese (black). Denotes the presence of manganese oxyhydroxide staining on bone surfaces. Graded as (1) heavy indicating surface staining of more than 50% of the bone surface (may be continuous or discontinuous), or (2) patchy indicating discontinuous coverage over less than 50% of the surface. |
| | Stain pattern (of mineral). Indicates the general pattern of mineral staining or deposition on the surface of bone. Recording as: (1) spotted or diffuse patches (may be present as irregular or random spots comprising multiple patches a few millimetres in diameter, or more focussed and slightly larger 'leopard' spotting ); (2) a mat or continuous surface of mineral with a surface coverage generally greater than 400 mm2. |
| | Tide mark. This indicates the presence of a longitudinal mineral stain. Stains are visible as single or multiple linear deposits of manganese and/or iron oxy-hydroxide phases, and mark a contact boundary between the bone surface and surrounding sediment, and indicate the resting orientation of the bone during precipitation of the stains [2]. Recorded as (1) present or (0) absent. |

| | |
|---|---|
| **Fracture Pattern** | Peri-mortem trauma. Identification of fracture patterns consistent with biomechanical markers of green or wet bone failure, using classification criteria from the forensic [3-7] and archaeological literature [8, 9]. Nomenclature based on cross-sectional morphology of fractured ends as presented by Galloway [10-13] consistent with markers of tensile- compressive failure. Fractures are recorded as (1) transverse, (2) spiral, (3) oblique, (4) butterfly, (5) segmental or (6) other (comminuted, longitudinal incomplete, greenstick, torus etc.). |
| | Post-mortem fractures. Identification of fracture patterns consistent with dry bone breakage using mechanical and gross-morphological classification criteria [6, 8]. Nomenclature based on cross-sectional morphology of fractured ends from Marshall [14] consistent with markers of biomechanically incompetent failure. Fractures are recorded as (1) transverse dry, (2) step or columnar, (3) oblique dry, (4) y-shaped, (5) flaked, (6) longitudinal, (7) other. |
| | Crushing. Evidence of localised surface compression with retention of comminuted fragments. Recorded as (1) present or (0) absent. |
| | Recent fracture or edge wear. Evidence of recent damage or abrasion to dry bone as evidenced by mismatch between internal structures or cortex at fresh break points being differentiated by showing as pale buff to off-white in cross- section. Recorded as (1) present or (0) absent. |
| **Surface Effects** | Cracking. The presence of incomplete surface disruptions which are observed in cases of sub-aerial (external) weathering [2, 15-21] and sub-surface burial environments [22, 23]. Cracking is recorded as: (1) transverse, across the long axis of a bone or perpendicular to longitudinal cracks; (2) longitudinally along the primary axis of the bone; (3) following the bone grain; (4) other |
| | Crack penetration. The extent of penetration into cortical structure, as observed in plan and cross section. Recorded as: (1) superficial where cracking penetrates less than 25% of the cortex as seen in cross section, or observed in plan; (2) deep, where cracks penetrate more than 25% of the cortex as seen in cross section (may extend through cortex as split lines) |

| | |
|---|---|
| | Patination (mosaic cracking). Superficial cracking or crazing across an area greater than 1cm2. Recorded as (1) present or (0) absent. |
| | Delamination/peeling. The presence of rough homogeneously altered cortical bone, with fibrous texture evidenced. Splinters of bone may be present in adhesion or removed, and areas of exfoliation noted. Recorded as (1) present or (0) absent. |
| | Bleaching (localised or hemi-surface). Recorded as (1) present or (0) absent. |
| **Cortical Removal** | Areas of possible gross invertebrate modification of the available cortical surface, consistent with the criteria of Dirks [24] and Backwell [25]. These can occur as (1) focussed or singular spots of outer cortex, (2) multifocal defects, or (3) diffuse areas of radular damage observed under low magnification. |
| | Striations. Areas of fine radular damage observed under low magnification, consistent with the criteria of Dirks [24] and Backwell [25]. These can occur as (1) single striae, (2) multiple clusters, or (3) diffuse/random in distribution. |
| **Pitting** | Areas of possible gross invertebrate modification of the available cortical surface, consistent with the criteria of Dirks [24] and Backwell [25]. Pitting up to 2mm in diameter, which occurs as round, ovoid or sub-rectangular defects in plan. Recorded as (1) diffuse or (2) occurring in clusters or multi-focal areas. |
| | Position of pitting. Recorded as (1) random or diffuse, (2) adjacent to a joint surface, or (3) distal (mid-diaphyseal) to a joint surface or epiphysis. |
| **Furrow or gouge** | Short, parallel, and linear or straight marks that may be perpendicular or transverse to the long axis of the bone. Recorded as (F) furrow or (G) gouge; (1) present or (0) absent. |
| **Modification of mineral deposit** | Pit defects or areas of cortical removal which penetrates pre-existing mineral surface deposits or concretions (iron or manganese). Recorded as (1) yes (0) no. |
| **Destruction (underlying surface exposed)** | Areas of cortical removal consistent with invertebrate modification, sediment abrasion or other mechanisms. Recorded as occurring at (E) epiphyses or the joint surface, or (N) non-epiphyseal (diaphyseal or other cortical surface). Extent recorded as (1) single surface or (2) multiple surfaces affected. |

| | |
|---|---|
| | Coffin wear. The patterned, localized destruction of margins of joint surfaces brought about by contact with a hard substrate during decomposition. Colloquially this is referred to as coffin wear. Areas affected include the posterior portions of several elements, including the occipital portion of the cranium, the vertebral spines/arches, the scapulae, the pelvis, and the limb bones whilst in supine or anatomical position [22]. Recorded as (1) present or (0) absent. |
| **Fluvial transport markers** | The presence of trace criteria characteristic of fluvial transport. These comprise: (T) thinning; (S) smoothing; (P) polish; (F) frosting; and (W) window or aperture formation. Identification criteria derived from forensic [26-28] and palaeontological sources [29-31]. Individual coded criteria recorded as (1) present or (0) absent. |
| **Bore hole** | Deep circular or ovoid defects greater than 2mm in diameter, perpendicular to, or running parallel to the bone surface [25, 32]. Recorded as (1) present or (0) absent. |
| **Cut or chop marks** | The presence of trace criteria characteristic of cutting, hacking or chopping. These comprise: (C) cut marks; (P) peeling or shaved defects; (N) point insertions or notched defects; (S) slot fractures; (M) chop marks or scoop defects [33-38]. Individual coded criteria recorded as (1) present or (0) absent. |
| **Carnivore modification** | The presence of trace criteria characteristic of carnivore modification of bone. These comprise: (B) bone cylinders; (P) tooth pits; (S) tooth scores; (E) end scalloping; (G) gastric corrosion [39, 40]. Individual coded criteria recorded as (1) present or (0) absent. |
| **Rodent** | Localised or widespread multiple striated defects to the cortical surface and exposed bone edges [40]. Recorded as (1) present or (0) absent. |
| **Burnt** | Presence of thermal alteration as evidenced by burn line, charring or calcination [41, 42]. Recorded as (1) present or (0) absent. |

## 1.10: Cave Ha 3 Archive

Please click here https://kcw.q-ten.net/appendix/a1.10_archive_spreadsheet_cave_ha_3.xlsx for the Cave Ha 3 archive spreadsheet. This link will automatically download the relevant file.

## 1.11: Georeferenced Taphonomy Tables

### *1.11.1 Cave Ha 3 Attribute Spreadsheets*

Please click here https://kcw.q-ten.net/appendix/a1.11.1_cave_ha_3_attribute_spreadsheet.xlsx for the attribute spreadsheets. This link will automatically download the relevant file.

### *1.11.2 Heaning Wood Attribute Spreadsheets*

Please click here https://kcw.q-ten.net/appendix/a1.11.2_heaning_wood_attribute_spreadsheet.xlsx for the attribute spreadsheets. This link will automatically download the relevant file.

# APPENDIX TWO: CAVE HA 3 QUANTIFICATION

## 2.1: Cave Ha 3 Master Spreadsheet

Please click here

https://kcw.q-ten.net/appendix/a2.1_cave_ha_3_specimen_spreadsheet.xlsx for the Cave Ha 3 master spreadsheet. This link will automatically download the relevant file.

# APPENDIX THREE: CAVE HA 3 DEMOGRAPHICS

## 3.1: Metrics

### *3.1.1: Individual 1*

Table 3.1: Metrics for Cave Ha 3 Individual 1

| M# | Description | L mm | R mm | M# | Description | L mm | R mm |
|---|---|---|---|---|---|---|---|
| 1 | Maximum cranial length | / | / | 40 | Humerus maximum length | / | / |
| 2 | Maximum cranial breadth | / | / | 41 | Humerus epicondylar breadth | / | / |
| 3 | Bizygomatic diameter | / | / | 42 | Humerus vertical head diameter | / | / |
| 4 | Basion-bregma height | / | / | 43 | Humerus maximum midshaft dia | / | / |
| 5 | Cranial base length | / | / | 44 | Humerus minimum midshaft dia | / | / |
| 6 | Basion-prosthion length | / | / | 45 | Radius maximum length | / | 223 |
| 7 | Maxillo-alveolar breadth | / | / | 46 | Radius A-P midshaft diameter | / | / |
| 8 | Maxillo-alveolar length | / | / | 47 | Radius M-L midshaft diameter | / | / |
| 9 | Biauricular breadth | / | / | 48 | Ulna maximum length | / | / |
| 10 | Upper facial height | / | / | 49 | Ulna A-P diameter | / | / |
| 11 | Minimum frontal breadth | / | / | 50 | Ulna M-L diameter | / | / |
| 12 | Upper facial breadth | / | / | 51 | Ulna physiological length | / | 225* |
| 13 | Nasal height | / | / | 52 | Ulna minimum circumference | / | / |
| 14 | Nasal breadth | / | / | 53 | Sacrum anterior length | / | / |
| 15 | Orbital breadth | / | / | 54 | Sacrum anterior superior breadth | 104.4 | |
| 16 | Orbital height | / | / | 55 | Sacrum max transverse base dia | 54.4 | |
| 17 | Biorbital breadth | / | / | 56 | Os coxae height | / | / |
| 18 | Interorbital breadth | / | / | 57 | Os coxae iliac breadth | / | / |
| 19 | Frontal chord | / | / | 58 | Os coxae pubis length | / | / |
| 20 | Parietal chord | / | / | 59 | Os coxae ischium length | / | / |
| 21 | Occipital chord | / | / | 60 | Femur maximum length | 401 | / |
| 22 | Foramen mangum length | / | / | 61 | Femur bicondylar length | 400 | / |
| 23 | Foramen magnum breadth | / | / | 62 | Femur epicondylar breadth | 73.8 | / |
| 24 | Mastoid length | / | / | 63 | Femur maximum head diameter | 39.5* | / |
| 25 | Chin height | / | / | 64 | Femur A-P subtrochanteric dia | / | / |
| 26 | Height of mandibular body | / | / | 65 | Femur M-L subtrochanteric dia | / | / |
| 27 | Breadth of mandibular body | / | / | 66 | Femur A-P midshaft diameter | / | / |
| 28 | Biogonial width | / | / | 67 | Femur M-L midshaft diameter | / | / |
| 29 | Bicondylar breadth | / | / | 68 | Femur midshaft circumference | / | / |
| 30 | Minimum ramus breadth | / | / | 69 | Tibia length | / | / |

| | | | | | | | |
|---|---|---|---|---|---|---|---|
| 31 | Maximum ramus breadth | / | / | 70 | Tibia max prox epiphyseal breadth | / | / |
| 32 | Maximum ramus height | / | / | 71 | Tibia max distal epihyseal breadth | / | / |
| 33 | Mandibular length | / | / | 72 | Tibia max dia at nutrient foramen | / | / |
| 34 | Mandibular angle | / | / | 73 | Tibia M-L dia at nutrient foramen | / | / |
| 35 | Clavicle maximum length | / | 134.3 | 74 | Tibia circum at nutrient foramen | / | / |
| 36 | Clavicle A-P midshaft diameter | / | 11.47 | 75 | Fibula maximum length | / | / |
| 37 | Clavicle S-I midshaft diameter | / | 8.83 | 76 | Fibula maximum dia at midshaft | / | / |
| 38 | Scapular height | / | / | 77 | Calcaneus maximum length | 69.03* | 73.6 |
| 39 | Scapular breadth | / | / | 78 | Calcaneus middle breadth | 33.87 | 42.6 |

*partial

Red = fractured/damaged

Femoral VHA (L) = 79.70 mm

### *3.1.2: Individual 2*

Table 3.2: Metrics for Cave Ha 3 Individual 2

| **Specimen ID** | **Bone** | **Side** | **Metric** |
|---|---|---|---|
| CH3.13.116 | UL | R | Max Length = 91.53mm (Partial) |
| CH3.70.114 | HU | L | Max length = 117.6mm (partial) |
| CH3.42.101 | FE | R | Max length = 152.7 mm (partial due to tufa obstruction/fracture) |
| CH3.42.488 | | | |
| CH3.77.239 | $PE_{IL}$ | R | Max Iliac Length = 55.8mm Iliac Width = 50.9 mm (partial) |
| CH3.12.10 | $CR_{fr}$ | | Partial frontal cord = 55.57mm |
| CH3.12.105 | $CR_{fr}$ | L | based on CH3.12.10/005 measurements |
| CH3.62.7 | CRM | L | |
| *CH3.12.3* | *$RdM_1$* | | MD =7.53mm BL = 7.13mm |
| *CH3.12.3* | *$RdM_2$* | | MD = 9.6 mm BL = 9.13 |
| *CH3.12.3* | *$LdM_1$* | | MD = 7.83mm BL = 7.03mm |
| *CH3.12.3* | *$LdM_2$* | | MD= 10.27 mm BL = 9.1mm |
| *CH3.12.3* | *$LM_1$* | | |
| CH3.62.7 | CRM | L | |
| | *$LdM^1$* | | *MD = 10.9mm LB= 8mm Crown =4.4mm* |
| | *$LdM^2$* | | *MD = 11.9mm LB= 8.8mm Crown = 5.4mm* |
| CH3.42.100 | FE | L | Max length = 152 mm (partial) |
| CH3.73.69 | TI | L | Combined measurement = 139.7mm length |
| CH3.73.68 | TI | L | |

### *3.1.3: Individual 3*

Table 3.3: Metrics for Cave Ha 3 Individual 3

| Specimen ID | Bone | Side | Metric |
|---|---|---|---|
| CH3.76.238 | SC | L | Scapular Width = 34.00mm Mid Dia Glenoidal Surface = 9mm Spine Length = 29.00mm |
| CH3.73.36 | $LdM_1$ | L | Crown Height = 6.4mm Root = R1/4 |
| CH3.73.224 | Cro | R | Max length = 35.7mm max Width = 24.6mm No Fusion |
| CH3.73.233 | R1 | R | Length = 30.2mm |
| CH3.73.67 | TI | L | Combined length = 91.6mm (complete fracture limits measurement) |
| CH3.73.39 | TI | L | |
| CH3.73.99 | RA | L | Partial max length = 54.3mm |
| CH3.73.98 | RA | R | Partial Length = 43.5mm |
| CH3.73.97 | UL | R | Partial Length = 59.1mm |
| CH3.70.245 | PEil | L | Max iliac length = 46.2mm Max iliac Width = 42.9mm (Damage obscuring measurements) |

### *3.1.4: Individual 4*

Table 3.4: Metrics for Cave Ha 3 Individual 4

| Specimen ID | Bone | Assessment |
|---|---|---|
| CH3.28.107/033 | CRt | Squama Height = 26.2mm Squama Width = 32.53mm |
| CH3.39.475/031 | UL | Max length = 60.5mm |
| CH34.478/032 | RA | Max Length = 52.53 |
| CH3.37.476/038 | UL | Max length = 59.5mm (Partial) |
| CH3.34.477/040 | RA | Max length = 51.6mm |
| CH3.37.474 | HU | Max length = 62.00mm Distal width = 15.06mm (Partial width) |
| CH3.37.481/039 | FI | Max length = 58.77mm |
| CH3.37.472/029 | FE | Max length = 73.8mm Distal width = 15.9mm (Partial width) |
| CH3.34.480/041 | TI | Max length = 60.9mm (Partial) |
| CH3.34.479/028 | TI | Max length = 63.6mm |
| CH3.37.473/027 | FE | Max length = 74.8mm Distal width = 18.07mm |
| CH3.42/204 | SC | Spine (partial)= 21.4mm Length (partial) =27.2mm |
| CH3.32.16/025 | CRp | Height cord =55.1mm Width cord = 74.2mm |
| CH3.32.15/026 | CRp | Height cord =57.2mm Width cord = 74.9mm |
| CH3.37.471/035 | SC | Spine (partial)= 20.5mm Length (partial) =24.4mm Width =17.2mm |
| CH3.28.106/042 | CRf | Height cord = 55.1mm Width Cord = 44.27mm |
| CH3.28/224 | CRt | Squama Width = 29.57mm |

# APPENDIX FOUR: CAVE HA 3 TAPHONOMY

## Appendix 4.1: Individual 1

Table 4.1.1: Fragments from Individual 1 with peri-mortem crushing.

| Bone Code | Bone ID | Side |
|---|---|---|
| CH3.77.96 | PE | R |
| CH3.73.221 | R1 | R |
| CH3.73.220 | RA | R |
| CH3.69.72 | FE | L |
| CH3.63.92 | LV3 | unsided |
| CH3.64.444 | R11 | R |
| CH3.65.82 | HU | R |
| CH3.73.62 | MPH 4 prox | L |
| CH3.65.74 | CL | L |
| CH3.14.40 | CAL | L |

Please click here https://kcw.q-ten.net/appendix/a4.1_cave_ha_3_individual_1_taphonomy.xlsx for all frequency tables relating to Individual 1 taphonomy. This link will automatically download the relevant file.

## Appendix 4.2: Individual 2

Table 4.2.1: Fragments excluded from Individual 2 GIS mapping.

| Bone Code | Bone ID | Side | Reason for exclusion |
|---|---|---|---|
| CH3.73.230 | LV | U/S | Uncertainty around position |
| CH3.73.232 | TV | U/S | Uncertainty around position |
| CH3.73.231 | TV | U/S | Uncertainty around position |
| CH3.63.490 | TV | U/S | Uncertainty around position |
| CH3.63.491 | TV | U/S | Uncertainty around position |
| CH3.63.492 | LV | U/S | Uncertainty around position |
| CH3.64.497 | R | R | Uncertainty around position |
| CH3.70.494 | R | R | Uncertainty around position |
| CH3.64.496 | R | R | Uncertainty around position |
| CH3.70 | R | L | Uncertainty around position |
| CH3.70 | R | L | Uncertainty around position |
| CH3.70 | R | L | Uncertainty around position |
| CH3.42.498 | R | L | Uncertainty around position |
| CH3.70.485 | R | L | Uncertainty around position |
| CH3.76.493 | R | R | Uncertainty around position |

Please click here https://kcw.q-ten.net/appendix/a4.2_cave_ha_3_individual_2_taphonomy.xlsx for all frequency tables relating to Individual 2 taphonomy. This link will automatically download the relevant file.

## Appendix 4.3: Individual 3

Table 4.3.1: Fragments from Individual 3 with peri-mortem crushing.

| Bone Code | Bone ID | Side |
|---|---|---|
| CH3.76.238 | SC | L |
| CH3.73.98 | RA | R |

Please click here https://kcw.q-ten.net/appendix/a4.3_cave_ha_3_individual_3_taphonomy.xlsx for all frequency tables relating to Individual 3 taphonomy. This link will automatically download the relevant file.

# Appendix 4.4: Individual 4

Table 4.4.1: Fragments excluded from Individual 4 GIS mapping.

| Bone Code | Bone ID | Side | Reason for exclusion |
|---|---|---|---|
| CH3.32.29 | $CR_{fg}$ | U/S | Unplaceable |
| CH3.37.469 | $CR_{fg}$ | U/S | Unplaceable |
| CH3.38.108 | $CR_{fg}$ | U/S | Unplaceable |
| CH3.37.486 | R | L | Uncertainty around position |
| CH3.37.484 | R | L | Uncertainty around position |

Table 4.4.2: Fragments from Individual 4 with peri-mortem crushing.

| Bone Code | Bone ID | Side |
|---|---|---|
| CH3.34.477 | RA | R |
| CH3.42 | SC | R |

Please click here https://kcw.q-ten.net/appendix/a4.4_cave_ha_3_individual_4_taphonomy.xlsx for all frequency tables relating to Individual 4 taphonomy. This link will automatically download the relevant file.

# APPENDIX FIVE: HEANING WOOD QUANTIFICATION

## 5.1: Heaning Wood Master Spreadsheet

Please click here https://kcw.q-ten.net/appendix/a5.1_heaning_wood_master_spreadsheet.xlsx for the Heaning Wood master spreadsheet. This link will automatically download the relevant file.

## 5.2: Heaning Wood Unassigned Fragments

Please click here https://kcw.q-ten.net/appendix/a5.2_heaning_wood_unassigned_fragments.xlsx for the spreadsheet of unassigned fragments. This link will automatically download the relevant file.

# APPENDIX SIX: HEANING WOOD DEMOGRPAHICS

## 6.1: Individuals E and F X-Rays

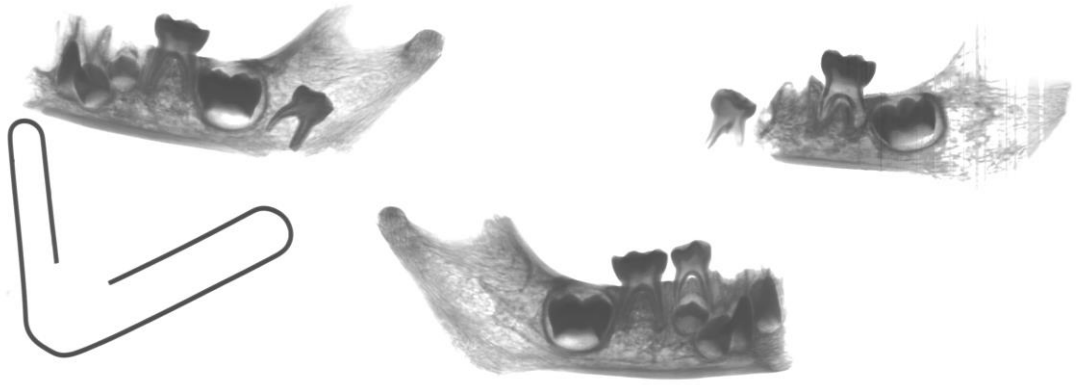

Figure 6.1: X-rays of HBC012 (E),HBC260 (E) and HBC238 (F) (left to right)

Figure 6.2: X-rays of HBC237 (E), HBC252 (E) and HBC256 (F) (left to right)

# APPENDIX SEVEN: HEANING WOOD TAPHONOMY

## Appendix 7.1: Individual A

Please click here https://kcw.q-ten.net/appendix/a7.1_heaning_wood_individual_a_taphonomy.xlsx for all frequency tables relating to Individual A taphonomy. This link will automatically download the relevant file.

## Appendix 7.2: Individual D

Please click here https://kcw.q-ten.net/appendix/a7.2_heaning_wood_individual_d_taphonomy.xlsx for all frequency tables relating to Individual D taphonomy. This link will automatically download the relevant file.

## Appendix 7.3: Individual B

Please click here https://kcw.q-ten.net/appendix/a7.3_heaning_wood_individual_b_taphonomy.xlsx for all frequency tables relating to Individual B taphonomy. This link will automatically download the relevant file.

## Appendix 7.4: Individual C

Please click here https://kcw.q-ten.net/appendix/a7.4_heaning_wood_individual_c_taphonomy.xlsx for all frequency tables relating to Individual C taphonomy. This link will automatically download the relevant file.

## Appendix 7.5: Individual E

Please click here https://kcw.q-ten.net/appendix/a7.5_heaning_wood_individual_e_taphonomy.xlsx for all frequency tables relating to Individual E taphonomy. This link will automatically download the relevant file.

## Appendix 7.6: Individual G

Please click here https://kcw.q-ten.net/appendix/a7.6_heaning_wood_individual_g_taphonomy.xlsx for all frequency tables relating to Individual G taphonomy. This link will automatically download the relevant file.